

Palladium-mediated C–H Functionalization of Aliphatic Amines via High Valent Palladium(IV) Intermediates

William George Whitehurst

Trinity College

University of Cambridge



This dissertation is submitted for the Degree of Doctor of Philosophy

Department of Chemistry

University of Cambridge

Lensfield Road

Cambridge

CB2 1EW

May 2020

Declaration

This thesis is submitted in partial fulfilment of the requirements for the Degree of Doctor of Philosophy. It describes the work carried out in the Department of Chemistry from October 2016 to March 2020. This dissertation is the result of my own work and includes nothing which is the outcome of work done in collaboration except where indicated in the text.

William G. Whitehurst

14th May 2020

Statement of Length

This dissertation does not exceed the word limit of 60,000 words as set by the Degree Committee for the Faculty of Physics and Chemistry.

William G. Whitehurst

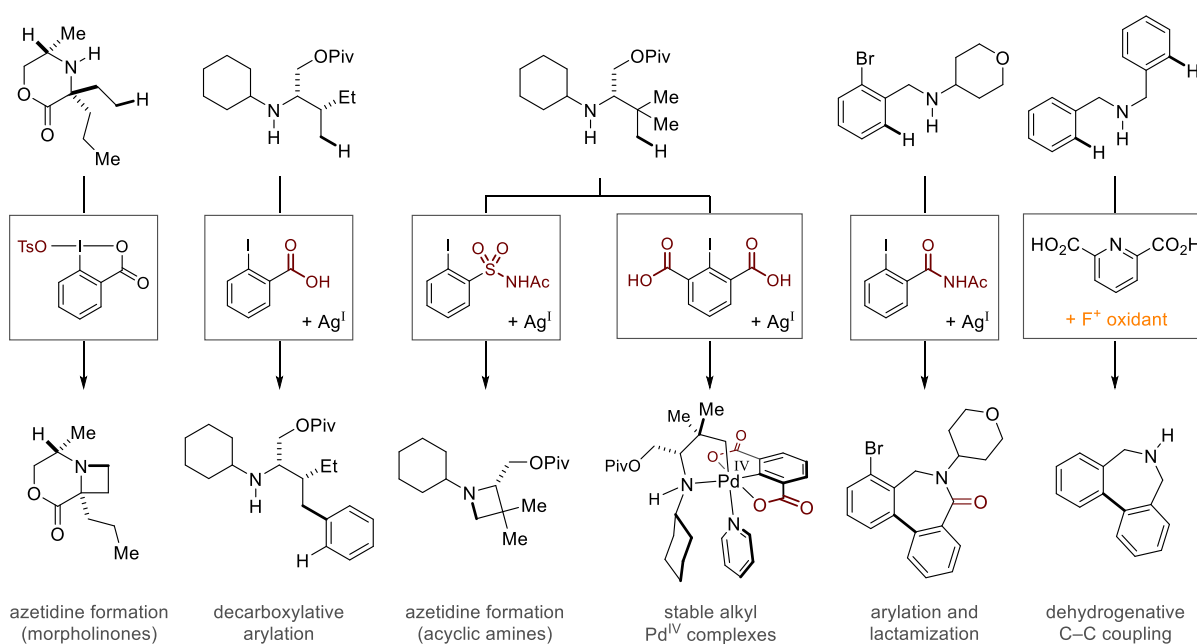
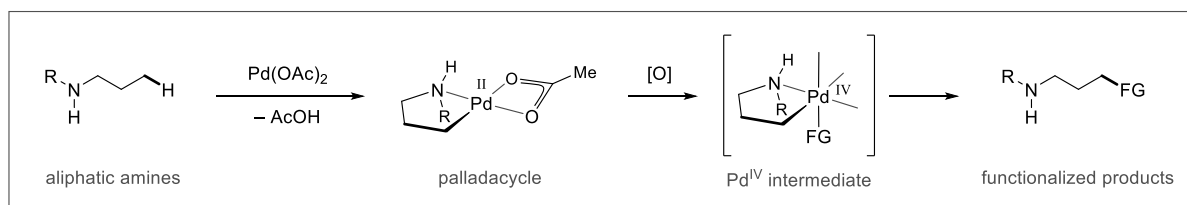
14th May 2020

Abstract: Palladium-mediated C–H Functionalization of Aliphatic Amines via High Valent Palladium(IV) Intermediates

William George Whitehurst

The search for new and distinct disconnection strategies is one of the foremost challenges in synthetic organic chemistry. To this end, transition metal-catalyzed C–H functionalization represents a current area of research which aims to develop transformations that directly convert C–H bonds to C–C or C–heteroatom bonds, often enabling the synthesis of functionalized products that are not readily accessible using classical synthetic methods.

The work disclosed in this thesis concerns the Pd-mediated C–H functionalization of unprotected aliphatic amines, in which the amine nitrogen coordinates to the Pd centre to promote cyclometalation to the key palladacycle intermediate. Specifically, research focused on the design and optimization of novel oxidants that would provide mild and general conditions to oxidize amine-derived palladacycles to high valent Pd^{IV} intermediates capable of undergoing a variety of reductive elimination pathways to afford a diverse range of functionalized products.



Hypervalent iodine(III) reagents were initially investigated as oxidants in the development of a Pd-catalyzed intramolecular γ C–H amination process to form azetidine products from hindered cyclic amines. Following this, aryl halides containing coordinating groups at the *ortho* position were discovered as efficient palladacycle oxidants in which the *ortho*-group pre-coordinates to the palladium centre to facilitate the oxidative addition of the carbon–halogen bond. Employing 2-halobenzoic acid reagents, a Pd-catalyzed γ C–H arylation of acyclic secondary amines was developed involving in situ decarboxylation of the aryl group. Conversely, exchanging the *ortho*-carboxylic group for an acyl sulfonamide resulted in a switch in the selectivity of reductive elimination to form azetidines. Subsequently, organometallic studies using an aryl iodide reagent containing two *ortho*-carboxylic acid groups provided access to isolable aminoalkyl Pd^{IV} complexes that were stable at room temperature, allowing for the study of the structure and reactivity of these previously elusive high valent intermediates.

In addition to C(sp³)–H functionalization of all-alkyl amines, C(sp²)–H functionalization of benzylamines was investigated, with a modified aryl iodide reagent enabling a Pd-catalyzed C–H arylation-lactamization process to form a 7-membered ring lactam product. Finally, a stoichiometric study on benzylamine-derived palladacycles led to the discovery of an unprecedented dehydrogenative intramolecular C–C coupling reaction under oxidative conditions employing 2,6-pyridinedicarboxylic acid and an electrophilic fluorine oxidant. Preliminary investigations provided support for a Pd^{IV}-mediated C–H activation step preceding C–C bond formation.

Acknowledgements

My deepest thanks to Professor Matthew Gaunt for giving me the opportunity to work in his Group. You have cultivated an amazing environment for scientific research that I was honoured to be a part of. I am profoundly grateful for the guidance and support you have given to me over the years and have learnt a great deal from your approach to conducting and communicating research. Perhaps someday I will reach your level of skill at Chemdraw.

Thanks to all the members of the Gaunt group who I have crossed paths with. Though you may not realise it, every one of you has had a positive influence on me as a scientist and as a person. Special thanks to Manuel and Chuan for taking me under their wing in the first year and for providing my first experience of novel organic chemistry actually working. Henry, not only was it a pleasure working with you on a project but I have cherished our many discussions over the years. Nils, given your likely discomfort in reading acknowledgements, I will just say that it was awesome working with you, though I think I have now heard AC/DC's Thunderstruck enough for one lifetime! Roopender – speaking with you over the years, it is apt that this work is towards a “Doctor of Philosophy”. I just always thought it was funny that ‘hard work never goes unrewarded’ came from the laziest postdoc I’ve ever known. Finally, thanks to Antonio, Jesus, Henry and Roopender for proof-reading this thesis.

Many thanks to Nic, Naomi and Carlos for your support and hard work in maintaining the labs. Thanks to Duncan and Andrew for all your help and advice with NMR experiments. Thanks to Dr. Bond for conducting all the X-ray crystallographic analysis and to the University of Cambridge and EPSRC Mass Spectrometry Services for obtaining HRMS data. Thanks to the EPSRC for funding my PhD studies. Above all, thanks to my family for their unwavering support.

Abbreviations

‡	denotes a transition state
%wt	percentage weight purity
(±)	racemic mixture
$[\alpha]_D^T$	specific (optical) rotation
Å	angstrom, 1×10^{-10} m
Ac	acetyl
aq.	aqueous
APAO	acetyl-protected aminomethyl oxazoline
AQ	8-aminoquinoline (auxiliary)
Ar	generic description for an aryl group
atm	atmosphere
BDE	bond dissociation energy
BINOL	1,1'-bi-2-naphthol
Bn	benzyl
Boc	<i>tert</i> -butoxycarbonyl
bpy	2,2'-bipyridine
BQ	1,4-benzoquinone
Bu	butyl
Bz	benzoyl
C	Celsius
<i>c</i>	concentration
cal	calories
cat.	catalytic
CMD	concerted metalation-deprotonation
cod	1,5-cyclooctadiene
Cy	cyclohexyl
δ	chemical shift relative to a defined standard
DCE	1,2-dichloroethane
DCM	dichloromethane
DFT	density functional theory
DG	directing group
DME	1,2-dimethoxyethane
DMAP	4-dimethylaminopyridine
DMF	dimethylformamide
DMSO	dimethylsulfoxide
DiPEA	<i>N,N</i> -diisopropylethylamine
d.r.	diastereomeric ratio
E ⁽⁺⁾	generic description for an electrophile
<i>ee</i>	enantiomeric excess
equiv	equivalent
e.r.	enantiomeric ratio
ESI	electrospray ionisation
Et	ethyl
eu	entropy unit ($\text{cal K}^{-1} \text{mol}^{-1}$)
<i>fac</i>	facial
Fc	ferrocenium
FG	functional group

g	gram
GC-MS	gas chromatography-mass spectrometry
Gly	glycine
Grubbs II	Grubbs catalyst 2 nd generation
h	hour
HFIP	hexafluoro-2-propanol
HMDS	hexamethyldisilazide
HPLC	high performance liquid chromatography
(HR)MS	(high resolution) mass spectrometry
HTIB	hydroxy(tosyloxy)iodobenzene
Hz	Hertz
<i>i</i>	iso
IBA	2-iodosylbenzoic acid
Int	intermediate
IR	infrared
<i>J</i>	coupling constant
k	kilo or rate constant
K	degrees Kelvin or equilibrium constant
KIE	kinetic isotope effect
L	litre or generic description for a ligand
Leu	leucine
μ	micro
M	mega or moles per litre or generic symbol for metal atom
<i>m</i>	meta
m	milli
Me	methyl
Mes	2,4,6-trimethylphenyl (mesityl)
min	minute
mol	mole
M.p.	melting point
MPAA	mono- <i>N</i> -protected amino acid
Ms	methanesulfonyl
M.S.	molecular sieves
μW	microwave irradiation
m/z	mass-to-charge ratio
[N]	generic symbol for an amine-derived <i>N</i> -directing group
<i>n</i>	normal
n.d.	not determined
NFSI	<i>N</i> -fluorobenzenesulfonimide
NFTPT	<i>N</i> -fluoro-2,4,6-trimethylpyridinium triflate
NMP	<i>N</i> -methyl-2-pyrrolidone
NMR	nuclear magnetic resonance
NOE	nuclear Overhauser effect
Ns	4-nitrobenzenesulfonyl
Nu ⁽⁻⁾ or Nuc	generic description for a nucleophile
<i>o</i>	ortho
[O]	generic description for an oxidant
obs	observed (from experiment)
<i>p</i>	para
Ph	phenyl

Phe	phenylalanine
PhI(DMM)	phenyl iodonium dimethylmalonate
phen	phenanthroline
Phth	1,3-dihydro-1,3-dioxoisindolyl (phthalimido)
pin	pinacol
Piv	pivaloyl
ppm	parts per million
Pr	propyl
pyr	pyridine
quant.	quantitative (yield)
R	generic description for a carbon-containing group
rac	racemic
Ref.	reference
R _f	retention factor
rt	room temperature
s	second
SM	starting material
S _N 1	unimolecular nucleophilic substitution
S _N 2	bimolecular nucleophilic substitution
T	temperature
<i>t</i>	tertiary (tert)
TBS	<i>tert</i> -butyldimethylsilyl
TCE	1,1,2,2-tetrachloroethane
TDG	transient directing group
Tf	trifluoromethanesulfonyl (triflyl)
TFA	trifluoroacetic acid or trifluoroacetate
THF	tetrahydrofuran
TIPS	triisopropylsilyl
TLC	thin layer chromatography
TMP	2,2,6,6-tetramethylpiperidine
TMS	trimethylsilyl
Tol	tolyl
TS	transition state
Ts	4-toluenesulfonyl (tosyl)
V	volt
Val	valine
X	generic description for a halide, pseudohalide, or counter anion

Table of Contents

Declaration	i
Statement of Length	i
Abstract: Palladium-mediated C–H Functionalization of Aliphatic Amines via High Valent Palladium(IV) Intermediates	ii
Acknowledgements	iv
Abbreviations	v
Table of Contents	viii
1. Introduction	1
1.1. C–H Functionalization by Transition Metal-mediated C–H Activation	1
1.1.1. Definitions of C–H Functionalization and C–H Activation	1
1.1.2. Overview: Concept, Challenges and Opportunities	1
1.1.3. C–H Activation: Mechanisms of C–H Bond Cleavage	2
1.1.4. Cyclometalation: Directed C–H Activation	4
1.1.5. C(sp ²)–H versus C(sp ³)–H Activation	6
1.2. Palladium-mediated Directed C–H Activation	8
1.2.1. CMD Mediated by Palladium(II) Carboxylate Complexes	8
1.2.2. Mechanisms of Palladacycle Functionalization & Catalytic Manifolds	10
1.2.3. Pd ^{II} -catalyzed C(sp ³)–H Functionalization of Aliphatic Amines	11
1.3. Organometallic Chemistry of Alkyl Pd ^{IV} Complexes	40
1.3.1. Synthesis of Alkyl Pd ^{IV} Complexes & Mechanisms of Oxidation	42
1.3.2. Pd ^{IV} -mediated C–C Bond Reductive Elimination	45
1.3.3. Pd ^{IV} -mediated C(sp ³)–heteroatom Bond Reductive Elimination	48
2. Pd-catalyzed γ C(sp ³)–H Amination to Form Azetidines	55
2.1. Background & Previous Work	55
2.2. Project Aims	61
2.3. Results & Discussion	62

2.3.1. Diastereopure Chiral Morpholinone Substrates	62
2.3.2. Acyclic Substrates	67
2.4. Summary	69
3. Pd-catalyzed C–H Functionalization by <i>ortho</i> -DG-assisted Oxidative Addition	71
3.1. Background & Project Aims	71
3.2. Results & Discussion	75
3.2.1. Stoichiometric Palladacycle Studies	75
3.2.2. Development of Catalysis & Reaction Scope	84
3.2.3. <i>ortho</i> -DG-assisted Oxidative Addition	90
3.3. Summary	95
4. Stable Alkyl Pd ^{IV} Complexes Derived from Cyclopalladated Amines & Oximes	97
4.1. Background & Project Aims	97
4.2. Results & Discussion	100
4.2.1. Synthesis & Reactivity of Stable Aminoalkyl Pd ^{IV} Complexes	100
4.2.2. Synthesis of an Oxime-derived Alkyl Pd ^{IV} Complex	104
4.2.3. Mechanism of the Nucleophile-mediated Reductive Elimination	106
4.2.4. Pincer-ligated Aryl Pd ^{IV} Complexes: Evidence for Pd ^{IV} -mediated C–H Activation	111
4.3. Summary	119
5. Conclusions & Outlook	121
6. Experimental	129
6.1. General Information	129
6.2. Experimental Procedures	131
6.2.1. Pd-catalyzed γ C(sp ³)–H Amination to form Azetidines	131
6.2.2. Pd-catalyzed C–H Functionalization by <i>ortho</i> -DG-assisted Oxidative Addition .	139
6.2.3. Stable Pd ^{IV} Complexes Derived from Cyclopalladated Amines & Oximes	164
7. References	178

Table of Contents

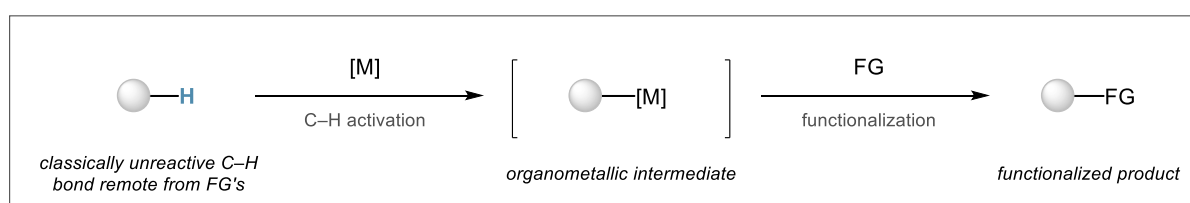
Appendix I: Miscellaneous Experimental Procedures	190
Appendix II: Supplementary Data	230
Appendix III: ^1H , ^{13}C and ^{19}F NMR Spectra	271
Appendix IV: Published Work.....	373

1. Introduction

1.1. C–H Functionalization by Transition Metal-mediated C–H Activation

1.1.1. Definitions of C–H Functionalization and C–H Activation

C–H functionalization is a class of chemical transformation involving the conversion of C–H bonds within organic molecules into other types of bonds in order to modify the carbon framework (C–C bond formation) or install functional groups (C–heteroatom bond formation). While a multitude of reactions fall into this broad definition, the work in this thesis specifically focuses on C–H functionalization reactions proceeding via transition metal mediated C–H activation (Scheme 1). C–H activation is defined as the stoichiometric or catalytic reaction of a transition metal complex with classically unreactive C–H bonds of hydrocarbons to form products or catalytic intermediates containing a new metal–carbon bond.^{1–3} The metal–carbon bond is a versatile synthetic intermediate due to the plethora of reactivity modes available to the metal centre, such as insertion, β -hydride elimination, transmetalation or oxidation, that can occur prior to bond-forming reductive elimination. Types of C–H functionalization that fall outside of this definition of C–H activation include (i) reactions that do not form an organometallic complex resulting from C–H bond cleavage (e.g. electrophilic aromatic substitution, insertion of metal carbenes or nitrenes, and radical hydrogen atom abstraction processes), and (ii) reactions that do not involve transition metal complexes (e.g. directed *ortho*-metalation of arenes by organolithium bases).

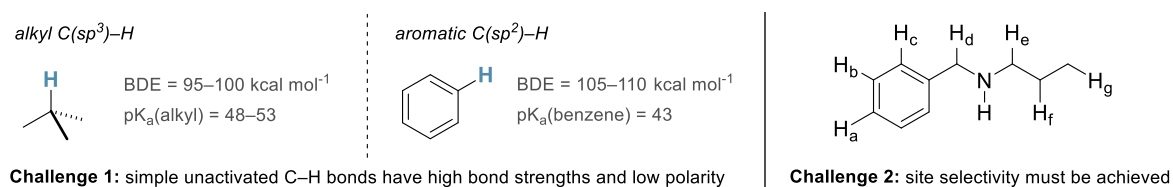


Scheme 1. Transition metal-mediated C–H activation. [M] = transition metal complex; FG = functional group.

1.1.2. Overview: Concept, Challenges and Opportunities

C–H functionalization is a highly attractive strategy for chemical synthesis, given that it utilizes the most abundant type of bond found in organic molecules: the carbon–hydrogen bond. Consequently, compared to more straightforward synthetic approaches involving the coupling

of pre-functionalized nucleophilic and electrophilic partners, such as in nucleophilic substitution or metal-catalyzed cross-coupling reactions, C–H functionalization offers a fundamentally more direct approach to constructing and derivatizing molecules. Nonetheless, despite its conceptual appeal, C–H functionalization presents two significant challenges to the realization of efficient and useful processes (Scheme 2).^{4–7} Firstly, C–H bonds have high bond strengths (bond dissociation energy, BDE(alkyl) = 95–100 kcal mol^{–1}, BDE(aryl) = 105–110 kcal mol^{–1}),^{8,9} and C–H bonds remote from functional groups have low polarity (pK_a(alkyl) = 48–53, pK_a(benzene) = 43).¹⁰ Secondly, the ubiquity of C–H bonds, despite being a primary advantage of the C–H functionalization approach, presents a formidable challenge given that the conditions of the reaction must be sufficiently discerning to react with one particular C–H bond in the presence of many other C–H bonds with similar properties.



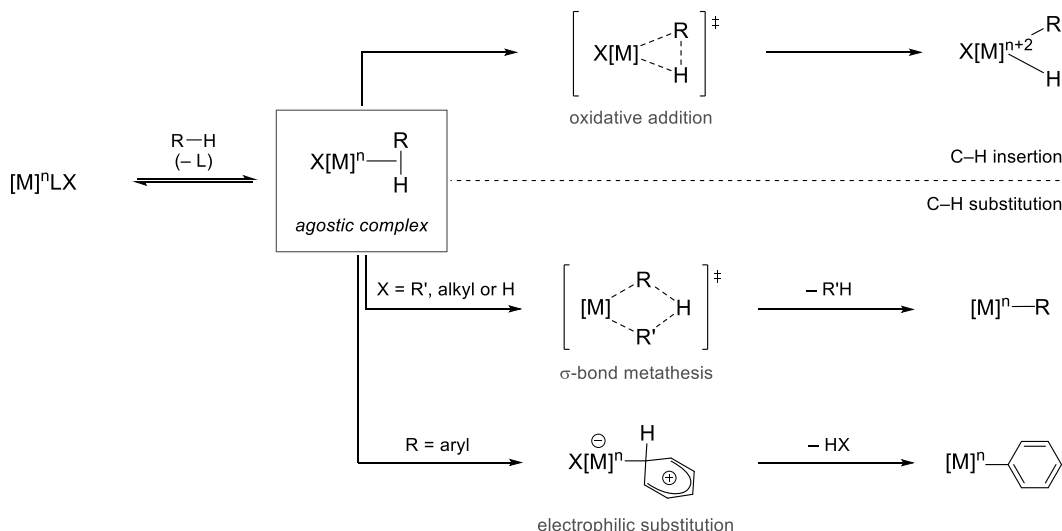
Scheme 2. Challenges of C–H functionalization: (1) C–H bond strength and polarity, and (2) site selectivity.

While reactive free radicals were known for more than a century to functionalize C–H bonds in alkanes, it was not until the 1950's and the increasing interest in organo-transition metal chemistry that the challenge of both reactivity and selectivity could be adequately met.^{3,11,12} In particular, mild C–H activation with transition metal complexes was readily demonstrated for a range of d-block elements, indicating the diverse applicability of such a mechanistic paradigm and the potential for exploiting the distinct properties of different metals. To date, several decades of research have led to increasingly efficient and selective catalytic systems that have established C–H functionalization as a powerful alternative disconnection strategy for the synthetic chemist.

1.1.3. C–H Activation: Mechanisms of C–H Bond Cleavage

Central to the development of C–H activation has been the understanding of possible mechanisms by which C–H bond cleavage can occur. In general terms, following ligand displacement to form an agostic interaction, there are two limiting scenarios for transition

metal-mediated C–H activation: insertion or substitution (Scheme 3).^{3,13–16} Insertion proceeds by an oxidative addition mechanism, whereas substitution is classically associated with either a σ -bond metathesis or electrophilic substitution mechanism.

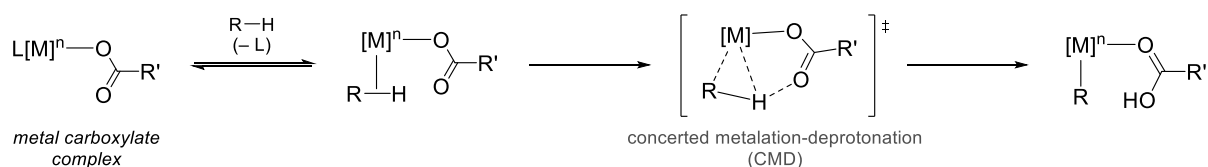


Scheme 3. C–H activation mechanisms: oxidative addition, σ -bond metathesis and electrophilic substitution.

Oxidative addition is typical of low valent, electron-rich late transition metals (Fe^0 , Ru^0 , Co^I , Rh^I , $Ir^{I/III}$) that can accommodate the +2 increase in oxidation state and coordination number.³ The insertion of the metal can occur for alkyl or aryl C–H bonds, resulting in the concomitant formation of M–H and M–C bonds. The concerted three-centred transition state comprises “forward” charge transfer from the filled σ C–H orbital to an empty metal d orbital, and “reverse” charge transfer from a filled metal d-orbital to the σ^* of the C–H bond.¹⁴ σ -Bond metathesis is a concerted substitution mechanism and is common for d^0 early transition metals (Groups 3, 4, Lanthanides and Actinides) where oxidative addition is not possible due to the lack of valence d-orbital electrons.³ The substitution process occurs via a concerted four-centre transition state that exchanges the bonds between a hydrocarbon moiety and a metal–alkyl or metal–hydride complex. Conversely, electrophilic substitution is a stepwise substitution mechanism that is associated with highly electrophilic late and post-transition metals (Pd^{II} , $Pt^{II/IV}$, Au^{III} , Hg^{II}).³ The mechanism is limited to aromatic C–H bonds, given that electrophilic attack by the metal complex leads to a new metal-carbon bond to form a cationic Wheland-type intermediate prior to deprotonation of the *ipso* C–H bond by an anionic ligand on the metal.

Recently, computational investigation into the mechanism of C–H activation across a range of transition metals has suggested that C–H bond cleavage is better represented by a

continuum of electrophilic, ambiphilic, and nucleophilic pathways leading to novel mechanisms for C–H activation being proposed.^{14,17} Significantly, in accordance with the discovery of carboxylate salts as beneficial additives for C–H activation,¹⁵ another prominent mechanistic pathway was identified pertaining to a substitution mechanism with characteristics of both σ -bond metathesis and electrophilic substitution. It is now widely understood that Lewis basic heteroatom-containing ligands can substantially lower the activation barrier to cleaving C–H bonds at a metal centre by acting as an internal base. The ambiphilic mechanism – known as concerted metalation–deprotonation (CMD, Scheme 4) – involves simultaneous interaction between the Lewis acidic metal and the C–H bond, and of the C–H proton with the nucleophilic internal base. For a bound carboxylate, CMD occurs via a concerted six-membered transition state leading to concomitant metalation and proton transfer.¹⁵ Notably, the concertedness of the mechanism allows for the activation of both alkyl and aryl C–H bonds. When a suitable internal base ligand is present, CMD is the major activation pathway for a range of transition metals including Pd^{II}, Ir^{III}, Rh^{III}, Co^{III} and Ru^{II}.

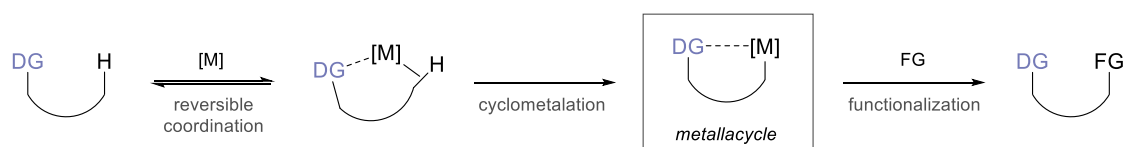


Scheme 4. Mechanism of concerted metalation-deprotonation (CMD) involving a carboxylate as internal base.

1.1.4. Cyclometalation: Directed C–H Activation

The development of new reactions using C–H activation relies on successfully achieving high levels of site selectivity, that is, the activation of a particular C–H bond over all others in the molecule. Control of site selectivity is crucial for a synthetically useful process because it avoids the formation of regioisomeric mixtures which may be difficult to separate. While a number of catalytic systems have obtained selectivity on the basis of the steric or electronic properties of the substrate,^{18–21} the approach that has attracted by far the most interest has been the use of directing groups (DG, Scheme 5).^{22–30} The directing group reversibly coordinates to the metal centre to promote intramolecular conversion of a proximal C–H bond to a metal–C bond in a process known as cyclometalation. The directing group favours C–H activation both in terms of kinetics, by increasing the local effective concentration of the metal complex, as well as thermodynamics, by stabilising the metallacycle intermediate by chelation.^{19,30} In

general, there is a strong kinetic and thermodynamic preference for cyclometalation via a 5-membered ring metallacycle, though 4- to 7-membered ring metallacycles are also readily formed.²⁹ Cyclometalation may be a reversible or irreversible process, depending on the type of directing group, transition metal and reaction conditions. Lastly, the resulting cyclometalation complex may undergo derivatization (or “functionalization”) to complete the overall directed C–H functionalization process.



Scheme 5. Directed C–H Activation: reversible coordination, cyclometalation and functionalization.

Stoichiometric cyclometalation was first reported in the early 1960's,^{29–31} initially with Group 10 transition metals (1963-1965: Ni, Pd, Pt)^{32,33} to form *ortho*-metalated complexes of azobenzenes, followed by various phosphorus-directed metallacycles of other platinum group metals (1967-1969: Ir, Rh, Ru; Figure 1).^{34–36} An important consequence of directing groups was that alkyl group C(sp³)–H activation also became possible under mild conditions, allowing for the isolation of metallacycles resulting from the cleavage of benzylic (Hartwell, 1970)³⁷ and later methyl C(sp³)–H bonds (Shaw, 1978).³⁸

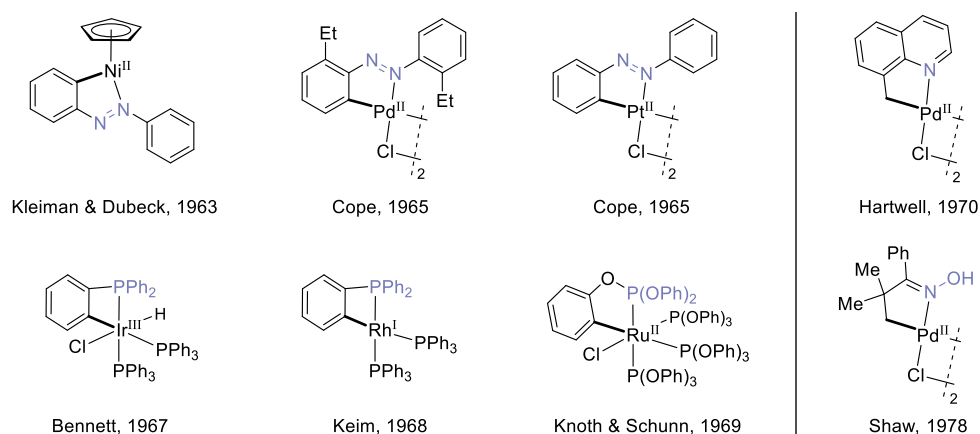
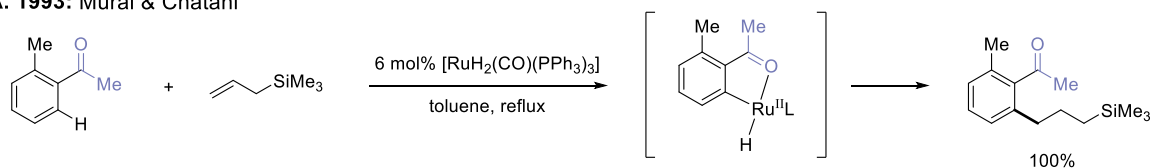


Figure 1. Early examples of cyclometalation complexes. Left: C(sp²) metallacycles. Right: C(sp³) metallacycles.

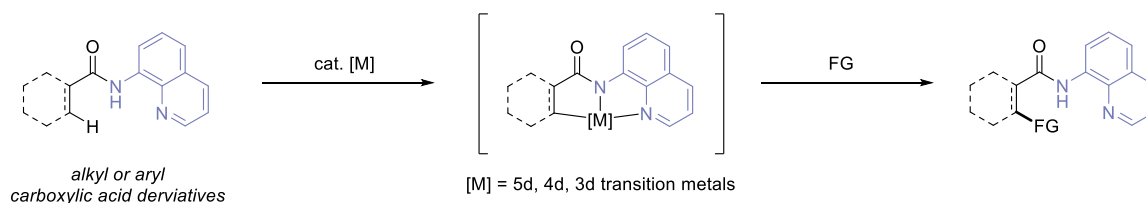
However, it was not until the 1990's that directing groups became widely used in the development of *catalytic* C–H activation processes. In 1993, seminal work by Murai and Chatani³⁹ reported the Ru-catalysed coupling of aryl ketones with olefins, providing the first

example of an efficient catalytic C–H activation process in which high selectivity, yields and good scope were attained (Scheme 6a). The reaction proceeds via a ketone-directed oxidative addition of a Ru^0 catalyst into the *ortho* C–H bond, forming a ruthenacycle intermediate which can react with olefins to form *ortho*-alkylated products. Over the subsequent decades, a significant number of directing groups were designed for transition metal-catalysed C–H activation, enabling a wide array of different C–H functionalization processes. In this regard, arguably the most widely employed directing group to date has been the venerable 8-aminoquinoline amide (AQ) auxiliary, first reported by Daugulis in 2005 for Pd-catalyzed C–H arylation (Scheme 6b).⁴⁰ The AQ auxiliary is a uniquely versatile directing group for C–H activation,^{41–47} having been used for a range transition metals across the periodic table including first-row metals, for both $\text{C}(\text{sp}^2)\text{--H}$ and $\text{C}(\text{sp}^3)\text{--H}$ activation, for a variety of different bond formations, as well as in the activation of structurally complex intermediates towards the synthesis of natural products.^{48–50}

A. 1993: Murai & Chatani



B. 8-Aminoquinoline amide directing group (Daugulis)



Scheme 6. Transition metal-catalyzed directed C–H activation: (a) Murai & Chatani's Ru-catalyzed *ortho*-C–H alkylation, and (b) Daugulis' 8-aminoquinoline amide directing group.

1.1.5. $\text{C}(\text{sp}^2)\text{--H}$ versus $\text{C}(\text{sp}^3)\text{--H}$ Activation

Within the field of C–H activation a clear distinction is made between the activation of aromatic $\text{C}(\text{sp}^2)\text{--H}$ and alkyl $\text{C}(\text{sp}^3)\text{--H}$ bonds. Although transition metal complexes are capable of cleaving both types of C–H bond, activation of aromatic $\text{C}(\text{sp}^2)\text{--H}$ bonds is generally much more facile than for alkyl $\text{C}(\text{sp}^3)\text{--H}$ bonds (Figure 2). Notably, this reactivity difference between C–H bonds is generally consistent regardless of the mechanism of activation. While $\text{C}(\text{sp}^2)\text{--H}$ bonds are typically more acidic and less hindered than $\text{C}(\text{sp}^3)\text{--H}$ bonds, an additional

reason for the diminished activation barrier for aromatic C(sp²)–H bonds stems from the fact that the π -system of the arene can interact with the metal centre to preassemble a reactive conformation, facilitating the formation of an agostic interaction and hence C–H activation.^{2,20,51} Interestingly, activation of alkenyl C(sp²)–H bonds has been significantly less explored than for aromatic systems due to the competitive reactivity of alkenes themselves as well as their proximal C(sp³)–H bonds.^{52,53} Indeed, C(sp³)–H bonds which are adjacent to unsaturated arene or alkene groups, such as benzylic or allylic C–H bonds, are also readily cleaved by metals and are considered as electronically-activated C(sp³)–H bonds due to their low bond strength and increased acidity (BDE(allylic C–H) = 85–90 kcal mol⁻¹, pK_a = 43)^{9,10} compared to electronically unactivated C(sp³)–H bonds. In particular, allylic C–H activation is often extremely facile due to the ready formation of π -allyl complexes and typically does not require the assistance of a directing group.^{4,54} Finally, comparing types of unbiased C(sp³)–H bonds, methyl groups are more readily activated over methylene groups on the basis of sterics, and inner-sphere C–H bond cleavage at tertiary centres is very rare.⁵⁵ A general reactivity trend for metal-mediated directed C–H activation is shown in Figure 2.

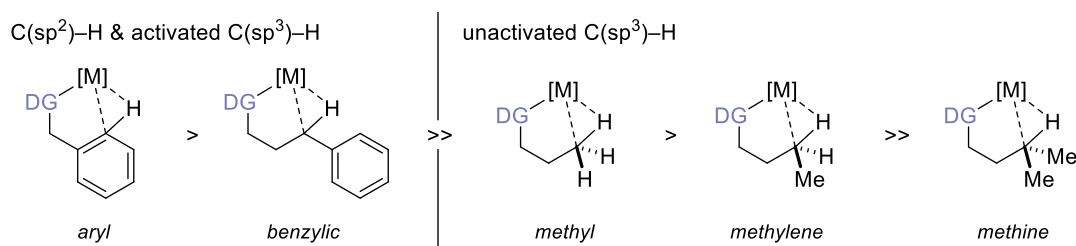
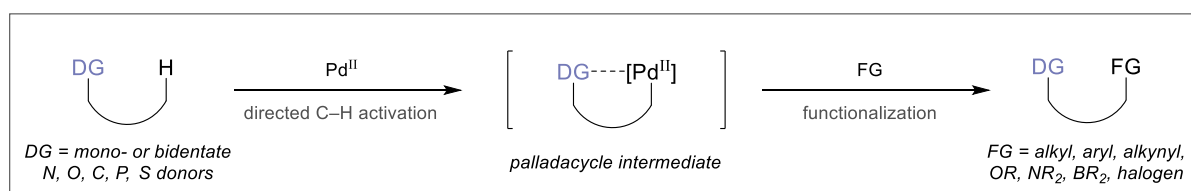


Figure 2. Reactivity trend for metal-mediated cyclometalation (alkenyl and allylic cases excluded for clarity).

1.2. Palladium-mediated Directed C–H Activation

To date, palladium has been the most widely employed element for metal-mediated or -catalyzed directed C–H functionalization (Scheme 7).^{5,9,18,30,31,41,44,45,56–65} The reason for its prevalence can be attributed to two important factors. Firstly, Pd^{II} complexes bearing carboxylate ligands are among the most active species for cleaving C–H bonds, being able to activate both C(sp²)–H and C(sp³)–H bonds with high levels of efficiency. In fact, Pd^{II} complexes are largely unrivalled in the context of more challenging directed C(sp³)–H activation;^{45,58,59,63,65} whereas essentially all other transition metals require the use of strongly coordinating bidentate directing groups, or high temperature or harshly acidic conditions to cleave unactivated alkyl C(sp³)–H bonds, Pd^{II} complexes can mediate C(sp³)–H activation with a broad range of directing groups (including weakly coordinating monodentate DG's)³¹ under mild, functional group tolerant conditions. Secondly, the metallacycles resulting from C–H activation (termed, palladacycles)^{66–71} have a distinctly versatile reactivity in that bond-forming reductive elimination can occur through a variety of oxidative, reductive as well as redox neutral pathways, meaning that multiple different mechanisms are often possible for a particular type of bond formation. This mechanistic flexibility afforded by palladium has facilitated the development of catalytic transformations, establishing palladium catalysis as the foremost approach for metal-mediated directed C–H functionalization.

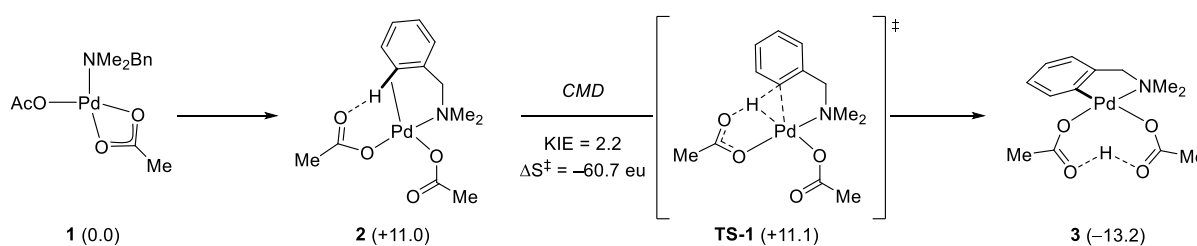


Scheme 7. Pd-mediated directed C–H activation: broad applicability to a variety of DG's and bond formations.

1.2.1. CMD Mediated by Palladium(II) Carboxylate Complexes

C–H activation by a CMD mechanism is available to a variety of transition metals. However, it is apparent that palladium is uniquely placed in the Periodic Table to satisfy the requirements of the ambiphilic mechanism across a range of substrate classes. Notably, while palladium can readily access oxidation states between 0 and +4, C–H activation almost exclusively occurs at a square planar Pd^{II} centre.^{5,31,72}

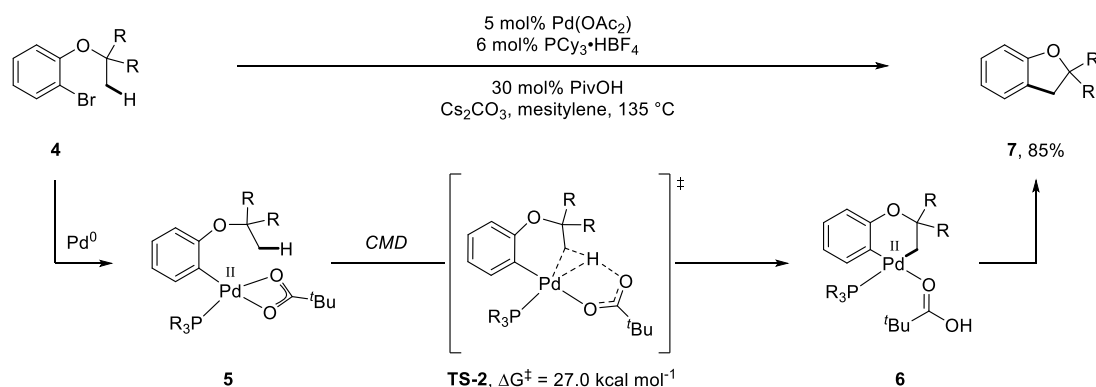
A pioneering experimental study into the mechanism of palladium(II) acetate-mediated C(sp²)-H activation was carried out by Ryabov in 1985 on the *ortho*-palladation of *N,N*-dimethylbenzylamine in chloroform (Scheme 8).^{73,74} Ryabov proposed that coordinatively unsaturated complex **1** forms prior to C-H activation. The cleavage of the C-H bond had an associated kinetic isotope effect (KIE, $k_{\text{H}}/k_{\text{D}}$) of 2.2 and a large, negative activation entropy of $-60.7 \text{ cal K}^{-1} \text{ mol}^{-1}$ indicative of a highly ordered transition state (**TS-1**). Consequently, Ryabov suggested that the transition state features concerted Pd-C bond formation and acetate-assisted C-H bond cleavage (i.e. CMD).^{28,73,75} A computational study of the reaction by Davies and Macgregor⁷⁶ in 2005 supported the proposal of CMD, highlighting the importance of the agostic C-H complex **2** that precedes near-barrierless C-H bond cleavage to **3**. Notably, the study did not find evidence supporting the formation of a Wheland-type intermediate characteristic of a stepwise electrophilic substitution mechanism.



Scheme 8. Mechanism for palladium(II) acetate-mediated C(sp²)-H activation of *N,N*-dimethylbenzylamine. Computed energies shown in parentheses in kcal mol⁻¹. “eu” = cal K⁻¹ mol⁻¹.

Recently, more detailed studies on Pd^{II}-mediated aromatic C(sp²)-H activation have attributed the broad applicability of the CMD mechanism to the potential for significant asynchronicity in the transition state.^{17,77} For example, C-H bond cleavage can either be more or less advanced than Pd-C bond formation depending on the relative electrophilicity of the Pd^{II} centre and electronic properties of the substrate. Conversely, such a detailed analysis of CMD has not been conducted for alkyl C(sp³)-H activation, with the mechanism being largely derived by analogy with sp² systems. An early study that implicated a CMD mechanism for Pd^{II}-mediated C(sp³)-H activation was conducted by Fagnou⁷⁸ in 2007 for a Pd⁰-catalyzed intramolecular C-H arylation to form dihydrobenzofuran products (**7**, Scheme 9). DFT studies were conducted from Pd^{II} intermediate **5** formed from the oxidative addition of a phosphine-ligated Pd⁰ complex into the C-Br bond of **4**, with a low energy transition state (**TS-2**, $\Delta G^\ddagger = 27.0 \text{ kcal mol}^{-1}$) being found involving carboxylate-assisted CMD of the pendant methyl group to form 6-membered palladacycle **6**. An alternative mechanism involving C(sp³)-H oxidative

addition was considered but ruled out on the basis of the instability of the resulting alkyl,hydride-Pd^{IV} intermediate ($\Delta G = 47.7 \text{ kcal mol}^{-1}$ relative to **5**).

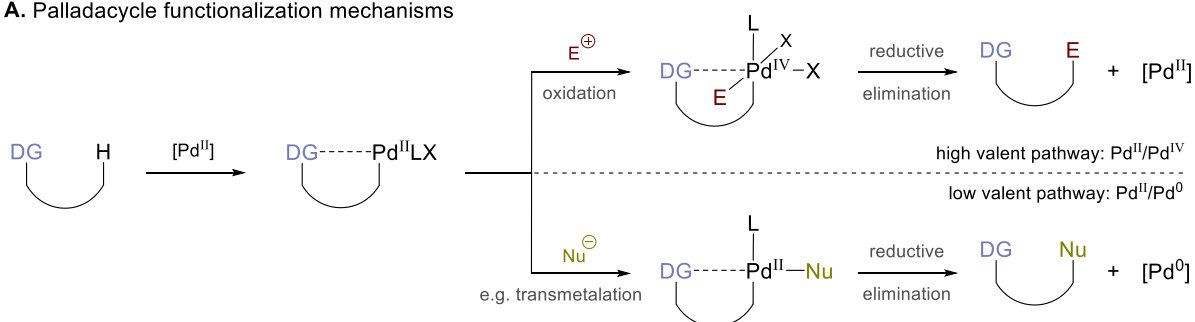


Scheme 9. Mechanism of Pd^{II}-mediated C(sp³)-H activation: computational studies conducted by Fagnou.

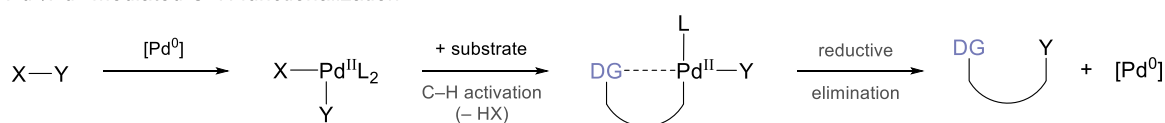
1.2.2. Mechanisms of Palladacycle Functionalization & Catalytic Manifolds

The Pd^{II} metallacycle formed upon directed C-H activation contains a Pd-C bond which can be functionalized by one of two general mechanistic pathways – the “high valent” or “low valent” pathway – depending on the types of intermediates formed prior to reductive elimination (Scheme 10).^{5,31,59} The high valent pathway involves oxidation of the Pd^{II} metallacycle to form a Pd^{IV} intermediate, typically by employing an electrophilic organohalide or iodine(III) reagent. These reactive Pd^{IV} species can mediate a range of reductive elimination pathways, including C-C as well as more challenging C-heteroatom bond formations. Notably,

A. Palladacycle functionalization mechanisms



B. Pd⁰/Pd^{II}-mediated C-H functionalization



Scheme 10. Palladacycle functionalization: (a) high valent & low valent pathways and (b) Pd⁰/Pd^{II} mechanism.

under certain conditions, aromatic C(sp²)-palladacycles also have the possibility to form higher speciation Pd^{III}/Pd^{III} dimers upon oxidation, which have been associated with more facile bimetallic oxidation and reductive elimination processes.^{79–82} On the other hand, the low valent pathway involves a redox-neutral step, such as transmetalation of a nucleophilic coupling partner or insertion of an unsaturated reagent such as an alkene, followed by reductive elimination.

In the context of catalytic processes, the high valent pathway results in the formation of a Pd^{II} by-product that is at the required oxidation state to mediate another C–H activation. Conversely, the low valent pathway releases a Pd⁰ by-product that must undergo oxidation to Pd^{II} by a reagent known as the terminal oxidant to turnover the catalytic cycle. The terminal oxidant is typically a Cu^{II} or Ag^I additive, benzoquinone or simply oxygen.⁵ In catalysis, the low valent mechanism is generally limited to C–C bond formation given that C–H activation requires a vacant site of coordination and thus does not usually tolerate the strongly donating and bulky phosphines required to promote C–heteroatom bond reductive elimination from a Pd^{II} centre.⁸³ An exception to the use of phosphine ligands in C–H activation concerns a less common catalytic manifold wherein the steps of the low valent pathway are reversed (Pd⁰/Pd^{II} mechanism),^{31,59} such as in the intramolecular C(sp³)–H arylation of Fagnou (above, Scheme 9). Here, an electron-rich Pd⁰ complex first undergoes oxidative addition to Pd^{II}, followed by C–H activation and reductive elimination. Although the Pd⁰/Pd^{II} manifold is an effective terminal oxidant-free low valent strategy, particularly for undirected C(sp²)–H arylation,⁸⁴ for directed C(sp³)–H activation this mechanism is typically limited to activated benzylic positions or intramolecular transformations.⁶⁰

1.2.3. Pd^{II}-catalyzed C(sp³)–H Functionalization of Aliphatic Amines

Aliphatic amines are essential molecules for society, in particular due to their high representation in bio-active molecules such as alkaloid natural products and pharmaceutical agents (Figure 3).^{85–90} While the polar nitrogen-containing functional group of aliphatic amines and their derivatives often plays a key role in the interactions with biomolecules such as proteins through hydrogen bonding, the nucleophilic character of amines also provides an opportunity for interaction with transition metals for exploiting in catalytic processes. Pd^{II}-catalyzed C(sp³)–H functionalization directed by amine-derived monodentate or bidentate nitrogen directing groups has emerged as a powerful method to streamline the synthesis of complex

aliphatic amines by the site-selective modification of the hydrocarbon framework.^{59,65} A general catalytic cycle for this process is shown in Scheme 11. Starting from a catalyst-bound nitrogen-containing aliphatic molecule, directed C–H activation by a Pd^{II} centre via carboxylate-assisted CMD first takes place to form a palladacycle containing a cyclometalated amine derivative. The palladacycle is then functionalized via a high valent Pd^{II}/Pd^{IV} or low valent Pd^{II}/Pd⁰ mechanism to form the derivatised product, which is released from the catalyst by the binding of another substrate molecule. Catalytic reactions are categorised based on the type of directing group strategy that is used. In general, there are three main sub-classes:⁶⁵ (i) pre-installed amine-derived directing groups, (ii) in situ-formed and cleaved (transient) directing groups and (iii) native amine-directed (or DG-free) strategy.

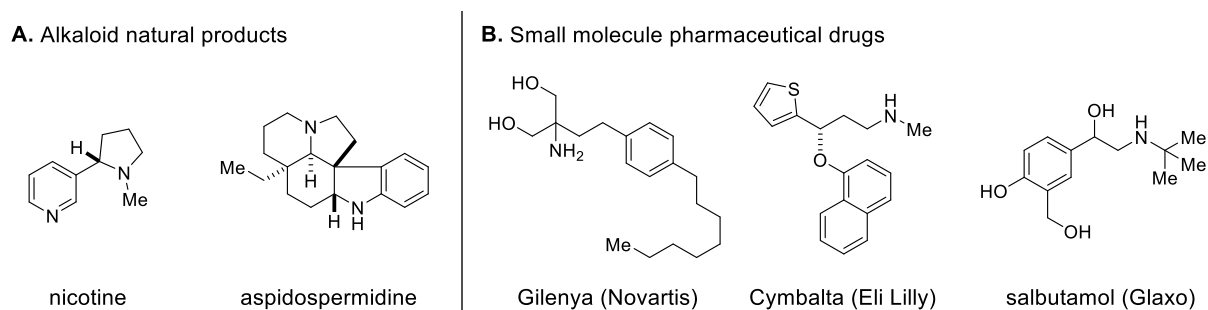
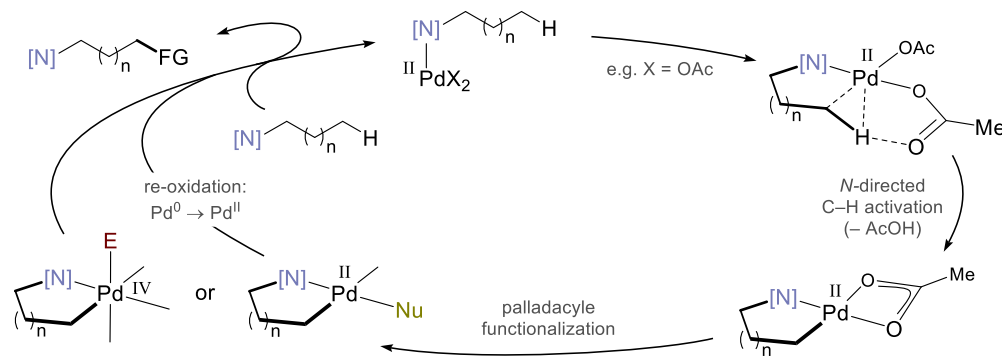


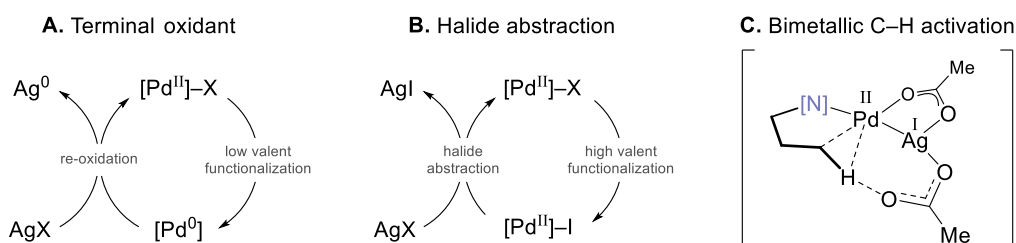
Figure 3. Bio-active aliphatic amines: (a) alkaloid natural products; (b) small molecule pharmaceutical drugs.



Scheme 11. General catalytic cycle for Pd^{II}-catalyzed C(sp³)–H functionalization of aliphatic amines. [N] = amine-derived *N*-directing group.

Before entering a discussion of the relevant literature, an important aspect to highlight about Pd^{II}-mediated C–H activation is the frequent use of stoichiometric Ag^I salt additives in the reaction conditions of catalytic processes. While not an ideal additive due to the relatively high cost and associated toxicity of silver salts, it is evident that Ag^I additives have broadly

resulted in improved catalytic efficiency for a wide variety of cases, and in some instances are essential for the transformation, which has enabled the realization of increasingly challenging catalytic processes.^{59,65} On the one hand, rudimentary roles of Ag^I salts include their use as terminal oxidants in low valent functionalizations, or as halide abstractors in high valent functionalizations using aryl or alkyl iodide reagents that result in unreactive Pd^{II}–iodide complexes being formed (Scheme 12).⁹¹ On the other hand, recent analysis has attributed their widespread use to a more intimate role in catalysis, with the proposal that Ag^I is involved in heterobimetallic interactions with Pd^{II} to facilitate the C–H bond cleavage.^{92–95} Although the majority of evidence to date has been from computational studies, there is increasing support in favour of this privileged role of silver in C–H activation making it an important consideration in mechanistic discussion.

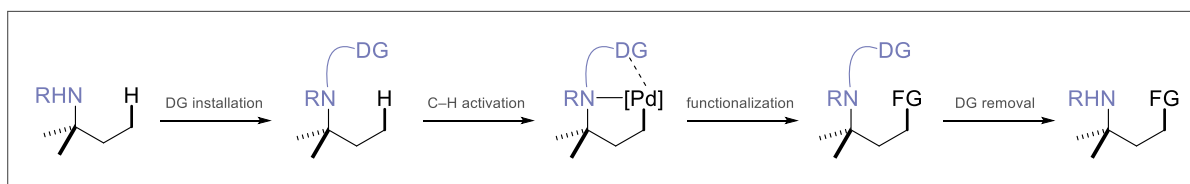


Scheme 12. Roles of silver(I) salts: (a) terminal oxidant, (b) halide abstraction, (c) bimetallic C–H activation.

1.2.3.1. Amine-derived Directing Group Strategy

The original and most explored approach to Pd-catalyzed amine C–H functionalization has been the amine-derived directing group strategy (Scheme 13).^{40,65} The strategy involves the prior installation of a DG through a covalent linkage to the amine nitrogen, with the DG being an electron-withdrawing or chelating moiety that facilitates directed C–H activation by the palladium catalyst. After functionalization, the DG is removed in a subsequent step to reveal the final product. The drawbacks of the strategy are that two (or more) steps are added to the synthetic sequence and that the use of a DG, if not recovered, leads to stoichiometric waste. Nonetheless, there are several benefits to using pre-installed directing groups. Firstly, DG installation typically converts the amine into an amide or sulfonamide, which protects the amine-nitrogen and significantly increases the thermal and chemical stability of the substrate. Secondly, DG's often provide a dominant interaction with the catalyst, making the catalytic processes tolerant of other coordinating functional groups. Thirdly, the DG can be modified at will in order to improve catalytic efficiency or alter site selectivity. Overall, despite its

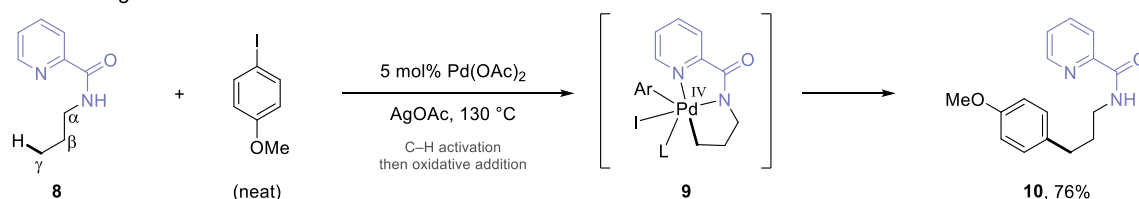
shortcomings, the amine-derived directing group strategy is the most straightforward approach to catalytic C–H activation, resulting in its widespread use for amine functionalization.



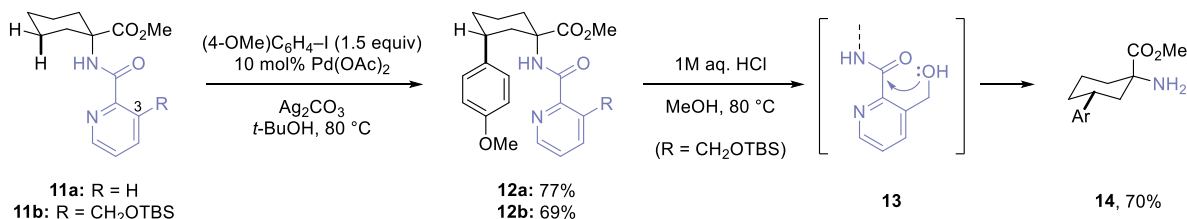
Scheme 13. Amine-derived directing group strategy: DG installation and removal required.

The first example of Pd-catalyzed C(sp³)–H functionalization of an aliphatic amine derivative was reported by Daugulis⁴⁰ in 2005, in which substrates bearing the picolinamide directing group (**8**) underwent C–H arylation when using aryl iodides in the presence of AgOAc (Scheme 14A). The picolinamide DG is a strongly coordinating bidentate auxiliary that forms a 5-membered ring chelate with the Pd^{II} catalyst, promoting the formation of both the

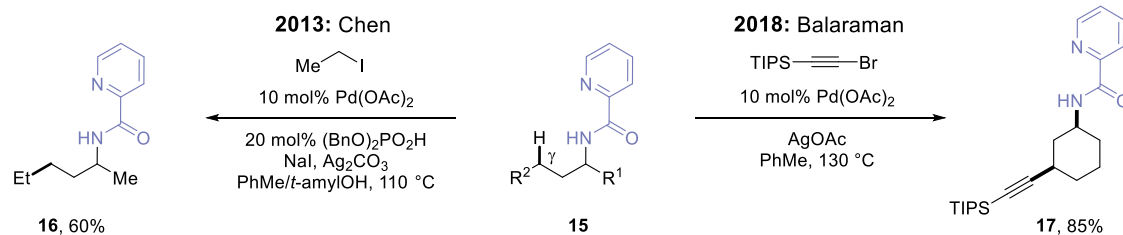
A. 2005: Daugulis



B. 2011: Chen



C. C–H alkylation & alkynylation

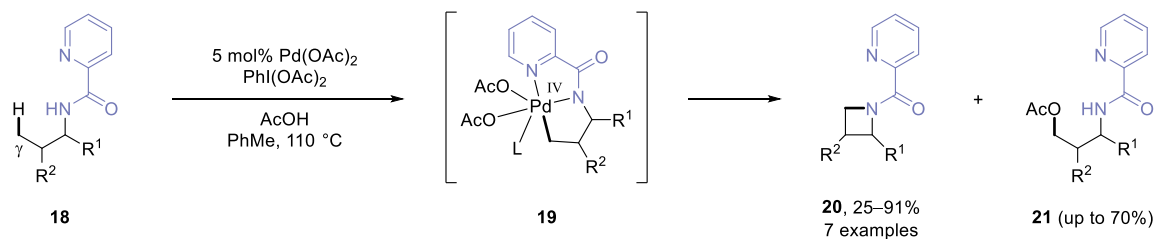
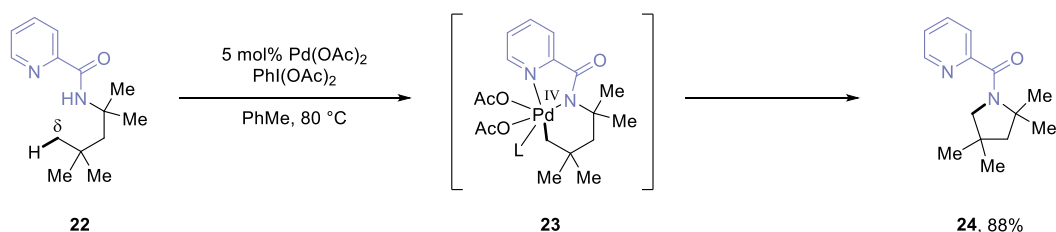
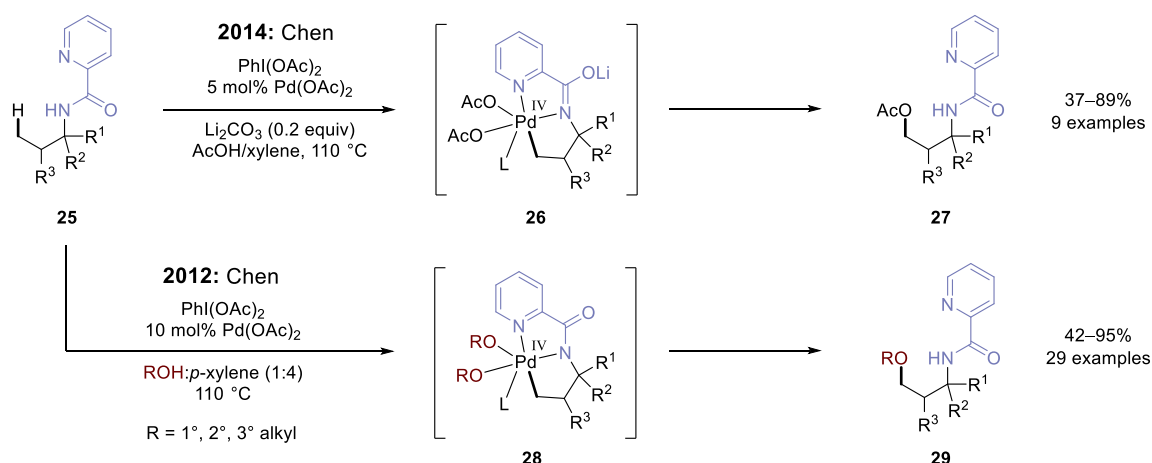


Scheme 14. Pd-catalyzed picolinamide-directed C(sp³)–H activation: C–C bond-forming reactions.

palladacycle as well as the subsequent oxidative functionalization. Selective mono-arylation was observed with complete selectivity for the γ position, indicating the preference of the DG to promote cyclometalation via a 5-membered palladacycle to form a 5,5-bicycle around the metal centre. Oxidative addition of the aryl iodide to the palladacycle forms putative Pd^{IV} intermediate **9**, which undergoes C(sp³)-C(sp²) bond reductive elimination to give arylated product **10**. Although good catalytic efficiency was achieved, undesirable features of the reaction were the use of aryl iodide as solvent and the high reaction temperature (130 °C).

Following the seminal work of Daugulis, in 2011 Chen⁹⁶ developed an improved protocol for the picolinamide-directed γ C(sp³)-H arylation (Scheme 14B). The reaction was conducted with only a small excess of aryl iodide (1.5 equivalents) and at a lower temperature of 80 °C. The reaction was demonstrated for γ -methylene activation of cyclohexylamine derivatives (**11**) to afford products bearing the aryl group on the same face as the picolinamide DG (**12**). Alkenyl iodides could also be employed under slightly modified conditions to provide γ -alkenylenated products. Significantly, Chen found that the picolinamide DG within product **12a** could not be hydrolytically cleaved in satisfactory yield, presumably due to the steric hindrance of the quaternary centre adjacent to the amide nitrogen. Consequently, a modified picolinamide DG was designed, containing a silyl-protected hydroxymethyl substituent at the 3-position of the pyridine ring (**11b**). After conducting the C-H arylation (**12b**), the modified DG could be cleaved under acidic aqueous conditions (1 M aq. HCl, MeOH, 80 °C) wherein the deprotected alcohol attacks the proximal carbonyl to cleave the amide linkage (**13**) and release the desired primary amine product **14**. Subsequently, other C-C bond forming processes were developed with picolinamide-protected substrates (**15**, Scheme 14C), such as alkylation with primary alkyl iodides (**16**; Chen, 2013)⁹⁷ and alkynylation using a TIPS-protected alkynyl bromide (**17**; Balaraman, 2018).⁹⁸ Interestingly, the alkylation procedure employed an unusual dibenzyl phosphate additive, which was proposed to act as a phase transfer catalyst to solubilize the Ag^I salt. Increased Ag^I concentration was thought to assist in the reaction between the palladacycle and alkyl iodide by weakening of the C-I bond, thus facilitating the oxidation of the Pd^{II} centre.

Alongside the development of C-C bond-forming reactions, the picolinamide DG was also used to mediate C-heteroatom bonding-forming reactions. In 2012, Chen⁹⁹ reported the intramolecular γ C-H amination of picolinamide-containing substrates (**18**) to form strained azetidine products (**20**) by employing PhI(OAc)₂ as oxidant (Scheme 15A). The mechanism involves oxidation of the palladacycle by PhI(OAc)₂ to form a Pd^{IV} intermediate bearing acetate ligands (**19**), which can undergo C-N bond reductive elimination of the deprotonated amide of

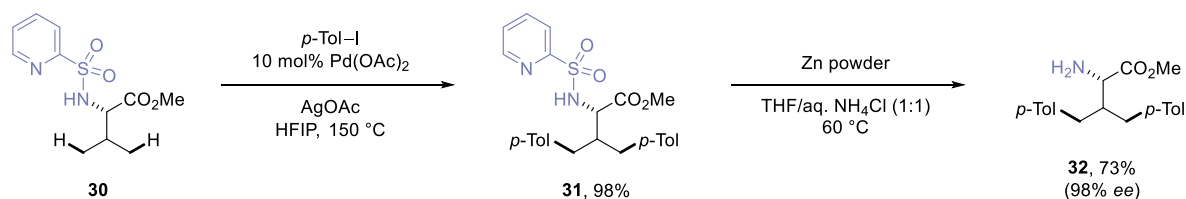
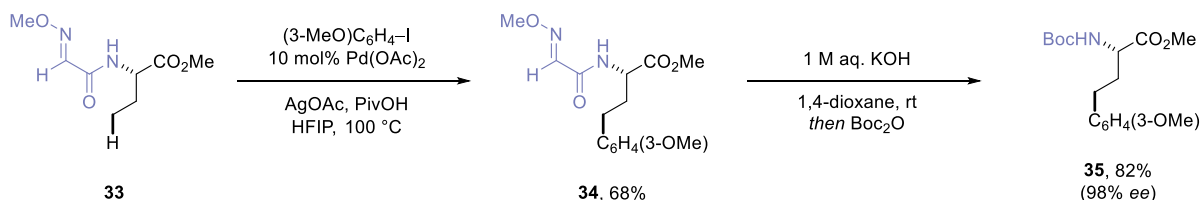
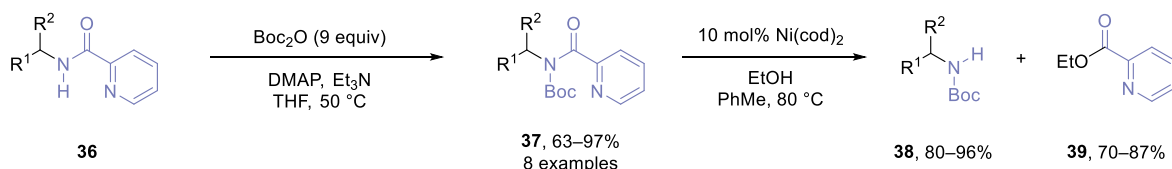
A. 2012: Chen**B. 2012:** Daugulis (& Chen)**C. C–H acetoxylation & alkoxylation****Scheme 15.** Pd-catalyzed picolinamide-directed C(sp³)-H activation: C–heteroatom bond-forming reactions.

the DG onto the carbon of the activated γ position. The by-product (**21**) resulting from competing C–O bond reductive elimination from the Pd^{IV} intermediate was also observed in the majority of cases as the minor product, indicating the significant challenge associated with Pd^{IV} chemistry for selective bond-forming reductive elimination. Notably, the yield of cyclized azetidine product correlated with the degree of branching along the activated alkyl chain, and in fact, for an example with no β -substituent (**18**: R¹ = CO₂Me, R² = H), the acetoxylated product became the major product (70% C–O, 25% C–N). In the same article,⁹⁹ Chen reported the formation of pyrrolidines using the same conditions via activation of the δ position, which was simultaneously reported by Daugulis.¹⁰⁰ Given that the favoured position of activation is the γ position, substrates for the pyrrolidine-forming reaction required γ -substitution (e.g. **22**) to block this position and thus prevent undesired side-reactions. Analogous to the azetidine

formation, the homologous 6-membered palladacycle is oxidized by $\text{PhI}(\text{OAc})_2$ to form a Pd^{IV} intermediate (**23**) which promotes cyclization to the pyrrolidine (**24**).

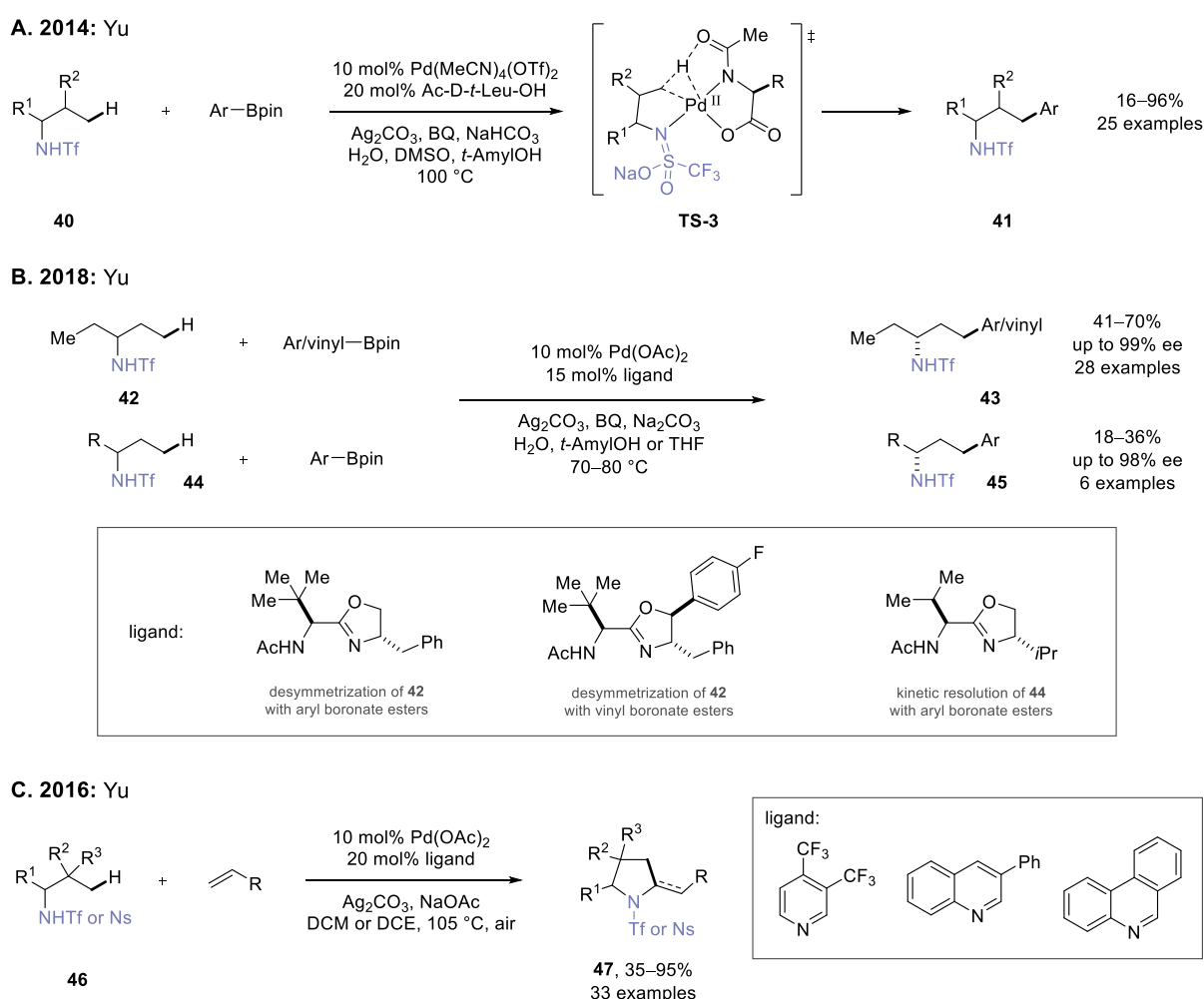
A selective γ C–H acetoxylation reaction using the picolinamide DG was later developed by Chen¹⁰¹ (**25** to **27**, Scheme 15C). Although $\text{PhI}(\text{OAc})_2$ was once again used, selectivity for acetoxylation over intramolecular amination was improved by the addition of a sub-stoichiometric amount of Li_2CO_3 . The role of Li_2CO_3 was not elucidated, but it was proposed that Li^+ could favour the imidate resonance form of the picolinamide (**26**) and thus minimize C–N bond reductive elimination, which requires an anionic *N*-ligand.^{102,103} The ability to modify the Pd^{IV} intermediate was also exploited by Chen for a γ C–H alkoxylation reaction.¹⁰⁴ Using $\text{PhI}(\text{OAc})_2$ in the presence of an alcohol co-solvent, the putative Pd^{IV} intermediate was found to undergo ligand exchange with alkoxide ligands (**28**) prior to reductive elimination, enabling the formation of alkoxyated products (**29**) in good yield. Only trace quantities of azetidine or acetoxyated by-products were observed under the optimized reaction conditions, and primary, secondary and tertiary alcohol coupling partners could all be employed.

While the picolinamide represented a major advance for the C–H functionalization of aliphatic amines, Chen's original study in 2011⁹⁶ (Scheme 14B) highlighted the difficulty in removing the DG. As a result, in 2013, two new DG's were developed that could be cleaved under mild conditions. Carretero¹⁰⁵ reported the sulfonamide analogue of the picolinamide DG (**30**, Scheme 16A) and demonstrated that efficient catalysis could be achieved for a γ C–H arylation procedure. The arylated product (**31**) was subjected to weakly acidic conditions to cleave the sulfonamide bond and furnish the unprotected amine (**32**). Simultaneously, Ma¹⁰⁶ reported the 2-methoxyiminoacetyl DG (**33**, Scheme 16B). After conducting a Pd-catalyzed γ C–H arylation (**34**), the directing group was cleaved under basic conditions at room temperature and the product isolated as the Boc-protected amine (**35**). Significantly, in both cases where amino acid derivatives were used as substrates, no erosion of the defined α -stereocentre was observed upon isolation after the DG removal. Following these studies, two further examples of cleavable DG's were disclosed, namely the 5-methylisoxazole-3-carboxamide (MICA)¹⁰⁷ and benzothiazole-2-sulfonyl (Bts)¹⁰⁸ DG's. Very recently, Maes¹⁰⁹ reported an improved removal protocol for the picolinamide DG (Scheme 16C). The picolinamide was derivatised with Boc_2O followed by Ni-catalyzed transesterification to give the Boc-protected amine product (**38**) and ethyl 2-picolinate (**39**). The protocol was demonstrated for a variety of substrates containing functional groups sensitive to acidic or basic hydrolysis conditions. In addition, **39** could be recycled for use in further amidation reactions of aliphatic amines.

A. 2013: Carretero**B. 2013: Ma****C. Improved protocol for picolinamide DG removal (2019, Maes)****Scheme 16.** Development of cleavable DG's and improved removal protocol for the picolinamide DG.

In 2014, Yu¹¹⁰ demonstrated that monodentate nitrogen-DG's could also promote directed C(sp³)-H activation in the presence of a mono-*N*-protected amino acid (MPAA) ligand (Scheme 17A). Yu employed *N*-triflyl protected amines (**40**) and aryl boronate ester coupling partners in combination with Ag₂CO₃, 1,4-benzoquinone and Na₂CO₃ additives to enable a Pd-catalyzed γ C-H arylation process (**41**) proceeding via a low valent Pd^{II}/Pd⁰ mechanism. The ligand that provided the highest catalytic efficiency was *N*-acetyl-protected *tert*-leucine, and significantly, no reaction was observed in the absence of the ligand. Subsequently, the essential role of the MPAA ligand was elucidated using computational methods, in which the carbonyl of the *N*-acetyl group was found to act as the internal base in the CMD step (**TS-3**).^{111,112} Crucially, the increased basicity of the *N*-acetyl amide relative to acetate vastly improves the activity of the Pd^{II} catalyst by reducing the barrier to C-H bond cleavage. In 2018, Yu¹¹³ reported an enantioselective variant of the γ C-H arylation reaction of triflamide substrates (Scheme 17B). A series of chiral acetyl-protected aminomethyl oxazoline (APAO) ligands were developed to enable either an enantioselective ethyl group desymmetrization (**42** to **43**) or a kinetic resolution of non-symmetric triflamides (**44** to **45**). γ -Alkenylation could also be achieved using vinyl boronate esters, and overall, the functionalized products were produced in good yield and high enantioselectivity. Finally, Yu developed a pyrrolidine-forming reaction

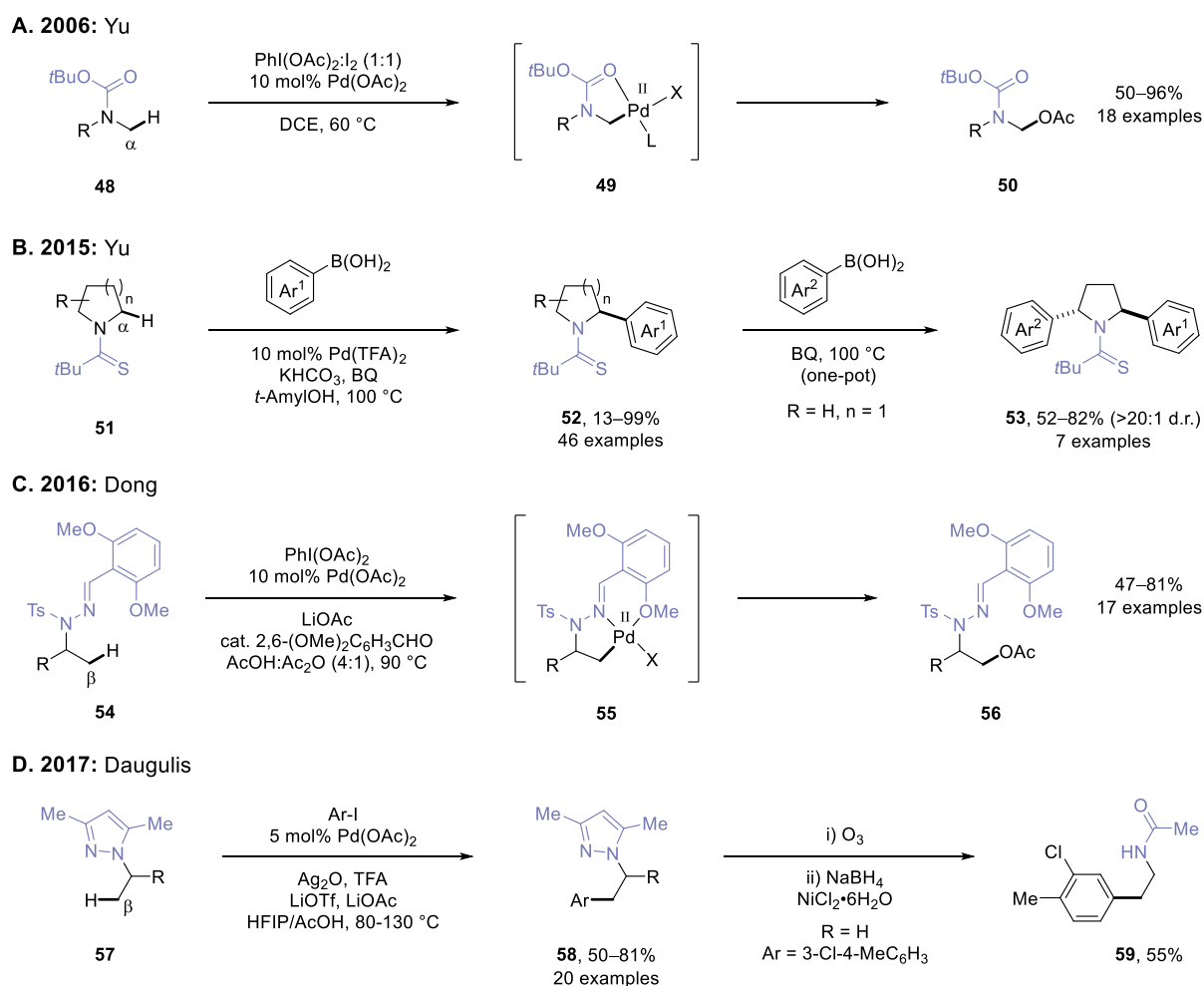
from the γ -C–H activation of *N*-triflyl or -nosyl protected amines (**46**) using activated acrylate or styrene coupling partners (Scheme 17C).¹¹⁴ A modified catalyst system was employed, involving a pyridine or quinoline-based ligand instead of an MPAA. A selection of three different ligands were used depending on the class of substrate in order to obtain high yields across a broad range of aliphatic amine derivatives with varying substitution patterns. In terms of mechanism, the reaction initially produces γ -alkenylated intermediates by a low valent Pd^{II}/Pd⁰ mechanism, via cyclopalladation, olefin insertion and β -H elimination, which subsequently undergo in situ cyclization via Michael addition or oxidative aza-Wacker cyclization to give the saturated or unsaturated pyrrolidine derivatives (**47**), respectively.



Scheme 17. Pd-catalyzed C–H functionalization directed by sulfonamide-protected aliphatic amines.

A series of DG's have been developed which promote the activation of C–H bonds at positions other than the γ -position relative to the amine nitrogen. An early example of such a case was the α C–H acetoxylation of Boc-protected amines (**48**) by Yu¹¹⁵ in 2006 (Scheme

18A). While the use of $\text{PhI}(\text{OAc})_2$ as oxidant alone gave no reaction, the combination of 1:1 $\text{PhI}(\text{OAc})_2$ and I_2 (leading to in situ formation of iodine monoacetate, IOAc) provided α -acetoxyated products (**50**) in good to high yields. The reaction was found to functionalize α -methyl groups only and not α -methylene groups, resulting in the proposal of Boc-directed C–H activation via a 5-membered palladacycle (**49**) as opposed to an alternative radical pathway. Later, in 2015 Yu¹¹⁶ developed a Pd-catalyzed α -C–H arylation of saturated azacycles and acyclic *N*-methylamines using a more strongly coordinating *tert*-butyl thioamide directing group (**51**, Scheme 18B). The reaction employed aryl boronic acids as arylating agents, which provided the α -arylated products (**52**) with high mono-arylation selectivity. Interestingly, 1,4-benzoquinone was found to be the most effective terminal oxidant, whereas Ag^{I} salts led to deleterious oxidation of the thioamide to an unreactive amide by-product. Due to the exquisite mono-selectivity of the reaction, a one-pot α, α' di-arylation procedure was developed to provide hetero-difunctionalized pyrrolidines (**53**). Notably, exclusive *trans* stereoselectivity (>20:1 d.r.)



Scheme 18. Pd-catalyzed α and β C–H functionalization of aliphatic amine derivatives.

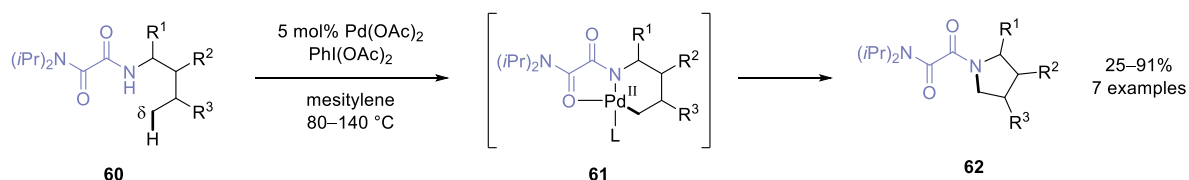
was observed in all cases as a result of a highly stereoselective second C–H activation wherein the steric interaction between the *t*-Bu of the thioamide and α -aryl substituent is minimized. Yu¹¹⁷ later developed an enantioselective α -arylation of thioamides by employing a chiral BINOL-derived phosphoric acid ligand.

More recently, β C–H functionalization procedures have been developed. For example, in 2016 Dong¹¹⁸ reported the β C–H acetoxylation of *N*-alkyl tosylhydrazone substrates (**54**), which were readily accessed in a one-pot, three-step synthetic procedure from free primary amines (Scheme 18C). The reaction was proposed to occur via a 6,5-bicyclic palladacycle intermediate (**55**) that provided exclusive selectivity for β -methyl group activation, followed by oxidative functionalization with $\text{PhI}(\text{OAc})_2$. In 2017, Daugulis¹¹⁹ reported an alternative β -directing auxiliary in the form of *N*-alkyl pyrazoles (**57**, Scheme 18D). A β C–H arylation reaction was developed using aryl iodides, with a 3,5-dimethyl substitution pattern on the pyrazole being found to provide the highest yields of arylated products (**58**). Subsequent ozonolysis with reductive work-up afforded the corresponding β -phenethylamine as the *N*-Ac-protected product (**59**).

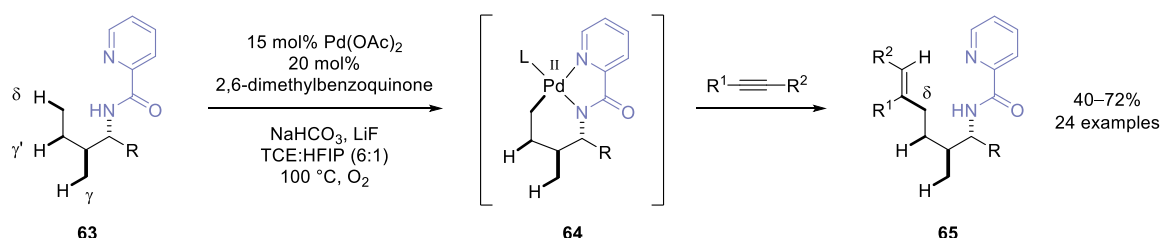
The more remote δ -position of aliphatic amines can also be accessed with the amine-derived DG strategy. In 2014, Yao and Zhao¹²⁰ reported an oxalyl amide DG (**60**) that acts as a bidentate *N,O*-ligand for Pd (Scheme 19A). Using $\text{PhI}(\text{OAc})_2$, intramolecular δ C–H amination was achieved via a 5,6-bicyclic palladacycle (**61**) to give pyrrolidine derivatives (**62**). In general, the yields of cyclized products correlated with the degree of substitution along the alkyl chain undergoing C–H activation, reflecting the impact of the Thorpe-Ingold effect in favouring the intramolecular C–N bond reductive elimination from the putative Pd^{IV} intermediate over competing pathways such as acetoxylation. Nonetheless, for the linear *n*-butylamine derived substrate (**60**, $\text{R}^1 = \text{R}^2 = \text{R}^3 = \text{H}$), the pyrrolidine was still obtained in a reasonable 25% yield. In later reports, the oxalyl amide DG was also found to enable γ C(sp³)–H functionalization processes, such as arylation^{121,122} and acetoxylation,¹²³ indicating that transformations proceeding via a 5,5-bicyclic palladacycle are also readily promoted under different reaction conditions. Conversely, δ -selective C–H alkenylation with internal alkyne coupling partners was reported by Shi¹²⁴ in 2016, wherein picolinamide-containing substrates (**63**) were functionalized at a δ -methyl position in the presence of γ -methyl and γ -methylene C–H bonds (Scheme 19B). Deuteration studies showed that C–H activation at the typically favoured γ -position was reversible under the reaction conditions. Consequently, the δ -selectivity was explained by the Curtin-Hammett principle, in which the 5- and 6-membered palladacycles are in equilibrium but with the less stable 6-membered palladacycle (**64**) being more reactive

towards insertion by the alkyne. The 8-membered palladacycle resulting from alkyne insertion into **64** undergoes protodemetalation by AcOH or HFIP to furnish the γ -alkenylated product (**65**), liberating a Pd^{II} centre and thus providing a rare example of a redox-neutral Pd^{II}/Pd^{II} functionalization mechanism.

A. 2014: Yao & Zhao



B. 2016: Shi

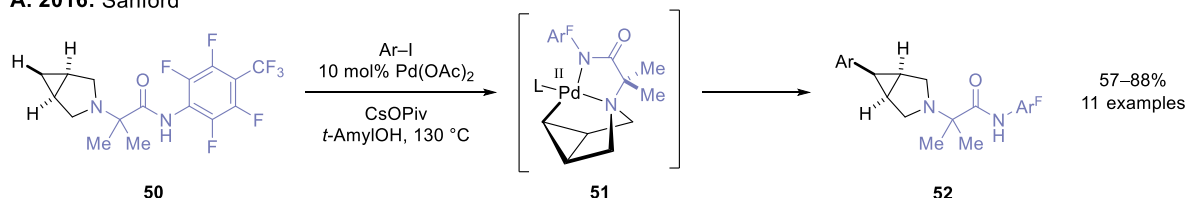


Scheme 19. Pd-catalyzed δ C–H functionalization of aliphatic amine derivatives.

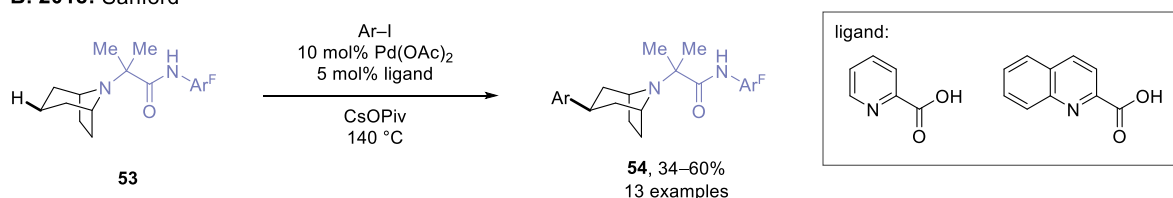
In 2016, Sanford¹²⁵ reported the transannular C–H arylation of saturated aza-heterocycles (Scheme 20A). The remote functionalization was achieved using an unusual tertiary amine-based bidentate DG containing a pendant fluorinated arylamide moiety (**50**). The DG selectively promoted the activation of γ C–H bonds within the cyclic amine to form a transannular palladacycle (**51**), which was functionalized using aryl iodide coupling partners to provide γ -arylated derivatives (**52**). Notably, CsOPiv was used to abstract iodide from the Pd centre to turn over the catalytic cycle, whereas more commonly employed Ag^I salts led to undesired α -oxidation of the substrate to the iminium. In general, the C–H activation was facilitated by the use of bicyclic amine substrates that could stabilize the resulting boat conformation of the cyclopalladated amine, though a simple piperidine-derived substrate was also employed with good efficiency (55% yield). Additionally, the protocol was demonstrated for the late-stage functionalization of pharmaceutical drugs, with γ -arylated derivatives of varenicline and cytosine being prepared. In 2018, Sanford¹²⁶ developed a second-generation set of conditions for the transannular C–H arylation, whereby the yield of the reaction could be improved by the addition of a 2-picolinic acid or 2-quinaldic acid ligand (**53** to **54**, Scheme 20B). The ligand was found to be responsible for recovering the catalyst from an insoluble

material that formed during the reaction, but was suggested to not be involved in reducing the barrier to rate-limiting C–H activation based on the similar KIE's observed in the presence and absence of ligand ($k_H/k_D = 3.2$ and 3.3 , respectively). However, the increased catalytic efficiency resulted in a noticeably improved scope of the reaction, allowing for previously unreactive tropane and homotropane cores to be directly functionalized for the first time.

A. 2016: Sanford



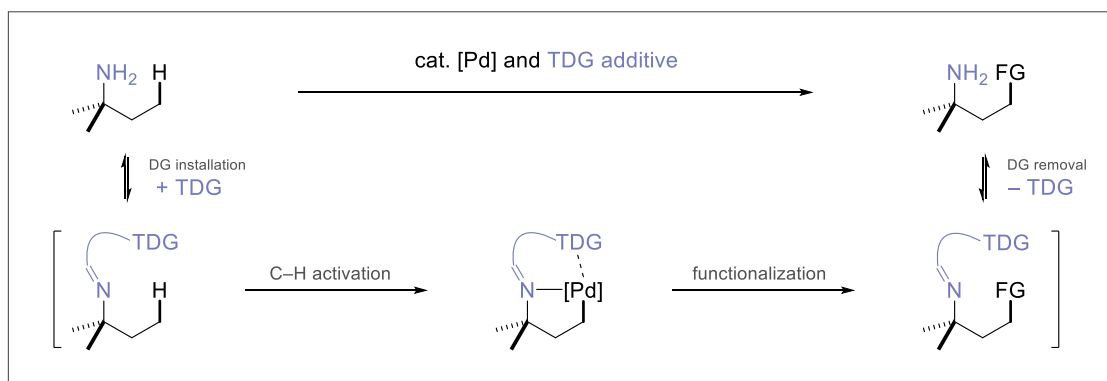
B. 2018: Sanford



Scheme 20. Transannular C–H activation of saturated aza-heterocycles by Sanford.

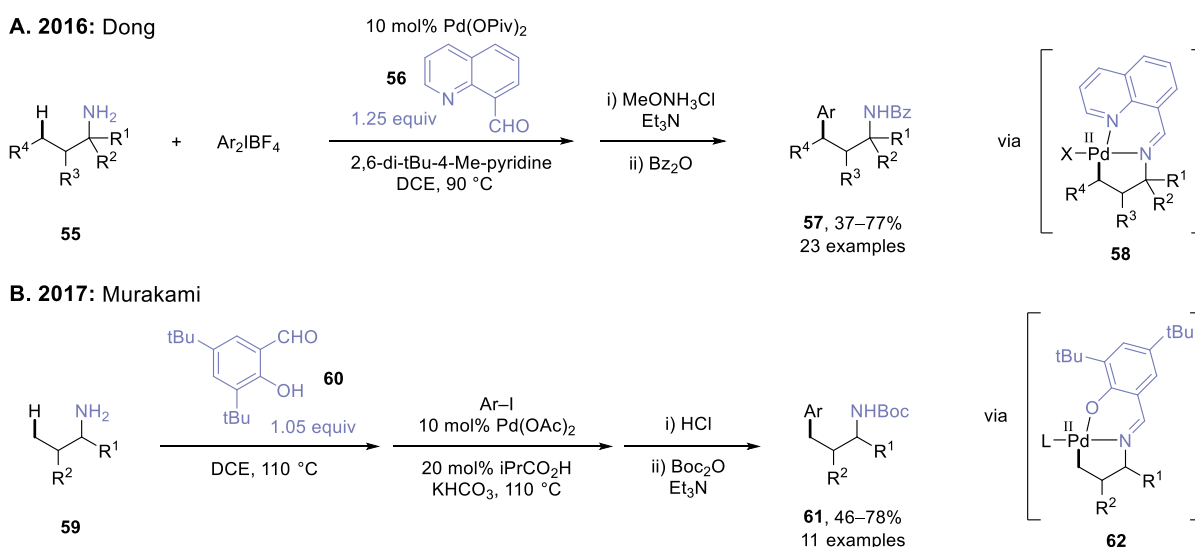
1.2.3.2. Transient Directing Group Strategy

The transient directing group (TDG) strategy^{127–133} involves the in situ installation and removal of a DG, enabling auxiliary-controlled C–H activation to be conducted in a one-pot procedure (Scheme 21). Although the strategy was originally developed in the late 1990's for Rh-catalyzed olefin hydroacylation processes,¹³⁴ it was not until 2016 that TDG's were exploited for Pd-catalyzed $\text{C}(\text{sp}^3)\text{--H}$ functionalization with the report of benzylic C–H arylation of *o*-tolualdehydes by Yu.¹³⁵ In terms of aliphatic amine functionalization, a reversible covalent linkage between the amine nitrogen and a TDG additive forms a temporary mono- or bidentate DG, most commonly involving reversible imine formation between a primary amine substrate and TDG-containing aldehyde. Depending on the reaction efficiency, the TDG additive may be used in stoichiometric or catalytic quantities. Overall, the TDG strategy maintains the benefits of the amine-derived DG approach, but overcomes the major limitation relating to added steps for DG installation and removal. Nonetheless, TDG's remain in their infancy for Pd-catalyzed amine functionalization and have only been demonstrated for C–H arylation processes to date, indicating that further research is required to improve the scope of transformations available to this type of strategy.



Scheme 21. Transient directing group (TDG) strategy: reversible in situ installation and removal of the DG.

One of the first examples of a TDG strategy for Pd-catalyzed amine $C(sp^3)\text{--}H$ functionalization was reported by Dong¹³⁶ in 2016 (Scheme 22A). Primary amines (**55**) were directly combined with a stoichiometric amount of quinoline-8-carbaldehyde (**56**) in the presence of the Pd^{II} catalyst, a pyridine base and diaryliodonium salt coupling partners. The in situ-formed imine promoted γ C–H activation to form a 6,5-bicyclic palladacycle (**58**), which underwent oxidative functionalization to give arylated products in protected form (**57**) after methoxyamine work-up and benzoylation. In 2017, Murakami¹³⁷ developed a similar strategy using a bulky 3,5-di-*tert*-butylsalicylaldehyde TDG (**60**) for the γ C–H arylation of primary amines using aryl iodides (Scheme 22B). The optimised protocol involved prior formation of the imine by the heating of the free amines (**59**) with TDG **60**, followed by the sequential addition of the Pd^{II} catalyst and reagents for the arylation process. The TDG once again



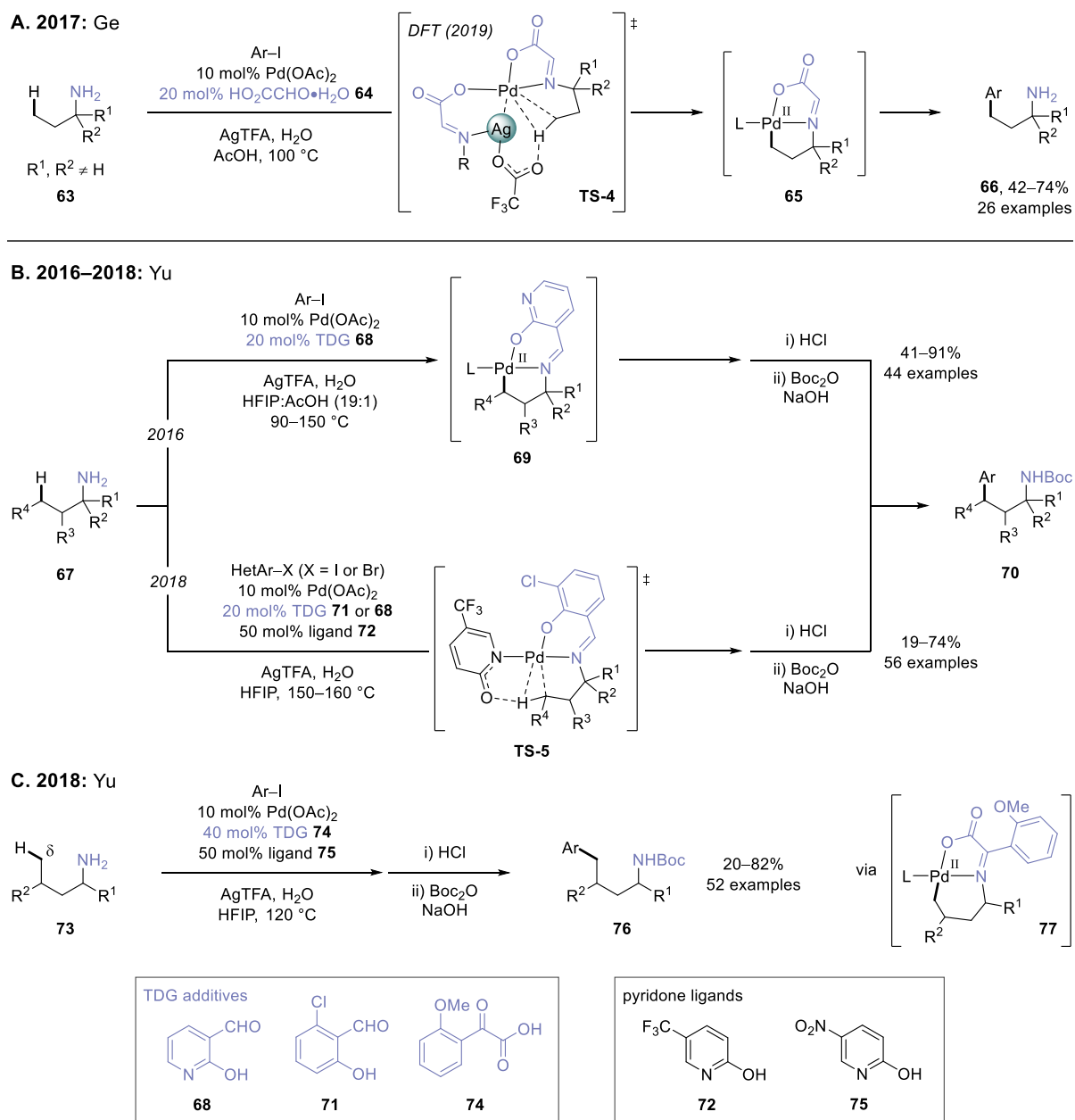
Scheme 22. Imine-based transient directing group strategies using stoichiometric TDG additives.

promoted selective γ -functionalization via a 6,5-bicyclic palladacycle (**62**), with the amine products (**61**) being isolated after acidic work-up and Boc-protection. Interestingly, in both the cases of Dong and Murakami, although decreasing the equivalency of the TDG additive to sub-stoichiometric amounts led to diminished yields, the yields were found to be greater than the TDG loading suggesting that reversible exchange of the TDG between product and substrate molecules was occurring during the reaction.

In 2017, Ge¹³⁸ reported a γ C–H arylation of α -tertiary primary amines (**63**) using catalytic quantities of a TDG additive (Scheme 23A). Using aryl iodides, AgTFA and 10 mol% Pd(OAc)₂, 20 mol% of inexpensive glyoxylic acid monohydrate (**64**) was used as the TDG additive to provide moderate to good yields of γ -arylated products (**66**) via a carboxy-imine intermediate. The optimised conditions required the addition of water (4 equivalents) to promote the dynamic exchange of the TDG by reversible imine formation and hydrolysis. The directed C–H activation proceeded via a 5,5-bicyclic palladacycle (**65**), which was confirmed under stoichiometric palladium conditions by the isolation of a stable pyridine-ligated complex (**65**; R¹ = R² = Me, L = pyridine). Significantly, the Pd-catalyzed reaction gave 0% yield in the absence of the AgTFA additive. Subsequently, in 2019, further mechanistic studies by Wang and Dang⁹⁵ elucidated the essential role of the Ag^I salt through in situ mass spectroscopy and DFT analysis. In particular, it was deduced that C–H activation was facilitated by a bimetallic Pd^{II}/Ag^I CMD mechanism (**TS-4**) as opposed to a more straightforward monometallic Pd^{II}-mediated CMD step ($\Delta\Delta G^\ddagger = 5.0$ kcal mol⁻¹).

Around the same time as Ge, Yu¹³⁹ also developed a catalytic TDG method for the γ C–H arylation of primary amines, once again employing aryl iodides in combination with AgTFA (**67** to **70**, Scheme 23B). The first-generation conditions, reported in 2016, involved the use of 20 mol% 2-hydroxynicotinaldehyde (**68**) as the TDG additive which enabled γ C–H activation via a 6,5-bicyclic palladacycle (**69**). Notably, the scope of Yu's reaction was significantly broader than Ge's method, given that α -tertiary substitution was not required and that more challenging γ -methylene activation was also made possible. However, a limitation to the reaction was that γ -methylene C–H arylation was not sufficiently robust to allow for the coupling of heteroaryl iodides. With the discovery of electron-poor 2-pyridone ligands as more active carboxylate surrogates for Pd^{II}-mediated C–H activation,^{140,141} Yu¹⁴² reported a second-generation reaction employing 6-chlorosalicylaldehyde (**71**) as the TDG additive with a separate pyridone ligand (**72**). DFT studies on the mechanism of the pyridone-assisted functionalization have confirmed that C–H bond cleavage is facilitated by the ligated anionic pyridone acting as the internal base in the CMD mechanism (**TS-5**).¹⁴¹ Crucially, the greater

activity afforded by the pyridone ligand enabled a significantly improved scope with heteroaryl iodide coupling partners, as well as the use of previously unreactive heteroaryl bromides.



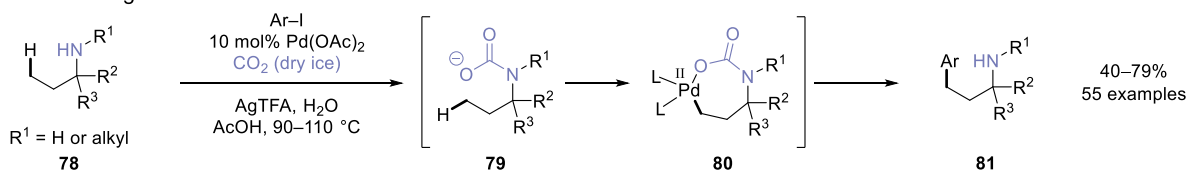
Scheme 23. Imine-based transient directing groups using catalytic TDG additives by (a) Ge and (b, c) Yu.

While developing the second-generation reaction, Yu¹⁴² discovered that δ C–H activation could be achieved by simply altering the size of the chelate of the TDG (Scheme 23C). Whereas the formation of a 6-membered chelate with TDG **68** and **71** gave exclusively γ C–H activation, using ketoacid **74** as the TDG resulted in a 5-membered chelate that promoted δ C–H activation via a 5,6-bicyclic palladacycle (**77**). Using a slightly modified pyridone ligand

(**75**), the C–H arylation procedure transformed α,γ -disubstituted primary amines (**73**) to δ -arylated products (**76**) in generally good yield and high diastereoselectivity (up to >10:1 d.r.). Conversely, low yields (ca. 20%) were obtained in the absence of γ -substitution (**73**: $R^2 = H$) and for δ -methylene C–H arylation.

In 2018, Young¹⁴³ reported a distinct TDG approach using carbon dioxide for in situ protection of aliphatic amines (**78**) as *N*-carbamate salts (**79**, Scheme 24). Using otherwise similar conditions to Ge and Yu, the CO₂-mediated conditions provided an efficient C–H arylation procedure to afford γ -arylated derivatives (**81**). Significantly, given that imine formation was not invoked, Young's reaction could functionalize both primary, and for the first time with TDG's, secondary amine substrates. For primary amines, 1–2 equivalents of CO₂ in the form of dry ice were used, while secondary amines required a higher loading of 30 equivalents of CO₂. In terms of mechanism, it was proposed that the initially formed carbamate (**79**) promotes γ C–H activation via a putative 7-membered palladacycle intermediate (**80**). However, it should be noted that complex **80** was neither directly observed nor isolated.

2018: Young

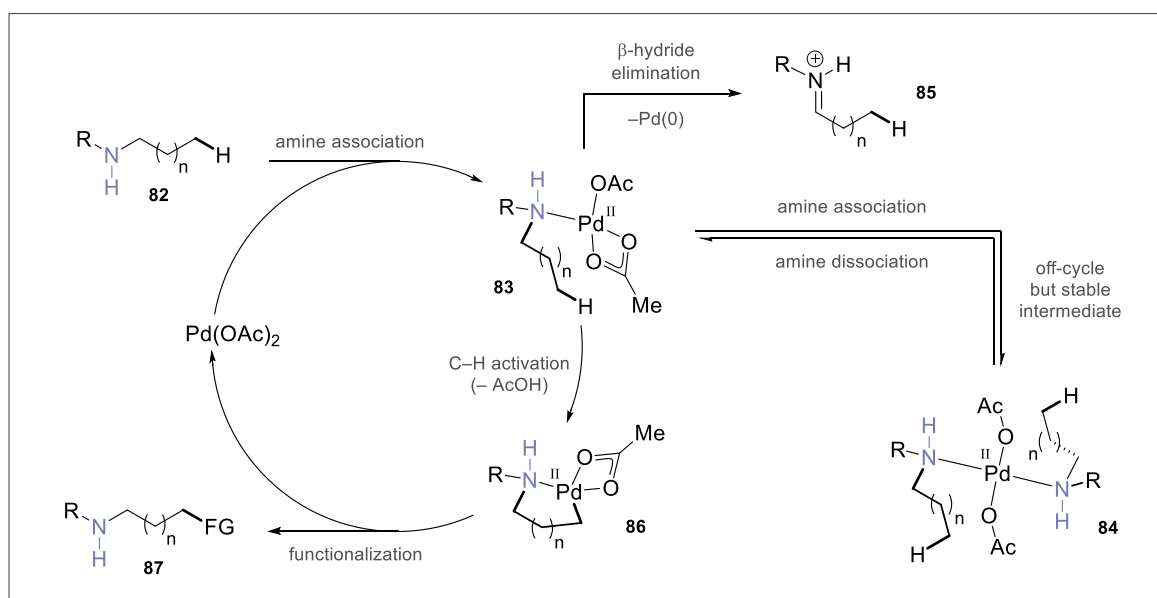


Scheme 24. Carbon dioxide-mediated γ C–H arylation via an in situ-formed carbamate TDG.

1.2.3.3. Native Amine-directed Strategy

The native amine-directed strategy exploits the innate coordinating ability of the amine nitrogen within unprotected amine substrates to direct the Pd^{II} catalyst for C–H activation.⁶⁵ As a result, the strategy does not require the addition of exogenous DG's or TDG additives and is therefore conceptually the most straightforward and atom efficient approach to directed amine functionalization. A general catalytic cycle is shown in Scheme 25 using Pd(OAc)₂ as catalyst.⁶⁵ The first step involves binding of the Lewis basic free amine (**82**) to the Pd^{II} centre to form a mono-amine Pd^{II} complex (**83**). The κ^2 -carboxylate ligand within **83** can interconvert to a κ^1 -carboxylate to reveal a vacant site of coordination, promoting C–H activation to form a palladacycle containing the cyclometalated amine (**86**). Complex **86** then undergoes functionalization to furnish the derivatized amine product (**87**) and return the active catalyst. However, despite its simplicity, the native amine-directed strategy is associated with two main

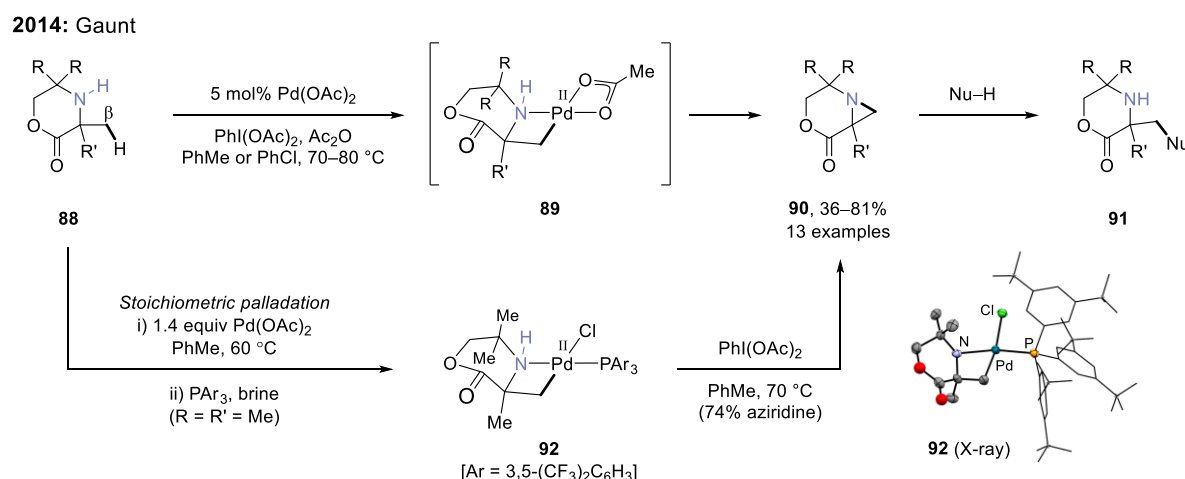
challenges which must be overcome to achieve catalysis.⁶⁵ Firstly, aliphatic amines have a high affinity for Pd^{II} centres and often associate twice to form thermodynamically stable *trans* bis-amine Pd^{II} complexes (**84**).¹⁴⁴ Significantly, because **84** is coordinatively saturated in the square plane, the bis-amine complex is unable to undergo cyclometalation and is therefore an off-cycle intermediate. Secondly, the mono-amine complex **83** is susceptible to Pd^{II}-mediated β -hydride elimination that results in oxidative degradation of the amine substrate as well as reduction of the catalyst after reductive elimination from the Pd–hydride intermediate. As a result of these unique challenges, although the stoichiometric activation of unprotected amines was among the first reported examples of cyclometalation,^{74,145} catalysis using a native amine-directed strategy was not achieved until almost a decade after Daugulis' seminal example of a catalytic DG-mediated process.^{40,146}



Scheme 25. Native amine-directed C–H functionalization of aliphatic amines: catalytic cycle & challenges.

The first example of a Pd-catalyzed C(sp³)–H functionalization directed by an unprotected aliphatic amine was reported in 2014 by Gaunt¹⁴⁶ (Scheme 26). The reaction conditions included the use of Pd(OAc)₂ as catalyst and PhI(OAc)₂ as oxidant, resulting in an intramolecular β methyl C–H amination process to furnish strained aziridine products (**90**). Key to the success of the catalytic process was the use of hindered cyclic secondary amines known as morpholinones (**88**) wherein the positions α -to-nitrogen were fully substituted (**88**: R, R' \neq H). Employing these substrates had the effect of both destabilizing the unreactive bis-amine Pd^{II} complex due to steric congestion, as well as preventing degradation of the substrate by

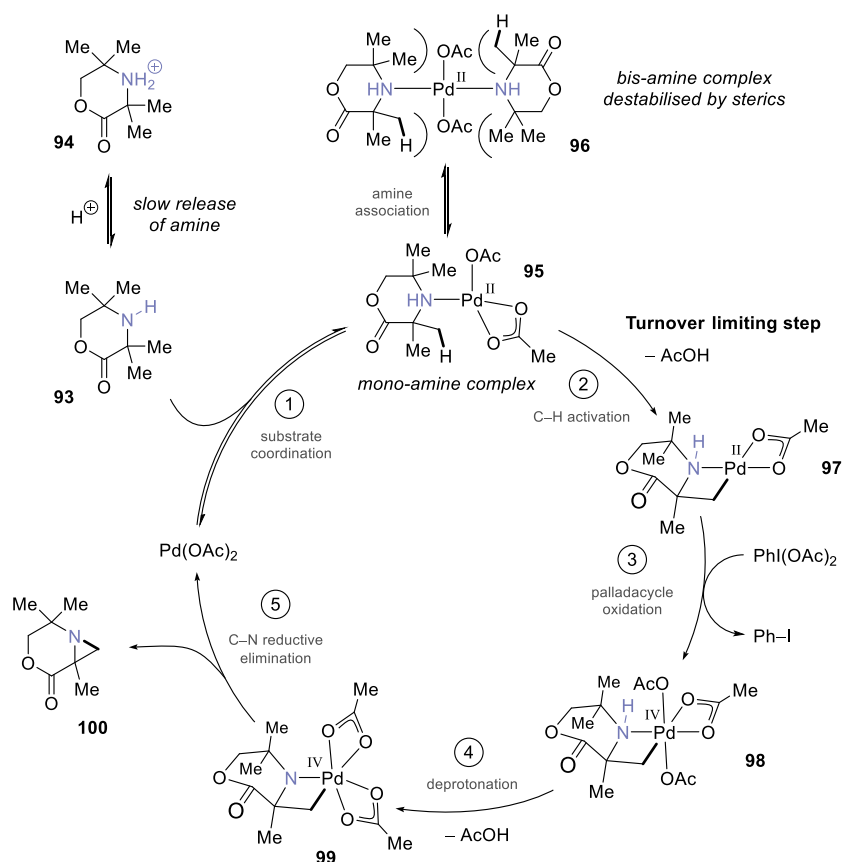
offering no possible sites for β -hydride elimination. Notably, the reaction was thought to proceed via a four-membered palladacycle (**89**), which was confirmed under stoichiometric palladium conditions by the formation of a stable phosphine-ligated complex (**92**). Although four-membered *C,N*-palladacycles had been previously isolated,^{71,147} Gaunt's example was the first to be formed through a C–H activation mechanism. Exposure of **92** to $\text{PhI}(\text{OAc})_2$ yielded the aziridine via oxidative functionalization, demonstrating the unusual reductive elimination event from a putative Pd^{IV} intermediate to form the aziridine product. Subsequently, the hindered aziridines could be ring-opened by different nucleophiles such as thiolate, azide, fluoride or electron-rich heterocycles to provide diversely β -functionalized aliphatic amines (**91**). In 2016, the Pd-catalyzed aziridine formation was incorporated into a continuous flow set-up, allowing for large quantities of hindered aziridines to readily synthesized.¹⁴⁸



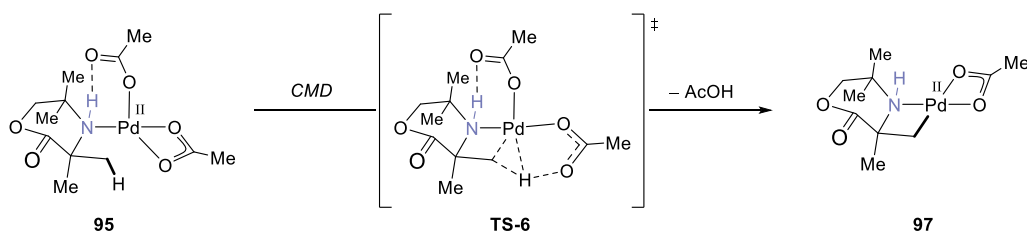
Scheme 26. Intramolecular β C–H amination of hindered secondary amines to form aziridines.

In 2015, a more detailed investigation into the mechanism of the aziridine-forming reaction was reported by Gaunt.¹⁴⁹ The first step of the catalytic cycle was proposed to be coordination of the amine substrate (**93**) to the Pd^{II} catalyst to form the mono-amine complex (**95**; Step 1, Scheme 27), which would be followed by either unproductive binding of a second equivalent of amine (**96**) or productive C–H activation to the four-membered ring palladacycle (**97**, Step 2). Kinetic analysis found that the reaction was first order in Pd catalyst, zero order in $\text{PhI}(\text{OAc})_2$ and had complex order in amine substrate, changing from -1 order at low reaction conversion to first order at high conversion. These kinetic data indicated that the turnover limiting step (TOLS) occurred prior to oxidation of the palladacycle, and that the bis-amine Pd^{II} complex (**96**) was indeed an off-cycle intermediate. A primary KIE was observed for the

reaction ($k_H/k_D = 3.8$) which showed that C–H activation was the TOLS. Interestingly, computational DFT analysis of the transition state for cyclopalladation via CMD (TS-6) revealed the importance of a hydrogen-bonding interaction between a κ^1 -acetate and the N–H bond of the ligated amine which assisted in the assembly of the reactive conformation for C–H activation (Scheme 28). Additionally, dispersion-interaction analysis rationalized the observed regioselectivity for methyl group activation proximal to the carbonyl of the lactone on the basis of the greater acidity of the C–H bonds relative to the distal methyl groups in **93**. Next, oxidation of the palladacycle by $\text{PhI}(\text{OAc})_2$ was suggested to access a tri-acetate bound Pd^{IV} intermediate



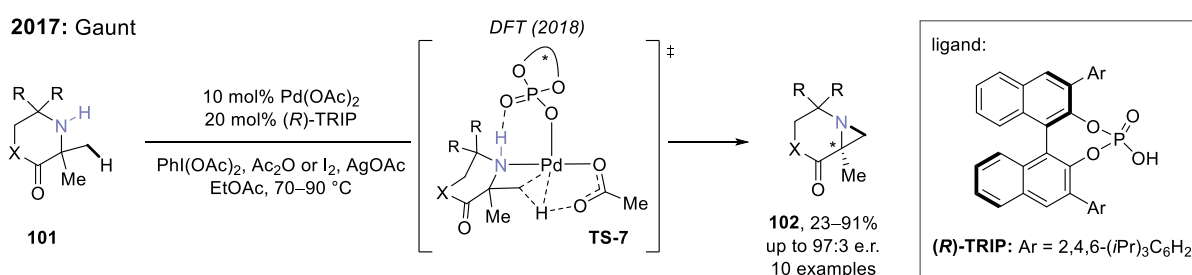
Scheme 27. Mechanism of the Pd-catalyzed intramolecular β C–H amination to form aziridines.



Scheme 28. Computational DFT analysis of the transition state for native amine-directed $\text{C}(\text{sp}^3)\text{--H}$ activation.

(**98**; Step 3) that could undergo product-forming reductive elimination. Once again, DFT analysis provided crucial insight, in which a low energy pathway was calculated proceeding by N–H deprotonation (**99**; Step 4) prior to intramolecular C–N bond reductive elimination to the aziridine (**100**; Step 5). Conversely, higher energy pathways were calculated for direct reductive elimination from intermediate **98**, or for initial amine de-coordination followed by outer-sphere S_N2 attack of the activated β -position. The mechanistic studies led to a re-evaluation of the catalytic reaction conditions. In particular, it was found that the addition of 20 equivalents of acetic acid resulted in a dramatically increased reaction rate, presumably due to protonation of the amine substrate (**94**) lowering the concentration of free amine (**93**) and thus disfavoring formation of the off-cycle bis-amine complex.

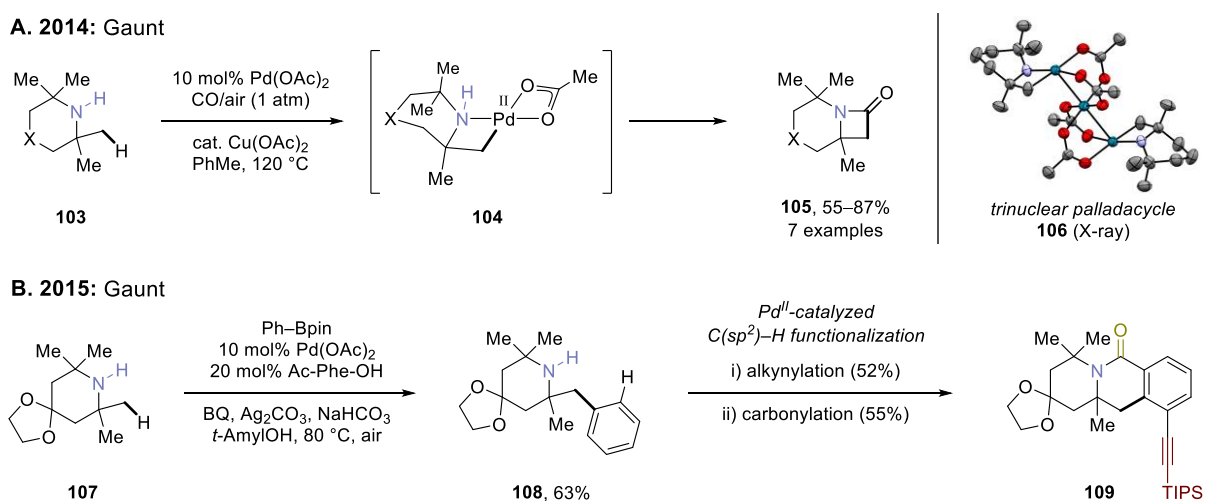
In 2017, an enantioselective version of the aziridine-forming reaction was developed involving the activation of prochiral methyl groups in α -dimethyl substituted morpholinones and piperazinones (**101**, Scheme 29).¹⁵⁰ Under slightly modified conditions that included a chiral BINOL-derived phosphoric acid ligand (*R*)-TRIP, the corresponding enantioenriched aziridines (**102**) were accessed in good yield and high enantioselectivity (up to 97:3 e.r.). Later, computational DFT studies by Zhang¹⁵¹ elucidated the enantio-determining transition state for the C–H activation (**TS-7**), whereby the chiral phosphoric acid was found to act as an anionic spectator ligand that is hydrogen-bonded to the amine(NH), creating a chiral environment for an acetate-assisted CMD process.



Scheme 29. Enantioselective Pd-catalyzed aziridine-forming reaction using a chiral phosphoric acid ligand.

In 2014, Gaunt¹⁴⁶ also developed a catalytic β C–H carbonylation process of hindered tetramethylpiperidine (TMP) substrates (**103**, Scheme 30A). The reaction once again proceeded via a four-membered palladacycle (**104**), which was functionalized by a low valent mechanism involving CO insertion and C(O)–N bond reductive elimination to afford β -lactam products (**105**). Catalytic Cu(OAc)₂ was used to re-generate the Pd^{II} catalyst with air being used as the terminal oxidant. Notably, the palladacycle could be isolated under stoichiometric palladium

conditions as the acetate-bridged trinuclear complex in the solid state (**106**). Shortly after, in 2015, Gaunt¹⁵² reported a β C–H arylation process of TMP substrates employing boronic acid coupling partners (**107** to **108**, Scheme 30B). Crucially, a MPAA ligand (*N*-acetyl phenylalanine) was required to ensure good yields of the β -arylated products along with 1,4-benzoquinone and Ag₂CO₃ as other essential additives. The product utility was demonstrated by conducting two subsequent amine-directed *ortho* C(sp²)–H functionalizations to access complex polycyclic amine derivatives (**109**).

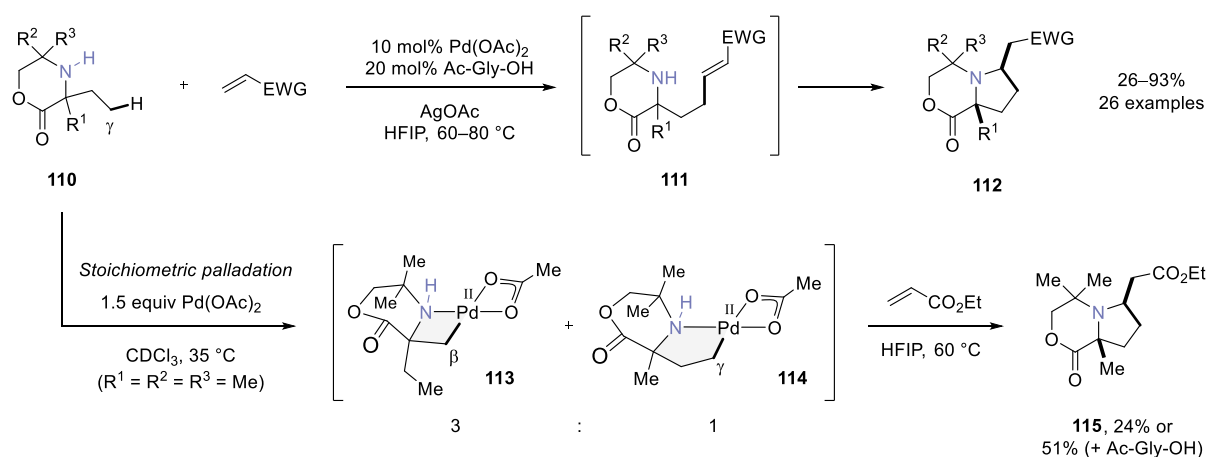


Scheme 30. Pd-catalyzed β C–H (a) carbonylation and (b) arylation of hindered tetramethylpiperidine substrates.

While the first examples of the native amine-directed strategy all involved β C–H activation of hindered secondary amines, it was later shown that γ C–H activation was possible as well. In 2017, Gaunt¹⁵³ reported the γ C–H alkenylation of morpholinones (**110**) using electron-poor olefin coupling partners, which proceeded via the γ -alkenylated intermediate (**111**) followed by a diastereoselective aza-Michael addition to form stereo-defined pyrrolidine products (**112**, Scheme 31A). Similar to the β C–H arylation of TMP substrates, addition of an MPAA ligand (*N*-acetyl glycine) led to improved reaction yields in the catalytic transformation. In order to probe the selectivity for β versus γ C–H activation within hindered secondary amines, an intramolecular competition experiment was conducted under stoichiometric palladium conditions without the MPAA ligand using a morpholinone containing appropriately disposed β -methyl and γ -methyl groups proximal to the lactone carbonyl (**110**: R¹ = R² = R³ = Me). By NMR analysis of the resulting palladacycles, a 3:1 ratio of β : γ C–H activation was observed, demonstrating a preference for the formation of a four-membered palladacycle (**113**) over a five-membered palladacycle (**114**). However, upon subjecting the mixture of

palladacycles to ethyl acrylate in HFIP at 60 °C, only the pyrrolidine product was formed (**115**, 24%). Conversely, the yield of **115** increased to 51% in the presence of *N*-acetyl glycine, indicating that the MPAA ligand had altered the ratio of the two palladacycles (**113**:**114**). The result of the stoichiometric functionalization was explained by deuterium labelling studies, which revealed that C–H activation was in fact reversible in the presence of the MPAA ligand but was irreversible in its absence.

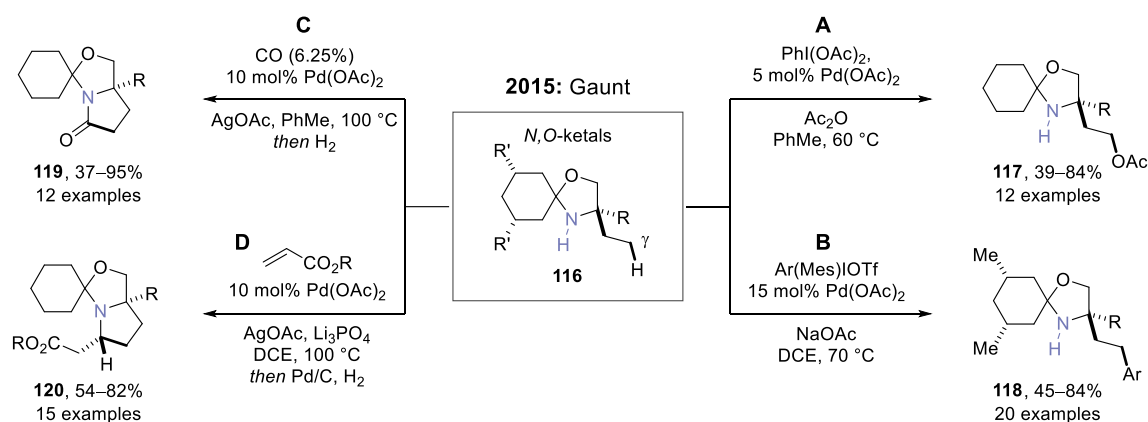
2017: Gaunt



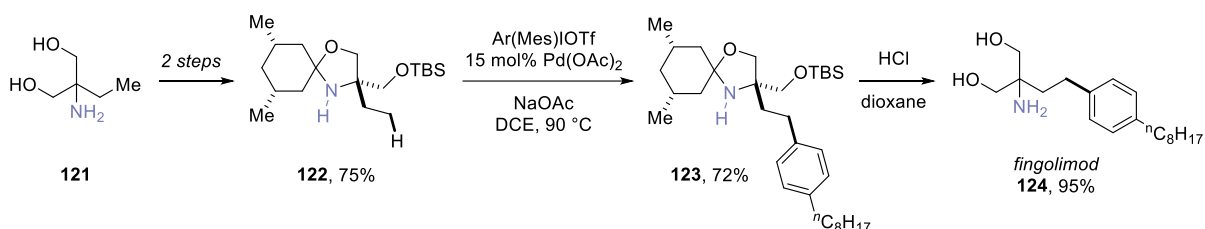
Scheme 31. Pd-catalyzed γ C–H alkenylation & competition between β and γ -methyl group activation.

In 2015, Gaunt¹⁵⁴ reported a series of Pd-catalyzed γ C–H functionalization processes for sterically hindered *N,O*-ketals (**116**, Scheme 32). The products of the transformations could be converted to amino alcohols under acidic aqueous conditions. Using oxidative Pd^{II}/Pd^{IV} catalysis, γ C–H acetoxylation with PhI(OAc)₂ (**117**) and γ C–H arylation with diaryliodonium salts (**118**) were developed. Notably, the arylation procedure employed dimethyl-substituted *N,O*-ketal substrates (**116**: R' = Me) which provided higher yields relative to the simple cyclohexanone-derived *N,O*-ketals. Conversely, using low-valent Pd^{II}/Pd⁰ catalysis, γ C–H carbonylation (**119**) and γ C–H alkenylation (**120**) procedures were developed. In both cases, the reactions produced small quantities of the unsaturated 5-membered ring by-product containing a double bond between the β and γ positions, and therefore sequential hydrogenation steps were used to convert the by-products to the desired saturated equivalents. The utility of the *N,O*-ketal functionalization strategy was showcased in the four-step synthesis of the pharmaceutical drug fingolimod (**124**), a treatment for multiple sclerosis (Scheme 32E). Starting from a commercial amino-diol (**121**), the *N,O*-ketal substrate (**122**) was synthesized in two steps by ketone condensation and silyl protection, followed by the Pd-catalyzed γ C–H

arylation process to access the arylated derivative (**123**). Finally, global deprotection under acidic conditions provided fingolimod (**124**) in excellent yield.



E. Synthesis of fingolimod using a C–H functionalization approach

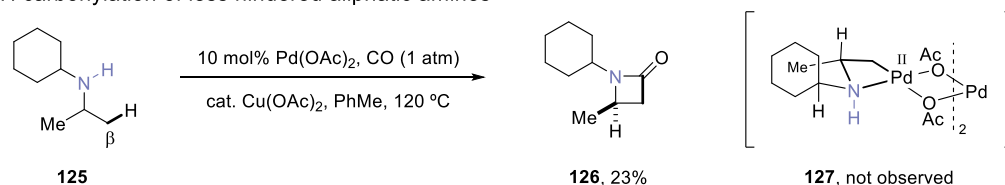


Scheme 32. Pd-catalyzed γ C–H (a) acetoxylation, (b) arylation, (c) carbonylation and (d) alkenylation of *N,O*-ketal substrates. (e) Application of the γ C–H arylation in the four-step synthesis of fingolimod.

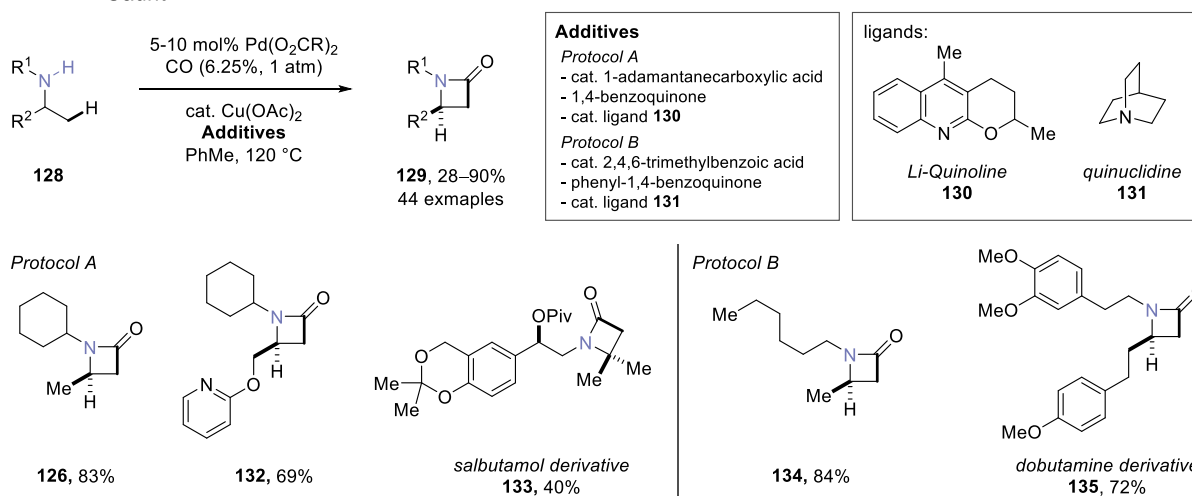
In general, Pd-catalyzed C–H functionalization of aliphatic amines is effective for hindered substrates because the off-cycle bis-amine Pd^{II} complex is significantly destabilized by steric repulsions, promoting the formation of a coordinatively unsaturated intermediate that can undergo C–H activation. However, the ability to functionalize less hindered amines is typically more desirable given that these types of amines are more commonly encountered in molecules of interest, such as pharmaceutical drugs. Preliminary investigations by Gaunt¹⁵⁵ on the functionalization of less hindered amines indicated that catalytic β C–H carbonylation was potentially viable (Scheme 33A). For example, using the previously developed catalytic conditions for TMP substrates,¹⁴⁶ *N*-cyclohexylisopropylamine (**125**) underwent β C–H carbonylation to the β -lactam (**126**) in 23% yield. While this was a promising initial result, it was found that the putative palladacycle intermediate (**127**) could not be observed indicating that an alternative mechanism could be operating (*vide infra*). In 2016, Gaunt¹⁵⁵ reported an optimized method for the synthesis of β -lactams (Scheme 33B). Extensive screening of the reaction conditions enabled the discovery of efficient catalytic conditions, which included the

addition of a hindered acid additive (1-adamantanecarboxylic acid or 2,4,6-trimethylbenzoic acid), benzoquinone (1,4-benzoquinone or phenyl-1,4-benzoquinone) and a monodentate *N*-donor ligand (Li-quinoline **130** or quinuclidine **131**). Significantly, the transformation displayed broad scope, which was enabled by the development of two protocols that were used depending on whether more substituted (Protocol A) or less substituted (Protocol B, Scheme 33B) amine substrates were being employed. Under the improved conditions, *N*-cyclohexylisopropylamine was carbonylated in 83% yield (**126**). Moreover, a wide range of functionally diverse aliphatic amines were tolerated in the reaction (**132–135**), including complex pharmaceutical compounds such as salbutamol (**133**) and dobutamine (**135**).

A. β C–H carbonylation of less hindered aliphatic amines



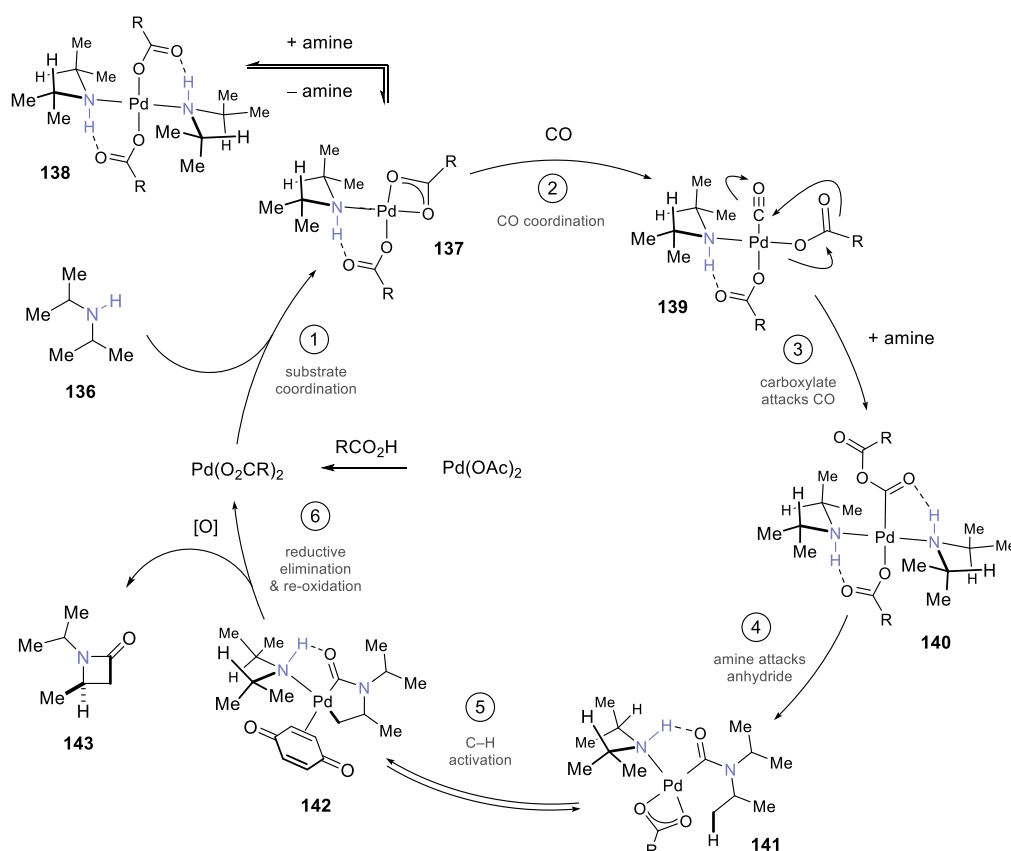
B. 2016: Gaunt



Scheme 33. Pd-catalyzed β C–H carbonylation: (a) preliminary result and (b) optimized catalytic reaction.

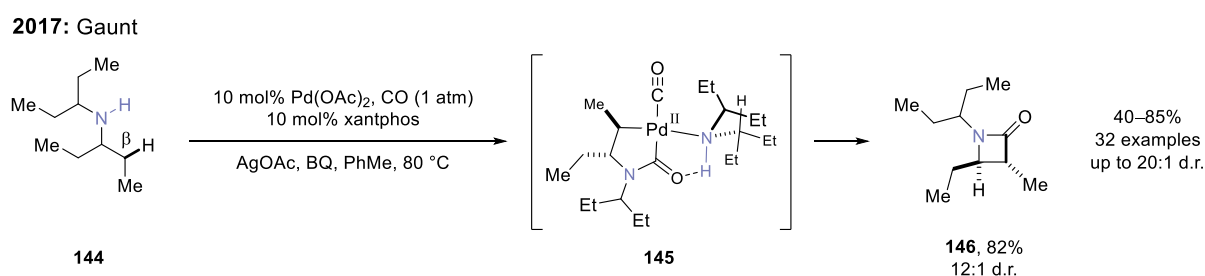
The mechanism of the β C–H carbonylation reaction was extensively explored in order to explain the generality of the reaction and the role of different additives.¹⁵⁵ In particular, computational DFT analysis was used to support each step of the proposed mechanism (Scheme 34). Firstly, the amine (**136**) binds to the Pd-carboxylate catalyst, forming a mono-amine complex (**137**, Step 1) which is in equilibrium with the bis-amine complex (**138**). CO then coordinates to form a Pd-carbonyl complex (**139**, Step 2), wherein a low energy pathway was calculated involving attack of the carboxylate onto the CO ligand (Step 3). The resulting Pd-

anhydride intermediate (**140**) was proposed to undergo attack by the amine onto the proximal Pd-acyl moiety to form a Pd-carbamoyl complex (**141**, Step 4), which was also supported computationally. During this step, the bulky acid additive was suggested to favour attack of the proximal carbonyl over attack of the distal carbonyl of the Pd-anhydride, which was necessary given that distal attack would give an *N*-acylated by-product. Notably, *N*-acetylation was a major by-product in the absence of the bulky acid additive. Next, a relatively facile C–H activation process from **141** was predicted *in silico* ($\Delta G^\ddagger = +25.6 \text{ kcal mol}^{-1}$, Step 5) wherein the reactive conformation is reinforced by a hydrogen-bond between the second equivalent of bound amine and the *N*-acyl moiety, resulting in a 5-membered *N*-acyl palladacycle (**142**). Additionally, deuterium labelling studies revealed that the C–H activation was reversible. Finally, benzoquinone-assisted reductive elimination affords the β -lactam product (**143**, Step 6) and gives a Pd^0 intermediate that is re-oxidized to the Pd^{II} carboxylate active catalyst. Here, the Pd^0 complex was thought to be stabilized by the addition of the *N*-donor ligand (**130** or **131**) prior to re-oxidation by the Cu co-catalyst.



Scheme 34. Proposed mechanism for the β C–H carbonylation of less hindered amines.

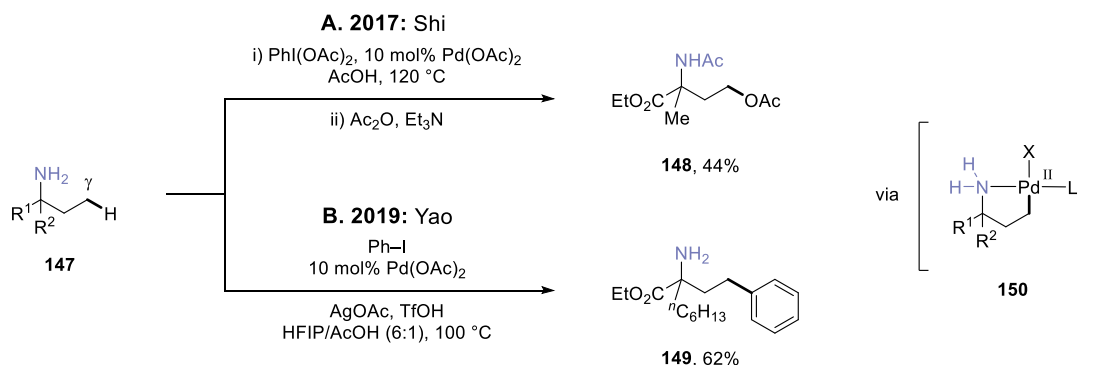
The original report for β C–H carbonylation of less hindered amines was generally only effective for β -methyl activation. In 2017, an efficient β -methylene carbonylation was reported,¹⁵⁶ in which the use of bisphosphine ligand xantphos was found to give high yields of *trans* di-substituted β -lactams (**144** to **146**, Scheme 35). While the reaction was thought to proceed via an analogous Pd-carbamoyl intermediate (**145**), the role of the xantphos ligand, outside of stabilizing Pd⁰ species, was unclear. Interestingly, control reactions showed that the mono-phosphine oxide variant of xantphos was as effective as xantphos itself (80%, **146**), whereas the di-phosphine oxide led to a large drop-off in yield (23%).



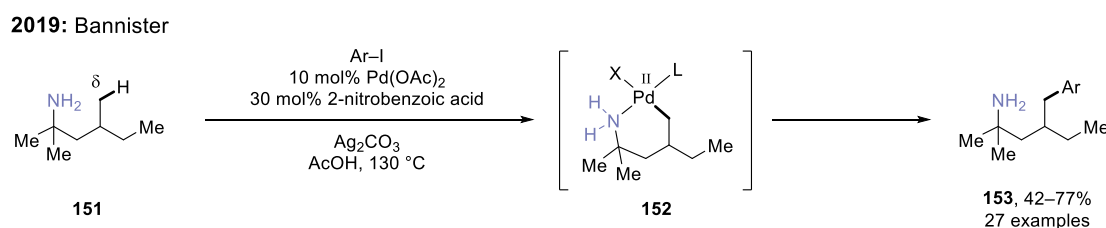
Scheme 35. β -Methylene carbonylation of less hindered aliphatic amines using xantphos as ligand.

Recently, primary amines have also been employed in the native amine-directed strategy for C–H functionalization. Given that primary amines are significantly more coordinating than secondary amines, in general, acidic solvents have been used in order to protonate the primary amine substrate and thus lower the concentration of free amine that could form off-cycle bis-amine complexes. The first example of native primary amine-directed functionalization was reported by Shi¹⁵⁷ in 2017, which simply used PhI(OAc)₂ and catalytic Pd(OAc)₂ in acetic acid at 120 °C to obtain γ -acetoxylated products (**147** to **148**, Scheme 36A). Notably, the conditions were found to partially acetylate the amine-nitrogen during the course of the reaction, and therefore global acetylation was conducted as a second step. Crucially, the control reaction employing an *N*-acetylated starting material gave zero conversion, supporting the intermediacy of the primary amine-directed five-membered ring palladacycle (**150**). In 2019, Yao¹⁵⁸ reported a γ C–H arylation of unprotected primary amines using aryl iodides (**147** to **149**, Scheme 36B). Yao¹⁵⁹ also reported an alternative arylation procedure using diaryliodonium salts in a separate work. In the same year, Bannister¹⁶⁰ reported the δ C–H arylation of primary amines using aryl iodide coupling partners in the presence of an electron-poor 2-nitrobenzoic acid ligand (**151** to **153**, Scheme 37). By analogy with the γ C–H functionalization processes, the reaction was proposed to proceed via the six-membered

palladacycle intermediate (**152**). Overall, although primary amine-directed C–H functionalization has been shown to be possible under relatively forcing conditions (acidic solvent and high temperatures), it is important to note that the reactions have much narrower scope than for the TDG strategies presented previously, indicating that the native primary amine functional group is generally less effective at mediating C–H activation compared to the in situ-formed TDG's.



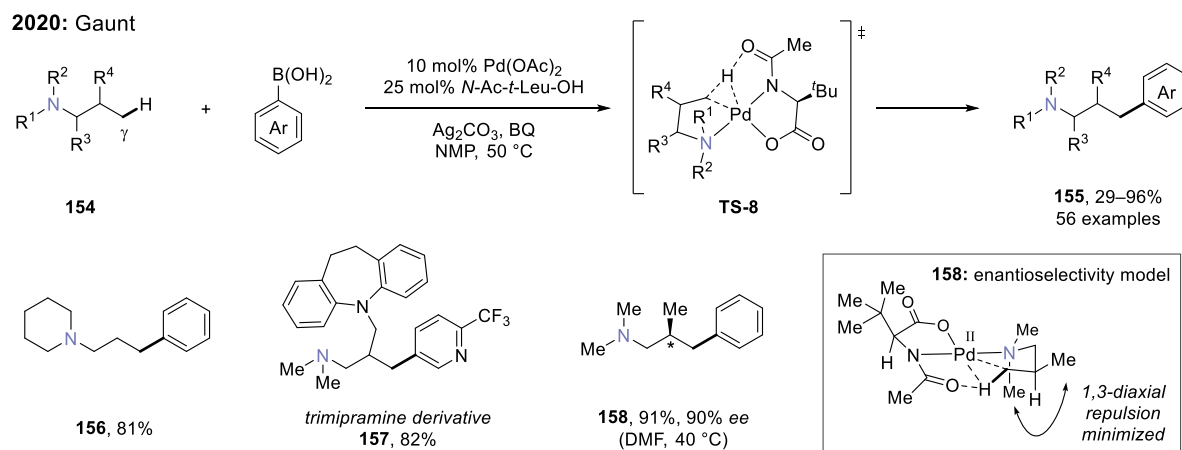
Scheme 36. Pd-catalyzed γ C–H functionalization of primary amines: (a) acetoxylation and (b) arylation.



Scheme 37. Pd-catalyzed δ C–H arylation of unprotected primary amines.

Very recently, Gaunt¹⁶¹ reported a Pd-catalyzed tertiary amine-directed C–H functionalization (Scheme 38). Tertiary aliphatic amines are particularly challenging substrates given their sensitivity to undergo oxidative degradation through facile Pd^{II} -mediated β -hydride elimination. However, it was found that employing an MPAA ligand (*N*-acetyl *tert*-leucine) suppressed this deleterious side reaction, and instead promoted efficient C–H activation at the γ -position (**TS-8**). Using boronic acid coupling partners in combination with Ag_2CO_3 and 1,4-benzoquinone additives, a wide array of tertiary amines (**154**) were transformed to their γ -arylated derivatives (**155**). The substrate scope included the functionalization of simple commercial amines (**156**) as well as more complex pharmaceutical drug compounds such as trimipramine (**157**). Moreover, since the ligand employed was chiral (and enantiopure),

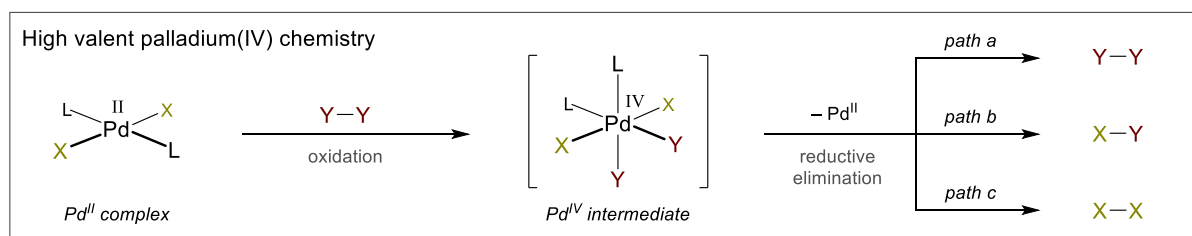
subjecting prochiral tertiary amines to the conditions resulted in enantioenriched chiral amine products (**158**). For the methyl group desymmetrization of amine leading to **158**, the observed enantioselectivity was proposed to result from the chair-like transition state of the C–H activation step, wherein the pseudo-axial *N*-methyl group is positioned away from the bulky *tert*-Bu group of the ligand and the spectating γ -methyl group is positioned in the pseudo-equatorial position to avoid a repulsive 1,3-diaxial interaction.



Scheme 38. Pd-catalyzed γ C–H arylation of tertiary aliphatic amines using an MPAA ligand.

1.3. Organometallic Chemistry of Alkyl Pd^{IV} Complexes

High valent Pd^{IV} complexes^{70,72,162–167} have intrigued chemists for decades by virtue of their distinct electronic and structural properties relative to more commonly encountered Pd^{II} and Pd⁰ complexes. Pd^{IV} complexes are accessed by the oxidation of Pd^{II} complexes and have d⁶ occupancy, octahedral geometry and are diamagnetic (Scheme 39). Classically, Pd^{IV} complexes have been viewed as extremely reactive and elusive intermediates given their lower stability compared to Pt^{IV} complexes.^{70,168} In particular, Pd^{IV} intermediates have a strong tendency to undergo reductive elimination processes, making these high valent species valuable as intermediates in catalytic processes. However, there are often multiple different reductive elimination pathways that are available to the Pd^{IV} intermediate. For example, the anionic ligands transferred by the oxidant may reductively eliminate to effect the reverse reaction back to starting materials (Path a, Scheme 39), two different adjacent ligands may couple to form a different product (Path b), or alternatively, two *trans* ligands may undergo reductive elimination via more a complex mechanism involving ligand isomerization or an outer-sphere process (Path c). Consequently, studying the structure and reactivity of well-defined Pd^{IV} complexes has become important for understanding ways of controlling the selectivity of reductive elimination for the development of catalytic processes.



Scheme 39. Pd^{IV} complexes: access by oxidation of Pd^{II} complexes and decomposition by reductive elimination.

Alkyl Pd^{IV} complexes – organometallic complexes containing one or more σ -bound alkyl ligands – are important intermediates in catalytic transformations of organic molecules, such as in Pd-catalyzed C(sp³)–H functionalization reactions. Yet, due to the transient nature of Pd^{IV} species, it was not until relatively recently that stable, crystallographically characterized examples of alkyl Pd^{IV} complexes were isolated. Early indications for the observation of these complexes occurred in the late 1970's by Yamamoto¹⁶⁹ and early 1980's by Stille,¹⁷⁰ wherein phosphine-ligated alkyl Pd^{II} complexes were reacted with halogens or alkyl halides. Notably, although phosphines are effective ligands for Pd^{II} centres, they are generally less effective for

stabilizing Pd^{IV} centres and consequently stable high valent complexes were not isolated. Conversely, harder nitrogen-based multidentate ligands proved to be better suited for stabilizing the hard Lewis acidic Pd^{IV} centre. In 1986, pioneering work by Canty¹⁷¹ reported the first example of an isolable alkyl Pd^{IV} complex, containing a 2,2'-bipyridyl supporting ligand and *fac*-Me₃Pd^{IV} organometallic group, with an iodide completing the octahedral coordination sphere (PdIme₃(bpy), **159**, Figure 4). Shortly after, in 1987, Canty^{172,173} found that *fac*-tridentate “tripodal” supporting ligands gave increased stability, with the use of a neutral tris(pyrazol-1-yl)methane ligand giving a stable cationic alkyl Pd^{IV} complex ([PdMe₃{(pz)₃CH}]I, **160**). In 1994,^{174,175} the isoelectronic anionic tris(pyrazol-1-yl)borate ligand was employed to generate the neutral tripodal ligand-supported Pd^{IV} complex (PdMe₃{(pz)₃BH}, **161**). Interestingly, it was not until 2000¹⁷⁶ that a phosphine-ligated alkyl Pd^{IV} complex was characterized by crystallography. The complex was synthesized by Canty through the displacement of a Pd^{IV}-bound triflate with PMe₂Ph to give a cationic phosphine-Pd^{IV} product ([PdMe₃(phen)(PMe₂Ph)][OTf], **162**). In 2003, Cámpora¹⁷⁷ moved away from the *fac*-trialkyl ligand arrangement and instead synthesised a new type of stable Pd^{IV} complex containing a cyclometalated (C_{alkyl},C_{aryl}) group known as a cycloneophyl ligand (**163**). Finally, in 2010, Vicente¹⁷⁸ reported the first example of an isolable Pd^{IV} complex containing a *mer*-tridentate pincer ligand (**164**).

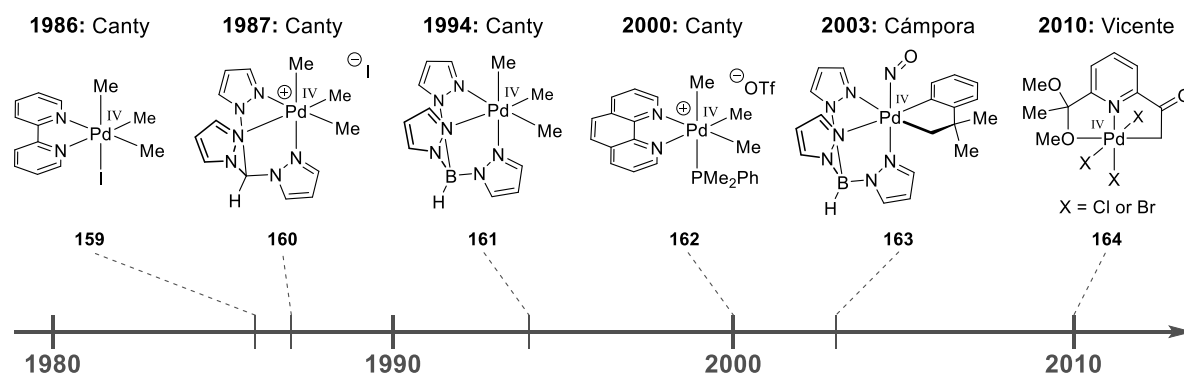


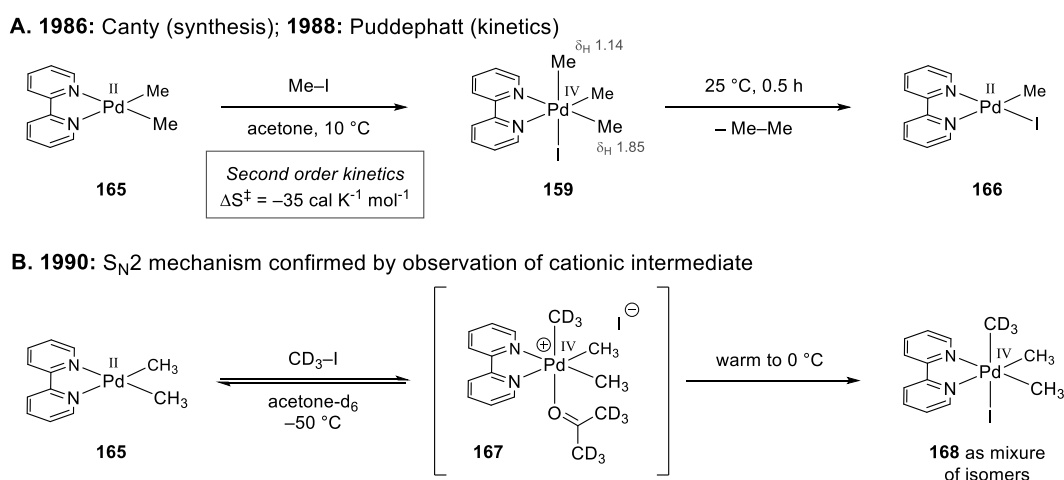
Figure 4. The evolution of stable alkyl Pd^{IV} complexes: seminal examples (1986–2010).

A series of factors affect the stability of Pd^{IV} complexes.¹⁶⁷ Firstly, rigid ligand scaffolds that reinforce the octahedral geometry result in more stable complexes compared to using flexible ligands. Accordingly, bipyridine is more stabilizing than tetramethylethylenediamine (tmeda), while phenanthroline is more stabilizing than bipyridine. Secondly, tridentate ligands are significantly more stabilizing than bidentate ligands, which is a result of the fact that

reductive elimination typically requires coordinative unsaturation to occur (see: Section 1.3.3.). As a direct comparison, while complex **159** slowly decomposes above $-10\text{ }^{\circ}\text{C}$ in solution, complex **161** is stable up to at least $80\text{ }^{\circ}\text{C}$.^{171,175} Thirdly, more electron-rich (Lewis basic) ligands offer greater stability for the electron-poor Pd^{IV} centre. For example, the anionic $[(\text{pz})_3\text{BH}]^-$ ligand is more stabilizing than the neutral $(\text{pz})_3\text{CH}$ ligand. Finally, cyclometalated carbon ligands such as the cycloneophyl group increase the stability of the complex by increasing the barrier to reductive elimination. Whereas the *fac*- Me_3 group can undergo facile reductive elimination of ethane, intramolecular $\text{C}(\text{sp}^3)\text{--C}(\text{sp}^2)$ bond reductive elimination of the cycloneophyl group to form a strained benzocyclobutane is a much less favoured process.

1.3.1. Synthesis of Alkyl Pd^{IV} Complexes & Mechanisms of Oxidation

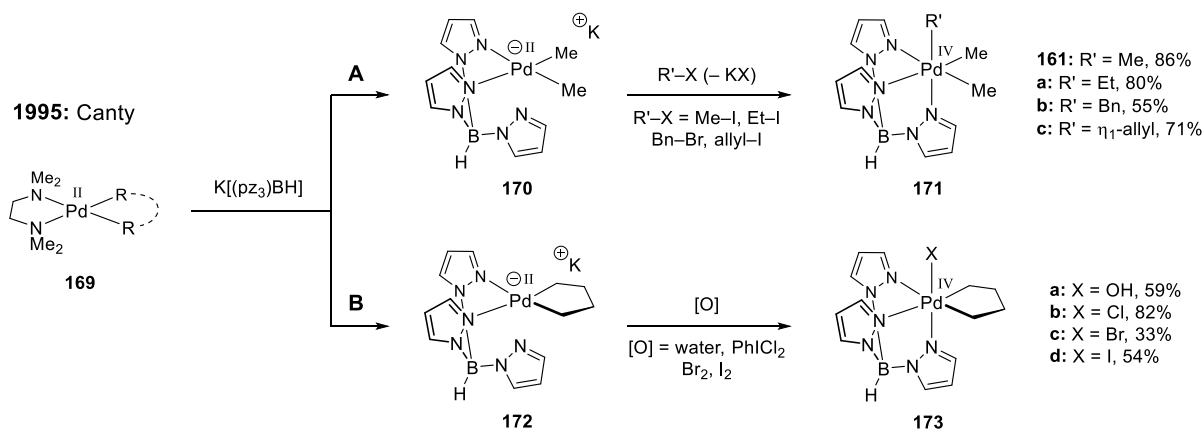
The most common approach to synthesizing alkyl Pd^{IV} complexes has been to employ alkyl halide reagents to oxidize the Pd^{II} centre to a Pd^{IV} centre. Canty's original synthesis¹⁷¹ of $\text{PdIme}_3(\text{bpy})$ (**159**) involved subjecting $\text{PdMe}_2(\text{bpy})$ (**165**) to methyl iodide in acetone which led to instantaneous formation of **159** (Scheme 40A). The *fac*-arrangement of methyl ligands gave rise to a 2:1 ratio of methyl protons in the ^1H NMR spectrum ($\delta_{\text{H}} = 1.85, 6\text{H}; 1.14, 3\text{H}$). After 30 minutes at room temperature, the complex had completely decomposed to ethane and $\text{PdIme}(\text{bpy})$ (**166**). The kinetics of the oxidation were later analysed by Puddephatt,^{179,180} who found that the reaction had overall second order kinetics (first order in **165** and Me-I) and a large negative entropy of activation ($\Delta S^{\ddagger} = -35\text{ cal K}^{-1}\text{ mol}^{-1}$). Together, these observations strongly indicated an $\text{S}_{\text{N}}2$ mechanism, which was later confirmed using ^1H NMR at low temperature to directly observe the cationic intermediate (**167**) resulting from the reversible



Scheme 40. Synthesis of $\text{PdIme}_3(\text{bpy})$ and elucidation of the mechanism of oxidation.

attack of **165** on methyl iodide (Scheme 40B).¹⁷³ Using methyl iodide- d_3 , scrambling of the CH_3 and CD_3 ligands was observed both within the cationic intermediate (**167**) and final Pd^{IV} product (**168**).

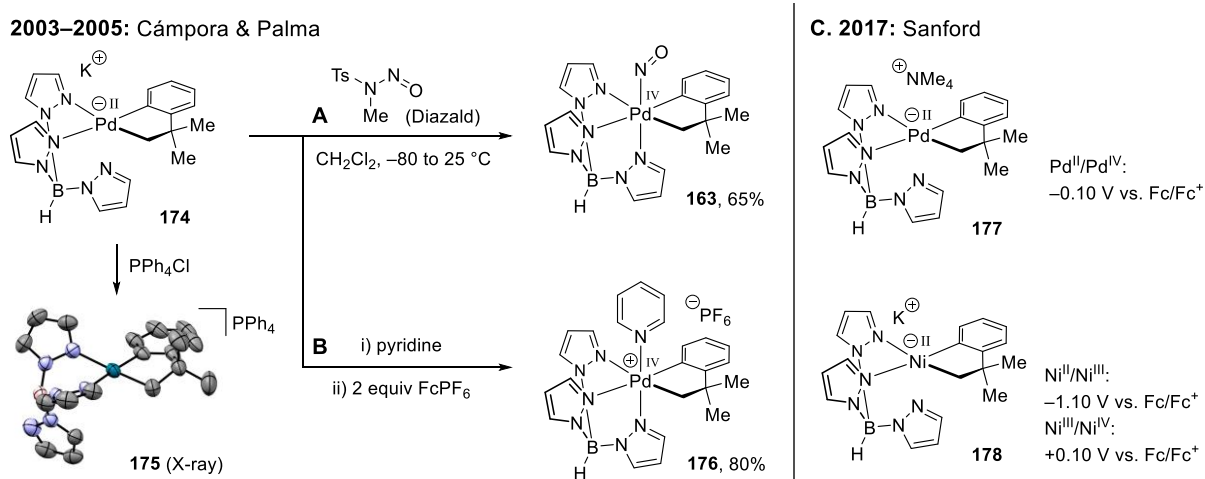
Canty's synthesis of tripodal ligand-supported Pd^{IV} complexes was also achieved using alkyl halides.¹⁷⁵ For example, starting from the dimethyl (tmeda) Pd^{II} precursor, tmeda was first displaced by the more coordinating $[(pz)_3BH]^-$ ligand to form an anionic Pd^{II} complex (**169** to **170**, Scheme 41A). The $[(pz)_3BH]^-$ ligand is known as a "scorpionate" ligand,¹⁸¹ given that it binds to Pd^{II} in a bidentate fashion while leaving the third pyrazolyl group "tail" primed to capture the Pd^{IV} centre upon oxidation. Canty showed that a series of activated alkyl halide reagents could be employed, providing access to the methyl, ethyl, benzyl and η^1 -allyl Pd^{IV} complexes (**161**, **171a–c**). In an analogous manner, an anionic pallada(II)cyclopentane complex (**172**) was oxidized by a series of two-electron oxidants such as halogens, a hypervalent iodine reagent or even water to access hydroxy, chloride, bromide or iodide Pd^{IV} complexes (**173a–d**, Scheme 41B).^{182,183} The oxidation of **172** by water (releasing H_2 gas) is particularly unusual given that H_2O is not typically considered as an oxidant. As such, the reaction demonstrated the unique ability of the scorpionate ligand to significantly facilitate the oxidation from Pd^{II} to Pd^{IV} .



Scheme 41. Synthesis of $[(pz)_3BH]$ -ligated Pd^{IV} complexes: (a) alkyl halides or (b) other two-electron oxidants.

Cámpora and Palma showed that high valent cycloneophyl-ligated Pd^{IV} complexes could be synthesized by either two-electron¹⁷⁷ or one-electron oxidants.¹⁸⁴ Interestingly, the negatively charged Pd^{II} complex containing the tripodal borate ligand (**174**) could be crystallized after counter-cation exchange (**175**), allowing for the observation of the primed Pd^{II} -bound scorpionate ligand in the solid-state.¹⁸⁴ Subjecting **174** to one equivalent of Diazald, a two-electron oxidant, provided the nitrosyl Pd^{IV} complex (**163**, Scheme 42A). Conversely,

using 2 equivalents of $[\text{Cp}_2\text{Fe}][\text{PF}_6]$ (FcPF_6) as an outer-sphere one-electron oxidant in the presence pyridine yielded the cationic Pd^{IV} complex (**176**, Scheme 42B). The added pyridine played a crucial role in stabilizing the resulting Pd^{IV} product by completing the octahedral coordination sphere, with the oxidation being additionally facilitated by the use of a more electron-rich pyridine such as DMAP. Later, cyclic voltammetry (CV) studies by Sanford¹⁸⁵ on the tetramethylammonium salt of the Pd^{II} precursor complex (**177**) in acetonitrile/pyridine showed a single oxidation wave with an onset potential of -0.10 V versus Fc/Fc^+ corresponding to the $\text{Pd}^{\text{II}}/\text{Pd}^{\text{IV}}$ redox couple. Significantly, the fact that two separate one-electron oxidation events were not observed by CV was in agreement with the known instability of the Pd^{III} oxidation state. Conversely, when conducting CV on the Ni^{II} analogue (**178**) in acetonitrile, Sanford observed two distinct oxidation processes with onset potentials of -1.10 and $+0.10$ V versus Fc/Fc^+ , corresponding to the $\text{Ni}^{\text{II}}/\text{Ni}^{\text{III}}$ and $\text{Ni}^{\text{III}}/\text{Ni}^{\text{IV}}$ redox couples.

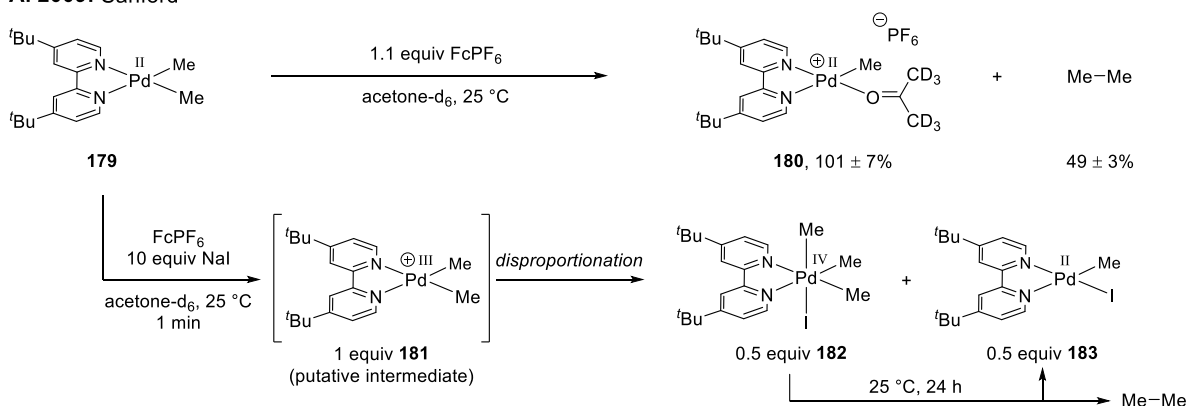


Scheme 42. Synthesis of cycloneophyl Pd^{IV} complexes by oxidation with (a) Diazald or (b) FcPF_6 ; (c) Cyclic voltammetry studies comparing the redox properties of cycloneophyl Pd^{II} and Ni^{II} complexes.

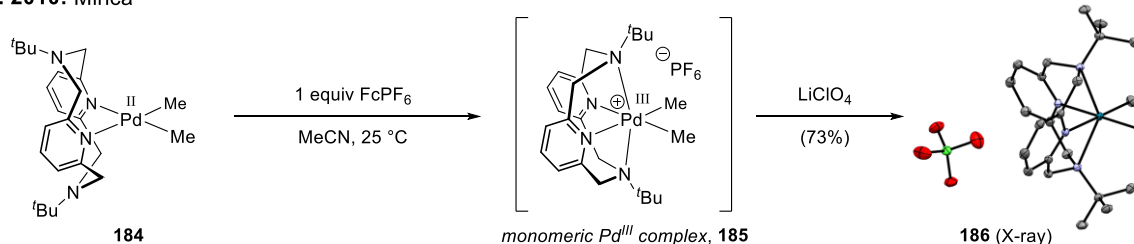
The mechanism of sequential one-electron oxidations of alkyl Pd^{II} complexes to Pd^{IV} complexes was first explored by Sanford¹⁸⁶ (Scheme 43A). Reacting $\text{PdMe}_2(\text{tBu}_2\text{bpy})$ (**179**) with FcPF_6 in acetone- d_6 led to quantitative formation of the solvated cationic Pd^{II} complex containing one methyl ligand (**180**) and approximately 50% yield of ethane. Upon repeating the reaction in the presence of 10 equivalents of NaI , instantaneous formation of a 1:1 mixture was observed comprising the stable trimethylated Pd^{IV} iodide complex (**182**) and a Pd^{II} complex bearing one methyl and one iodide ligand (**183**). After 24 h, decomposition of the Pd^{IV} complex led to the overall generation of one equivalent of **183** and half an equivalent of ethane.

Consequently, it was proposed that FcPF_6 mediates a single electron oxidation of **179** to a putative cationic Pd^{III} intermediate (**181**), which rapidly undergoes disproportionation with a second molecule of **181** to give the observed products **182** and **183** in the presence of excess iodide. Although the Pd^{III} intermediate was not directly observed, a timely subsequent study by Mirica¹⁸⁷ provided the first example of an isolable monomeric Pd^{III} complex (Scheme 43B). A dimethyl Pd^{II} precursor ligated to a tetradentate N4-donor ligand bound in a bidentate manner (**184**) was oxidized with one equivalent of FcPF_6 to furnish a stable cationic Pd^{III} complex (**185**). Upon oxidation, the tetradentate N4 ligand filled the two axial positions within **185** to form a distorted octahedral complex. Notably, counter-anion exchange enabled structural determination of the monomeric Pd^{III} complex by X-ray crystallography (**186**).

A. 2009: Sanford



B. 2010: Mirica

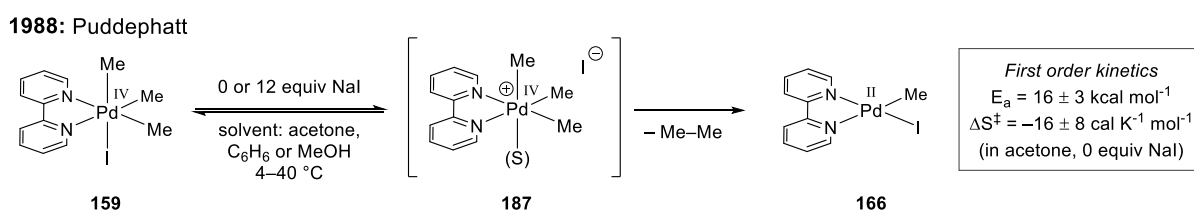


Scheme 43. (a) Sequential one-electron oxidation mechanism. (b) Isolation of an alkyl Pd^{III} complex.

1.3.2. Pd^{IV} -mediated C–C Bond Reductive Elimination

One of the most important uses of stable alkyl Pd^{IV} complexes is for the study of reductive elimination mechanisms for different ligand systems and types of bond formation. In 1988, Puddephatt¹⁷⁹ conducted the first studies on C–C bond reductive elimination from a Pd^{IV} centre using Canty's original bipyridyl Pd^{IV} complex (**159**, Scheme 44). The reductive elimination quantitatively produced ethane and the Pd^{II} by-product (**166**), being studied in a variety of

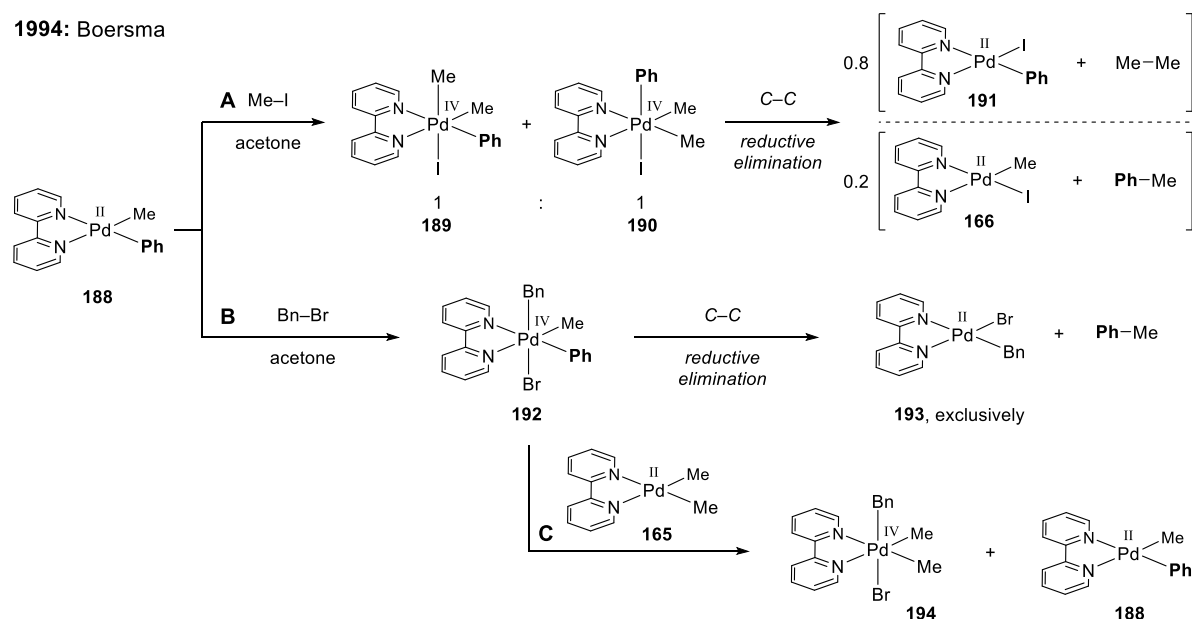
solvents in the presence or absence of excess NaI. The reaction was found to have a first order kinetic profile and was inhibited by excess NaI, indicating that the reaction involved reversible dissociation of iodide prior to a concerted C–C bond reductive elimination. Furthermore, the reaction occurred faster in more polar solvents, supporting the intermediacy of a charged intermediate following iodide dissociation (**187**). The activation parameters were obtained in the case of acetone solvent and absence of added iodide: $E_a = 16 \pm 3 \text{ kcal mol}^{-1}$, $\Delta S^\ddagger = -16 \pm 8 \text{ cal K}^{-1} \text{ mol}^{-1}$. The low activation energy reflected the facile formation of ethane, while the negative activation entropy was attributed to the re-organisation of solvent upon the formation of a charged intermediate.



Scheme 44. Mechanism of reductive elimination from PdIVMe₃(bpy).

The synthesis of differentially substituted trialkyl Pd^{IV} complexes enabled the selectivity of C–C bond reductive elimination to be analysed for the bipyridyl-supported Pd^{IV} complexes. In 1994, Boersma¹⁸⁸ reacted PdMePh(bpy) (**188**) with methyl iodide to form PdIMe₂Ph(bpy) as a 1:1 mixture of configurational isomers (**189**, **190**; Scheme 45A). A preference for methyl group reductive elimination was observed, giving a 4:1 ratio of ethane to toluene along with the associated Pd^{II} by-products (**191** and **166**, respectively). Conversely, reacting **188** with benzyl bromide gave a single isomer of a Pd^{IV} complex that contained three different carbon ligands: methyl, phenyl and benzyl (**192**). Reductive elimination from **192** exclusively produced toluene and Pd^{II} complex **193**. Overall, while the involvement of the methyl group in the reductive elimination was generally favoured, there was no clear explanation for the selectivity of C–C bond formation. Moreover, the mechanism was further complicated by the fact that the Pd^{IV} complexes could undergo facile exchange processes of the alkyl ligands. For example, subjecting PdBrMePhBn(bpy) (**192**) to PdMe₂(bpy) (**165**) led to rapid transfer of the benzyl and bromide ligands to form the more stable (less encumbered) Pd^{IV} complex PdBrMe₂Bn(bpy) (**194**) and the respective Pd^{II} by-product PdMePh(bpy) (**188**, Scheme 45C).

1994: Boersma

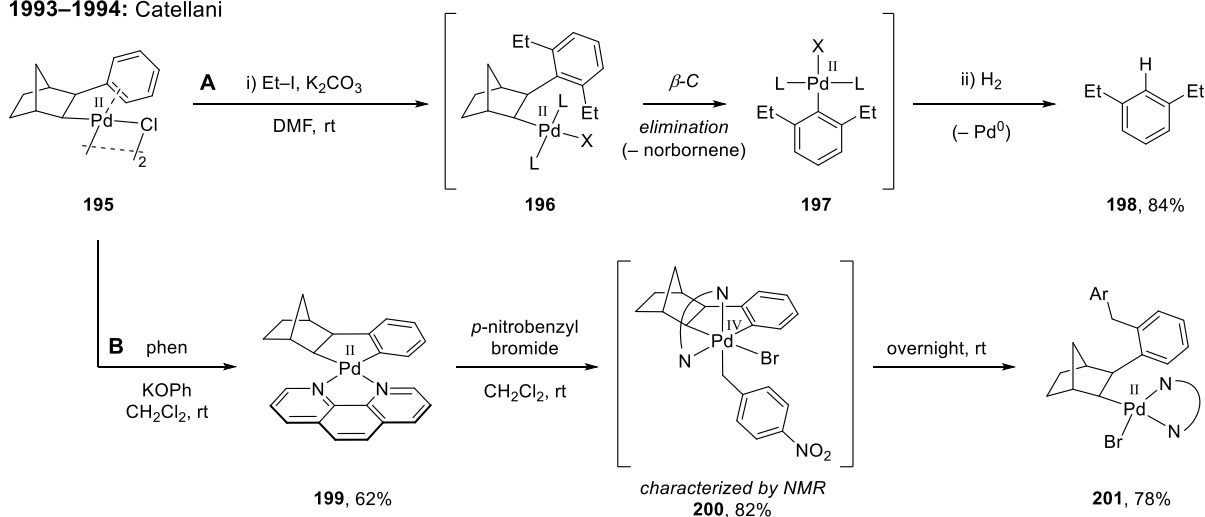


Scheme 45. Selectivity of C–C bond reductive elimination from (a) $\text{Pd}^{\text{IV}}\text{Me}_2\text{Ph}(\text{bpy})$ and (b) $\text{Pd}^{\text{IV}}\text{BrMePhBn}(\text{bpy})$. (c) Alkyl ligand exchange processes between Pd^{IV} centres.

One of the first cases where C–C bond reductive elimination from an alkyl Pd^{IV} intermediate was implicated in a catalytic process was for the Catellani reaction,^{165,189,190} which was developed over several years in the early 1990's through stoichiometric organometallic studies. The reaction originated from the observation of Inoue¹⁹¹ that the insertion of an aryl Pd^{II} complex into norbornene results in an alkyl Pd^{II} product that is stable to β -hydride elimination due to the absence of *syn*- β hydrogens (**195**, Scheme 46). However, it was the pioneering studies of Catellani^{189,192–195} which identified that these arylnorbornenylpalladium(II) complexes could promote *ortho* C–H functionalization processes in the presence of suitable electrophiles. For example, reacting dimeric Pd^{II} complex **195** with ethyl iodide in the presence of K_2CO_3 led to di-*ortho*-alkylation of the pendant aryl group (Scheme 46A).¹⁹² Moreover, due to the steric encumbrance of the resulting intermediate (**196**), spontaneous β -carbon elimination occurred to release norbornene and provide a new doubly alkylated σ -aryl Pd^{II} complex (**197**). Finally, hydrogenolysis of the Pd–C bond liberated the 1,3-diethylated arene (**198**). The mechanism of the norbornene-assisted C–H functionalization was extensively studied by Catellani. Subjecting **195** to KOPh with added phenanthroline ligand enabled the isolation of the palladacyclic complex (**199**),¹⁹³ unequivocally confirming this as an intermediate in the reaction pathway (Scheme 46B). Then, reacting palladacycle **199** with *p*-nitrobenzyl bromide led to the formation of a Pd^{IV} complex (**200**) that was stable for several hours at room temperature, allowing for characterization of the high valent complex by NMR spectroscopy.¹⁹⁵

Interestingly, **200** was the first example of an observable Pd^{IV} complex containing a metallacycle. C–C bond reductive elimination from **200** resulted in the exclusive coupling of the benzyl and aromatic groups (**201**), which was in contrast to the bond-forming selectivity of the trialkyl bipyridyl- Pd^{IV} complexes that disfavoured the coupling of the benzyl group (e.g. **192** to **193**). Following the seminal work of Catellani, a vast array of catalytic transformations were developed that utilized the directing ability of norbornene for the synthesis of poly-substituted aromatic derivatives.^{190,196} Notably, the methodological development of Catellani-type processes remains an active field of research up to the current day,¹⁹⁰ reflecting the remarkable versatility of this type of reactivity mode.

1993–1994: Catellani

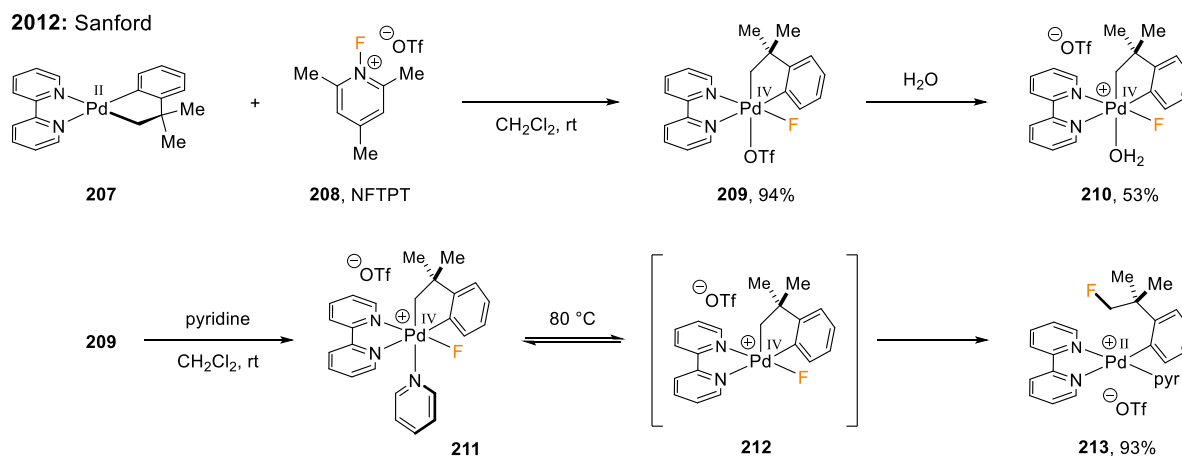


Scheme 46. Development of the Catellani reaction: (a) norbornene-assisted *ortho*-C–H alkylation. (b) Evidence for a cyclometalated alkyl Pd^{IV} intermediate and the formation of an observable benzyl Pd^{IV} complex.

1.3.3. Pd^{IV} -mediated $\text{C}(\text{sp}^3)$ –heteroatom Bond Reductive Elimination

In the late 1990's, studies began to focus on $\text{C}(\text{sp}^3)$ –heteroatom bond reductive elimination from alkyl Pd^{IV} intermediates. However, obtaining selectivity for the desired C–heteroatom bond formation over competing C–C coupling proved challenging. For example, Canty¹⁹⁷ found that simply reacting $\text{PdMe}_2(\text{bpy})$ (**165**) with benzoyl peroxide led to an unstable $\text{Me}_2\text{Pd}^{\text{IV}}$ intermediate (**202**) that underwent both C–C and C–O bond reductive eliminations to give a 60:40 mixture of ethane and methyl benzoate (Scheme 47A). Later, a more detailed study¹⁹⁸ involved the synthesis of a $\text{Me}_3\text{Pd}^{\text{IV}}$ benzoate complex (**203**) from the oxidation of **165** with Me-I followed by halide abstraction with $\text{Ag}[\text{O}_2\text{CPh}]$, but reductive elimination gave only ethane (Scheme 47B). Conversely, around the same time, Goldberg^{199,200} demonstrated that a

Cámpora and Palma¹⁷⁷ forming cycloneophyl Pd^{IV} complexes (e.g. **163**, Scheme 42), Sanford synthesized an analogous Pd^{IV} fluoride complex supported by a bipyridyl ligand (**209**) by reacting the Pd^{II} precursor (**207**) with *N*-fluoro-2,4,6-trimethylpyridinium triflate (NFTPT, **208**). Complex **209** was formed as a single isomer in near-quantitative yield by the oxidative transfer of fluoride and triflate groups from **208** to **207**. **209** was found to have notable stability to moisture and, rather than hydrolysing the Pd–F bond as was often observed in Pd^{II} complexes,²⁰³ the addition of water to **209** simply displaced the labile triflate ligand to form a cationic Pd^{IV} aquo complex (**210**). Alternatively, subjecting **209** to pyridine gave the pyridine-ligated cationic Pd^{IV} complex (**211**), which underwent clean C(sp³)–F bond reductive elimination at 80 °C to give the fluorinated σ-aryl Pd^{II} complex (**213**). Significantly, **213** was the sole product of the reductive elimination and hence C(sp²)–F coupling involving the aromatic group was not detected. From kinetic experiments, the C–F bond formation from **211** was found to have a first order kinetic profile and had negative first order dependency with respect to added pyridine. Consequently, Sanford proposed initial dissociation of pyridine to form a cationic 5-coordinate intermediate (**212**), followed by inner sphere C–F bond reductive elimination. An alternative mechanism involving fluoride dissociation from **212** followed by outer-sphere nucleophilic attack by fluoride was ruled out on the basis that this would require the formation of a dicationic 14-electron Pd^{IV} intermediate that would be highly disfavoured.

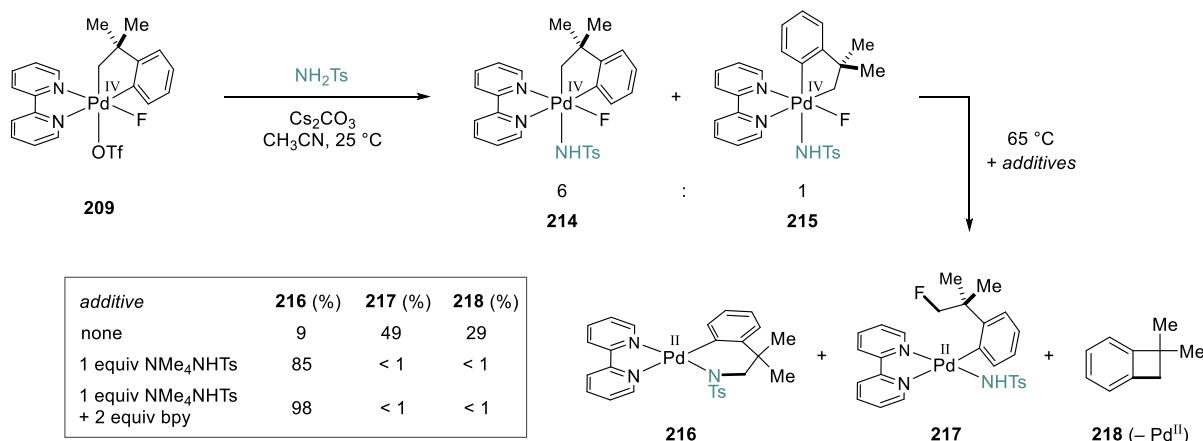


Scheme 48. C(sp³)–F bond reductive elimination from cycloneophyl Pd^{IV} complex: synthesis and mechanism.

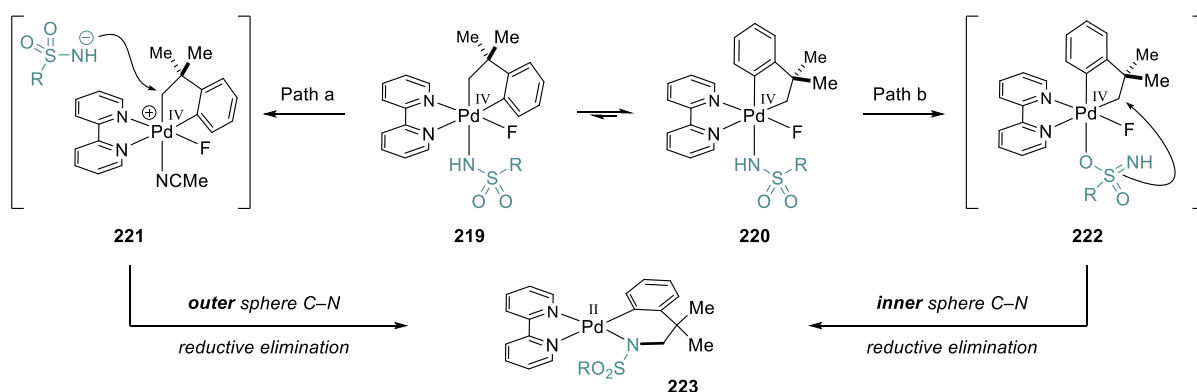
Sanford²⁰⁴ next explored Pd^{IV}-mediated C(sp³)–N bond reductive elimination. Subjecting the stable high valent cycloneophyl complex **209** to NH₂Ts and Cs₂CO₃ resulted in instantaneous ligand exchange of the triflate ligand for NHTs, forming two isomeric Pd^{IV}–NHTs complexes in a 6:1 ratio (Scheme 49A). The NHTs ligand was *trans* to the methylene of

the cycloneophyl group in the major isomer (**214**) and *trans* to the σ -aryl of the cycloneophyl in the minor isomer (**215**). Heating the isomeric Pd^{IV} complexes resulted in a mixture of reductive elimination pathways, in which the desired C(sp³)–N bond formation occurred in only 9% yield to form the palladacyclic product (**216**) after internal *N*-displacement of the fluoride ligand. Interestingly, the major pathway was in fact C(sp³)–F bond reductive elimination (**217**, 49%), with intramolecular C–C bond reductive elimination also taking place in 29% yield to form the benzocyclobutane product (**218**). However, as was previously observed in the case of Pt^{IV} chemistry^{199,200} (Scheme 47C), Sanford found that adding extra nucleophile to the reaction greatly improved the efficiency and selectivity of the desired bond formation. Adding 1 equivalent of soluble NMe₄NHTs, the yield of **216** increased to 85% and only traces of side-products **217** and **218** were formed. Furthermore, adding 2 equivalents of bipyridine ligand as well provided a further increase in the yield of **216** to 98%. Kinetic studies showed that the reaction was first order in the Pd^{IV} complexes (**214**, **215**) and zero order in added nucleophile (NMe₄NHTs), indicating that a dissociative ionization of the *N*-nucleophile followed by outer-

A. 2014: Sanford



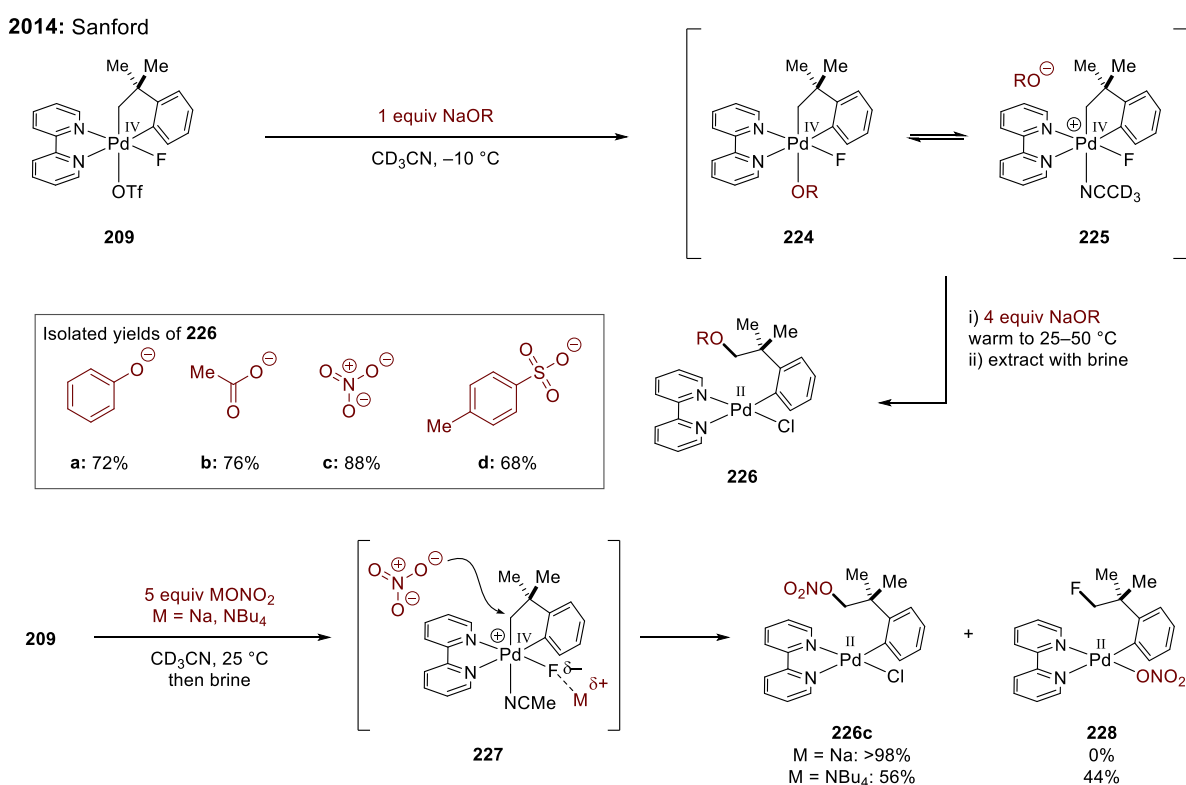
B. 2016: Sanford & Zimmerman (DFT)



Scheme 49. C(sp³)–N bond reductive elimination from a cycloneophyl Pd^{IV} complex.

sphere attack of the cationic Pd^{IV} complex was the likely mechanism. Indeed, later computational DFT studies by Zimmerman¹⁰³ calculated a low energy pathway involving an outer-sphere mechanism (**221** to **223**), originating from the major isomeric form of the Pd^{IV} intermediate (**219**; Path a, Scheme 49B). However, DFT analysis also revealed an alternative pathway which was similar in energy starting from the minor Pd^{IV} isomer (**220**), involving *N*-to-*O* ligand isomerization of the sulfonamide followed by intramolecular attack of the pendant nitrogen within a neutral 6-coordinate intermediate (**222**, Path b).

The same cycloneophyl Pd^{IV} complex (**209**) could also be used to study $\text{C}(\text{sp}^3)\text{--O}$ bond reductive elimination.^{205,206} Adding 1 equivalent of a range of oxyanion nucleophiles as their sodium salts (NaOR , $\text{R} = \text{Ph}$, Ac , NO_2 , Ts) to **209** at $-10\text{ }^\circ\text{C}$ in CD_3CN gave rise to an equilibrium mixture of the neutral oxyanion-ligated complexes (**224**) and the cationic acetonitrile-bound complex (**225**, Scheme 50). Subsequently, adding an excess of the nucleophiles, raising the temperature to between $25\text{--}50\text{ }^\circ\text{C}$ and then washing with brine resulted in exclusive formation of $\text{C}(\text{sp}^3)\text{--O}$ coupled products that were isolated as alkyl Pd^{II} chloride complexes in 68–88% yield (**226a–d**). From kinetic experiments, the reductive elimination was once again first order in the Pd^{IV} complex and zero order in added nucleophile. Crucially, given that the oxyanion ligand cannot isomerize to a different coordination mode to promote an inner-

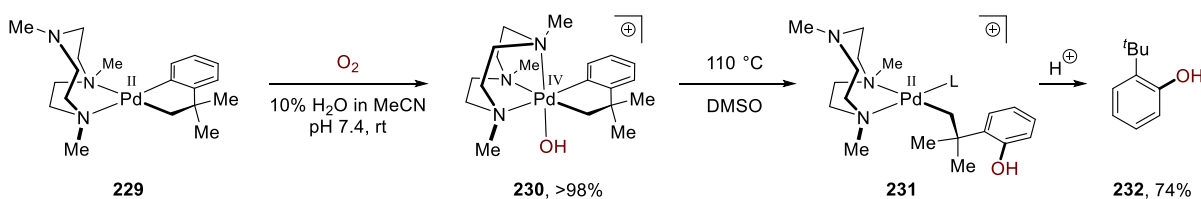


Scheme 50. $\text{C}(\text{sp}^3)\text{--O}$ bond reductive elimination from a cycloneophyl Pd^{IV} complex.

sphere reductive elimination mechanism, it was proposed that the mechanism occurred simply via outer-sphere nucleophilic attack of the cationic Pd^{IV} intermediate. In addition, a notable effect of the counter-cation of the oxyanion was observed. For example, reacting **209** with NaONO_2 and NBu_4ONO_2 at 25 °C led to exclusively $\text{C}(\text{sp}^3)\text{--O}$ bond reductive elimination in the former case (>98% **226c**) but gave a mixture of $\text{C}(\text{sp}^3)\text{--O}$ and $\text{C}(\text{sp}^3)\text{--F}$ reductive elimination in the latter case (56% **226c**, 44% **228**). Using ^{19}F NMR, a 1:1 interaction was observed between the Lewis acidic Na^+ cation and the Lewis basic $\text{Pd}^{\text{IV}}\text{--F}$ (**227**), whereas no interaction was observed for the tetrabutylammonium salt. Based on the experimental results, this Lewis acid-base interaction was proposed to inhibit $\text{C}(\text{sp}^3)\text{--F}$ bond reductive elimination.

Compared to Sanford's study on $\text{C}(\text{sp}^3)\text{--O}$ bond formation, divergent reactivity was observed by Mirica²⁰⁷ wherein a cycloneophyl-ligated Pd^{IV} complex underwent selective aromatic $\text{C}(\text{sp}^2)\text{--O}$ bond reductive elimination as opposed to alkyl group reductive elimination. Oxidation of a Pd^{II} complex supported by a scorpionate-type Me_3tacn ligand ($\text{Me}_3\text{tacn} = N,N',N''$ -trimethyl-1,4,7-triazacyclononane; **229**) by dioxygen led to quantitative formation of a cationic Pd^{IV} hydroxide complex (**230**, Scheme 51). Heating **230** in DMSO to 110 °C resulted in exclusive $\text{C}(\text{sp}^2)\text{--O}$ bond reductive elimination (**231**), presumably via an inner-sphere mechanism, which gave the phenol product (**232**) after protodemetalation. Crucially, the $\text{C}(\text{sp}^3)\text{--O}$ reductive elimination product was not detected. However, it was not clear whether this alternative reactivity could be attributed to the difference in supporting ligand (Me_3tacn versus bpy) or was a feature of hydroxide reductive elimination, given that the use of NaOH or NMe_4OH with Sanford's complex (**209**) gave a complicated mixture of products.²⁰⁵

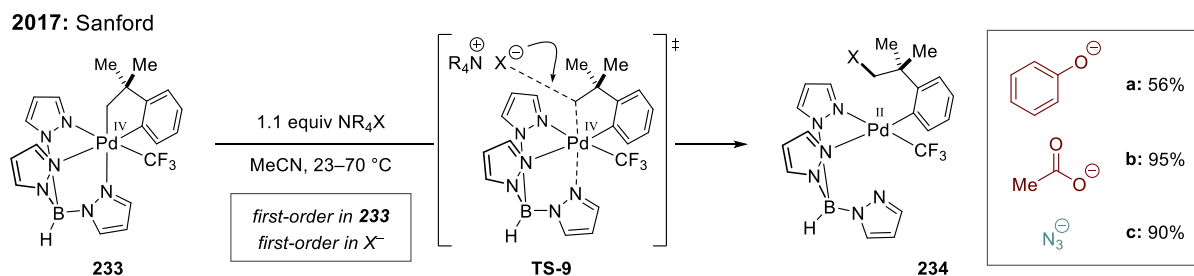
2014: Mirica



Scheme 51. $\text{C}(\text{sp}^2)\text{--O}$ bond reductive elimination from cycloneophyl $\text{Pd}^{\text{IV}}(\text{Me}_3\text{tacn})$ complex.

Finally, Sanford¹⁸⁵ showed that Pd^{IV} complexes which do not contain ligands that readily dissociate (to form 5-coordinate cationic intermediates) can also undergo nucleophile-mediated reductive elimination by direct outer-sphere attack of the neutral six-coordinate Pd^{IV} complex. For example, a Pd^{IV} centre ligated by a cycloneophyl group, $[(\text{pz})_3\text{BH}]$ and CF_3 ligands was attacked by *O*- and *N*-centred nucleophiles to form $\text{C}(\text{sp}^3)\text{--heteroatom}$ coupled

products (**234**) in good to high yields (Scheme 52). Notably, in this instance, kinetic studies revealed that the reductive elimination was first order in both **233** and added nucleophile, supporting a straightforward S_N2 mechanism involving the six-coordinate Pd^{IV} complex (**TS-9**).

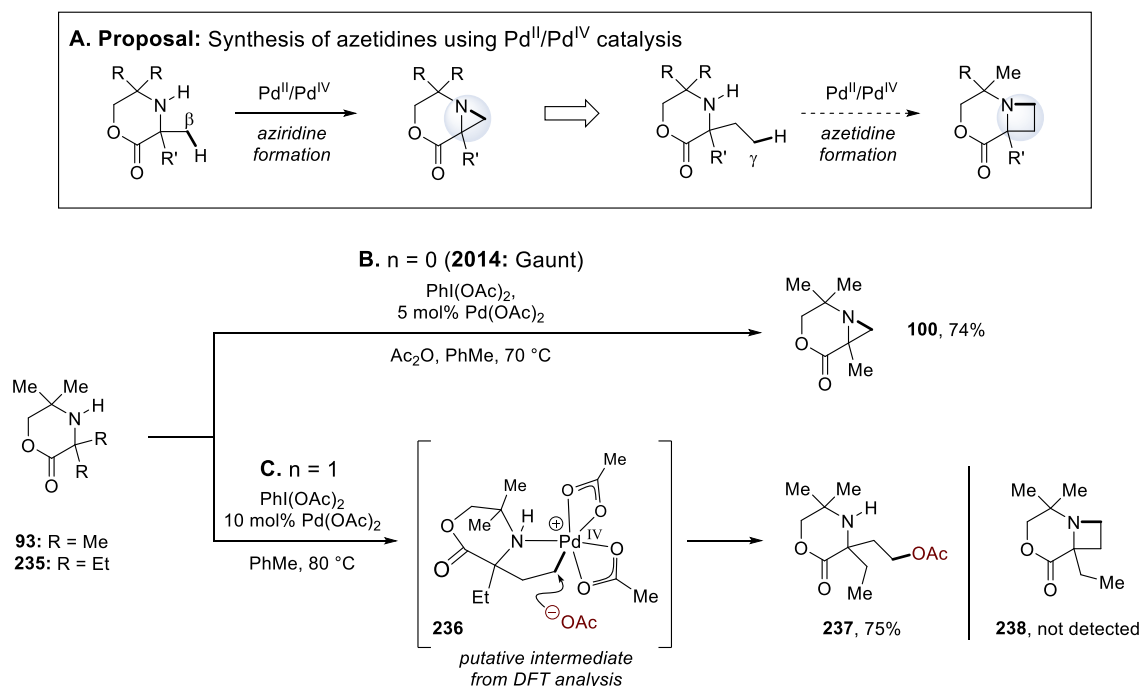


Scheme 52. C(sp³)-heteroatom reductive elimination by outer-sphere attack of a 6-coordinate Pd^{IV} complex.

2. Pd-catalyzed γ C(sp³)–H Amination to Form Azetidines

2.1. Background & Previous Work

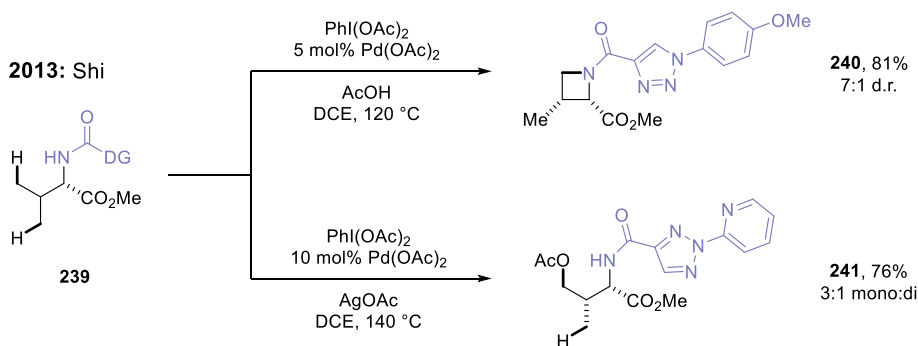
Following the discovery of the Pd-catalyzed aziridine formation by the intramolecular β C–H amination of hindered secondary amines,¹⁴⁶ it was thought that the homologous γ C–H amination process could be possible under similar conditions using Pd^{II}/Pd^{IV} catalysis (Scheme 53A). Crucially, the γ functionalization would result in the formation of four-membered ring azetidine products in a single step,²⁰⁸ which would be a valuable transformation given that classical methods for azetidine synthesis typically require highly functionalized precursors capable of mediating an internal displacement that are often challenging and time-consuming to prepare.^{209–212} However, while it was previously shown that subjecting morpholinone **93** to PhI(OAc)₂ and catalytic Pd(OAc)₂ gave exclusively aziridine formation (**100**, 74%; Scheme 53B),¹⁴⁶ reaction of the α -diethyl homologue (**235**) gave exclusively γ C–H acetoxylation (**237**, 75%; conducted by Dr M. Nappi; Scheme 53C) with no detectable amount of the desired azetidine (**238**) being formed. For the γ -acetoxylation process, computational DFT analysis carried out by Dr B. G. N. Chappell calculated that the favoured reductive elimination pathway involved outer-sphere attack by acetate onto a cationic Pd^{IV} intermediate (**236**), which was



Scheme 53. (a) Proposal for azetidine formation. Comparison of (b) β versus (c) γ C–H functionalization using PhI(OAc)₂ as oxidant. Reaction C conducted by Dr M. Nappi. DFT study conducted by Dr B. G. N. Chappell.

analogous to the mechanistic proposal of Sanford²⁰⁵ from the study of C(sp³)–O bond reductive elimination from stable Pd^{IV} complexes (see Section 1.3.3.). The Pd-catalyzed γ C–H acetoxylation of hindered secondary amines was later re-optimized and studied in detail using kinetic and computational analysis to gain further insight into the divergent selectivity for reductive elimination from aminoalkyl Pd^{IV} intermediates.²¹³

Evidently, intramolecular γ C–H amination proved to be less favoured than for the aziridine-forming β -functionalization reaction, and thus a distinct approach was necessary in order to mediate a selective azetidine formation over competing reductive elimination pathways. Previously, in 2016, Shi²¹⁴ had demonstrated that the selectivity of reductive elimination from a Pd^{IV} centre could be controlled by varying the type of DG that was used (Scheme 54). Using PhI(OAc)₂ and catalytic Pd(OAc)₂, substrates containing triazole amide-based DG's (**239**) selectively produced either azetidine products (**240**) when using a bidentate variant of the DG, or γ -acetoxylation (**241**) when using a tridentate variant containing a tethered pyridine. Although the specific reason for this switch in bond-forming selectivity was unclear, the reactions demonstrated the ability to favour azetidine formation based on the ligand environment around the Pd^{IV} centre. Nonetheless, the strategy of Shi could not be applied within a native amine-directed strategy due to the requirement for chelating auxiliary groups.

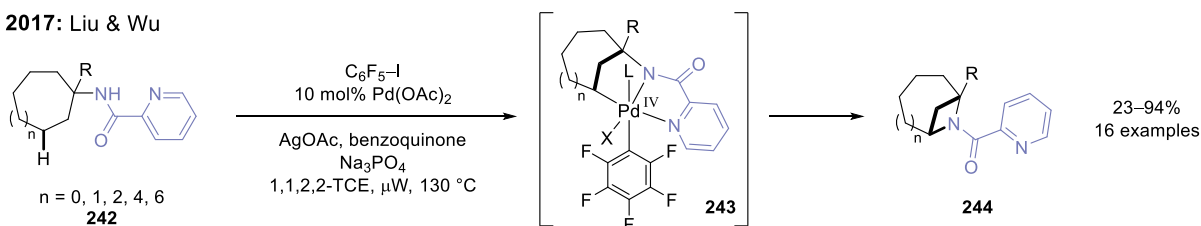


Scheme 54. Controlling the selectivity of reductive elimination through choice of directing group.

In parallel with the current work was the report by Liu and Wu,²¹⁵ which showed that reductive elimination could alternatively be controlled by the choice of oxidant (Scheme 55). Rather than using PhI(OAc)₂, pentafluoriodobenzene (C₆F₅I) was employed as part of a picolinamide-directed γ -methylene functionalization reaction to promote intramolecular C–N bond reductive elimination, forming bicyclic azetidine products (**242** to **244**). Importantly, the putative Pd^{IV} intermediate (**243**) resulting from oxidative addition contained the highly electron-withdrawing pentafluorophenyl ligand that did not undergo C–C bond reductive

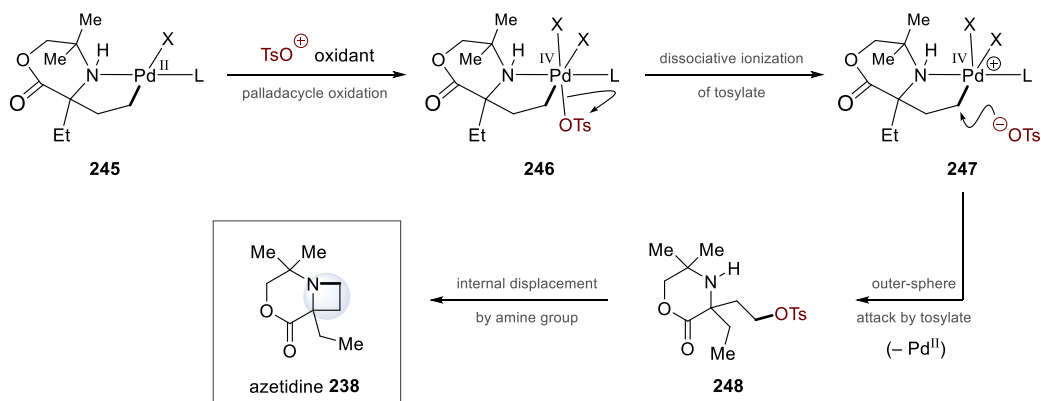
elimination (arylation) or acetoxylation (from AgOAc), but instead provided high selectivity for the desired cyclization process.

2017: Liu & Wu



Scheme 55. Reagent-controlled reductive elimination to promote intramolecular C(sp³)–N bond formation.

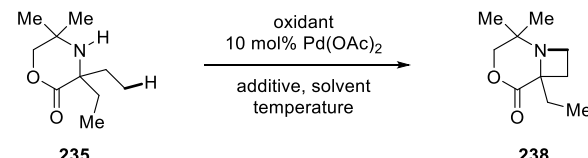
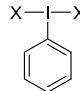
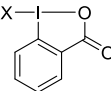
The ability to control the selectivity of reductive elimination from aminoalkyl Pd^{IV} intermediates derived from native amine-directed C–H activation remained an unsolved challenge. In the search for a suitable oxidant that could promote selective azetidine formation, it was hypothesized that, rather than aiming for a direct C–N bond forming process, the reductive elimination of a leaving group could instead be used to form an intermediate that would be prone to cyclization. Specifically, installation of a tosylate group was an attractive strategy given that it would exploit the proclivity of aminoalkyl Pd^{IV} intermediates to undergo outer-sphere C–O bond reductive elimination pathways (Scheme 56). For example, oxidative transfer of a tosylate group to the amine-derived palladacycle (**245**) would result in a Pd^{IV} intermediate (**246**) which could undergo dissociative ionization followed by S_N2-type attack of the Pd^{IV}-bound alkyl group (**247**). The resulting γ C–H tosyloxylation product (**248**) would then spontaneously cyclize to form the azetidine derivative (**238**).



Scheme 56. Proposed strategy for azetidine formation: γ C–H tosyloxylation followed by internal displacement.

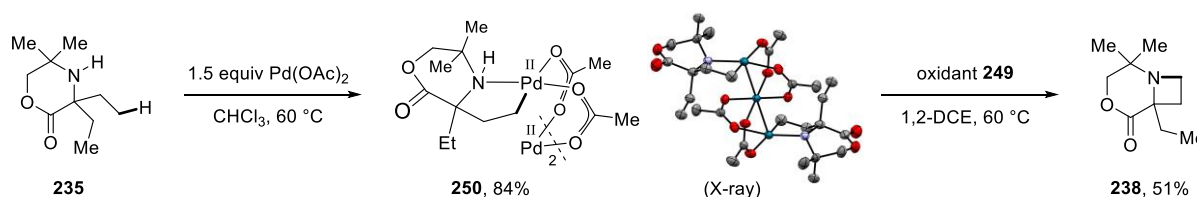
The preliminary experiments for the Pd-catalyzed γ C–H amination of hindered secondary amine **235** were conducted by Dr M. Nappi and Dr C. He. Firstly, simply combining $\text{PhI}(\text{OAc})_2$ with TsOH as an additive (two equivalents each) in PhMe at 80 °C gave none of the desired azetidine product (**238**; Table 1, entry 1), indicating that free TsOH was not beneficial for reactivity. However, employing a pre-formed tosylated iodine(III) reagent hydroxy(tosyloxy)iodobenzene (HTIB, also known as Koser's reagent)²¹⁶ provided the first observation of **238**, albeit in 6% yield (entry 2). Using AgOAc as an additive with HTIB increased the yield to 27% (entry 3). Meanwhile, cyclic iodonium oxidants²¹⁷ were also tested, with 2-iodosylbenzoic acid (IBA) giving 17% yield when used with AgOAc (entry 4). Notably, exchanging IBA for a tosylated cyclic iodonium oxidant (**249**), originally reported by Zhdankin²¹⁸ in 1994, increased the yield to 52% (entry 5). The reaction was optimized by Dr M. Nappi and Dr C. He using oxidant **249** to provide the azetidine product in 81% yield, which included increasing the equivalency of **249** and AgOAc to three equivalents each, lowering the temperature to 60 °C and changing the solvent to 1,2-DCE (entry 6). The control reaction removing the palladium catalyst gave no yield of **238** as was expected (entry 7), though removing the AgOAc additive also significantly hindered the reaction with only traces of azetidine formed (entry 8). While the specific role of AgOAc was not elucidated, the in situ formation of AgOTs was ruled out by a further control reaction exchanging AgOAc for AgOTs

Table 1. Reaction Discovery and Optimisation.^a

					
<div style="display: flex; justify-content: space-around; align-items: center;"> <div style="text-align: center;">  <p>$\text{PhI}(\text{OAc})_2$: X = OAc HTIB: X = OTs</p> </div> <div style="text-align: center;">  <p>IBA: X = OH 249: X = OTs</p> </div> </div>					
Entry	Oxidant (equiv)	Additive (equiv)	<i>T</i> (°C)	Solvent	Yield (%) ^b
1	$\text{PhI}(\text{OAc})_2$ (2)	TsOH (2)	80	PhMe	0
2	HTIB (2)	–	80	PhMe	6
3	HTIB (2)	AgOAc (2)	80	PhMe	27
4	IBA (2)	AgOAc (2)	80	PhMe	17
5	249 (2)	AgOAc (2)	80	PhMe	52
6	249 (3)	AgOAc (3)	60	1,2-DCE	81
7 ^c	249 (3)	AgOAc (3)	60	1,2-DCE	0
8	249 (3)	–	60	1,2-DCE	trace
9	249 (3)	AgOTs (3)	60	1,2-DCE	0

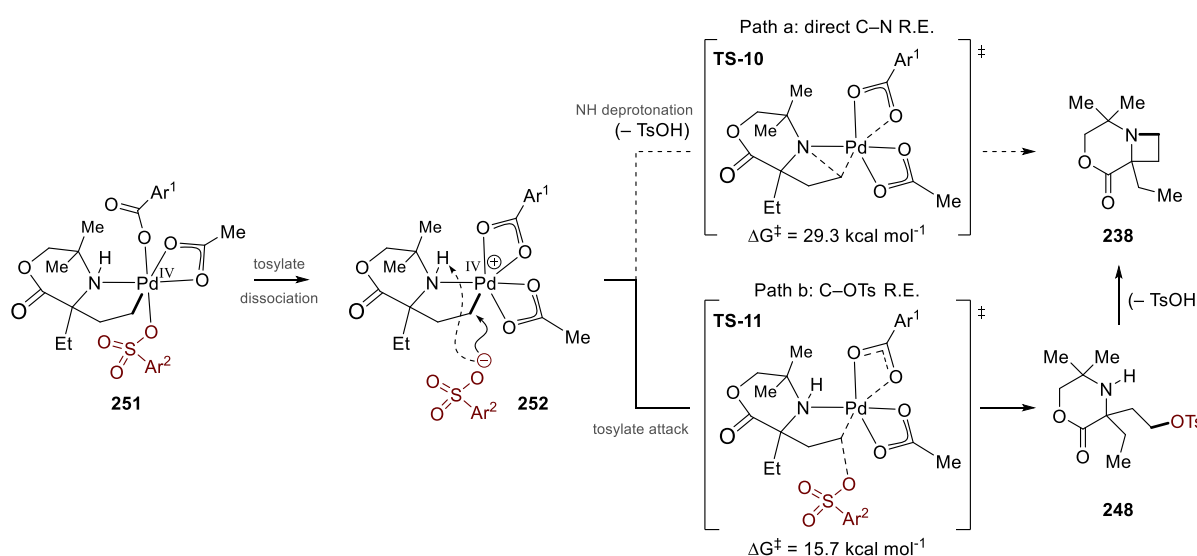
^aReactions were conducted by Dr M. Nappi and Dr C. He. ^bYields were determined by ¹H NMR using 1,1,2,2-tetrachloroethane or Ph₃CH as internal standard. ^cNo Pd(OAc)₂.

that provided 0% yield (entry 9). Finally, a stoichiometric palladium experiment was conducted by Dr C. He, wherein the 5-membered palladacycle was synthesized as the trinuclear acetate-bridged complex (**250**) in 84% yield by subjecting **235** to 1.5 equivalents of Pd(OAc)₂ in chloroform at 60 °C (Scheme 57). Reacting complex **250** with oxidant **249** in 1,2-DCE at 60 °C gave the azetidine (**238**) in 51% yield, confirming the intermediacy of the palladacycle as well as indicating that the silver(I) additive was not essential for the palladacycle oxidation nor for the product-forming reductive elimination step.



Scheme 57. Stoichiometric palladation of **235** and reaction with oxidant **249**. Reactions conducted by Dr C. He.

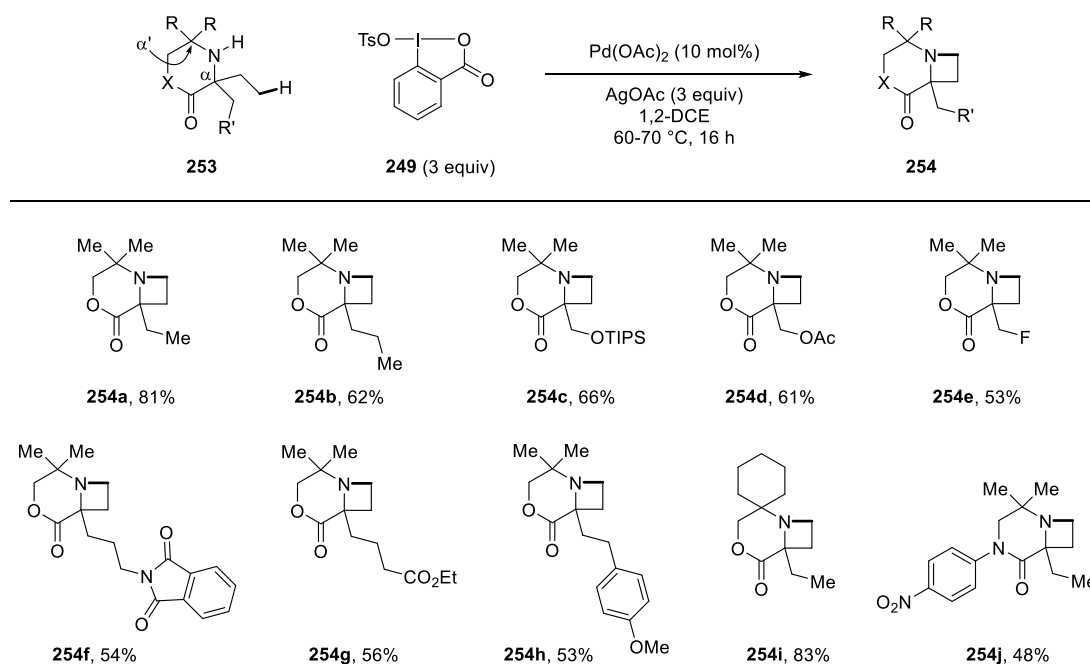
Having discovered an effective method for azetidine formation, computational DFT analysis was conducted by Dr B. G. N. Chappell to elucidate the reaction pathway (Scheme 58). Following oxidation of the palladacycle by oxidant **249**, a low energy pathway was calculated involving dissociation of the tosylate ligand from the Pd^{IV} intermediate (**251**) to generate the corresponding cationic Pd^{IV} species (**252**). From **252**, two potential reductive elimination mechanisms were calculated: (i) amine(NH) deprotonation followed by direct



Scheme 58. Computational DFT analysis of possible reductive elimination pathways. Conducted by Dr B. G. N. Chappell. Ar¹ = 2-I-C₆H₄CO₂H, Ar² = 4-Me-C₆H₄.

C–N bond reductive elimination ($\Delta G^\ddagger = 29.3 \text{ kcal mol}^{-1}$, **TS-10**; Path a) and (ii) outer-sphere attack by the displaced tosylate ($\Delta G^\ddagger = 15.7 \text{ kcal mol}^{-1}$, **TS-11**; Path b). In line with our proposed strategy, C–OTs bond reductive elimination via an outer-sphere mechanism (Path b) was found to be significantly lower in energy.

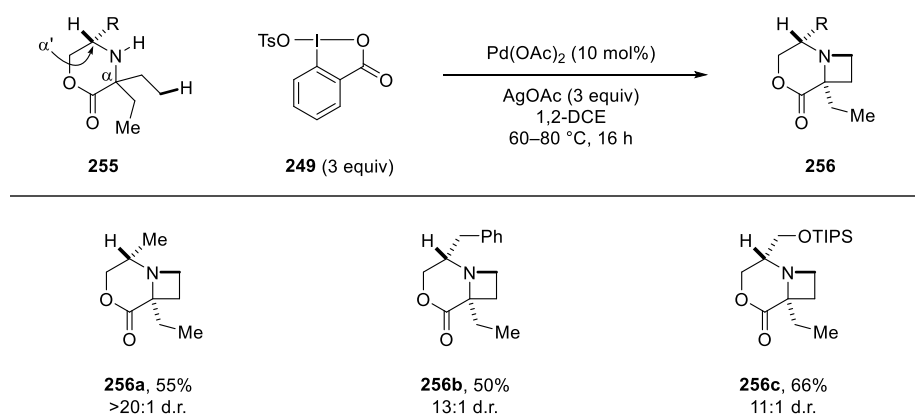
The scope of hindered secondary amines was explored by Dr M. Nappi and Dr C. He (Scheme 59). Maintaining the α -ethyl group required for γ C–H activation, the second α substituent was varied with alkyl chains containing different functional groups such as protected alcohols, fluoride, phthalimide, ester and aryl groups, providing the desired azetidines in good to excellent yield (**254a–h**, 53–81%). The α' -position distal to the lactone carbonyl was also changed from a geminal dimethyl group to a spirocyclic cyclohexyl moiety (**254i**, 83%). Finally, changing the morpholinone core for an aryl-substituted piperazinone core provided the azetidine in moderate yield (**254j**, 48%).



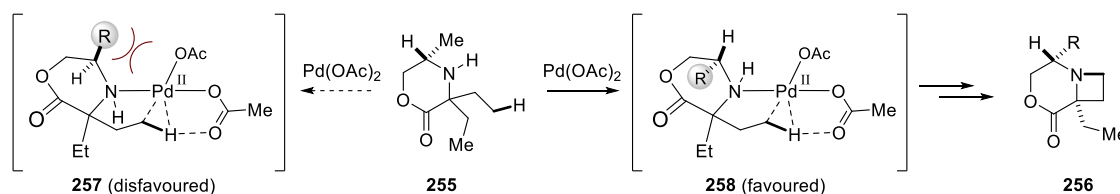
Scheme 59. Scope of amines with fully substituted α and α' positions. Yields are for isolated products. Reactions conducted by Dr M. Nappi and Dr C. He.

Significantly, Dr C. He discovered that the γ C–H amination reaction also extended to chiral amino acid-derived substrates containing α -gem-diethyl substitution (**255**, Scheme 60). These substrates contained an α' -H substituent that was previously found to be incompatible with the more oxidizing $\text{PhI}(\text{OAc})_2$ reagent due to deleterious oxidation of the amine,^{146,213} highlighting the improved chemoselectivity of oxidant **249**. Moreover, while the azetidines

were obtained in moderate yields for substrates derived from alanine, phenylalanine and serine (**256a–c**, 50–66%), the azetidine products were produced with high diastereoselectivity (up to >20:1 d.r.) resulting from the desymmetrization of the α -gem-diethyl group, providing essentially enantio- and diastereopure chiral products. In each case, the major diastereomer was formed from the activation of the ethyl chain *syn* to the α' -H substituent, presumably as a result of the Pd^{II} catalyst binding to the least hindered face of the secondary amine leading to C–H activation from this face of the morpholinone (**257** versus **258**, Scheme 61).



Scheme 60. Scope of amino acid-derived amines. Yields are for isolated products. All reactions by Dr C. He.



Scheme 61. Rationale for the observed diastereoselectivity of the γ C–H activation.

2.2. Project Aims

Upon joining the project of the Pd-catalyzed γ C–H amination, several areas of research remained to be explored. Firstly, we were interested in further investigating the scope of chiral amino acid-derived morpholinone substrates (Figure 5A). Given that the reaction selectively activated the alkyl chain on the least hindered face of the chiral morpholinones, we aimed to synthesize isomerically pure substrates that maintained a suitably displaced γ C–H bond on the least hindered face (*anti* to the amino acid-derived R-group) but with various “spectator” alkyl groups containing different functionality on the more hindered face. Consequently, it was

necessary to develop a diastereoselective synthetic protocol in order to access these substrate molecules. Secondly, it was planned to test the reaction on acyclic secondary amine substrates (Figure 5B). For previously reported Pd-catalyzed C–H functionalization reactions employing unprotected secondary amines, the scope of acyclic substrates had been extremely limited. However, the specific reason for this difficulty was unclear and therefore it was planned to use the azetidine-forming reaction as a means to further study this area of chemical space.

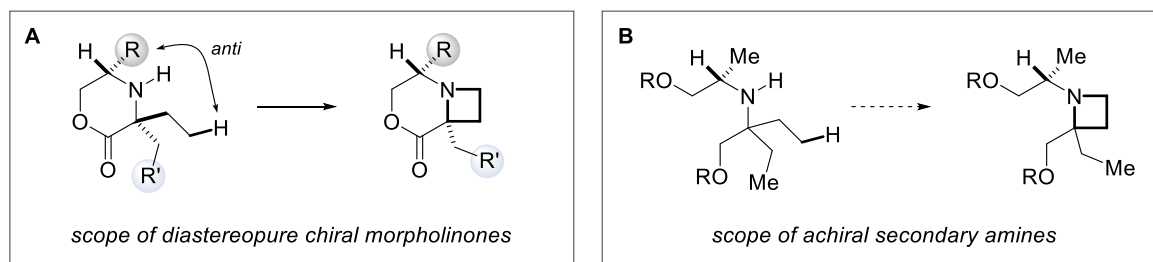


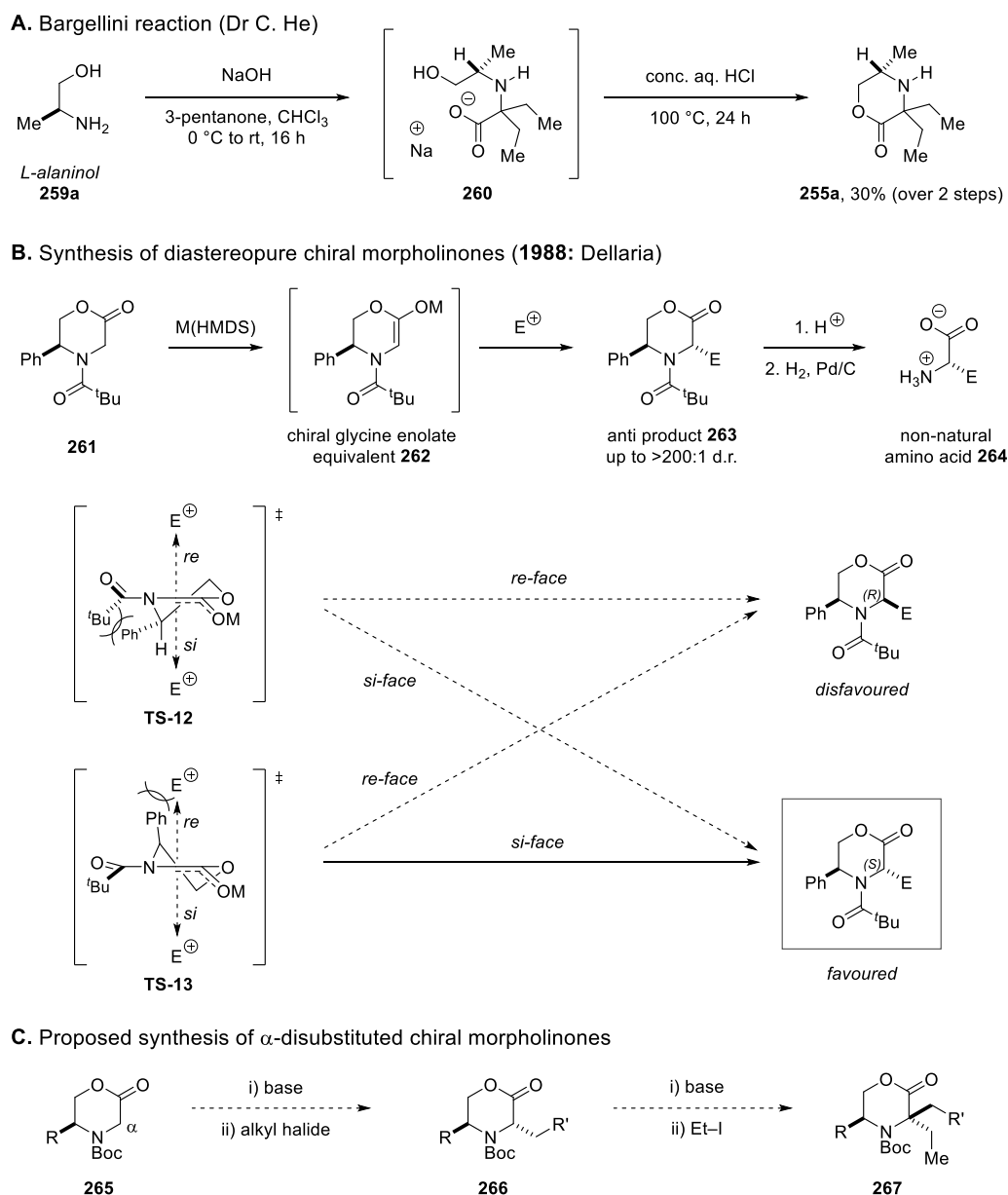
Figure 5. Project aims for the Pd-catalyzed γ C–H amination reaction.

2.3. Results & Discussion

2.3.1. Diastereopure Chiral Morpholinone Substrates

Previously, hindered secondary amines derived from amino acids containing the α -gem-diethyl group could be synthesized using the Bargellini reaction.²¹⁹ For example, the morpholinone derived from alanine (**255a**) was prepared by reacting L-alaninol (**259a**) with 3-pentanone and chloroform in the presence of sodium hydroxide, initially forming a sodium carboxylate intermediate (**260**) that was cyclized under high temperature acidic conditions (concentrated aq. HCl, 100 °C; Scheme 62A). However, given that we required a stereoselective synthesis for morpholinones containing two different α substituents, the Bargellini reaction could not be used because it would not be able to adequately control diastereoselectivity. Consequently, we searched for an alternative synthetic approach.

In 1988, Dellaria^{220,221} reported the diastereoselective alkylation of glycine enolate equivalents formed from morpholinones (**262**) for the synthesis of non-natural amino acids (Scheme 62B). The transformation was simultaneously reported by Williams^{222,223} using a similar method. In particular, highly diastereoselective alkylations were observed for the *N*-Boc-protected phenylglycine-derived morpholinone (**261**) when using lithium or sodium hexamethyldisilazide at low temperatures (–78 to –100 °C), which gave diastereo- and enantio-



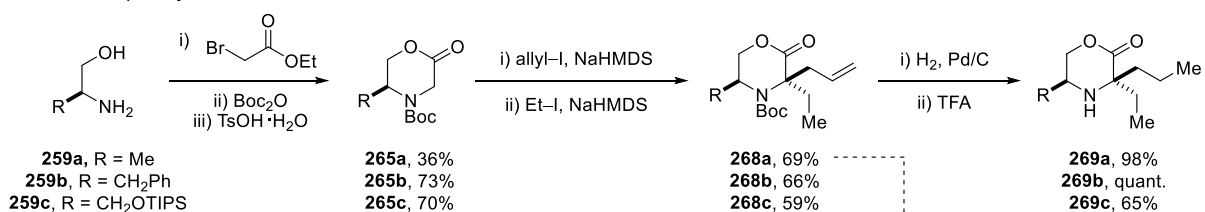
Scheme 62. (a) Example of the Bargellini reaction. (b) Literature precedence for stereoselective synthesis of chiral morpholinones and (c) application to α -disubstituted morpholinones. Reaction A conducted by Dr C. He.

pure alkylated products (**263**, up to >200:1 d.r.). Unprotected non-natural amino acids (**264**) could be generated in two steps by lactone hydrolysis and hydrogenolysis. The model for stereoinduction was reasoned on the basis of kinetic control, with four transition states being possible: *re/si*-**TS-12** and *re/si*-**TS-13**.²²¹ Transition states *re/si*-**TS-13** are favoured over *re/si*-**TS-12** on the basis of A(1,3) strain wherein the pseudo-axial amino acid-derived phenyl group avoids unfavourable steric clashing with the *tert*-butyl of the Boc protecting group. *si*-**TS-13** is then favoured over *re*-**TS-13** as the electrophile approaches from the least hindered face of the enolate. We planned to utilize Dellaria's stereoselective alkylation method to generate α -

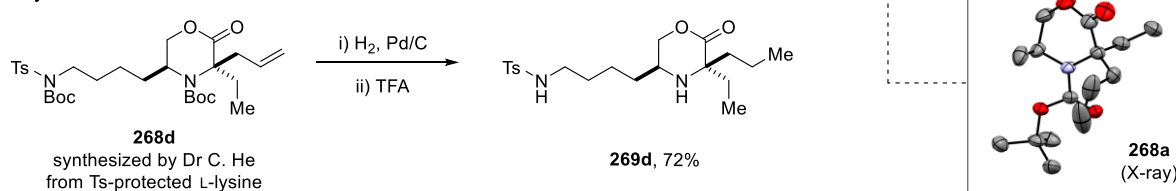
disubstituted chiral morpholinones as single isomers by carrying out two sequential alkylation steps on morpholinones derived from several different amino acids (**265**, Scheme 62C). Notably, α -ethylation would be carried out as the final alkylation step (**266** to **267**) in order to place an ethyl chain on the least hindered face of the morpholinone, as required for the Pd-mediated C–H activation.

Amino acid-derived morpholinones containing simple α -*n*-propyl α -ethyl substitution were first synthesized. Starting from L-alaninol, L-phenylalaninol and TIPS-protected L-serinol (**259a–c**), a sequential 3-step alkylation–Boc-protection–cyclisation protocol afforded the morpholinone cores (**265a–c**, Scheme 63A). Next, using the conditions developed by Dellaria, allylation followed by ethylation provided the α -dialkylated morpholinones in diastereomerically pure form after chromatography (**268a–c**). The crystal structure of **268a** revealed the expected pseudo-axial orientation of the alanine-derived α' -methyl group, as dictated by the A(1,3) strain of the *N*-Boc group, and importantly confirmed the relative stereochemistry of the α -alkyl substituents. Hydrogenation and Boc deprotection furnished the desired substrate molecules (**269a–c**). Following a similar synthetic sequence, the α -allyl α -ethyl intermediate derived from *N*-Ts-protected L-lysine was prepared by Dr C. He. As before, hydrogenation and Boc deprotection provided the desired amine substrate (**269d**, Scheme 63B).

A. Alanine, phenylalanine and serine derivatives



B. Lysine derivative

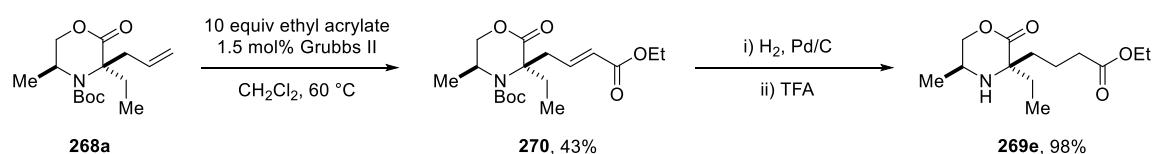


Scheme 63. Synthesis of morpholinone substrates derived from (a) alanine, phenylalanine, serine and (b) lysine.

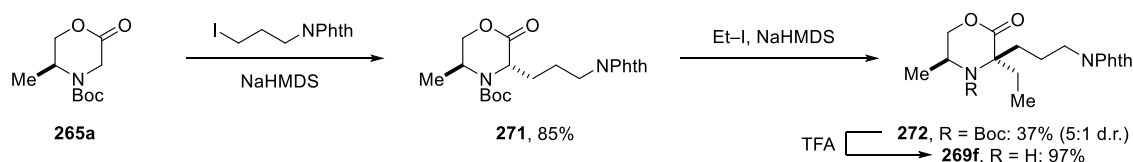
Using different synthetic intermediates, alanine-derived morpholinones with alkyl substituents containing functional groups were also accessed. For example, α -allyl α -ethyl-substituted intermediate **268a** underwent an olefin cross metathesis reaction with ethyl acrylate using Grubbs II catalyst to give the α,β -unsaturated ester derivative (**270**), which was

hydrogenated and deprotected to give amine substrate **269e** containing an alkyl ester substituent (Scheme 64A). Meanwhile, an alkyl phthalimide substituent was incorporated by using an alkyl iodide containing a terminal phthalimide in the alkylation sequence of parent morpholinone **265a** (Scheme 64B). Although the doubly alkylated product (**272**) was formed with moderate diastereoselectivity (5:1 d.r.), the major desired diastereomer was chromatographically isolated in synthetically useful 37% yield and deprotected to give the amine substrate (**269f**).

A. Alkyl ester substituent



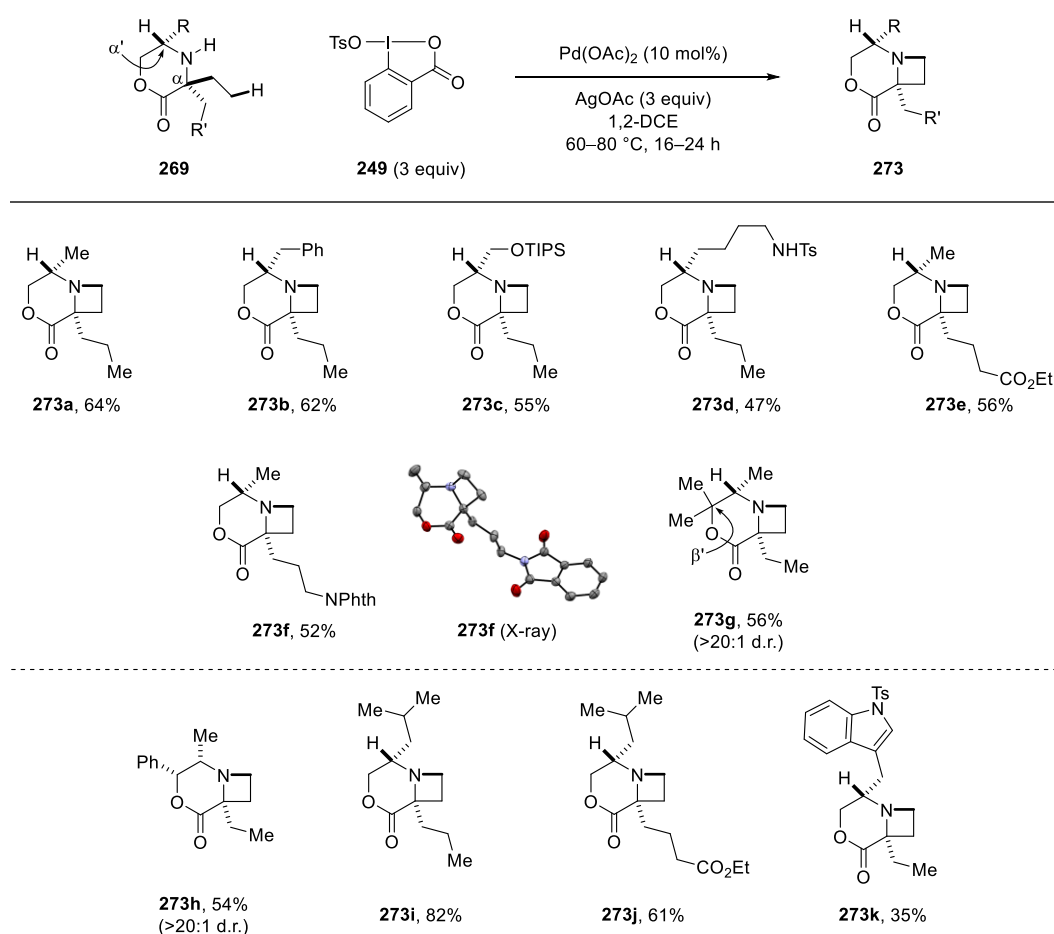
B. Alkyl phthalimide substituent



Scheme 64. Synthesis of alanine-derived morpholinones containing (a) ester and (b) phthalimide groups.

The synthesised chiral diastereopure morpholinones were subjected to the previously described Pd-catalyzed γ C–H amination conditions (Scheme 65). Alanine, phenylalanine and serine-derived substrates containing α -*n*-propyl α -ethyl substitution afforded the azetidine products in moderate to good yields (**273a–c**, 55–64%). Lysine-derived substrate gave a synthetically useful yield of the azetidine (**273d**, 47%), though was noticeably less reactive presumably on account of having a coordinating NH-Ts-containing side chain. Alkyl ester and phthalimide functional groups were well tolerated under the reaction conditions in the chiral alanine-derived substrates (**273e–f**, 52–56%). Azetidine **273f** was crystalline and hence analysed by X-ray characterization of a single crystal. The conformation of the six-membered ring showed a characteristic twist-boat, while the azetidine had the expected puckered conformation with an angle of pucker of 20.5°. Notably, the mass balance for the reactions was between 70–80%, indicating substrate decomposition (from β -H elimination or amine *N*-oxidation) was occurring in all cases under the conditions. A more substituted morpholinone core containing *gem*-dimethyl substitution at the β' -position (**269g**) was subjected in the reaction to test whether the mass balance could be improved by sterically protecting the α' -position, though the azetidine product was formed in essentially the same yield as for the simple

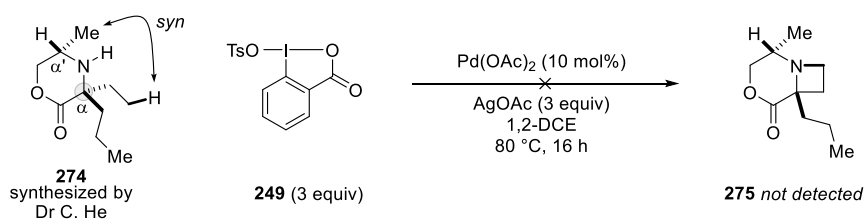
alanine-derived substrate, once again with excellent diastereoselectivity (**273g**, 56% yield, >20:1 d.r.). Several other chiral morpholinone substrates were synthesized and employed in the Pd-catalyzed reaction by Dr M. Nappi and Dr C. He (Scheme 65, bottom). A derivative of norephedrine containing α' -methyl and β' -phenyl substitution afforded the azetidine in good yield and excellent diastereoselectivity (**273h**, 54%, >20:1 d.r.). Derivatives of leucine generally were optimal substrates for the reaction, giving high yields of azetidines (**273i–j**, 61–82%), while a Ts-protected tryptophan derivative gave a synthetically useful yield (**273k**, 35%).



Scheme 65. Extended scope of amino acid-derived chiral morpholinones.

Azetidines **273h–273j** were synthesized by Dr M. Nappi. Azetidine **273k** was synthesized by Dr C. He.

A morpholinone containing α -*n*-propyl α -ethyl substitution derived from alanine, but containing the ethyl chain on the more hindered face *syn* to the alanine-derived methyl group, was synthesized by Dr C. He (**274**). As expected, under the Pd-catalyzed conditions the corresponding azetidine was not detected (**275**, Scheme 66).

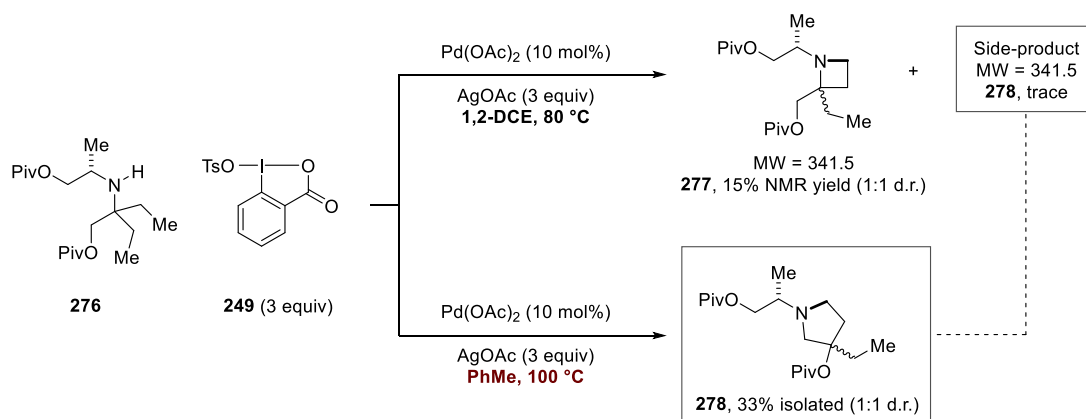


Scheme 66. α -Ethyl substitution on the more hindered face of the morpholinone gave no reaction.

2.3.2. Acyclic Substrates

We were interested in employing acyclic substrates in the Pd-catalyzed γ C–H amination reaction in order to move away from the privileged morpholinone scaffold and towards more commonly encountered classes of amine. Specifically, the greater conformational flexibility of acyclic amines relative to cyclic substrates such as morpholinones makes C–H activation more challenging due to the greater entropic penalty to cyclometalation. Furthermore, the resulting palladacycle is less rigid and therefore it is also more difficult to achieve the Pd^{II} to Pd^{IV} oxidation step. With these considerations in mind, we first tested a hindered acyclic secondary amine (**276**) that was synthesized from reductive ring-opening and Piv-protection of the α -diethyl substituted alanine-derived morpholinone (**255a**). Importantly, substrate **276** contained the same substitution pattern around the amine nitrogen as was in the reactive morpholinone substrates and thus was thought to give the highest chance of maintaining productive reactivity.

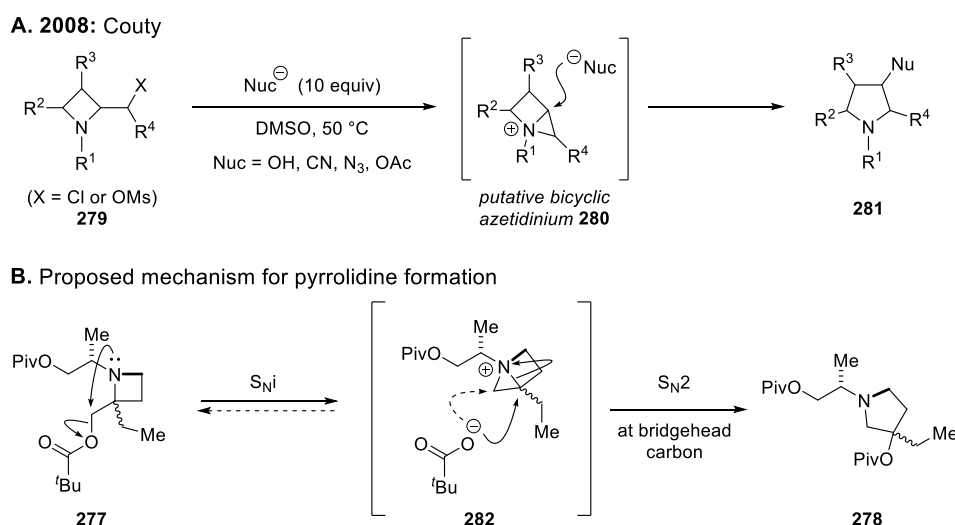
Subjecting amine **276** to the Pd-catalyzed conditions as developed previously (80 °C, 1,2-DCE) gave a low yield of the azetidine product (**277**, 15% by NMR; Scheme 67). Notably, unlike the morpholinone substrates, **277** was formed as a 1:1 mixture of diastereomers indicating that the cyclic structure was crucial for inducing stereoselectivity. Although the



Scheme 67. Investigation of morpholinone-derived acyclic amine: observation of rearranged pyrrolidine product.

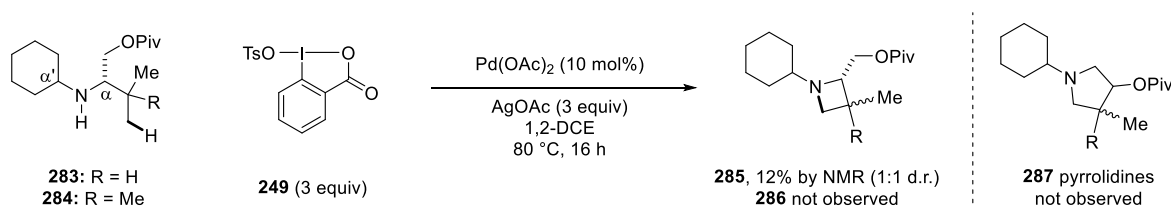
conversion was low, a trace amount of another product with the same molecular weight was observed when analysing the crude reaction mixture by GC-MS. Subsequently, upon repeating the reaction at higher temperature (100 °C, PhMe) the trace side-product was found to increase significantly in yield, with the azetidine (**277**) no longer being observed. After purifying the reaction by silica gel chromatography, the new product was identified as the ring-expanded pyrrolidine product containing a β -quaternary centre (**278**, 33% isolated, 1:1 d.r.).

With respect to the mechanism of the pyrrolidine formation, it was proposed that the reaction proceeded via the intermediacy of the azetidine given that this product was observed under the lower temperature conditions. Upon searching the literature for similar types of ring expansion, we found that the expansion of (α -chloromethyl) and (α -(OMs)-methyl)azetidines (**279**) to 3-substituted pyrrolidines (**281**) had previously been reported (Scheme 68A).^{211,224} Although a concerted mechanism was originally proposed, a study by Couty²²⁵ in 2008 strongly favoured a stepwise mechanism on the basis that external nucleophiles (e.g. OH^- , CN^- , N_3^- , AcO^-) could intercept the putative bicyclic azetidinium intermediate (**280**) to form diversely functionalized pyrrolidines. By analogy with Couty's observations, it is proposed that the initially formed azetidine **277** undergoes an internal displacement of the pivalate group present within the alkyl substituent of the azetidine, forming a 3,4-bicyclic azetidinium intermediate (**282**, Scheme 68B). The displaced pivalate anion may then attack the unsubstituted position of the three-membered ring, re-forming starting material, or attack the bridgehead position to form the observed pyrrolidine product (**278**). The release of ring strain should provide a thermodynamic driving force for conversion of **277** to **278**.



Scheme 68. (a) Couty's ring expansion of azetidines and (b) proposed mechanism from literature precedence.

In order to test the limit of the Pd-catalyzed γ C–H amination reaction, less hindered acyclic secondary amines derived from valine (**283**) and *tert*-leucine (**284**) were employed (Scheme 69). These substrates contained two potential sites for β -H elimination, with one hydrogen substituent at each of the α and α' positions, making them more vulnerable to Pd-mediated decomposition. Nonetheless, pleasingly, under the standard catalytic conditions the azetidine was formed for the valine-derived substrate, albeit in low yield (**285**, 12% by NMR, 1:1 d.r.). Conversely, the azetidine was not observed for the more substituted *tert*-leucine-derived substrate (**286**), and in both cases, the rearranged pyrrolidine product was not observed (**287**). Overall, despite not providing a synthetically useful yield, the observation of azetidine **285** provided a crucial indication that a wider range of aliphatic amines could potentially be functionalized using a high valent Pd^{II}/Pd^{IV}-catalyzed C–H functionalization strategy.



Scheme 69. Investigation of acyclic amines derived from valine and *tert*-leucine.

2.4. Summary

The current chapter disclosed the investigation into the scope of the Pd-catalyzed intramolecular γ C–H amination of hindered aliphatic amines that was discovered by Dr M. Nappi and Dr C. He. The reaction was effective for a range of cyclic morpholinone substrates, providing access to an array of densely substituted azetidine derivatives. Following the earlier report of β C–H amination to form aziridines via four-membered ring palladacycle intermediates, the present work demonstrated a novel strategy for favouring intramolecular C–N bond formation from five-membered ring palladacycles over other competing bond-forming processes. Specifically, a cyclic iodine(III) tosylate oxidant was used to access a Pd^{IV} intermediate capable of undergoing selective C–OTs reductive elimination, installing a tosylate leaving group at the γ -position that was spontaneously displaced by the amine nitrogen. The reaction exploited the relative facility of the outer-sphere reductive elimination mechanism that is possible for anionic oxygen ligands from Pd^{IV} intermediates, as opposed to a direct C–N bond reductive elimination that was found to be disfavoured from five-membered ring palladacycles.

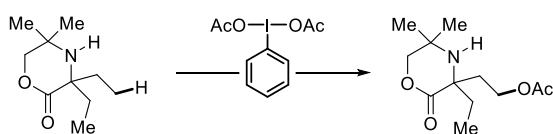
Perhaps the most important implication from the work was that high valent Pd^{II}/Pd^{IV} catalysis was demonstrated for the first time to tolerate substrates containing hydrogen substituents adjacent to the amine nitrogen. In previous studies, hypervalent iodine(III) oxidants had been found to rapidly degrade these types of less substituted amine, and therefore the cyclic iodine(III) reagent proved to be highly chemoselective for oxidizing the palladacycle without significant background oxidation of the substrate. Consequently, chiral morpholinones derived from amino acids containing one α -H substituent could be functionalized in good yield, generating diastero- and enantiopure azetidine derivatives that would be difficult to otherwise synthesize in isomerically pure form. Building on the improved scope of the azetidine-forming reaction, the limit of the Pd catalysis was tested by employing acyclic secondary amine substrates, which had proven to be challenging for the native amine-directed C–H functionalization strategy due to their lower reactivity towards cyclometalation. Interestingly, the azetidine products of Piv-protected amino-diol substrates derived from morpholinones were found to readily undergo ring-expansion processes in situ under the Pd-catalysed conditions. Although this transformation was not extensively explored, further optimisation could provide a new method for the synthesis of substituted pyrrolidines. Moreover, a less hindered valine-derived secondary amine with two hydrogen substituents adjacent to the amine nitrogen provided a low but promising yield of the corresponding azetidine, providing the first example of an oxidative C–H functionalization on an unprotected amine substrate that is not a morpholinone or derived from a morpholinone. Significantly, this result provided the basis for subsequent research described in the following sections, which aimed to expand the scope of aliphatic amine-directed Pd^{II}/Pd^{IV}-catalyzed C–H functionalization reactions.

3. Pd-catalyzed C–H Functionalization by *ortho*-DG-assisted Oxidative Addition

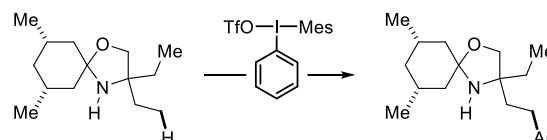
3.1. Background & Project Aims

Since the advent of the native amine-directed C–H functionalization strategy, a variety of Pd-catalyzed γ C(sp³)–H functionalization processes proceeding via the high valent Pd^{II}/Pd^{IV} manifold were developed. The transformations included (A) γ -acetoxylation of hindered secondary amines using PhI(OAc)₂,^{154,213} (B) γ -arylation of *N,O*-ketals using diaryliodonium salts¹⁵⁴ and (C) γ C–H amination of morpholinones using a cyclic iodine(III) tosylate reagent (Scheme 70).²²⁶ Notably, in all cases hypervalent iodine reagents were employed, which react with the intermediate five-membered ring palladacycles via an outer-sphere S_N2 oxidation mechanism analogous to that of alkyl halide reagents (Scheme 70D).^{227,228} However, while the iodine(III) oxidants could readily oxidize a range of palladacyclic intermediates derived from cyclic hindered secondary amines, a fundamental limitation was that less hindered (and more nucleophilic) amines were prone to directly reacting with the oxidant through the nitrogen lone pair leading to deleterious substrate oxidation to form imines.^{229–231} Therefore, the oxidant must be sufficiently reactive to oxidize the palladacycle while avoiding degradation of the amine substrate, but for less hindered amines this window for productive reactivity becomes vanishingly small. Consequently, while less hindered amines have been demonstrated to be cyclopalladated under stoichiometric conditions,⁷¹ the scope of catalytic transformations has been limited due to incompatibility with known oxidants. Overall, outside of hindered morpholinone or *N,O*-ketal substrates, the discovery of a mild and general method for accessing aminoalkyl Pd^{IV} intermediates under catalytic conditions has remained an unsolved problem.

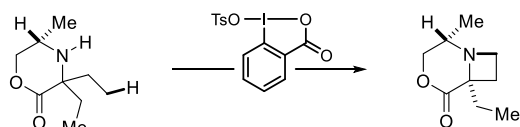
A. PhI(OAc)₂: acetoxylation



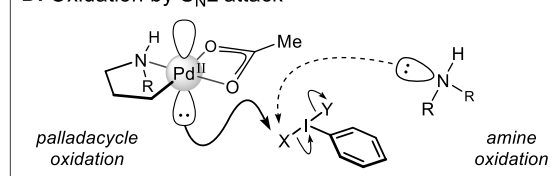
B. Ar(Mes)I–OTf: arylation



C. Cyclic iodine(III) tosylate: amination

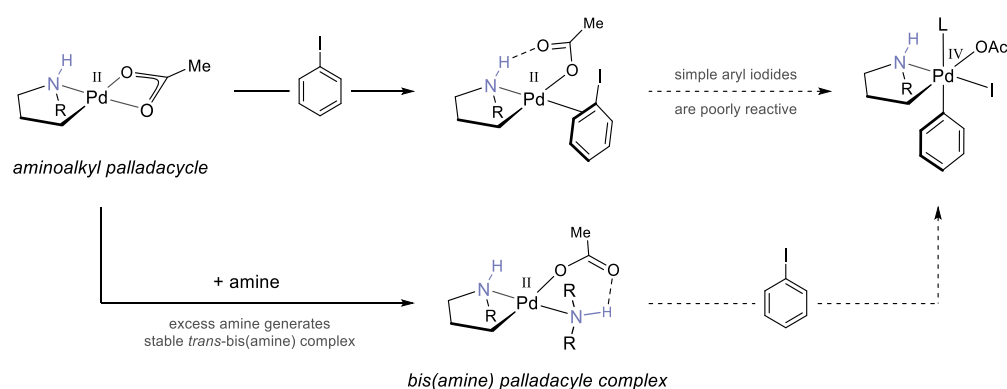


D. Oxidation by S_N2 attack



Scheme 70. Summary of Pd^{II}/Pd^{IV}-catalyzed methods for aliphatic amine-directed γ C(sp³)–H functionalization.

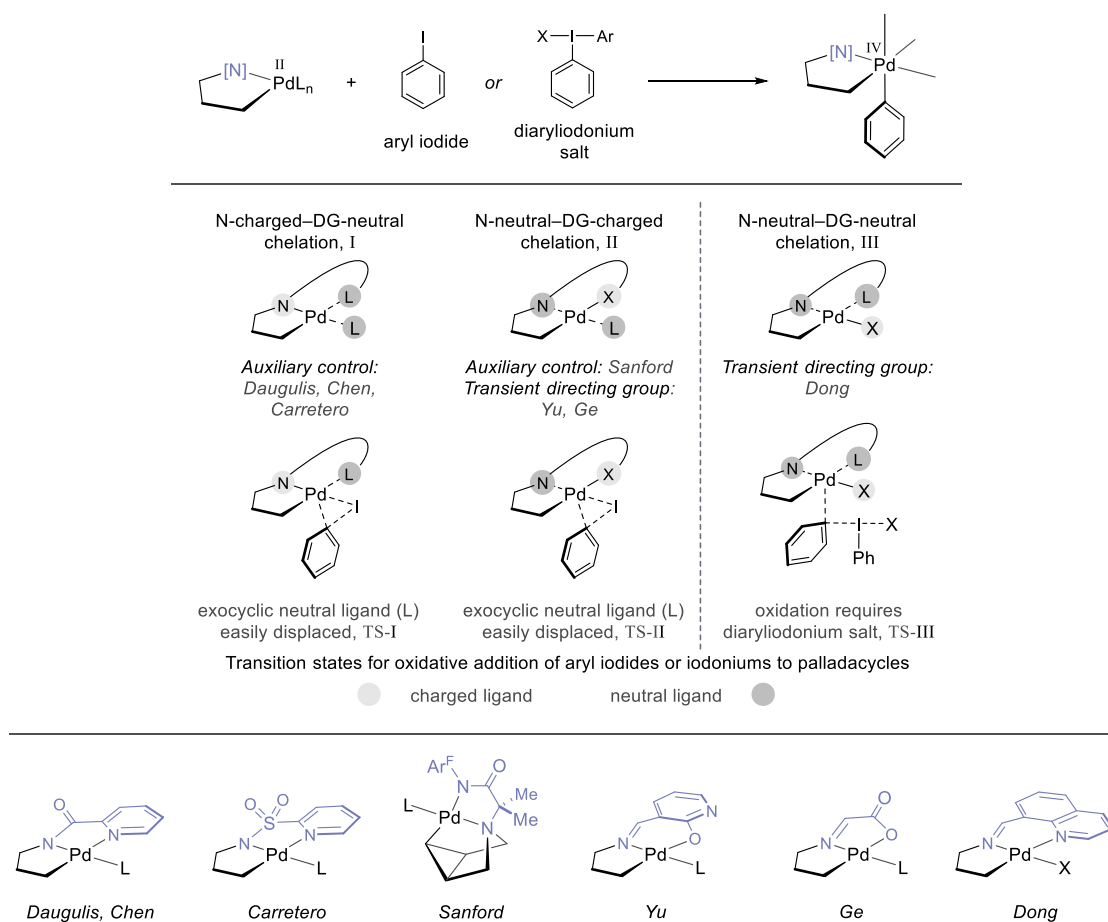
In the search for a general method for aminoalkyl palladacycle oxidation, we considered whether milder oxidants reacting via an oxidative addition mechanism at the metal centre could provide a more selective reactivity mode. Given that the amine nitrogen cannot mediate an oxidative addition mechanism, there should no longer be an incompatibility between the substrate and oxidant. To date, aryl iodides have been the most commonly used reagent in Pd-catalyzed C–H functionalization reactions and react via oxidative addition to the Pd^{II} metallacycle, resulting in an aryl Pd^{IV} intermediate that typically leads to arylation of the substrate via C–C bond reductive elimination.^{59,65} Despite their prevalence in the literature, aryl iodides have not yet been reported as coupling partners in a native amine-directed C–H functionalization process. While aryl iodides are indeed less reactive than their hypervalent iodine counterparts, a more fundamental reason for their lack of reactivity stems from the mechanistic requirements of the oxidative addition (Scheme 71). Importantly, oxidative insertion of the C–I bond is known to proceed via an intermediate wherein the aryl iodide is coordinated to the metal through the iodine atom or π -system of the aryl group.^{70,232,233} Therefore, unlike the outer-sphere S_N2 mechanism for hypervalent iodine reagents, aryl iodides require a vacant site of coordination in order to oxidize the Pd^{II} centre. Under catalytic conditions whereby the amine is in effective excess, coordination of the aryl iodide to the aminoalkyl palladacycle would be in competition with the binding of a second equivalent of amine substrate. However, crucially, amine coordination would form a coordinatively saturated and thermodynamically stable^{69,144} *trans*-bis(amine) palladacycle complex that would be unlikely to react with aryl iodides.



Scheme 71. Aryl iodides are mild oxidants but have not been reported to react with aminoalkyl palladacycles.

Cognizant of the necessary requirements for the oxidative addition of aryl iodides to palladacycle intermediates, we surveyed the literature of auxiliary-controlled C(sp³)–H

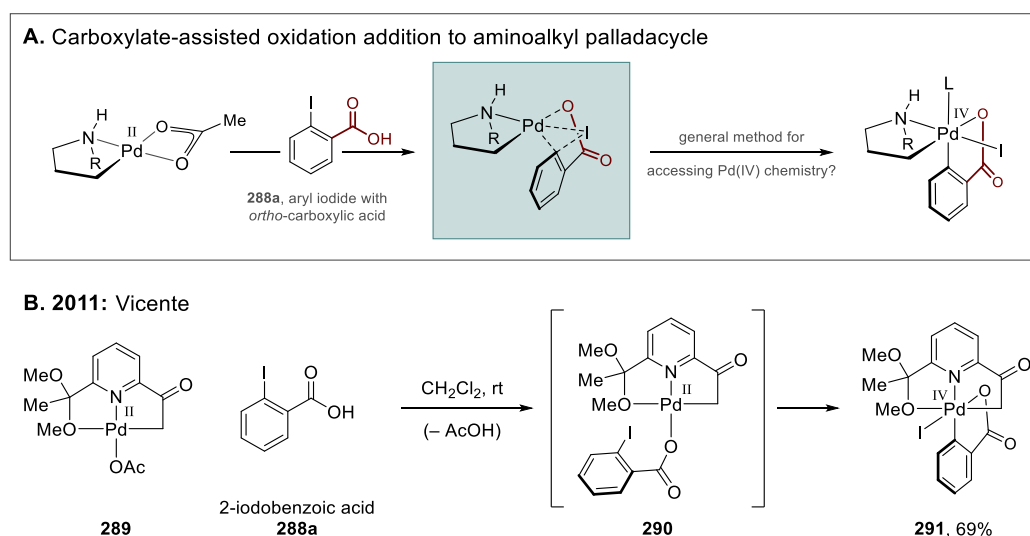
arylation reactions of amine derivatives and found that a clear trend emerged regarding the types of DG that were employed with aryl iodide reagents (Scheme 72). For example, aryl iodides were first reported with bidentate directing groups containing an anionic nitrogen group and neutral chelating group (denoted as Type I DG's), such as the picolinamide DG used by Daugulis⁴⁰ and Chen⁹⁶ or 2-pyridylsulfonamide DG of Carretero.¹⁰⁵ The palladacycles that result from these Type I DG's contain an exocyclic neutral ligand that may be displaced by the aryl iodide prior to oxidative addition (TS-I). Alternatively, bidentate DG's containing a neutral nitrogen group and charged chelating group (Type II) are also successfully employed with aryl iodides given that the exocyclic ligand is once again a neutral ligand that is able to be displaced (TS-II). Type II DG's were employed by Sanford¹²⁵ in the transannular C–H arylation of cyclic aliphatic amines and in the TDG strategies of Yu¹³⁹ and Ge.¹³⁸ Finally, a third type of bidentate DG containing a neutral nitrogen group as well as a neutral chelating ligand (Type III) was used in the TDG strategy of Dong.¹³⁶ In this distinct scenario, the palladacycle contains an exocyclic ligand that is anionic, and hence there is no ligand that can be displaced by the neutral aryl



Scheme 72. Comparison of Pd-catalyzed C(sp³)–H arylation reactions promoted by amine-derived DG's.

iodide reagent without forming a cationic complex. As a result, diaryliodonium salts were required to achieve the oxidative C–H arylation reaction (TS-III). Significantly, the bis(amine) palladacycle complex is analogous to the Type III DG scenario of Dong, given that the stable *trans* arrangement of amine ligands means that there is no labile neutral ligand that can be readily displaced by the aryl iodide.

Following work on the Pd-catalyzed γ C–H amination reaction, stoichiometric studies were conducted (*vide infra*) wherein it was serendipitously discovered that an aryl iodide containing an *ortho*-carboxylic acid group (2-iodobenzoic acid, **288a**) – the side product generated from the oxidation of the palladacycle by the cyclic iodine(III) tosylate oxidant **249** – could itself oxidize aminoalkyl palladacycles to form functionalized amine products (Scheme 73A). The oxidation was reasoned to proceed by the coordination of the *ortho*-carboxylate to the Pd^{II} metallacycle, allowing the C–I bond to more readily interact with the metal centre via an intramolecular oxidative addition mechanism. As a result, the carboxylate-assisted oxidative addition effectively surmounted the issues facing aryl iodides as oxidants for native amine-directed C–H functionalization, namely, their mild reactivity compared with more oxidizing hypervalent iodine reagents and the weak interaction of simple aryl iodides with the palladacycle. Notably, Vicente²³⁴ had previously demonstrated the ability of 2-iodobenzoic acid (**288a**) to oxidize an *ONC*-pincer Pd^{II} complex (**289**) to the corresponding Pd^{IV} complex (**291**) by coordination of the *ortho*-carboxylate group of the aryl iodide (**290**), providing observation of the oxidative addition to the metal centre (Scheme 73B). However, the facile oxidation mode had so far not been utilized within a Pd-catalyzed C–H functionalization reaction.



Scheme 73. (a) Carboxylate-assisted oxidation addition of 2-iodobenzoic acid to aminoalkyl palladacycles. (b) Vicente's synthesis of a stable Pd^{IV} *ONC*-pincer complex by employing 2-iodobenzoic acid.

A series of project aims were set out to explore the oxidative addition chemistry of aminoalkyl palladacycles. Firstly, stoichiometric studies were conducted to analyse the efficiency of the palladacycle functionalization using 2-iodobenzoic acid and to explore the selectivity of bond-forming reductive elimination under various conditions (Figure 6A). Secondly, we aimed to exploit the mild nature of the aryl iodide oxidant to develop a catalytic process for the C–H functionalization of less hindered aliphatic amines than those previously employed in native amine-directed functionalization (Figure 6B). Thirdly, we investigated the effect of replacing the *ortho*-carboxylic acid group with different coordinating DG's in order to explore the generality and versatility of the *ortho*-directed oxidative addition reactivity mode (Figure 6C).

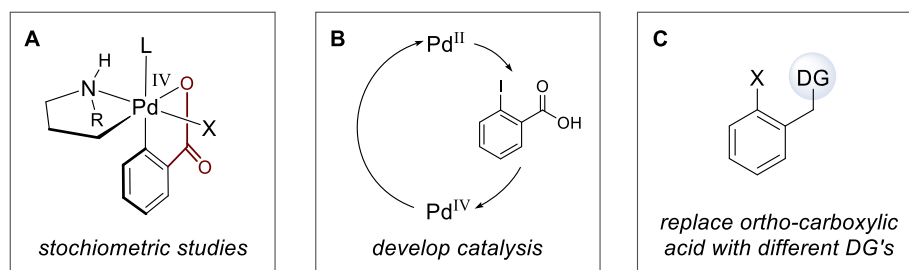


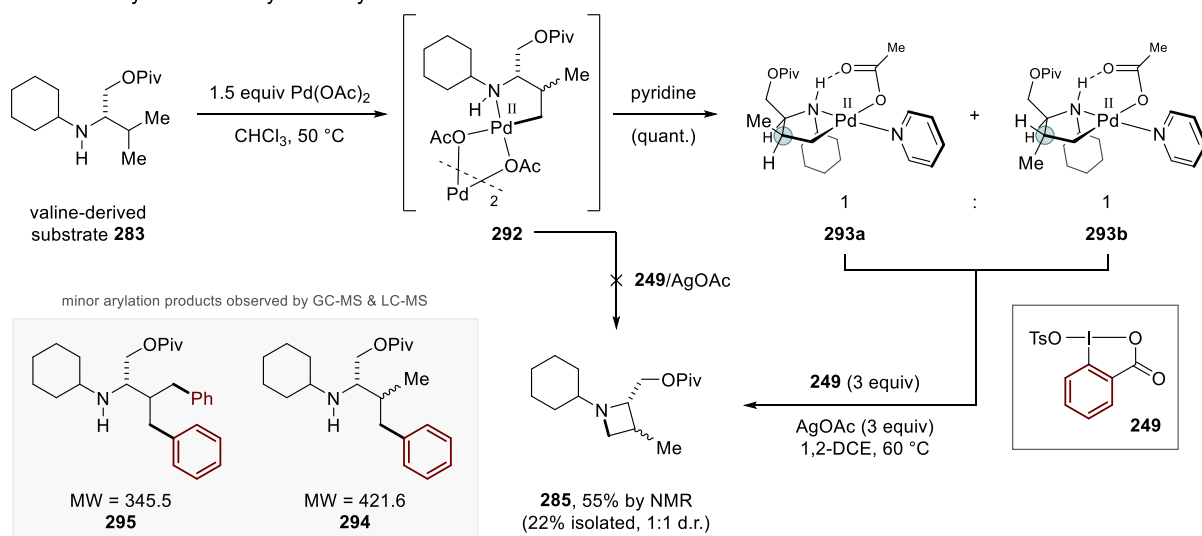
Figure 6. Project aims for the carboxylate-assisted oxidative addition to aminoalkyl palladacycles.

3.2. Results & Discussion

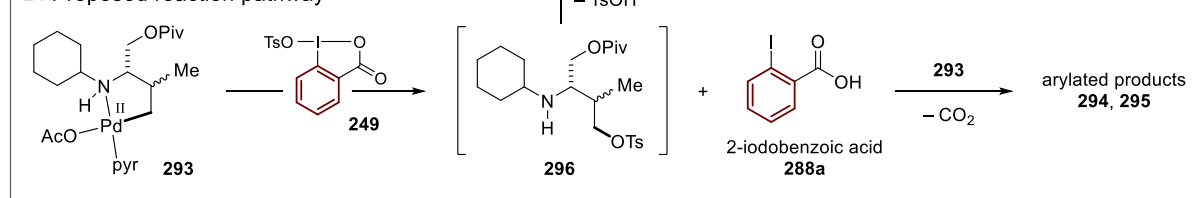
3.2.1. Stoichiometric Palladacycle Studies

As disclosed previously in Section 2.3.2., the acyclic valine-derived amine substrate **283** provided a low but notable 12% yield of the azetidine product in the Pd-catalyzed γ C–H amination reaction. As a result, we were curious whether the low efficiency of the reaction was related to the C–H activation step or palladacycle functionalization step. An experiment with stoichiometric palladium was conducted to study each of these mechanistic steps. The acetate-bridged trinuclear palladacycle (**292**) was synthesized by subjecting amine **283** to 1.5 equivalents of Pd(OAc)₂ in chloroform at 50 °C (Scheme 74A). Although the ¹H NMR spectrum of **292** was complicated as a result of interconversion between species of different nuclearity in solution, the spectrum could be resolved by the addition of pyridine as a coordinating ligand. The resolved ¹H NMR spectrum showed that a diastereomeric mixture of monomeric palladacycles had formed in quantitative yield in a 1:1 ratio (**293a**:**293b**). Next, the mixture of

A. Discovery of decarboxylative arylation reaction



B. Proposed reaction pathway



Scheme 74. Cyclopalladation of amine **283** and reaction with oxidant **249**: (a) discovery of minor arylated by-products and (b) proposed reaction pathway involving 2-iodobenzoic acid as arylating agent.

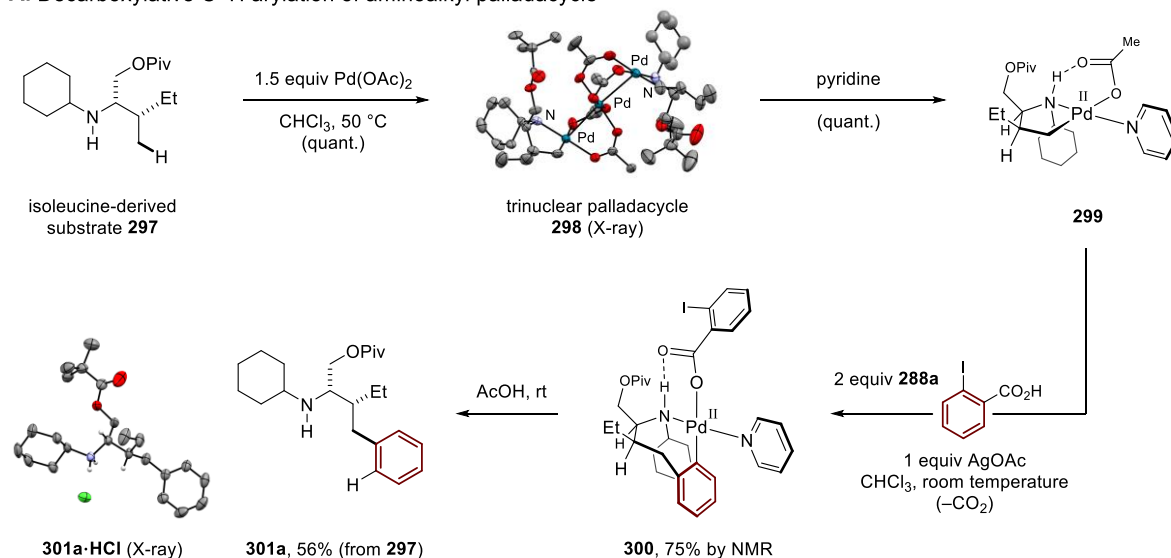
palladacycles (**293**) was reacted with the cyclic iodine(III) tosylate oxidant (**249**) in the presence of AgOAc at 60 °C and was found to give the corresponding azetidine product in 55% yield by NMR (**285**, 22% isolated, 1:1 d.r.). While the stoichiometric experiment had seemingly demonstrated that both the activation and functionalization steps of the mechanism were proceeding with good efficiency, it was subsequently found that subjecting the trinuclear palladacycle directly to oxidant **249** in the absence of pyridine gave no yield of azetidine **285**, indicating that the pyridine ligand could be involved in lowering the barrier to palladacycle oxidation by the stabilization of the resulting Pd^{IV} intermediate.¹⁸⁴ Consequently, it was concluded that oxidant **249** was not sufficiently reactive to efficiently oxidize the palladacycle derived from amine **283** under catalytic conditions, in which pyridine would not be present. Nonetheless, a more significant observation from this study was that minor arylation by-products (mono- and di-arylation, **294** and **295**) were also formed in the reaction between the pyridine-ligated palladacycles (**293**) and **249**, being observed by GC-MS and LC-MS analysis (Scheme 74A). Moreover, chromatographic separation and analysis by NMR of these arylation

products indicated that the phenyl groups were being incorporated at remote γ -positions rather than, for example, at nitrogen. Notably, the only potential source of an aromatic group was from the iodine(III) oxidant **249**. As a result, a reaction pathway was proposed wherein the pyridine-ligated palladacycles (**293**) were first oxidized by oxidant **249**, generating the γ -tosyloxylation product (**296**) that would spontaneously cyclize to the azetidine (**285**) as well as an equivalent of 2-iodobenzoic acid (**288a**) as a by-product of the oxidant (Scheme 74B). It was thought that aryl iodide **288a** could react with a palladacycle (**293**) to generate the mono-arylation product (**294**) which could then activate and functionalize once more to generate the di-arylation product (**295**). Interestingly, if this hypothesis was correct, the palladacycle functionalization step would involve in situ decarboxylation of the aryl iodide reagent, meaning that the *ortho*-carboxylic acid group was acting as a type of traceless DG.

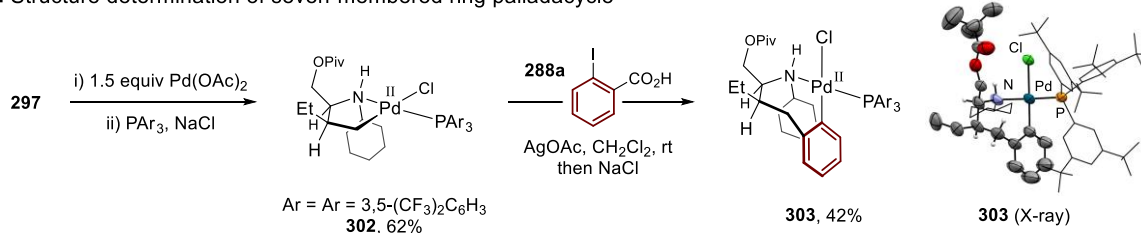
In order to confirm the proposed reaction pathway, another stoichiometric experiment was carried out but, this time, employing an isoleucine-derived substrate (**297**) that only has one γ -methyl group, so as to remove the possibility of diastereomeric mixtures and multiply functionalized products. Subjecting amine **297** to 1.5 equivalents of $\text{Pd}(\text{OAc})_2$ led to quantitative γ C–H activation to give the trinuclear palladacycle (**298**) as a green crystalline solid (Scheme 75A). The solid-state structure of **298** was elucidated by X-ray diffraction of a single crystal. Adding pyridine to **298** provided the monomeric pyridine-ligated palladacycle (**299**), which was reacted with 2 equivalents of 2-iodobenzoic acid (**288a**) in the presence of 1 equivalent of AgOAc in chloroform. Remarkably, at room temperature, full conversion of complex **299** was observed after one hour, generating a new Pd complex that contained a 1,2-disubstituted aromatic group incorporated into the amine and with a second equivalent of 2-iodobenzoic acid ligated to the Pd centre that was engaged in hydrogen bonding to the N–H bond of the bound secondary amine (**300**, 75% by NMR). Changing the solvent from chloroform to acetic acid and stirring at room temperature released the γ -arylated amine product (**301a**, 56% from **297**), which was confirmed by single crystal X-ray crystallographic analysis of the HCl salt. While the intermediate Pd complex was initially thought to be an alkyl Pd^{IV} complex that is stable at room temperature, it was later discovered that the complex was in fact an unusual seven-membered ring Pd^{II} metallacycle (**300**). The identity of **300** was revealed by repeating the stoichiometric reaction with a triarylphosphine-ligated palladacycle (**302**), leading to the formation of a chromatographically stable, but more importantly crystalline, complex that could be characterised by X-ray diffraction of a single crystal (**303**, Scheme 75B; phosphine-ligated complexes were synthesized by J. H. Blackwell). Significantly, the stoichiometric experiment demonstrated that a facile carboxylate-assisted oxidative addition

occurs between aminoalkyl palladacycles and 2-iodobenzoic acid. Furthermore, the formation of the seven-membered ring palladacycle intermediate, resulting from $C(sp^3)-C(sp^2)$ bond formation and extrusion of a molecule of CO_2 , provided direct observation of a novel mode of reactivity involving the decarboxylative arylation of γ -cyclopalladated amines.

A. Decarboxylative C–H arylation of aminoalkyl palladacycle

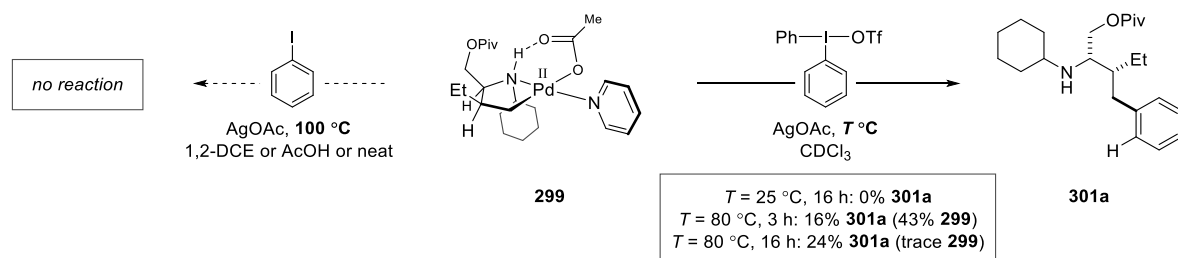


B. Structure determination of seven-membered ring palladacycle



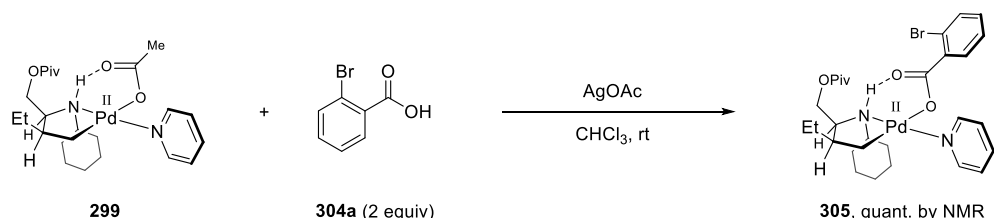
Scheme 75. (a) Carboxylate-assisted oxidative addition resulted in 7-membered ring palladacycle. (b) Structure determination of PAR_3 -ligated 7-membered ring palladacycle. Reactions in (b) conducted by J. H. Blackwell.

For comparison, palladacycle **299** was subjected to iodobenzene in the presence of $AgOAc$. However, stirring the reaction at 100 °C in 1,2-DCE or AcOH, or conducting the reaction in iodobenzene as solvent, gave no conversion to the arylated product **301a** (Scheme 76). Additionally, palladacycle **299** was reacted with diphenyliodonium triflate. While no reaction occurred at room temperature, heating to 80 °C resulted in slow conversion to **301a** (16% after 3 h, 24% after 16 h by NMR). Notably, the mass balance of the reaction was poor, with only traces of the starting palladacycle **299** remaining after 16 h at 80 °C. Overall, the use of 2-iodobenzoic acid with $AgOAc$ was found to be uniquely effective at oxidizing the palladacycle under mild conditions, leading to decarboxylative arylation in good efficiency.



Scheme 76. Subjecting palladacycle **299** to iodobenzene and diphenyliodonium triflate.

Given that the decarboxylative arylation was an unexpected and unprecedented transformation, we were interested to explore the mechanism of the reaction. Firstly, support for the formation of a putative high valent Pd^{IV} intermediate was obtained by subjecting palladacycle **299** to 2-bromobenzoic acid (**304a**, Scheme 77). In the presence of AgOAc in chloroform at room temperature, the reaction did not lead to the formation of arylation product **301a**, but rather the formation of the Pd^{II} benzoate complex (**305**) wherein the acetate ligand had been displaced by 2-bromobenzoate. Given the higher propensity of aryl iodides to undergo oxidative addition compared to aryl bromides,²³³ the fact that the functionalization was not observed strongly supports oxidative addition as a mechanistic step. Moreover, the observed coordination of the benzoic acid to the Pd^{II} centre provides evidence for the coordination of the *ortho*-carboxylic acid group prior to oxidative addition.

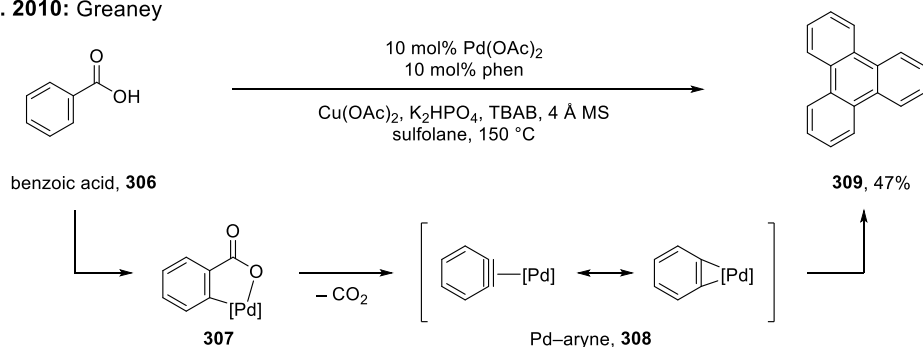


Scheme 77. Support for a putative Pd^{IV} intermediate: subjecting palladacycle **299** to 2-bromobenzoic acid.

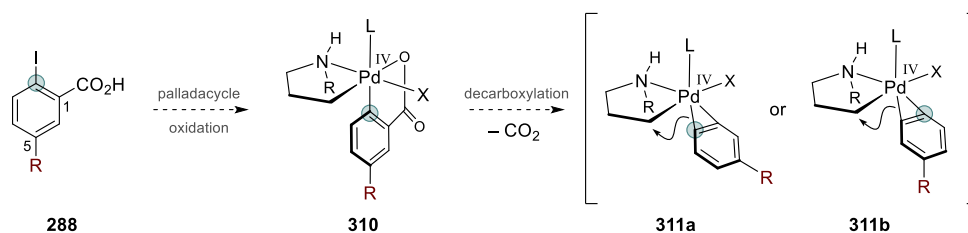
Next, we considered the possibility of aryne formation resulting from the metal-mediated elimination of CO₂ and iodide from 2-iodobenzoic acid. In 2010, Greaney²³⁵ reported a Pd-catalyzed trimerization reaction of benzoic acid (**306**) to triphenylene (**309**) under forcing high temperature conditions (150 °C, sulfolane; Scheme 78A). The reaction was proposed to proceed via carboxylate-directed cyclometalation (**307**) followed by decarboxylation to form a reactive Pd^{II}-aryne intermediate (**308**) that would undergo trimerization. While the mechanistic proposal was not supported by experiment, the work highlighted the possibility of generating

aryne or aryne-like intermediates from a cyclopalladated benzoic acid. By analogy, it was hypothesized that the Pd^{IV} intermediate (**310**) formed from the oxidation of the aminoalkyl palladacycle by a *substituted* aryl iodide (**288**) could potentially undergo decarboxylation at the high valent metal centre to generate a pair of regioisomeric Pd^{IV} -aryne complexes (**311a** and **311b**, Scheme 78B). Importantly, C–C bond reductive elimination could occur from either the position of the iodide (**311a**) or the carboxylate (**311b**) leading to a mixture of regioisomeric products forming. To determine the regioselectivity, 2-iodo-5-methylbenzoic acid (**288b**) was reacted with palladacycle **299** with AgOAc in chloroform at room temperature (Scheme 78C).

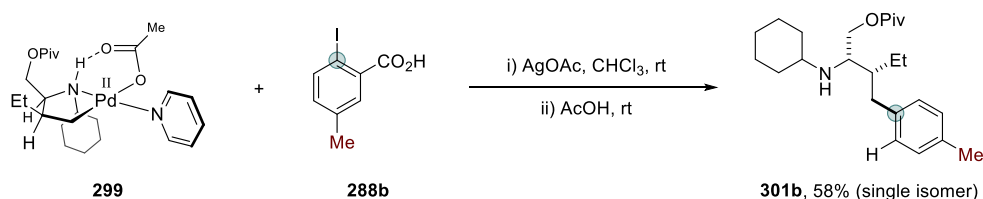
A. 2010: Greaney



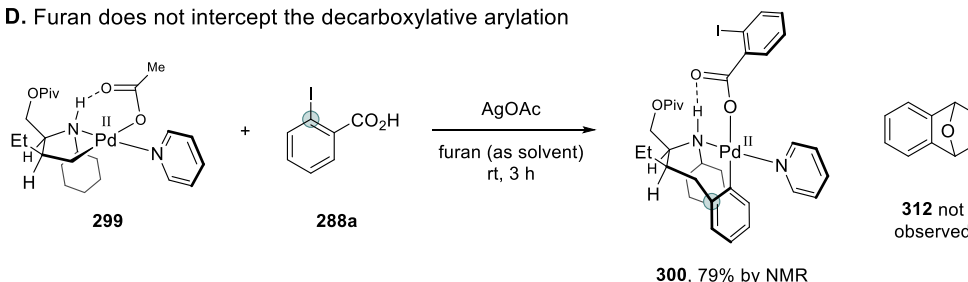
B. Hypothesis: aryne formation would result in a mixture of regioisomers



C. Decarboxylative arylation produces a single isomer



D. Furan does not intercept the decarboxylative arylation



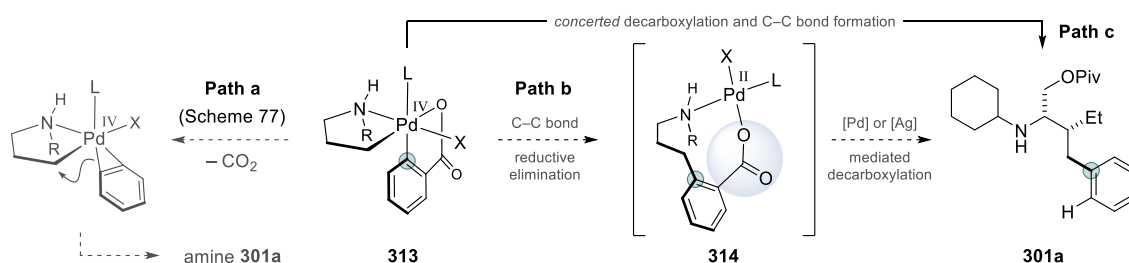
Scheme 78. (a) Literature precedent for Pd-aryne formation from the decarboxylation of cyclopalladated benzoic acid. (b)–(d) Investigating the possibility of aryne formation in the decarboxylative arylation of complex **299**.

After protodemetalation by AcOH, the arylated product containing a *para*-methyl substituent was isolated (**301b**, 58%), with no other arylated amine products being detected. Hence, the reaction was completely regioselective, with the C–C bond being formed at the position of the C–I bond in the aryl iodide reagent. Additionally, to check for transient aryne intermediates, furan – a well-known aryne trapping reagent or “aryophile”^{236,237} – was used as the solvent for the decarboxylative arylation reaction between **299** and **288a** (Scheme 78D). However, the seven-membered ring Pd^{II} complex formed in similar yield in furan as in chloroform (**300**, 79% by NMR in furan; c.f. 75% in chloroform), with the cycloaddition product of benzyne and furan (**312**) not being observed. Taken together, these mechanistic control experiments suggested that aryne intermediates were not being formed in the reaction.

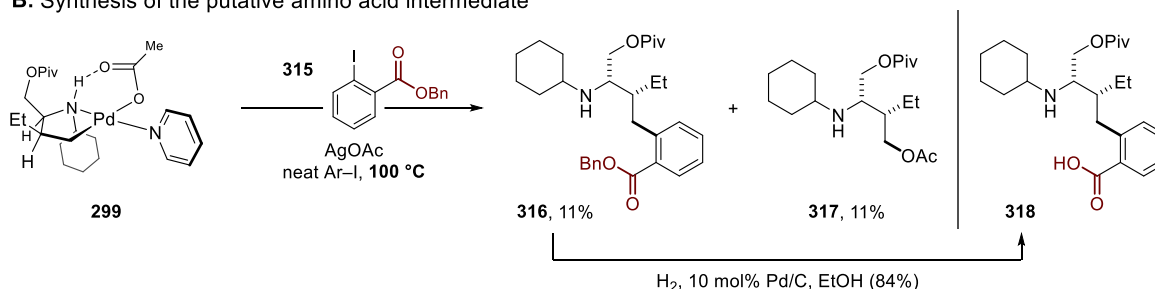
Next, we planned to investigate the mechanism of CO₂ extrusion in the decarboxylative arylation. There are two possible points in the reaction pathway at which decarboxylation could occur. Firstly, decarboxylation from the Pd^{IV} intermediate formed upon carboxylate-assisted oxidative addition could occur to generate a Pd-aryne complex, but given that the formation of aryne species was not supported experimentally, this pathway was ruled out (Scheme 79A, Path a). Secondly, C–C bond reductive elimination could occur from the initially formed Pd^{IV} intermediate to give a Pd^{II}-bound amino acid (**314**), which could then undergo decarboxylation mediated by a Pd^{II} or Ag^I metal centre, or by a combination of the two (Path b). Significantly, while Pd^{II} and Ag^I-catalyzed decarboxylation reactions were extensively reported in the literature,^{238–240} the reactions required elevated temperatures in all cases (>100 °C). The high reaction temperatures signified a divergence from the current work, in which decarboxylation occurred at room temperature. Consequently, a third mechanistic possibility was proposed, wherein decarboxylation and C–C bond reductive elimination occur in concert from the Pd^{IV} intermediate (Path c). In order to distinguish between the stepwise and concerted reaction pathways (Paths b and c), the putative amino acid intermediate of the stepwise mechanism was synthesized by reacting palladacycle **299** with benzyl 2-iodobenzoate (**315**) – an ester-protected variant of the *ortho*-carboxylate oxidant that was employed in order to prevent in situ decarboxylation (Scheme 79B). While the *ortho*-ester functional group was far less effective than the *ortho*-carboxylate at promoting the functionalization, the desired arylated product (**316**) could be obtained in 11% yield when using the aryl iodide as solvent in the presence of AgOAc at 100 °C. The acetoxylated product (**317**) was also obtained in 11% yield as a by-product of the reaction. Hydrogenation of the benzyl-protected intermediate gave the free amino acid (**318**). Subjecting **318** to 1 equivalent of Pd(OAc)₂ with AgOAc (0–1 equivalent) gave no reaction at room temperature, but stirring the reactions at 80 °C led to quantitative conversion

to a dimeric palladacycle in which γ -methylene C–H activation had occurred (**319**, Scheme 79C). The structure of the dimeric complex was confirmed by X-ray crystallography. Furthermore, subjecting **318** to the complete reaction conditions used previously, including 2-iodobenzoic acid **288a** (1.5 equiv $\text{Pd}(\text{OAc})_2$, 1 equiv AgOAc , 2 equiv **288a**, 2 equiv pyridine in CDCl_3 at room temperature), gave no reaction. Given that the *ortho*-carboxylate remained intact, it was concluded that amino acid **318** was not an intermediate in the decarboxylative arylation, and that decarboxylation must occur prior to C–C bond reductive elimination. Therefore, it was proposed that the most likely mechanism involved *concerted* decarboxylation and C–C bond reductive elimination from a high valent Pd^{IV} centre (Path c).

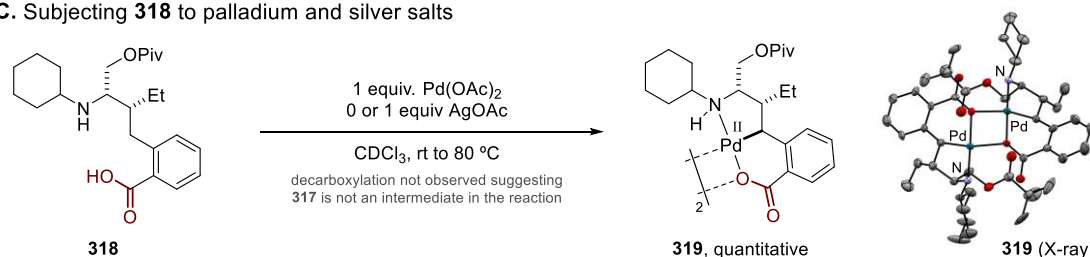
A. Hypothesis: stepwise reductive elimination followed by decarboxylation (or concerted decarboxylative arylation)



B. Synthesis of the putative amino acid intermediate



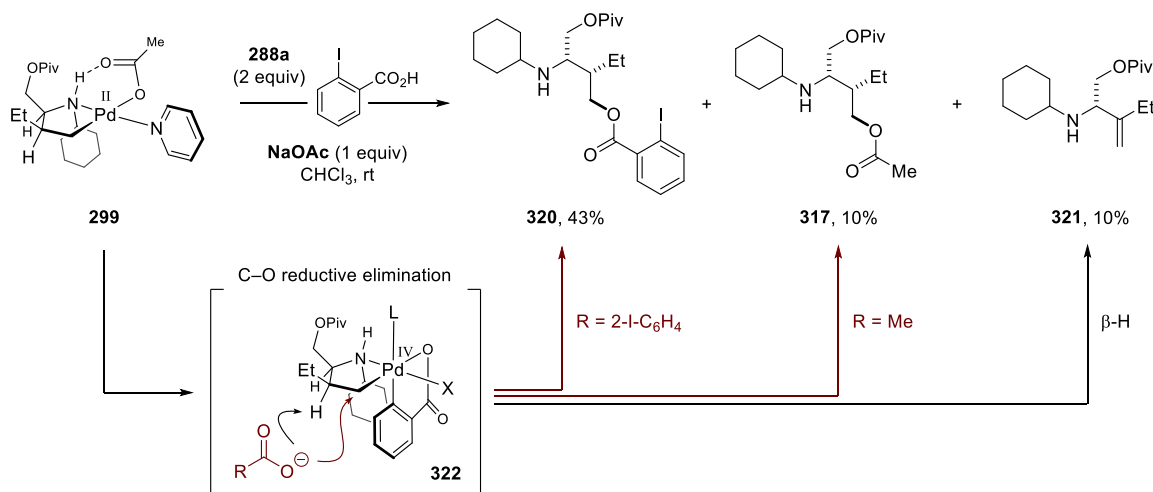
C. Subjecting **318 to palladium and silver salts**



Scheme 79. (a) Mechanism involving stepwise C–C bond reductive elimination to an amino acid followed by Pd^{II} - or Ag^{I} -mediated decarboxylation. (b) Synthesis of amino acid **318** and (c) reaction with Pd^{II} and Ag^{I} salts.

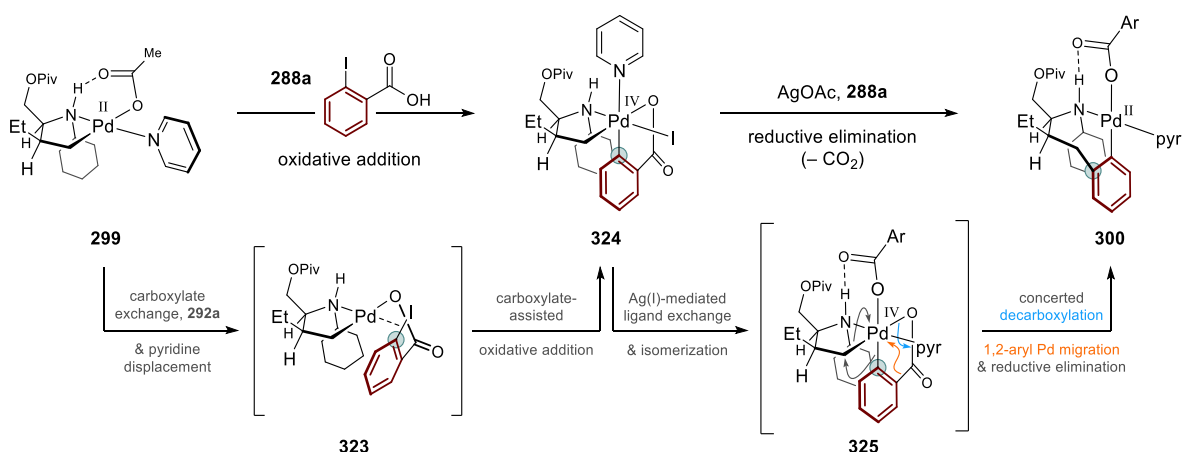
The final mechanistic control experiment concerned the role of the silver salt additive. Exchanging AgOAc for NaOAc , we were surprised to observe a complete switch in the selectivity of reductive elimination, with a mixture of C–O coupled products being formed that

incorporated either 2-iodobenzoate (**320**, 43%) or acetate (**317**, 10%) at the γ -position of the amine (Scheme 80). A terminal alkene product was also formed in the reaction (**321**, 10%). Crucially, given that the C–I bond was present in **320** and that mixture of C–O coupled products were formed, C–O bond reductive elimination was proposed to occur via external nucleophilic attack of the putative Pd^{IV} intermediate (**322**).²⁰⁵ Alternatively, carboxylate-mediated deprotonation of the β -C–H bond could explain the formation of the alkene by-product.



Scheme 80. Exchange of AgOAc for NaOAc led to C–O bond reductive elimination.

Overall, taking into account all the experimental observations, a working hypothesis of the mechanism for the Pd-/Ag-mediated decarboxylative arylation is shown in Scheme 81. The aminoalkyl palladacycle (**299**) first undergoes ligand exchange with 2-iodobenzoic acid (**288a**), forming an intermediate from which carboxylate-assisted oxidative addition can take place following the dissociation of pyridine (**323**). The resulting Pd^{IV} intermediate (**324**) contains a Pd–I bond which is proposed to undergo Ag^{I} -mediated iodide abstraction to install a carboxylate ligand on the Pd^{IV} centre (**325**), triggering a reductive elimination sequence involving concerted decarboxylation and C–C bond formation. During the reductive elimination, the Pd centre undergoes a 1,2-aryl migration²⁴¹ to produce the observed seven-membered ring palladacycle complex (**300**). A recent computational study by Wang and Dang⁹⁵ found evidence for a Ag^{I} salt in facilitating C–C bond reductive elimination from a metalacyclic Pd^{IV} intermediate, highlighting an additional role of Ag^{I} in Pd-catalyzed C–H functionalization reactions. The current work additionally represents an example wherein the presence of a silver salt causes a complete switch in the selectivity of bond-forming reductive elimination.



Scheme 81. Working mechanistic hypothesis for the carboxylate-assisted decarboxylative arylation reaction.

3.2.2. Development of Catalysis & Reaction Scope

We investigated the possibility of developing a catalytic process for the decarboxylative arylation reaction. Gratifyingly, employing amine **297** with 1.5 equivalents of 2-iodobenzoic acid, 10 mol% $\text{Pd}(\text{OAc})_2$, 2 equivalents of AgOAc in chloroform at 80 °C for 16 hours gave 51% yield of the γ -arylated product (**301a**) with 8% yield of the C–O coupled by-product (**328–I**; Table 2, entry 1). The amine starting material was also recovered in 35% yield, indicating almost complete mass balance ($>90\%$) and thus minimal substrate decomposition under the catalytic conditions. Interestingly, using 2-bromobenzoic acid (**304a**) improved the yield of **301a** to 63%, again with C–O coupling as a minor by-product (7% **328–Br**, entry 2). Conversely, employing 2-chlorobenzoic acid (**326**) or 2-(OTf)-benzoic acid (**327**) gave no conversion to functionalized products (entries 3–4). Use of Pd catalysts with bulkier carboxylate ligands such as $\text{Pd}(\text{O}_2\text{CMes})_2$ or $\text{Pd}(\text{OPiv})_2$ gave slight increases in yield of **301a** (67% and 69%, respectively; entries 5–6), with commercial $\text{Pd}(\text{OPiv})_2$ being selected for the remaining optimization reactions. On the other hand, use of AgOPiv resulted in diminished yield relative to AgOAc (entries 7–8). Additionally, pre-forming the silver salt of 2-bromobenzoic acid was not beneficial, giving 50% yield of **301a** when used with $\text{Pd}(\text{OPiv})_2$ (entry 9). Finally, increasing the equivalency of 2-bromobenzoic acid to 2 equivalents and extending the reaction time to 20 hours gave a final optimized yield of **301a** of 74% (70% isolated yield). Removing the Pd catalyst resulted in no conversion (entry 11), whereas removing the AgOAc additive gave 6% of the C–O coupled product (**328–Br**, entry 12) but none of the arylated product (**301a**), as would be expected from the results of the stoichiometric studies. Looking to develop a silver-free γ C–H acyloxylation reaction, we tested different

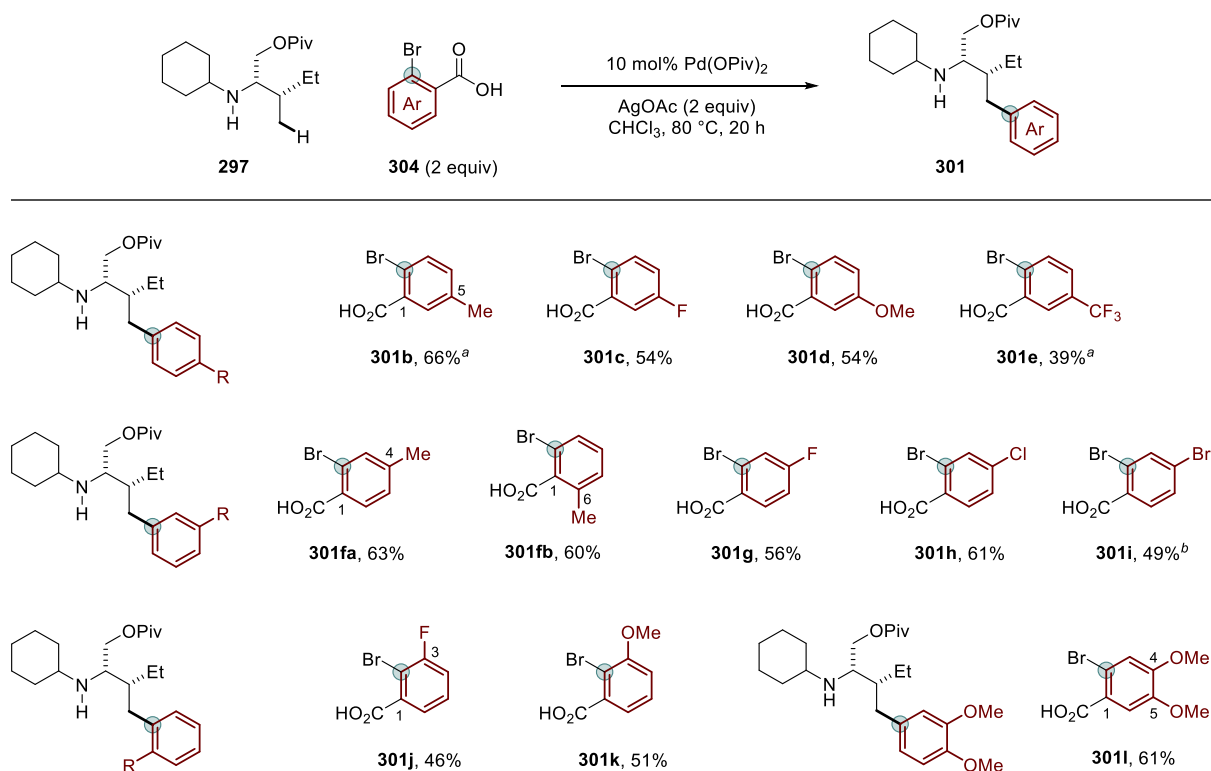
inorganic base additives. Adding 2 equivalents of NaOAc improved the yield of **328-Br** to 10%, while using CsOPiv provided a further increase to 20% (13% isolated yield of **328-Br**, entry 14). Nonetheless, despite further screening of reaction conditions, we were unable to increase the yield to a satisfactory level. Presumably, the absence of the silver salt meant that the halogen abstraction from the Pd catalyst as required for catalytic turnover was either not occurring (as in the case of NaOAc, TON = 1) or not occurring efficiently (as in the case of CsOPiv, TON = 2). As discussed previously, the silver salt may also play a role in facilitating the C–H activation step through bimetallic interactions with the Pd catalyst.⁹⁵ Ultimately, the likely multi-faceted role of the silver salt could explain the diminished catalytic efficiency of the C–O bond-forming reaction relative to the decarboxylative arylation process.

Table 2. Optimization of catalytic reactions for C–C and C–O bond formation.

Entry	Ar–X	Pd(O ₂ CR) ₂	Additive	297 (%)	301a (%)	328–X (%)
1	I	Pd(OAc) ₂	AgOAc	35	51	8
2	Br	Pd(OAc) ₂	AgOAc	17	63	7
3	Cl	Pd(OAc) ₂	AgOAc	96	0	0
4	OTf	Pd(OAc) ₂	AgOAc	100	0	0
5	Br	Pd(O₂CMes)₂	AgOAc	27	67	5
6	Br	Pd(OPiv)₂	AgOAc	24	69	4
7	Br	Pd(OPiv) ₂	AgOPiv	25	57	7
8	Br	Pd(OAc) ₂	AgOPiv	19	48	5
9	–	Pd(OPiv) ₂	Ag(O₂C-2-Br-C₆H₄)^a	37	50	7
10 ^b	Br	Pd(OPiv) ₂	AgOAc	18	74 (70) ^c	6
11	Br	–	AgOAc	100	0	0
12	Br	Pd(OPiv) ₂	–	81	0	6
13 ^b	Br	Pd(OPiv) ₂	NaOAc	85	0	10
14 ^b	Br	Pd(OPiv) ₂	CsOPiv	78	0	20 (13) ^c

Percentage yields obtained from ¹H NMR analysis of the crude reaction mixtures against an internal standard (1,1,2,2-tetrachloroethane). ^aSynthesized by Dr. G. N. Hermann. ^b2 equiv Ar–Br, 20 h reaction time. ^cIsolated yield after chromatography.

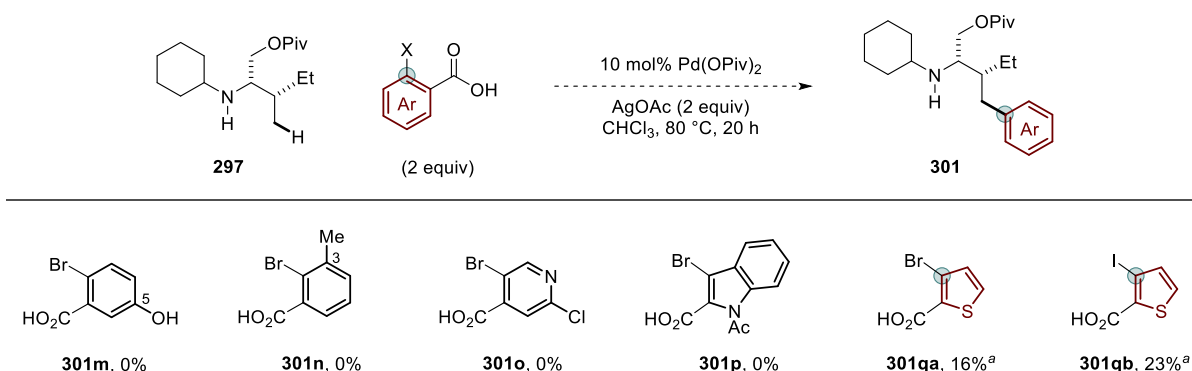
Having optimized catalytic conditions for the C–C bond-forming decarboxylative arylation, we next explored the scope of the reaction. The scope with respect to substituted 2-bromobenzoic acid reagents (**304**) was found to be relatively broad for the γ -arylation of amine **297** (Scheme 82). In all cases, minor side-products arising from C–O coupling were formed in <10% yield but no general trend related to electronic properties was identified. 5-Substituted aryl bromide reagents giving rise to *para*-substituted arylated amines were well tolerated (**301b–e**, 39–66%). Notably, the electron-withdrawing CF₃ substituent gave a diminished yield (39%), potentially indicating that the bromobenzoic acid (used in stoichiometric quantities) could be acting as the internal base in the CMD mechanism of C–H activation as more acidic reagents would be predicted to be less effective in this role. The synthesis of *meta*-substituted arylation products was also demonstrated, with 4-methyl-2-bromobenzoic acid and 6-methyl-bromobenzoic acid both resulting in the same *meta*-methyl product after decarboxylation with similar efficiency (**301fa**, 63%; **301fb**, 60%). 4-Substituted aryl bromides bearing different halide substituents (F, Cl, Br) were also well tolerated (**301g–i**, 49–61%). 3-Substituted aryl bromides, wherein the 3-substituent is positioned *ortho* to the C–Br bond, could be tolerated for spatially small groups such as fluoride or methoxy (**301j–k**, 46–51%) that would not



Scheme 82. Scope of substituted 2-bromobenzoic acid reagents in the γ -arylation of **297**. Yields are of isolated products. ^aReaction conducted by J. H. Blackwell. ^b2.5 equiv aryl bromide and 2.5 equiv AgOAc were used.

significantly affect the interaction with the Pd centre as required for oxidative addition. Finally, a more highly substituted 4,5-dimethoxy arylation product was obtained in good yield (**301l**, 61%).

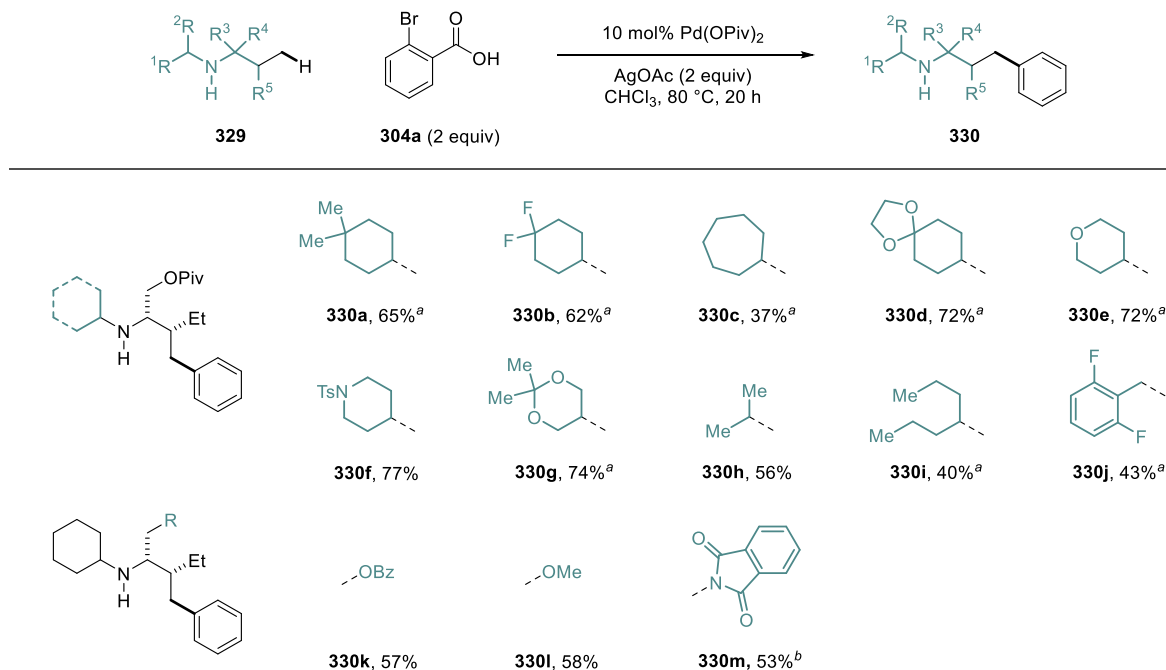
Several substituted aryl bromide reagents were also found to be ineffective in the decarboxylative arylation (Scheme 83). For example, a coordinating free-hydroxyl functional group (**301m**, 0%) and sterically encumbered 3-methyl substituted reagent were found to shut down the reaction (**301n**, 0%). Moreover, heteroaryl bromide reagents derived from 2-chloropyridine or *N*-acetyl-protected indole gave no yield of the arylated products (**301o–p**, 0%). Conversely, 3-bromothiophene-2-carboxylic acid produced a low but promising yield of the heteroarylated product (**301qa**, 16% by NMR), which could be slightly increased when using the analogous aryl iodide reagent (**301qb**, 23% by NMR). Although the low efficiency of heteroaryl halide reagents represented a drawback of the reaction, the fact that 5-membered ring thiophenyl halides were observed to undergo the decarboxylative arylation process highlighted a potential starting point for future work into expanding the scope of coupling partners.



Scheme 83. Unreactive or poorly reactive (hetero)aryl halides. ^aYield determined by ¹H NMR against standard.

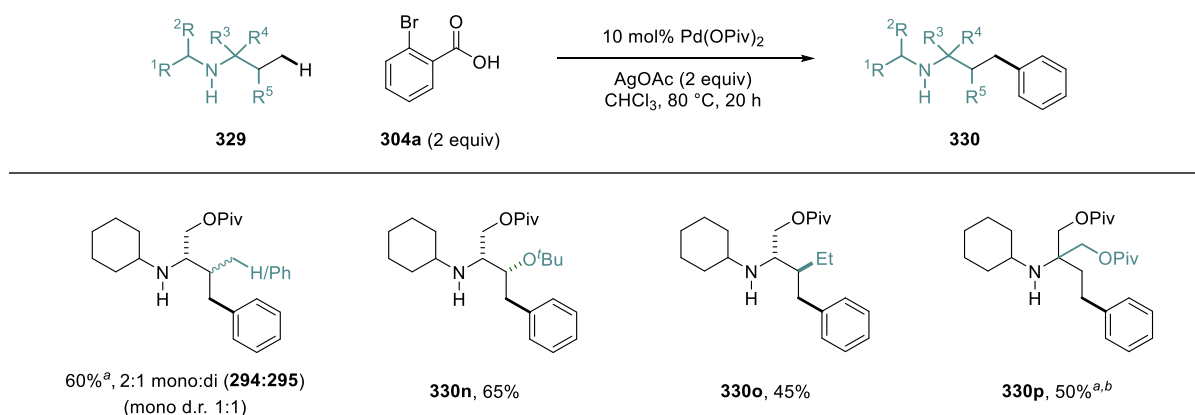
The scope of aliphatic amines was explored, starting with substrates derived from the isoleucine scaffold (Scheme 84). Varying the “spectator” substituent of the secondary amine that was not undergoing C–H activation, it was found that a range of cyclic alkyl groups could be tolerated, including those bearing fluoride, protected ketone, ether, sulfonamide and protected-diol functional groups (**330a–g**, 37–77%). Acyclic, branched alkyl groups also provided arylated products in moderate to good yield (**330h–i**, 40–56%). Generally, branching at both the α and α' positions of the aliphatic amine was required for catalytic reactivity, though a 2,6-difluorobenzyl alkyl group was found to provide a moderate yield of arylated product (**330j**, 43%). Varying the α -substituent of the alkyl chain undergoing C–H activation, it was

found that changing the Piv protecting group for benzoyl or methyl was well tolerated (**330k–l**, 57–58%). In addition, a substrate containing a phthalimide functional group provided the corresponding arylation product in good yield (**330m**, 53%).



Scheme 84. Scope of aliphatic amines (isoleucine derivatives) with 2-bromobenzoic acid. Yields are of isolated products. ^aReaction conducted by J. H. Blackwell. ^bReaction temperature was 70 °C.

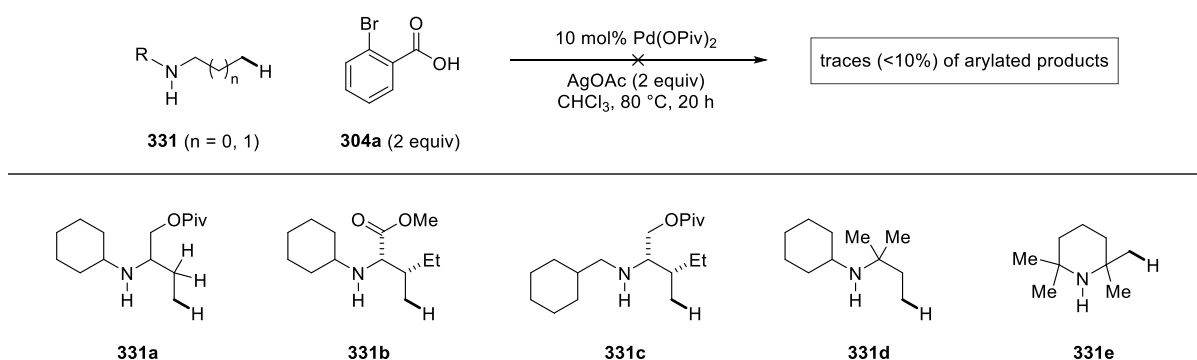
The scope of other amino acid-derived secondary amines was also investigated (Scheme 85). For example, a valine-derived substrate gave the arylated product in good yield, though was formed as a mixture of mono- and di-arylated products as was observed in the preliminary



Scheme 85. Scope of aliphatic amines (other amino amino-acid derivatives). Yields are of isolated products. ^aYield determined by ¹H NMR against internal standard. ^bReaction conducted by J. H. Blackwell.

stoichiometric studies (60% by NMR, 2:1 mono:di, **294:295**; mono d.r. 1:1). A *tert*-butyl-protected threonine-derived substrate provided the arylated product in good yield (**330n**, 65%), while the unnatural diastereomer of the isoleucine scaffold gave a moderate yield (45%, **330o**). Finally, an α -tertiary amine substrate was also found to be a suitable substrate for the reaction (**330p**, 50% by NMR; reaction conducted by J. H. Blackwell).

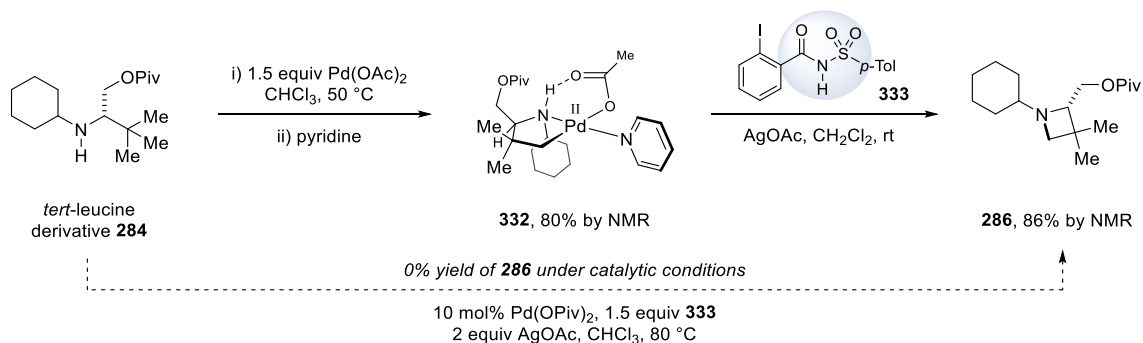
During the studies on the scope of aliphatic amines, several unreactive substrates were identified (Scheme 86). For example, a drawback of the reaction was that both α and β substitution was required along the chain undergoing C–H activation. Hence, amine **331a** with no β -substituent gave zero yield in the reaction. The lack of reactivity was attributed to the higher barrier to cyclometalation for substrates containing less alkyl branching. Additionally, an α -ester substituent was also not tolerated (**331b**), with the α -amino ester position undergoing epimerization during the reaction. A less substituted amine containing an α -methylene unit (**331c**) was unreactive with only 63% of the substrate recovered, indicating degradative β -H elimination. A hindered secondary amine derived from *tert*-amyl amine was also unreactive (**331d**), though the reason for this was unclear. It was possible that the electron-withdrawing effect of the proximal oxygen atom in the amino alcohol substrates most commonly employed could benefit the reaction by making the amine nitrogen less electron-rich, and therefore disfavour over-coordination to the Pd centre to form the off-cycle bis(amine) complex. Finally, tetramethylpiperidine (**331e**) was tried as a substrate and found to be unreactive. Given that the β C–H activation of **331e** was known to be efficient under catalytic conditions, the lack of product formation indicated that 2-bromobenzoic acid was unable to functionalize the intermediate four-membered ring palladacycle.



Scheme 86. Unreactive aliphatic amines in the Pd-catalyzed decarboxylative arylation reaction.
331d was synthesized by Dr. G. N. Hermann.

3.2.3. *ortho*-DG-assisted Oxidative Addition

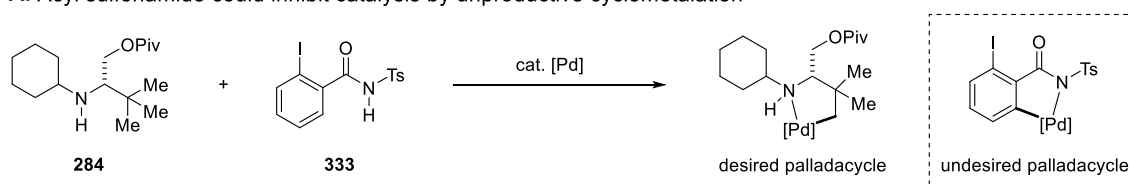
We were interested in exploring the effect of changing the *ortho*-carboxylic acid group in the aryl halide reagent for another group which could also facilitate the oxidative addition to the palladacycle but would not undergo a decarboxylation process. Given that the decarboxylation was thought to trigger the C–C bond reductive elimination, exchange of the carboxylate could lead to different reductive elimination pathways being promoted. As a starting point, the *ortho*-carboxylic acid was changed to an *ortho*-acyl sulfonamide as the pK_a values of these functional groups are known to be very similar ($pK_a \sim 5$).²⁴² A stoichiometric experiment employing a secondary amine derived from *tert*-leucine (**284**) was carried out, in which the pyridine-ligated palladacycle (**332**, 80% yield from **284**) was subjected to an aryl iodide containing an *ortho*-*N*-tosylbenzamide group (**333**, Scheme 87). In the presence of AgOAc, full conversion of palladacycle **332** was observed at room temperature and resulted in the formation of the azetidine product (**286**) in 86% yield by NMR. The facile oxidative functionalization of the palladacycle demonstrated that the *ortho*-directed oxidative addition reactivity mode was likely being maintained for the acyl sulfonamide group. Moreover, the azetidine was formed as the sole amine-containing product, indicating that complete selectivity for intramolecular C–N bond reductive elimination was obtained using reagent **333**. The switch in the selectivity of reductive elimination upon changing the *ortho*-DG in the aryl iodide reagent represented a novel approach to promoting different types of bond formation from a common palladacycle intermediate. However, upon employing aryl iodide **333** under catalytic conditions (10 mol% Pd(OPiv)₂, 1.5 equiv **333**, 2 equiv AgOAc, CHCl₃, 80 °C), it was found that none of the azetidine **286** was formed. Given that not even a trace of azetidine was observed, it was apparent that aryl iodide **333** was somehow disrupting the Pd-catalyzed cyclometalation.



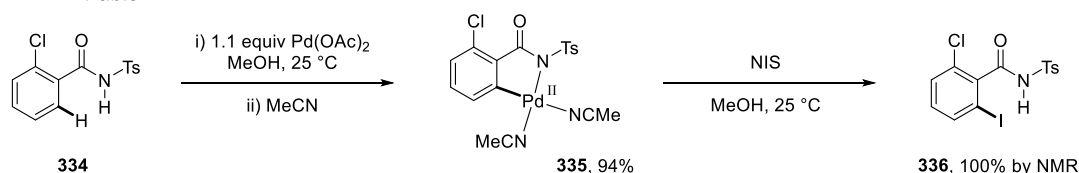
Scheme 87. Use of an aryl iodide reagent containing an *ortho*-*N*-tosylbenzamide group.

It was posited that the catalytic reaction was being inhibited by unproductive acyl sulfonamide-directed cyclometalation within the aryl iodide reagent (Scheme 88A). Given that the amine (**284**) and aryl iodide (**333**) would both be present in stoichiometric amounts during catalysis, the palladium catalyst would be distributed between the desired amine-directed palladacycle and undesired acyl sulfonamide-directed palladacycle. If the undesired palladacycle predominated under the reaction conditions, then no reaction would occur. In 2014, Fabis²⁴³ reported that *N*-tosylbenzamides (**334**) could promote a facile room temperature *ortho*-palladation, with a bis(acetonitrile)-ligated palladacycle (**335**) being isolated in 94% yield under stoichiometric conditions (Scheme 88B). Functionalization of palladacycle **335** was shown with *N*-iodosuccinimide (NIS) to quantitatively afford the *ortho*-iodinated product (**336**). A series of room temperature catalytic transformations were developed by Fabis, as well as a stoichiometric radio-iodination procedure using [¹²⁵I]NIS.^{243,244} Overall, the studies of Fabis demonstrated the effectiveness of the *N*-tosylbenzamide group as an *ortho*-DG and therefore support the notion of catalyst deactivation within our amine functionalization reaction. Looking to overcome the incompatibility of *N*-sulfonylbenzamide reagents, we proposed to invert the acyl sulfonamide group to give the isomeric *N*-acylbenzenesulfonamide reagent (Scheme 88C). It was thought that the modified reagent would destabilize the resulting palladacycle by having a larger SO₂ unit (relative to a carbonyl) within the backbone of the palladacycle that would

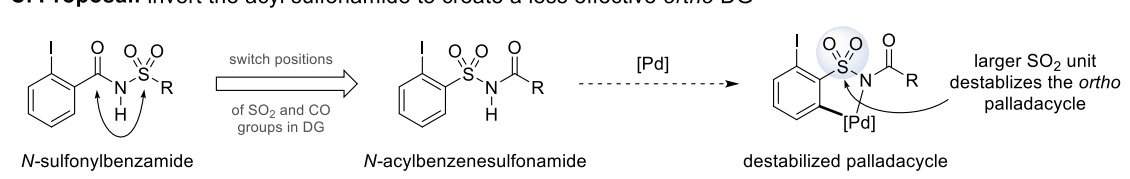
A. Acyl sulfonamide could inhibit catalysis by unproductive cyclometalation



B. 2014: Fabis



C. Proposal: invert the acyl sulfonamide to create a less effective *ortho* DG

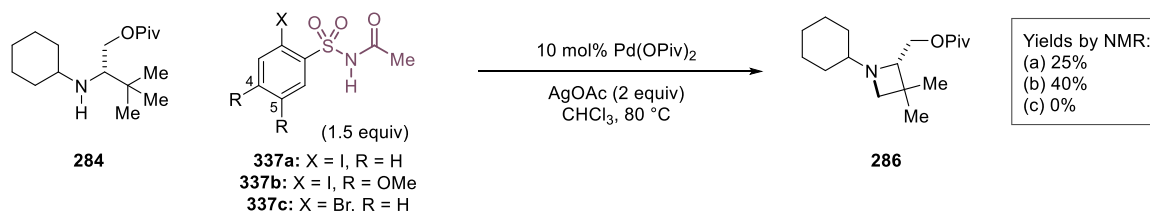


Scheme 88. (a) Proposed catalyst deactivation by sulfonamide-directed cyclometalation. (b) Precedent for *N*-tosylbenzamides as *ortho*-DG's for Pd-mediated C–H activation. (c) Strategy to overcome catalyst inhibition.

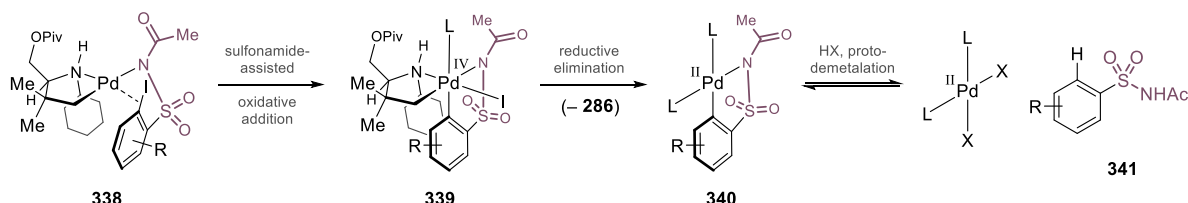
distort the structure of the chelate. Notably, there are no examples of *N*-acylbenzenesulfonamide reagents undergoing Pd-catalyzed C–H activation in the literature, though one example of Rh-catalyzed *ortho*-arylation has been reported.²⁴⁵ Nonetheless, if the formation of the undesired acyl sulfonamide-directed palladacycle could be sufficiently disfavoured, then the Pd-catalyzed amine functionalization should in theory proceed.

Gratifyingly, employing aryl iodide reagents containing the *ortho* *N*-acetylbenzenesulfonamide group did indeed provide catalytic turnover in the C–H functionalization of amine **284**, with complete selectivity for the formation of azetidine **286** being maintained (Scheme 89A). Using the simplest variant of the aryl iodide reagent (**337a**), 25% yield of azetidine **286** was obtained. Interestingly, 4,5-dimethoxy substitution of the aryl iodide (**337b**) led to an increased yield of 40%. Conversely, employing the analogous aryl bromide reagent (**337c**) gave no yield of the azetidine, indicating that the *N*-acetylbenzenesulfonamide was less effective in assisting the oxidation of the aminoalkyl palladacycle than the *ortho*-carboxylic acid group. Considering the mechanism of the catalytic azetidine formation, it is proposed that the acyl sulfonamide mediates an *ortho*-directed oxidative addition to the palladacycle (**338**) to form a putative bis(cyclometalated) Pd^{IV} intermediate (**339**, Scheme 89B). Presumably, the cyclopalladated aromatic group is prevented from undergoing C(sp²)–C(sp³) bond reductive elimination due to the relatively strong binding of the acyl sulfonamide group to the Pd^{IV} centre. Instead, C–I reductive elimination (followed by cyclization) or direct C–N bond reductive elimination occurs to form azetidine **286** as well as a Pd^{II} by-product that would still contain the cyclopalladated aromatic group (**340**). In order

A. Catalytic turnover enabled with *ortho*-*N*-acetylbenzenesulfonamide reagents



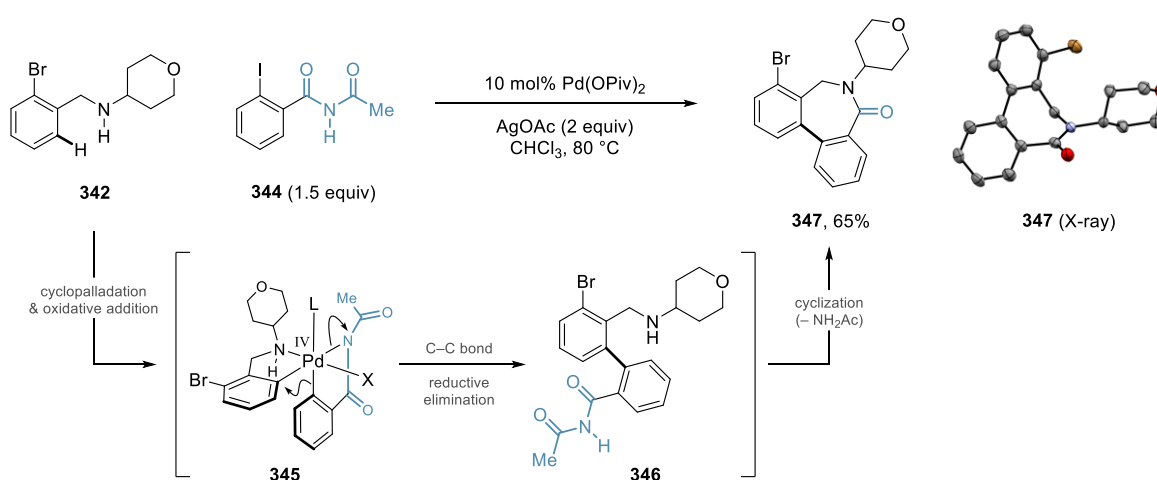
B. Proposed mechanism: *ortho*-sulfonamide assistance



Scheme 89. (a) Achieving catalytic turnover using *N*-acetylbenzenesulfonamides and (b) proposed mechanism.

to conversion to a functionalized amine product (Scheme 90B). Based on the molecular weight identified by LC-MS analysis of the reaction mixture, the product was proposed to be an *ortho*-arylated benzylamine in which the acyl sulfonamide group remained intact (**343**). The ^1H NMR spectrum showed broad signals, presumably due to restricted rotation about the biaryl linkage, which precluded quantitative analysis of the reaction.

While studying benzylamine functionalization, it was discovered that a modified aryl iodide reagent containing an *ortho*-*N*-acetylbenzamide (imide) group resulted in the formation of an interesting seven-membered ring lactam product (Scheme 91). Under catalytic conditions, the reaction between benzylamine **342** and the *ortho*-imide aryl iodide reagent **344** provided a dibenzoazepinone product in good yield (**347**, 65%). Lactam **347** was a crystalline solid and thus the solid-state structure was elucidated by X-ray diffraction of a single crystal, which revealed the defined bowl-like structure of the seven-membered ring core. Taking into account the previous observation of arylated product **343**, the proposed mechanism involves amine-directed *ortho*-palladation and imide-assisted oxidative addition to form a putative Pd^{IV} intermediate (**345**). The weakly bound imide DG is thought to readily dissociate from the Pd^{IV} centre to trigger a C–C bond reductive elimination to form the *ortho*-arylated product (**346**), which subsequently undergoes in situ lactamization to the observed dibenzoazepinone product (**347**). Although the Pd-catalyzed C–H arylation-lactamization process was not further explored, the reaction provided an important proof-of-concept for the application of *ortho*-DG-assisted oxidative addition for the functionalization of aromatic benzylamine substrates. In the preparation of this thesis, the formation of dibenzoazepinone products via Pd-catalyzed *ortho*-C–H arylation and lactamization of free benzylamines was reported by Young²⁴⁷ using *ortho*-ester aryl iodide reagents.



Scheme 91. Aryl iodide containing *ortho*-imide DG led to the formation of a 7-membered ring lactam product.

3.3. Summary

The current chapter disclosed the discovery and development of a Pd-catalyzed γ C–H arylation of secondary aliphatic amines. Preliminary stoichiometric studies revealed a facile carboxylate-assisted oxidative addition of 2-iodobenzoic acid to aminoalkyl palladacycles. In the presence of a Ag^{I} additive, decarboxylative C–C bond reductive elimination from a putative Pd^{IV} intermediate generated a seven-membered ring palladacycle which was protodemetalated to give the γ -arylated amine product. Mechanistic control experiments discounted the involvement of aryne intermediates and provided evidence for an unprecedented room temperature decarboxylation step at a high valent Pd^{IV} centre. Significantly, in the absence of a silver salt, C–C bond reductive elimination did not occur and, instead, the Pd^{IV} intermediate was intercepted by external carboxylate nucleophiles, thus demonstrating the crucial role of Ag^{I} in determining the selectivity of reductive elimination.

Having identified a novel reactivity mode for aminoalkyl palladacycle functionalization, a catalytic reaction was developed and optimized for the decarboxylative arylation process wherein the *ortho*-carboxylate group acts as a traceless directing group. The Pd-catalyzed reaction represents the first example in which less hindered acyclic aliphatic amines have undergone native amine-directed C–H functionalization under catalytic conditions. It was found that 2-bromobenzoic acid reagents provided improved catalytic efficiency compared to 2-iodobenzoic acids, with a broad range of functional substituents being tolerated in the aryl component in the reaction. Meanwhile, a variety of secondary aliphatic amines derived from chiral amino acids provided moderate to good yields of arylated products. However, the main drawback of the reaction was that substrates required both α and β substitution along the alkyl chain undergoing C–H activation in order to allow for the efficient formation of the palladacycle. This requirement highlighted the limit of native amine-directed C–H activation using a simple Pd^{II} carboxylate catalyst. Substrates with less branching would likely require the assistance of a ligand which could lower the barrier to cyclopalladation, such as an MPAA or pyridone ligand. Accordingly, a future objective following the current work would be to incorporate a ligand-assisted C–H activation within an oxidative $\text{Pd}^{\text{II}}/\text{Pd}^{\text{IV}}$ -catalyzed C–H functionalization of aliphatic amines.

The *ortho*-carboxylic acid group within the aryl iodide oxidant was exchanged for other types of directing groups in order to investigate the generality of the *ortho*-DG-assisted oxidative addition to aminoalkyl palladacycles. Notably, under stoichiometric conditions, aryl iodides containing *ortho*-acyl sulfonamide groups were found to effectively recapitulate the

facile and mild reactivity of the benzoic acid reagents, though the selectivity of reductive elimination was different, this time exclusively forming the cyclized azetidine product. In terms of catalytic activity, although *ortho*-*N*-sulfonylbenzamide aryl iodides provided zero yield of the azetidine product, isomeric *N*-acylbenzenesulfonamide aryl iodides provided the azetidine in moderate yield, providing a proof-of-concept for the extension of the *ortho*-DG-assisted oxidative addition reactivity to catalytic C–heteroatom bond-forming processes. Finally, the reactivity of the aryl iodide reagents was tested in the context of benzylamine C(sp²)–H functionalization. Under catalytic conditions, surprisingly, 2-iodobenzoic acid showed no reactivity for aromatic functionalization, whereas the newly developed 2-iodo-*N*-acetylbenzenesulfonamide reagent gave the *ortho*-arylated product in which the acyl sulfonamide DG remained intact. Conversely, a more useful transformation was observed when employing a modified aryl iodide containing an *ortho*-imide DG, in which cyclization of the initially formed arylated product led to the formation of a seven-membered ring dibenzazepinone product. Overall, the *ortho*-DG-assisted oxidative addition reactivity mode was demonstrated as an efficient and modular approach to palladacycle functionalization, and it is envisioned that other substrate classes such as carboxylic acids, amides or imines could also be functionalized using this approach.

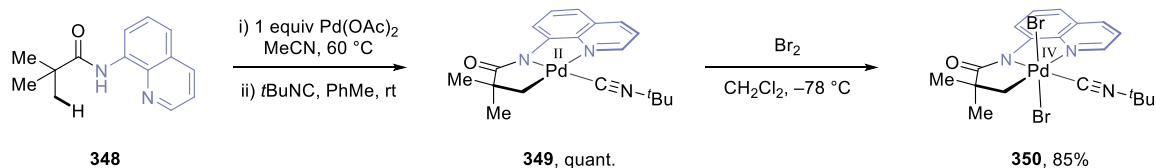
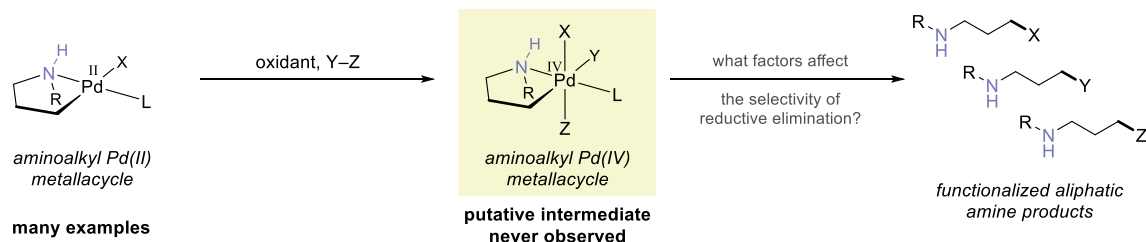
4. Stable Alkyl Pd^{IV} Complexes Derived from Cyclopalladated Amines & Oximes

4.1. Background & Project Aims

Alkyl Pd^{IV} complexes have been frequently invoked in the proposed mechanisms of Pd-catalyzed directed C(sp³)–H functionalization reactions.^{59,65} However, direct observation of these putative high valent intermediates has been incredibly scarce, presumably due to the propensity of Pd^{IV} complexes to undergo reductive elimination processes. While pioneering organometallic studies by Canty and Sanford have elucidated the key mechanistic features of several different reductive elimination pathways using stable alkyl Pd^{IV} complexes,^{167,204,205} these complexes have contained methyl or cycloneophyl alkyl ligands that do not effectively represent cyclometalated substrates that are found in Pd^{II}/Pd^{IV}-catalyzed reactions.⁵⁹ Consequently, there is a dearth of information about the structure and reactivity of alkyl Pd^{IV} intermediates being formed from the oxidation of cyclopalladated substrates. Acquiring such information would provide crucial insight into ways of controlling the efficiency and selectivity of product-forming reductive elimination in a catalytic scenario and thus inspire novel approaches to the development of Pd-catalyzed C–H functionalization reactions.

To the best of our knowledge, there is only a single example of an isolated alkyl Pd^{IV} complex containing a cyclometalated substrate that has been used in a catalytic transformation. In 2010, as part of a study to develop β C–H arylation and alkylation reactions of carboxylic acid derivatives containing the bidentate 8-aminoquinolinamide DG, Daugulis²⁴⁸ showed that an isocyanide-ligated palladacycle (**349**) synthesized from a pivalic acid-derived substrate (**348**) underwent oxidation by bromine at low temperature to form the *trans*-dibromide Pd^{IV} complex (**350**, Scheme 92A). Complex **350** decomposed within hours at 0 °C in solution, though the complex could be crystallized to unequivocally confirm its structure by X-ray crystallography. Nonetheless, there are currently no examples of an alkyl Pd^{IV} complex derived from a cyclopalladated substrate containing a monodentate nitrogen DG.

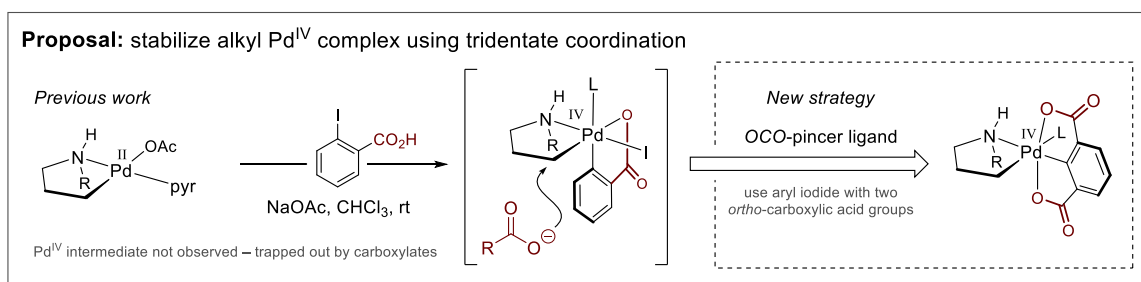
Given the Gaunt group's long-standing interest in native amine-directed C(sp³)–H functionalization, we aimed to investigate the synthesis of stable and isolable aminoalkyl Pd^{IV} complexes from cyclopalladated aliphatic amines (Scheme 92B). Although aminoalkyl Pd^{IV} intermediates have been invoked in numerous catalytic cycles by our group,^{146,154,213,226,249} to date, we have never been able to observe these highly reactive intermediates. Conversely, many examples of the respective alkyl Pd^{II} metallacycles have been synthesized under stoichiometric

A. 2010: Daugulis**B. Aminoalkyl Pd^{IV} complexes: commonly invoked, but never observed**

Scheme 92. (a) A rare example of an isolated alkyl Pd^{IV} intermediate containing a cyclometalated substrate molecule. (b) A stable and isolable aminoalkyl Pd^{IV} metallacycle complex remains unreported in the literature.

conditions, and have often provided an invaluable method of exploring palladacycle reactivity without the requirement for catalytic turnover.²⁴⁹ Given that controlling the selectivity of reductive elimination has frequently been noted as a significant challenge in native amine-directed C–H functionalization under oxidative conditions,^{226,249} it was thought that the undertaking of an organometallic study into the synthesis and reactivity of aminoalkyl Pd^{IV} complexes would more clearly identify the controlling factors in the context of aliphatic amine functionalization.

Previous work on carboxylate-assisted oxidative addition of aryl halides to aminoalkyl palladacycles provided the foundation of our proposed strategy for synthesizing stable Pd^{IV} complexes (Scheme 93). Specifically, the observation that subjecting an aminoalkyl palladacycle to a combination of 2-iodobenzoic acid and sodium acetate led to a mixture of functionalized products resulting from C–O bond reductive elimination indicated that a Pd^{IV} intermediate was being formed, but was sufficiently reactive to couple directly with carboxylate



Scheme 93. Proposal for the synthesis of stable Pd^{IV} complexes using carboxylate-assisted oxidative addition.

nucleophiles present in the reaction mixture. Consequently, we proposed to stabilize the Pd^{IV} intermediate by exchanging the 2-iodobenzoic acid reagent for an aryl iodide containing two *ortho*-carboxylic acid groups that would potentially form a Pd^{IV} complex containing a trianionic *OCO*-pincer ligand. It was thought that the highly electron-rich and chelating pincer ligand would adequately stabilize the Pd^{IV} centre to allow for isolation of the complex.

The project aims that were set out for the organometallic study are summarized in Figure 7. Firstly, we aimed to synthesize a series of pincer-stabilized alkyl Pd^{IV} complexes which would serve as model complexes for our studies (Figure 7A). Secondly, we planned to explore the reactivity of the high valent complexes. In particular, we were most interested in exploring the feasibility of different C–heteroatom bond reductive eliminations that are known to be promoted by the outer-sphere attack of nucleophilic species (Figure 7B). If reactivity could be obtained with high levels of efficiency and selectivity, we planned to study the mechanism of the reductive elimination in detail in order to compare with previous organometallic studies related to Pd^{IV}-mediated C(sp³)–heteroatom bond formations.^{204,205} Finally, we planned to investigate the isolation of pincer-stabilized aryl Pd^{IV} complexes derived from cyclopalladated benzylamine substrates (Figure 7C). Given that aromatic palladacycles had previously been found to be unreactive towards carboxylate-assisted oxidative addition (see: Section 3.2.3.), we also aimed to explore variations to the pincer ligand scaffold and thus observe the effect that ligand changes would have on the structure, stability and reactivity of the resulting Pd^{IV} complexes.

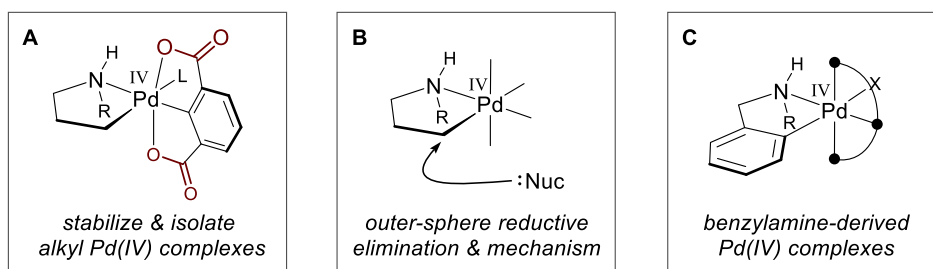


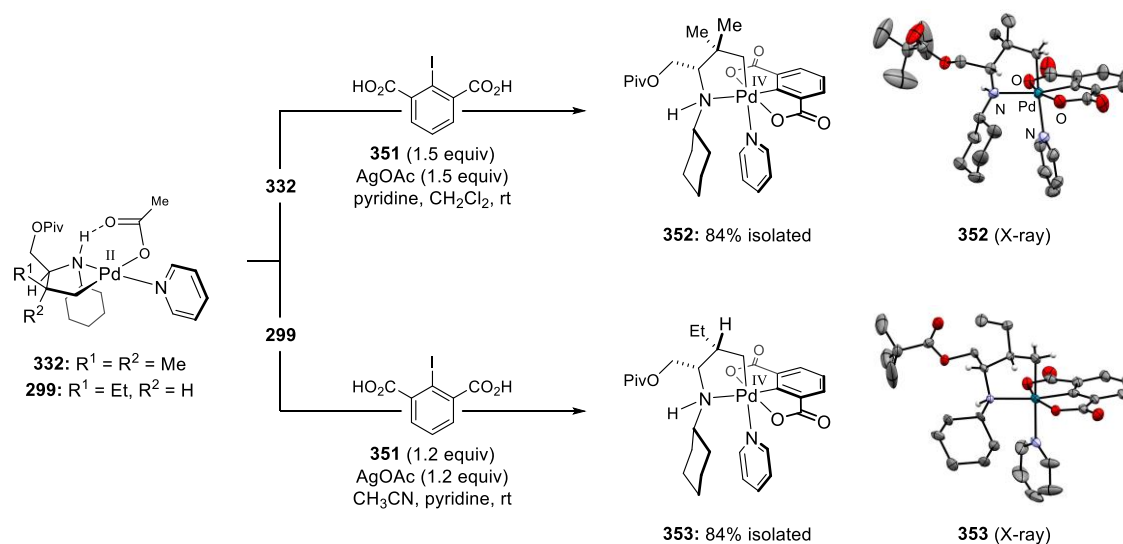
Figure 7. Project aims for an organometallic study into the synthesis and reactivity of alkyl Pd^{IV} complexes.

4.2. Results & Discussion

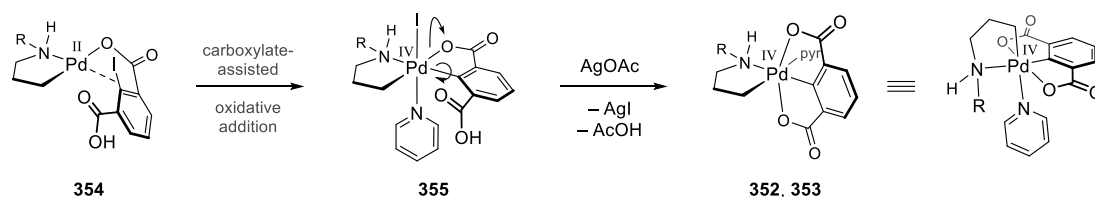
4.2.1. Synthesis & Reactivity of Stable Aminoalkyl Pd^{IV} Complexes

We started by investigating our proposed strategy to employ an aryl iodide containing two *ortho*-carboxylic acid groups. Two different pyridine-ligated Pd^{II} metallacycles were used as starting materials that were synthesized as part of previous studies – one that contained a cyclometalated amine derived from *tert*-leucine (**332**) and another derived from isoleucine (**299**, Scheme 94A). The two palladacycles are isomeric at the β -position relative to the amine nitrogen, with complex **332** having a *gem*-dimethyl group and **299** having ethyl and hydrogen substituents. Subjecting the palladacycles (**332** and **299**) to 2-iodo-1,3-benzenedicarboxylic acid (**351**) in the presence of AgOAc and pyridine at room temperature led to quantitative conversion to new species, as was observed by ¹H NMR analysis of the crude reaction mixtures. Notably, the products contained several downfield-shifted ¹H NMR signals indicating that, if the palladacycles had remained intact, oxidation of the Pd centre had likely taken place. Conversely, an upfield shift of the amine(NH) signals was also observed (e.g. δ_{H} 3.49 ppm in **352** compared to 5.42 ppm in **332**), indicating that the N–H bond was no longer involved in an

A. Synthesis of alkyl Pd^{IV} complexes from cyclopalladated amines



B. Proposed mechanism of formation of Pd^{IV} complexes



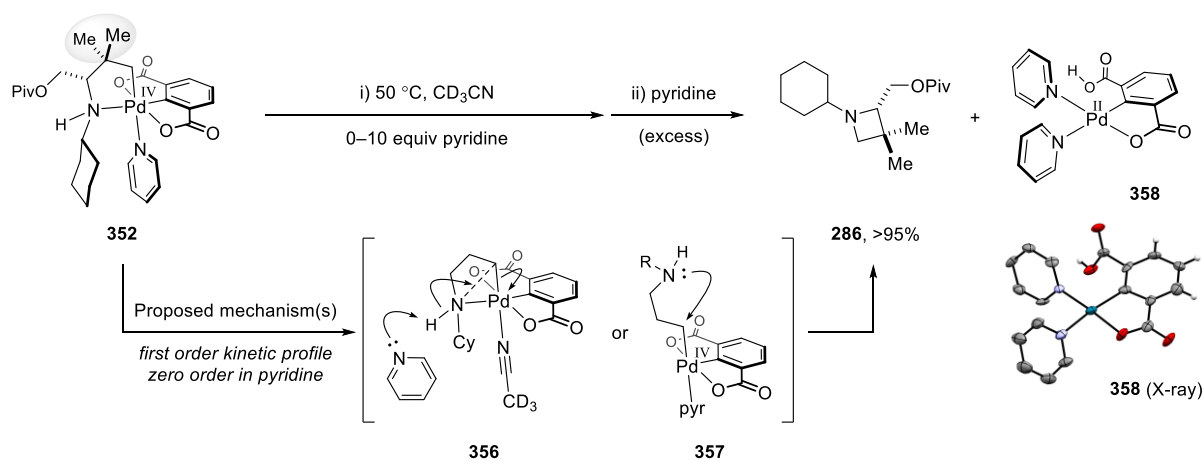
Scheme 94. (a) Synthesis of stable aminoalkyl Pd^{IV} complexes and (b) proposed mechanism of their formation.

intramolecular hydrogen-bonding interaction, as in the starting Pd^{II} complexes. Gratifyingly, isolation and crystallization of the products (**352** and **353**, both isolated in 84% yield) provided unequivocal confirmation of their structures by X-ray diffraction of single crystals as the desired aminoalkyl Pd^{IV} complexes. From the solid-state structures, the σ -aryl dicarboxylate group is bound in a meridional tridentate fashion to the octahedral Pd^{IV} centre, forming the expected *OCO*-pincer ligand scaffold. Interestingly, the pyridine ligand is *trans* to the Pd^{IV}-bound alkyl group of the cyclometalated amine, as opposed to being *trans* to the neutral amine(NH) ligand. This is in contrast to what is commonly observed in square planar Pd^{II} complexes in which the neutral ligands are typically found *trans* to one another, such as in bis(amine) Pd^{II} complexes.^{69,144} As a result of the strong trans influence of the highly donating alkyl group, the pyridine ligand is weakly bound to the Pd^{IV} centre, which is reflected in the observed loss of the pyridine ligand upon exposing the Pd^{IV} complexes to vacuum for extended periods of time. Full characterization of the complexes in the solution phase was conducted by NMR spectroscopy in CDCl₃, with 2D NOESY NMR of **353** confirming that the observed solid-state configuration was maintained in solution. Furthermore, both complexes were found to be indefinitely stable in the solid-state when stored at 5 °C.

The proposed mechanism of formation for the aminoalkyl Pd^{IV} complexes is shown in Scheme 94B. Given that the oxidation process occurs at room temperature, it is proposed that aryl iodide **351** oxidizes the Pd^{II} centre by a carboxylate-assisted oxidative addition (**354**), which in the presence of pyridine, forms the putative Pd^{IV} intermediate **355**. A ligand isomerization process involving rotation about the Pd–C(sp²) bond of the σ -aryl ligand then takes place, which is likely facilitated by a silver-mediated iodide abstraction from the Pd^{IV} centre. The resulting complex is the *OCO*-pincer-ligated Pd^{IV} complex containing the observed configuration of ligands around the metal centre (**352**, **353**).

Having synthesized a pair of isomeric aminoalkyl Pd^{IV} complexes, we next investigated their reactivity. In the case of complex **352**, it became apparent that intramolecular C–N bond reductive elimination was favoured, forming the azetidine (**286**, Scheme 95). For example, stirring complex **352** at 50 °C as a solution in acetonitrile led to quantitative conversion to **286**. The reaction was also promoted at room temperature by the presence of acidic or basic additives. Conversely, stirring isomeric complex **353** at 50 °C led to a complex mixture of decomposition products. As a result, the tendency of **352** to undergo cyclization is attributed to the *gem*-dialkyl effect.²⁵⁰ In particular, the X-ray structures show that the palladacycle of **352** containing the branched β -*gem*-dimethyl group results in a decrease in the bite angle (N_{amine}–Pd–C_{alkyl} = 82.4° in **352** c.f. 84.0° in **353**), which brings the amine nitrogen and γ -activated alkyl

group into closer proximity and thus could facilitate the reductive elimination of these ligands. The mechanism of the C–N bond reductive elimination was briefly explored by studying the kinetics of the reaction in the presence of added pyridine (0, 5 and 10 equivalents). Following the reactions by ¹H NMR spectroscopy, the reductive elimination was observed to have a first order kinetic profile and was zero order in pyridine (Figure 8). Consequently, assuming that reductive elimination occurs from a coordinatively unsaturated Pd^{IV} intermediate, as is generally observed,^{103,204,205} and that the tridentate *OCO*-pincer ligand is unlikely to dissociate, we propose that the mechanism proceeds via dissociation of the labile pyridine ligand, forming solvent-ligated intermediate **356**, followed by pyridine-mediated deprotonation of the



Scheme 95. Aminoalkyl Pd^{IV} complex **352** underwent intramolecular C(sp³)–N bond reductive elimination.

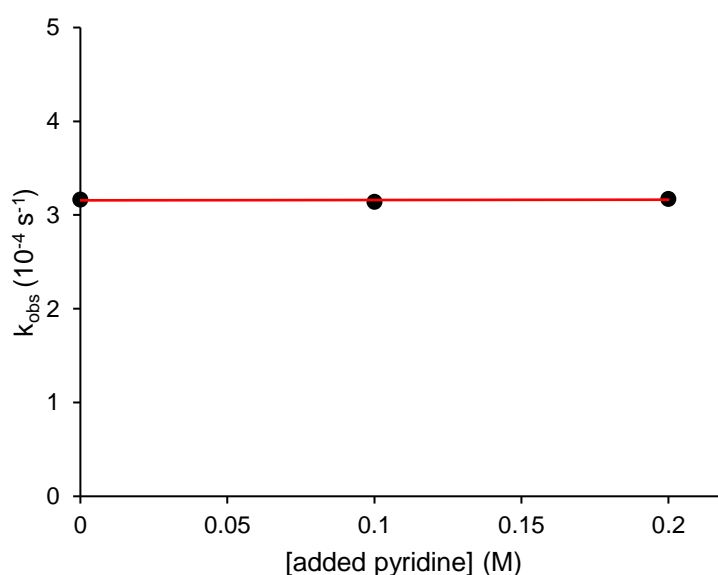
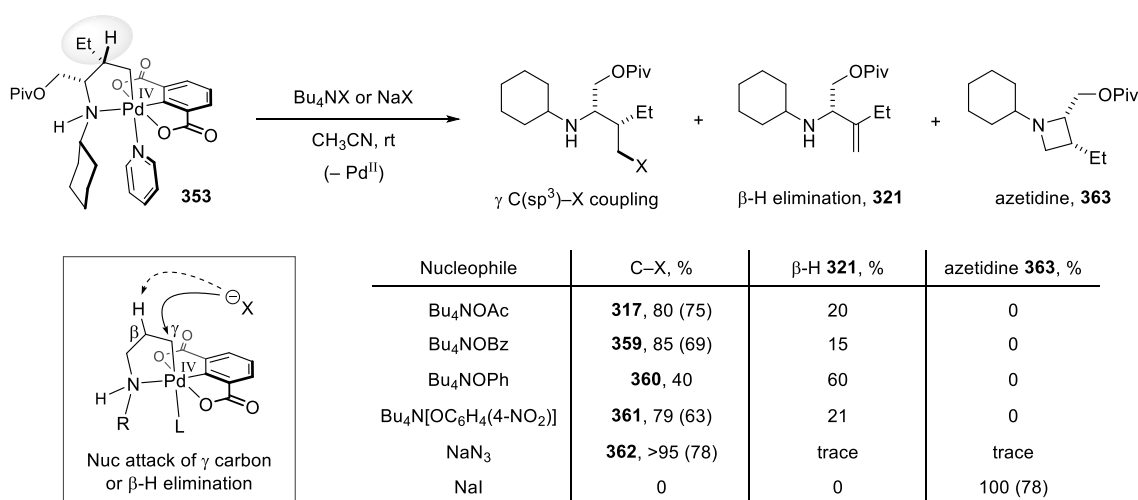


Figure 8. Plot of rate constant (k_{obs}) against concentration of added pyridine for the thermal decomposition of complex **352**. T = 50 °C; [**352**] = 0.02 M in CD₃CN; [added pyridine] = 0.0, 0.1, 0.2 M (0–10 equivalents).

amine(NH) to trigger the C–N bond reductive elimination. An alternative mechanism involving dissociation of the amine nitrogen prior to outer-sphere S_N2-type C–N bond formation (**357**), which would also be consistent with the kinetic data, is deemed less likely given that the *gem*-dialkyl effect should disfavour cyclization in this case by increasing the barrier to amine dissociation. During the course of the azetidine formation, it was found that an insoluble solid formed which was thought to be the organometallic Pd^{II} by-product. Upon addition of excess pyridine and recrystallization of the solid material, the compound was identified as a bis(pyridyl) Pd^{II} complex by X-ray diffraction (**358**, Scheme 95). Interestingly, the *OCO*-pincer ligand is bound in a bidentate coordination mode with one of the carboxylate arms twisted 64° out-of-plane of the aromatic ring to accommodate the binding of a second molecule of pyridine.

Next, we investigated the reactivity of the Pd^{IV} complexes to external nucleophiles in order to explore the viability of different types of C–heteroatom bond formation. However, the fully substituted β-position of complex **352** hindered the γ-position to attack by nucleophiles and instead led to predominantly cyclization rather than intermolecular γ-functionalization. On the other hand, it was found that the less substituted backbone in complex **353** allowed for nucleophile-mediated reductive elimination to proceed with good efficiency (Scheme 96). For example, subjecting **353** to soluble tetrabutylammonium salts of acetate, benzoate, phenoxide and *p*-nitrophenoxide in acetonitrile at room temperature gave moderate to high yields of the C–O coupled products (**317**, **359–361**). While full conversion of **353** occurred in all cases, the remaining mass balance was attributed to the formation of the olefin by-product **321** resulting from β-H elimination. Notably, the ratio of C–O bond formation to β-H elimination correlated with the basicity of the anionic nucleophile, varying between 85:15 C–O:β-H for Bu₄NOBz to a 40:60 ratio for Bu₄NOPh (pK_a(BzOH) = 4.25, pK_a(PhOH) = 10.0 in water).¹⁰ Based on the observed trend, it is plausible that the nucleophile mediates the β-H elimination process via an outer-sphere *anti* 1,2-elimination process, though an inner-sphere Pd^{IV}-mediated *syn* 1,2-elimination cannot be ruled out.²⁵¹ While sodium salts of the oxyanions generally gave lower conversion, highly nucleophilic counter-anions such as azide and iodide were effective as their sodium salts. Sodium azide gave almost complete selectivity for C–N bond formation (**362**, 78% isolated yield), with only traces of olefin **321** being observed, whereas sodium iodide formed only the azetidine product (**363**, 78% isolated yield), presumably after rapid cyclization of the initially formed γ C–I coupled product. Overall, the study demonstrated the viability of the outer-sphere attack mechanism for a variety of *O*- and *N*-nucleophiles on Pd^{IV} intermediates containing a cyclometalated amine, affording access to a more diverse range of γ-functionalized products than had previously been reported in Pd-catalyzed amine functionalizations.

Importantly, intermolecular C–N reductive elimination had been obtained for the first time in the reaction of **353** with sodium azide. Nonetheless, the intimate mechanism of the nucleophile-mediated reductive elimination was not amenable for study with the current system, given that the reactions were complicated by product mixtures in the case of the tetrabutylammonium salts, or by the low solubility of the nucleophiles or reaction by-products in the case of the sodium salts. As a result, we designed a different alkyl Pd^{IV} complex supported by the *OCO*-pincer ligand that would be more suited to the purpose of mechanistic experiments.



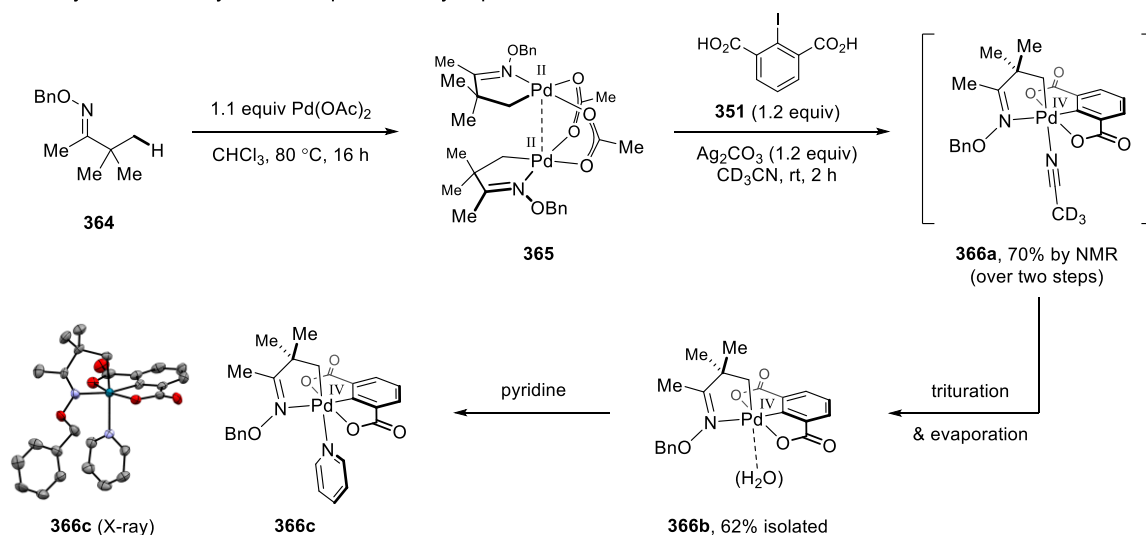
Scheme 96. Aminoalkyl Pd^{IV} complex **353** underwent nucleophile-mediated reductive elimination. Relative product ratios C–X coupling: β -H elimination determined by ¹H NMR; isolated yields in parentheses.

4.2.2. Synthesis of an Oxime-derived Alkyl Pd^{IV} Complex

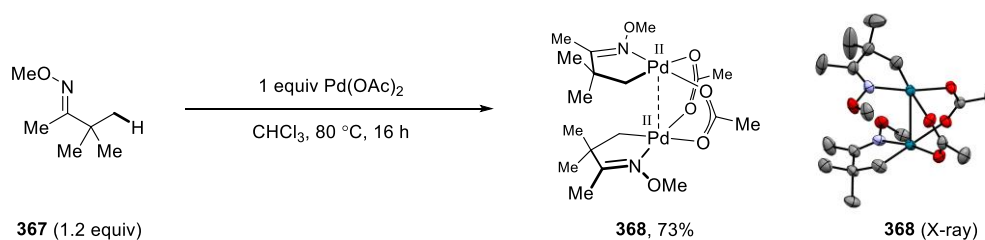
We selected an oxime substrate as a surrogate for the aliphatic amines present in the aminoalkyl Pd^{IV} complexes. Analogously to the amines, the oxime acts as a monodentate-nitrogen DG and should in theory behave similarly in the Pd-mediated reactions. However, crucially, the cyclometalated oxime is unable to undergo intramolecular C–N bond reductive elimination, allowing for β -H elimination to be blocked with alkyl substituents without promoting an undesired cyclization process. Accordingly, the non-volatile *O*-benzyl oxime derivative of pinacolone was chosen as the model substrate (**364**, Scheme 97A). Subjecting **364** to 1.1 equivalents of Pd(OAc)₂ in chloroform at 80 °C provided the dinuclear acetate-bridged palladacycle (**365**), which was directly reacted with aryl iodide **351** and Ag₂CO₃ in acetonitrile-d₃. After two hours at room temperature, full conversion to a new complex was observed by ¹H NMR spectroscopy, which was proposed to be the acetonitrile-ligated *OCO*-pincer Pd^{IV}

complex (**366a**, 70% by NMR from **364**). Purification of Pd^{IV} complex **366a** by trituration in hexanes (under air) followed by evaporation of the solvent and drying under vacuum enabled isolation of the material, though elemental analysis clearly indicated that loss of the acetonitrile ligand had occurred (low %N) with a molecule of water taking its place (**366b**, 62% isolated yield). The monohydrate Pd^{IV} complex **366b** was found to be indefinitely stable in the solid state when stored at 5 °C. Although neither complex **366a** nor **366b** could be successfully crystallized, ligation of pyridine gave a crystalline derivative which could be structurally characterized by X-ray diffraction of a single crystal (**366c**). As expected, complex **366c** has a structure that is analogous to the aminoalkyl Pd^{IV} complexes **352** and **353**.

A. Synthesis of alkyl Pd^{IV} complex from cyclopalladated oxime



B. Crystallization of an acetate-bridged dimeric cyclopalladated alkyl oxime



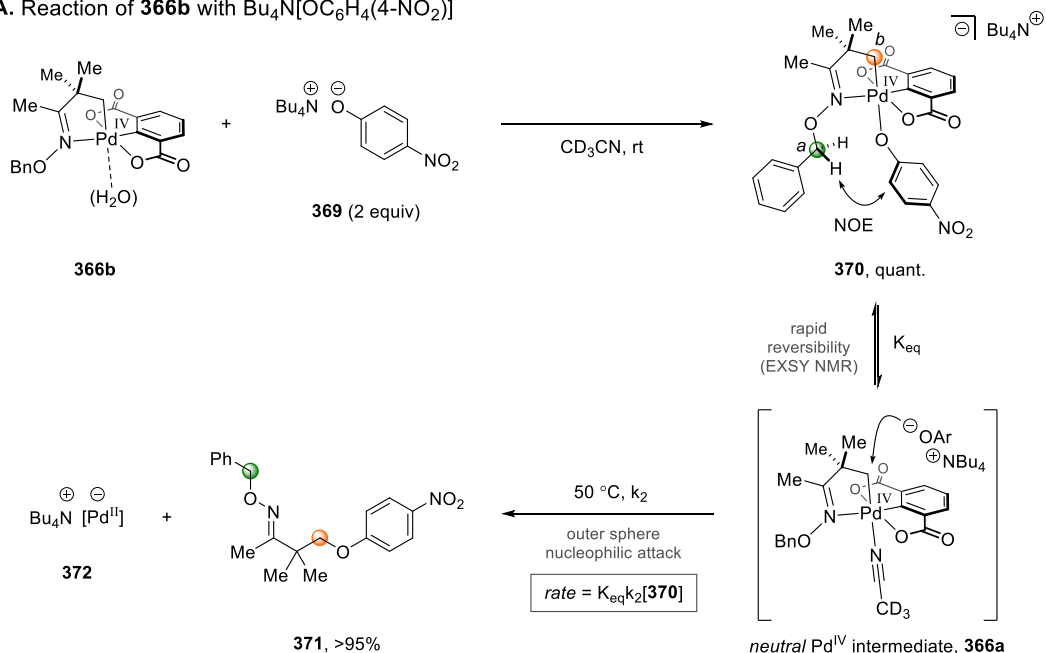
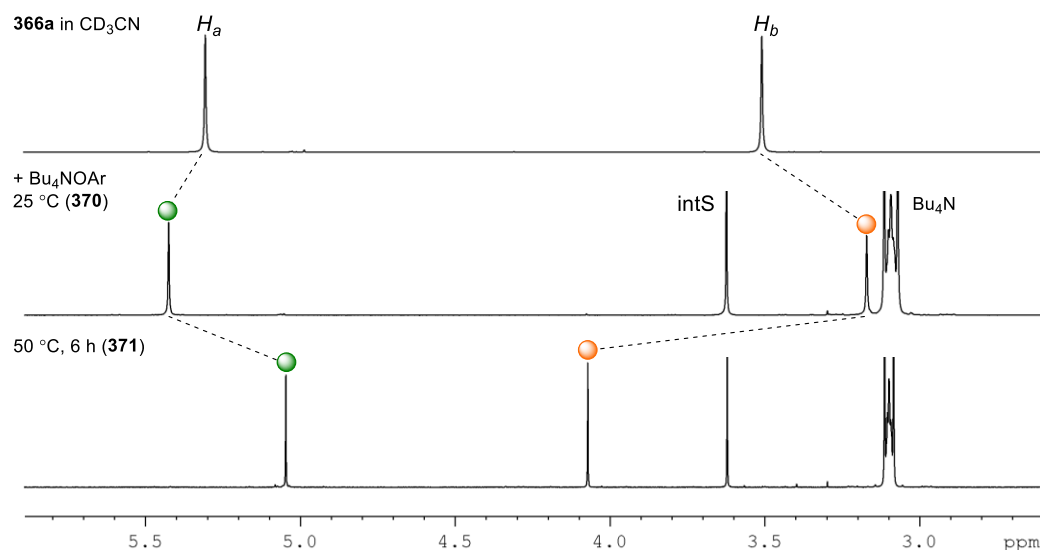
Scheme 97. (a) Synthesis of an oxime-derived alkyl Pd^{IV} complex. (b) Crystal structure of Pd^{II} metallacycle.

As an aside, the solid-state structure of a cyclopalladated alkyl oxime as the acetate-bridged Pd^{II} dimer complex has never been reported in the literature. Therefore, while complex **365** was found not to be crystalline, the *O*-methyl pinacolone oxime palladacycle was synthesized (**367** to **368**, 73%) and crystallized to reveal the structure by X-ray crystallography

(Scheme 97B). The solid-state structure of complex **368** has a Pd–Pd distance of 2.909 Å and contains eclipsed cyclometalated oxime units with head-to-tail orientation.

4.2.3. Mechanism of the Nucleophile-mediated Reductive Elimination

The reaction between oxime-derived Pd^{IV} complex **366b** and tetrabutylammonium *p*-nitrophenoxide (**369**) was selected to study the mechanism of the nucleophile-mediated reductive elimination, as the reaction was found to give quantitative yield of functionalized product with a rate of reaction that was convenient for kinetic measurements. To a solution of complex **366b** in CD₃CN at room temperature (forming solvent-ligated **366a** in situ), 2 equivalents of **369** were added (Scheme 98A). Monitoring the reaction by ¹H NMR, an instantaneous shift in the signals of the Pd^{IV} complex occurred, indicating a new organometallic species had formed (Scheme 98B). In particular, the benzylic protons of the oxime (*H_a*, green circles) had shifted slightly downfield (from δ_H 5.30 ppm in **366a** to 5.43 ppm in **370**), whereas a larger upfield shift was observed for the Pd^{IV}-bound methylene protons (*H_b*, orange circles; from δ_H 3.52 in **366a** to 3.10 in **370**). Moreover, the two equivalents of *p*-nitrophenoxide **369** had split into a 1:1 ratio of signals, with 1 equivalent becoming associated with the Pd complex and 1 equivalent remaining as free, unbound nucleophile. Significantly, a 2D ¹H–¹H NOESY NMR experiment revealed a cross-peak between the oxime benzylic protons and the aromatic protons of the associated *p*-nitrophenoxide, signalling the binding of the phenoxide nucleophile to form a negatively-charged Pd^{IV} complex (**370**). To the best of our knowledge, anionic Pd^{IV} complexes have rarely been characterized in the literature outside of homoleptic [Pd^{IV}X₆]^{2–} complexes.^{252,253} The NOESY spectrum also showed exchange (EXSY) cross-peaks relating to rapid exchange of free and bound *p*-nitrophenoxide ligand on the NMR timescale. Unfortunately, due to the propensity of complex **370** to undergo reductive elimination, particularly in non-polar solvents, crystals suitable for X-ray crystallography were not obtained. However, full characterization as a solution in CD₃CN by NMR spectroscopy, as well as high resolution mass spectrometry data, were consistent with the proposed structure of **370**. Heating the reaction to 50 °C for 6 h led to quantitative conversion to the β-functionalized oxime product (**371**, >95% yield) along with the Pd^{II} by-product (**372**), presumably as a tetrabutylammonium salt. Based on the previous work of Sanford studying C(sp³)–O bond reductive elimination from bipyridine-supported cycloneophyl Pd^{IV} complexes (see Section 1.3.3.),²⁰⁵ we proposed an analogous mechanism involving reversible dissociation of *p*-nitrophenoxide from complex **370**

A. Reaction of **366b** with Bu₄N[OC₆H₄(4-NO₂)]B. Reaction monitoring by ¹H NMR of C(sp³)-O reductive elimination from **370**

Scheme 98. (a) Reaction of **366b** with nucleophile **369**. (b) Reaction monitoring by ¹H NMR spectroscopy.

to form the putative solvent-ligated Pd^{IV} intermediate (**366a**), which is then attacked by the oxyanion nucleophile in an S_N2 fashion at the activated β-position of the oxime to form the C–O bond. Notably, while in the case of Sanford, a neutral six-coordinate nucleophile-bound Pd^{IV} complex underwent oxyanion dissociation to form a coordinatively unsaturated *cationic* intermediate, our system involved an *anionic* starting Pd^{IV} complex that reacts via a neutral intermediate. The key feature of this reaction mechanism is the reversible binding of the nucleophile (K_{eq}) prior to the outer-sphere nucleophilic attack (k₂), which is associated with a

zero order kinetic dependence on the nucleophile and thus overall first order kinetic behaviour (rate = $K_{\text{eq}}k_2[\mathbf{370}]$). Conversely, direct nucleophilic attack of a six-coordinate Pd^{IV} intermediate would have first order dependence on the nucleophile and overall second order behaviour.¹⁸⁵ While the rapid exchange of bound and free *p*-nitrophenoxide ligand was observed by EXSY NMR, we undertook kinetic experiments to elucidate the order of the reaction in nucleophile **369**.

Monitoring the course of the reaction by ¹H NMR for the reductive elimination from **370** in CD₃CN at 50 °C, a first order kinetic profile was observed (Figure 9). Complex **370** cleanly converted to oxime product **371** without any intermediate being observed. Varying the amount of added nucleophile **369** (1–7 equivalents of unbound **369**), we observed a negligible change in the observed rate constant (k_{obs} , Figure 10). Therefore, the reaction was zero order in nucleophile **369** and first order in Pd^{IV} complex **370**. These experiments were in accordance with the findings of Sanford²⁰⁵ and thus strongly supported the proposed reaction mechanism involving dissociation of the *p*-nitrophenoxide ligand followed by bond-forming outer-sphere nucleophilic attack.

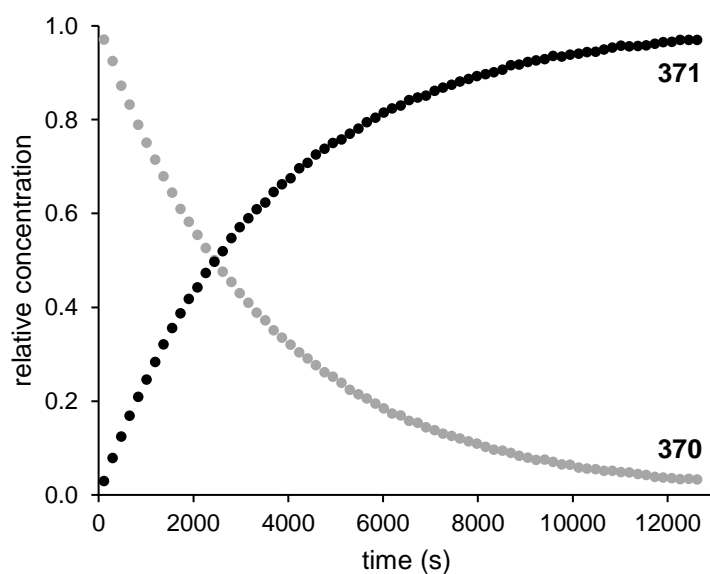


Figure 9. Concentration-time plot for the reaction of Pd^{IV} complex **370** to oxime **371**.
T = 50 °C; [**370**] = 0.02 M in CD₃CN; [unbound **369**] = 0.02 M (1 equivalent).

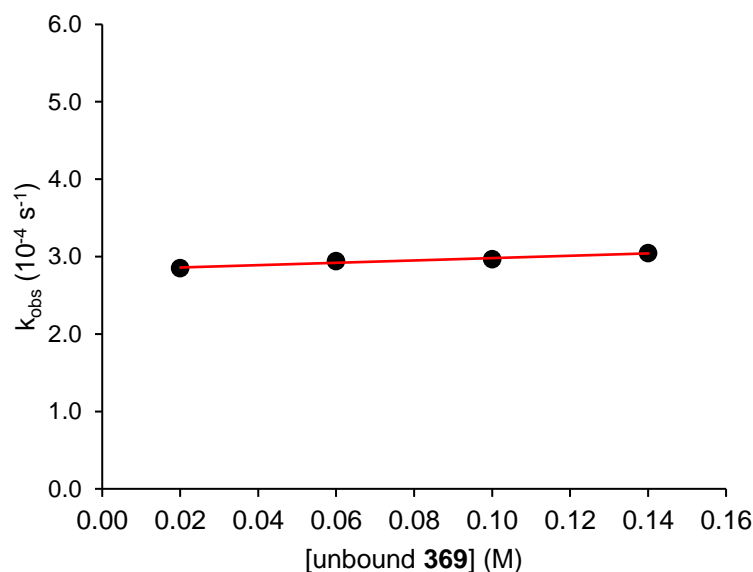


Figure 10. Plot of rate constant (k_{obs}) versus concentration of excess nucleophile **369** for the reaction of **370** to oxime **371**. T = 50 °C; [**370**] = 0.02 M in CD₃CN; [unbound **369**] = 0.02, 0.06, 0.10, 0.14 M (1–7 equivalents).

In order to confirm the presence of the solvent-ligated intermediate and rule out the kinetically indistinguishable mechanism of direct inner-sphere C–O bond reductive elimination from a six-coordinate Pd^{IV} complex, the effect of adding pyridine to the reaction was investigated. Given that pyridine is a strongly coordinating ligand, its presence should significantly slow the reaction by increasing the barrier to forming the putative intermediate (**366a**). For this study, the reaction was conducted in non-coordinating CDCl₃ solvent rather than CD₃CN to more clearly observe the effect of adding a coordinating additive. Adding 0, 1 or 3 equivalents of pyridine, a stepwise decrease in the rate of reductive elimination was observed (Figure 11). Notably, the reaction yields were not significantly affected by the added pyridine, with >90% yield of oxime **371** being obtained in all cases. The difference in the initial rate for the reactions involving 1 and 3 equivalents of pyridine was approximately three-fold, relating to a negative first order dependence of pyridine as would be expected for a reaction mechanism requiring pyridine dissociation prior to reductive elimination. In addition, the reaction rate in CDCl₃ in the absence of pyridine was significantly higher than when the reaction was conducted in CD₃CN, further indicating the inhibiting effect of coordinating additives. Overall, this study strongly supports the formation of a coordinatively unsaturated (in CDCl₃) or solvent-ligated intermediate (in CD₃CN) in the reaction.

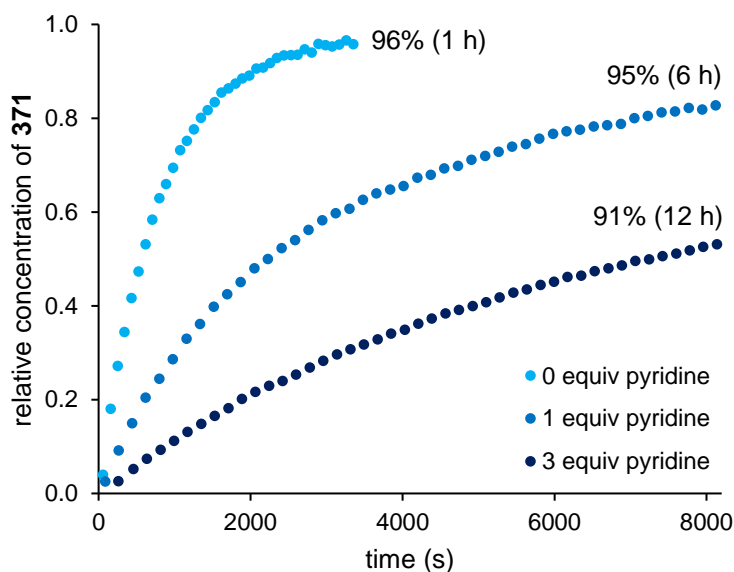


Figure 11. Concentration-time plot for the reaction of **370** to oxime **371** in the presence of pyridine. T = 50 °C; [370] = 0.01 M in CDCl₃; [unbound **369**] = 0.01 M; [pyridine] = 0, 0.01, 0.03 M (0–3 equivalents).

Finally, we measured the rate of reaction at different temperatures to determine the activation parameters for the C–O reductive elimination, ΔH^\ddagger and ΔS^\ddagger (Figure 12). Conducting the reductive elimination of **370** in CD₃CN in the presence of 1 equivalent of unbound nucleophile **369**, the rate constants were obtained over a temperature range between 40–60 °C with 5 °C intervals. From the plot of $\ln(k_{\text{obs}}/T)$ versus $1/T$, the activation parameters were calculated as $\Delta H^\ddagger_{\text{obs}} = +24.3 \pm 0.2 \text{ kcal mol}^{-1}$ and $\Delta S^\ddagger_{\text{obs}} = +0.4 \pm 0.6 \text{ cal K}^{-1} \text{ mol}^{-1}$. Notably, given that the proposed mechanism involves two elementary steps – dissociation of the nucleophile followed by outer-sphere attack – the activation parameters represent the sum of the equilibrium value of the initial dissociation step plus the activation value of the rate-determining S_N2 step ($\Delta X^\ddagger_{\text{obs}} = \Delta X^\circ_{\text{diss}} + \Delta X^\ddagger_{\text{SN2}}$, X = H or S).²⁵⁴ Hence, while the relatively small value for $\Delta H^\ddagger_{\text{obs}}$ reflects the overall facility of the reductive elimination, the near-zero value for $\Delta S^\ddagger_{\text{obs}}$ requires the analysis of each elementary step. As such, the dissociation of the nucleophile is predicted to have a large positive ΔS value and the S_N2 attack step is predicted to have a large negative ΔS value,²⁵⁵ which overall would result in a $\Delta S^\ddagger_{\text{obs}}$ value that is small in magnitude. Comparatively, unimolecular inner-sphere reductive elimination or bimolecular outer-sphere attack of a six-coordinate Pd^{IV} complex would both proceed via more ordered transition states which would be expected to have a large negative ΔS^\ddagger value. Notably, small ΔS^\ddagger values ($<10 \text{ cal K}^{-1} \text{ mol}^{-1}$) have previously been observed by Milstein²⁵⁴ and Hartwig²⁵⁶ for Ir-mediated processes involving two elementary steps with opposing values of ΔS .

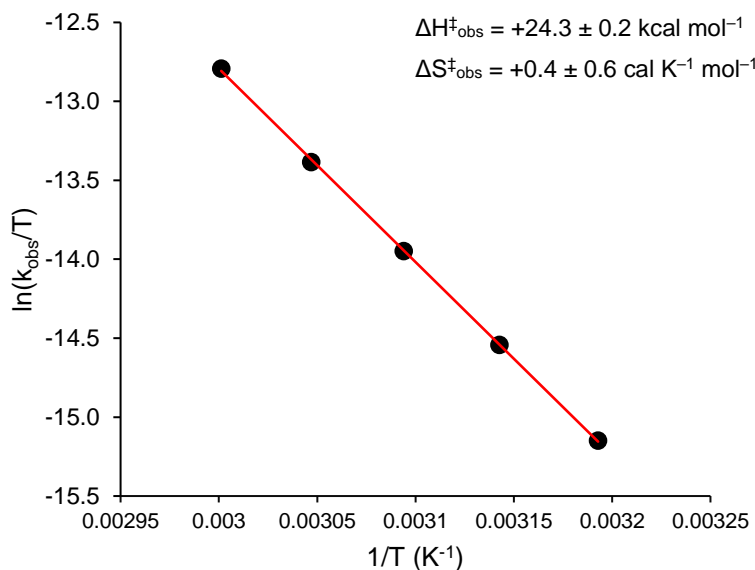


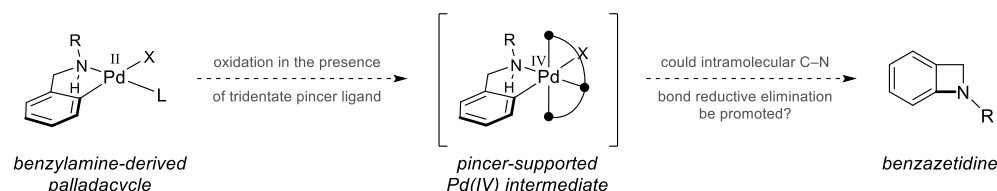
Figure 12. Temperature dependence & determination of activation parameters for the reaction of **370** to oxime **371**: plot of $\ln(k_{\text{obs}}/T)$ versus $1/T$. $T = 40, 45, 50, 55, 60\text{ }^{\circ}\text{C}$; $[\mathbf{370}] = 0.02\text{ M}$ in CD_3CN ; $[\text{unbound } \mathbf{369}] = 0.02\text{ M}$.

4.2.4. Pincer-ligated Aryl Pd^{IV} Complexes: Evidence for Pd^{IV}-mediated C–H Activation

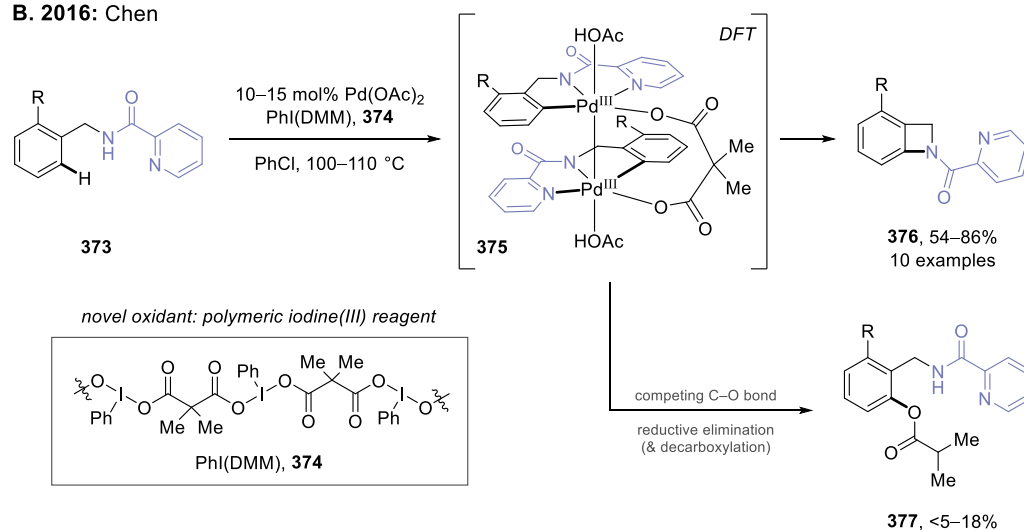
The *OCO*-pincer-supported alkyl Pd^{IV} complexes enabled a range of different C(sp³)–heteroatom bond reductive eliminations to be directly observed to provide diversely functionalized amine and oxime products. While the pincer ligand effectively stabilised the Pd^{IV} centre as a highly electron-donating ligand scaffold, its tridentate meridional coordination mode also kinetically stabilized the high valent complexes by limiting the possibilities for a low energy decomposition pathway arising from coordinative unsaturation. Consequently, we were interested in investigating pincer-stabilized aryl Pd^{IV} complexes derived from cyclopalladated benzylamines. In theory, aromatic palladacycles should additionally stabilize the Pd^{IV} complex by removing the option of a facile nucleophile-mediated outer-sphere reductive elimination pathway given that S_N2 of the activated C(sp²) position is not possible. Therefore, if a stable Pd^{IV} complex containing an *ortho*-cyclometalated benzylamine could be accessed, it was thought that more challenging reductive elimination pathways could be promoted. In particular, we aimed to investigate whether intramolecular C(sp²)–N bond reductive elimination to form a highly strained benzazetidine product was possible from the pincer-supported Pd^{IV} centre (Scheme 99A). Benzazetidines are highly rigid organic molecules with potential application, for example, as novel nitrogen-containing drug scaffolds.^{257–259} However, to date, there are very few methods to access these strained bicycles.^{259–262} In fact, the first practical synthetic method

for the synthesis of benzazetidines was only recently reported in 2016 by Chen,²⁶² who employed an auxiliary-controlled Pd-catalyzed C–H functionalization strategy (Scheme 99B). Benzylamine substrates protected with the picolinamide DG (**373**) were converted to the corresponding benzazetidine products (**376**) in moderate to good yield using a palladium catalyst with a novel polymeric iodine(III) oxidant derived from dimethylmalonic acid, PhI(DMM) (**374**). An acyloxylation product formed from C–O reductive elimination followed by decarboxylation (**377**) was also formed as a minor by-product in the reaction. Computational DFT analysis by Chen²⁶² supported the formation of a dimeric Pd^{III} intermediate (**375**), in which the two high valent Pd centres are bridged by the dimethylmalonate ligand transferred from the oxidant. Given that there is no straightforward reductive elimination pathway of a simple monodentate anionic ligand within intermediate **375**, the challenging intramolecular C–N bond formation is made possible. Although the reaction effectively demonstrated that reductive elimination of a strained benzazetidine product was possible from a high valent Pd centre, the requirement for the picolinamide DG ultimately limits the utility of the reaction. However, the bidentate DG played a crucial role not only in promoting the C–H activation, but also in controlling the selectivity of the reductive elimination. Conversely, methods to control

A. Use pincer-ligated Pd^{IV} complex to promote challenging C–N bond reductive elimination



B. 2016: Chen

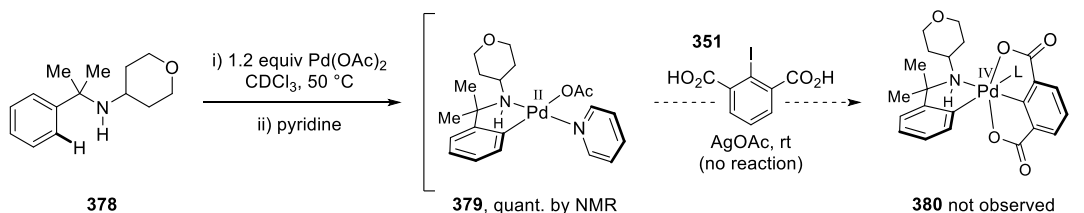


Scheme 99. (a) Benzazetidine formation from cyclopalladated benzylamine. (b) Chen's benzazetidine synthesis.

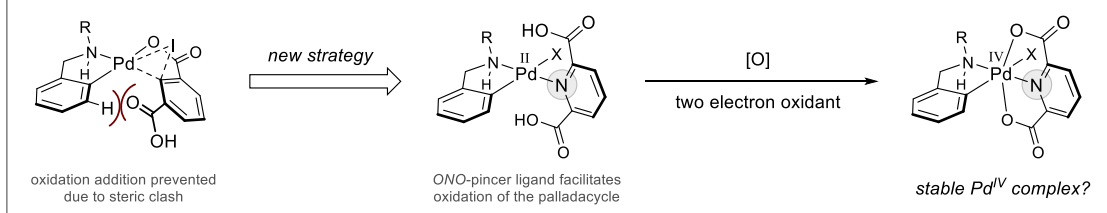
reductive elimination for native functional group-directed transformations remains a significant challenge which we hoped to address in the current study.

Given that a branched benzylic position was thought to provide an additional driving force for promoting cyclization to the benzazetidine, benzylamine **378** containing a benzylic *gem*-dimethyl group was selected for our studies (Scheme 100A). As for the alkyl systems, the pyridine-ligated palladacycle (**379**) was first synthesized from amine **378** using stoichiometric Pd(OAc)₂ and was obtained in quantitative yield by NMR. However, subjecting complex **379** to 2-iodo-1,3-benzenedicarboxylic acid (**351**) with AgOAc gave no conversion to the predicted Pd^{IV} complex (**380**), with the starting palladacycle remaining unreacted. The lack of reactivity was attributed to the greater steric profile of the aromatic palladacycle compared to palladacycles resulting from methyl group activation, leading to a steric clash between the aryl iodide reagent and the backbone of the σ -aryl group that could hinder the carboxylate-assisted oxidative addition (Scheme 100B). Consequently, we proposed to employ a modified pincer ligand containing a neutral pyridine core, namely 2,6-pyridinedicarboxylic acid, which in the presence of a suitable two-electron oxidant could result in the formation of an *ONO*-pincer-supported Pd^{IV} complex. Rather than relying on a carboxylate-assisted oxidative addition, the

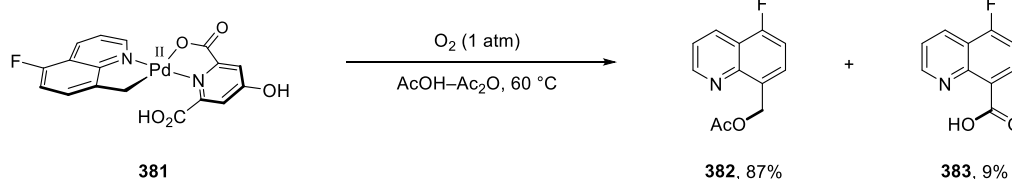
A. Aryl iodide **351** does not react with benzylamine-derived palladacycle



B. Proposal: employ modified *ONO*-pincer to assist oxidation of palladacycle



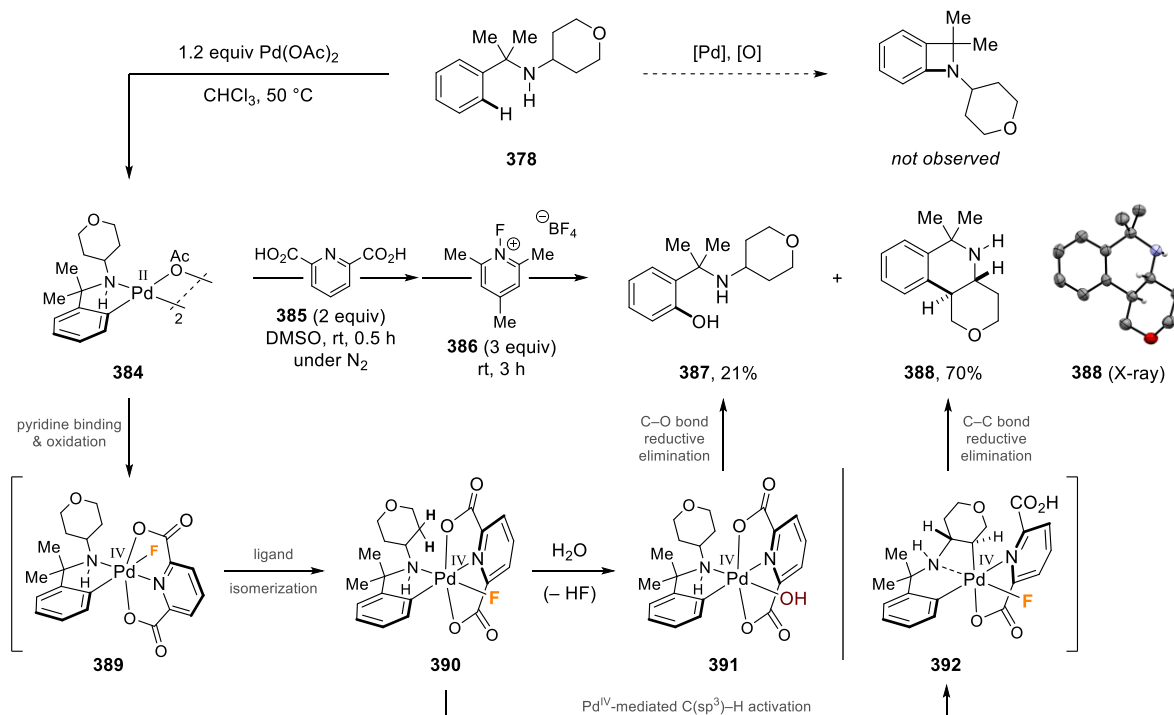
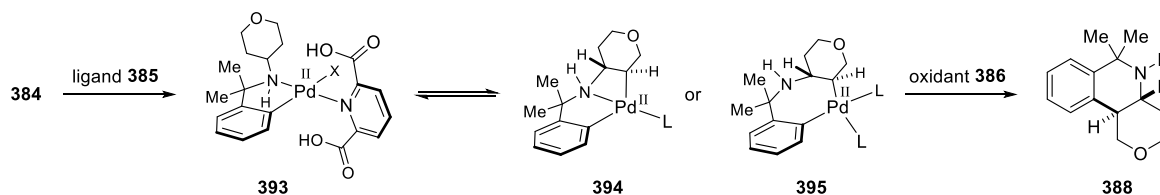
C. 2008: Vedernikov



Scheme 100. (a) Access to an *OCO*-pincer aryl Pd^{IV} complex was unsuccessful. (b) Proposal for a modified *ONO*-pincer ligand. (c) 2,6-Pyridinedicarboxylic acid ligands have been shown to facilitate oxidation.

pyridine-based pincer could potentially coordinate to the Pd^{II} metallacycle to preassemble a reactive conformation in order to assist in the oxidation of the metal centre. The proposed strategy was inspired by work from Vedernikov,²⁶³ who previously showed the effect of 2,6-pyridinedicarboxylic acid ligands in facilitating the oxidation of palladacycles (Scheme 100C). For example, a palladacycle derived from 5-fluoro-8-methylquinoline ligated with 4-hydroxypyridine-2,6-dicarboxylic acid (**381**) was exposed to oxygen under atmospheric pressure in AcOH-Ac₂O solvent at 60 °C. Under these mildly oxidizing conditions, the acetoxylated product (**382**) was obtained in high yield via a putative high valent Pd intermediate,²⁶⁴ along with a minor carboxylic acid product (**383**) formed from competing over-oxidation. Conversely, no reaction was observed in the absence of the pyridine ligand highlighting its essential role in the reaction. Based on this stoichiometric result, a catalytic reaction was developed for benzylic C–H acetoxylation of 8-methylquinoline substrates.²⁶³

Our studies for the *ONO*-pincer strategy employed the acetate-bridged palladacycle dimer **384** as the starting point (formed from **378** and Pd(OAc)₂), which was first subjected to the 2,6-pyridinedicarboxylic acid ligand (**385**) in DMSO for 0.5 h at room temperature before adding an oxidant (Scheme 101A). Highly polar solvent was required to maintain solubility of the palladacycle once bound with the pincer ligand. Upon screening a variety of oxidants, it was found that electrophilic fluorine reagents resulted in high levels of conversion of the palladacycle. For example, *N*-fluoro-2,4,6-trimethylpyridinium tetrafluoroborate (**386**) gave full conversion of the palladacycle after 3 hours at room temperature. However, a stable Pd^{IV} complex was not observed, and instead a mixture of two reductive elimination products was obtained. The minor product was identified as the *ortho*-hydroxylated product (**387**, 21% yield). On the other hand, the major product was identified as having a molecular weight corresponding to the cyclized benzazetidine, though analysis of the isolated compound by NMR revealed that a different structure had formed in which the β-methylene position within the tetrahydropyranyl substituent had undergone activation (**388**, 70% yield). Major product **388** was a crystalline solid allowing for analysis by X-ray crystallography, which revealed its structure as the cyclized hydroisoquinoline resulting from C–C bond formation between the aromatic *ortho*-position and the β-methylene position. Notably, amine **388** was formed as a single diastereomer with a *trans*-junction connecting the hydroisoquinoline and tetrahydropyran ring systems. Although neither a stable Pd^{IV} complex nor a benzazetidine product was observed, the formation of **388** was a highly unusual transformation that warranted further investigation. Crucially, no reaction was observed in the absence of ligand **385**, with the starting palladacycle **384** remaining unreacted in the presence of oxidant **386** alone in DMSO at room temperature.

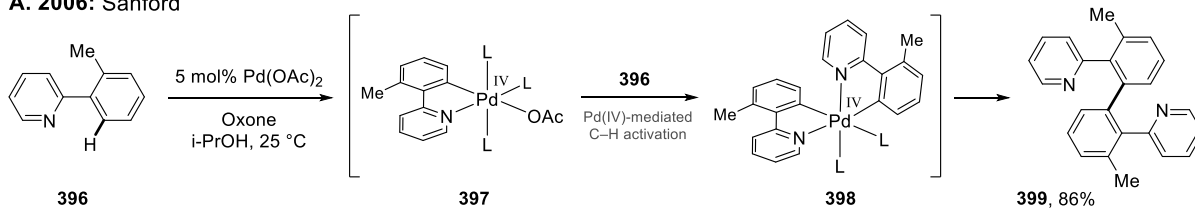
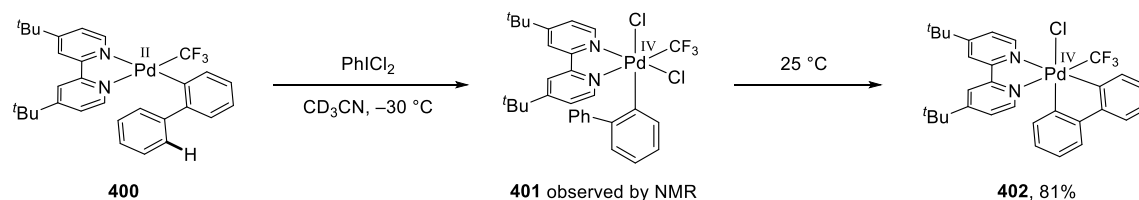
A. Benzazetidine not observed: unexpected formation of hydroisoquinoline product**B. Alternative mechanism:** C(sp³)-H activation at Pd^{II} centre (disfavoured)

Scheme 101. (a) Unexpected formation of hydroisoquinoline, proposed mechanism of formation via Pd^{IV}-mediated β C(sp³)-H activation and (b) alternative mechanism via Pd^{II}-mediated β C(sp³)-H activation.

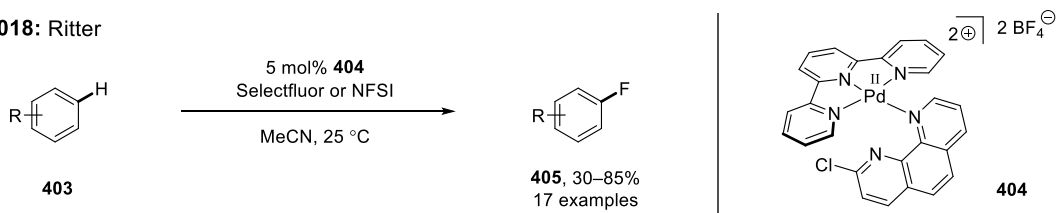
Considering the mechanism of the reaction, it was proposed that binding of the pyridine ligand and oxidation would first give a Pd^{IV} fluoride complex supported by an *ONO*-pincer ligand (**389**, Scheme 101A). Ligand isomerization (**390**) and hydrolysis of the Pd-F bond by trace water would then lead to a Pd^{IV} hydroxide complex (**391**) that could undergo C(sp²)-O bond reductive elimination to give the hydroxylated product **387**. Given that the reaction was conducted in dry DMSO under N₂, the hydrolysis process could be minimized, and instead the Pd^{IV} fluoride complex **390** could potentially undergo a Pd^{IV}-mediated β C(sp³)-H activation to form an intermediate (**392**) capable of promoting C(sp²)-C(sp³) bond reductive elimination to give the hydroisoquinoline **388**. Pd^{IV}-mediated C-H activation is an extremely rare phenomenon, with only a handful of cases being reported in the literature (*vide infra*).⁷² As a result, it is unclear exactly how the C-H activation occurs at the Pd^{IV} centre, though it is

plausible that one of the carboxylate substituents of the *ONO*-pincer acts as an internal base to assist in the C–H bond cleavage.²⁶⁵ Because of the rarity of Pd^{IV}-mediated C–H activation, an alternative mechanism for the formation of **388** could be that the pincer-ligated Pd^{II} complex (**393**) undergoes β C(sp³)–H activation *prior* to oxidation of the palladacycle (Scheme 101B). The Pd^{II}-mediated C–H activation would lead to a strained 5,4-bicyclic palladacycle (**394**) or, if the amine nitrogen dissociates, a seven-membered ring palladacycle (**395**). Oxidation of these palladacycle intermediates could then result in the observed intramolecular C–C bond formation. However, this low valent activation mechanism is disfavoured given that the electron-rich Pd^{II} metallacycle **393** would not be expected to undergo such a challenging methylene C(sp³)–H activation at room temperature. While both of the resulting metallacycles (**394**, **395**) are highly destabilized due to ring strain or the instability of the large ring metallacycle, C–H activation could be imagined to be more readily accommodated at an octahedral Pd^{IV} centre which is not limited to having a co-planar arrangement of ligands as in square planar Pd^{II} complexes. Therefore, although further investigation is required to distinguish between the two proposed mechanisms, the formation of hydroisoquinoline **388** is currently thought to most likely occur via a Pd^{IV}-mediated C–H activation process.

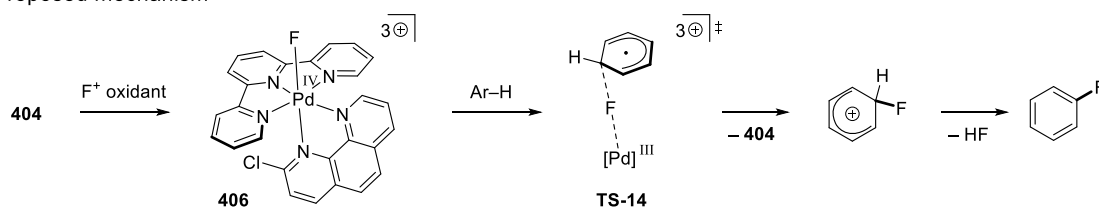
While C(sp³)–H activation has never been directly observed at a Pd^{IV} centre, Pd^{IV}-mediated C(sp²)–H activation has been examined in several studies by Sanford. For example, an early indication of the possibility of high valent C–H activation was reported in 2006²⁶⁶ in a Pd-catalyzed dimerization of 2-phenylpyridine substrates (**396** to **399**, Scheme 102A). The reaction employed Pd(OAc)₂ as catalyst and oxone as the oxidant in alcohol solvent at 25 °C. Mechanistic control experiments indicated that the first C–H activation occurred at a Pd^{II} centre, followed by oxidation (**397**) and a second C–H activation at a Pd^{IV} centre to give a putative bis(cyclometalated) Pd^{IV} complex (**398**) that can undergo C–C bond reductive elimination. Double C–H activation at a Pd^{II} centre was discounted given that a second C–H activation was not detected in deuterium labelling studies using the *ortho*-metalated Pd^{II} complex of **396**. Later, in 2011, Sanford²⁶⁷ conducted an organometallic study reporting the first direct observation of C–H activation at a Pd^{IV} centre (Scheme 102B). A bipyridyl-ligated aryl Pd^{II} complex containing a pendant phenyl group (**400**) was oxidized by PhICl₂ at –30 °C to obtain a Pd^{IV} dichloride intermediate (**401**) which, upon warming to 25 °C, underwent C(sp²)–H activation of the pendant phenyl group to form a stable cyclometalated Pd^{IV} complex (**402**). Notably, a later study²⁶⁵ found that the high valent C–H activation was accelerated in the presence of an acetate ligand, indicating that a carboxylate-assisted C–H activation process analogous to that of Pd^{II}-mediated CMD is also possible at a Pd^{IV} centre.

A. 2006: Sanford**B. 2011: Sanford****Scheme 102.** Sanford's Pd^{IV}-mediated C(sp²)–H activation: (a) a catalytic reaction & (b) organometallic study.

Another noteworthy example of high valent Pd-mediated C–H activation was the non-directed Pd-catalyzed aromatic C–H fluorination reported by Ritter²⁶⁸ in 2018 (Scheme 103). The reaction employed a specifically designed dicationic Pd^{II} complex as catalyst (**404**) in combination with electrophilic fluorine reagents (Selectfluor or NFSI) to enable the direct fluorination of arene substrates (**403**) to fluorinated derivatives (**405**). Significantly, the reaction was also effective for the late stage fluorination of several drug molecules, thus showing the potential utility of the transformation. The proposed mechanism involved initial oxidation of the dicationic Pd^{II} catalyst (**404**) to form a tricationic Pd^{IV} fluoride complex (**406**). Based on prior mechanistic studies,²⁶⁹ the Pd^{IV} complex **406** was proposed to mediate an outer-sphere fluoride-coupled electron transfer event (**TS-14**) to transfer the fluoride ligand to the arene substrate and reform the Pd^{II} complex **404**. Crucially, in contrast to Sanford's studies, no

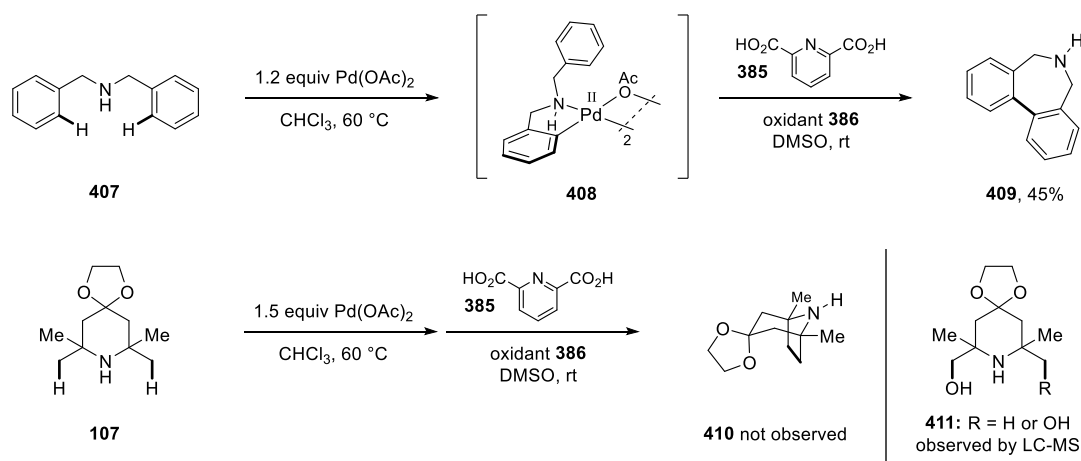
2018: Ritter

Proposed mechanism

**Scheme 103.** Ritter's C(sp²)–H fluorination and the proposed high valent Pd outer-sphere C–H activation.

organometallic intermediate resulting from C–H activation was invoked in the proposed outer-sphere mechanism. Therefore, while Ritter's mechanism seems less relevant for the current work involving a proposed alkyl C(sp³)–H activation at a high valent Pd centre, the ability of Pd^{IV} fluoride complexes to promote unusual one-electron functionalization processes cannot be ruled out as a potential reaction pathway.

The scope of the Pd^{IV} *ONO*-pincer chemistry was briefly explored using substrates that would potentially undergo two sequential C(sp²)–H activations or two C(sp³)–H activations (Scheme 104). Firstly, the acetate-bridged palladacycle dimer of dibenzylamine was synthesized (**407** to **408**). Subjecting complex **408** to ligand **385** and oxidant **386** in DMSO at room temperature, pleasingly the desired dihydro-dibenzazepine product (**409**) was formed in 45% yield, potentially as a result of a second *ortho* C(sp²)–H activation at a Pd^{IV} centre followed by C–C bond reductive elimination. Secondly, a tetramethylpiperidine substrate (**107**), known to undergo efficient β C(sp³)–H activation to form a four-membered palladacycle,¹⁴⁶ was subjected to stoichiometric Pd(OAc)₂ followed by the addition of reagents **385** and **386**. In this instance, the second C–H activation to form bicyclic amine product **410** was not observed and, instead, mono- and di-hydroxylated products (**411**) were observed by LC-MS analysis of the crude reaction mixture, along with protodemetalation of the palladacycle to reform starting amine **107**. However, it was possible that the use of a cyclic piperidine starting material did not allow for sufficient conformational flexibility for the second C–H activation to take place. Nonetheless, while the all-alkyl system was unreactive in the current example, the fact that the cyclized product was observed for dibenzylamine indicates that the reaction is not specific to a single palladacycle and could potentially enable the modification of a broad range of benzylamines. Further studies into this novel transformation are required to provide a clearer



Scheme 104. Testing the Pd^{IV}-mediated C–H activation on dibenzylamine and tetramethylpiperidine substrates.

picture of the mechanism and scope of the reaction, as well as provide information that could aid in the design of a catalytic process exploiting this reactivity mode.

4.3. Summary

The current chapter disclosed the synthesis and reactivity of stable alkyl Pd^{IV} complexes derived from cyclopalladated amines and oximes. Stable aminoalkyl Pd^{IV} complexes were synthesized from pyridine-ligated Pd^{II} metallacycles derived from secondary amines by employing an aryl iodide reagent containing two *ortho*-carboxylic acid groups. The oxidation reactions occurred at room temperature by a carboxylate-assisted oxidative addition process that resulted in the formation of Pd^{IV} complexes supported by an *OCO*-pincer ligand. Two aminoalkyl Pd^{IV} complexes were synthesized with varying degrees of substitution along the backbone of the activated amine. For the Pd^{IV} complex containing a fully substituted β *gem*-dimethyl group, intramolecular C–N bond reductive elimination was favoured to form the azetidine product. Conversely, the Pd^{IV} complex containing a mono-substituted β -position within the activated amine had a lower tendency to cyclize but instead could be intercepted by various *O*- and *N*-nucleophiles to form diversely γ -functionalized amine products. Notably, a side product resulting from β -H elimination was observed in the nucleophile-promoted reductive elimination reactions, with the extent of the side reaction correlating with the basicity of the added nucleophile. Consequently, the Pd^{IV} complexes provided crucial insight into the different factors affecting the efficiency and selectivity of reductive elimination of functionalized aliphatic amines, which has important implications for the design of novel catalytic processes in the context of Pd^{II}/Pd^{IV}-catalyzed functionalization of aliphatic amines.

While the amine-derived Pd^{IV} complexes were not suitable for conducting a detailed study of the mechanism of reductive elimination due to competing side reactions and the complexity of the NMR spectra, an analogous oxime-derived Pd^{IV} complex provided a more straightforward test case. Subjecting an acetonitrile-ligated oxime Pd^{IV} complex to tetrabutylammonium *p*-nitrophenoxide as nucleophile resulted in displacement of the acetonitrile for the nucleophile and the formation of an anionic Pd^{IV} complex. Heating the nucleophile-bound Pd^{IV} complex led to quantitative reductive elimination of the C–O coupled product. Kinetic experiments provided evidence for rapid and reversible nucleophile dissociation and the formation of a neutral five-coordinate or solvent-ligated Pd^{IV} complex prior to C–O bond reductive elimination by outer-sphere S_N2 attack of the oxyanion nucleophile.

Finally, the formation of a stable aryl Pd^{IV} complex was investigated by the oxidation of a cyclopalladated secondary benzylamine substrate bearing an *N*-tetrahydropyranyl group. Significantly, while 2-iodo-1,6-benzenedicarboxylic acid was unreactive with the benzylamine-derived palladacycle, a different approach employing 2,6-pyridinedicarboxylic acid as an *ONO*-pincer ligand in combination with an *N*-fluoropyridinium oxidant was found to give full conversion of the palladacycle at room temperature. Unexpectedly, a cyclized hydroisoquinoline product was obtained resulting from the dehydrogenative C–C coupling between the benzylamine *ortho*-position and the β -position of the pendant tetrahydropyranyl substituent within the aliphatic amine. The reaction was proposed to occur by a Pd^{IV}-mediated β C(sp³)–H activation, though further studies are required to confirm this mechanistic proposal. Notably, under the same conditions, the palladacycle derived from dibenzylamine reacted in an analogous manner to form a cyclized dihydro-dibenzazepine product, indicating the potential generality of the novel high valent Pd-mediated transformation.

5. Conclusions & Outlook

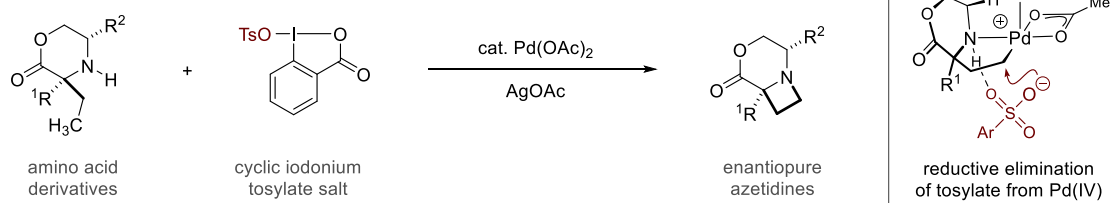
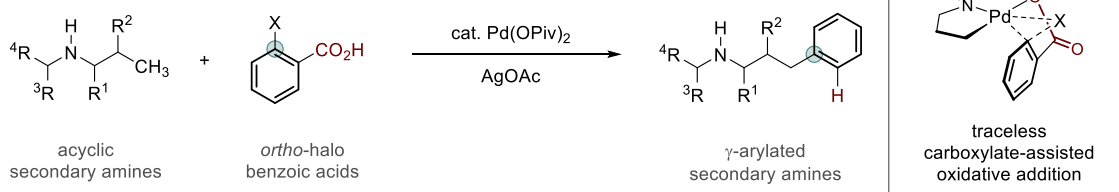
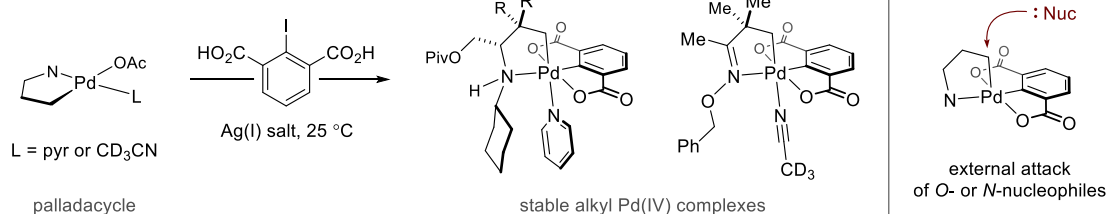
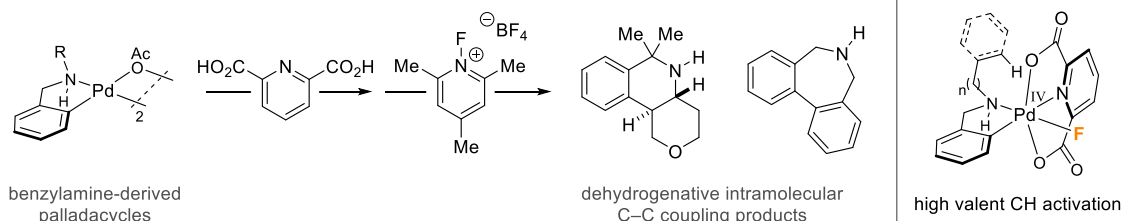
Pd-catalyzed directed C(sp³)-H functionalization has been a focus of research in synthetic organic chemistry for nearly two decades and has enabled a diverse range of functional group incorporations across numerous substrate classes, including carboxylic acids, carbonyl compounds, amines, and their derivatives. Within this context, native amine-directed C(sp³)-H functionalization has provided a direct method of accessing functionalized aliphatic amines without the requirement for directing groups or directing group additives by exploiting the innate coordinating ability of the amine nitrogen to promote cyclometalation. Although the early work in this area focused on the functionalization of hindered, cyclic secondary amines, significant advances were made in the discoveries of a Pd-catalyzed β -C(sp³)-H carbonylation process to form β -lactams and the γ -arylation of tertiary aliphatic amines using a mono-*N*-protected amino acid ligand, both of which showed significantly improved substrate scopes relative to the original work using the native amine-directed strategy. Nonetheless, a fundamental limitation to these broader scoping catalytic reactions was that they were limited to C-C bond forming processes, and thus C-heteroatom bond formations remained limited to reactions employing hindered cyclic amines.

An effective strategy to install heteroatomic functional groups had been to utilize the facile reductive elimination chemistry of Pd^{IV} complexes formed by the oxidation of the amine-directed Pd^{II} metallacycle. However, the formation of aminoalkyl Pd^{IV} intermediates typically required the use of strong and indiscriminate oxidants that are only compatible with extremely hindered amines with fully substituted α and α' centres adjacent to the amine nitrogen. As such, there was no mild and selective method for accessing Pd^{IV} complexes in the context of native amine-directed C-H functionalization using less substituted aliphatic amine substrates. Furthermore, in the absence of a directing group auxiliary that can be modified to alter the efficiency and selectivity of reductive elimination from high valent intermediates, the selectivity of product-forming reductive elimination for native amine functionalization had largely been substrate dependent and often gave undesired product mixtures through multiple competing reductive elimination processes. Consequently, the discovery of a reagent or ligand to control the selectivity of reductive elimination from aminoalkyl Pd^{IV} complexes remained a significant unmet challenge.

The current work aimed to address the aforementioned shortcomings in the native amine-directed strategy, in particular, with the primary objective of uncovering new and general methods for accessing Pd^{IV} chemistry. The first project that was discussed involved

intramolecular γ C(sp³)–H amination to form strained four-membered ring azetidines and employed a cyclic iodine(III) tosylate reagent as a novel oxidant in Pd-catalyzed C–H functionalization. The reaction was initially developed for the functionalization of hindered morpholinone substrates as a novel approach for promoting cyclization from a five-membered ring aminoalkyl palladacycle over other competing pathways such as γ -acetoxylation. Given the facility of C–O bond forming processes from the oxidation of the five-membered palladacycle via outer-sphere reductive elimination pathways, the high selectivity for cyclization to the azetidine was achieved by using an oxidant that transferred a tosylate leaving group to the amine that would lead to spontaneous cyclization, rather than aiming for a direct C–N bond reductive elimination that was prohibitively high in energy. However, the current work found that the cyclic iodine(III) tosylate oxidant was sufficiently mild such that it could tolerate morpholinone substrates derived from chiral amino acid starting materials that contained an α -H substituent – a class of substrate that was readily decomposed in the presence of a previously employed iodine(III) oxidant, PhI(OAc)₂ (Scheme 105A). The resulting azetidine formation for the chiral substrates occurred with high diastereoselectivity to provide diastereo- and enantiopure azetidine derivatives. Although the oxidant had improved compatibility with secondary amine substrates, acyclic amines were functionalized in low yields, which was attributed to the lower reactivity of the aminoalkyl palladacycles formed from these substrates relative to those derived from cyclic morpholinones. Therefore, while the scope of the high valent Pd^{II}/Pd^{IV} catalysis was slightly improved to include chiral morpholinone substrates, a general method to access Pd^{IV} intermediates was yet to be discovered.

Following the intramolecular γ C(sp³)–H amination process, it was serendipitously discovered that an aryl iodide reagent bearing an *ortho*-carboxylic acid group led to a facile carboxylate-assisted oxidative addition of five-membered ring palladacycles formed from the γ -methyl activation of acyclic secondary amines. In the presence of a Ag^I additive, decarboxylative C–C bond reductive elimination occurred to furnish γ -arylated products, with mechanistic control studies supporting a novel mechanism involving decarboxylation at a Pd^{IV} centre. Conversely, the absence of a Ag^I salt led to a complete switch in the selectivity of reductive elimination to give C–O coupled products resulting from the external nucleophilic attack of the activated γ -position within the Pd^{IV} intermediate by 2-iodobenzoate or acetate as *O*-centred nucleophiles. Crucially, the intramolecularization of the oxidation process enabled the weakly oxidizing aryl iodide reagent to be an efficient oxidant that was completely selective for the metal centre over the amine substrate, allowing the oxidant to be employed in a catalytic scenario in which the unprotected amine was present in stoichiometric quantities. Accordingly,

A. Intramolecular C(sp³)-H amination of hindered secondary amines to azetidines

B. C(sp³)-H arylation of secondary amines by carboxylate-assisted oxidative addition

C. Stable Pd^{IV} complexes: diverse γ -functionalization by external nucleophilic attack

D. Pd^{IV}-mediated C(sp³)-H & C(sp²)-H activation from cyclopalladated benzylamines


Scheme 105. Key research findings: (a) enantiopure azetidine synthesis, (b) decarboxylative γ C-H arylation by carboxylate-assisted oxidative addition & (c) synthesis of stable alkyl Pd^{IV} complexes derived from cyclometalated amines and oximes. (d) Evidence for Pd^{IV}-mediated C-H activation.

a Pd-catalyzed reaction was developed for the decarboxylative γ C(sp³)-H arylation process, wherein it was found that the optimal conditions involved the use of 2-bromobenzoic acid reagents rather than 2-iodobenzoic acids (Scheme 105B). A wide range of substituted 2-bromobenzoic acids were tolerated in the reaction and the scope of secondary aliphatic amines included substrates with a variety of different spectating functional groups, demonstrating the excellent functional group tolerance of high valent Pd^{II}/Pd^{IV} catalysis. However, a drawback of the reaction was that amine substrates required branching along the chain undergoing C-H activation at both the α and β positions in order for efficient reactivity to be achieved, indicating

the low efficiency of γ C–H activation for less hindered amines under the reaction conditions. Nonetheless, the facile mode of palladacycle oxidation was an important advance in high valent Pd-catalyzed amine functionalization and represented a potentially general method of accessing Pd^{IV} chemistry within this context. Furthermore, subsequent studies that exchanged the *ortho*-carboxylic acid for an acyl sulfonamide group again changed the selectivity of reductive elimination to give azetidine products, showing the versatility of the *ortho*-DG-assisted oxidative addition in being able to mediate both C–C as well as different C–heteroatom bond-forming reductive elimination processes.

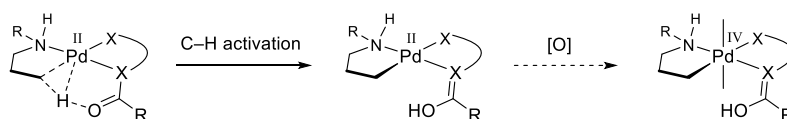
The final project concerned the synthesis of a new class of alkyl Pd^{IV} complexes derived from cyclopalladated aliphatic amines and oximes (Scheme 105C). Transiently formed Pd^{IV} complexes have frequently been invoked as catalytic intermediates in Pd-catalyzed C–H functionalization reactions, but there are sparingly few examples where the Pd^{IV} intermediate has been directly observed. Moreover, in the case of the native amine-directed strategy, a Pd^{IV} complex resulting from the oxidation of a cyclopalladated aliphatic amine had never been observed. Consequently, we were interested in isolating an example of an aminoalkyl Pd^{IV} complex to gain information about the structure and reactivity of these important yet elusive intermediates. An aryl iodide reagent containing two *ortho*-carboxylic acid groups was employed, leading to a carboxylate-assisted oxidative addition wherein the resulting Pd^{IV} intermediate was captured by the second carboxylate substituent to form an *OCO*-pincer-ligated Pd^{IV} complex. A pair of aminoalkyl Pd^{IV} complexes were synthesized that were stable at room temperature in the solid state and in solution. The amine-derived complexes differed in their substitution patterns at the β -position of the activated alkyl chain of the amine, one with *gem*-dimethyl substitution and one with ethyl and hydrogen substituents, which allowed for several different reductive elimination pathways to be investigated, including C–O and C–N bond reductive eliminations as well as β -hydride elimination from a Pd^{IV} centre. Additionally, the intimate mechanism of C–O bond reductive elimination was elucidated using an analogous oxime-derived alkyl Pd^{IV} complex, which confirmed that an outer-sphere S_N2 attack mechanism, commonly observed for high valent Group 10 transition metals, was indeed operative for the *OCO*-pincer ligated complexes. Following the use of the *OCO*-pincer ligand to stabilize the Pd^{IV} centre, the analogous *ONO*-pincer ligand containing a pyridine core was utilized in an attempt to stabilize high valent benzylamine-derived aromatic palladacycles that were unreactive to carboxylate-assisted oxidative addition. However, upon subjecting benzylamine-derived Pd^{II} metallacycles to 2,6-pyridinedicarboxylic acid as ligand and an electrophilic fluorine reagent as a two-electron oxidant, rather than obtaining a pincer-stabilized

aryl Pd^{IV} complex, an unexpected dehydrogenative C–C coupling process was observed to form cyclized products (Scheme 105D). The reactions were proposed to proceed by a second C–H activation event at a Pd^{IV} centre, with the transformation being demonstrated for both a C(sp²)–C(sp³) coupling and for a C(sp²)–C(sp²) coupling. While further investigation into the reaction scope and mechanism is required, unprecedented Pd-mediated reactivity had been discovered under stoichiometric conditions in which a pendant alkyl or aromatic group of a cyclopalladated benzylamine undergoes a C–H activation process under oxidative conditions leading to an intramolecular C–C coupling.

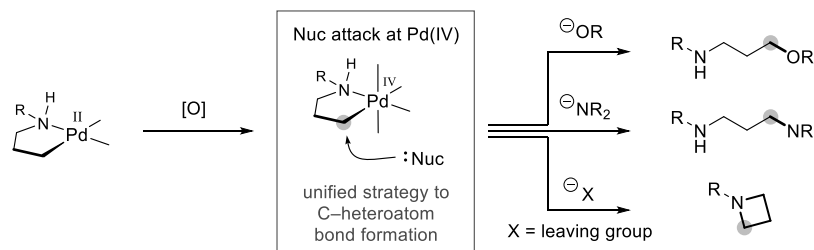
The conclusions drawn from the current work highlight several avenues for future work. Firstly, while the catalytic reactions that were developed led to progress in the scope of aliphatic amines that could be efficiently functionalized under high valent Pd^{II}/Pd^{IV} catalysis, particularly in the case of acyclic secondary amines for the decarboxylative γ C–H arylation process, a notable limitation was that a high degree of branching along the alkyl chain was still required for γ C–H activation to take place under catalytic conditions, with less substituted substrates beyond a certain limit undergoing no reaction or decomposition. Significantly, this limit to the reaction scope indicated the point at which the carboxylate ligand-mediated C–H activation started to be outcompeted by undesired processes such as bis(amine) complex formation or β -hydride elimination, which could not be effectively controlled by simple carboxylate ligands around the Pd^{II} centre. Directing group auxiliaries were originally developed exactly for the purpose of ensuring more efficient cyclometalation, though this strategy represents the antithesis of the native functional group-directed approach and thus does not hold the solution. On the other hand, more recently, ligands that can facilitate the C–H activation step have been developed and have been used both in auxiliary-controlled as well as native functional group-directed transformations to improve the catalyst efficiency.^{59,65} Typically, these ligands mimic the action of the carboxylate ligand as the internal base in the Pd^{II}-mediated CMD mechanism and lead to improved reactivity by having increased basicity relative to carboxylates, with prominent examples including mono-*N*-protected amino acids and pyridone ligands. Moreover, our group recently reported the Pd-catalyzed γ C(sp³)–H arylation of tertiary amines using an MPAA ligand with boronic acid coupling partners,¹⁶¹ demonstrating the feasibility of incorporating ligand assistance into the native amine-directed strategy. However, thus far, ligands have not been successfully incorporated into a high valent Pd^{II}/Pd^{IV}-catalyzed process for amine functionalization. Therefore, a key objective for future work would be to screen for ligands which can assist in the C–H activation in the presence of, for example, *ortho*-DG-containing aryl halide reagents which have been developed in the current work, in order to

facilitate cyclopalladation while still maintaining the facile mode of palladacycle oxidation (Scheme 106A). Alternatively, a ligand or oxidizing reagent could be developed comprising features that would facilitate both cyclopalladation and oxidation in a single component. If solved, the development of a truly general $\text{Pd}^{\text{II}}/\text{Pd}^{\text{IV}}$ -catalyzed amine functionalization would enable the regioselective late-stage installation of polar heteroatomic functional groups into complex amines such as drugs or drug fragments that is not possible with current synthetic methods.

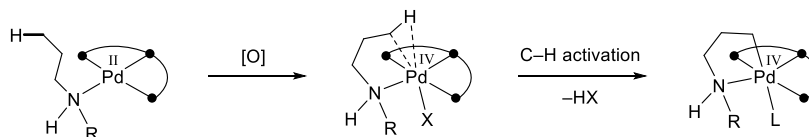
A. Development of ligand compatible with $\text{Pd}^{\text{II}}/\text{Pd}^{\text{IV}}$ catalysis



B. Diverse nucleophile-mediated reductive elimination from a Pd^{IV} centre



C. High valent Pd^{IV} -mediated directed $\text{C}(\text{sp}^3)\text{-H}$ activation



Scheme 106. Future work for the development of $\text{Pd}^{\text{II}}/\text{Pd}^{\text{IV}}$ -catalyzed C–H functionalization of amines.

Secondly, regarding the scope of C–heteroatom bond-forming processes, to date, C–H functionalization methods have generally focused on developing individual transformations that install one type of heteroatomic functional group, such as acetoxylation or intramolecular amination, and therefore are limited to relatively few types of groups that can be incorporated. Conversely, methods such as Pd-catalyzed C–heteroatom cross-couplings or allylic substitution reactions can incorporate a diverse range coupling partners to form a much broader range of products. Pd-catalyzed C–H functionalization has, to some extent, addressed this matter by using $\text{Pd}^{\text{II}}/\text{Pd}^{\text{IV}}$ catalysis to install a leaving group²⁷⁰ or form a strained ring intermediate^{146,271} that can subsequently be reacted with a nucleophile of choice as part of separate step. In fact, in the context of the native amine-directed approach, this strategy was exploited in the

intramolecular β C(sp³)–H amination process to form aziridines,¹⁴⁶ which could be ring-opened with nucleophiles to form β -functionalized derivatives. However, despite being a seminal contribution, this strategy is not considered as a general solution for diverse heteroatom incorporation into amine substrates given that (i) β C(sp³)–H activation is currently limited to extremely hindered tetramethylpiperidine or morpholinone substrates, and (ii) for γ C(sp³)–H functionalization, installation of a leaving group and cyclization would lead to a four-membered ring azetidine product that would be poorly reactive towards nucleophilic ring-opening reactions. Therefore, as was explored in the organometallic studies of stable aminoalkyl Pd^{IV} complexes, a potential solution could be to intercept high valent Pd^{IV} intermediates with external nucleophiles as part of a unified catalytic approach that exploits the facility of outer-sphere reductive elimination processes from alkyl Pd^{IV} complexes (Scheme 106B). Given the availability of nucleophilic coupling partners and the robustness of outer-sphere S_N2-type reactivity, a much wider range of products could be obtained than would be possible via individually optimized C–heteroatom bond formations. Nonetheless, for this strategy to be successful, a novel catalyst would likely be required that does not contain a labile and nucleophilic ligand such as a carboxylate which could lead to a competing and potentially undesired C–O bond reductive elimination and thus product mixtures. Consequently, an alternative, albeit less precedented, strategy could be to use a sacrificial oxidant to promote a Pd^{IV}-mediated C–H activation to form a high valent cyclometalation complex which could then undergo the nucleophile-mediated reductive elimination. Though further investigation is required, the current work has highlighted the potential for a Pd^{IV} centre to mediate both alkyl as well as aromatic C–H activation of amine substrates. Overall, although the development of a diverse C–heteroatom bond-forming functionalization remains a relatively distant target, the achievement of such an objective would significantly advance the scope and utility of C–H functionalization processes.

Thirdly and finally, as was alluded to before, C–H activation at a high valent Pd^{IV} centre remains a frontier of research in the field of Pd-catalyzed C–H functionalization.⁷² In parallel to developing ligands that facilitate C–H activation at a Pd^{II} centre, an alternative option is to develop ligands that promote the formation of Pd^{IV} intermediates prior to activation, with the more Lewis acidic and reactive Pd^{IV} centre being used to facilitate the C–H bond cleavage (Scheme 106C). Currently, Pd^{IV}-mediated C–H activation has not been exploited in a Pd-catalyzed C(sp³)–H functionalization reaction. In terms of aliphatic amine functionalization, future work in this area should build on the current findings employing pincer ligands and aim to develop well-defined organometallic systems which would allow for the efficiency,

selectivity and mechanism of the oxidative C–H activation to be studied in greater detail. Meanwhile, development of catalytic systems could be conducted by screening different combinations of chelating ligands and oxidants in the presence of various amine substrates in order to discover novel high valent transformations. If successful, the development of catalytic processes involving Pd^{IV}-mediated C(sp³)–H activation would establish a new class of reaction in the field directed C–H functionalization with a complementary mode of reactivity that could afford new opportunities for amine functionalization.

6. Experimental

6.1. General Information

NMR spectra were recorded in deuterated solvents using a Bruker AM 400 (400 MHz) or Avance 500 (500 MHz) at 298 K (unless otherwise stated). Chemical shifts (δ) are reported in parts per million (ppm) relative to tetramethylsilane. Signals were referenced to the residual solvent peak (CHCl_3 at 7.26 and 77.16 ppm, DMSO at 2.50 and 39.52 ppm, MeOD at 3.31 and 49.00 ppm, CD_3CN at 1.94 and 118.26 ppm and $(\text{CD}_3)_2\text{CO}$ at 2.05 and 29.84 ppm for ^1H and ^{13}C NMR respectively). Coupling constants are reported in Hertz (Hz). Abbreviations for splitting patterns are as follows: s, singlet; d, doublet; t, triplet; q, quartet; m, multiplet; br., broad. Where coincident coupling constants have been observed, the apparent (app.) multiplicity of the proton resonance has been reported. Spectra were analysed using Bruker TopSpin software and kinetic experiments were processed using Bruker Dynamics Center. For novel compounds, proton and carbon assignments were deduced using 2D NMR methods (COSY, DEPT-135, HSQC, HMBC and NOESY). Note: diastereotopic protons located on the same carbon atom are labelled, for example, **1-H_a**, **1-H_b** (arbitrarily unless known). Diastereotopic carbons are labelled (arbitrarily unless known) for example **1**, **1'** etc., where **1'** and **2'** are located on the same diastereotopic face. For a mixture of two diastereomers, assignments are labelled as **1**, **2**, **3** and **1***, **2***, **3*** etc. to denote the signals of each diastereomer. ^1H NMR analysis of crude reaction mixtures was determined with reference to 1,1,2,2-tetrachloroethane as an internal standard.

High-resolution mass spectra (HRMS) were measured on a Micromass Q-TOF spectrometer or Waters XEVO GII-S Q-TOF spectrometer at the Department of Chemistry, University of Cambridge or on a Thermo Scientific LTQ Orbitrap XL at the EPSRC Mass Spectrometry Service, University of Swansea. Infrared (IR) spectra were recorded on a Perkin Elmer 1FT-IR Spectrometer or Thermo Fisher Nicolet Summit PRO FTIR Spectrometer as solids or films, either through direct application or deposited as solutions in CHCl_3 , with absorptions reported in wavenumbers (cm^{-1}). Melting points (m.p.) were recorded using a Gallenkamp melting-point apparatus and are reported uncorrected. Optical rotations were measured on a Perkin Elmer 343 Polarimeter using a sodium lamp (λ 589 nm, D-line). X-ray crystallography was performed on a Nonius Kappa CCD or Bruker D8-QUEST PHOTON-100 at the University of Cambridge Chemistry X-ray Laboratory (by Dr. Andrew Bond). Elemental analysis was obtained using a Perkin Elmer 240 Elemental Analyzer (by Stephen Young).

Tetrahydrofuran, toluene, hexane, diethyl ether, acetonitrile and dichloromethane were dried and distilled using standard methods (Perrin, D. D.; Armarego, W. L. F. *Purification of Laboratory Chemicals*; Pergamon Press: Oxford, 1997). For Pd-catalyzed reactions, chloroform purchased from Sigma Aldrich was used (anhydrous, stabilised with 0.5–1% EtOH; filtered through basic alumina before use). Pd(OAc)₂ (Pd 45.9–48.4%, needles), Pd(OPiv)₂ and AgOAc (anhydrous, 99%) were purchased from Alfa Aesar. All commercial reagents were purchased at the highest quality and used without further purification.

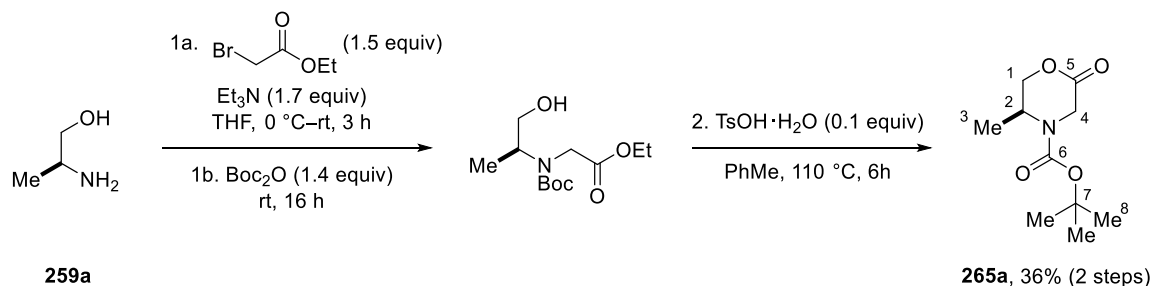
Unless otherwise stated, all reactions were carried out in oven-dried glassware under nitrogen atmosphere. Pd-mediated or -catalysed reactions were conducted in glass microwave vials with PTFE/silicone septa. All other reactions, unless otherwise stated, were conducted in round-bottomed flasks with rubber septa. Syringes were used to transfer air- and moisture-sensitive chemicals between reaction vessels. TLC was performed using E. Merck silica gel 60 F254 pre-coated plates (0.25 mm) and visualised under UV light (254 nm) and KMnO₄ staining. GC-MS analysis was carried out using a Shimadzu QP2010-SE fitted with a BPX5 column (10 m, 0.1 mm, 0.1 µm film). LC-MS analysis was carried out using a Shimadzu LCMS-2020. Purification by column chromatography used Merck Flash Silica Gel 60 (230–400 mesh). Isolute SCX-2 resin was purchased from Biotage.

6.2. Experimental Procedures

6.2.1. Pd-catalyzed γ C(sp³)-H Amination to form Azetidines

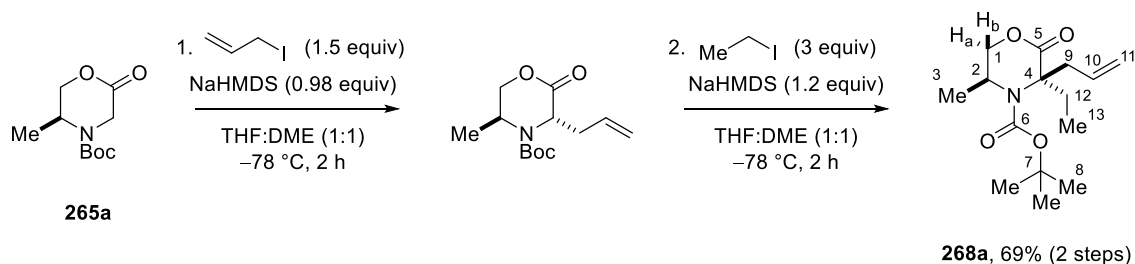
Representative Example of Chiral Morpholinone Synthesis

tert-Butyl (S)-5-methyl-2-oxomorpholine-4-carboxylate (**265a**)



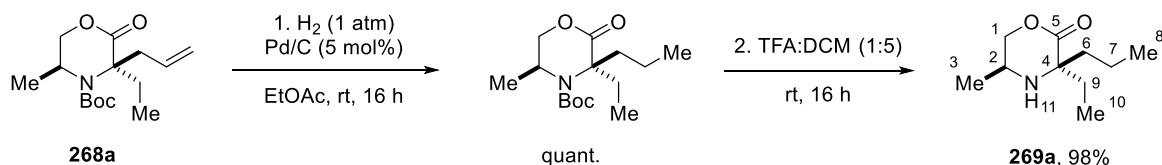
To a solution of L-alaninol (**259a**, 3.76 g, 50 mmol, 1 equiv) and triethylamine (12 mL, 85 mmol, 1.7 equiv) in THF (100 mL) at 0 °C was added ethyl bromoacetate (12.53 g, 75 mmol, 1.5 equiv) dropwise. The reaction was warmed to room temperature with stirring for 3 h. The resulting suspension was re-cooled to 0 °C, filtered and the solids washed with cold THF (100 mL). Di-*tert*-butyl dicarbonate (15.3 g, 70 mmol, 1.4 equiv) was added to the combined filtrates and stirred at room temperature overnight. The solvent was removed *in vacuo* and the crude residue dissolved in toluene (250 mL) before washing with sat. aq. NaHCO₃ and brine (100 mL each). The organic phase was separated, dried over MgSO₄ and filtered.

p-Toluenesulfonic acid monohydrate (950 mg, 5 mmol, 0.1 equiv) was added to the solution in toluene (diluted to 0.5 L total volume) and heated under reflux using Dean–Stark apparatus for 6 h. After cooling to room temperature, the reaction mixture was washed with water (100 mL) and the organic phase separated, dried over MgSO₄, filtered and evaporated. The crude material was purified by silica gel flash chromatography (10–30% ethyl acetate in hexanes) to give the title compound as a colourless solid (**265a**, 3.84 g, 17.8 mmol, 36% yield over 2 steps). **M.p.** 82–84 °C; lit.²⁷² 85–86 °C. $[\alpha]_D^{25.0} +1.0^\circ$ (*c* 1.0, CHCl₃); lit.²⁷² $[\alpha]_D^{25.0} +6.96^\circ$ (*c* 2.21, CHCl₃). **¹H NMR** (400 MHz, CDCl₃) δ 4.43 (dd, *J* = 11.6, 3.4 Hz, 1H, **1-H_a**), 4.31 – 4.11 (m, 3H, **1-H_b**, **2**, **4-H_a**), 4.05 (d, *J* = 18.7 Hz, 1H, **4-H_b**), 1.46 (s, 9H, **8**), 1.26 (d, *J* = 6.6 Hz, 3H, **3**). **¹³C NMR** (101 MHz, CDCl₃) δ 167.4 (**5**), 153.5 (**6**), 81.4 (**7**), 71.3 (**1**), 45.5 (**2**), 43.8 (**4**), 28.5 (**8**), 15.9 (**3**). **IR** (neat, cm⁻¹) 2975, 1749, 1684, 1414, 1387, 1363, 1240, 1198, 1156, 1101, 1042, 870, 769. **HRMS** *m/z* (ESI) calcd for C₁₀H₁₈N₁O₄ [*M*+*H*]⁺ 216.1230, found 216.1231.

***tert*-Butyl (3*R*,5*S*)-3-allyl-3-ethyl-5-methyl-2-oxomorpholine-4-carboxylate (**268a**)**

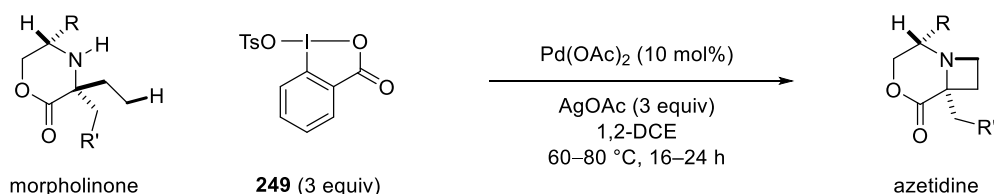
To a solution of *tert*-butyl (*S*)-5-methyl-2-oxomorpholine-4-carboxylate (**265a**, 1.08 g, 5 mmol, 1 equiv) in THF:DME (1:1, 10 mL) at $-78\text{ }^{\circ}\text{C}$ was added NaHMDS (2 M in THF, 2.45 mL, 4.9 mmol, 0.98 equiv) dropwise. After stirring at $-78\text{ }^{\circ}\text{C}$ for 0.5 h, neat allyl iodide (1.26 g, 7.5 mmol, 1.5 equiv) was added dropwise. The reaction was stirred at $-78\text{ }^{\circ}\text{C}$ for a further 2 h before being quenched at $-78\text{ }^{\circ}\text{C}$ with sat. aq. NH_4Cl (10 mL) and warming to room temperature. The reaction mixture was diluted with diethyl ether (100 mL) and the organic phase separated. The aqueous phase was re-extracted with diethyl ether (2 x 50 mL) and the combined organics dried over MgSO_4 , filtered and evaporated.

The crude material was dissolved in THF:DME (1:1, 10 mL) and cooled to $-78\text{ }^{\circ}\text{C}$. NaHMDS (2 M in THF, 3 mL, 6 mmol, 1.2 equiv) was added dropwise. After stirring at $-78\text{ }^{\circ}\text{C}$ for 0.5 h, neat ethyl iodide (2.34 g, 15 mmol, 3 equiv) was added dropwise. The reaction was stirred at $-78\text{ }^{\circ}\text{C}$ for a further 2 h before being quenched at $-78\text{ }^{\circ}\text{C}$ with sat. aq. NH_4Cl (10 mL) and warming to room temperature. The reaction mixture was diluted with diethyl ether (100 mL) and the organic phase separated. The aqueous phase was re-extracted with diethyl ether (2 x 50 mL) and the combined organics dried over MgSO_4 , filtered and evaporated. The crude material was purified by silica gel flash chromatography (0–15% ethyl acetate in hexanes) to give the title compound as a colourless solid (**268a**, 0.977 g, 3.45 mmol, 69% yield over 2 steps). **M.p.** 39–41 $^{\circ}\text{C}$. $[\alpha]_D^{25.0} -20.2^{\circ}$ (*c* 1.0, CHCl_3). **^1H NMR** (400 MHz, CDCl_3) δ 5.71 – 5.57 (m, 1H, **10**), 5.14 – 5.03 (m, 2H, **11**), 4.51 (dd, *J* = 11.3, 2.3 Hz, 1H, **1-H_a**), 4.33 (br. s, 1H, **2**), 4.05 (d, *J* = 11.3 Hz, 1H, **1-H_b**), 3.12 (br. s, 1H, **9-H_a**), 3.00 – 2.89 (m, 1H, **9-H_b**), 2.34 – 2.09 (m, 2H, **12**), 1.48 (s, 9H, **8**), 1.19 (d, *J* = 6.8 Hz, 3H, **3**), 0.93 (dd, *J* = 7.6, 1.1 Hz, 3H, **13**). **^{13}C NMR** (101 MHz, CDCl_3) δ 170.8 (**5**), 153.2 (**6**), 134.4 (**10**), 119.1 (**11**), 80.7 (**7**), 70.2 (**1**), 67.9 (**4**), 46.6 (**2**), 39.1 (**9**), 31.9 (**12**), 28.6 (**8**), 18.1 (**3**), 9.5 (**13**). **IR** (neat, cm^{-1}) 2984, 2939, 1733, 1694, 1475, 1461, 1439, 1367, 1338, 1312, 1267, 1192, 1162, 1100, 1062, 928, 769. **HRMS** *m/z* (ESI) calcd for $\text{C}_{15}\text{H}_{26}\text{N}_1\text{O}_4$ [*M*+*H*] $^{+}$ 284.1856, found 284.1858.

(3*R*,5*S*)-3-Ethyl-5-methyl-3-propylmorpholin-2-one (269a)

A solution of *tert*-butyl (3*R*,5*S*)-3-allyl-3-ethyl-5-methyl-2-oxomorpholine-4-carboxylate (**268a**, 829 mg, 2.93 mmol, 1 equiv) in ethyl acetate (30 mL) was subjected to three cycles of vacuum/nitrogen backfill. Palladium on activated carbon (Pd/C, 10 wt%, 156 mg, 0.15 mmol, 5 mol%) was added in one portion, the atmosphere exchanged for hydrogen and the reaction stirred at room temperature overnight. The reaction was filtered through Celite and concentrated *in vacuo* to give the hydrogenated product as a colourless solid (835 mg, 2.93 mmol, quantitative yield).

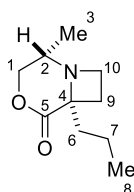
The hydrogenated product (797 mg, 2.79 mmol) was dissolved in dichloromethane (18 mL) and trifluoroacetic acid (3.6 mL) added. The reaction was stirred at room temperature overnight, concentrated *in vacuo*, basified with sat. aq. NaHCO₃ and the product extracted with dichloromethane (2 x 50 mL). The combined organics were dried over MgSO₄, filtered and evaporated to give the title compound as a pale yellow oil (**269a**, 509 mg, 2.75 mmol, 98% yield). [α]_D^{25.0} −6.0° (*c* 1.0, CHCl₃). ¹H NMR (400 MHz, CDCl₃) δ 4.22 (dd, *J* = 10.5, 3.1 Hz, 1H, **1-H_a**), 3.92 (app. t, *J* = 10.5 Hz, 1H, **1-H_b**), 3.37 – 3.26 (m, 1H, **2**), 2.01 – 1.89 (m, 1H, **9-H_a**), 1.81 – 1.62 (m, 2H, **6-H_a**, **9-H_b**), 1.62 – 1.48 (m, 1H, **7-H_a**), 1.47 – 1.36 (m, 1H, **6-H_b**), 1.35 – 1.18 (m, 2H, **7-H_b**, **11**), 1.07 (d, *J* = 6.3 Hz, 3H, **3**), 0.97 – 0.88 (m, 6H, **8**, **10**). ¹³C NMR (101 MHz, CDCl₃) δ 173.6 (**5**), 76.2 (**1**), 63.3 (**4**), 44.1 (**2**), 41.6 (**6**), 32.4 (**9**), 17.6 (**7**), 17.3 (**3**), 14.4 (**8**), 8.1 (**10**). IR (neat, cm^{−1}) 3334, 2963, 2875, 1725, 1462, 1316, 1213, 1180, 1146, 1114, 1046, 766, 727. HRMS *m/z* (ESI) calcd for C₁₀H₂₀N₁O₂ [M+H]⁺ 186.1489, found 186.1486.

Pd-catalyzed Azetidine Formation

General Procedure A. The morpholinone substrate (1 equiv), Pd(OAc)₂ (10 mol%), oxidant **249** (3 equiv) and silver acetate (3 equiv) in dry 1,2-dichloroethane (0.1 M) were heated in a sealed tube at 60 or 80 °C under air atmosphere for 16–24 h. The reaction was cooled to room

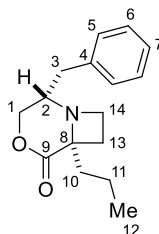
temperature, filtered through Celite (eluting with dichloromethane) and basified with sat. aq. NaHCO_3 . The aqueous phase was re-extracted with dichloromethane and the combined organics dried over MgSO_4 , filtered and evaporated. The crude material was purified by silica gel flash chromatography.

(2*S*,6*S*)-2-Methyl-6-propyl-4-oxa-1-azabicyclo[4.2.0]octan-5-one (273a)



(3*R*,5*S*)-3-Ethyl-5-methyl-3-propylmorpholin-2-one (**269a**, 56 mg, 0.30 mmol) was subjected to General Procedure A with heating at 80 °C for 20 h. The crude material was purified by silica gel flash chromatography (10–40% ethyl acetate in hexanes) to provide the title compound as a pale yellow oil (**273a**, 35 mg, 0.191 mmol, 64% yield). $[\alpha]_D^{25.0} -42.1^\circ$ (*c* 1.0, CHCl_3). ^1H NMR (400 MHz, CDCl_3) δ 4.15 (dd, $J = 11.4, 3.3$ Hz, 1H, **1-H_a**), 4.05 – 3.96 (m, 1H, **1-H_b**), 3.69 – 3.60 (m, 1H, **10-H_a**), 3.02 – 2.86 (m, 2H, **2, 10-H_b**), 2.78 – 2.68 (m, 1H, **9-H_a**), 2.32 – 2.22 (m, 1H, **9-H_b**), 1.88 – 1.71 (m, 2H **6-H_a, 6-H_b**), 1.50 – 1.30 (m, 2H, **7-H_a, 7-H_b**), 0.97 (d, $J = 6.4$ Hz, 3H, **3**), 0.93 (t, $J = 7.3$ Hz, 3H, **8**). ^{13}C NMR (101 MHz, CDCl_3) δ 175.1 (**5**), 71.8 (**1**), 68.0 (**4**), 59.0 (**2**), 51.6 (**10**), 43.6 (**6**), 28.4 (**9**), 17.0 (**7**), 16.7 (**3**), 14.3 (**8**). IR (neat, cm^{-1}) 2961, 2932, 2873, 1743, 1468, 1353, 1257, 1187, 1119, 1042, 1031, 789. HRMS *m/z* (ESI) calcd for $\text{C}_{10}\text{H}_{18}\text{N}_1\text{O}_2$ $[\text{M}+\text{H}]^+$ 184.1332, found 184.1331.

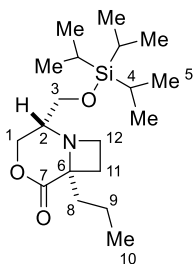
(2*S*,6*S*)-2-Benzyl-6-propyl-4-oxa-1-azabicyclo[4.2.0]octan-5-one (273b)



(3*R*,5*S*)-5-Benzyl-3-ethyl-3-propylmorpholin-2-one (**269b**, 78 mg, 0.30 mmol) was subjected to General Procedure A with heating at 80 °C for 20 h. The crude material was purified by silica gel flash chromatography (5–20% ethyl acetate in hexanes) to provide the title compound as a pale yellow oil (**273b**, 48 mg, 0.185 mmol, 62% yield). $[\alpha]_D^{25.0} -131.7^\circ$ (*c* 0.9, CHCl_3). ^1H

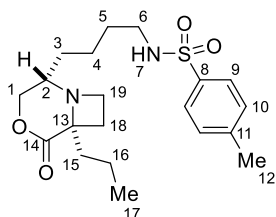
NMR (400 MHz, CDCl₃) δ 7.32 – 7.26 (m, 2H, **6**), 7.25 – 7.14 (m, 3H, **5**, **7**), 4.19 (dd, J = 11.5, 3.5 Hz, 1H, **1-H_a**), 4.02 (app. t, J = 11.1 Hz, 1H, **1-H_b**), 3.37 – 3.26 (m, 1H, **14-H_a**), 3.08 – 2.97 (m, 1H, **2**), 2.89 – 2.80 (m, 1H, **14-H_b**), 2.70 – 2.58 (m, 2H, **3-H_a**, **13-H_a**), 2.53 (dd, J = 13.3, 6.6 Hz, 1H, **3-H_b**), 2.29 – 2.18 (m, 1H, **13-H_b**), 1.83 – 1.65 (m, 2H, **10-H_a**, **10-H_b**), 1.52 – 1.34 (m, 2H, **11-H_a**, **11-H_b**), 0.94 (app. t, J = 7.2 Hz, 3H, **12**). **¹³C NMR** (101 MHz, CDCl₃) δ 175.4 (**9**), 137.6 (**4**), 129.5 (**5**), 128.6 (**6**), 126.7 (**7**), 70.0 (**1**), 68.2 (**8**), 65.3 (**2**), 52.7 (**14**), 43.5 (**10**), 39.0 (**3**), 28.0 (**13**), 16.9 (**11**), 14.3 (**12**). **IR** (neat, cm⁻¹) 2960, 2874, 1746, 1455, 1362, 1288, 1187, 1147, 1106, 1046, 756, 701. **HRMS** m/z (ESI) calcd for C₁₆H₂₂NO₂ [M+H]⁺ 260.1645, found 260.1646.

(2*R*,6*S*)-6-Propyl-2-(((triisopropylsilyl)oxy)methyl)-4-oxa-1-azabicyclo[4.2.0]octan-5-one (273c)



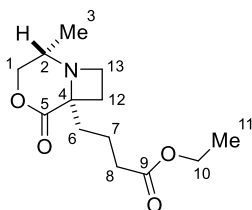
(3*R*,5*R*)-3-Ethyl-3-propyl-5-(((triisopropylsilyl)oxy)methyl)morpholin-2-one (**269c**, 107 mg, 0.30 mmol) was subjected to General Procedure A with heating at 60 °C for 24 h. The crude material was purified by silica gel flash chromatography (0–10% ethyl acetate in hexanes) to provide the title compound as a colourless oil (**273c**, 59 mg, 0.166 mmol, 55% yield). [α]_D^{25.0} –35.8° (c 1.5, CHCl₃). **¹H NMR** (400 MHz, CDCl₃) δ 4.50 (dd, J = 11.4, 3.6 Hz, 1H, **1-H_a**), 4.06 (app. t, J = 11.2 Hz, 1H, **1-H_b**), 3.71 – 3.55 (m, 2H, **3-H_a**, **12-H_a**), 3.42 – 3.33 (m, 1H, **3-H_b**), 3.07 (dd, J = 17.7, 8.2 Hz, 1H, **12-H_b**), 2.99 – 2.89 (m, 1H, **2**), 2.75 – 2.64 (m, 1H, **11-H_a**), 2.33 – 2.23 (m, 1H, **11-H_b**), 1.83 – 1.65 (m, 2H, **8-H_a**, **8-H_b**), 1.48 – 1.33 (m, 2H, **9-H_a**, **9-H_b**), 1.15 – 0.98 (m, 21H, **4**, **5**), 0.93 (app. t, J = 7.3 Hz, 3H, **10**). **¹³C NMR** (101 MHz, CDCl₃) δ 175.5 (**7**), 69.2 (**1**), 68.2 (**6**), 65.3 (**2**), 63.7 (**3**), 52.8 (**12**), 43.4 (**8**), 28.4 (**11**), 18.1 (**5**), 16.9 (**9**), 14.3 (**10**), 11.9 (**4**). **IR** (neat, cm⁻¹) 2942, 2867, 1751, 1465, 1333, 1289, 1162, 1115, 1048, 1029, 882, 810, 682. **HRMS** m/z (ESI) calcd for C₁₉H₃₈NO₃Si [M+H]⁺ 356.2615, found 356.2618.

4-Methyl-N-(4-((2*S*,6*S*)-5-oxo-6-propyl-4-oxa-1-azabicyclo[4.2.0]octan-2-yl)butyl)benzenesulfonamide (273d)



N-(4-((3*S*,5*R*)-5-Ethyl-6-oxo-5-propylmorpholin-3-yl)butyl)-4-methylbenzenesulfonamide (**269d**, 39.6 mg, 0.10 mmol) was subjected to General Procedure A with heating at 80 °C for 20 h. The crude material was purified by silica gel flash chromatography (40–80% ethyl acetate in hexanes) to provide the title compound as a pale yellow oil (**273d**, 18.5 mg, 0.046 mmol, 47% yield). $[\alpha]_D^{25.0}$ -41.0° (*c* 0.9, CHCl₃). **¹H NMR** (400 MHz, CDCl₃) δ 7.74 (d, *J* = 8.2 Hz, 2H, **9**), 7.31 (d, *J* = 8.2 Hz, 2H, **10**), 4.60 – 4.48 (m, 1H, **7**), 4.15 (dd, *J* = 11.7, 3.5 Hz, 1H, **1-H_a**), 3.98 (app. t, *J* = 11.2 Hz, 1H, **1-H_b**), 3.63 – 3.51 (m, 1H, **19-H_a**), 3.04 – 2.88 (m, 3H, **6-H_a**, **6-H_b**, **19-H_b**), 2.75 – 2.60 (m, 2H, **2**, **18-H_a**), 2.43 (s, 3H, **12**), 2.31 – 2.21 (m, 1H, **18-H_b**), 1.85 – 1.63 (m, 2H, **15-H_a**, **15-H_b**), 1.54 – 1.17 (m, 8H, **3-H_a**, **3-H_b**, **4-H_a**, **4-H_b**, **5-H_a**, **5-H_b**, **16-H_a**, **16-H_b**), 0.93 (app. t, *J* = 7.2 Hz, 3H, **17**). **¹³C NMR** (101 MHz, CDCl₃) δ 175.1 (**14**), 143.6 (**11**), 137.1 (**8**), 129.9 (**10**), 127.2 (**9**), 70.1 (**1**), 68.5 (**13**), 63.5 (**2**), 53.5 (s), 43.5 (**15**), 42.9 (**6**), 32.1 (**3**), 29.8 (**5**), 28.2 (**18**), 22.9 (**4**), 21.7 (**12**), 17.0 (**16**), 14.3 (**17**). **IR** (neat, cm⁻¹) 3278, 2930, 2868, 1740, 1462, 1326, 1159, 1094, 1042, 816, 668. **HRMS** *m/z* (ESI) calcd for C₂₀H₃₁N₂O₄S [M+H]⁺ 395.1999, found 395.1999.

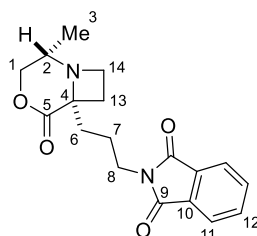
Ethyl 4-((2*S*,6*S*)-2-methyl-5-oxo-4-oxa-1-azabicyclo[4.2.0]octan-6-yl)butanoate (273e)



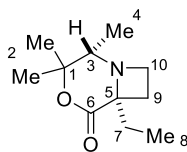
Ethyl 4-((3*R*,5*S*)-3-ethyl-5-methyl-2-oxomorpholin-3-yl)butanoate (**269e**, 77 mg, 0.30 mmol) was subjected to General Procedure A with heating at 80 °C for 24 h. The crude material was purified by silica gel flash chromatography (10–60% ethyl acetate in hexanes) to provide the title compound as a pale yellow oil (**273e**, 43 mg, 0.168 mmol, 56% yield). $[\alpha]_D^{25.0}$ -65.2° (*c* 1.0, CHCl₃). **¹H NMR** (400 MHz, CDCl₃) δ 4.21 – 4.08 (m, 3H, **1-H_a**, **10**), 4.00 (t, *J* = 11.0 Hz,

1H, **1-H_b**), 3.67 – 3.59 (m, 1H, **13-H_a**), 3.03 – 2.95 (m, 1H, **13-H_b**), 2.95 – 2.85 (m, 1H, **2**), 2.77 – 2.67 (m, 1H, **12-H_a**), 2.38 – 2.26 (m, 3H, **8-H_a**, **8-H_b**, **12-H_b**), 1.95 – 1.66 (m, 4H, **6-H_a**, **6-H_b**, **7-H_a**, **7-H_b**), 1.25 (t, $J = 7.1$ Hz, 3H, **11**), 0.97 (d, $J = 6.4$ Hz, 3H, **3**). ¹³C NMR (101 MHz, CDCl₃) δ 175.0 (**5**), 173.2 (**9**), 71.8 (**1**), 67.6 (**4**), 60.5 (**10**), 59.0 (**2**), 51.7 (**13**), 40.4 (**6**), 34.1 (**8**), 27.7 (**12**), 19.1 (**7**), 16.9 (**3**), 14.4 (**11**). **IR** (neat, cm⁻¹) 2970, 2875, 1734, 1449, 1376, 1253, 1177, 1145, 1095, 1037. **HRMS** m/z (ESI) calcd for C₁₃H₂₂N₁O₄ [M+H]⁺ 256.1543, found 256.1544.

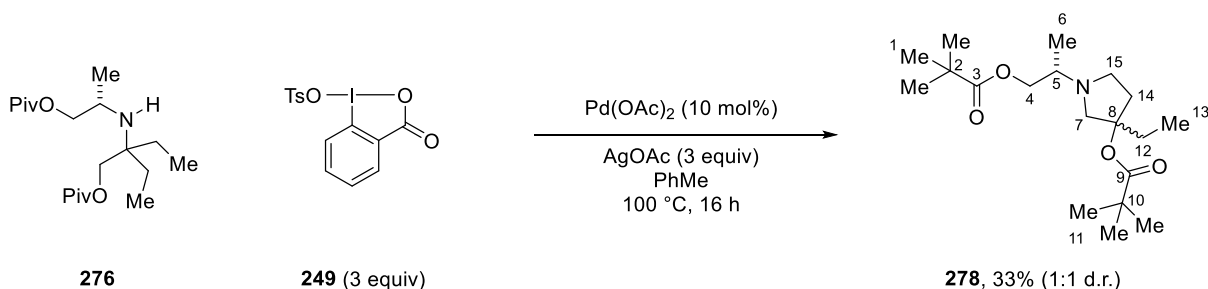
2-(3-((2*S*,6*S*)-2-Methyl-5-oxo-4-oxa-1-azabicyclo[4.2.0]octan-6-yl)propyl)isoindoline-1,3-dione (273f)



2-(3-((3*R*,5*S*)-3-Ethyl-5-methyl-2-oxomorpholin-3-yl)propyl)isoindoline-1,3-dione (**269f**, 99 mg, 0.30 mmol) was subjected to General Procedure A with heating at 80 °C for 24 h. The crude material was purified by silica gel flash chromatography (10–90% ethyl acetate in hexanes) to provide the title compound as a colourless solid (**273f**, 51 mg, 0.155 mmol, 52% yield). **M.p.** 127–129 °C. $[\alpha]_D^{25.0} -44.4^\circ$ (c 1.5, CHCl₃). ¹H NMR (400 MHz, CDCl₃) δ 7.87 – 7.79 (m, 2H, **11**), 7.75 – 7.67 (m, 2H, **12**), 4.16 (dd, $J = 11.5, 3.3$ Hz, 1H, **1-H_a**), 4.00 (app. t, $J = 11.2$ Hz, 1H, **1-H_b**), 3.77 – 3.67 (m, 2H, **8-H_a**, **8-H_b**), 3.63 – 3.54 (m, 1H, **14-H_a**), 3.01 – 2.82 (m, 2H, **2**, **14-H_b**), 2.74 – 2.63 (m, 1H, **13-H_a**), 2.32 – 2.20 (m, 1H, **13-H_b**), 1.93 – 1.75 (m, 4H, **6-H_a**, **6-H_b**, **7-H_a**, **7-H_b**), 0.95 (d, $J = 6.4$ Hz, 3H, **3**). ¹³C NMR (101 MHz, CDCl₃) δ 174.9 (**5**), 168.5 (**9**), 134.1 (**12**), 132.2 (**10**), 123.4 (**11**), 71.8 (**1**), 67.3 (**4**), 59.0 (**2**), 51.5 (**14**), 38.1 (**6**), 37.9 (**8**), 27.7 (**13**), 22.9 (**7**), 16.8 (**3**). **IR** (neat, cm⁻¹) 2963, 2927, 2851, 1772, 1741, 1707, 1396, 1360, 1187, 1036, 752, 719. **HRMS** m/z (ESI) calcd for C₁₈H₂₁N₂O₄ [M+H]⁺ 329.1496, found 329.1497.

(2S,6S)-6-Ethyl-2,3,3-trimethyl-4-oxa-1-azabicyclo[4.2.0]octan-5-one (273g)

(*S*)-3,3-Diethyl-5,6,6-trimethylmorpholin-2-one (60 mg, 0.30 mmol) was subjected to General Procedure A with heating at 80 °C for 20 h. The crude material was purified by silica gel flash chromatography (10–50% ethyl acetate in hexanes) to provide the title compound as a colourless oil (**273g**, 33 mg, 0.167 mmol, 56% yield). $[\alpha]_D^{25.0} +11.6^\circ$ (*c* 1.0, CHCl₃). ¹H NMR (400 MHz, CDCl₃) δ 3.78 – 3.63 (m, 1H, **10-H_a**), 3.00 – 2.78 (m, 3H, **3**, **10-H_b**, **9-H_a**), 2.40 – 2.30 (m, 1H, **9-H_b**), 2.07 – 1.87 (m, 2H, **7-H_a**, **7-H_b**), 1.38 (s, 3H, **2**), 1.37 (s, 3H, **2'**), 1.15 (app. t, *J* = 7.4 Hz, 3H, **8**), 0.97 (d, *J* = 6.3 Hz, 3H, **4**). ¹³C NMR (101 MHz, CDCl₃) δ 175.4 (**6**), 85.7 (**1**), 66.8 (**5**), 65.7 (**3**), 49.3 (**10**), 32.8 (**7**), 27.9 (**2**), 27.4 (**9**), 20.8 (**2'**), 14.9 (**4**), 7.9 (**8**). IR (neat, cm⁻¹) 2975, 2939, 2879, 1729, 1455, 1390, 1287, 1206, 1128, 1089, 1021, 960, 732, 700. HRMS *m/z* (ESI) calcd for C₁₁H₂₀N₁O₂ [M+H]⁺ 198.1489, found 198.1485.

*Synthesis of Rearranged Pyrrolidine Product***3-Ethyl-1-((*S*)-1-(pivaloyloxy)propan-2-yl)pyrrolidin-3-yl pivalate (278)**

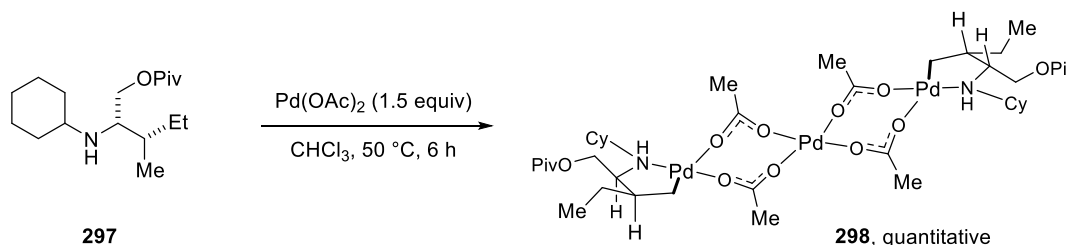
(*S*)-2-Ethyl-2-((1-(pivaloyloxy)propan-2-yl)amino)butyl pivalate (**276**, 103 mg, 0.3 mmol, 1 equiv), Pd(OAc)₂ (6.7 mg, 0.03 mmol, 10 mol%), oxidant **249** (376 mg, 0.9 mmol, 3 equiv) and silver acetate (150 mg, 0.9 mmol, 3 equiv) in toluene (3 mL) were heated to 100 °C for 16 h. The reaction was cooled to room temperature, filtered through Celite (eluting with dichloromethane) and basified with sat. aq. NaHCO₃ (5 mL). The aqueous phase was re-extracted with dichloromethane (3 x 20 mL). The combined organics were dried over MgSO₄, filtered and evaporated. The crude material was purified by silica gel flash chromatography (10–50% ethyl acetate in hexanes) to give the title compound as a pale orange oil (**278**, 34 mg, 0.10 mmol, 33% yield, 1:1 d.r., isolated as a mixture of diastereomers). *Note: only minor*

deviations in the ^1H NMR signals for the two diastereomers; hence ^1H assignments correspond to signals from both diastereomers. Separate assignments are made for the ^{13}C signals. ^1H NMR (400 MHz, CDCl_3) δ 4.21 – 4.11 (m, 2H, **4-H_a**), 4.02 – 3.91 (m, 2H, **4-H_b**), 3.09 – 2.96 (m, 2H, **7-H_a**), 2.94 – 2.75 (m, 4H, **7-H_b**, **15-H_a**), 2.73 – 2.61 (m, 4H, **5**, **15-H_b**), 2.19 – 2.04 (m, 4H, **12-H_a**, **14-H_a**), 2.00 – 1.86 (m, 4H, **12-H_b**, **14-H_b**), 1.22 (s, 18H, **1** or **11**), 1.19 (s, 18H, **1** or **11**), 1.13 (app. d, $J = 6.4$ Hz, 6H, **6**), 0.86 (app. t, $J = 7.4$ Hz, 6H, **13**). ^{13}C NMR (101 MHz, CDCl_3) δ 178.3 (two signals, **3/3*** or **9/9***), 177.9 (**3** or **9**), 177.8 (**3*** or **9***), 89.0 (**8**), 88.9 (**8***), 67.1 (two signals, **4/4***), 62.5 (**7**), 62.2 (**7***), 57.2 (two signals, **5/5***), 50.3 (**15**), 49.9 (**15***), 39.1 (two signals, **2/2*** or **10/10***), 38.8 (two signals, **2/2*** or **10/10***), 36.8 (**14**), 36.5 (**14***), 30.0(0) (**12**), 29.9(5) (**12***), 27.2(1) (two signals, **1/1*** or **11/11***), 27.1(8) (two signals, **1/1*** or **11/11***), 15.6 (**6**), 15.5 (**6***), 8.2 (two signals, **13/13***). IR (neat, cm^{-1}) 2972, 2878, 1725, 1481, 1461, 1397, 1366, 1282, 1148, 1034, 864, 769. HRMS m/z (ESI) calcd for $\text{C}_{19}\text{H}_{36}\text{N}_1\text{O}_4$ $[\text{M}+\text{H}]^+$ 342.2639, found 342.2642.

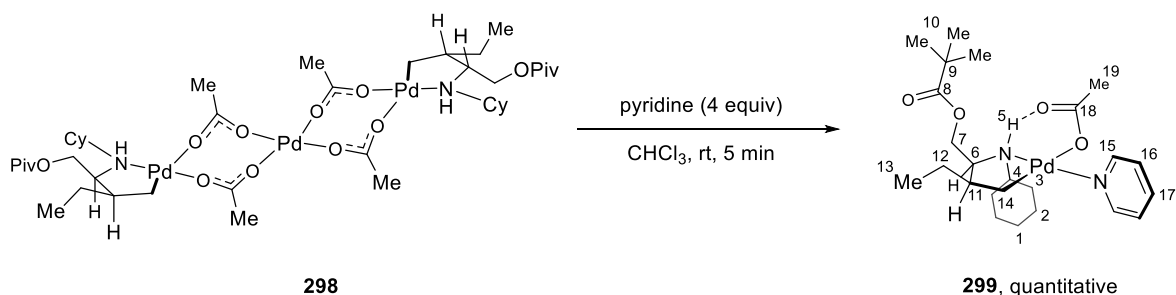
6.2.2. Pd-catalyzed C–H Functionalization by *ortho*-DG-assisted Oxidative Addition

Stoichiometric Studies Employing 2-Halobenzoic Acids

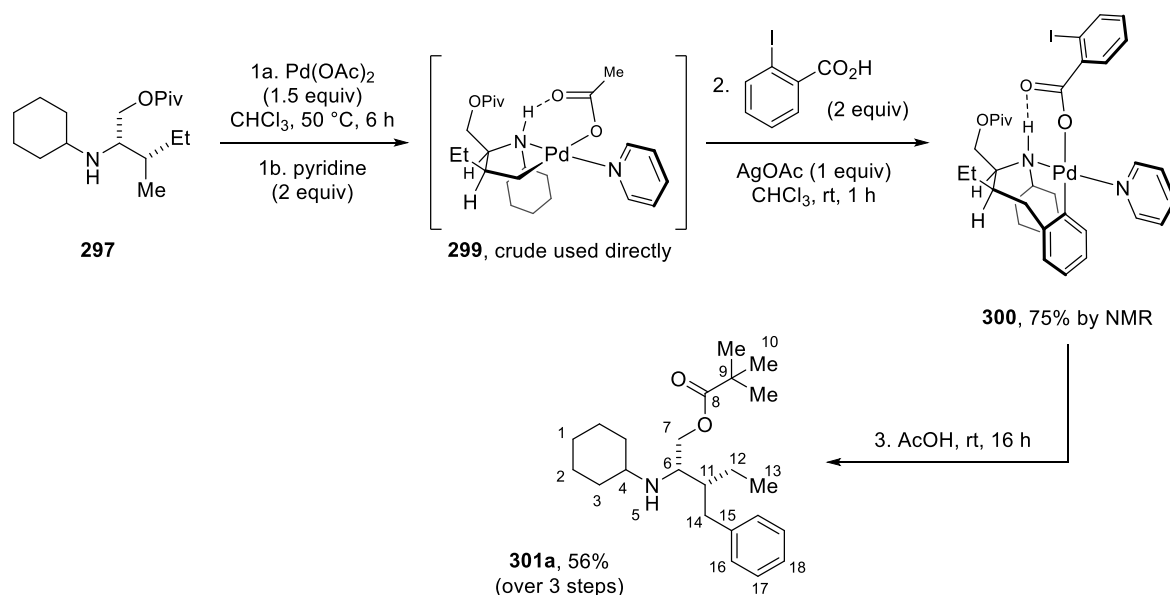
Trinuclear palladacycle **298**



To a solution of (2*S*,3*S*)-2-(cyclohexylamino)-3-methylpentyl pivalate (**297**, 142 mg, 0.50 mmol, 1 equiv) in CHCl_3 (5 mL) in air at room temperature was added $\text{Pd}(\text{OAc})_2$ (168 mg, 0.75 mmol, 1.5 equiv). The reaction was stirred at 50 $^\circ\text{C}$ for 6 h. After cooling to room temperature, CHCl_3 was evaporated, hexane (10 mL) added, and the solution passed through a pad of Celite. The solvent was evaporated to give the title compound as a green foam (**298**, 280 mg, 0.25 mmol, quantitative yield). IR (film, cm^{-1}) 2933, 1730, 1576, 1396, 1338, 1281, 1145, 1033, 697. **Elemental Analysis** calcd for $\text{C}_{42}\text{H}_{76}\text{N}_2\text{O}_{12}\text{Pd}_3$ C: 45.03 H: 6.84 N: 2.50, found C: 44.96 H: 6.84 N: 2.72.

Pyridine-ligated palladacycle **299**

To a solution of trinuclear palladacycle **298** (56.0 mg, 0.05 mmol, 1 equiv) in CHCl₃ (1 mL) was added pyridine (16 μ L, 0.2 mmol, 4 equiv) and the reaction stirred at room temperature for 5 minutes. The solvent was removed *in vacuo*, and Et₂O (10 mL) added. The resulting suspension was filtered through Celite and the filtrate concentrated *in vacuo*. Hexane (10 mL) was added followed by filtration again through Celite. Removal of the solvent and drying under high vacuum gave the title compound as a yellow oil (53.0 mg, 0.10 mmol, quantitative yield). **¹H NMR** (400 MHz, CDCl₃) δ 8.60 (d, J = 5.1 Hz, 2H, **15**), 7.74 (t, J = 7.6 Hz, 1H, **17**), 7.31 – 7.24 (m, 2H, **16**), 6.27 (d, J = 6.7 Hz, 1H, **5**), 4.70 (app. t, J = 11.2 Hz, 1H, **7-H_a**), 4.43 (dd, J = 11.2, 2.8 Hz, 1H, **7-H_b**), 3.13 – 3.03 (m, 1H, **6**), 2.72 – 2.60 (m, 2H, **3-H_a**, **4**), 2.24 – 2.09 (m, 2H, **3'-H_a**, **11**), 1.92 (s, 3H, **18**), 1.88 – 1.70 (m, 3H, **2-H_a**, **2'-H_a**, **14-H_a**), 1.66 – 1.53 (m, 3H, **1-H_a**, **3-H_b**, **14-H_b**), 1.47 – 1.05 (m, 15H, **1-H_b**, **2-H_b**, **2'-H_b**, **3'-H_b**, **10**, **12-H_{a,b}**), 0.91 (t, J = 7.3 Hz, 3H, **13**). **¹³C NMR** (101 MHz, CDCl₃) δ 178.9 (**8**), 177.1 (**18**), 151.7 (**15**), 137.4 (**17**), 124.8 (**16**), 64.9 (**6**), 62.9 (**7**), 59.9 (**4**), 47.2 (**11**), 38.9 (**9**), 35.2 (**3**), 32.0 (**3'**), 27.4 (**10**), 26.9 (**14**), 26.2 (**2**), 26.1 (**2'**), 25.5 (**1**), 24.1 (**12**), 23.9 (**19**), 13.2 (**13**). **IR** (film, cm⁻¹) 2930, 2857, 1729, 1588, 1448, 1381, 1327, 1283, 1155, 1041, 759. **HRMS** m/z (ESI) calcd for C₂₂H₃₇N₂O₂¹⁰⁶Pd₁ [M–OAc]⁺ 467.1884, found 467.1883.

(2*S*,3*R*)-3-Benzyl-2-(cyclohexylamino)pentyl pivalate (301a)

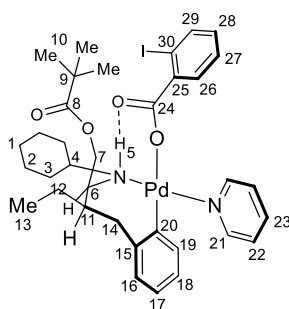
A solution of (2*S*,3*S*)-2-(cyclohexylamino)-3-methylpentyl pivalate (**297**, 28.3 mg, 0.10 mmol, 1 equiv) and Pd(OAc)₂ (33.7 mg, 0.15 mmol, 1.5 equiv) in CHCl₃ (1 mL) was stirred in a sealed vial at 50 °C for 6 h. The reaction was cooled to room temperature, passed through a Celite plug and pyridine (16 µL, 0.20 mmol, 2 equiv) added. The reaction was concentrated *in vacuo* to give the crude pyridine-ligated palladacycle (**299**), which was used directly in the next step.

The crude palladacycle **299** was re-dissolved in CHCl₃ (1 mL) followed by addition of 2-iodobenzoic acid (49.6 mg, 0.20 mmol, 2 equiv) and AgOAc (16.7 mg, 0.10 mmol, 1 equiv). The reaction was stirred at room temperature for 1 h, passed through a Celite plug and concentrated *in vacuo*. 1,1,2,2-tetrachloroethane (1 equiv) was added as internal standard, and the crude material was analysed by ¹H NMR at room temperature as a solution in CDCl₃. Seven-membered palladacycle **300** was observed in 75% yield.

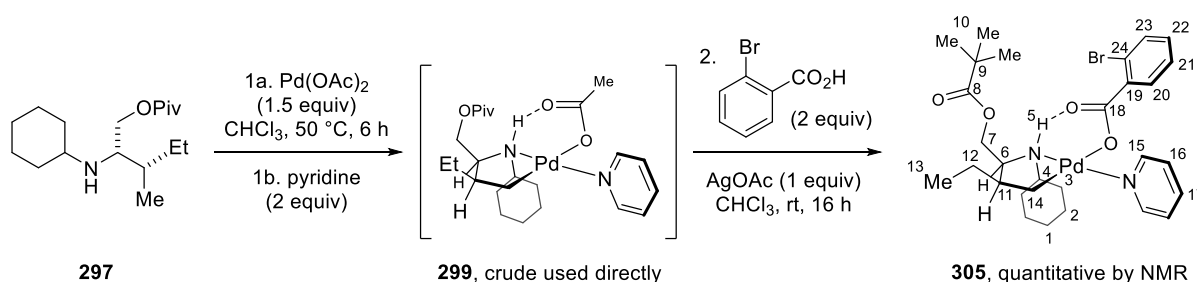
After removal of the chloroform from Step 2, crude **300** was dissolved in AcOH (1 mL) and stirred at room temperature overnight. The solvent was removed *in vacuo*, followed by addition of DCM (10 mL) and washing with sat. aq. NaHCO₃ (10 mL). The organic phase was separated, dried over MgSO₄, filtered and the solvent evaporated. The crude material was purified by silica gel flash chromatography (5–10% EtOAc in hexanes) to give arylated product **301a** as a pale yellow oil (20.0 mg, 0.056 mmol, 56% yield over 3 steps). [α]_D^{24.0} –11.5° (*c* 1.0, CHCl₃). ¹H NMR (400 MHz, CDCl₃) δ 7.30 – 7.23 (m, 2H, **17**), 7.21 – 7.13 (m, 3H, **16**, **18**), 4.12 (dd, *J* = 11.1, 5.8 Hz, 1H, **7-H_a**), 4.00 (dd, *J* = 11.1, 6.1 Hz, 1H, **7-H_b**), 3.01 – 2.91 (m, 1H, **6**), 2.84 (dd, *J* = 13.6, 6.4 Hz, 1H, **14-H_a**), 2.58 – 2.48 (m, 1H, **4**), 2.44 (dd, *J* = 13.6, 7.9 Hz, 1H, **14-H_b**), 1.88 – 1.66 (m, 5H, **2-H_a**, **2'-H_a**, **3-H_a**, **3'-H_a**, **11**), 1.63 – 1.55 (m, 1H, **1-H_a**), 1.46

– 1.01 (m, 17 H, **1-H_a**, **2-H_b**, **2'-H_b**, **3-H_b**, **3'-H_b**, **5**, **10**, **12-H_{a,b}**), 0.90 (t, $J = 7.4$ Hz, 3H, **13**). ^{13}C NMR (101 MHz, CDCl_3) δ 178.6 (**8**), 141.9 (**15**), 129.2 (**16**), 128.4 (**17**), 125.8 (**18**), 64.9 (**7**), 54.5 (**4**), 54.0 (**6**), 44.1 (**11**), 38.9 (**9**), 36.2 (**14**), 34.4 (**3'**), 34.1 (**3**), 27.3 (**10**), 26.2 (**1**), 25.2(3) (**2**), 25.1(5) (**2'**), 22.2 (**12**), 12.5 (**13**). IR (film, cm^{-1}) 2960, 2927, 2853, 1729, 1479, 1451, 1282, 1154, 1032, 735, 699. HRMS m/z (ESI) calcd for $\text{C}_{23}\text{H}_{38}\text{N}_1\text{O}_2$ $[\text{M}+\text{H}]^+$ 360.2897, found 360.2900.

Pyridine-ligated 7-membered ring palladacycle **300**

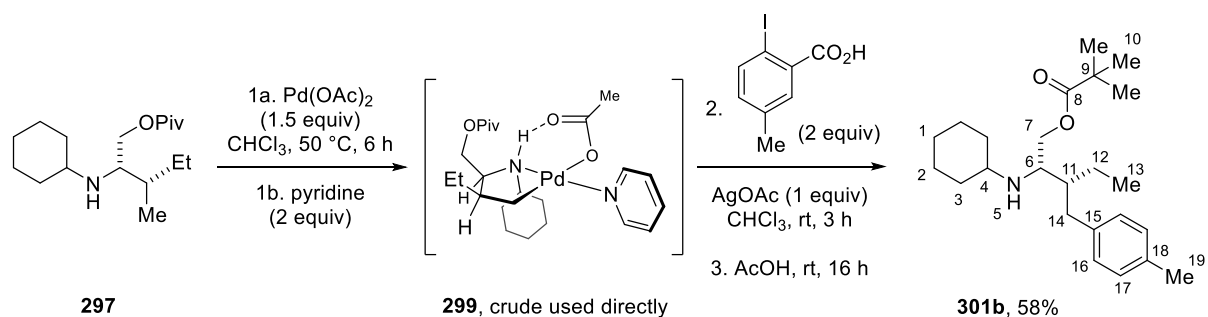


In a separate experiment, a purified sample was prepared by dissolving a portion of crude **300** in CHCl_3 and passing through a short plug of silica gel, eluting with CHCl_3 . The resulting solution was concentrated *in vacuo* and the residue triturated in hexane. The mother liquor (containing **300**) was separated, filtered through Celite and the solvent removed, giving the title compound as a viscous yellow oil. ^1H NMR (400 MHz, CDCl_3) δ 8.60 (d, $J = 4.8$ Hz, 2H, **21**), 7.85 (d, $J = 7.4$ Hz, 1H, **26**), 7.72 – 7.64 (m, 2H, **23**, **29**), 7.33 – 7.26 (m, 1H, **28**), 7.24 – 7.17 (m, 2H, **22**), 7.02 – 6.92 (m, 2H, **19**, **27**), 6.90 – 6.80 (m, 2H, **16**, **17**), 6.76 – 6.70 (m, 1H, **18**), 6.37 (d, $J = 9.5$ Hz, 1H, **5**), 5.34 (dd, $J = 11.8$, 6.1 Hz, 1H, **7-H_a**), 5.19 (dd, $J = 11.8$, 2.0 Hz, 1H, **7-H_b**), 3.92 (dd, $J = 13.3$, 9.5 Hz, 1H, **14-H_a**), 3.62 – 3.51 (m, 1H, **3-H_a**), 3.41 – 3.30 (m, 1H, **6**), 2.64 (d, $J = 13.3$ Hz, 1H, **14-H_b**), 2.03 – 1.43 (m, 9H, **1-H_a**, **2-H_a**, **2'-H_a**, **3-H_b**, **3'-H_a**, **4**, **11**, **12-H_{a,b}**), 1.35 – 0.87 (m, 16H, **1-H_b**, **2-H_b**, **2'-H_b**, **3'-H_b**, **10**, **13**). ^{13}C NMR (101 MHz, CDCl_3) δ 178.5 (**8**), 152.7 (**21**), 148.9 (**25**), 147.5 (**20**), 146.5 (**15**), 139.9 (**26**), 137.5 (**23**), 134.4 (**19**), 130.1 (**27**), 129.7 (**29**), 127.5 (**28**), 126.5 (**16**), 124.9 (**18**), 124.6 (**22**), 123.9 (**17**), 93.5 (**30**), 64.7 (**7**), 60.6 (**6**), 56.4 (**4**), 40.9 (**11**), 38.7 (**9**), 36.7 (**14**), 34.7 (**3**), 30.8 (**3'**), 28.2 (**12**), 27.1 (**10**), 25.6 (**2**), 25.3 (**2'**), 24.9 (**1**), 12.9 (**13**). Note: significant broadening of ^{13}C signals of the 2-I-benzoate ligand. ^{13}C signal for $\text{C}=\text{O}$ (carbon **24**) could not be distinguished from the baseline. IR (film, cm^{-1}) 2929, 2858, 1724, 1571, 1547, 1449, 1367, 1281, 1146, 1013, 908, 728, 691. HRMS m/z (ESI) calcd for $\text{C}_{28}\text{H}_{41}\text{N}_2\text{O}_2^{106}\text{Pd}_1$ $[\text{M}-(2\text{-I-benzoate})]^+$ 543.2197, found 543.2200.

Pyridine-ligated palladacycle with 2-bromobenzoate ligand (**305**)

A solution of (2*S*,3*S*)-2-(cyclohexylamino)-3-methylpentyl pivalate (**297**, 28.3 mg, 0.10 mmol, 1 equiv) and Pd(OAc)₂ (33.7 mg, 0.15 mmol, 1.5 equiv) in CHCl₃ (1 mL) was stirred in a sealed vial at 50 °C for 6 h. The reaction was cooled to room temperature, passed through a Celite plug and pyridine (16 µL, 0.20 mmol, 2 equiv) added. The reaction was concentrated *in vacuo* to give the crude pyridine-ligated palladacycle (**299**) which was used directly in the next step.

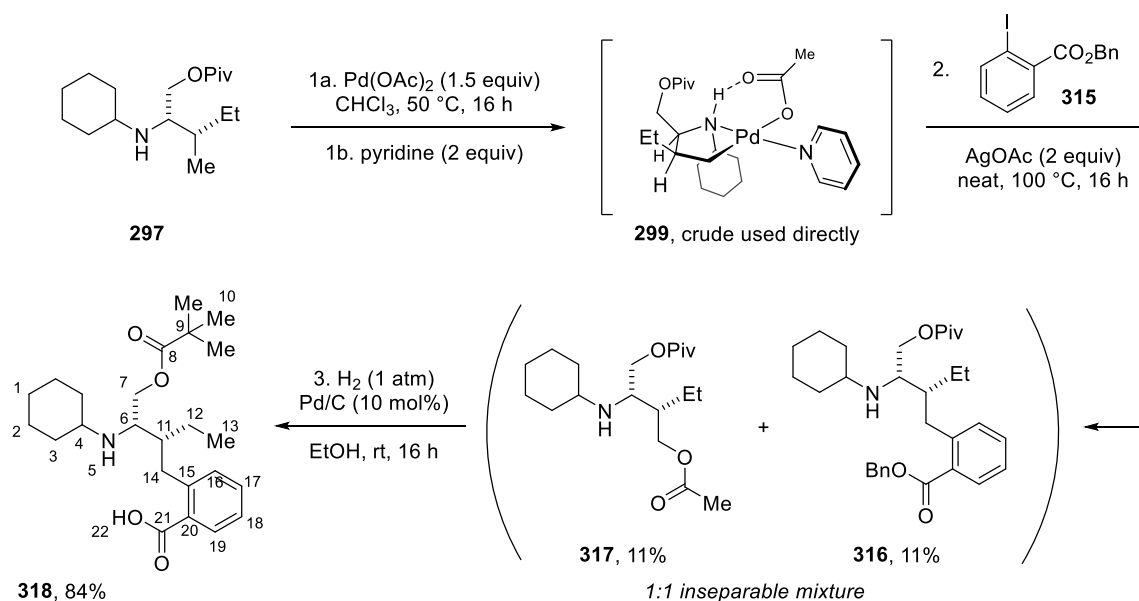
The crude palladacycle **299** was re-dissolved in CHCl₃ (1 mL), followed by addition of 2-bromobenzoic acid (40.2 mg, 0.20 mmol, 2 equiv) and AgOAc (16.7 mg, 0.10 mmol, 1 equiv). The reaction was stirred at room temperature overnight, passed through a Celite plug and concentrated *in vacuo*. Analysis of the reaction mixture by NMR indicated 2-bromobenzoate-ligated palladacycle had formed (**305**, quantitative yield against internal standard). A purified sample was prepared separately by dissolving a portion of crude **305** in hexanes and filtering through a short plug of Celite (carried out twice). The solvent was removed *in vacuo* to give the title compound as a colourless oil. **¹H NMR** (400 MHz, CDCl₃) δ 8.72 (dd, *J* = 5.2 Hz, 2H, **15**), 7.75 (t, *J* = 7.5 Hz, 1H, **17**), 7.51 – 7.43 (m, 2H, **20**, **23**), 7.33 – 7.28 (m, 2H, **16**), 7.21 (t, *J* = 7.4 Hz, 1H, **21**), 7.08 (td, *J* = 7.8, 1.6 Hz, 1H, **22**), 6.01 (d, *J* = 6.4 Hz, 1H, **5**), 4.76 (t, *J* = 11.2 Hz, 1H, **7-H_a**), 4.48 (dd, *J* = 11.2, 2.8 Hz, 1H, **7-H_b**), 3.22 – 3.13 (m, 1H, **6**), 2.89 – 2.77 (m, 1H, **4**), 2.72 – 2.63 (m, 1H, **3-H_a**), 2.38 – 2.29 (m, 1H, **3'-H_a**), 2.27 – 2.16 (m, 1H, **11**), 1.96 – 1.57 (m, 6H, **1-H_a**, **2-H_a**, **2'-H_a**, **3-H_b**, **14-H_{a,b}**), 1.50 – 1.09 (m, 15H, **1-H_b**, **2-H_b**, **2'-H_b**, **3'-H_b**, **10**, **12-H_{a,b}**), 0.96 (t, *J* = 7.3 Hz, 3H, **13**). **¹³C NMR** (101 MHz, CDCl₃) δ 178.9 (**8**), 173.2 (**18**, extracted from ¹H–¹³C HMBC NMR spectrum), 151.7 (**15**), 141.6 (**19**, extracted from ¹H–¹³C HMBC NMR spectrum), 137.3 (**17**), 132.9 (**23**), 129.4 (**20**), 129.0 (**22**), 126.8 (**21**), 124.7 (**16**), 119.7 (**24**), 64.4 (**6**), 62.7 (**7**), 60.0 (**4**), 47.4 (**11**), 39.0 (**9**), 34.9 (**3**), 32.1 (**3'**), 27.4 (**10**), 27.2 (**14**), 26.1(3) (**2**), 26.0(7) (**2'**), 25.5 (**1**), 24.1 (**12**), 13.2 (**13**). **IR** (film, cm⁻¹) 2932, 1727, 1604, 1448, 1366, 1282, 1153, 1039, 749. **HRMS** *m/z* (ESI) calcd for C₂₂H₃₇N₂O₂¹⁰⁶Pd₁ [M–(2-Br-benzoate)]⁺ 467.1884, found 467.1891.

(2*S*,3*R*)-2-(Cyclohexylamino)-3-(4-methylbenzyl)pentyl pivalate (301b)

A solution of (2*S*,3*S*)-2-(cyclohexylamino)-3-methylpentyl pivalate (**297**, 28.3 mg, 0.10 mmol, 1 equiv) and Pd(OAc)₂ (33.7 mg, 0.15 mmol, 1.5 equiv) in CHCl₃ (1 mL) was stirred in a sealed vial at 50 °C for 6 h. The reaction was cooled to room temperature, passed through a Celite plug and pyridine (16 µL, 0.20 mmol, 2 equiv) added. The reaction was concentrated *in vacuo* to give the crude pyridine-ligated palladacycle (**299**), which was used directly in the next step.

The crude palladacycle **299** was re-dissolved in CHCl₃ (1 mL), followed by addition of 2-iodo-5-methylbenzoic acid (52.4 mg, 0.20 mmol, 2 equiv) and AgOAc (16.7 mg, 0.10 mmol, 1 equiv). The reaction was stirred at room temperature for 3 h, passed through a Celite plug and concentrated *in vacuo*.

AcOH (1 mL) was added to the crude residue, and the reaction stirred at room temperature overnight. The solvent was removed *in vacuo*, followed by addition of dichloromethane (10 mL) and washing with sat. aq. NaHCO₃ (10 mL). The organic phase was separated, dried over MgSO₄, filtered and the solvent evaporated. Purification by silica gel flash chromatography (5% Et₂O in DCM) gave arylated derivative as a pale yellow oil (**301b**, *single regioisomer*, 21.5 mg, 0.058 mmol, 58% yield). $[\alpha]_D^{24.2}$ -14.1 (*c* 1.0, CHCl₃). ¹H NMR (400 MHz, CDCl₃) δ 7.10 – 7.02 (m, 4H, **16**, **17**), 4.10 (dd, *J* = 11.1, 5.8 Hz, 1H, **7-H_a**), 3.97 (dd, *J* = 11.1, 6.2 Hz, 1H, **7-H_b**), 2.96 – 2.90 (m, 1H, **6**), 2.78 (dd, *J* = 13.7, 6.5 Hz, 1H, **14-H_a**), 2.49 (tt, *J* = 10.2, 3.6 Hz, 1H, **4**), 2.40 (dd, *J* = 13.7, 7.8 Hz, 1H, **14-H_b**), 2.31 (s, 3H, **19**), 1.87 – 1.67 (m, 5H, **2-H_a**, **2'-H_a**, **3-H_a**, **3'-H_a**, **11**), 1.63 – 1.55 (m, 1H, **1-H_a**), 1.51 – 0.99 (m, 17H, **1-H_a**, **2-H_b**, **2'-H_b**, **3-H_b**, **3'-H_b**, **5**, **10**, **12-H_{a,b}**), 0.90 (t, *J* = 7.4 Hz, 3H, **13**). ¹³C NMR (126 MHz, CDCl₃) δ 178.7 (**8**), 138.8 (**15**), 135.3 (**18**), 129.0(8) (**16 or 17**), 129.0(6) (**16 or 17**), 65.1 (**7**), 54.4 (**4**), 53.9 (**6**), 44.2 (**11**), 38.9 (**9**), 35.7 (**14**), 34.4 (**3'**), 34.2 (**3**), 27.4 (**10**), 26.1 (**1**), 25.3 (**2**), 25.2 (**2'**), 22.2 (**12**), 21.1 (**19**), 12.5 (**13**). IR (film, cm⁻¹) 2957, 2937, 1730, 1450, 1147, 801. HRMS *m/z* (ESI) calcd for C₂₄H₄₀N₁O₂ [M+H]⁺ 374.3054, found 374.3054.

2-((2*R*,3*S*)-3-(Cyclohexylamino)-2-ethyl-4-(pivaloyloxy)butyl)benzoic acid (**318**)

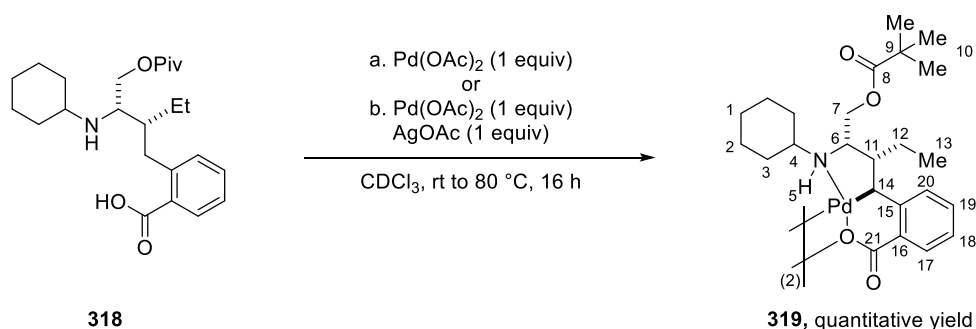
A solution of (2*S*,3*S*)-2-(cyclohexylamino)-3-methylpentyl pivalate (**297**, 567 mg, 2.00 mmol, 1 equiv) and Pd(OAc)₂ (673 mg, 3.00 mmol, 1.5 equiv) in CHCl₃ (20 mL) was stirred in a sealed vessel at 50 °C for 16 h. The reaction was cooled to room temperature, filtered through a pad of Celite and pyridine (310 µL, 4.00 mmol, 2 equiv) added to the filtrate. The reaction was concentrated *in vacuo* to give the crude pyridine-ligated palladacycle (**299**), which was used directly in the next step.

A mixture of crude **299**, benzyl 2-iodobenzoate (**315**, 2 mL) and silver acetate (668 mg, 4.00 mmol, 2 equiv) was heated at 100 °C in a sealed vial overnight. The reaction was cooled to room temperature, diluted with dichloromethane (50 mL) and filtered through a pad of Celite. The filtrate washed with sat. aq. NaHCO₃ (50 mL) and the organics separated, dried over MgSO₄, filtered and the solvent removed *in vacuo*. The crude material was purified by silica gel flash chromatography (column 1: 5–15% EtOAc in hexanes; column 2: 5–10% Et₂O in DCM), giving an inseparable 1:1 mixture (183 mg, pale yellow oil) of the desired arylated product (**316**, 0.22 mmol, 11% yield) and acetoxylated product (**317**, 0.22 mmol, 11% yield).

The mixture of **316** and **317** was dissolved in EtOH (10 mL) and Pd/C (10 wt%, 21 mg, 0.02 mmol, 10 mol%) added under nitrogen. The atmosphere was exchanged for hydrogen, and the reaction stirred under a balloon of hydrogen at room temperature overnight. The reaction was filtered through a pad of Celite and the solvent removed *in vacuo*. The crude residue was purified by silica gel flash chromatography (2–10% MeOH in dichloromethane) to furnish the title compound as a colourless crystalline solid (**318**, 75 mg, 0.19 mmol, 84% yield). $[\alpha]_D^{26.4} - 53.7^\circ$ (*c* 0.7, MeOH). ¹H NMR (400 MHz, MeOD) δ 7.71 (dd, *J* = 7.6, 1.3 Hz, 1H, **19**), 7.33

(td, $J = 7.4$, 1.5 Hz, 1H, **17**), 7.28 – 7.20 (m, 2H, **16**, **18**), 4.46 (dd, $J = 12.5$, 4.0 Hz, 1H, **7-H_a**), 4.28 (dd, $J = 12.5$, 7.7 Hz, 1H, **7-H_b**), 3.50 – 3.44 (m, 1H, **6**), 3.35 (dd, $J = 13.7$, 6.2 Hz, 1H, **14-H_a**), 2.97 (tt, $J = 11.4$, 3.7 Hz, 1H, **4**), 2.61 (dd, $J = 13.7$, 7.4 Hz, 1H, **14-H_b**), 2.19 – 2.02 (m, 2H, **3-H_a**, **11**), 1.91 – 1.73 (m, 3H, **2-H_a**, **2'-H_a**, **3'-H_a**), 1.69 – 1.49 (m, 4H, **1-H_a**, **3-H_b**, **12-H_{a,b}**), 1.35 – 1.15 (m, 13H, **1-H_b**, **2-H_b**, **2'-H_b**, **3'-H_b**, **10**), 1.04 (t, $J = 7.4$ Hz, 3H, **13**). ^{13}C NMR (101 MHz, MeOD) δ 179.2 (**8**), 176.9 (**21**), 140.0 (**15**), 139.0 (**20**), 131.7 (**16**), 130.9 (**19**), 130.5 (**17**), 127.6 (**18**), 63.2 (**7**), 58.2 (**4**), 56.9 (**6**), 45.2 (**11**), 39.8 (**9**), 34.6 (**14**), 30.9 (**3**), 28.9 (**3'**), 27.5 (**10**), 26.0 (**1**), 25.8 (**2**), 25.6 (**2'**), 24.7 (**12**), 12.6 (**13**). IR (neat, cm^{-1}) 2969, 2856, 1731, 1580, 1558, 1370, 1149. HRMS m/z (ESI) calcd for $\text{C}_{24}\text{H}_{38}\text{N}_1\text{O}_4$ $[\text{M}+\text{H}]^+$ 404.2795, found 404.2792.

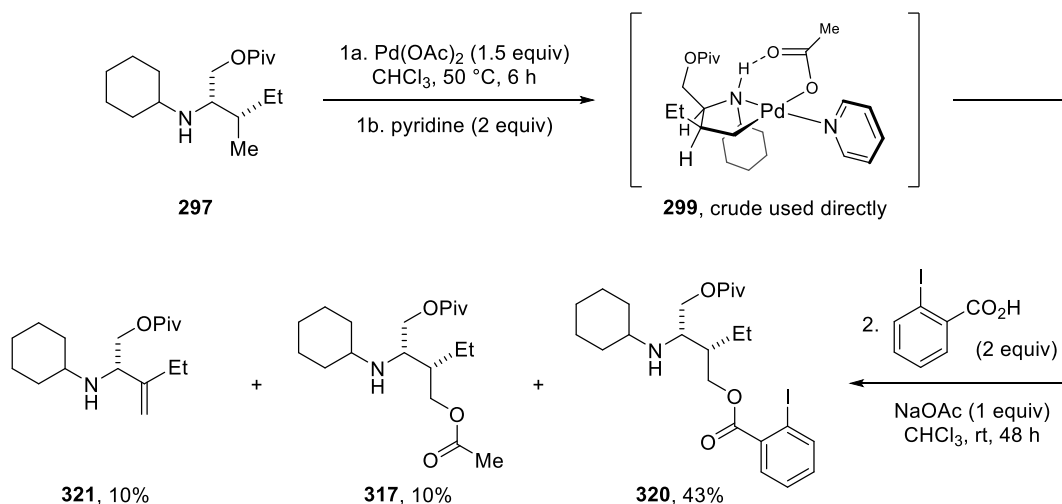
6,5-Bicyclic palladacycle dimer **319**



A solution of 2-((2*R*,3*S*)-3-(cyclohexylamino)-2-ethyl-4-(pivaloyloxy)butyl)benzoic acid (**318**, 8.1 mg, 0.02 mmol, 1 equiv) and $\text{Pd}(\text{OAc})_2$ (4.5 mg, 0.02 mmol, 1 equiv) in CDCl_3 (0.5 mL) was stirred at room temperature for 6 h. Analysis of the reaction by ^1H NMR indicated that **318** had displaced acetate from $\text{Pd}(\text{OAc})_2$, but that negligible conversion had occurred (trace **319**). The reaction was subsequently heated at 80 °C overnight. After cooling to room temperature, the mixture was filtered through a plug of Celite. Analysis by NMR indicated formation of cyclometallated complex **319** (quantitative yield against internal standard, single diastereomer). The same result was obtained following the above procedure with addition of 1 equivalent of AgOAc . ^1H NMR (400 MHz, CDCl_3) δ 7.47 (d, $J = 7.4$ Hz, 1H, **17**), 7.23 – 7.15 (m, 2H, **19**, **20**), 7.11 (t, $J = 6.9$ Hz, 1H, **18**), 5.17 (t, $J = 11.2$ Hz, 1H, **7-H_a**), 4.65 (dd, $J = 11.2$, 2.2 Hz, 1H, **7-H_b**), 4.44 (d, $J = 8.7$ Hz, 1H, **5**), 4.23 (d, $J = 11.4$ Hz, 1H, **14**), 3.50 – 3.40 (m, 1H, **6**), 2.80 (d, $J = 11.4$ Hz, 1H, **3-H_a**), 2.74 – 2.59 (m, 2H, **4**, **11**), 2.20 – 2.10 (m, 1H, **3'-H_a**), 1.86 – 1.67 (m, 3H, **2-H_a**, **2'-H_a**, **12-H_a**), 1.65 – 1.43 (m, 2H, **1-H_a**, **3-H_b**), 1.35 – 1.01 (m, 17H, **1-H_b**, **2-H_b**, **2'-H_b**, **3'-H_b**, **10**, **12-H_b**, **13**). ^{13}C NMR (101 MHz, CDCl_3) δ 178.8 (**8**), 173.7 (**21**), 145.7

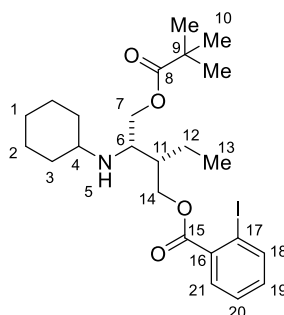
(**15**), 136.8 (**16**), 130.7 (**17**), 130.3 (**19**), 123.2 (**18**), 120.8 (**20**), 62.9 (**7**), 62.8 (**6**), 59.7 (**4**), 46.8 (**11**), 39.2 (**14**), 39.1 (**9**), 34.9 (**3**), 32.2 (**3'**), 27.5 (**10**), 26.1 (**2'**), 25.9 (**2**), 25.5 (**1**), 21.2 (**12**), 14.0 (**13**). **IR** (neat, cm^{-1}) 3217, 2932, 2855, 1730, 1630, 1594, 1576, 1545, 1446, 1302, 1282, 1141, 730. **Elemental Analysis** calcd for $\text{C}_{48}\text{H}_{70}\text{N}_2\text{O}_8\text{Pd}_2$ C: 56.75 H: 6.95 N: 2.76, found C: 56.85 H: 7.17 N 2.87.

γ -Functionalized amine products **320**, **317** and **321**

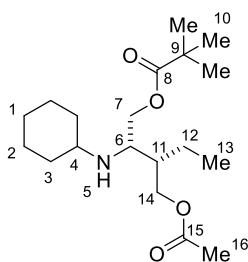


A solution of (2*S*,3*S*)-2-(cyclohexylamino)-3-methylpentyl pivalate (**297**, 57 mg, 0.20 mmol, 1 equiv) and $\text{Pd}(\text{OAc})_2$ (67 mg, 0.3 mmol, 1.5 equiv) in CHCl_3 (2 mL) was stirred in a sealed vial at 50 °C for 6 h. The reaction was cooled to room temperature, passed through a Celite plug and pyridine (32 μL , 0.40 mmol, 2 equiv) added. The reaction was concentrated *in vacuo* to give the crude pyridine-ligated Pd(II) metallacycle (**299**) which was used directly in the next step.

The crude palladacycle **299** was re-dissolved in CHCl_3 (2 mL), followed by addition of 2-iodobenzoic acid (99 mg, 0.40 mmol, 2 equiv) and NaOAc (16 mg, 0.20 mmol, 1 equiv). The reaction was stirred at room temperature for 48 h, passed through a Celite plug and concentrated *in vacuo*. The crude residue contained a mixture of three products (**320**, **317** and **321**), which were separated by silica gel flash chromatography (column 1: 0–10% Et_2O in DCM; column 2: 5–20% EtOAc in hexanes).

(2S,3S)-3-(Cyclohexylamino)-2-ethyl-4-(pivaloyloxy)butyl 2-iodobenzoate (320)

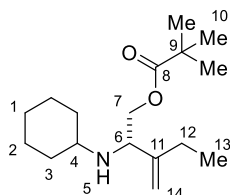
The title compound was isolated as a pale yellow oil (**320**, 46 mg, 0.087 mmol, 43% yield). $[\alpha]_D^{25.0} -5.6^\circ$ (*c* 2.0, CHCl₃). ¹H NMR (400 MHz, CDCl₃) δ 7.99 (d, *J* = 7.9 Hz, 1H, **18**), 7.77 (dd, *J* = 7.7, 1.6 Hz, 1H, **21**), 7.40 (t, *J* = 7.7 Hz, 1H, **20**), 7.15 (td, *J* = 7.9, 1.6 Hz, 1H, **19**), 4.44 (dd, *J* = 11.1, 6.6 Hz, 1H, **14-H_a**), 4.37 (dd, *J* = 11.1, 4.8 Hz, 1H, **14-H_b**), 4.15 (dd, *J* = 11.2, 5.8 Hz, 1H, **7-H_a**), 4.03 (dd, *J* = 11.2, 5.8 Hz, 1H, **7-H_b**), 3.13 – 3.07 (m, 1H, **6**), 2.49 (tt, *J* = 10.1, 3.8 Hz, 1H, **4**), 1.92 – 1.63 (m, 5H, **2-H_a**, **2'-H_a**, **3-H_a**, **3'-H_a**, **11**), 1.63 – 1.51 (m, 2H, **1-H_a**, **12-H_a**), 1.48 – 1.34 (m, 1H, **12-H_b**), 1.30 – 0.82 (m, 18H, **1-H_b**, **2-H_b**, **2'-H_b**, **3-H_b**, **3'-H_b**, **5**, **10**, **13**). ¹³C NMR (101 MHz, CDCl₃) δ 178.6 (**8**), 166.7 (**15**), 141.5 (**18**), 135.5 (**16**), 132.7 (**19**), 130.9 (**21**), 128.1 (**20**), 94.1 (**17**), 65.7 (**14**), 65.0 (**7**), 54.6 (**4**), 53.9 (**6**), 41.9 (**11**), 39.0 (**9**), 34.6 (**3'**), 34.1 (**3**), 27.4 (**10**), 26.2 (**1**), 25.2 (**2**), 25.0 (**2'**), 20.1 (**12**), 12.6 (**13**). IR (neat, cm⁻¹) 2966, 2928, 2854, 1729, 1463, 1287, 1250, 1152, 1106, 1017, 743. HRMS *m/z* (ESI) calcd for C₂₄H₃₇I₁N₁O₄ [M+H]⁺ 530.1762, found 530.1752.

(2S,3S)-3-(Acetoxymethyl)-2-(cyclohexylamino)pentyl pivalate (317)

The title compound was isolated as a colourless oil (**317**, 7.1 mg, 0.021 mmol, 10% yield). $[\alpha]_D^{25.0} +17.8^\circ$ (*c* 0.4, CHCl₃). ¹H NMR (400 MHz, CDCl₃) δ 4.19 – 4.07 (m, 3H, **7-H_a**, **14-H_{a,b}**), 3.98 (dd, *J* = 11.3, 6.1 Hz, 1H, **7-H_b**), 3.02 – 2.96 (m, 1H, **6**), 2.46 (tt, *J* = 10.1, 3.7 Hz, 1H, **4**), 2.04 (s, 3H, **16**), 1.86 – 1.66 (m, 5H, **2-H_a**, **2'-H_a**, **3-H_a**, **3'-H_a**, **11**), 1.62 – 1.43 (m, 2H, **1-H_a**, **12-H_a**), 1.39 – 0.92 (m, 19H, **1-H_b**, **2-H_b**, **2'-H_b**, **3-H_b**, **3'-H_b**, **5**, **10**, **12-H_b**, **13**). ¹³C NMR (101 MHz, CDCl₃) δ 178.7 (**8**), 171.3 (**15**), 65.0 (**7**), 64.4 (**14**), 54.5 (**4**), 53.9 (**6**), 41.7

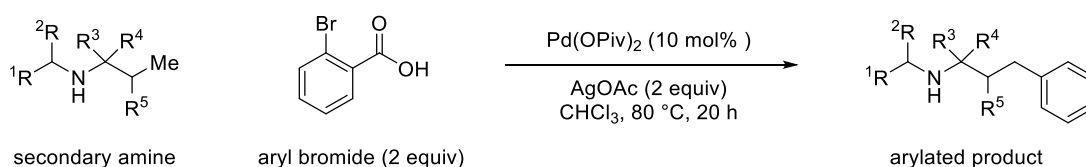
(**11**), 39.0 (**9**), 34.5 (**3'**), 34.1 (**3**), 27.4 (**10**), 26.2 (**1**), 25.2 (**2**), 25.0 (**2'**), 21.2 (**16**), 20.2 (**12**), 12.5 (**13**). **IR** (neat, cm^{-1}) 2966, 2929, 2858, 1732, 1481, 1367, 1283, 1234, 1154, 1034. **HRMS** m/z (ESI) calcd for $\text{C}_{19}\text{H}_{36}\text{N}_1\text{O}_4$ $[\text{M}+\text{H}]^+$ 342.2639, found 342.2642.

(S)-2-(Cyclohexylamino)-3-methylenepentyl pivalate (321)

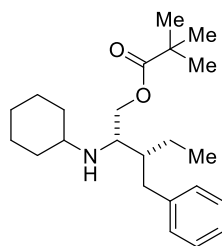


The title compound was isolated as a colourless oil (**321**, 5.6 mg, 0.020 mmol, 10% yield). $[\alpha]_D^{25.0} +19.8^\circ$ (c 0.4, CHCl_3). **^1H NMR** (400 MHz, CDCl_3) δ 5.03 (br. s, 1H, **14-H_a**), 4.93 (d, $J = 1.2$ Hz, 1H, **14-H_b**), 4.10 (dd, $J = 10.9, 5.4$ Hz, 1H, **7-H_a**), 3.95 (dd, $J = 10.9, 7.5$ Hz, 1H, **7-H_b**), 3.56 – 3.49 (m, 1H, **6**), 2.38 (tt, $J = 10.2, 3.6$ Hz, 1H, **4**), 2.15 – 1.87 (m, 3H, **3-H_a**, **12-H_{a,b}**), 1.82 – 1.66 (m, 3H, **2-H_a**, **2'-H_a**, **3'-H_a**), 1.62 – 1.54 (m, 1H, **1-H_a**), 1.29 – 0.87 (m, 18H, **1-H_b**, **2-H_b**, **2'-H_b**, **3-H_b**, **3'-H_b**, **5**, **10**, **13**). **^{13}C NMR** (101 MHz, CDCl_3) δ 178.4 (**8**), 149.6 (**11**), 111.2 (**14**), 66.7 (**7**), 59.4 (**6**), 53.7 (**4**), 38.9 (**9**), 34.8 (**3'**), 33.3 (**3**), 27.4 (**10**), 26.3 (**1**), 25.4 (**2**), 25.0 (**2'**), 24.9 (**12**), 12.3 (**13**). **IR** (neat, cm^{-1}) 2966, 2929, 2851, 1733, 1481, 1283, 1151, 1035, 798. **HRMS** m/z (ESI) calcd for $\text{C}_{17}\text{H}_{32}\text{N}_1\text{O}_2$ $[\text{M}+\text{H}]^+$ 282.2428, found 282.2431.

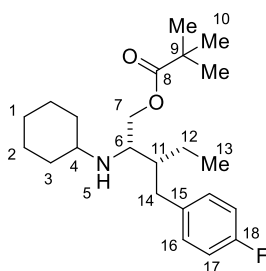
Pd-catalyzed Decarboxylative γ C(sp³)-H Arylation



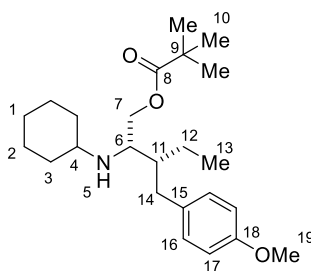
General Procedure B. To a 2–5 mL microwave vial containing a 10 mm magnetic stirrer bar were added $\text{Pd}(\text{OPiv})_2$ (3.1 mg, 0.01 mmol, 10 mol%), AgOAc (33.4 mg, 0.2 mmol, 2 equiv) and aryl bromide (0.2 mmol, 2 equiv). Under air, a solution of amine (0.1 mmol, 1 equiv) in CHCl_3 (1 mL) was added via syringe and the vial sealed with a crimp cap with silicone/PTFE septum. The vial was placed in an oil bath pre-heated to 80 °C, and the reaction stirred at this temperature for 20 h. After cooling to room temperature, the reaction was filtered through a short plug of Celite and the filtrate concentrated *in vacuo*. The crude residue was purified by silica gel flash chromatography, wherein the arylated product was separated from remaining starting material and minor C–O acyloxylation by-product.

(2*S*,3*R*)-3-Benzyl-2-(cyclohexylamino)pentyl pivalate (301a)

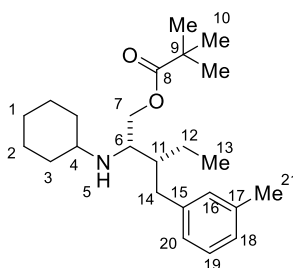
Synthesised using General Procedure B from (2*S*,3*S*)-2-(cyclohexylamino)-3-methylpentyl pivalate (**297**, 28.3 mg, 0.10 mmol) and 2-bromobenzoic acid. Purification by silica gel flash chromatography (5–10% EtOAc in hexanes) gave the title compound as a pale yellow oil (**301a**, 25.1 mg, 0.070 mmol, 70% yield). Spectral data were presented previously in the Experimental.

(2*S*,3*R*)-2-(Cyclohexylamino)-3-(4-fluorobenzyl)pentyl pivalate (301c)

Synthesised using General Procedure B from (2*S*,3*S*)-2-(cyclohexylamino)-3-methylpentyl pivalate (**297**, 28.3 mg, 0.10 mmol) and 2-bromo-5-fluorobenzoic acid. Purification by silica gel flash chromatography (2–5% EtOAc in hexanes) gave the title compound as a pale yellow oil (**301c**, 20.4 mg, 0.054 mmol, 54% yield). $[\alpha]_D^{22.7} -11.8^\circ$ (*c* 1.0, CHCl₃). **¹H NMR** (400 MHz, CDCl₃) δ 7.11 (dd, *J* = 8.5, 5.5 Hz, 2H, **16**), 6.95 (app. t, *J* = 8.5 Hz, 2H, **17**), 4.09 (dd, *J* = 11.1, 6.0 Hz, 1H, **7-H_a**), 3.97 (dd, *J* = 11.1, 6.0 Hz, 1H, **7-H_b**), 2.94 – 2.88 (m, 1H, **6**), 2.80 (dd, *J* = 13.8, 6.6 Hz, 1H, **14-H_a**), 2.54 – 2.44 (m, 1H, **4**), 2.41 (dd, *J* = 13.8, 7.7 Hz, 1H, **14-H_b**), 1.88 – 1.65 (m, 5H, **2-H_{a,b}**, **3-H_a**, **3'-H_a**, **11**), 1.64 – 1.54 (m, 1H, **1-H_a**), 1.44 – 0.96 (m, 17H, **1-H_b**, **2'-H_{a,b}**, **3-H_b**, **3'-H_b**, **5**, **10**, **12-H_{a,b}**), 0.90 (t, *J* = 7.4 Hz, 3H, **13**). **¹³C NMR** (101 MHz, CDCl₃) δ 178.6 (**8**), 161.3 (d, $^1J_{CF}$ = 243 Hz, **18**), 137.6 (d, $^4J_{CF}$ = 3.3 Hz, **15**), 130.4 (d, $^3J_{CF}$ = 7.7 Hz, **16**), 115.1 (d, $^2J_{CF}$ = 20.9 Hz, **17**), 64.9 (**7**), 54.3 (**4**), 53.8 (**6**), 44.4 (**11**), 38.9 (**9**), 35.4 (**14**), 34.6 (**3'**), 34.3 (**3**), 27.3 (**10**), 26.2 (**1**), 25.2 (**2**), 25.1 (**2'**), 22.1 (**12**), 12.5 (**13**). **¹⁹F NMR** (376 MHz, CDCl₃) δ -118.9. **IR** (film, cm⁻¹) 2960, 2925, 2854, 1729, 1509, 1460, 1282, 1222, 1155. **HRMS** *m/z* (ESI) calcd for C₂₃H₃₇F₁N₁O₂ [*M*+*H*]⁺ 378.2803, found 378.2800.

(2*S*,3*R*)-2-(Cyclohexylamino)-3-(4-methoxybenzyl)pentyl pivalate (301d)

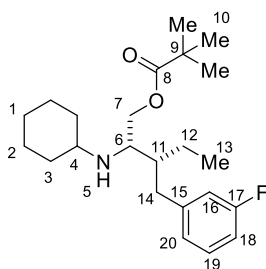
Synthesised using General Procedure B from (2*S*,3*S*)-2-(cyclohexylamino)-3-methylpentyl pivalate (**297**, 28.3 mg, 0.10 mmol) and 2-bromo-5-methoxybenzoic acid. Purification by silica gel flash chromatography (2–5% Et₂O in DCM) gave the title compound as a pale yellow oil (21.1 mg, 0.054 mmol, 54% yield). $[\alpha]_D^{22.7} -9.0^\circ$ (*c* 1.0, CHCl₃). **¹H NMR** (400 MHz, CDCl₃) δ 7.07 (d, *J* = 8.5 Hz, 2H, **16**), 6.82 (d, *J* = 8.5 Hz, 2H, **17**), 4.09 (dd, *J* = 11.1, 5.9 Hz, 1H, **7-H_a**), 3.97 (dd, *J* = 11.1, 6.2 Hz, 1H, **7-H_b**), 3.79 (s, 3H, **19**), 2.95 – 2.89 (m, 1H, **6**), 2.75 (dd, *J* = 13.8, 6.6 Hz, 1H, **14-H_a**), 2.53 – 2.44 (m, 1H, **4**), 2.39 (dd, *J* = 13.8, 7.8 Hz, 1H, **14-H_b**), 1.87 – 1.65 (m, 5H, **2-H_a**, **2'-H_a**, **3-H_a**, **3'-H_a**, **11**), 1.63 – 1.55 (m, 1H, **1-H_a**), 1.45 – 0.97 (m, 17H, **1-H_b**, **2-H_b**, **2'-H_b**, **3-H_b**, **3'-H_b**, **5**, **10**, **12-H_{a,b}**), 0.90 (t, *J* = 7.4 Hz, 3H, **13**). **¹³C NMR** (101 MHz, CDCl₃) δ 178.7 (**8**), 157.8 (**18**), 133.9 (**15**), 130.1 (**16**), 113.8 (**17**), 65.1 (**7**), 55.4 (**19**), 54.4 (**4**), 53.9 (**6**), 44.4 (**11**), 38.9 (**9**), 35.3 (**14**), 34.6 (**3'**), 34.4 (**3**), 27.4 (**10**), 26.3 (**1**), 25.3 (**2**), 25.2 (**2'**), 22.2 (**12**), 12.5 (**13**). **IR** (film, cm⁻¹) 2927, 2855, 1728, 1512, 1461, 1282, 1246, 1155, 1037. **HRMS** *m/z* (ESI) calcd for C₂₄H₄₀N₁O₃ [M+H]⁺ 390.3003, found 390.2995.

(2*S*,3*R*)-2-(Cyclohexylamino)-3-(3-methylbenzyl)pentyl pivalate (301f)

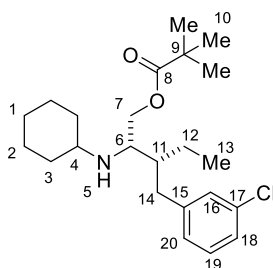
Synthesised using General Procedure B from (2*S*,3*S*)-2-(cyclohexylamino)-3-methylpentyl pivalate (**297**, 28.3 mg, 0.10 mmol) and either 2-bromo-4-methylbenzoic acid or 2-bromo-6-methylbenzoic acid. Purification by silica gel flash chromatography (0–10% EtOAc in hexanes) gave the title compound as a pale yellow oil. Using 2-bromo-4-methylbenzoic acid: 23.4 mg, 0.063 mmol, 63% yield (**301fa**). Using 2-bromo-6-methylbenzoic acid: 22.5 mg, 0.060 mmol,

60% yield (**301fb**). $[\alpha]_D^{22.7} -10.8^\circ$ (*c* 1.0, CHCl₃). **¹H NMR** (400 MHz, CDCl₃) δ 7.16 (app. t, *J* = 7.9 Hz, 1H, **19**), 7.01 – 6.94 (m, 3H, **16**, **18**, **20**), 4.10 (dd, *J* = 11.1, 6.0 Hz, 1H, **7-H_a**), 3.98 (dd, *J* = 11.1, 6.0 Hz, 1H, **7-H_b**), 2.95 – 2.89 (m, 1H, **6**), 2.77 (dd, *J* = 13.6, 6.8 Hz, 1H, **14-H_a**), 2.54 – 2.38 (m, 2H, **4**, **14-H_b**), 2.32 (s, 3H, **21**), 1.87 – 1.68 (m, 5H, **2-H_{a,b}**, **3-H_a**, **3'-H_a**, **11**), 1.65 – 1.49 (m, 2H, **1-H_a**, **5**), 1.46 – 0.99 (m, 16H, **1-H_b**, **2'-H_{a,b}**, **3-H_b**, **3'-H_b**, **10**, **12-H_{a,b}**), 0.91 (t, *J* = 7.4 Hz, 3H, **13**). **¹³C NMR** (101 MHz, CDCl₃) δ 178.6 (**8**), 141.8 (**15**), 137.8 (**17**), 130.0 (**16**), 128.2 (**19**), 126.6 (**18**), 126.2 (**20**), 65.0 (**7**), 54.4 (**4**), 53.9 (**6**), 44.1 (**11**), 38.9 (**9**), 36.1 (**14**), 34.6 (**3'**), 34.3 (**3**), 27.4 (**10**), 26.3 (**1**), 25.2(4) (**2**), 25.1(7) (**2'**), 22.2 (**12**), 21.5 (**21**), 12.5 (**13**). **IR** (film, cm⁻¹) 2960, 2926, 2854, 1729, 1479, 1460, 1282, 1154. **HRMS** *m/z* (ESI) calcd for C₂₄H₄₀N₁O₂ [M+H]⁺ 374.3054, found 374.3055.

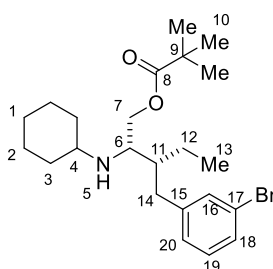
(2*S*,3*R*)-2-(Cyclohexylamino)-3-(3-fluorobenzyl)pentyl pivalate (301g**)**



Synthesised using General Procedure B from (2*S*,3*S*)-2-(cyclohexylamino)-3-methylpentyl pivalate (**297**, 28.3 mg, 0.10 mmol) and 2-bromo-4-fluorobenzoic acid. Purification by silica gel flash chromatography (5% EtOAc in hexanes) provided the title compound as a pale yellow oil (**310g**, 21.3 mg, 0.056 mmol, 56% yield). $[\alpha]_D^{25.0} -12.0^\circ$ (*c* 1.0, CHCl₃). **¹H NMR** (400 MHz, CDCl₃) δ 7.26 – 7.17 (m, 1H, **19**), 6.94 (d, *J* = 7.6 Hz, 1H, **20**), 6.90 – 6.83 (m, 2H, **16**, **18**), 4.09 (dd, *J* = 11.1, 6.0 Hz, 1H, **7-H_a**), 3.97 (dd, *J* = 11.1, 6.0 Hz, 1H, **7-H_b**), 2.95 – 2.88 (m, 1H, **6**), 2.84 (dd, *J* = 13.6, 6.5 Hz, 1H, **14-H_a**), 2.54 – 2.39 (m, 2H, **4**, **14-H_b**), 1.87 – 1.66 (m, 5H, **2-H_{a,b}**, **3-H_a**, **3'-H_a**, **11**), 1.64 – 1.55 (m, 1H, **1-H_a**), 1.46 – 0.97 (m, 17H, **1-H_b**, **2'-H_{a,b}**, **3-H_b**, **3'-H_b**, **5**, **10**, **12-H_{a,b}**), 0.90 (t, *J* = 7.4 Hz, 3H, **13**). **¹³C NMR** (101 MHz, CDCl₃) δ 178.6 (**8**), 163.0 (d, ¹*J*_{CF} = 245 Hz, **17**), 144.7 (d, ³*J*_{CF} = 7.1 Hz, **15**), 129.7 (d, ³*J*_{CF} = 8.3 Hz, **19**), 124.9 (d, ⁴*J*_{CF} = 2.7 Hz, **20**), 115.9 (d, ²*J*_{CF} = 20.8 Hz, **16**), 112.7 (d, ²*J*_{CF} = 21.0, **18**), 64.8 (**7**), 54.3 (**4**), 53.9 (**6**), 44.1 (**11**), 38.9 (**9**), 36.0 (**14**), 34.6 (**3'**), 34.4 (**3**), 27.4 (**10**), 26.3 (**1**), 25.2 (**2**), 25.1 (**2'**), 22.1 (**12**), 12.5 (**13**). **¹⁹F NMR** (376 MHz, CDCl₃) δ -115.0. **IR** (film, cm⁻¹) 2959, 2927, 2851, 1729, 1589, 1480, 1449, 1282, 1153, 781. **HRMS** *m/z* (ESI) calcd for C₂₃H₃₇F₁N₁O₂ [M+H]⁺ 378.2803, found 378.2802.

(2*S*,3*R*)-3-(3-Chlorobenzyl)-2-(cyclohexylamino)pentyl pivalate (301h)

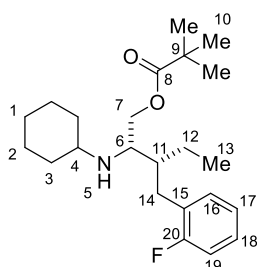
Synthesised using General Procedure B from (2*S*,3*S*)-2-(cyclohexylamino)-3-methylpentyl pivalate (**297**, 28.3 mg, 0.10 mmol) and 2-bromo-4-chlorobenzoic acid. Purification by silica gel flash chromatography (0–10% EtOAc in hexanes) gave the title compound as a pale yellow oil (**301h**, 24.2 mg, 0.061 mmol, 61% yield). $[\alpha]_D^{25.0} -15.3^\circ$ (*c* 1.0, CHCl₃). **¹H NMR** (400 MHz, CDCl₃) δ 7.23 – 7.12 (m, 3H, **16**, **18**, **19**), 7.04 (app. d, *J* = 7.3 Hz, 1H, **20**), 4.08 (dd, *J* = 11.1, 6.1 Hz, 1H, **7-H_a**), 3.97 (dd, *J* = 11.1, 6.1 Hz, 1H, **7-H_b**), 2.93 – 2.87 (m, 1H, **6**), 2.82 (dd, *J* = 13.7, 6.8 Hz, 1H, **14-H_a**), 2.54 – 2.38 (m, 2H, **4**, **14-H_b**), 1.87 – 1.66 (m, 5H, **2-H_{a,b}**, **3-H_a**, **3'-H_a**, **11**), 1.64 – 1.55 (m, 1H, **1-H_a**), 1.46 – 0.98 (m, 17H, **1-H_b**, **2'-H_{a,b}**, **3-H_b**, **3'-H_b**, **5**, **10**, **12-H_{a,b}**), 0.91 (t, *J* = 7.3 Hz, 3H, **13**). **¹³C NMR** (101 MHz, CDCl₃) δ 178.6 (**8**), 144.2 (**15**), 134.1 (**17**), 129.6 (**19**), 129.3 (**16**), 127.4 (**20**), 126.1 (**18**), 64.7 (**7**), 54.3 (**4**), 53.8 (**6**), 44.1 (**11**), 38.9 (**9**), 35.9 (**14**), 34.6 (**3'**), 34.3 (**3**), 27.4 (**10**), 26.3 (**1**), 25.2 (**2**), 25.1 (**2'**), 22.1 (**12**), 12.5 (**13**). **IR** (film, cm⁻¹) 2959, 2929, 2851, 1729, 1478, 1282, 1153, 769. **HRMS** *m/z* (ESI) calcd for C₂₃H₃₇ClN₁O₂ [M+H]⁺ 394.2507, found 394.2506.

(2*S*,3*R*)-3-(3-Bromobenzyl)-2-(cyclohexylamino)pentyl pivalate (301i)

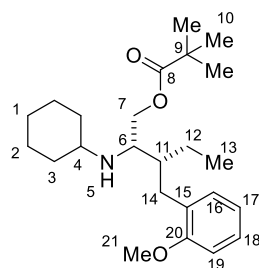
Synthesised using General Procedure B (**note**: 2.5 equiv aryl bromide and 2.5 equiv AgOAc were used) from (2*S*,3*S*)-2-(cyclohexylamino)-3-methylpentyl pivalate (**297**, 28.3 mg, 0.10 mmol) and 2,4-dibromobenzoic acid. Purification by silica gel flash chromatography (5–10% EtOAc in hexanes) gave the title compound as a pale yellow oil (**301i**, 21.3 mg, 0.049 mmol, 49% yield). $[\alpha]_D^{25.0} -14.8^\circ$ (*c* 1.0, CHCl₃). **¹H NMR** (400 MHz, CDCl₃) δ 7.35 – 7.28 (m, 2H,

16, 18), 7.17 – 7.06 (m, 2H, **19, 20**), 4.08 (dd, $J = 11.1, 6.1$ Hz, 1H, **7-H_a**), 3.96 (dd, $J = 11.1, 6.1$ Hz, 1H, **7-H_b**), 2.93 – 2.86 (m, 1H, **6**), 2.81 (dd, $J = 13.7, 6.8$ Hz, 1H, **14-H_a**), 2.53 – 2.38 (m, 2H, **4, 14-H_b**), 1.86 – 1.66 (m, 5H, **2-H_a, 2'-H_a, 3-H_a, 3'-H_a, 11**), 1.64 – 1.55 (m, 1H, **1-H_a**), 1.47 – 0.97 (m, 17H, **1-H_b, 2-H_b, 2'-H_b, 3-H_b, 3'-H_b, 5, 10, 12-H_{a,b}**), 0.91 (t, $J = 7.3$ Hz, 3H, **13**). ^{13}C NMR (101 MHz, CDCl_3) δ 178.6 (**8**), 144.5 (**15**), 132.2 (**16**), 129.9 (**19**), 129.0 (**18**), 127.9 (**20**), 122.5 (**17**), 64.7 (**7**), 54.3 (**4**), 53.7 (**6**), 44.1 (**11**), 38.9 (**9**), 35.9 (**14**), 34.6 (**3'**), 34.3 (**3**), 27.4 (**10**), 26.3 (**1**), 25.2 (**2**), 25.1 (**2'**), 22.1 (**12**), 12.5 (**13**). IR (film, cm^{-1}) 2956, 2929, 2852, 1728, 1477, 1281, 1153, 770. HRMS m/z (ESI) calcd for $\text{C}_{23}\text{H}_{37}\text{Br}_1\text{N}_1\text{O}_2$ $[\text{M}+\text{H}]^+$ 438.2002, found 438.2005.

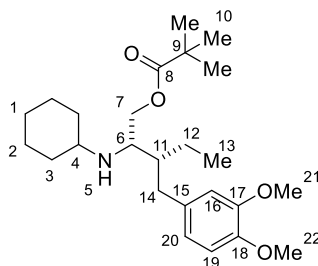
(2*S*,3*R*)-2-(Cyclohexylamino)-3-(2-fluorobenzyl)pentyl pivalate (301j)



Synthesised using General Procedure B from (2*S*,3*S*)-2-(cyclohexylamino)-3-methylpentyl pivalate (**297**, 28.3 mg, 0.10 mmol) and 2-bromo-3-fluorobenzoic acid. Purification by silica gel flash chromatography (5–10% EtOAc in hexanes) gave the title compound as a pale yellow oil (**301j**, 17.4 mg, 0.046 mmol, 46% yield). $[\alpha]_D^{22.7} -11.9^\circ$ (c 1.0, CHCl_3). ^1H NMR (400 MHz, CDCl_3) δ 7.20 – 7.12 (m, 2H, **16, 18**), 7.07 – 6.95 (m, 2H, **17, 19**), 4.10 (dd, $J = 11.1, 6.1$ Hz, 1H, **7-H_a**), 4.00 (dd, $J = 11.1, 6.1$ Hz, 1H, **7-H_b**), 2.97 – 2.91 (m, 1H, **6**), 2.85 (dd, $J = 13.7, 6.3$ Hz, 1H, **14-H_a**), 2.55 – 2.45 (m, 2H, **4, 14-H_b**), 1.89 – 1.67 (m, 5H, **2-H_a, 2'-H_a, 3-H_a, 3'-H_a, 11**), 1.63 – 1.56 (m, 1H, **1-H_a**), 1.47 – 0.99 (m, 17H, **1-H_b, 2-H_b, 2'-H_b, 3-H_b, 3'-H_b, 5, 10, 12-H_{a,b}**), 0.90 (t, $J = 7.4$ Hz, 3H, **13**). ^{13}C NMR (101 MHz, CDCl_3) δ 178.7 (**8**), 161.5 (d, $^1J_{\text{CF}} = 245$ Hz, **20**), 131.6 (d, $^3J_{\text{CF}} = 5.2$ Hz, **16**), 128.8 (d, $^2J_{\text{CF}} = 15.7$ Hz, **15**), 127.6 (d, $^3J_{\text{CF}} = 8.1$ Hz, **18**), 123.9 (d, $^4J_{\text{CF}} = 3.4$ Hz, **17**), 115.4 (**19**), 64.9 (**7**), 54.3 (**4**), 54.0 (**6**), 42.8 (**11**), 38.9 (**9**), 34.6 (**3'**), 34.3 (**3**), 29.7 (d, $^3J_{\text{CF}} = 1.4$ Hz, **14**), 27.3 (**10**), 26.3 (**1**), 25.3 (**2**), 25.2 (**2'**), 22.3 (**12**), 12.4 (**13**). ^{19}F NMR (376 MHz, CDCl_3) δ -117.6. IR (film, cm^{-1}) 2960, 2927, 2854, 1729, 1492, 1454, 1283, 1229, 1154, 754. HRMS m/z (ESI) calcd for $\text{C}_{23}\text{H}_{37}\text{F}_1\text{N}_1\text{O}_2$ $[\text{M}+\text{H}]^+$ 378.2803, found 378.2804.

(2*S*,3*R*)-2-(Cyclohexylamino)-3-(2-methoxybenzyl)pentyl pivalate (301k)

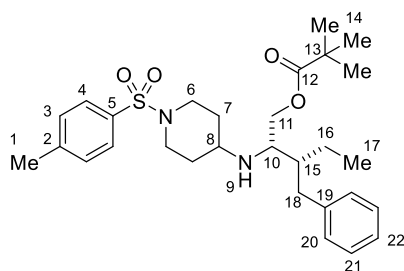
Synthesised using General Procedure B from (2*S*,3*S*)-2-(cyclohexylamino)-3-methylpentyl pivalate (**297**, 28.3 mg, 0.10 mmol) and 2-bromo-3-methoxybenzoic acid. Purification by silica gel flash chromatography (5–10% Et₂O in DCM) gave the title compound as a pale yellow oil (**301k**, 19.7 mg, 0.051 mmol, 51% yield). $[\alpha]_D^{22.7} -5.8^\circ$ (*c* 1.0, CHCl₃). ¹H NMR (400 MHz, CDCl₃) δ 7.17 (app. t, *J* = 7.8 Hz, 1H, **18**), 7.11 (d, *J* = 7.1 Hz, 1H, **16**), 6.87 (app. t, *J* = 7.4 Hz, 1H, **17**), 6.83 (d, *J* = 8.2 Hz, 1H, **19**), 4.12 (dd, *J* = 11.0, 5.9 Hz, 1H, **7-H_a**), 4.00 (dd, *J* = 11.0, 6.3 Hz, 1H, **7-H_b**), 3.80 (s, 3H, **21**), 2.99 – 2.92 (m, 1H, **6**), 2.85 (dd, *J* = 13.4, 5.8 Hz, 1H, **14-H_a**), 2.57 – 2.48 (m, 1H, **4**), 2.41 (dd, *J* = 13.4, 8.1 Hz, 1H, **14-H_b**), 1.90 – 1.79 (m, 3H, **3-H_a**, **3'-H_a**, **11**), 1.78 – 1.68 (m, 2H, **2-H_a**, **2'-H_a**), 1.64 – 1.56 (m, 1H, **1-H_a**), 1.45 – 0.99 (m, 17H, **1-H_b**, **2-H_b**, **2'-H_b**, **3-H_b**, **3'-H_b**, **5**, **10**, **12-H_{a,b}**), 0.88 (t, *J* = 7.4 Hz, 3H, **13**). ¹³C NMR (101 MHz, CDCl₃) δ 178.7 (**8**), 157.7 (**20**), 131.0 (**16**), 130.1 (**15**), 127.1 (**18**), 120.3 (**17**), 110.3 (**19**), 65.4 (**7**), 55.2 (**21**), 54.5 (**4**), 54.2 (**6**), 42.3 (**11**), 38.9 (**9**), 34.5 (**3'**), 34.3 (**3**), 30.8 (**14**), 27.4 (**10**), 26.3 (**1**), 25.3(3) (**2**), 25.2(8) (**2'**), 22.7 (**12**), 12.5 (**13**). IR (film, cm⁻¹) 2926, 2854, 1728, 1494, 1465, 1285, 1242, 1155, 1032, 751. HRMS *m/z* (ESI) calcd for C₂₄H₄₀N₁O₃ [M+H]⁺ 390.3003, found 390.3003.

(2*S*,3*R*)-2-(Cyclohexylamino)-3-(3,4-dimethoxybenzyl)pentyl pivalate (301l)

Synthesised using General Procedure B from (2*S*,3*S*)-2-(cyclohexylamino)-3-methylpentyl pivalate (**297**, 28.3 mg, 0.10 mmol) and 2-bromo-4,5-dimethoxybenzoic acid. Purification by silica gel flash chromatography (5–20% EtOAc in hexanes) gave the title compound as a pale

yellow oil (**301l**, 25.8 mg, 0.061 mmol, 61% yield). $[\alpha]_D^{25.0} -15.2^\circ$ (*c* 1.0, CHCl₃). ¹H NMR (400 MHz, CDCl₃) δ 6.78 (d, *J* = 7.9 Hz, 1H, **19**), 6.74 – 6.67 (m, 2H, **16**, **20**), 4.10 (dd, *J* = 11.1, 6.1 Hz, 1H, **7-H_a**), 3.97 (dd, *J* = 11.1, 6.1 Hz, 1H, **7-H_b**), 3.88 – 3.83 (m, 6H, **21**, **22**), 2.96 – 2.89 (m, 1H, **6**), 2.75 (dd, *J* = 13.6, 6.7 Hz, 1H, **14-H_a**), 2.54 – 2.45 (m, 1H, **4**), 2.40 (dd, *J* = 13.6, 7.6, 1H, **14-H_b**), 1.90 – 1.66 (m, 5H, **2-H_{a,b}**, **3-H_a**, **3'-H_a**, **11**), 1.64 – 1.55 (m, 1H, **1-H_a**), 1.46 – 0.99 (m, 17H, **1-H_b**, **2'-H_{a,b}**, **3-H_b**, **3'-H_b**, **5**, **10**, **12-H_{a,b}**), 0.91 (t, *J* = 7.4 Hz, 3H, **13**). ¹³C NMR (101 MHz, CDCl₃) δ 178.6 (**8**), 148.8 (**17**), 147.3 (**18**), 134.6 (**15**), 121.0 (**20**), 112.6 (**16**), 111.3 (**19**), 65.1 (**7**), 56.1 (**21** or **22**), 55.9 (**21** or **22**), 54.4 (**4**), 53.9 (**6**), 44.4 (**11**), 38.9 (**9**), 35.9 (**14**), 34.6 (**3'**), 34.4 (**3**), 27.4 (**10**), 26.3 (**1**), 25.3 (**2**), 25.2 (**2'**), 22.2 (**12**), 12.5 (**13**). IR (film, cm⁻¹) 2959, 2927, 2852, 1727, 1515, 1463, 1281, 1261, 1237, 1155, 1031, 765. HRMS *m/z* (ESI) calcd for C₂₅H₄₂N₁O₄ [M+H]⁺ 420.3108, found 420.3108.

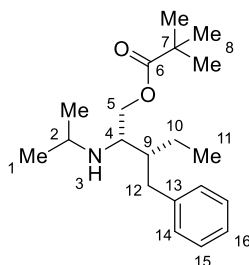
(2*S*,3*R*)-3-Benzyl-2-((1-tosylpiperidin-4-yl)amino)pentyl pivalate (330f**)**



Synthesised using General Procedure B from (2*S*,3*S*)-3-methyl-2-((1-tosylpiperidin-4-yl)amino)pentyl pivalate (**329f**, 43.8 mg, 0.10 mmol) and 2-bromobenzoic acid. Purification by silica gel flash chromatography (10–20% EtOAc in hexanes) gave the title compound as a colourless oil (**330f**, 39.8 mg, 0.077 mmol, 77% yield). $[\alpha]_D^{24.0} -7.6^\circ$ (*c* 1.0, CHCl₃). ¹H NMR (400 MHz, CDCl₃) δ 7.64 (d, *J* = 8.1 Hz, 2H, **4**), 7.32 (d, *J* = 8.1 Hz, 2H, **3**), 7.27 – 7.21 (m, 2H, **21**), 7.19 – 7.13 (m, 1H, **22**), 7.09 (d, *J* = 7.5 Hz, 2H, **20**), 4.02 (dd, *J* = 11.1, 6.0 Hz, 1H, **11-H_a**), 3.93 (dd, *J* = 11.1, 6.0 Hz, 1H, **11-H_b**), 3.65 – 3.56 (m, 2H, **6-H_a**, **6'-H_a**), 2.84 – 2.77 (m, 1H, **10**), 2.71 (dd, *J* = 13.7, 7.0 Hz, 1H, **18-H_a**), 2.53 – 2.36 (m, 7H, **1**, **6-H_b**, **6'-H_b**, **8**, **18-H_b**), 1.87 – 1.75 (m, 2H, **7-H_a**, **7'-H_a**), 1.74 – 1.65 (m, 1H, **15**), 1.48 – 1.06 (m, 14H, **7-H_b**, **7'-H_b**, **9**, **14**, **16-H_{a,b}**), 0.88 (t, *J* = 7.4 Hz, 3H, **17**). ¹³C NMR (101 MHz, CDCl₃) δ 178.6 (**12**), 143.6 (**2**), 141.6 (**19**), 133.2 (**5**), 129.7 (**3**), 129.1 (**20**), 128.4 (**21**), 127.8 (**4**), 126.0 (**22**), 64.3 (**11**), 53.9 (**10**), 51.2 (**8**), 45.1 (**6**), 45.0 (**6'**), 43.9 (**15**), 38.9 (**13**), 36.1 (**18**), 32.8 (**7**), 32.3 (**7'**), 27.3 (**14**), 22.1 (**16**), 21.6 (**1**), 12.5 (**17**). IR (film, cm⁻¹) 2964, 2932, 2875, 1725, 1479, 1340,

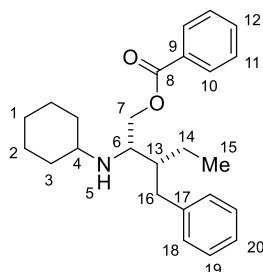
1284, 1164, 1092, 1047, 934, 727. **HRMS** m/z (ESI) calcd for $C_{29}H_{43}N_2O_4S_1$ $[M+H]^+$ 515.2938, found 515.2931.

(2S,3R)-3-Benzyl-2-(isopropylamino)pentyl pivalate (330h)



Synthesised using General Procedure B from (2S,3S)-2-(isopropylamino)-3-methylpentyl pivalate (**329h**, 24.3 mg, 0.10 mmol) and 2-bromobenzoic acid. Purification by silica gel flash chromatography (4–10% EtOAc in hexanes) gave the title compound as a colourless oil (**330h**, 17.9 mg, 0.056 mmol, 56% yield). $[\alpha]_D^{24.0} -1.8^\circ$ (c 1.0, $CHCl_3$). **1H NMR** (400 MHz, $CDCl_3$) δ 7.30 – 7.24 (m, 2H, **15**), 7.20 – 7.13 (m, 3H, **14**, **16**), 4.12 (dd, $J = 11.1, 5.9$ Hz, 1H, **5-H_a**), 3.98 (dd, $J = 11.1, 5.9$ Hz, 1H, **5-H_b**), 2.96 – 2.86 (m, 2H, **2**, **4**), 2.82 (dd, $J = 13.6, 6.6$ Hz, 1H, **12-H_a**), 2.45 (dd, $J = 13.6, 7.7$ Hz, 1H, **12-H_b**), 1.82 – 1.71 (m, 1H, **9**), 1.47 – 1.09 (m, 12H, **3**, **8**, **10-H_{a,b}**), 1.03 (app. t, $J = 6.5$ Hz, 6H, **1**, **1'**), 0.91 (t, $J = 7.4$ Hz, 3H, **11**). **^{13}C NMR** (101 MHz, $CDCl_3$) δ 178.6 (**6**), 141.9 (**13**), 129.2 (**14**), 128.4 (**15**), 125.9 (**16**), 64.9 (**5**), 54.3 (**4**), 46.2 (**2**), 44.2 (**9**), 38.9 (**7**), 36.2 (**12**), 27.4 (**8**), 23.9 (**1**), 23.7 (**1'**), 22.3 (**10**), 12.5 (**11**). **IR** (film, cm^{-1}) 2963, 2933, 1730, 1479, 1463, 1380, 1282, 1154, 737, 699. **HRMS** m/z (ESI) calcd for $C_{20}H_{34}N_1O_2$ $[M+H]^+$ 320.2584, found 320.2587.

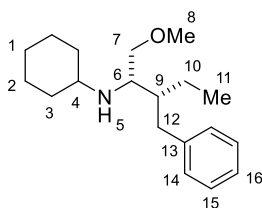
(2S,3R)-3-Benzyl-2-(cyclohexylamino)pentyl benzoate (330k)



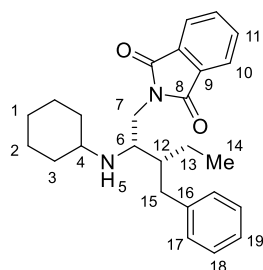
Synthesised using General Procedure B from (2S,3S)-2-(cyclohexylamino)-3-methylpentyl benzoate (**329k**, 30.3 mg, 0.10 mmol) and 2-bromobenzoic acid. Purification by silica gel flash chromatography (5% EtOAc in hexanes) gave the title compound as a colourless oil (**330k**, 21.5

mg, 0.057 mmol, 57% yield). $[\alpha]_D^{24.0} +10.4^\circ$ (*c* 1.0, CHCl₃). **¹H NMR** (400 MHz, CDCl₃) δ 7.99 (d, *J* = 7.9 Hz, 2H, **10**), 7.57 (app. t, *J* = 7.4 Hz, 1H, **12**), 7.44 (app. t, *J* = 7.7 Hz, 2H, **11**), 7.30 – 7.24 (m, 2H, **19**), 7.22 – 7.15 (m, 3H, **18**, **20**), 4.37 (dd, *J* = 11.1, 5.9 Hz, 1H, **7-H_a**), 4.23 (dd, *J* = 11.1, 6.2 Hz, 1H, **7-H_b**), 3.12 – 3.06 (m, 1H, **6**), 2.87 (dd, *J* = 13.7, 6.7 Hz, 1H, **16-H_a**), 2.60 – 2.49 (m, 2H, **4**, **16-H_b**), 1.90 – 1.79 (m, 3H, **3-H_a**, **3'-H_a**, **13**), 1.78 – 1.67 (m, 2H, **2-H_a**, **2'-H_a**), 1.64 – 1.56 (m, 1H, **1-H_a**), 1.53 – 1.01 (m, 8H, **1-H_b**, **2-H_b**, **2'-H_b**, **3-H_b**, **3'-H_b**, **5**, **14-H_{a,b}**), 0.94 (t, *J* = 7.4 Hz, 3H, **15**). **¹³C NMR** (101 MHz, CDCl₃) δ 166.8 (**8**), 141.9 (**17**), 133.1 (**12**), 130.4 (**9**), 129.7 (**10**), 129.2 (**18**), 128.5 (**11**), 128.4 (**19**), 125.9 (**20**), 65.8 (**7**), 54.5 (**4**), 54.1 (**6**), 44.4 (**13**), 36.3 (**16**), 34.6 (**3'**), 34.3 (**3**), 26.3 (**1**), 25.2(4) (**2**), 25.1(8) (**2'**), 22.4 (**14**), 12.5 (**15**). **IR** (film, cm⁻¹) 2931, 2852, 1719, 1451, 1271, 1112, 1026, 710. **HRMS** *m/z* (ESI) calcd for C₂₅H₃₄N₁O₂ [M+H]⁺ 380.2584, found 380.2585.

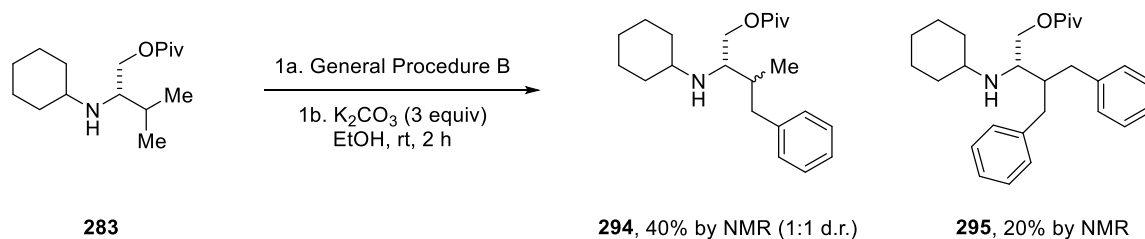
N-((2*S*,3*R*)-3-Benzyl-1-methoxypentan-2-yl)cyclohexanamine (**330l**)



Synthesised using General Procedure B from *N*-((2*S*,3*S*)-1-methoxy-3-methylpentan-2-yl)cyclohexanamine (**329l**, 21.3 mg, 0.10 mmol) and 2-bromobenzoic acid. Purification by silica gel flash chromatography (10–20% EtOAc in hexanes) gave the title compound as a pale yellow oil (**330l** 16.8 mg, 0.058 mmol, 58% yield). $[\alpha]_D^{24.0} +1.1^\circ$ (*c* 1.0, CHCl₃). **¹H NMR** (400 MHz, CDCl₃) δ 7.30 – 7.24 (m, 2H, **15**), 7.20 – 7.13 (m, 3H, **14**, **16**), 3.43 (dd, *J* = 9.5, 4.7 Hz, 1H, **7-H_a**), 3.34 – 3.25 (m, 4H, **7-H_b**, **8**), 2.99 – 2.88 (m, 2H, **6**, **12-H_a**), 2.54 – 2.44 (m, 1H, **4**), 2.29 (dd, *J* = 13.6, 8.9 Hz, 1H, **12-H_b**), 1.92 – 1.67 (m, 5H, **2-H_a**, **2'-H_a**, **3-H_a**, **3'-H_a**, **9**), 1.64 – 1.56 (m, 1H, **1-H_a**), 1.37 – 0.98 (m, 8H, **1-H_b**, **2-H_b**, **2'-H_b**, **3-H_b**, **3'-H_b**, **5**, **10-H_{a,b}**), 0.86 (t, *J* = 7.4 Hz, 3H, **11**). **¹³C NMR** (101 MHz, CDCl₃) δ 142.5 (**13**), 129.3 (**14**), 128.3 (**15**), 125.7 (**16**), 73.5 (**7**), 59.0 (**8**), 54.6 (**6**), 54.1 (**4**), 43.5 (**9**), 36.2 (**12**), 34.8 (**3'**), 34.1 (**3**), 26.4 (**1**), 25.5 (**2**), 25.4 (**2'**), 22.6 (**10**), 12.4 (**11**). **IR** (film, cm⁻¹) 2925, 2852, 1494, 1450, 1109, 734, 699. **HRMS** *m/z* (ESI) calcd for C₁₉H₃₂N₁O₁ [M+H]⁺ 290.2478, found 290.2480.

2-((2*S*,3*R*)-3-Benzyl-2-(cyclohexylamino)pentyl)isoindoline-1,3-dione (**330m**)

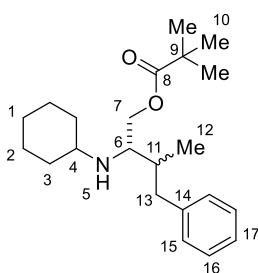
Synthesised using General Procedure B (**note**: reaction temperature was 70 °C) from 2-((2*S*,3*S*)-2-(cyclohexylamino)-3-methylpentyl)isoindoline-1,3-dione (**329m**, 32.8 mg, 0.10 mmol) and 2-bromobenzoic acid. Purification by silica gel flash chromatography (column 1: 5–10% EtOAc in hexanes; column 2: 2–10% Et₂O in DCM) gave the title compound as a colourless oil (**330m**, 21.4 mg, 0.053 mmol, 53% yield). $[\alpha]_D^{24.0} +8.6^\circ$ (*c* 1.0, CHCl₃). ¹H NMR (400 MHz, CDCl₃) δ 7.85 – 7.78 (m, 2H, **10**), 7.74 – 7.68 (m, 2H, **11**), 7.20 – 7.14 (m, 2H, **18**), 7.13 – 7.07 (m, 3H, **17**, **19**), 3.70 (dd, *J* = 13.6, 5.8 Hz, 1H, **7-H_a**), 3.59 (dd, *J* = 13.6, 8.1 Hz, 1H, **7-H_b**), 3.10 – 3.03 (m, 1H, **6**), 2.83 (dd, *J* = 13.6, 6.4 Hz, 1H, **15-H_a**), 2.50 – 2.40 (m, 2H, **4**, **15-H_b**), 1.75 – 1.61 (m, 4H, **2-H_a**, **3-H_a**, **3'-H_a**, **12**), 1.59 – 1.45 (m, 3H, **1-H_a**, **2'-H_a**, **13-H_a**), 1.44 – 1.32 (m, 1H, **13-H_b**), 1.29 – 0.93 (m, 8H, **1-H_b**, **2-H_b**, **2'-H_b**, **3-H_b**, **5**, **14**), 0.92 – 0.79 (m, 1H, **3'-H_b**). ¹³C NMR (101 MHz, CDCl₃) δ 168.9 (**8**), 142.0 (**16**), 134.0 (**11**), 132.2 (**9**), 129.1 (**17**), 128.3 (**18**), 125.8 (**19**), 123.3 (**10**), 54.4 (**4**), 54.3 (**6**), 44.6 (**12**), 39.8 (**7**), 36.1 (**15**), 34.5 (**3**), 34.0 (**3'**), 26.2 (**1**), 25.0 (**2**), 24.9 (**2'**), 22.8 (**13**), 12.6 (**14**). IR (film, cm⁻¹) 2928, 2851, 1771, 1710, 1432, 1395, 722. HRMS *m/z* (ESI) calcd for C₂₆H₃₃N₂O₂ [M+H]⁺ 405.2537, found 405.2535.

Arylation of L-valine derivative **283**

(*S*)-2-(Cyclohexylamino)-3-methylbutyl pivalate (**283**, 53.9 mg, 0.20 mmol) was subjected to General Procedure B (**note**: scale was doubled), using 2-bromobenzoic acid as the arylating agent. To hydrolyse C–O coupled by-products, the crude material was re-dissolved in EtOH (2 mL) and K₂CO₃ (83 mg, 0.60 mmol, 3 equiv) added. The reaction was stirred at room

temperature for 2 h. The solvent was removed *in vacuo* and the resulting material analysed by ^1H NMR, indicating 40% yield mono-arylation (**294**, 1:1 d.r.), 20% di-arylation (**295**) and 39% remaining starting material (**283**). Purification by silica gel flash chromatography (0–10% Et_2O in dichloromethane) enabled isolation of the arylated products. Mono-arylation: **294** (**diastereomer 1**), colourless oil (8.9 mg, 0.026 mmol, 13% yield); **294** (**diastereomer 2**), colourless oil (7.0 mg, 0.020 mmol, 10% yield). Diarylation: **295**, colourless oil (12.4 mg, 0.029 mmol, 15% yield).

(2*S*,3*R*/*S*)-2-(Cyclohexylamino)-3-methyl-4-phenylbutyl pivalate (294)

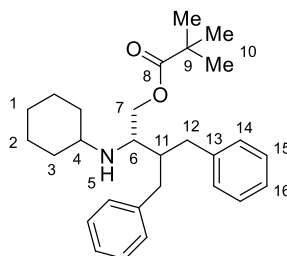


Diastereomer 1. $[\alpha]_D^{25.0} -6.1^\circ$ (*c* 0.5, CHCl_3). ^1H NMR (400 MHz, CDCl_3) δ 7.30 – 7.23 (m, 2H, **16**), 7.21 – 7.12 (m, 3H, **15**, **17**), 4.11 – 3.99 (m, 2H, **7-H_{a,b}**), 2.91 – 2.81 (m, 2H, **6**, **13-H_a**), 2.51 (tt, *J* = 10.3, 3.8 Hz, 1H, **4**), 2.36 (dd, *J* = 13.3, 9.3 Hz, 1H, **13-H_b**), 2.03 – 1.92 (m, 1H, **11**), 1.91 – 1.67 (m, 4H, **2-H_a**, **2'-H_a**, **3-H_a**, **3'-H_a**), 1.64 – 1.55 (m, 1H, **1-H_a**), 1.32 – 0.98 (m, 15H, **1-H_b**, **2-H_b**, **2'-H_b**, **3-H_b**, **3'-H_b**, **5**, **10**), 0.85 (d, *J* = 6.9 Hz, 3H, **12**). ^{13}C NMR (101 MHz, CDCl_3) δ 178.7 (**8**), 141.6 (**14**), 129.2 (**15**), 128.4 (**16**), 125.9 (**17**), 65.3 (**7**), 56.6 (**6**), 54.7 (**4**), 39.6 (**11**), 38.9 (**9**), 37.1 (**13**), 34.7 (**3**), 34.3 (**3'**), 27.4 (**10**), 26.3 (**1**), 25.3 (**2**), 25.1 (**2'**), 14.6 (**12**). IR (neat, cm^{-1}) 2927, 2850, 1729, 1479, 1455, 1282, 1156, 1031, 742, 699. HRMS *m/z* (ESI) calcd for $\text{C}_{22}\text{H}_{36}\text{N}_1\text{O}_2$ $[\text{M}+\text{H}]^+$ 346.2741, found 346.2743.

Diastereomer 2. $[\alpha]_D^{25.0} +3.3^\circ$ (*c* 0.5, CHCl_3). ^1H NMR (400 MHz, CDCl_3) δ 7.30 – 7.25 (m, 2H, **16**), 7.21 – 7.14 (m, 3H, **15**, **17**), 4.21 (dd, *J* = 11.3, 5.1 Hz, 1H, **7-H_a**), 4.02 (dd, *J* = 11.3, 5.9 Hz, 1H, **7-H_b**), 2.92 (dd, *J* = 13.3, 4.7 Hz, 1H, **13-H_a**), 2.79 (app. q, *J* = 5.2 Hz, 1H, **6**), 2.47 (tt, *J* = 10.2, 3.7 Hz, 1H, **4**), 2.32 (dd, *J* = 13.3, 9.9 Hz, 1H, **13-H_b**), 1.97 – 1.80 (m, 2H, **3-H_a**, **11**), 1.78 – 1.66 (m, 3H, **2-H_a**, **2'-H_a**, **3'-H_a**), 1.63 – 1.55 (m, 1H, **1-H_a**), 1.37 – 0.97 (m, 15H, **1-H_b**, **2-H_b**, **2'-H_b**, **3-H_b**, **3'-H_b**, **5**, **10**), 0.86 (d, *J* = 6.9 Hz, 3H, **12**). ^{13}C NMR (101 MHz, CDCl_3) δ 178.8 (**8**), 141.5 (**14**), 129.2 (**15**), 128.4 (**16**), 125.9 (**17**), 64.9 (**7**), 57.2 (**6**), 54.6 (**4**), 39.7 (**11**), 39.0 (**9**), 37.9 (**13**), 34.5 (**3**), 34.2 (**3'**), 27.4 (**10**), 26.3 (**1**), 25.3 (**2**), 25.1 (**2'**), 15.4

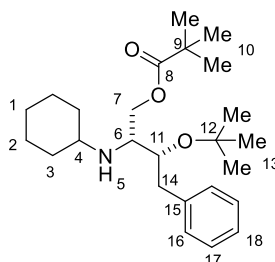
(**12**). **IR** (neat, cm^{-1}) 2963, 2927, 2854, 1729, 1479, 1454, 1282, 1155, 1033, 700. **HRMS** m/z (ESI) calcd for $\text{C}_{22}\text{H}_{36}\text{N}_1\text{O}_2$ $[\text{M}+\text{H}]^+$ 346.2741, found 346.2743.

(S)-3-Benzyl-2-(cyclohexylamino)-4-phenylbutyl pivalate (295)



$[\alpha]_D^{25.0} -2.5^\circ$ (c 1.0, CHCl_3). **^1H NMR** (400 MHz, CDCl_3) δ 7.29 – 7.21 (m, 4H, **14**, **14'**), 7.20 – 7.07 (m, 6H, **15**, **15'**, **16**, **16'**), 4.13 (dd, $J = 11.1$, 6.6 Hz, 1H, **7-H_a**), 4.03 (dd, $J = 11.1$, 5.9 Hz, 1H, **7-H_b**), 2.90 – 2.78 (m, 2H, **6**, **12-H_a**), 2.72 (dd, $J = 13.7$, 6.5 Hz, 1H, **12'-H_a**), 2.56 – 2.45 (m, 2H, **12-H_b**, **12'-H_b**), 2.41 (tt, $J = 10.1$, 3.6 Hz, 1H, **4**), 2.26 – 2.17 (m, 1H, **11**), 1.82 – 1.52 (m, 5H, **1-H_a**, **2-H_a**, **2'-H_a**, **3-H_a**, **3'-H_a**), 1.32 – 1.10 (m, 13H, **1-H_b**, **2-H_b**, **2'-H_b**, **5**, **10**), 1.07 – 0.95 (m, 2H, **3-H_b**, **3'-H_b**). **^{13}C NMR** (101 MHz, CDCl_3) δ 178.6 (**8**), 141.5 (**13'**), 141.2 (**13'**), 129.1(9) (**15**), 129.1(7) (**15'**), 128.5 (**14**), 128.4 (**14'**), 126.0(3) (**16**), 125.9(6) (**16'**), 64.8 (**7**), 54.4 (**4**), 53.4 (**6**), 44.5 (**11**), 38.9 (**9**), 36.0 (**12**), 35.8 (**12'**), 34.5 (**3'**), 34.2 (**3**), 27.4 (**10**), 26.2 (**1**), 25.2 (**2'**), 25.1 (**2**). **IR** (neat, cm^{-1}) 2928, 2854, 1729, 1453, 1282, 1151, 1031, 749. **HRMS** m/z (ESI) calcd for $\text{C}_{28}\text{H}_{40}\text{N}_1\text{O}_2$ $[\text{M}+\text{H}]^+$ 422.3054, found 422.3048.

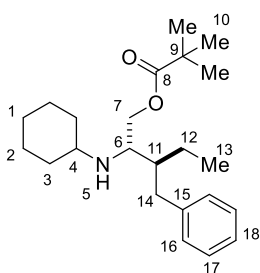
(2R,3R)-3-(tert-Butoxy)-2-(cyclohexylamino)-4-phenylbutyl pivalate (330n)



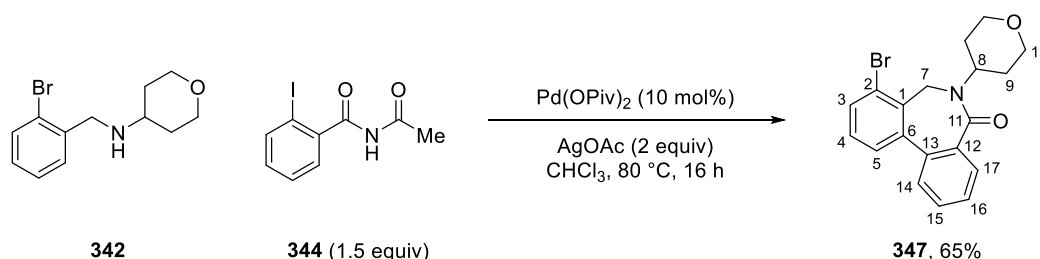
Synthesised using General Procedure B from (2R,3R)-3-(tert-butoxy)-2-(cyclohexylamino)-butyl pivalate (**329n**, 32.8 mg, 0.10 mmol) and 2-bromobenzoic acid. Purification by silica gel flash chromatography (5–10% EtOAc in hexanes) gave the title compound as a colourless amorphous solid (**330n**, 26.3 mg, 0.065 mmol, 65% yield). $[\alpha]_D^{24.0} -18.1^\circ$ (c 1.0, CHCl_3). **^1H NMR** (400 MHz, CDCl_3) δ 7.29 – 7.23 (m, 2H, **17**), 7.22 – 7.14 (m, 3H, **16**, **18**), 4.17 (dd, $J = 10.7$, 5.4 Hz, 1H, **7-H_a**), 3.92 (dd, $J = 10.7$, 8.0 Hz, 1H, **7-H_b**), 3.83 – 3.76 (m, 1H, **11**), 3.09

(dd, $J = 13.4, 7.8$ Hz, 1H, **14-H_a**), 2.82 – 2.76 (m, 1H, **6**), 2.69 (dd, $J = 13.4, 5.5$ Hz, 1H, **14-H_b**), 2.53 (tt, $J = 10.2, 3.8$ Hz, 1H, **4**), 1.89 – 1.67 (m, 4H, **2-H_a**, **2'-H_a**, **3-H_a**, **3'-H_a**), 1.64 – 1.56 (m, 1H, **1-H_a**), 1.47 – 1.01 (m, 24H, **1-H_b**, **2-H_b**, **2'-H_b**, **3-H_b**, **3'-H_b**, **5**, **10**, **13**). ^{13}C NMR (101 MHz, CDCl_3) δ 178.4 (**8**), 140.0 (**15**), 129.6 (**16**), 128.4 (**17**), 126.1 (**18**), 74.0 (**12**), 72.8 (**11**), 63.8 (**7**), 54.8 (**4**), 54.6 (**6**), 39.0 (**9**), 38.8 (**14**), 34.7 (**3'**), 34.1 (**3**), 28.8 (**13**), 27.3 (**10**), 26.3 (**1**), 25.3 (**2**), 25.1 (**2'**). IR (film, cm^{-1}) 2973, 2927, 2854, 1731, 1453, 1364, 1282, 1152, 1085, 744, 699. HRMS m/z (ESI) calcd for $\text{C}_{25}\text{H}_{42}\text{N}_1\text{O}_3$ $[\text{M}+\text{H}]^+$ 404.3159, found 404.3158.

(2*S*,3*S*)-3-Benzyl-2-(cyclohexylamino)pentyl pivalate (**330o**)



Synthesised using General Procedure B from (2*S*,3*R*)-2-(cyclohexylamino)-3-methylpentyl pivalate (**329o**, 28.3 mg, 0.10 mmol) and 2-bromobenzoic acid. Purification by silica gel flash chromatography (column 1: 5–10% EtOAc in hexanes; column 2: 5–10% Et₂O in dichloromethane) gave the title compound as a colourless oil (**330o**, 16.3 mg, 0.045 mmol, 45% yield). $[\alpha]_D^{24.0} +0.4^\circ$ (c 1.0, CHCl_3). ^1H NMR (400 MHz, CDCl_3) δ 7.30 – 7.23 (m, 2H, **17**), 7.21 – 7.13 (m, 3H, **16**, **18**), 4.15 (dd, $J = 11.1, 6.0$ Hz, 1H, **7-H_a**), 4.03 (dd, $J = 11.1, 6.0$ Hz, 1H, **7-H_b**), 2.94 – 2.88 (m, 1H, **6**), 2.74 (dd, $J = 13.8, 6.0$ Hz, 1H, **14-H_a**), 2.53 – 2.36 (m, 2H, **4**, **14-H_b**), 1.87 – 1.76 (m, 1H, **3-H_a**), 1.76 – 1.63 (m, 4H, **2-H_a**, **2'-H_a**, **3'-H_a**, **11**), 1.61 – 1.54 (m, 1H, **1-H_a**), 1.53 – 1.41 (m, 1H, **12-H_a**), 1.34 – 0.93 (m, 16H, **1-H_b**, **2-H_b**, **2'-H_b**, **3-H_b**, **3'-H_b**, **5**, **10**, **12-H_b**), 0.87 (t, $J = 7.3$ Hz, 3H, **13**). ^{13}C NMR (101 MHz, CDCl_3) δ 178.7 (**8**), 141.8 (**15**), 129.2 (**16**), 128.4 (**17**), 125.9 (**18**), 65.2 (**7**), 54.7 (**4**), 53.9 (**6**), 44.3 (**11**), 39.0 (**9**), 36.1 (**14**), 34.6 (**3'**), 34.2 (**3**), 27.4 (**10**), 26.3 (**1**), 25.3 (**2**), 25.1 (**2'**), 22.2 (**12**), 12.3 (**13**). IR (film, cm^{-1}) 2929, 2854, 1729, 1479, 1451, 1282, 1154, 738, 699. HRMS m/z (ESI) calcd for $\text{C}_{23}\text{H}_{38}\text{N}_1\text{O}_2$ $[\text{M}+\text{H}]^+$ 360.2897, found 360.2899.

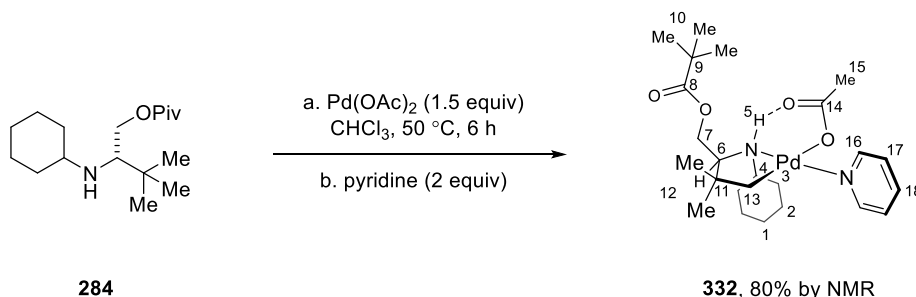
*Pd-catalyzed Formation of Dibenzoazepinone Product***8-Bromo-6-(tetrahydro-2H-pyran-4-yl)-6,7-dihydro-5H-dibenzo[*c,e*]azepin-5-one (347)**

To a 2–5 mL microwave vial containing a 10 mm magnetic stirrer bar were added Pd(OPiv)_2 (3.1 mg, 0.02 mmol, 10 mol%), AgOAc (33.4 mg, 0.2 mmol, 2 equiv) and aryl iodide **344** (43.4 mg, 0.15 mmol, 1.5 equiv). Under air, a solution of amine **342** (27.0 mg, 0.1 mmol, 1 equiv) in CHCl_3 (1 mL) was added via syringe and the vial sealed with a crimp cap with silicone/PTFE septum. The vial was placed in an oil bath pre-heated to 80 °C, and the reaction stirred at this temperature for 16 h. After cooling to room temperature, the reaction was filtered through a short plug of Celite and the filtrate concentrated *in vacuo*. The crude residue was purified by silica gel flash chromatography (10–40% ethyl acetate in hexanes) to give the title compound as a colourless crystalline solid (**347**, 24.0 mg, 0.065 mmol, 65% yield). $^1\text{H NMR}$ (400 MHz, CDCl_3) δ 7.99 (d, $J = 7.5$ Hz, 1H, **3**), 7.61 (d, $J = 8.0$ Hz, 1H, **17**), 7.57 – 7.47 (m, 3H, **4**, **14**, **15**), 7.43 (d, $J = 7.3$ Hz, 1H, **5**), 7.29 (t, $J = 7.8$ Hz, 1H, **16**), 4.87 – 4.76 (m, 2H, **7-H_a**, **8**), 4.16 – 4.05 (m, 2H, **7-H_b**, **10-H_a**), 3.99 (dd, $J = 11.5$, 4.5 Hz, 1H, **10'-H_a**), 3.57 (t, $J = 11.0$ Hz, 1H, **10-H_b**), 3.48 (t, $J = 11.0$ Hz, 1H, **10'-H_b**), 2.23 (qd, $J = 11.9$, 4.6 Hz, 1H, **9-H_a**), 2.10 (qd, $J = 11.9$, 4.6 Hz, 1H, **9'-H_a**), 1.75 – 1.67 (m, 1H, **9-H_b**), 1.50 – 1.43 (m, 1H, **9'-H_b**). $^{13}\text{C NMR}$ (101 MHz, CDCl_3) δ 168.3 (**11**), 141.3 (**1**), 138.4 (**6**), 136.6 (**12**), 135.1 (**13**), 132.4 (**17**), 130.7 (**4**), 130.4 (**3**), 129.7 (**16**), 129.0 (**5**), 128.4 (two signals overlapping, **14**, **15**), 121.6 (**2**), 67.8 (**10'**), 67.5 (**10**), 51.9 (**8**), 44.9 (**7**), 31.7 (**9'**), 30.4 (**9**). **IR** (neat, cm^{-1}) 2964, 2837, 1628, 1442, 1285, 1143, 1084, 1001, 855, 755. **HRMS** m/z (ESI) calcd for $\text{C}_{19}\text{H}_{19}\text{BrN}_1\text{O}_2$ $[\text{M}+\text{H}]^+$ 372.0599, found 372.0592.

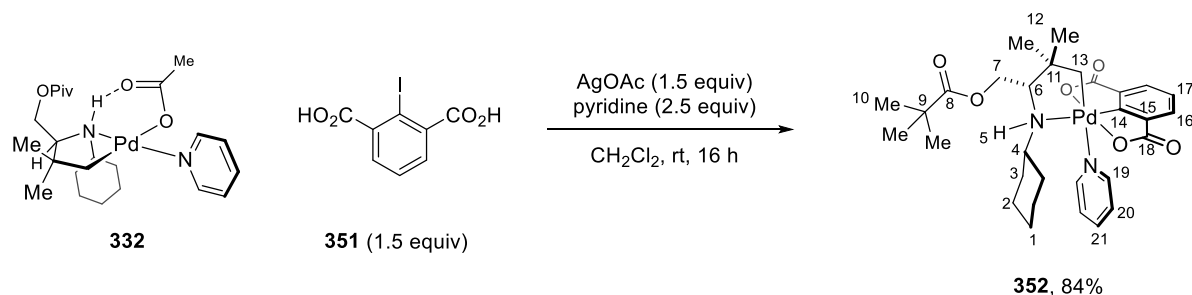
6.2.3. Stable Pd^{IV} Complexes Derived from Cyclopalladated Amines & Oximes

Synthesis of Amine-derived Alkyl Pd^{IV} Complexes

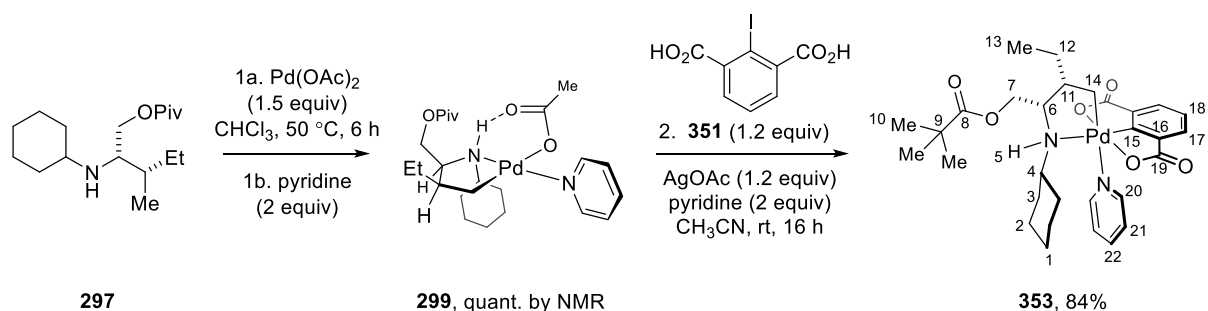
Pyridine-ligated palladacycle **332**



A solution of (*S*)-2-(cyclohexylamino)-3,3-dimethylbutyl pivalate (**284**, 283 mg, 1.00 mmol, 1 equiv) and Pd(OAc)₂ (337 mg, 1.50 mmol, 1.5 equiv) in chloroform (10 mL) was stirred under air in a sealed vial at 50 °C for 6 h. The reaction was cooled to room temperature, passed through a pad of Celite and pyridine (161 μL, 2.00 mmol, 2 equiv) added. The reaction was concentrated *in vacuo* to give the crude pyridine-ligated palladacycle **332**. The material was triturated in hexanes and the suspension filtered through Celite (repeated three times). The filtrate was concentrated *in vacuo* and dried under vacuum to afford **332** as a viscous yellow oil (80% yield by NMR). ¹H NMR (400 MHz, CDCl₃) δ 8.54 – 8.49 (m, 2H, **16**), 7.72 (tt, *J* = 7.6, 1.6 Hz, 1H, **18**), 7.29 – 7.24 (m, 2H, **17**), 5.42 (d, *J* = 9.0 Hz, 1H, **5**), 4.33 (dd, *J* = 12.2, 4.2 Hz, 1H, **7-H_a**), 4.05 (dd, *J* = 12.2, 6.4 Hz, 1H, **7-H_b**), 2.71 – 2.56 (m, 2H, **4**, **6**), 2.26 – 2.19 (m, 2H, **3-H_{a,b}**), 1.95 (s, 3H, **15**), 1.91 – 1.82 (m, 3H, **2-H_a**, **3'-H_a**, **13-H_a**), 1.81 – 1.56 (m, 3H, **1-H_a**, **2'-H_a**, **3'-H_b**), 1.46 (s, 3H, **12**), 1.32 (d, *J* = 8.2 Hz, 1H, **13-H_b**), 1.25 – 1.20 (m, 12H, **1-H_b**, **2-H_b**, **2'-H_b**, **10**), 0.94 (s, 3H, **12'**). ¹³C NMR (101 MHz, CDCl₃) δ 178.3 (**8**), 177.7 (**14**), 152.3 (**16**), 137.1 (**18**), 124.8 (**17**), 69.2 (**6**), 64.9 (**7**), 62.1 (**4**), 45.7 (**11**), 38.8 (**9**), 38.1 (**13**), 35.1 (**3**), 31.1 (**3'**), 28.2 (**12'**), 27.2 (**10**), 25.9 (**2'**), 25.7 (**2**), 25.4 (**1**), 25.2 (**12**), 24.4 (**15**). IR (film, cm⁻¹) 2956, 2929, 2857, 1728, 1603, 1557, 1448, 1364, 1278, 1148, 1033, 758, 696. HRMS *m/z* (ESI) calcd for C₂₂H₃₇N₂O₂Pd₁ [M–OAc]⁺ 467.1884, found 467.1890.

Amine-derived Pd^{IV} complex **352**

332 (0.80 mmol, 1 equiv) was dissolved in dichloromethane (10 mL) and pyridine added (161 μ L, 2.00 mmol, 2.5 equiv). The solution was transferred to a vial containing 2-iodo-1,3-benzenedicarboxylic acid (**351**, 350 mg, 1.20 mmol, 1.5 equiv) and AgOAc (200 mg, 1.20 mmol, 1.5 equiv). The resulting suspension was stirred at room temperature for 16 h. The reaction was filtered through a pad of Celite and the filtrate concentrated *in vacuo*. The residue was dissolved in dichloromethane (100 mL) and washed with sat. aq. NaHCO₃ (50 mL). The organic phase was separated, and the aqueous phase re-extracted with dichloromethane (100 mL). The combined organics were dried over MgSO₄, filtered and concentrated *in vacuo* to give the product as a solution (<5 mL) in residual dichloromethane. The complex was precipitated by adding hexanes (50 mL). The precipitate was isolated by decanting the mother liquor to afford Pd^{IV} complex **352** as an off-white solid (425 mg, 0.673 mmol, 84% yield). ¹H NMR (600 MHz, CDCl₃) δ 8.77 (d, J = 4.5 Hz, 2H, **19**), 7.81 (t, J = 7.2 Hz, 1H, **21**), 7.49 (dd, J = 7.5, 1.3 Hz, 1H, **16**), 7.46 – 7.37 (m, 3H, **16'**, **20**), 7.19 (t, J = 7.5 Hz, 1H, **17**), 4.48 (dd, J = 12.9, 3.6 Hz, 1H, **7-H_a**), 4.18 (dd, J = 12.9, 3.4 Hz, 1H, **7-H_b**), 3.58 (d, J = 6.5 Hz, 1H, **13-H_a**), 3.49 (d, J = 10.3 Hz, 1H, **5**), 3.23 (dt, J = 10.4, 3.5 Hz, 1H, **6**), 2.89 (d, J = 6.5 Hz, 1H, **13-H_b**), 2.87 – 2.76 (m, 1H, **4**), 2.05 – 1.97 (m, 1H, **3-H_a**), 1.70 – 1.60 (m, 2H, **2-H_a**, **3'-H_a**), 1.48 – 1.38 (m, 2H, **1-H_a**, **2'-H_a**), 1.25 – 1.10 (m, 16H, **3-H_b**, **10**, **12**, **12'**), 1.10 – 0.94 (m, 2H, **1-H_b**, **2-H_b**), 0.61 (qtd, J = 12.0, 2.3 Hz, 1H, **3'-H_b**), 0.45 (qt, J = 13.1, 3.1 Hz, 1H, **2'-H_b**). ¹³C NMR (101 MHz, CDCl₃) δ 178.1 (**8**), 177.1 (**18**), 176.6 (**18'**), 165.1 (**14**), 148.2 (**19**), 139.2 (**21**), 134.1 (**15**), 133.9 (**15'**), 133.3 (**16**), 133.1 (**16'**), 126.3 (**17**), 126.0 (**20**), 65.0 (**13**), 63.0 (**6**), 61.6 (**7**), 57.9 (**4**), 46.6 (**11**), 39.0 (**9**), 32.3 (**3'**), 31.0 (**3**), 28.1 (**12'**), 27.3 (**10**), 25.4 (**1**), 25.3 (**2'**), 25.1 (**2**), 22.5 (**12**). IR (neat, cm⁻¹) 2936, 2856, 1728, 1662, 1614, 1569, 1447, 1287, 1148, 1117, 1068, 1011, 937, 755. Elemental analysis calcd for C₃₀H₄₀N₂O₆Pd₁: C: 57.10 H: 6.39 N: 4.44, found C: 56.79 H: 6.45 N: 4.45.

Amine-derived Pd^{IV} complex **353**

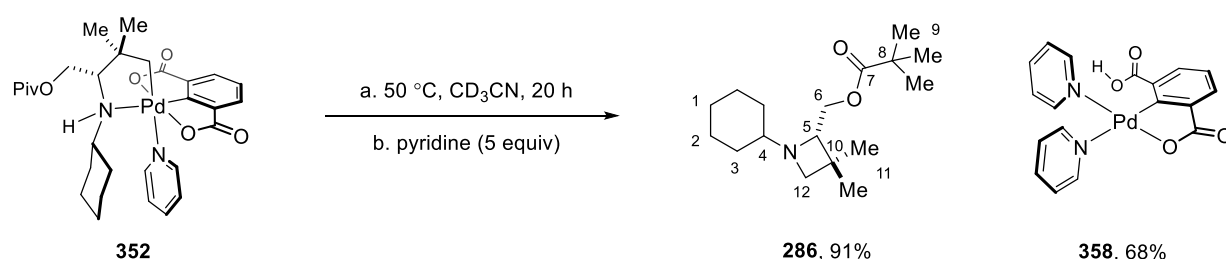
A solution of (2*S*,3*S*)-2-(cyclohexylamino)-3-methylpentyl pivalate (**297**, 283 mg, 1.00 mmol, 1 equiv) and Pd(OAc)₂ (337 mg, 1.50 mmol, 1.5 equiv) in chloroform (10 mL) was stirred under air in a sealed vial at 50 °C for 6 h. The reaction was cooled to room temperature, passed through a Celite plug and pyridine (161 μL, 2.00 mmol, 2 equiv) added. The reaction was concentrated *in vacuo* to give the crude pyridine-ligated palladacycle **299**. The material was triturated in hexane and the suspension filtered through Celite. The filtrate was concentrated *in vacuo* and dried under vacuum to afford **299** as a viscous yellow oil (quantitative yield by NMR; spectral data reported previously in the Experimental).

299 (1.00 mmol, 1 equiv) was dissolved in acetonitrile (10 mL) and pyridine added (161 μL, 2.00 mmol, 2 equiv). The solution was transferred to a vial containing 2-iodo-1,3-benzenedicarboxylic acid (**351**, 350 mg, 1.20 mmol, 1.2 equiv) and AgOAc (200 mg, 1.20 mmol, 1.2 equiv) in acetonitrile (10 mL). The resulting suspension was stirred under air at room temperature for 16 h, changing colour from bright yellow to off-white. The reaction was filtered through a pad of Celite and the filtrate concentrated *in vacuo*. The residue was dissolved in dichloromethane (200 mL) followed addition of pyridine (0.2 mL) and water (100 mL). The organic phase was separated, and the aqueous phase re-extracted twice with dichloromethane (100 mL each). The combined organics were dried over MgSO₄, filtered and the solvent removed *in vacuo* to give the crude product as a yellow residue. The complex was precipitated by adding Et₂O (5 mL) followed by hexanes (50 mL). Separation of the precipitate by decanting the mother liquor afforded Pd^{IV} complex **353** as an off-white solid (530 mg, 0.840 mmol, 84% yield). ¹H NMR (600 MHz, CDCl₃) δ 8.70 – 8.64 (m, 2H, **20**), 7.82 (tt, *J* = 7.7, 1.4 Hz, 1H, **22**), 7.56 (dd, *J* = 7.5, 1.3 Hz, 1H, **17**), 7.47 – 7.39 (m, 3H, **17'**, **21**), 7.23 (t, *J* = 7.5 Hz, 1H, **18**), 4.51 – 4.41 (m, 2H, **7-H_{a,b}**), 3.65 (d, *J* = 6.1 Hz, 1H, **5**), 3.42 (dd, *J* = 12.2, 6.6 Hz, 1H, **14-H_a**), 3.39 – 3.32 (m, 1H, **6**), 3.01 (t, *J* = 5.8 Hz, 1H, **14-H_b**), 2.69 – 2.56 (m, 2H, **4**, **11**), 2.16 – 2.07 (m, 1H, **3-H_a**), 1.74 – 1.64 (m, 2H, **2-H_a**, **3'-H_a**), 1.57 – 1.42 (m, 4H, **1-H_a**, **2'-H_a**, **12-H_{a,b}**), 1.26 – 1.17 (s, 9H, **10**), 1.15 – 0.99 (m, 5H, **1-H_b**, **2-H_b**, **13**), 0.97 – 0.80 (m, 3H, **2'-H_b**,

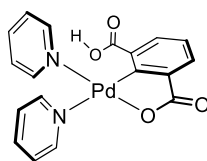
3-H_b, 3'-H_b). ¹³C NMR (101 MHz, CDCl₃) δ 179.1 (**8**), 177.2 (**19**), 176.8 (**19'**), 164.3 (**15**), 148.2 (**20**), 139.1 (**22**), 134.4 (**16**), 134.2 (**16'**), 133.3 (**17'**), 133.2 (**17**), 126.4 (**18**), 126.1 (**21**), 63.1 (**7**), 59.6 (**6**), 59.2 (**4**), 56.7 (**14**), 51.1 (**11**), 39.0 (**9**), 33.3 (**3'**), 31.6 (**3**), 27.4 (**10**), 25.6 (**2**), 25.2(9) (**1** or **2'**), 25.2(8) (**1** or **2'**), 23.2 (**12**), 12.7 (**13**). IR (film, cm⁻¹) 2934, 2855, 1727, 1658, 1603, 1568, 1447, 1289, 1144, 1115, 1057, 1013, 753, 699. **Elemental analysis** calcd for C₃₀H₄₀N₂O₆Pd₁ C: 57.10 H: 6.39 N: 4.44, found C: 56.72 H: 6.59 N: 4.14.

Thermal Decomposition of Alkyl Pd^{IV} Complex **352**

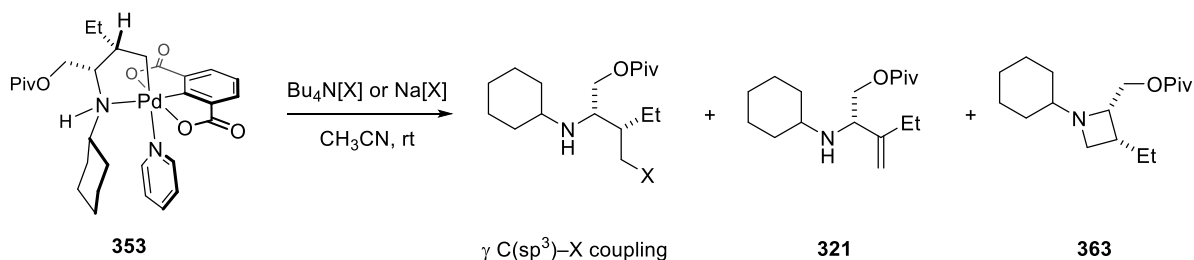
(S)-(1-Cyclohexyl-3,3-dimethylazetidin-2-yl)methyl pivalate (**286**)



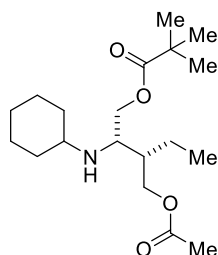
Amine-Pd^{IV} complex **352** (31.6 mg, 0.05 mmol) in acetonitrile-d₃ (2 mL) was stirred in a sealed tube at 50 °C for 20 h. After cooling to room temperature, the reaction was analysed by ¹H NMR. A single amine product was observed, indicating a selective reductive elimination event from the Pd^{IV} starting material. Pyridine (20 μ L, 0.25 mmol, 5 equiv) was added and the insoluble Pd^{II} product **358** isolated by filtration. The filtrate was concentrated *in vacuo*, and dichloromethane (20 mL) and sat. aq. NaHCO₃ (20 mL) added. The organic phase was washed, separated, and the aqueous phase was re-extracted with dichloromethane (20 mL). The combined organics were dried over MgSO₄, filtered and concentrated *in vacuo*. Purification by silica gel flash chromatography (10–15% ethyl acetate in hexanes) afforded azetidine product as a colourless oil (**286**, 12.9 mg, 0.045 mmol, 91% yield). [α]_D^{23.6} –54.3° (c 1.0, CHCl₃). ¹H NMR (400 MHz, CDCl₃) δ 4.23 (dd, *J* = 11.2, 4.7 Hz, 1H, **6-H_a**), 4.03 (dd, *J* = 11.2, 9.3 Hz, 1H, **6-H_b**), 3.15 (d, *J* = 7.0 Hz, 1H, **12-H_a**), 3.01 (dd, *J* = 9.3, 4.7 Hz, 1H, **5**), 2.62 (d, *J* = 7.0 Hz, 1H, **12-H_b**), 2.11 – 2.01 (m, 1H, **4**), 1.91 – 1.82 (m, 1H, **3-H_a**), 1.76 – 1.64 (m, 3H, **2-H_a**, **2'-H_a**, **3'-H_a**), 1.62 – 1.54 (m, 1H, **1-H_a**), 1.29 – 1.08 (m, 18 H, **1-H_b**, **2-H_b**, **2'-H_b**, **9**, **11**, **11'**), 1.08 – 0.88 (m, 2H, **3-H_b**, **3'-H_b**). ¹³C NMR (101 MHz, CDCl₃) δ 178.3 (**7**), 70.2 (**5**), 67.1 (**4**), 65.1 (**6**), 63.7 (**12**), 38.8 (**8**), 32.6 (**10**), 31.4 (**3**), 29.9 (**3'**), 29.1 (**11**), 27.4 (**9**), 26.0 (**1**), 24.8 (**2**, **2'**), 22.5 (**11'**). IR (film, cm⁻¹) 2929, 2855, 1732, 1480, 1462, 1368, 1281, 1148, 1033. HRMS *m/z* (ESI) calcd for C₁₇H₃₂N₁O₂ [M+H]⁺ 282.2428, found 282.2428.

Bis(pyridyl)-Pd^{II} By-product 358

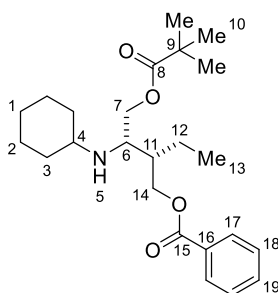
The filtered solid material was triturated in dichloromethane and recrystallized from boiling methanol to give the title compound as a colourless crystalline solid (**358**, 14.6 mg, 0.034 mmol, 68% yield). **IR** (film, cm⁻¹) 2922, 2750, 1707, 1602, 1448, 1349, 1260, 1135, 1065, 885, 766, 755, 695. **Elemental analysis** calcd for C₁₈H₁₄N₂O₄Pd₁ C: 50.43 H: 3.29 N: 6.53, found C: 50.01 H: 3.21 N: 6.29. *Note: DMSO-d₆ was the only NMR solvent that 358 had adequate solubility in. The ¹H NMR spectrum showed broad, unresolved signals, presumably due to the reversible displacement of pyridine by DMSO-d₆. Hence, NMR data are not reported. Structure was confirmed by X-ray crystallography.*

Reaction of Alkyl Pd^{IV} Complex 353 with Nucleophiles

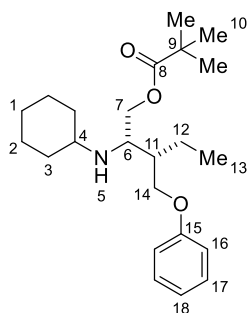
General Procedure C. Alkyl Pd^{IV} complex **353** (31.6 mg, 0.05 mmol, 1 equiv) and the tetrabutylammonium or sodium salt of the nucleophile (3–10 equiv) were stirred in acetonitrile (2–10 mL) at room temperature for 16 h. The solvent was then evaporated, followed by the addition of dichloromethane (20 mL) and sat. aq. NaHCO₃ (10 mL). The organic phase was separated, dried over MgSO₄, filtered and concentrated *in vacuo*. The crude material was analysed by ¹H NMR in CDCl₃ to determine the relative quantities of $\gamma \text{ C(sp}^3\text{)}\text{--X}$ coupling product, β -H elimination (**321**) and azetidine (**363**). Reactions were purified by silica gel flash chromatography.

(2*S*,3*S*)-3-(Acetoxymethyl)-2-(cyclohexylamino)pentyl pivalate (317)

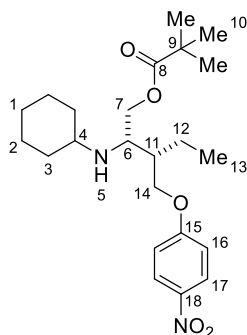
Following General Procedure C, complex **353** (0.05 mmol) was reacted with tetrabutylammonium acetate (45 mg, 0.15 mmol, 3 equiv) in acetonitrile (2 mL). The title compound was isolated by silica gel flash chromatography (10–20% Et₂O in hexanes) as a colourless oil (**317**, 12.8 mg, 0.037 mmol, 75% yield). The spectral data are presented previously in the Experimental section.

(2*S*,3*S*)-3-(Cyclohexylamino)-2-ethyl-4-(pivaloyloxy)butyl benzoate (359)

Following General Procedure C, complex **353** (0.05 mmol) was reacted with tetrabutylammonium benzoate (55 mg, 0.15 mmol, 3 equiv) in acetonitrile (2 mL). The title compound was isolated by silica gel flash chromatography (2–5% Et₂O in dichloromethane) as a colourless oil (**359**, 14.0 mg, 0.035 mmol, 69% yield). ¹H NMR (400 MHz, CDCl₃) δ 8.04 – 8.00 (m, 2H, **17**), 7.56 (tt, *J* = 7.4, 1.3 Hz, 1H, **19**), 7.44 (app. t, *J* = 7.4 Hz, 2H, **18**), 4.44 – 4.35 (m, 2H, **14-H_{a,b}**), 4.20 (dd, *J* = 11.2, 5.7 Hz, 1H, **7-H_a**), 4.05 (dd, *J* = 11.2, 5.9 Hz, 1H, **7-H_b**), 3.10 (td, *J* = 5.7, 4.2 Hz, 1H, **6**), 2.50 (tt, *J* = 10.0, 3.7 Hz, 1H, **4**), 1.91 – 1.64 (m, 5H, **2-H_a**, **2'-H_a**, **3-H_a**, **3'-H_a**, **11**), 1.63 – 1.51 (m, 2H, **1-H_a**, **12-H_a**), 1.49 – 1.37 (m, 1H, **12-H_b**), 1.30 – 0.95 (m, 18H, **1-H_b**, **2-H_b**, **2'-H_b**, **3-H_b**, **3'-H_b**, **5**, **10**, **13**). ¹³C NMR (101 MHz, CDCl₃) δ 178.6 (**8**), 166.7 (**15**), 133.0 (**19**), 130.5 (**16**), 129.6 (**17**), 128.6 (**18**), 65.0 (**7**), 64.8 (**14**), 54.5 (**4**), 54.1 (**6**), 42.0 (**11**), 39.0 (**9**), 34.5 (**3'**), 34.1 (**3**), 27.4 (**10**), 26.2 (**1**), 25.2 (**2**), 25.0 (**2'**), 20.3 (**12**), 12.6 (**13**). IR (film, cm⁻¹) 2964, 2928, 2853, 1717, 1451, 1271, 1150, 1111, 1027, 909, 731. HRMS *m/z* (ESI) calcd for C₂₄H₃₈N₁O₄ [M+H]⁺ 404.2795, found 404.2815.

(2*S*,3*S*)-2-(Cyclohexylamino)-3-(phenoxymethyl)pentyl pivalate (360)

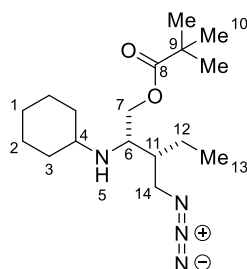
Following General Procedure C, complex **353** (0.05 mmol) was reacted with tetrabutylammonium phenoxide (51 mg, 0.15 mmol, 3 equiv) in acetonitrile (2 mL). The reaction mixture was purified by silica gel flash chromatography (2–10% Et₂O in hexanes) to give a 40:60 mixture of **360**:**321** (14.7 mg, 92% recovery). The NMR data of **360** were identified from the product mixture. ¹H NMR (400 MHz, CDCl₃) δ 7.32 – 7.26 (m, 2H, **17**), 6.98 – 6.89 (m, 3H, **16**, **18**), 4.23 (dd, *J* = 11.3, 5.5 Hz, 1H, **14-H_a**), 4.09 – 3.96 (m, 3H, **7-H_{a,b}**, **14-H_b**), 3.18 – 3.11 (m, 1H, **6**), 2.51 (tt, *J* = 10.1, 3.8 Hz, 1H, **4**), 1.96 – 0.87 (m, 26H, **1-H_{a,b}**, **2-H_{a,b}**, **2'-H_{a,b}**, **3-H_{a,b}**, **3'-H_{a,b}**, **5**, **10**, **11**, **12-H_{a,b}**, **13**). ¹³C NMR (101 MHz, CDCl₃) δ 178.7 (**8**), 159.1 (**15**), 129.5 (**17**), 120.7 (**18**), 114.7 (**16**), 67.4 (**14**), 65.4 (**7**), 54.7 (**4**), 54.4 (**6**), 42.4 (**11**), 39.0 (**9**), 34.5 (**3**), 34.2 (**3'**), 27.4 (**10**), 26.3 (**1**), 25.3 (**2**), 25.1 (**2'**), 20.3 (**12**), 12.6 (**13**).

(2*S*,3*S*)-2-(Cyclohexylamino)-3-((4-nitrophenoxy)methyl)pentyl pivalate (361)

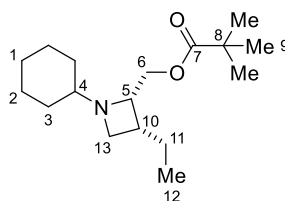
Following General Procedure C, complex **353** (0.05 mmol) was reacted with tetrabutylammonium *p*-nitrophenoxide (57 mg, 0.15 mmol, 3 equiv) in acetonitrile (2 mL). The title compound was isolated by silica gel flash chromatography (0–20% Et₂O in hexanes) as a colourless oil (**361**, 13.2 mg, 0.031 mmol, 63% yield). ¹H NMR (400 MHz, CDCl₃) δ 8.19 (d, *J* = 9.3 Hz, 2H, **17**), 6.96 (d, *J* = 9.3 Hz, 2H, **16**), 4.22 – 4.13 (m, 2H, **7-H_a**, **14-H_a**), 4.07 (dd, *J* = 9.2, 4.5 Hz, 1H, **14-H_b**), 4.01 (dd, *J* = 11.3, 6.6 Hz, 1H, **7-H_b**), 3.13 (td, *J* = 6.0, 4.0 Hz, 1H, **6**), 2.47 (tt, *J* = 10.2, 3.7 Hz, 1H, **4**), 1.92 – 1.84 (m, 1H, **11**), 1.83 – 1.39 (m, 7H, **1-H_a**, **2-H_a**,

2'-H_a, 3-H_a, 3'-H_a, 12-H_{a,b}), 1.30 – 0.84 (m, 17H, **1-H_b**, **2-H_b**, **2'-H_b**, **3-H_b**, **3'-H_b**, **10**, **13**). ¹³C NMR (101 MHz, CDCl₃) δ 178.6 (**8**), 164.2 (**15**), 141.6 (**18**), 126.1 (**17**), 114.6 (**16**), 68.4 (**14**), 65.0 (**7**), 54.6 (**4**), 54.0 (**6**), 42.3 (**11**), 39.0 (**9**), 34.5 (**3'**), 34.2 (**3**), 27.4 (**10**), 26.2 (**1**), 25.2 (**2**), 25.0 (**2'**), 20.1 (**12**), 12.6 (**13**). IR (film, cm⁻¹) 2964, 2928, 2853, 1723, 1593, 1513, 1340, 1260, 1152, 1111, 1015, 908, 845, 729. HRMS m/z (ESI) calcd for C₂₃H₃₇N₂O₅ [M+H]⁺ 421.2697, found 421.2697.

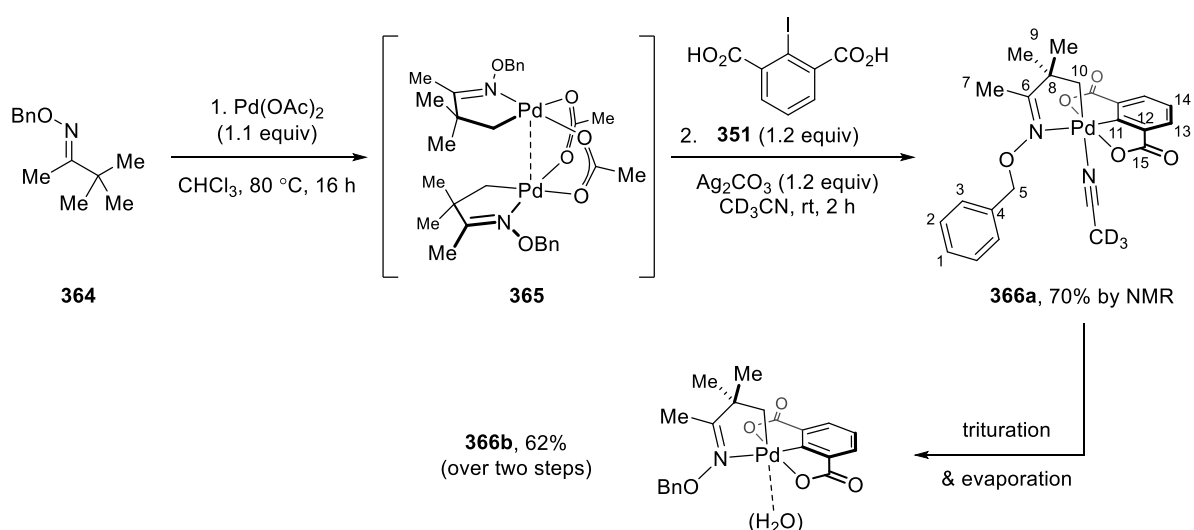
(2*S*,3*R*)-3-(Azidomethyl)-2-(cyclohexylamino)pentyl pivalate (362**)**



Following General Procedure C, complex **353** (0.05 mmol) was reacted with sodium azide (33 mg, 0.50 mmol, 10 equiv) in acetonitrile (10 mL). **Note:** work-up was conducted using ethyl acetate rather than dichloromethane. The title compound was isolated by silica gel flash chromatography (5% Et₂O in dichloromethane) as a colourless oil (**363**, 12.7 mg, 0.039 mmol, 78% yield). ¹H NMR (600 MHz, CDCl₃) δ 4.08 (dd, *J* = 11.2, 6.0 Hz, 1H, **7-H_a**), 3.99 (dd, *J* = 11.2, 6.0 Hz, 1H, **7-H_b**), 3.46 (dd, *J* = 12.1, 7.2 Hz, 1H, **14-H_a**), 3.35 (dd, *J* = 12.1, 6.2 Hz, 1H, **14-H_b**), 3.00 (td, *J* = 6.0, 4.0 Hz, 1H, **6**), 2.46 (tt, *J* = 10.3, 3.6 Hz, 1H, **4**), 1.89 – 1.84 (m, 1H, **3-H_a**), 1.78 – 1.67 (m, 3H, **2-H_a**, **2'-H_a**, **3'-H_a**), 1.62 – 1.55 (m, 2H, **1-H_a**, **11**), 1.52 – 1.44 (m, 1H, **12-H_a**), 1.33 – 0.90 (m, 18H, **1-H_b**, **2-H_b**, **2'-H_b**, **3-H_b**, **3'-H_b**, **10**, **12-H_b**, **13**), 0.73 (br. s, 1H, **5**). ¹³C NMR (101 MHz, CDCl₃) δ 178.6 (**8**), 64.8 (**7**), 54.6 (**4**), 53.8 (**6**), 52.0 (**14**), 42.4 (**11**), 39.0 (**9**), 34.6 (**3'**), 34.1 (**3**), 27.4 (**10**), 26.2 (**1**), 25.3 (**2**), 25.0 (**2'**), 20.5 (**12**), 12.4 (**13**). IR (film, cm⁻¹) 2962, 2927, 2853, 2095, 1727, 1450, 1280, 1148, 1033, 910, 733. HRMS m/z (ESI) calcd for C₁₇H₃₃N₄O₂ [M+H]⁺ 325.2598, found 325.2614.

((2*S*,3*R*)-1-Cyclohexyl-3-ethylazetidin-2-yl)methyl pivalate (363)

Following General Procedure C, complex **353** (0.05 mmol) was reacted with sodium iodide (38 mg, 0.25 mmol, 5 equiv) in acetonitrile (5 mL). The title compound was isolated by silica gel flash chromatography (10% ethyl acetate in hexanes) as a colourless oil (**363**, 11.0 mg, 0.039 mmol, 78% yield). ¹H NMR (400 MHz, CDCl₃) δ 4.18 (dd, *J* = 11.3, 4.8 Hz, 1H, **6-H_a**), 4.10 (dd, *J* = 11.3, 8.7 Hz, 1H, **6-H_b**), 3.38 (td, *J* = 8.4, 4.8 Hz, 1H, **5**), 3.10 (dd, *J* = 7.5, 2.9 Hz, 1H, **13-H_a**), 2.96 (app. t, *J* = 7.9 Hz, 1H, **13-H_b**), 2.19 (quintet of d, *J* = 7.9, 2.8 Hz, 1H, **10**), 2.07 (tt, *J* = 10.7, 3.5 Hz, 1H, **4**), 1.90 – 1.81 (m, 1H, **3-H_a**), 1.77 – 1.62 (m, 5H, **2-H_a**, **2'-H_a**, **3'-H_a**, **11-H_{a,b}**), 1.61 – 1.54 (m, 1H, **1-H_a**), 1.28 – 0.81 (m, 17H, **1-H_b**, **2-H_b**, **2'-H_b**, **3-H_b**, **3'-H_b**, **9**, **12**). ¹³C NMR (101 MHz, CDCl₃) δ 178.5 (**7**), 66.4 (**4**), 64.6 (**6**), 63.4 (**5**), 54.9 (**13**), 38.8 (**8**), 33.1 (**10**), 31.4 (**3**), 29.9 (**3'**), 27.3 (**9**), 26.1 (**1**), 24.8(0) (**2**), 24.7(9) (**2'**), 22.4 (**11**), 11.9 (**12**). IR (film, cm⁻¹) 2958, 2928, 2854, 1730, 1480, 1368, 1280, 1148, 1034, 980, 733. HRMS *m/z* (ESI) calcd for C₁₇H₃₂N₁O₂ [M+H]⁺ 282.2428, found 282.2442.

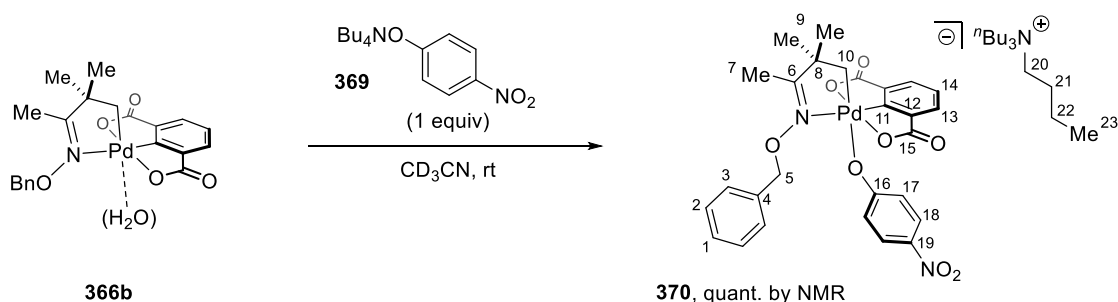
*Synthesis of Oxime-derived Alkyl Pd^{IV} Complex***Oxime-derived Pd^{IV} complex 366a/b**

A solution of (*E*)-3,3-dimethylbutan-2-one *O*-benzyl oxime (**364**, 61.6 mg, 0.30 mmol, 1 equiv) and Pd(OAc)₂ (74.1 mg, 0.33 mmol, 1.1 equiv) in chloroform (3 mL) was stirred under air in a

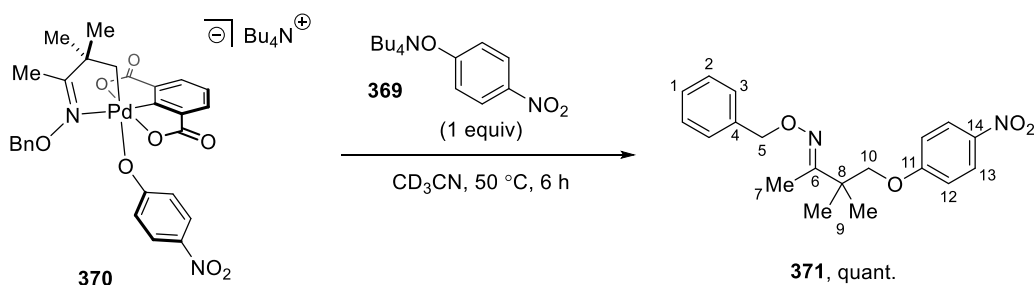
sealed vial at 80 °C for 16 h. The reaction was cooled to room temperature and passed through a pad of Celite. The filtrate was concentrated *in vacuo* to give the crude dimeric palladacycle **365** as a brown residue (75:25 mixture of **365**:**364** by NMR; used directly in next step).

Crude **365** was dissolved in CD₃CN (6 mL) and transferred to a vial containing 2-iodoisophthalic acid (**351**, 105 mg, 0.36 mmol, 1.2 equiv) and Ag₂CO₃ (99 mg, 0.36 mmol, 1.2 equiv). The resulting suspension was stirred under air at room temperature for 2 h (70% yield of **366a** by NMR). The reaction was filtered through a pad of Celite and the filtrate concentrated *in vacuo*. The residue was dissolved in dichloromethane (30 mL) and a spatula of K₂CO₃/MgSO₄ (1:1) added. After swirling the suspension for ca. 1 min, the reaction was filtered and concentrated *in vacuo*. The resulting yellow residue was diluted with hexanes (30 mL) to precipitate the product. Separation of the precipitate by decanting the mother liquor afforded alkyl Pd^{IV} complex **366b** as a pale-yellow solid (91.9 mg, 0.187 mmol, 62% yield). **IR** (film, cm⁻¹) 3308 (br., ν_{O-H}), 2940, 1637, 1614, 1570, 1306, 1156, 1119, 1018, 987, 744, 699. **Elemental analysis** calcd for C₂₁H₂₃N₁O₆Pd₁ C: 51.28 H: 4.71 N: 2.85, found C: 51.55 H: 4.59 N: 2.78. *Note: Elemental analysis of the isolated material indicated that the bound acetonitrile had been removed by evaporation (low %N), and that the complex obtained corresponded to the monohydrate 366b (associated water observed by IR). Unfortunately, attempts to crystallise 366b were unsuccessful and therefore the precise configuration of this complex is not known. Subsequent reactions using 366b were carried out in coordinating solvent, and/or with an added nucleophile, restoring a monomeric octahedral complex in solution.*

Spectral data for **366a** generated from dissolving isolated **366b** in CD₃CN are as follows: **¹H NMR** (400 MHz, CD₃CN) δ 7.59 – 7.54 (m, 2H, **3**), 7.49 – 7.35 (m, 6H, **1**, **2**, **13**, **14**), 5.30 (s, 2H, **5**), 3.52 (s, 2H, **10**), 1.85 (s, 3H, **7**), 1.19 (s, 6H, **9**). **¹³C NMR** (101 MHz, CD₃CN) δ 183.6 (**6**), 176.5 (**15**), 163.5 (**11**), 136.6 (**12**), 136.5 (**4**), 133.1 (**13**), 130.5 (**3**), 129.7 (**1**), 129.5 (**2**), 127.6 (**14**), 77.4 (**5**), 65.3 (**10**), 51.8 (**8**), 26.4 (**9**), 13.6 (**7**).

Reaction of Complex **366** with Nucleophile **369**Anionic alkyl Pd^{IV} complex **370**

To Pd^{IV} complex **366b** (20.0 mg, 0.041 mmol, 1 equiv) in acetonitrile-*d*₃ (0.7 mL; **366a** formed in solution) was added tetrabutylammonium *p*-nitrophenoxide **369** (15.5 mg, 0.041 mmol, 1 equiv) under air at room temperature. The resulting yellow solution was immediately transferred to an NMR tube for analysis. NMR spectra were recorded at 298 K. Quantitative conversion to a new species was observed. Based on ¹H, ¹³C, 2D COSY, HSQC, HMBC and NOESY NMR experiments and HRMS analysis, the product was identified as the anionic Pd^{IV} complex **370**. **¹H NMR** (400 MHz, CD₃CN) δ 7.79 (d, *J* = 9.2 Hz, 2H, **18**), 7.45 – 7.25 (m, 8H, **1**, **2**, **3**), 6.32 (d, *J* = 9.2 Hz, 2H, **17**), 5.43 (s, 2H, **5**), 3.18 (s, 2H, **10**), 3.14 – 3.05 (m, 8H, **20**), 1.98 (s, 3H, **7**), 1.67 – 1.56 (m, 8H, **21**), 1.36 (sextet, *J* = 7.4 Hz, 8H, **22**), 1.27 (s, 6H, **9**), 0.98 (t, *J* = 7.4 Hz, 12H, **23**). **¹³C NMR** (101 MHz, CD₃CN) δ 181.2 (**6**), 178.9 (**16**), 176.8 (**15**), 165.0 (**11**), 137.1 (**4**), 136.8 (**12**), 134.2 (**19**), 132.2 (**13**), 130.5 (**3**), 129.2(2) (**1**), 129.2(0) (**2**), 127.0 (**18**), 126.5 (**14**), 120.6 (**17**), 76.7 (**5**), 59.2 (1:1:1 t, ¹*J*_{C-N} = 2.9 Hz, **20**), 57.3 (**10**), 50.5 (**8**), 27.0 (**9**), 24.2 (**21**), 20.3 (1:1:1 t, ³*J*_{C-N} = 1.5 Hz, **22**), 13.7 (**23**), 13.5 (**7**). **HRMS** *m/z* (ESI) calcd for C₂₇H₂₅N₂O₈Pd₁ [Pd^{IV}]⁻ 611.0646, found 611.0649.

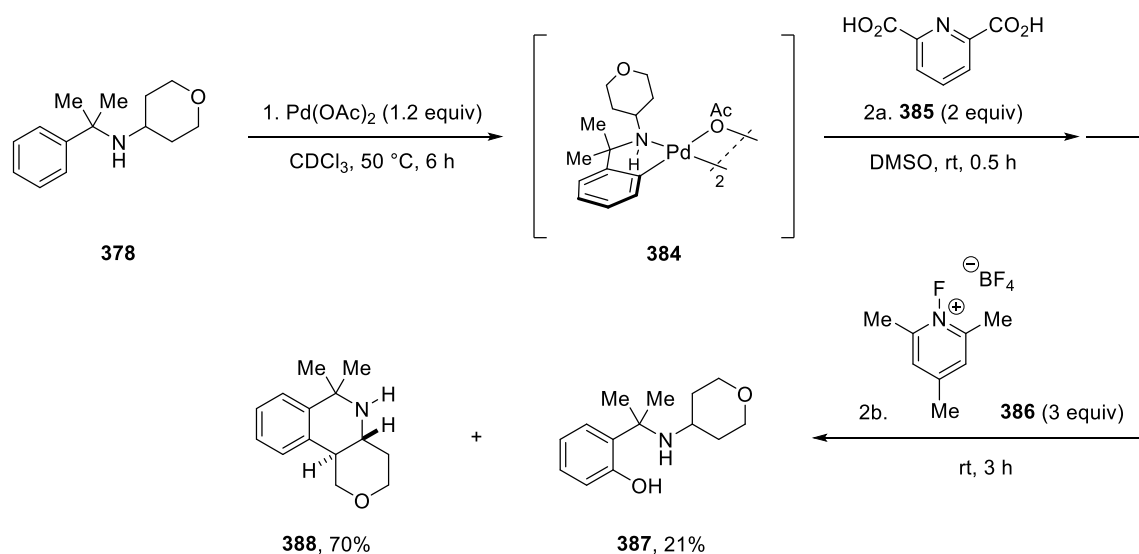
(E)-3,3-dimethyl-4-(4-nitrophenoxy)butan-2-one O-benzyl oxime (**371**)

To a vial containing Pd^{IV} complex **366b** (4.9 mg, 0.01 mmol, 1 equiv) and tetrabutylammonium *p*-nitrophenoxide **369** (7.6 mg, 0.02 mmol, 2 equiv) were added CD₃CN (0.5 mL) and anisole

(ca. 1 μ L, internal standard). The solution (containing 1 equiv **370** and 1 equiv **369** which instantaneously form) was transferred to a screw-top NMR tube and inserted into a pre-heated NMR spectrometer at 50 °C. Monitoring the reaction by ^1H NMR, after 6 h, **371** was obtained as the sole product in quantitative yield. *Note: 371 was isolated by column chromatography (0–10% diethyl ether in hexanes) from combined samples of the kinetic studies (see Appendix II).* Compound was a colourless oil. ^1H NMR (400 MHz, CDCl_3) δ 8.19 (d, J = 9.3 Hz, 2H, **13**), 7.35 – 7.26 (m, 5H, **1**, **2**, **3**), 6.92 (d, J = 9.3 Hz, 2H, **12**), 5.07 (s, 2H, **5**), 4.01 (s, 2H, **10**), 1.88 (s, 3H, **7**), 1.24 (s, 6H, **9**). ^{13}C NMR (101 MHz, CDCl_3) δ 164.4 (**11**), 160.4 (**6**), 141.6 (**14**), 138.4 (**4**), 128.4 (**2**), 128.2 (**3**), 127.7 (**1**), 126.0 (**13**), 114.7 (**12**), 75.8 (**5**), 75.2 (**10**), 41.2 (**8**), 23.1 (**9**), 11.0 (**7**). IR (film, cm^{-1}) 2972, 2929, 2874, 1607, 1593, 1512, 1497, 1341, 1262, 1112, 1035, 845, 752. HRMS m/z (ESI) calcd for $\text{C}_{19}\text{H}_{23}\text{N}_2\text{O}_4$ $[\text{M}+\text{H}]^+$ 343.1658, found 343.1656.

Functionalization of Benzylamine-derived Palladacycles

Synthesis of *ortho*-functionalized products **387** and **388**

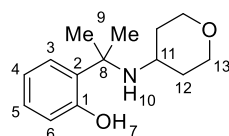


A solution of *N*-(2-phenylpropan-2-yl)tetrahydro-2H-pyran-4-amine (21.9 mg, 0.10 mmol, 1 equiv) and $\text{Pd}(\text{OAc})_2$ (26.9 mg, 0.12 mmol, 1.2 equiv) in CDCl_3 (2 mL) was heated at 50 °C in a sealed tube under air for 6 h. After cooling to room temperature, the chloroform was removed *in vacuo* to give the crude palladacycle dimer **384**.

Under a nitrogen atmosphere, pyridine-2,6-dicarboxylic acid (**385**, 33.4 mg, 0.20 mmol, 2 equiv) and dry DMSO (2 mL) were added to crude **384** and the reaction stirred at room temperature for 0.5 h. Following this, 1-fluoro-2,4,6-trimethylpyridinium tetrafluoroborate (**386**, 68.1 mg, 0.30 mmol, 3 equiv) was added and the reaction stirred at room temperature for

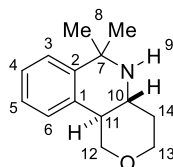
3 h. The DMSO was evaporated under a stream of air, and dichloromethane (20 mL) and NaHCO_3 (10 mL) added. The organic phase was washed, separated, dried over MgSO_4 , filtered and the solvent evaporated. The crude material was purified by silica gel flash chromatography (10–100% ethyl acetate in hexanes then 1–5% methanol in dichloromethane).

2-(2-((Tetrahydro-2H-pyran-4-yl)amino)propan-2-yl)phenol (**387**)

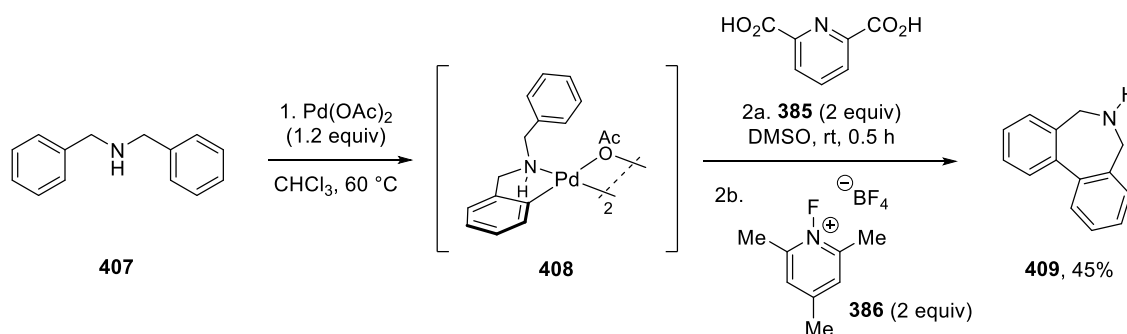


The title compound was isolated as a brown oil (**387**, 4.9 mg, 0.021 mmol, 21% yield). ^1H NMR (400 MHz, CDCl_3) δ 12.19 (br. s, 1H, **7**), 7.15 (t, $J = 7.7$ Hz, 1H, **5**), 7.08 (d, $J = 7.7$ Hz, 1H, **3**), 6.83 – 6.74 (m, 2H, **4**, **6**), 3.92 – 3.82 (m, 2H, **13-H_a**), 3.31 (t, $J = 11.6$ Hz, 2H, **13-H_b**), 2.81 (tt, $J = 11.0$, 4.2 Hz, 1H, **11**), 1.75 – 1.39 (m, 11H, **9**, **10**, **12-H_{a,b}**). ^{13}C NMR (101 MHz, CDCl_3) δ 157.7 (**1**), 130.7 (**2**), 128.8 (**5**), 125.6 (**3**), 119.0 (**4**), 117.4 (**6**), 67.0 (**13**), 57.8 (**8**), 49.7 (**11**), 35.1 (**12**), 28.9 (**9**). IR (neat, cm^{-1}) 3289, 2961, 2843, 1608, 1584, 1458, 1361, 1250, 1088, 755. HRMS m/z (ESI) calcd for $\text{C}_{14}\text{H}_{22}\text{N}_1\text{O}_2$ $[\text{M}+\text{H}]^+$ 236.1651, found 236.1660.

6,6-Dimethyl-3,4,4a,5,6,10b-hexahydro-1H-pyrano[4,3-c]isoquinoline (**388**)



The title compound was isolated as a yellow oil (**388**, 15.2 mg, 0.070 mmol, 70% yield). ^1H NMR (400 MHz, CDCl_3) δ 7.25 (dd, $J = 7.7$, 1.5 Hz, 1H, **6**), 7.20 (app. tt, $J = 7.5$, 1.0 Hz, 1H, **5**), 7.14 (app. td, $J = 7.2$, 1.5 Hz, 1H, **4**), 7.05 (app. dt, $J = 7.5$, 1.0 Hz, 1H, **3**), 4.57 (dd, $J = 11.0$, 4.4 Hz, 1H, **12-H_a**), 4.13 (dd, $J = 11.7$, 4.4 Hz, 1H, **13-H_a**), 3.56 (td, $J = 11.7$, 2.4 Hz, 1H, **13-H_b**), 3.30 (app. t, $J = 11.0$ Hz, 1H, **12-H_b**), 2.82 (td, $J = 10.6$, 3.8 Hz, 1H, **10**), 2.66 (td, $J = 10.4$, 4.8 Hz, 1H, **11**), 1.86 – 1.78 (m, 1H, **14-H_a**), 1.68 (app. qd, $J = 12.2$, 4.6 Hz, 1H, **14-H_b**), 1.51 (s, 3H, **8**), 1.50 (s, 3H, **8'**). ^{13}C NMR (101 MHz, CDCl_3) δ 144.2 (**2**), 133.7 (**1**), 126.7 (**6**), 126.5 (**5**), 126.0 (**4**), 124.2 (**3**), 69.7 (**12**), 67.7 (**13**), 54.2 (**7**), 51.8 (**10**), 44.1 (**11**), 33.6 (**14**), 32.6 (**8'**), 31.8 (**8**). IR (neat, cm^{-1}) 2962, 2844, 1440, 1362, 1148, 1084, 856, 757, 742. HRMS m/z (ESI) calcd for $\text{C}_{14}\text{H}_{20}\text{N}_1\text{O}_1$ $[\text{M}+\text{H}]^+$ 218.1545, found 218.1554.

6,7-Dihydro-5H-dibenzo[*c,e*]azepine (409)

A solution of dibenzylamine (19.2 μL , 0.10 mmol, 1 equiv) and $\text{Pd}(\text{OAc})_2$ (26.9 mg, 0.12 mmol, 1.2 equiv) in CHCl_3 (1 mL) was heated at $60\text{ }^\circ\text{C}$ in a sealed tube under air for 6 h. After cooling to room temperature, the chloroform was removed *in vacuo* to give the crude palladacycle dimer **408**.

Under a nitrogen atmosphere, pyridine-2,6-dicarboxylic acid (**385**, 33.4 mg, 0.20 mmol, 2 equiv) and dry DMSO (1 mL) were added to crude **408** and the reaction stirred at room temperature for 0.5 h. Following this, 1-fluoro-2,4,6-trimethylpyridinium tetrafluoroborate (**386**, 45.4 mg, 0.20 mmol, 2 equiv) was added and the reaction stirred at room temperature for 3 h. The DMSO was evaporated under a stream of air and the resulting residue was passed through a column of SCX-2 resin as a solution in dichloromethane. The material was purified by silica gel flash chromatography (2–10% methanol in dichloromethane) to give the title compound as a yellow oil (**409**, 8.8 mg, 0.045 mmol, 45% yield). ^1H NMR (400 MHz, CDCl_3) δ 7.55 – 7.39 (m, 8H), 4.04 (br. s, 1H), 3.76 (s, 4H). ^{13}C NMR (101 MHz, CDCl_3) δ 141.2, 135.1, 129.6, 128.6, 128.4, 128.1, 48.2. Spectral data were in accordance with the literature.²⁷³

7. References

- (1) Hartwig, J. F. *Organotransition Metal Chemistry - From Bonding to Catalysis*; University Science Books: Sausalito, CA, 2010.
- (2) Jazzar, R.; Hitce, J.; Renaudat, A.; Sofack-Kreutzer, J.; Baudoin, O. *Chem. Eur. J.* **2010**, *16*, 2654–2672.
- (3) Labinger, J. A.; Bercaw, J. E. *Nature* **2002**, *417*, 507–514.
- (4) Gensch, T.; Hopkinson, M. N.; Glorius, F.; Wencel-Delord, J. *Chem. Soc. Rev.* **2016**, *45*, 2900–2936.
- (5) Lyons, T. W.; Sanford, M. S. *Chem. Rev.* **2010**, *110*, 1147–1169.
- (6) Bergman, R. G. *Nature* **2007**, *446*, 391–393.
- (7) Shilov, A. E.; Shul'pin, G. B. *Chem. Rev.* **1997**, *97*, 2879–2932.
- (8) Blanksby, S. J.; Ellison, G. B. *Acc. Chem. Res.* **2003**, *36*, 255–263.
- (9) Xue, X.-S.; Ji, P.; Zhou, B.; Cheng, J.-P. *Chem. Rev.* **2017**, *117*, 8622–8648.
- (10) Bordwell, F. G. *Acc. Chem. Res.* **1988**, *21*, 456–463.
- (11) Arndtsen, B. A.; Bergman, R. G.; Mobley, T. A.; Peterson, T. H. *Acc. Chem. Res.* **1995**, *28*, 154–162.
- (12) Crabtree, R. H. *J. Organomet. Chem.* **2004**, *689*, 4083–4091.
- (13) Balcells, D.; Clot, E.; Eisenstein, O. *Chem. Rev.* **2010**, *110*, 749–823.
- (14) Ess, D. H.; Goddard, W. A.; Periana, R. A. *Organometallics* **2010**, *29*, 6459–6472.
- (15) Ackermann, L. *Chem. Rev.* **2011**, *111*, 1315–1345.
- (16) Periana, R. A.; Bhalla, G.; Tenn, W. J.; Young, K. J. H.; Liu, X. Y.; Mironov, O.; Jones, C. J.; Ziatdinov, V. R. *J. Mol. Catal. A Chem.* **2004**, *220*, 7–25.
- (17) Carrow, B. P.; Sampson, J.; Wang, L. *Isr. J. Chem.* **2019**, *59*, 1–30.
- (18) Neufeldt, S. R.; Sanford, M. S. *Acc. Chem. Res.* **2012**, *45*, 936–946.
- (19) Kuhl, N.; Hopkinson, M. N.; Wencel-Delord, J.; Glorius, F. *Angew. Chem. Int. Ed.* **2012**, *51*, 10236–10254.
- (20) Hartwig, J. F.; Larsen, M. A. *ACS Cent. Sci.* **2016**, *2*, 281–292.
- (21) Wedi, P.; van Gemmeren, M. *Angew. Chem. Int. Ed.* **2018**, *57*, 13016–13027.
- (22) Dehand, J.; Pfeffer, M. *Coord. Chem. Rev.* **1976**, *18*, 327–352.
- (23) Bruce, M. I. *Angew. Chem. Int. Ed.* **1977**, *16*, 73–86.
- (24) Constable, E. C. *Polyhedron* **1984**, *3*, 1037–1057.
- (25) Newkome, G. R.; Puckett, W. E.; Gupta, V. K.; Kiefer, G. E. *Chem. Rev.* **1986**, *86*, 451–489.

-
- (26) Omae, I. *Coord. Chem. Rev.* **1988**, *83*, 137–167.
- (27) Evans, D. W.; Baker, G. R.; Newkome, G. R. *Coord. Chem. Rev.* **1989**, *93*, 155–183.
- (28) Ryabov, A. D. *Chem. Rev.* **1990**, *90*, 403–424.
- (29) Albrecht, M. *Chem. Rev.* **2010**, *110*, 576–623.
- (30) Zhang, M.; Zhang, Y.; Jie, X.; Zhao, H.; Li, G.; Su, W. *Org. Chem. Front.* **2014**, *1*, 843.
- (31) Engle, K. M.; Mei, T. S.; Wasa, M.; Yu, J.-Q. *Acc. Chem. Res.* **2012**, *45*, 788–802.
- (32) Kleiman, J. P.; Dubeck, M. *J. Am. Chem. Soc.* **1963**, *85*, 1544–1545.
- (33) Cope, A. C.; Siekman, R. W. *J. Am. Chem. Soc.* **1965**, *87*, 3272–3273.
- (34) Bennett, M. A.; Milner, D. L. *Chem. Commun. (London)* **1967**, 581–582.
- (35) Keim, W. *J. Organomet. Chem.* **1968**, *14*, 179–184.
- (36) Knoth, W. H.; Schunn, R. A. *J. Am. Chem. Soc.* **1969**, *91*, 2400–2400.
- (37) Hartwell, G. E.; Lawrence, R. V.; Smas, M. J. *J. Chem. Soc. D* **1970**, 912–912.
- (38) Constable, A. G.; McDonald, W. S.; Sawkins, L. C.; Shaw, B. L. *J. Chem. Soc., Chem. Commun.* **1978**, 1061–1062.
- (39) Murai, S.; Kakiuchi, F.; Sekine, S.; Tanaka, Y.; Kamatani, A.; Sonoda, M.; Chatani, N. *Nature* **1993**, *366*, 529–531.
- (40) Zaitsev, V. G.; Shabashov, D.; Daugulis, O. *J. Am. Chem. Soc.* **2005**, *127*, 13154–13155.
- (41) Daugulis, O.; Do, H.-Q.; Shabashov, D. *Acc. Chem. Res.* **2009**, *42*, 1074–1086.
- (42) Corbet, M.; De Campo, F. *Angew. Chem. Int. Ed.* **2013**, *52*, 9896–9898.
- (43) Chen, Z.; Wang, B.; Zhang, J.; Yu, W.; Liu, Z.; Zhang, Y. *Org. Chem. Front.* **2015**, *2*, 1107–1295.
- (44) Daugulis, O.; Roane, J.; Tran, L. D. *Acc. Chem. Res.* **2015**, *48*, 1053–1064.
- (45) He, G.; Wang, B.; Nack, W. A.; Chen, G. *Acc. Chem. Res.* **2016**, *49*, 635–645.
- (46) Gandeepan, P.; Müller, T.; Zell, D.; Cera, G.; Warratz, S.; Ackermann, L. *Chem. Rev.* **2019**, *119*, 2192–2452.
- (47) Rej, S.; Ano, Y.; Chatani, N. *Chem. Rev.* **2020**, *120*, 1788–1887.
- (48) Yamaguchi, J.; Yamaguchi, A. D.; Itami, K. *Angew. Chem. Int. Ed.* **2012**, *51*, 8960–9009.
- (49) Abrams, D. J.; Provencher, P. A.; Sorensen, E. J. *Chem. Soc. Rev.* **2018**, *47*, 8925–8967.
- (50) Sinha, S. K.; Zanoni, G.; Maiti, D. *Asian J. Org. Chem.* **2018**, *7*, 1178–1192.
- (51) Baudoin, O. *Chem. Soc. Rev.* **2011**, *40*, 4902–4911.

- (52) Liu, M.; Yang, P.; Karunananda, M. K.; Wang, Y.; Liu, P.; Engle, K. M. *J. Am. Chem. Soc.* **2018**, *140*, 5805–5813.
- (53) Maraswami, M.; Loh, T.-P. *Synthesis* **2019**, *51*, 1049–1062.
- (54) Fernandes, R. A.; Nallasivam, J. L. *Org. Biomol. Chem.* **2019**, *17*, 8647–8672.
- (55) Ren, Z.; Dong, G. *Organometallics* **2016**, *35*, 1057–1059.
- (56) Chen, X.; Engle, K. M.; Wang, D.-H.; Yu, J.-Q. *Angew. Chem. Int. Ed.* **2009**, *48*, 5094–5115.
- (57) Dastbaravardeh, N.; Christakakou, M.; Haider, M.; Schnürch, M. *Synthesis* **2014**, *46*, 1421–1439.
- (58) Qiu, G.; Wu, J. *Org. Chem. Front.* **2015**, *2*, 169–178.
- (59) He, J.; Wasa, M.; Chan, K. S. L.; Shao, Q.; Yu, J.-Q. *Chem. Rev.* **2017**, *117*, 8754–8786.
- (60) Baudoin, O. *Acc. Chem. Res.* **2017**, *50*, 1114–1123.
- (61) Xu, Y.; Dong, G. *Chem. Sci.* **2018**, *9*, 1424–1432.
- (62) Saint-Denis, T. G.; Zhu, R.-Y.; Chen, G.; Wu, Q.-F.; Yu, J.-Q. *Science* **2018**, *359*, eaao4798.
- (63) Chu, J. C. K.; Rovis, T. *Angew. Chem. Int. Ed.* **2018**, *57*, 62–101.
- (64) Timsina, Y. N.; Gupton, B. F.; Ellis, K. C. *ACS Catal.* **2018**, *8*, 5732–5776.
- (65) He, C.; Whitehurst, W. G.; Gaunt, M. J. *Chem* **2019**, *5*, 1031–1058.
- (66) *Palladacycles: Synthesis, Characterization and Applications*; Dupont, J., Pfeffer, M., Eds.; Wiley-VCH: Weinheim, Germany, 2008.
- (67) *Palladacycles: Catalysis and Beyond*; Kapdi, A., Maiti, D., Eds.; Elsevier: Amsterdam, 2019.
- (68) Ryabov, A. D. *Synthesis* **1985**, *1985*, 233–252.
- (69) Dupont, J.; Consorti, C. S.; Spencer, J. *Chem. Rev.* **2005**, *105*, 2527–2571.
- (70) Sehnal, P.; Taylor, R. J. K.; Fairlamb, I. J. S. *Chem. Rev.* **2010**, *110*, 824–889.
- (71) Dickmu, G. C.; Smoliakova, I. P. *Coord. Chem. Rev.* **2020**, *409*, 213203.
- (72) Topczewski, J. J.; Sanford, M. S. *Chem. Sci.* **2015**, *6*, 70–76.
- (73) Ryabov, A. D.; Sakodinskaya, I. K.; Yatsimirsky, A. K. *J. Chem. Soc., Dalt. Trans.* **1985**, 2629–2638.
- (74) Cope, A. C.; Friedrich, E. C. *J. Am. Chem. Soc.* **1968**, *90*, 909–913.
- (75) Lapointe, D.; Fagnou, K. *Chem. Lett.* **2010**, *39*, 1118–1126.
- (76) Davies, D. L.; Donald, S. M. A.; Macgregor, S. A. *J. Am. Chem. Soc.* **2005**, *127*, 13754–13755.

- (77) Wang, L.; Carrow, B. P. *ACS Catal.* **2019**, *9*, 6821–6836.
- (78) Lafrance, M.; Gorelsky, S. I.; Fagnou, K. *J. Am. Chem. Soc.* **2007**, *129*, 14570–14571.
- (79) Powers, D. C.; Ritter, T. *Nat. Chem.* **2009**, *1*, 302–309.
- (80) Powers, D. C.; Ritter, T. *Acc. Chem. Res.* **2012**, *45*, 840–850.
- (81) Powers, D. C.; Lee, E.; Ariafield, A.; Sanford, M. S.; Yates, B. F.; Canty, A. J.; Ritter, T. *J. Am. Chem. Soc.* **2012**, *134*, 12002–12009.
- (82) Powers, I. G.; Uyeda, C. *ACS Catal.* **2017**, *7*, 936–958.
- (83) Hartwig, J. F. *Inorg. Chem.* **2007**, *46*, 1936–1947.
- (84) Lafrance, M.; Rowley, C. N.; Woo, T. K.; Fagnou, K. *J. Am. Chem. Soc.* **2006**, *128*, 8754–8756.
- (85) Wenkert, E. *Acc. Chem. Res.* **1968**, *1*, 78–81.
- (86) Stevens, R. V. *Acc. Chem. Res.* **1977**, *10*, 193–198.
- (87) Roughley, S. D.; Jordan, A. M. *J. Med. Chem.* **2011**, *54*, 3451–3479.
- (88) Cernak, T.; Dykstra, K. D.; Tyagarajan, S.; Vachal, P.; Krska, S. W. *Chem. Soc. Rev.* **2016**, *45*, 546–576.
- (89) Blakemore, D. C.; Castro, L.; Churcher, I.; Rees, D. C.; Thomas, A. W.; Wilson, D. M.; Wood, A. *Nat. Chem.* **2018**, *10*, 383–394.
- (90) Boström, J.; Brown, D. G.; Young, R. J.; Keserü, G. M. *Nat. Rev. Drug. Discov.* **2018**, *17*, 709–727.
- (91) Campeau, L.-C.; Parisien, M.; Jean, A.; Fagnou, K. *J. Am. Chem. Soc.* **2006**, *128*, 581–590.
- (92) Bay, K. L.; Yang, Y.-F.; Houk, K. N. *J. Organomet. Chem.* **2018**, *864*, 19–25.
- (93) Bhaskararao, B.; Singh, S.; Anand, M.; Verma, P.; Prakash, P.; C, A.; Malakar, S.; Schaefer, H. F.; Sunoj, R. B. *Chem. Sci.* **2020**, *11*, 208–216.
- (94) Anand, M.; Sunoj, R. B.; Schaefer, H. F. *J. Am. Chem. Soc.* **2014**, *136*, 5535–5538.
- (95) Feng, W.; Wang, T.; Liu, D.; Wang, X.; Dang, Y. *ACS Catal.* **2019**, *9*, 6672–6680.
- (96) He, G.; Chen, G. *Angew. Chem. Int. Ed.* **2011**, *50*, 5192–5196.
- (97) Zhang, S.-Y.; He, G.; Nack, W. A.; Zhao, Y.; Li, Q.; Chen, G. *J. Am. Chem. Soc.* **2013**, *135*, 2124–2127.
- (98) Landge, V. G.; Parveen, A.; Nandakumar, A.; Balaraman, E. *Chem. Commun.* **2018**, *54*, 7483–7486.
- (99) He, G.; Zhao, Y.; Zhang, S.; Lu, C.; Chen, G. *J. Am. Chem. Soc.* **2012**, *134*, 3–6.
- (100) Nades, E. T.; Daugulis, O. *J. Am. Chem. Soc.* **2012**, *134*, 7–10.
- (101) Li, Q.; Zhang, S.-Y.; He, G.; Nack, W. A.; Chen, G. *Adv. Synth. Catal.* **2014**, *356*,

- 1544–1548.
- (102) Hartwig, J. F. *Acc. Chem. Res.* **1998**, *31*, 852–860.
- (103) Pendleton, I. M.; Pérez-Temprano, M. H.; Sanford, M. S.; Zimmerman, P. M. *J. Am. Chem. Soc.* **2016**, *138*, 6049–6060.
- (104) Zhang, S.-Y.; He, G.; Zhao, Y.; Wright, K.; Nack, W. A.; Chen, G. *J. Am. Chem. Soc.* **2012**, *134*, 7313–7316.
- (105) Rodríguez, N.; Romero-Revilla, J. A.; Fernández-Ibáñez, M. Á.; Carretero, J. C. *Chem. Sci.* **2013**, *4*, 175–179.
- (106) Fan, M.; Ma, D. *Angew. Chem. Int. Ed.* **2013**, *52*, 12152–12155.
- (107) Pasunooti, K. K.; Banerjee, B.; Yap, T.; Jiang, Y.; Liu, C.-F. *Org. Lett.* **2015**, *17*, 6094–6097.
- (108) Zheng, Y.; Song, W.; Zhu, Y.; Wei, B.; Xuan, L. *J. Org. Chem.* **2018**, *83*, 2448–2454.
- (109) Biswas, S.; Bheemireddy, N. R.; Bal, M.; Van Steijvoort, B. F.; Maes, B. U. W. *J. Org. Chem.* **2019**, *84*, 13112–13123.
- (110) Chan, K. S. L.; Wasa, M.; Chu, L.; Laforteza, B. N.; Miura, M.; Yu, J.-Q. *Nat. Chem.* **2014**, *6*, 146–150.
- (111) Cheng, G. J.; Yang, Y. F.; Liu, P.; Chen, P.; Sun, T. Y.; Li, G.; Zhang, X.; Houk, K. N.; Yu, J.-Q.; Wu, Y. D. *J. Am. Chem. Soc.* **2014**, *136*, 894–897.
- (112) Engle, K. M. *Pure Appl. Chem.* **2016**, *88*, 119–138.
- (113) Shao, Q.; Wu, Q.-F.; He, J.; Yu, J.-Q. *J. Am. Chem. Soc.* **2018**, *140*, 5322–5325.
- (114) Jiang, H.; He, J.; Liu, T.; Yu, J.-Q. *J. Am. Chem. Soc.* **2016**, *138*, 2055–2059.
- (115) Wang, D.-H.; Hao, X.-S.; Wu, D.-F.; Yu, J.-Q. *Org. Lett.* **2006**, *8*, 3387–3390.
- (116) Spangler, J. E.; Kobayashi, Y.; Verma, P.; Wang, D.-H.; Yu, J.-Q. *J. Am. Chem. Soc.* **2015**, *137*, 11876–11879.
- (117) Jain, P.; Verma, P.; Xia, G.; Yu, J.-Q. *Nat. Chem.* **2017**, *9*, 140–144.
- (118) Huang, Z.; Wang, C.; Dong, G. *Angew. Chem. Int. Ed.* **2016**, *55*, 5299–5303.
- (119) Gulia, N.; Daugulis, O. *Angew. Chem. Int. Ed.* **2017**, *56*, 3630–3634.
- (120) Wang, C.; Chen, C.; Zhang, J.; Han, J.; Wang, Q.; Guo, K.; Liu, P.; Guan, M.; Yao, Y.; Zhao, Y. *Angew. Chem. Int. Ed.* **2014**, *53*, 9884–9888.
- (121) Han, J.; Zheng, Y.; Wang, C.; Zhu, Y.; Zeng, R.; Huang, Z.-B.; Zhao, Y. *J. Org. Chem.* **2015**, *80*, 9297–9306.
- (122) Han, J.; Zheng, Y.; Wang, C.; Zhu, Y.; Huang, Z.-B.; Zeng, R.; Zhao, Y. *J. Org. Chem.* **2016**, *81*, 5681–5689.
- (123) Liu, P.; Han, J.; Chen, C. P.; Shi, D. Q.; Zhao, Y. S. *RSC Adv.* **2015**, *5*, 28430–28434.

- (124) Xu, J.-W.; Zhang, Z.-Z.; Rao, W.-H.; Shi, B.-F. *J. Am. Chem. Soc.* **2016**, *138*, 10750–10753.
- (125) Topczewski, J. J.; Cabrera, P. J.; Saper, N. I.; Sanford, M. S. *Nature* **2016**, *531*, 220–224.
- (126) Cabrera, P. J.; Lee, M.; Sanford, M. S. *J. Am. Chem. Soc.* **2018**, *140*, 5599–5606.
- (127) Zhang, F.; Spring, D. R. *Chem. Soc. Rev.* **2014**, *43*, 6906–6919.
- (128) Zhao, Q.; Poisson, T.; Pannecoucke, X.; Besset, T. *Synthesis* **2017**, *49*, 4808–4826.
- (129) Rasheed, O. K.; Sun, B. *ChemistrySelect* **2018**, *3*, 5689–5708.
- (130) St John-Campbell, S.; Bull, J. A. *Org. Biomol. Chem.* **2018**, *16*, 4582–4595.
- (131) Bhattacharya, T.; Pimparkar, S.; Maiti, D. *RSC Adv.* **2018**, *8*, 19456–19464.
- (132) Niu, B.; Yang, K.; Lawrence, B.; Ge, H. *ChemSusChem* **2019**, *12*, 2955–2969.
- (133) Gandeepan, P.; Ackermann, L. *Chem* **2018**, *4*, 199–222.
- (134) Jun, C.-H.; Lee, H.; Hong, J.-B. *J. Org. Chem.* **1997**, *62*, 1200–1201.
- (135) Zhang, F.-L.; Hong, K.; Li, T.-J.; Park, H.; Yu, J.-Q. *Science* **2016**, *351*, 252–256.
- (136) Xu, Y.; Young, M. C.; Wang, C.; Magness, D. M.; Dong, G. *Angew. Chem. Int. Ed.* **2016**, *55*, 9084–9087.
- (137) Yada, A.; Liao, W.; Sato, Y.; Murakami, M. *Angew. Chem. Int. Ed.* **2017**, *56*, 1073–1076.
- (138) Liu, Y.; Ge, H. *Nat. Chem.* **2017**, *9*, 26–32.
- (139) Wu, Y.; Chen, Y. Q.; Liu, T.; Eastgate, M. D.; Yu, J.-Q. *J. Am. Chem. Soc.* **2016**, *138*, 14554–14557.
- (140) Wang, P.; Farmer, M. E.; Huo, X.; Jain, P.; Shen, P.-X.; Ishoey, M.; Bradner, J. E.; Wisniewski, S. R.; Eastgate, M. D.; Yu, J.-Q. *J. Am. Chem. Soc.* **2016**, *138*, 9269–9276.
- (141) Wang, P.; Verma, P.; Xia, G.; Shi, J.; Qiao, J. X.; Tao, S.; Cheng, P. T. W.; Poss, M. A.; Farmer, M. E.; Yeung, K.-S.; et al. *Nature* **2017**, *551*, 489–493.
- (142) Chen, Y.-Q.; Wang, Z.; Wu, Y.; Wisniewski, S. R.; Qiao, J. X.; Ewing, W. R.; Eastgate, M. D.; Yu, J.-Q. *J. Am. Chem. Soc.* **2018**, *140*, 17884–17894.
- (143) Kapoor, M.; Liu, D.; Young, M. C. *J. Am. Chem. Soc.* **2018**, *140*, 6818–6822.
- (144) Widenhoefer, R. A.; Buchwald, S. L. *Organometallics* **1996**, *15*, 3534–3542.
- (145) Fuchita, Y.; Hiraki, K.; Matsumoto, Y. *J. Organomet. Chem.* **1985**, *280*, C51–C53.
- (146) McNally, A.; Haffemayer, B.; Collins, B. S. L.; Gaunt, M. J. *Nature* **2014**, *510*, 129–133.
- (147) Arnek, R.; Zetterberg, K. *Organometallics* **1987**, *6*, 1230–1235.

- (148) Zakrzewski, J.; Smalley, A. P.; Kabeshov, M. A.; Gaunt, M. J.; Lapkin, A. A. *Angew. Chem. Int. Ed.* **2016**, *55*, 8878–8883.
- (149) Smalley, A. P.; Gaunt, M. J. *J. Am. Chem. Soc.* **2015**, *137*, 10632–10641.
- (150) Smalley, A. P.; Cuthbertson, J. D.; Gaunt, M. J. *J. Am. Chem. Soc.* **2017**, *139*, 1412–1415.
- (151) Zhang, J. *Org. Biomol. Chem.* **2018**, *16*, 8064–8071.
- (152) He, C.; Gaunt, M. J. *Angew. Chem. Int. Ed.* **2015**, *54*, 15840–15844.
- (153) He, C.; Gaunt, M. J. *Chem. Sci.* **2017**, *8*, 3586–3592.
- (154) Calleja, J.; Pla, D.; Gorman, T. W.; Domingo, V.; Haffemayer, B.; Gaunt, M. J. *Nat. Chem.* **2015**, *7*, 1009–1016.
- (155) Willcox, D.; Chappell, B. G. N.; Hogg, K.; Calleja, J.; Smalley, A.; Gaunt, M. J. *Science* **2016**, *354*, 851–857.
- (156) Cabrera-Pardo, J. R.; Trowbridge, A.; Nappi, M.; Ozaki, K.; Gaunt, M. J. *Angew. Chem. Int. Ed.* **2017**, *56*, 11958–11962.
- (157) Chen, K.; Wang, D.; Li, Z.-W.; Liu, Z.; Pan, F.; Zhang, Y.-F.; Shi, Z.-J. *Org. Chem. Front.* **2017**, *4*, 2097–2101.
- (158) Yuan, F.; Hou, Z.-L.; Pramanick, P. K.; Yao, B. *Org. Lett.* **2019**, *21*, 9381–9385.
- (159) Pramanick, P. K.; Zhou, Z.; Hou, Z.-L.; Yao, B. *J. Org. Chem.* **2019**, *84*, 5684–5694.
- (160) Lin, H.; Pan, X.; Barsamian, A. L.; Kamenecka, T. M.; Bannister, T. D. *ACS Catal.* **2019**, *9*, 4887–4891.
- (161) Rodrialvarez, J.; Nappi, M.; Azuma, H.; Flodén, N. J.; Burns, M. E.; Gaunt, M. J. *Nat. Chem.* **2020**, *12*, 76–81.
- (162) Hickman, A. J.; Sanford, M. S. *Nature* **2012**, *484*, 177–185.
- (163) Zhang, H.; Lei, A. *Dalt. Trans.* **2011**, *40*, 8745–8754.
- (164) Xu, L.-M.; Li, B.-J.; Yang, Z.; Shi, Z.-J. *Chem. Soc. Rev.* **2010**, *39*, 712–733.
- (165) Muñoz, K. *Angew. Chem. Int. Ed.* **2009**, *48*, 9412–9423.
- (166) Canty, A. J. *Platin. Met. Rev.* **1993**, *37*, 2–7.
- (167) Canty, A. J. *Acc. Chem. Res.* **1992**, *25*, 83–90.
- (168) Pope, W. J.; Peachey, S. J. *Proc. Chem. Soc.* **1907**, *23*, 86–87.
- (169) Ito, T.; Tsuchiya, H.; Yamamoto, A. *Bull. Chem. Soc. Jpn.* **1977**, *50*, 1319–1327.
- (170) Gillie, A.; Stille, J. K. *J. Am. Chem. Soc.* **1980**, *102*, 4933–4941.
- (171) Byers, P. K.; Canty, A. J.; Skelton, B. W.; White, A. H. *J. Chem. Soc., Chem. Commun.* **1986**, 1722–1724.
- (172) Byers, P. K.; Canty, A. J.; Skelton, B. W.; White, A. H. *J. Chem. Soc., Chem.*

- Commun.* **1987**, 1093–1095.
- (173) Byers, P. K.; Canty, A. J.; Skelton, B. W.; White, A. H. *Organometallics* **1990**, 9, 826–832.
- (174) Canty, A. J.; Honeyman, R. T.; Roberts, A. S.; Traill, P. R.; Colton, R.; Skelton, B. W.; White, A. H. *J. Organomet. Chem.* **1994**, 471, C8–C10.
- (175) Canty, A. J.; Jin, H.; Roberts, A. S.; Skelton, B. W.; Traill, P. R.; White, A. H. *Organometallics* **1995**, 14, 199–206.
- (176) Bayler, A.; Canty, A. J.; Edwards, P. G.; Skelton, B. W.; White, A. H. *J. Chem. Soc., Dalt. Trans.* **2000**, 3325–3330.
- (177) Cámpora, J.; Palma, P.; del Río, D.; Carmona, E.; Graiff, C.; Tiripicchio, A. *Organometallics* **2003**, 22, 3345–3347.
- (178) Vicente, J.; Arcas, A.; Juliá-Hernández, F.; Bautista, D. *Chem. Commun.* **2010**, 46, 7253–7255.
- (179) Byers, P. K.; Canty, A. J.; Crespo, M.; Puddephatt, R. J.; Scott, J. D. *Organometallics* **1988**, 7, 1363–1367.
- (180) Aye, K.-T.; Canty, A. J.; Crespo, M.; Puddephatt, R. J.; Scott, J. D.; Watson, A. A. *Organometallics* **1989**, 8, 1518–1522.
- (181) Trofimenko, S. *Chem. Rev.* **1993**, 93, 943–980.
- (182) Canty, A. J.; Fritsche, S. D.; Jin, H.; Skelton, B. W.; White, A. H. *J. Organomet. Chem.* **1995**, 490, C18–C19.
- (183) Canty, A. J.; Jin, H.; Roberts, A. S.; Skelton, B. W.; White, A. H. *Organometallics* **1996**, 15, 5713–5722.
- (184) Cámpora, J.; Palma, P.; del Río, D.; López, J. A.; Alvarez, E.; Connelly, N. G. *Organometallics* **2005**, 24, 3624–3628.
- (185) Camasso, N. M.; Canty, A. J.; Ariafard, A.; Sanford, M. S. *Organometallics* **2017**, 36, 4382–4393.
- (186) Lanci, M. P.; Remy, M. S.; Kaminsky, W.; Mayer, J. M.; Sanford, M. S. *J. Am. Chem. Soc.* **2009**, 131, 15618–15620.
- (187) Khusnutdinova, J. R.; Rath, N. P.; Mirica, L. M. *J. Am. Chem. Soc.* **2010**, 132, 7303–7305.
- (188) Markies, B. A.; Canty, A. J.; Boersma, J.; van Koten, G. *Organometallics* **1994**, 13, 2053–2058.
- (189) Catellani, M. *Synlett* **2003**, 298–313.
- (190) Cheng, H.-G.; Chen, S.; Chen, R.; Zhou, Q. *Angew. Chem. Int. Ed.* **2019**, 58, 5832–

5844.

- (191) Horino, H.; Arai, M.; Inoue, N. *Tetrahedron Lett.* **1974**, 8, 647–650.
- (192) Catellani, M.; Fagnola, M. C. *Angew. Chem. Int. Ed. Engl.* **1994**, 33, 2421–2422.
- (193) Catellani, M.; Chiusoli, G. P. *J. Organomet. Chem.* **1988**, 346, C27–C30.
- (194) Catellani, M.; Mann, B. E. *J. Organomet. Chem.* **1990**, 390, 251–255.
- (195) Bocelli, G.; Catellani, M.; Ghelli, S. *J. Organomet. Chem.* **1993**, 458, C12–C15.
- (196) Catellani, M.; Frignani, F.; Rangoni, A. *Angew. Chem. Int. Ed. Engl.* **1997**, 36, 119–122.
- (197) Canty, A. J.; Jin, H.; Skelton, B. W.; White, A. H. *Organometallics* **1998**, 37, 3975–3981.
- (198) Canty, A. J.; Denney, M. C.; Skelton, B. W.; White, A. H. *Organometallics* **2004**, 23, 1122–1131.
- (199) Williams, B. S.; Holland, A. W.; Goldberg, K. I. *J. Am. Chem. Soc.* **1999**, 121, 252–253.
- (200) Williams, B. S.; Goldberg, K. I. *J. Am. Chem. Soc.* **2001**, 123, 2576–2587.
- (201) Pawlikowski, A. V.; Getty, A. D.; Goldberg, K. I. *J. Am. Chem. Soc.* **2007**, 129, 10382–10393.
- (202) Racowski, J. M.; Gary, J. B.; Sanford, M. S. *Angew. Chem. Int. Ed.* **2012**, 51, 3414–3417.
- (203) Grushin, V. V. *Chem. Eur. J.* **2002**, 8, 1006–1014.
- (204) Pérez-Temprano, M. H.; Racowski, J. M.; Kampf, J. W.; Sanford, M. S. *J. Am. Chem. Soc.* **2014**, 136, 4097–4100.
- (205) Camasso, N. M.; Pérez-Temprano, M. H.; Sanford, M. S. *J. Am. Chem. Soc.* **2014**, 136, 12771–12775.
- (206) Canty, A. J.; Ariafard, A.; Camasso, N. M.; Higgs, A. T.; Yates, B. F.; Sanford, M. S. *Dalt. Trans.* **2017**, 46, 3742–3748.
- (207) Qu, F.; Khusnutdinova, J. R.; Rath, N. P.; Mirica, L. M. *Chem. Commun.* **2014**, 50, 3036–3039.
- (208) Zhang, M.; Wang, Q.; Peng, Y.; Chen, Z.; Wan, C.; Chen, J.; Zhao, Y.; Zhang, R.; Zhang, A.-Q. *Chem. Commun.* **2019**, 55, 13048–13065.
- (209) Cromwell, N. H.; Phillips, B. *Chem. Rev.* **1979**, 79, 331–358.
- (210) Brandi, A.; Cicchi, S.; Cordero, F. M. *Chem. Rev.* **2008**, 108, 3988–4035.
- (211) Couty, F.; Evano, G. *Synlett* **2009**, 3053–3064.
- (212) Mehra, V.; Lumb, I.; Anand, A.; Kumar, V. *RSC Adv.* **2017**, 7, 45763–45783.

- (213) Buettner, C. S.; Willcox, D.; Chappell, B. G. N.; Gaunt, M. J. *Chem. Sci.* **2019**, *10*, 83–89.
- (214) Ye, X.; He, Z.; Ahmed, T.; Weise, K.; Akhmedov, N. G.; Petersen, J. L.; Shi, X. *Chem. Sci.* **2013**, *4*, 3712–3716.
- (215) Zhao, J.; Zhao, X.-J.; Cao, P.; Liu, J.-K.; Wu, B. *Org. Lett.* **2017**, *19*, 4880–4883.
- (216) Koser, G. F.; Wettach, R. H. *J. Org. Chem.* **1977**, *42*, 1476–1478.
- (217) Shan, G.; Yang, X.; Zong, Y.; Rao, Y. *Angew. Chem. Int. Ed.* **2013**, *52*, 13606–13610.
- (218) Zhdankin, V. V.; Kuehl, C. J.; Bolz, J. T.; Formanek, M. S.; Simonsen, A. J. *Tetrahedron Lett.* **1994**, *35*, 7323–7326.
- (219) Lai, J. T. *Synthesis* **1984**, 122–123.
- (220) Dellaria, J. F.; Santarsiero, B. D. *Tetrahedron Lett.* **1988**, *29*, 6079–6082.
- (221) Dellaria, J. F.; Santarsiero, B. D. *J. Org. Chem.* **1989**, *54*, 3916–3926.
- (222) Williams, R. M.; Im, M.-N. *Tetrahedron Lett.* **1988**, *29*, 6075–6078.
- (223) Williams, R. M.; Sinclair, P. J.; Zhai, D.; Chen, D. *J. Am. Chem. Soc.* **1988**, *110*, 1547–1557.
- (224) Couty, F.; Durrat, F.; Prim, D. *Tetrahedron Lett.* **2003**, *44*, 5209–5212.
- (225) Durrat, F.; Sanchez, M. V.; Couty, F.; Evano, G.; Marrot, J. *Eur. J. Org. Chem.* **2008**, No. 19, 3286–3297.
- (226) Nappi, M.; He, C.; Whitehurst, W. G.; Chappell, B. G. N.; Gaunt, M. J. *Angew. Chem. Int. Ed.* **2018**, *57*, 3178–3182.
- (227) Deprez, N. R.; Sanford, M. S. *Inorg. Chem.* **2007**, *46*, 1924–1935.
- (228) Szabó, K. J. *J. Mol. Catal. A Chem.* **2010**, *324*, 56–63.
- (229) Müller, P.; Gilibert, D. M. *Tetrahedron* **1988**, *44*, 7171–7175.
- (230) Zhu, C.; Sun, C.; Wei, Y. *Synthesis* **2010**, 4235–4241.
- (231) Murai, K.; Kobayashi, T.; Miyoshi, M.; Fujioka, H. *Org. Lett.* **2018**, *20*, 2333–2337.
- (232) Senn, H. M.; Ziegler, T. *Organometallics* **2004**, *23*, 2980–2988.
- (233) Barrios-Landeros, F.; Hartwig, J. F. *J. Am. Chem. Soc.* **2005**, *127*, 6944–6945.
- (234) Vicente, J.; Arcas, A.; Juliá-Hernández, F.; Bautista, D. *Angew. Chem. Int. Ed.* **2011**, *123*, 7028–7031.
- (235) Cant, A. A.; Roberts, L.; Greaney, M. F. *Chem. Commun.* **2010**, 46, 8671–8673.
- (236) Stridfeldt, E.; Lindstedt, E.; Reitti, M.; Blid, J.; Norrby, P.-O.; Olofsson, B. *Chem. Eur. J.* **2017**, *23*, 13249–13258.
- (237) Idiris, F. I. M.; Jones, C. R. *Org. Biomol. Chem.* **2017**, *15*, 9044–9056.
- (238) Cornella, J.; Larrosa, I. *Synthesis* **2012**, *44*, 653–676.

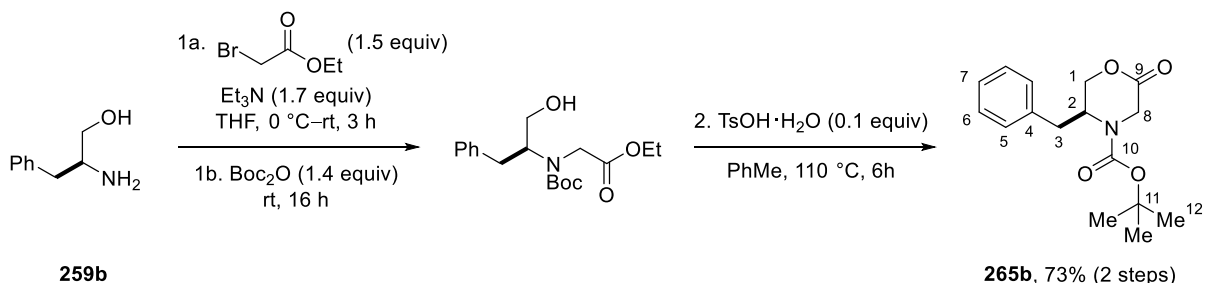
- (239) Perry, G. J. P.; Larrosa, I. *Eur. J. Org. Chem.* **2017**, 3517–3527.
- (240) Rodríguez, N.; Goossen, L. J. *Chem. Soc. Rev.* **2011**, *40*, 5030–5048.
- (241) Filatova, E. A.; Gulevskaya, A. V.; Pozharskii, A. F.; Ozeryanskii, V. A. *Tetrahedron* **2016**, *72*, 1547–1557.
- (242) Lassalas, P.; Gay, B.; Lasfargeas, C.; James, M. J.; Tran, V.; Vijayendran, K. G.; Brunden, K. R.; Kozlowski, M. C.; Thomas, C. J.; Smith, A. B.; et al. *J. Med. Chem.* **2016**, *59*, 3183–3203.
- (243) Péron, F.; Fossey, C.; Sopkova-de Oliveira Santos, J.; Cailly, T.; Fabis, F. *Chem. Eur. J.* **2014**, *20*, 7507–7513.
- (244) Dubost, E.; Babin, V.; Benoist, F.; Hébert, A.; Barbey, P.; Chollet, C.; Bouillon, J.-P.; Manrique, A.; Pieters, G.; Fabis, F.; et al. *Org. Lett.* **2018**, *20*, 6302–6305.
- (245) Ran, Y.; Yang, Y.; You, H.; You, J. *ACS Catal.* **2018**, *8*, 1796–1801.
- (246) Kapoor, M.; Chand-Thakuri, P.; Young, M. C. *J. Am. Chem. Soc.* **2019**, *141*, 7980–7989.
- (247) Chand-Thakuri, P.; Landge, V. G.; Kapoor, M.; Young, M. C. *J. Org. Chem.* **2020**, <https://dx.doi.org/10.1021/acs.joc.0c00542>.
- (248) Shabashov, D.; Daugulis, O. *J. Am. Chem. Soc.* **2010**, *132*, 3965–3972.
- (249) Whitehurst, W. G.; Blackwell, J. H.; Hermann, G. N.; Gaunt, M. J. *Angew. Chem. Int. Ed.* **2019**, *58*, 9054–9059.
- (250) Jung, M. E.; Piizzi, G. *Chem. Rev.* **2005**, *105*, 1735–1766.
- (251) Lloyd-Jones, G. C.; Slatford, P. A. *J. Am. Chem. Soc.* **2004**, *126*, 2690–2691.
- (252) Bruns, J.; van Gerven, D.; Klüner, T.; Wickleder, M. S. *Angew. Chem. Int. Ed.* **2016**, *55*, 8121–8124.
- (253) Kolter, M.; Koszinowski, K. *Chem. Eur. J.* **2016**, *22*, 15744–15750.
- (254) Blum, O.; Milstein, D. *J. Am. Chem. Soc.* **1995**, *117*, 4582–4594.
- (255) Meek, S. J.; Pitman, C. L.; Miller, A. J. M. *J. Chem. Educ.* **2016**, *93*, 275–286.
- (256) Boller, T. M.; Murphy, J. M.; Hapke, M.; Ishiyama, T.; Miyaura, N.; Hartwig, J. F. *J. Am. Chem. Soc.* **2005**, *127*, 14263–14278.
- (257) Wojciechowski, K. *Eur. J. Org. Chem.* **2001**, 3587–3605.
- (258) Sadana, A. K.; Saini, R. K.; Billups, W. E. *Chem. Rev.* **2003**, *103*, 1539–1602.
- (259) Didier, D.; Baumann, A. N.; Eisold, M. *Tetrahedron Lett.* **2018**, *59*, 3975–3987.
- (260) Salvio, R.; Placidi, S.; Sinibaldi, A.; Di Sabato, A.; Buscemi, D. C.; Rossi, A.; Antenucci, A.; Malkov, A.; Bella, M. *J. Org. Chem.* **2019**, *84*, 7395–7404.
- (261) Rocaboy, R.; Dailler, D.; Zellweger, F.; Neuburger, M.; Salomé, C.; Clot, E.; Baudoin,

- O. *Angew. Chem. Int. Ed.* **2018**, *57*, 12131–12135.
- (262) He, G.; Lu, G.; Guo, Z.; Liu, P.; Chen, G. *Nat. Chem.* **2016**, *8*, 1131–1136.
- (263) Zhang, J.; Khaskin, E.; Anderson, N. P.; Zavalij, P. Y.; Vedernikov, A. N. *Chem. Commun.* **2008**, 3625–3627.
- (264) Vedernikov, A. N. *Acc. Chem. Res.* **2012**, *45*, 803–813.
- (265) Maleckis, A.; Kampf, J. W.; Sanford, M. S. *J. Am. Chem. Soc.* **2013**, *135*, 6618–6625.
- (266) Hull, K. L.; Lanni, E. L.; Sanford, M. S. *J. Am. Chem. Soc.* **2006**, *128*, 14047–14049.
- (267) Racowski, J. M.; Ball, N. D.; Sanford, M. S. *J. Am. Chem. Soc.* **2011**, *133*, 18022–18025.
- (268) Yamamoto, K.; Li, J.; Garber, J. A. O.; Rolfes, J. D.; Boursalian, G. B.; Borghs, J. C.; Genicot, C.; Jacq, J.; van Gastel, M.; Neese, F.; et al. *Nature* **2018**, *554*, 511–514.
- (269) Brandt, J. R.; Lee, E.; Boursalian, G. B.; Ritter, T. *Chem. Sci.* **2014**, *5*, 169–179.
- (270) Xu, Y.; Yan, G.; Ren, Z.; Dong, G. *Nat. Chem.* **2015**, *7*, 829–834.
- (271) Zhuang, Z.; Yu, J.-Q. *Nature* **2020**, *577*, 656–659.
- (272) Baker, W. R.; Condon, S. L.; Spanton, S. *Tetrahedron Lett.* **1992**, *33*, 1573–1576.
- (273) France, S. P.; Aleku, G. A.; Sharma, M.; Mangas-Sanchez, J.; Howard, R. M.; Steflik, J.; Kumar, R.; Adams, R. W.; Slabu, I.; Crook, R.; et al. *Angew. Chem. Int. Ed.* **2017**, *56*, 15589–15593.
- (274) Zhou, J.; Fu, G. C. *J. Am. Chem. Soc.* **2003**, *125*, 12527–12530.
- (275) Rengasamy, R.; Curtis-Long, M. J.; Seo, W. D.; Jeong, S. H.; Jeong, I.-Y.; Park, K. H. *J. Org. Chem.* **2008**, *73*, 2898–2901.
- (276) Kelley, B. T.; Carroll, P.; Joullié, M. M. *J. Org. Chem.* **2014**, *79*, 5121–5133.
- (277) Karade, N. N.; Tiwari, G. B.; Shinde, S. V.; Gampawar, S. V.; Kondre, J. M. *Tetrahedron Lett.* **2008**, *49*, 3441–3443.
- (278) Jean, M.; Renault, J.; van de Weghe, P.; Asao, N. *Tetrahedron Lett.* **2010**, *51*, 378–381.
- (279) Alazet, S.; Preindl, J.; Simonet-Davin, R.; Nicolai, S.; Nanchen, A.; Meyer, T.; Waser, J. *J. Org. Chem.* **2018**, *83*, 12334–12356.
- (280) Hari, D. P.; Schouwey, L.; Barber, V.; Scopelliti, R.; Fadaei-Tirani, F.; Waser, J. *Chem. Eur. J.* **2019**, *25*, 9522–9528.
- (281) Kang, T.; Kim, Y.; Lee, D.; Wang, Z.; Chang, S. *J. Am. Chem. Soc.* **2014**, *136*, 4141–4144.
- (282) Peng, J.; Chen, C.; Xi, C. *Chem. Sci.* **2016**, *7*, 1383–1387.

Appendix I: Miscellaneous Experimental Procedures

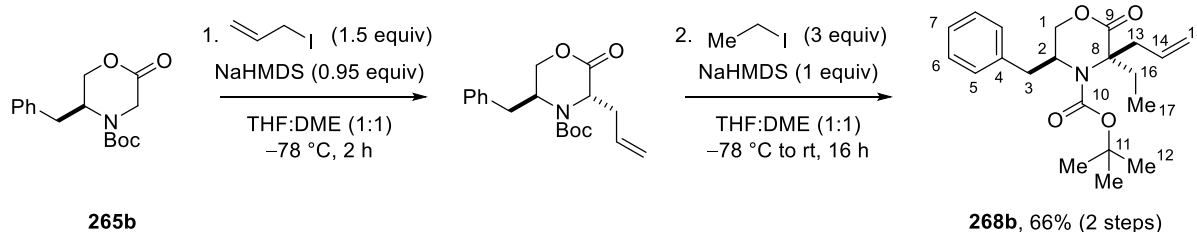
Synthesis of Chiral Morpholinone Substrates

tert-Butyl (S)-5-benzyl-2-oxomorpholine-4-carboxylate (**265b**)



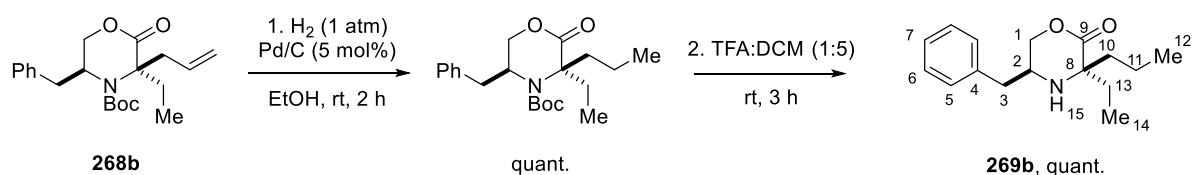
To a solution of L-phenylalaninol (**259b**, 1.51 g, 10 mmol 1 equiv) and triethylamine (2.4 mL, 17 mmol, 1.7 equiv) in THF (20 mL) at 0 °C was added ethyl bromoacetate (2.51 g, 15 mmol, 1.5 equiv) dropwise. The reaction was allowed to warm to room temperature with stirring for 3 h. The resulting suspension was cooled to 0 °C, filtered and the solids washed with cold THF (30 mL). Di-*tert*-butyl dicarbonate (3.06 g, 14 mmol, 1.4 equiv) was added to the combined filtrates and stirred at room temperature overnight. The solvent was removed *in vacuo* and the crude residue dissolved in toluene (50 mL) before washing with sat. aq. NaHCO₃ and brine (10 mL each). The organic phase was dried over MgSO₄ and filtered.

p-Toluenesulfonic acid monohydrate (190 mg, 1 mmol, 0.1 equiv) was added to the solution in toluene (diluted to 100 mL total volume) with heating under reflux using Dean-Stark apparatus for 6 h. After cooling to room temperature, the reaction mixture was washed with water (20 mL) and the organic phase separated, dried over MgSO₄, filtered and evaporated. The crude product was purified by silica gel flash chromatography (10–30% ethyl acetate in hexanes) to give the title compound as a colourless solid (**265b**, 2.12 g, 7.28 mmol, 73% yield over 2 steps). **M.p.** 94–96 °C; lit.²⁷² 95–96 °C. $[\alpha]_D^{25.0}$ –14.9° (*c* 1.0, CHCl₃); lit.²⁷² $[\alpha]_D^{25.0}$ –13.7° (*c* 2.45, CHCl₃). **¹H NMR** (400 MHz, CDCl₃) δ 7.36 – 7.28 (m, 2H, **6**), 7.28 – 7.13 (m, 3H, **5**, **7**), 4.38 – 4.07 (m, 5H, **1-H_a**, **1-H_b**, **2**, **8-H_a**, **8-H_b**), 3.00 (dd, *J* = 13.3, 3.8 Hz, 1H, **3-H_a**), 2.81 (dd, *J* = 13.3, 9.7 Hz, 1H, **3-H_b**), 1.46 (s, 9H, **12**). **¹³C NMR** (101 MHz, CDCl₃) δ 167.3 (**9**), 153.4 (**10**), 136.7 (**4**), 129.4 (**5**), 129.0 (**6**), 127.1 (**7**), 81.5 (**11**), 68.1 (**1**), 52.1 / 50.7 (**2**), 44.6 / 43.7 (**8**), 36.3 / 35.7 (**3**), 28.4 (**12**). *Note: ppm / ppm denotes rotameric forms giving rise to distinct shifts in ¹³C NMR spectrum.* **IR** (neat, cm^{–1}) 2978, 2933, 1759, 1698, 1407, 1381, 1369, 1344, 1292, 1225, 1167, 1117, 1007, 702. **HRMS** *m/z* (ESI) calcd for C₁₆H₂₂N₁O₄ [M+H]⁺ 292.1543, found 292.1546.

tert-Butyl (3R,5S)-3-allyl-5-benzyl-3-ethyl-2-oxomorpholine-4-carboxylate (268b)

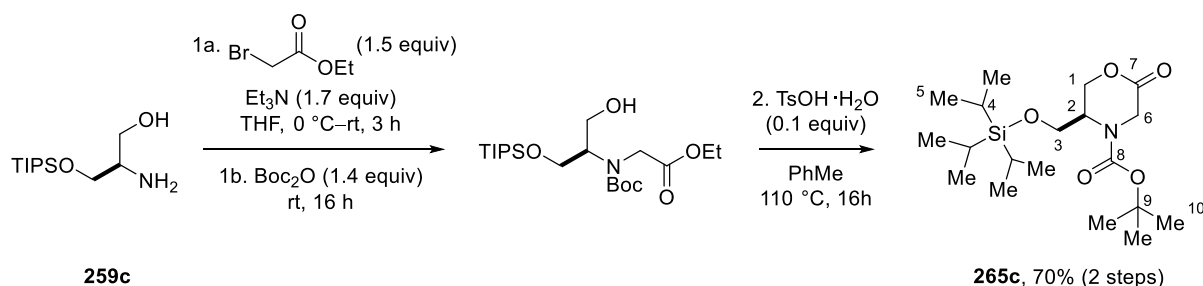
To a solution of *tert*-butyl (*S*)-5-benzyl-2-oxomorpholine-4-carboxylate (**265b**, 583 mg, 2 mmol, 1 equiv) in THF:DME (1:1, 4 mL) at $-78\text{ }^{\circ}\text{C}$ was added NaHMDS (2 M in THF, 0.95 mL, 1.9 mmol, 0.95 equiv) dropwise. After stirring at $-78\text{ }^{\circ}\text{C}$ for 0.5 h, neat allyl iodide (504 mg, 3 mmol, 1.5 equiv) was added dropwise. The reaction was stirred at $-78\text{ }^{\circ}\text{C}$ for a further 2 h before being quenched at $-78\text{ }^{\circ}\text{C}$ with sat. aq. NH_4Cl (5 mL) and warming to room temperature. The reaction mixture was diluted with diethyl ether (50 mL) and the organic phase separated. The aqueous phase was re-extracted with diethyl ether (2 x 30 mL) and the combined organics dried over MgSO_4 , filtered and evaporated.

The crude material was dissolved in THF:DME (1:1, 4 mL) and cooled once more to $-78\text{ }^{\circ}\text{C}$. NaHMDS (2 M in THF, 1 mL, 2 mmol, 1 equiv) was added dropwise and the reaction stirred at $-78\text{ }^{\circ}\text{C}$ for 0.5 h. Neat ethyl iodide (936 mg, 6 mmol, 3 equiv) was added dropwise at $-78\text{ }^{\circ}\text{C}$. Without removing the cooling bath, the reaction was allowed to warm slowly to room temperature overnight. Sat. aq. NH_4Cl (5 mL) was added followed by dilution with diethyl ether (50 mL). The organic phase was separated and the aqueous phase re-extracted with diethyl ether (2 x 30 mL). The combined organics were dried over MgSO_4 , filtered and evaporated. The crude material was purified by silica gel flash chromatography (10–30% ethyl acetate in hexanes) to give the title compound as a colourless oil (**268b**, 475 mg, 1.32 mmol, 66% yield over 2 steps). $[\alpha]_D^{25.0} -25.2^{\circ}$ (*c* 0.5, CHCl_3). $^1\text{H NMR}$ (400 MHz, CDCl_3) δ 7.35 – 7.27 (m, 2H, **6**), 7.27 – 7.15 (m, 3H, **5**, **7**), 5.83 – 5.63 (m, 1H, **14**), 5.22 – 5.05 (m, 2H, **15-H_a**, **15-H_b**), 4.51 – 4.08 (m, 2H, **1-H_a**, **2**), 3.99 (d, $J = 11.6\text{ Hz}$, 1H, **1-H_b**), 3.42 – 2.93 (m, 2H, **13-H_a**, **13-H_b**), 2.87 (dd, $J = 13.2, 3.2\text{ Hz}$, 1H, **3-H_a**), 2.68 (app. t, $J = 12.5\text{ Hz}$, 1H, **3-H_b**), 2.40 – 2.07 (m, 2H, **16-H_a**, **16-H_b**), 1.57 (s, 9H, **12**), 0.95 (app. t, $J = 7.6\text{ Hz}$, 3H, **17**). $^{13}\text{C NMR}$ (101 MHz, CDCl_3) δ 170.9 (**9**), 152.5 (**10**), 137.6 (**4**), 134.5 (**14**), 129.4 (**5**), 128.9 (**6**), 127.0 (**7**), 119.4 (**15**), 80.8 (**11**), 68.2 (**8**), 65.2 (**1**), 53.3 (**2**), 38.4 (**13**), 37.9 (**3**), 31.4 (**16**), 28.7 (**12**), 9.6 (**17**). IR (neat, cm^{-1}) 2978, 1746, 1700, 1456, 1368, 1326, 1285, 1271, 1163, 1108, 703. HRMS m/z (ESI) calcd for $\text{C}_{21}\text{H}_{30}\text{N}_1\text{O}_4$ $[\text{M}+\text{H}]^+$ 360.2169, found 360.2172.

(3*R*,5*S*)-5-Benzyl-3-ethyl-3-propylmorpholin-2-one (269b)

A solution of *tert*-butyl (3*R*,5*S*)-3-allyl-5-benzyl-3-ethyl-2-oxomorpholine-4-carboxylate (**268b**, 419 mg, 1.17 mmol, 1 equiv) in ethanol (10 mL) was subjected to three cycles of vacuum/nitrogen backfill. Palladium on activated carbon (Pd/C, 10 wt%, 62 mg, 0.059 mmol, 5 mol%) was added in one portion, the atmosphere exchanged for hydrogen and the reaction stirred at room temperature for 2 h. The reaction was filtered through Celite and concentrated *in vacuo* to give the product as a colourless oil (423 mg, 1.17 mmol, quantitative yield).

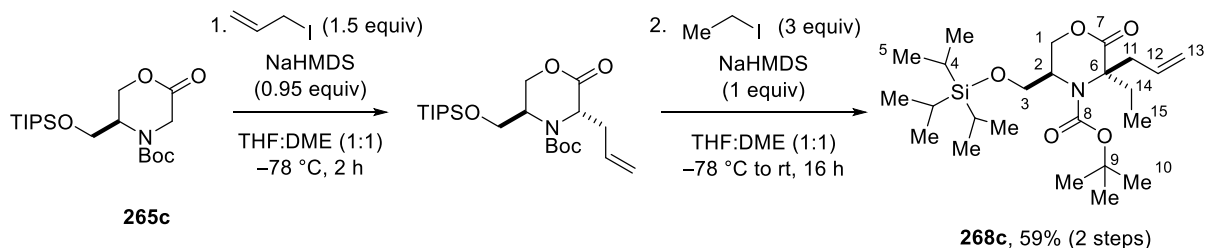
The hydrogenated product (423 mg, 1.17 mmol) was dissolved in dichloromethane (7.7 mL) and trifluoroacetic acid (1.5 mL) added. The reaction was stirred at room temperature for 3 h, concentrated *in vacuo*, basified with sat. aq. NaHCO₃ and organics extracted with dichloromethane (2 x 50 mL). The crude material was purified by silica gel flash chromatography (10–20% ethyl acetate in hexanes) to give the title compound as a colourless oil (**269b**, 306 mg, 1.17 mmol, quantitative yield). $[\alpha]_D^{25.0} -79.4^\circ$ (*c* 1.5, CHCl₃). ¹H NMR (400 MHz, CDCl₃) δ 7.37 – 7.30 (m, 2H, **6**), 7.30 – 7.23 (m, 1H, **7**), 7.23 – 7.17 (m, 2H, **5**), 4.24 (dd, *J* = 10.4, 3.0 Hz, 1H, **1-H_a**), 4.05 (app. t, *J* = 10.4 Hz, 1H, **1-H_b**), 3.47 – 3.34 (m, 1H, **2**), 2.73 (dd, *J* = 13.3, 4.8 Hz, 1H, **3-H_a**), 2.63 – 2.49 (m, 1H, **3-H_b**), 1.94 – 1.81 (m, 1H, **13-H_a**), 1.76 – 1.66 (m, 1H, **10-H_a**), 1.65 – 1.51 (m, 2H, **11-H_a**, **13-H_b**), 1.42 – 1.17 (m, 3H, **10-H_b**, **11-H_b**, **15**), 0.90 (app. t, *J* = 7.3 Hz, 3H, **12**), 0.67 (app. t, *J* = 7.4 Hz, 3H, **14**). ¹³C NMR (101 MHz, CDCl₃) δ 173.8 (**9**), 137.0 (**4**), 129.0(**5**) (**5**), 128.9(**5**) (**6**), 127.1 (**7**), 74.7 (**1**), 63.5 (**8**), 49.6 (**2**), 41.6 (**10**), 38.3 (**3**), 31.7 (**13**), 17.6 (**11**), 14.4 (**12**), 7.5 (**14**). IR (neat, cm⁻¹) 3332, 2962, 2874, 1732, 1456, 1317, 1294, 1198, 1154, 1044, 755, 701. HRMS *m/z* (ESI) calcd for C₁₆H₂₄NO₂ [M+H]⁺ 262.1802, found 262.1802.

***tert*-Butyl (*R*)-2-oxo-5-(((triisopropylsilyl)oxy)methyl)morpholine-4-carboxylate (**265c**)**

To a solution of (*R*)-2-amino-3-(((triisopropylsilyl)oxy)propan-1-ol (**259c**, 1.20 g, 4.85 mmol, 1 equiv; synthesized by Dr. C. He) and triethylamine (1.17 mL, 8.39 mmol, 1.7 equiv) in THF (10 mL) at 0 °C was added ethyl bromoacetate (1.20 g, 7.19 mmol, 1.5 equiv) dropwise. The reaction was allowed to warm to room temperature with stirring for 3 h. The resulting suspension was re-cooled to 0 °C, filtered and the solids washed with cold THF (20 mL). Di-*tert*-butyl dicarbonate (1.49 g, 6.83 mmol, 1.4 equiv) was added to the combined filtrates and stirred at room temperature overnight. The solvent was removed *in vacuo* and the crude residue dissolved in toluene (50 mL) before washing with sat. aq. NaHCO₃ and brine (10 mL each). The organic phase was dried over MgSO₄ and filtered.

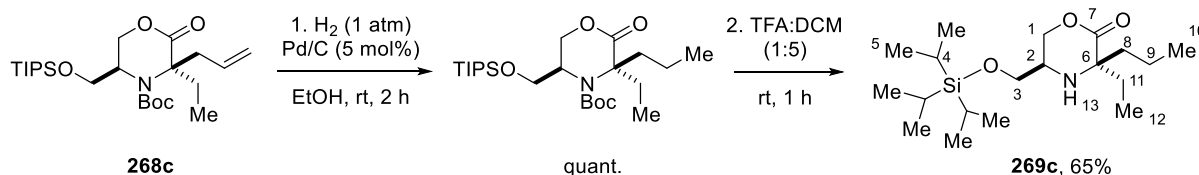
p-Toluenesulfonic acid monohydrate (92 mg, 0.48 mmol, 0.1 equiv) was added to the solution in toluene (diluted to 100 mL total volume) with heating under reflux using Dean–Stark apparatus overnight. After cooling to room temperature, the reaction mixture was washed with water (20 mL) and the organic phase separated, dried over MgSO₄, filtered and evaporated. The crude product was purified by silica gel flash chromatography (5–15% ethyl acetate in hexanes) to give the title compound as a colourless oil (**265c**, 1.32 g, 3.41 mmol, 70% yield over 2 steps). $[\alpha]_D^{25.0} +27.2^\circ$ (*c* 1.0, CHCl₃). ¹H NMR (400 MHz, CDCl₃) δ 4.64 (dd, *J* = 11.6, 3.3 Hz, 1H, **1-H_a**), 4.47 – 4.34 (d, *J* = 11.6 Hz, 1H, **1-H_b**), 4.26 (d, *J* = 18.2 Hz, 1H, **6-H_a**), 4.17 – 3.93 (m, 2H, **3-H_a**, **6-H_b**), 3.88 – 3.65 (m, 2H, **2**, **3-H_b**), 1.46 (s, 9H, **10**), 1.15 – 1.00 (m, 21H, **4**, **5**). ¹³C NMR (101 MHz, CDCl₃) δ 167.8 (**7**), 153.6 (**8**), 81.5 (**9**), 67.2 / 66.4 (**1**), 60.7 (**2**), 51.5 / 50.3 (**3**), 45.3 / 44.1 (**6**), 28.4 (**10**), 18.0(4) / 18.0(1) (**5**), 12.0 (**4**). Note: ppm / ppm denotes rotameric forms giving rise to distinct shifts in ¹³C NMR spectrum. IR (neat, cm⁻¹) 2943, 2867, 1763, 1702, 1464, 1407, 1369, 1344, 1289, 1246, 1165, 1112, 1058, 1006, 882, 770, 683. HRMS *m/z* (ESI) calcd for C₁₉H₃₈NO₅Si [M+H]⁺ 388.2514, found 388.2516.

***tert*-Butyl (3*R*,5*R*)-3-allyl-3-ethyl-2-oxo-5-(((triisopropylsilyl)oxy)methyl)morpholine-4-carboxylate (**268c**)**



To a solution of *tert*-butyl (*R*)-2-oxo-5-(((triisopropylsilyl)oxy)methyl)morpholine-4-carboxylate (**265c**, 775 mg, 2 mmol, 1 equiv) in THF:DME (1:1, 4 mL) at $-78\text{ }^{\circ}\text{C}$ was added NaHMDS (2 M in THF, 0.95 mL, 1.9 mmol, 0.95 equiv) dropwise. After stirring at $-78\text{ }^{\circ}\text{C}$ for 0.5 h, neat allyl iodide (504 mg, 3 mmol, 1.5 equiv) was added dropwise. The reaction was stirred at $-78\text{ }^{\circ}\text{C}$ for a further 2 h before being quenched at $-78\text{ }^{\circ}\text{C}$ with sat. aq. NH_4Cl (5 mL) and warming to room temperature. The reaction mixture was diluted with diethyl ether (50 mL) and the organic phase separated. The aqueous phase was re-extracted with diethyl ether (2 x 30 mL) and the combined organics dried over MgSO_4 , filtered and evaporated.

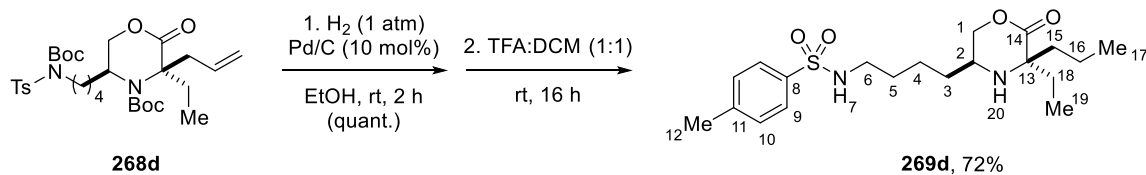
The crude material was dissolved in THF:DME (1:1, 4 mL) and cooled once more to $-78\text{ }^{\circ}\text{C}$. NaHMDS (2 M in THF, 1 mL, 2 mmol, 1 equiv) was added dropwise and the reaction stirred at $-78\text{ }^{\circ}\text{C}$ for 0.5 h. Neat ethyl iodide (936 mg, 6 mmol, 3 equiv) was added dropwise at $-78\text{ }^{\circ}\text{C}$. Without removing the cooling bath, the reaction was allowed to warm slowly to room temperature overnight. Sat. aq. NH_4Cl (5 mL) was added followed by dilution with diethyl ether (50 mL). The organic phase was separated and the aqueous phase re-extracted with diethyl ether (2 x 30 mL). The combined organics were dried over MgSO_4 , filtered and the solvent evaporated. The crude material was purified by silica gel flash chromatography (0–20% ethyl acetate in hexanes) to give the title compound as a colourless oil (**268c**, 536 mg, 1.18 mmol, 59% yield over 2 steps). $[\alpha]_D^{25.0} +20.3^{\circ}$ (c 1.0, CHCl_3). **^1H NMR** (400 MHz, CDCl_3) δ 5.67 – 5.48 (m, 1H, **12**), 5.14 – 4.98 (m, 2H, **13**), 4.58 (d, $J = 11.4$ Hz, 1H, **1-H_a**), 4.41 – 3.98 (m, 2H, **1-H_b**, **2**), 3.56 (dd, $J = 9.5, 5.1$ Hz, 1H, **3-H_a**), 3.49 (app. t, $J = 9.5$ Hz, 1H, **3-H_b**), 3.33 – 2.81 (m, 2H, **11-H_a**, **11-H_b**), 2.47 – 2.03 (m, 2H, **14-H_a**, **14-H_b**), 1.47 (s, 9H, **10**), 1.13 – 1.00 (m, 21H, **4**, **5**), 0.94 (app. t, $J = 7.6$ Hz, 3H, **15**). **^{13}C NMR** (101 MHz, CDCl_3) δ 171.0 (**7**), 152.6 (**8**), 134.1 (**12**), 119.3 (**13**), 80.8 (**9**), 68.2 (**6**), 64.5 (**1**), 60.8 (**3**), 52.1 (**2**), 38.7 (**11**), 31.6 (**14**), 28.5 (**10**), 18.1 / 18.0 (**5**), 12.0 (**4**), 9.6 (**15**). **IR** (neat, cm^{-1}) 2943, 2868, 1747, 1705, 1461, 1367, 1305, 1196, 1166, 1105, 1013, 882, 811, 771, 687. **HRMS** m/z (ESI) calcd for $\text{C}_{24}\text{H}_{46}\text{NO}_5\text{Si}$ $[\text{M}+\text{H}]^+$ 456.3140, found 456.3138.

(3*R*,5*R*)-3-Ethyl-3-propyl-5-(((triisopropylsilyl)oxy)methyl)morpholin-2-one (269c)

A solution of *tert*-butyl (3*R*,5*R*)-3-allyl-3-ethyl-2-oxo-5-(((triisopropylsilyl)oxy)methyl)-morpholine-4-carboxylate (**268c**, 486 mg, 1.07 mmol, 1 equiv) in ethanol (10 mL) was subjected to three cycles of vacuum/nitrogen backfill. Palladium on activated carbon (Pd/C, 10 wt%, 57 mg, 0.054 mmol, 5 mol%) was added in one portion, the atmosphere exchanged for hydrogen and the reaction stirred at room temperature for 2 h. The reaction was filtered through Celite and concentrated *in vacuo* to give the hydrogenated product as a colourless oil (488 mg, 1.07 mmol, quantitative yield).

The hydrogenated product (488 mg, 1.07 mmol) was dissolved in dichloromethane (7 mL) and trifluoroacetic acid (1.4 mL) added. The reaction was stirred at room temperature for 1 h, concentrated *in vacuo*, basified with sat. aq. NaHCO₃ and organics extracted with dichloromethane (2 x 50 mL). The crude material was purified by silica gel flash chromatography (0–10% ethyl acetate in hexanes) to give the title compound as a colourless oil (**269c**, 250 mg, 0.70 mmol, 65% yield). $[\alpha]_D^{25.0} -11.6^\circ$ (*c* 1.0, CHCl₃). ¹H NMR (400 MHz, CDCl₃) δ 4.30 (dd, *J* = 10.5, 3.4 Hz, 1H, **1-H_a**), 4.17 (app. t, *J* = 10.5 Hz, 1H, **1-H_b**), 3.74 (dd, *J* = 9.8, 4.4 Hz, 1H, **3-H_a**), 3.64 (dd, *J* = 9.8, 5.4 Hz, 1H, **3-H_b**), 3.32 – 3.24 (m, 1H, **2**), 2.00 – 1.84 (m, 2H, **11-H_a**, **13**), 1.83 (app. td, *J* = 12.1, 4.4 Hz, 1H, **8-H_a**), 1.71 – 1.60 (m, 1H, **11-H_b**), 1.60 – 1.39 (m, 2H, **8-H_b**, **9-H_a**), 1.36 – 1.19 (m, 1H, **9-H_b**), 1.17 – 0.99 (m, 21H, **4**, **5**), 0.96 – 0.88 (m, 6H, **10**, **12**). ¹³C NMR (101 MHz, CDCl₃) δ 173.8 (**7**), 72.4 (**1**), 63.7 (**3**), 62.7 (**6**), 50.1 (**2**), 41.5 (**8**), 32.4 (**11**), 18.1 (**5**), 17.6 (**9**), 14.4 (**10**), 12.0 (**4**), 8.0 (**12**). IR (neat, cm⁻¹) 3345, 2960, 2943, 2867, 1735, 1464, 1210, 1167, 1146, 1098, 1069, 882, 787, 682. HRMS *m/z* (ESI) calcd for C₁₉H₄₀N₁O₃Si₁ [M+H]⁺ 358.2772, found 358.2774.

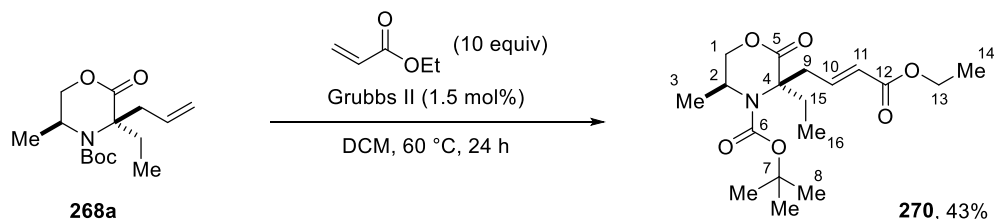
***N*-(4-((3*S*,5*R*)-5-Ethyl-6-oxo-5-propylmorpholin-3-yl)butyl)-4-methylbenzenesulfonamide (269d)**



A solution of *tert*-butyl (3*R*,5*S*)-3-allyl-5-(4-((*N*-(*tert*-butoxycarbonyl)-4-methylphenyl)sulfonamido)butyl)-3-ethyl-2-oxomorpholine-4-carboxylate (**268d**, 90 mg, 0.15 mmol, 1 equiv) in ethanol (5 mL) was subjected to three cycles of vacuum/nitrogen backfill. Palladium on activated carbon (Pd/C, 10 wt%, 25 mg, 0.015 mmol, 10 mol%) was added in one portion, the atmosphere exchanged for hydrogen and the reaction stirred at room temperature for 2 h. The reaction was filtered through Celite and concentrated *in vacuo* to give the hydrogenated product as a colourless oil (91 mg, 0.15 mmol, quantitative yield).

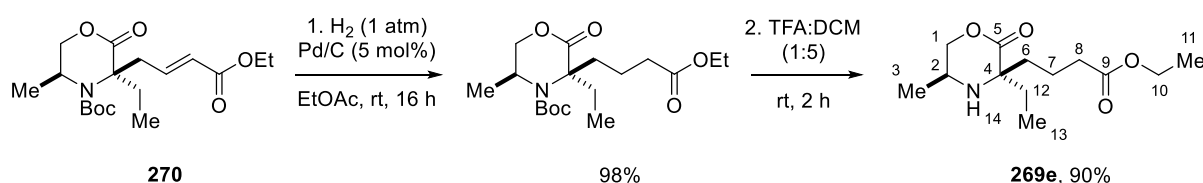
The hydrogenated product (91 mg, 0.15 mmol) was dissolved in dichloromethane (1 mL) and trifluoroacetic acid (1 mL) added. The reaction was stirred at room temperature overnight, concentrated *in vacuo*, basified with sat. aq. NaHCO₃ and the organics extracted with dichloromethane (3 x 20 mL). The crude material was purified by silica gel flash chromatography (50–80% ethyl acetate in hexanes) to give the title compound as a colourless oil (**269d**, 46 mg, 0.12 mmol, 72% yield). $[\alpha]_D^{25.0} -12.4^\circ$ (*c* 0.5, CHCl₃). ¹H NMR (400 MHz, CDCl₃) δ 7.76 – 7.71 (m, 2H, **9**), 7.29 (d, *J* = 8.1 Hz, 2H, **10**), 5.01 – 4.92 (m, 1H, **7**), 4.17 (dd, *J* = 10.5, 3.2 Hz, 1H, **1-H_a**), 3.88 (app. t, *J* = 10.6 Hz, 1H, **1-H_b**), 3.08 – 2.98 (m, 1H, **2**), 2.95 – 2.87 (m, 2H, **6-H_a**, **6-H_b**), 2.41 (s, 3H, **12**), 1.94 – 1.83 (m, 1H, **18-H_a**), 1.76 – 1.67 (m, 1H, **15-H_a**), 1.67 – 1.57 (m, 1H, **18-H_b**), 1.54 – 1.35 (m, 5H, **15-H_b**, **16-H_a**, **5-H_a**, **5-H_b**, **4-H_a**), 1.35 – 1.16 (m, 5H, **16-H_b**, **4-H_b**, **3-H_a**, **3-H_b**, **20**), 0.92 – 0.84 (m, 6H, **17**, **19**). ¹³C NMR (101 MHz, CDCl₃) δ 173.8 (**14**), 143.6 (**11**), 137.0 (**8**), 129.8 (**10**), 127.2 (**9**), 75.2 (**1**), 63.1 (**13**), 48.3 (**2**), 42.9 (**6**), 41.3 (**15**), 32.1 (**18**), 31.3 (**3**), 29.6 (**5**), 22.7 (**4**), 21.6 (**12**), 17.6 (**16**), 14.3 (**17**), 8.0 (**19**). IR (neat, cm⁻¹) 3278, 2963, 2873, 1723, 1458, 1326, 1213, 1158, 1094, 815, 750, 662. HRMS *m/z* (ESI) calcd for C₂₀H₃₃N₂O₄S₁ [M+H]⁺ 397.2156, found 397.2156.

***tert*-Butyl (3*R*,5*S*)-3-((*E*)-4-ethoxy-4-oxobut-2-en-1-yl)-3-ethyl-5-methyl-2-oxomorpholine-4-carboxylate (**270**)**



In a 20 mL vial equipped with magnetic stirrer, Grubbs' second generation catalyst (11 mg, 0.013 mmol, 1.5 mol%) and *tert*-butyl (3*R*,5*S*)-3-allyl-3-ethyl-5-methyl-2-oxomorpholine-4-carboxylate (**268a**, 241 mg, 0.85 mmol, 1 equiv) were combined, followed by the addition of dichloromethane (5 mL) and ethyl acrylate (0.9 mL, 8.5 mmol, 10 equiv). The vial was sealed and subjected to three cycles of vacuum/nitrogen backfill. The reaction was heated at 60 °C for 24 h before being cooled to room temperature, filtered through Celite and concentrated *in vacuo*. The crude material was purified by silica gel flash chromatography (0–20% ethyl acetate in hexanes) to give the title compound as a colourless solid (**270**, 130 mg, 0.37 mmol, 43% yield). **M.p.** 92–95 °C. $[\alpha]_D^{25.0}$ -78.1° (*c* 1.0, CHCl₃). **¹H NMR** (400 MHz, CDCl₃) δ 6.80 – 6.66 (m, 1H, **10**), 5.84 (d, *J* = 15.6 Hz, 1H, **11**), 4.52 (dd, *J* = 11.5, 2.8 Hz, 1H, **1-H_a**), 4.31 (br. s, 1H, **2**), 4.14 (q, *J* = 7.1 Hz, 2H, **13**), 4.06 (d, *J* = 11.3 Hz, 1H, **1-H_b**), 3.34 (br. s, 1H, **9-H_a**), 3.08 (dd, *J* = 13.4, 6.6 Hz, 1H, **9-H_b**), 2.34 – 2.16 (m, 2H, **15-H_a**, **15-H_b**), 1.47 (s, 9H, **8**), 1.23 (t, *J* = 7.1 Hz, 3H, **14**), 1.14 (d, *J* = 6.9 Hz, 3H, **3**), 0.93 (app. t, *J* = 7.6 Hz, 3H, **16**). **¹³C NMR** (101 MHz, CDCl₃) δ 170.2 (**5**), 166.1 (**12**), 152.7 (**6**), 144.3 (**10**), 125.2 (**11**), 81.2 (**7**), 70.2 (**1**), 67.4 (**4**), 60.2 (**13**), 46.9 (**2**), 37.0 (**9**), 31.6 (**15**), 28.5 (**8**), 17.8 (**3**), 14.4 (**14**), 9.4 (**16**). **IR** (neat, cm⁻¹) 2979, 2936, 1740, 1709, 1696, 1371, 1339, 1310, 1261, 1179, 1140, 1100, 1058, 1042, 963, 767. **HRMS** *m/z* (ESI) calcd for C₁₈H₃₀N₁O₆ [M+H]⁺ 356.2068, found 356.2069.

Ethyl 4-((3*R*,5*S*)-3-ethyl-5-methyl-2-oxomorpholin-3-yl)butanoate (269e**)**

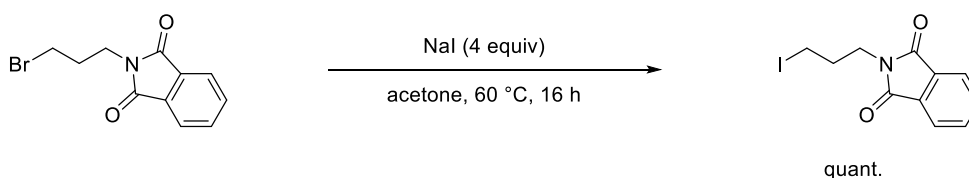


A solution of *tert*-butyl (3*R*,5*S*)-3-((*E*)-4-ethoxy-4-oxobut-2-en-1-yl)-3-ethyl-5-methyl-2-oxomorpholine-4-carboxylate (**270**, 130 mg, 0.37 mmol, 1 equiv) in ethyl acetate (10 mL) was subjected to three cycles of vacuum/nitrogen backfill. Palladium on activated carbon (Pd/C, 10

wt%, 20 mg, 0.019 mmol, 5 mol%) was added in one portion, the atmosphere exchanged for hydrogen and the reaction stirred at room temperature overnight. The reaction was filtered through Celite and concentrated to give the hydrogenated product as a colourless oil (128 mg, 0.36 mmol, 98% yield).

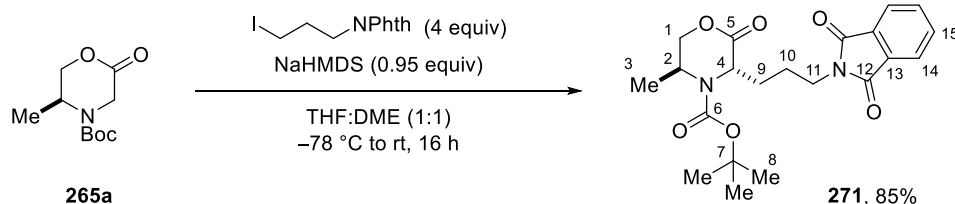
The hydrogenated product (128 mg, 0.36 mmol) was dissolved in dichloromethane (2.5 mL) and trifluoroacetic acid (0.47 mL) added. The reaction was stirred at room temperature for 2 h, concentrated *in vacuo*, basified with sat. aq. NaHCO₃ and the product extracted with dichloromethane (2 x 20 mL). The combined organics were dried over MgSO₄, filtered and the solvent evaporated. The crude material was purified by silica gel flash chromatography (50% ethyl acetate in hexanes) to give the title compound as a colourless oil (**269e**, 83 mg, 0.32 mmol, 90% yield). [α]_D^{25.0} -11.4° (*c* 0.5, CHCl₃). ¹H NMR (400 MHz, CDCl₃) δ 4.20 (dd, *J* = 10.5, 3.2 Hz, 1H, **1-H_a**), 4.10 (q, *J* = 7.2 Hz, 2H, **10**), 3.93 (app. t, *J* = 10.5 Hz, 1H, **1-H_b**), 3.37 – 3.26 (m, 1H, **2**), 2.37 – 2.19 (m, 2H, **8-H_a**, **8-H_b**), 1.99 – 1.83 (m, 2H, **7-H_a**, **12-H_a**), 1.82 – 1.72 (m, 1H, **6-H_a**), 1.72 – 1.61 (m, 1H, **12-H_b**), 1.61 – 1.39 (m, 3H, **7-H_b**, **6-H_b**, **14**), 1.23 (t, *J* = 7.2 Hz, 3H, **11**), 1.05 (d, *J* = 6.3 Hz, 3H, **3**), 0.91 (app. t, *J* = 7.5 Hz, 3H, **13**). ¹³C NMR (101 MHz, CDCl₃) δ 173.4 (**9**), 173.2 (**5**), 76.1 (**1**), 63.1 (**4**), 60.4 (**10**), 43.7 (**2**), 38.5 (**6**), 34.3 (**8**), 32.0 (**12**), 19.8 (**7**), 17.2 (**3**), 14.3 (**11**), 8.0 (**13**). IR (neat, cm⁻¹) 3329, 2971, 1732, 1462, 1377, 1318, 1184, 1095, 1050. HRMS *m/z* (ESI) calcd for C₁₃H₂₄NO₄ [M+H]⁺ 258.1700, found 258.1700.

2-(3-Iodopropyl)isoindoline-1,3-dione

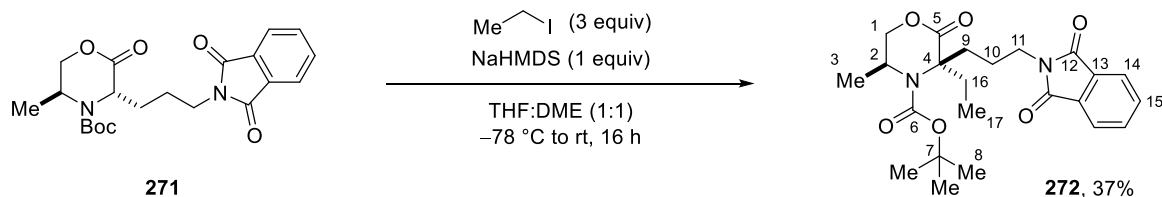


2-(3-Bromopropyl)isoindoline-1,3-dione (3 g, 11.2 mmol, 1 equiv) and sodium iodide (8.4 g, 55.8 mmol, 4 equiv) in acetone (25 mL) was heated to reflux and stirred overnight. After cooling to room temperature the solvent was removed *in vacuo* and dichloromethane (50 mL) and 10% aq. Na₂S₂O₃ (20 mL) added to the residue. The organic phase was separated, dried over MgSO₄, filtered and the solvent evaporated to give the title compound as a white powder (3.52 g, 11.2 mmol, quantitative yield). ¹H NMR (400 MHz, CDCl₃) δ 7.88 – 7.81 (m, 2H), 7.75 – 7.68 (m, 2H), 3.76 (t, *J* = 6.8 Hz, 2H), 3.16 (t, *J* = 7.2 Hz, 2H), 2.24 (app. quintet, *J* = 7.0 Hz, 2H). ¹³C NMR (101 MHz, CDCl₃) δ 168.4, 134.2, 132.1, 123.5, 38.8, 32.7, 1.3. Spectral data were in accordance with the literature.²⁷⁴

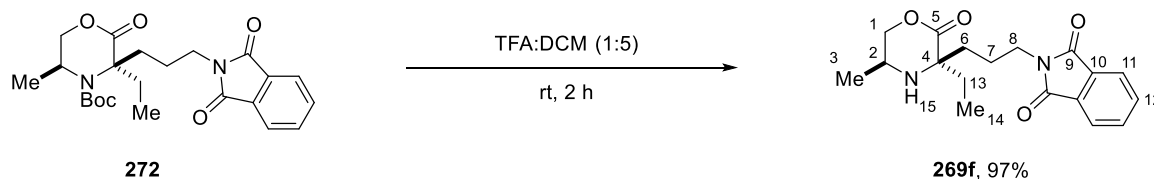
***tert*-Butyl (3*S*,5*S*)-3-(3-(1,3-dioxoisindolin-2-yl)propyl)-5-methyl-2-oxomorpholine-4-carboxylate (**271**)**



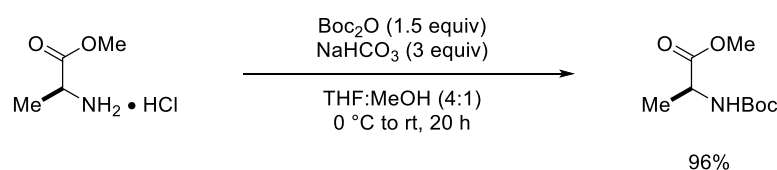
To a solution of *tert*-butyl (*S*)-5-methyl-2-oxomorpholine-4-carboxylate (**265a**, 280 mg, 1.30 mmol, 1 equiv) in THF:DME (1:1, 8 mL) at $-78\text{ }^{\circ}\text{C}$ was added NaHMDS (2 M in THF, 620 μL , 1.24 mmol, 0.95 equiv) dropwise. After stirring at $-78\text{ }^{\circ}\text{C}$ for 0.5 h, 2-(3-iodopropyl)isoindoline-1,3-dione (1.71 g, 5.43 mmol, 4 equiv) was added in one portion. Without removing the cooling bath, the reaction was allowed to warm slowly to room temperature overnight. Sat. aq. NH_4Cl (5 mL) was added followed by diethyl ether (30 mL). The organic phase was separated and the aqueous phase re-extracted with diethyl ether (2 x 20 mL). The combined organics were dried over MgSO_4 , filtered and the solvent evaporated. The crude product was purified by silica gel flash chromatography (10–40% ethyl acetate in hexanes) to give the title compound as a colourless sticky foam (**271**, 443 mg, 1.10 mmol, 85% yield). $[\alpha]_D^{25.0} +43.1^{\circ}$ (c 1.0, CHCl_3). $^1\text{H NMR}$ (400 MHz, CDCl_3) δ 7.86 – 7.80 (m, 2H, **14**), 7.74 – 7.68 (m, 2H, **15**), 4.52 (dd, $J = 11.9, 2.6$ Hz, 1H, **1-H_a**), 4.32 (br. s, 1H, **2**), 4.16 (d, $J = 11.9$ Hz, 1H, **1-H_b**), 4.13 – 4.06 (m, 1H, **4**), 3.71 (app. t, $J = 6.8$ Hz, 2H, **11**), 1.97 (br. s, 1H, **9-H_a**), 1.89 – 1.70 (m, 3H, **9-H_b**, **10-H_a**, **10-H_b**), 1.39 (br. s, 9H, **8**), 1.24 (d, $J = 6.8$ Hz, 3H, **3**). $^{13}\text{C NMR}$ (101 MHz, CDCl_3) δ 169.0 (**5**), 168.4 (**12**), 153.2 (**6**), 134.1 (**15**), 132.1 (**13**), 123.4 (**14**), 81.2 (**7**), 70.1 (**1**), 55.9 (**2**), 46.4 (**4**), 37.5 (**11**), 32.2 (**9**), 28.4 (**8**), 25.3 (**10**), 16.7 (**2**). IR (neat, cm^{-1}) 2975, 2933, 1782, 1751, 1710, 1694, 1398, 1372, 1280, 1171, 1131, 1065, 1033, 721. HRMS m/z (ESI) calcd for $\text{C}_{21}\text{H}_{27}\text{N}_2\text{O}_6$ $[\text{M}+\text{H}]^+$ 403.1864, found 403.1864.

***tert*-Butyl (3*R*,5*S*)-3-(3-(1,3-dioxoisindolin-2-yl)propyl)-3-ethyl-5-methyl-2-oxomorpholine-4-carboxylate (**272**)**

To a solution of *tert*-butyl (3*S*,5*S*)-3-(3-(1,3-dioxoisindolin-2-yl)propyl)-5-methyl-2-oxomorpholine-4-carboxylate (**271**, 427 mg, 1.06 mmol, 1 equiv) in THF:DME (1:1, 4 mL) at $-78\text{ }^{\circ}\text{C}$ was added NaHMDS (2 M in THF, 530 μL , 1.06 mmol, 1 equiv) dropwise. After stirring at $-78\text{ }^{\circ}\text{C}$ for 0.5 h, neat ethyl iodide (496 mg, 3.18 mmol, 3 equiv) was added dropwise. Without removing the cooling bath, the reaction was allowed to warm slowly to room temperature overnight. Sat. aq. NH_4Cl (5 mL) was added followed by dilution with diethyl ether (30 mL). The organic phase was separated and the aqueous phase re-extracted with diethyl ether (2 x 20 mL). The combined organics were dried over MgSO_4 , filtered and the solvent evaporated. The crude product was purified by silica gel flash chromatography (10–40% ethyl acetate in hexanes) to give the title compound as a colourless foam (**272**, 170 mg, 0.39 mmol, 37% yield). $[\alpha]_D^{25.0} -16.9^{\circ}$ (c 1.0, CHCl_3). $^1\text{H NMR}$ (400 MHz, CDCl_3) δ 7.85 – 7.79 (m, 2H, **14**), 7.72 – 7.66 (m, 2H, **15**), 4.53 (dd, $J = 11.5, 2.8\text{ Hz}$, 1H, **1-H_a**), 4.37 (br. s, 1H, **2**), 4.06 (dd, $J = 11.5, 1.1\text{ Hz}$, 1H, **1-H_b**), 3.77 – 3.63 (m, 2H, **11-H_a**, **11-H_b**), 2.52 – 2.15 (m, 3H, **9-H_a**, **9-H_b**, **16-H_a**), 2.14 – 2.03 (m, 1H, **16-H_b**), 1.60 – 1.49 (m, 2H, **10-H_a**, **10-H_b**), 1.40 (s, 9H, **8**), 1.24 (d, $J = 6.9\text{ Hz}$, 3H, **3**), 0.89 (app. t, $J = 7.6\text{ Hz}$, 3H, **17**). $^{13}\text{C NMR}$ (101 MHz, CDCl_3) δ 170.5 (**5**), 168.5 (**12**), 153.1 (**6**), 134.0 (**15**), 132.3 (**13**), 123.3 (**14**), 81.1 (**7**), 70.0 (**1**), 67.4 (**4**), 46.8 (**2**), 38.0 (**11**), 32.0 (br., **9**, **16**), 28.5 (**8**), 24.9 (**10**), 17.8 (**3**), 9.4 (**17**). **IR** (neat, cm^{-1}) 2975, 2937, 1772, 1741, 1712, 1693, 1437, 1397, 1369, 1314, 1170, 1088, 721. **HRMS** m/z (ESI) calcd for $\text{C}_{23}\text{H}_{31}\text{N}_2\text{O}_6$ $[\text{M}+\text{H}]^+$ 431.2177, found 431.2179.

2-(3-((3*R*,5*S*)-3-Ethyl-5-methyl-2-oxomorpholin-3-yl)propyl)isoindoline-1,3-dione (**269f**)

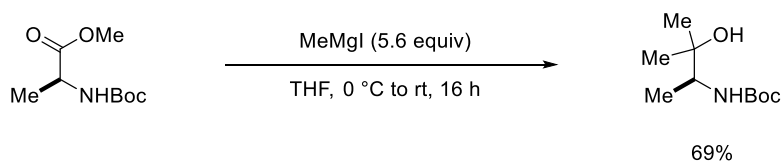
To a solution of *tert*-butyl (3*R*,5*S*)-3-(3-(1,3-dioxoisoindolin-2-yl)propyl)-3-ethyl-5-methyl-2-oxomorpholine-4-carboxylate (**272**, 150 mg, 0.35 mmol) in dichloromethane (2.3 mL) was added trifluoroacetic acid (0.46 mL). The reaction was stirred at room temperature for 2 h, concentrated *in vacuo*, basified with sat. aq. NaHCO₃ and the product extracted with dichloromethane (2 x 20 mL). The combined organics were dried over MgSO₄, filtered and the solvent evaporated to give the title compound as a colourless oil (**269f**, 113 mg, 0.34 mmol, 97% yield). $[\alpha]_D^{25.0}$ -4.8° (*c* 1.0, CHCl₃). ¹H NMR (500 MHz, CDCl₃) δ 7.86 – 7.81 (m, 2H, **11**), 7.73 – 7.68 (m, 2H, **12**), 4.18 (dd, *J* = 10.4, 3.1 Hz, 1H, **1-H_a**), 3.93 (app. t, *J* = 10.4 Hz, 1H, **1-H_b**), 3.75 – 3.66 (m, 2H, **8-H_a**, **8-H_b**), 3.37 – 3.27 (m, 1H, **2**), 2.02 – 1.90 (m, 2H, **13-H_a**, **7-H_a**), 1.90 – 1.83 (m, 1H, **6-H_a**), 1.72 – 1.62 (m, 2H, **13-H_b**, **7-H_b**), 1.51 – 1.43 (m, 1H, **6-H_b**), 1.28 (br. s, 1H, **15**), 1.04 (d, *J* = 6.3 Hz, 3H, **3**), 0.91 (app. t, *J* = 7.5 Hz, 3H, **14**). ¹³C NMR (126 MHz, CDCl₃) δ 173.1 (**5**), 168.5 (**9**), 134.0 (**12**), 132.3 (**10**), 123.4 (**11**), 76.0 (**1**), 63.2 (**4**), 43.8 (**2**), 38.2 (**8**), 36.4 (**6**), 32.0 (**13**), 24.0 (**7**), 17.3 (**3**), 8.0 (**14**). IR (neat, cm⁻¹) 3335, 2969, 2935, 1771, 1733, 1707, 1466, 1437, 1397, 1360, 1187, 1149, 1037, 720. HRMS *m/z* (ESI) calcd for C₁₈H₂₃N₂O₄ [M+H]⁺ 331.1652, found 331.1654.

Methyl (*tert*-butoxycarbonyl)-L-alaninate

To a solution of L-alanine methyl ester hydrochloride (7.83 g, 56.1 mmol, 1 equiv) in THF:MeOH (4:1, 150 mL) stirring under air at 0 °C was added NaHCO₃ (14.14 g, 168.3 mmol, 3 equiv) followed immediately by di-*tert*-butyl decarbonate (18.38 g, 84.2 mmol, 1.5 equiv). The reaction was warmed to room temperature and stirred for 20 h. Water (100 mL) and diethyl ether (200 mL) were added to the reaction and the organic phase separated. The aqueous phase was extracted with diethyl ether (2 x 300 mL). The combined organics were washed with sat. aq. NaHCO₃ (2 x 100 mL) and brine (2 x 100 mL), dried over MgSO₄, filtered and the solvent

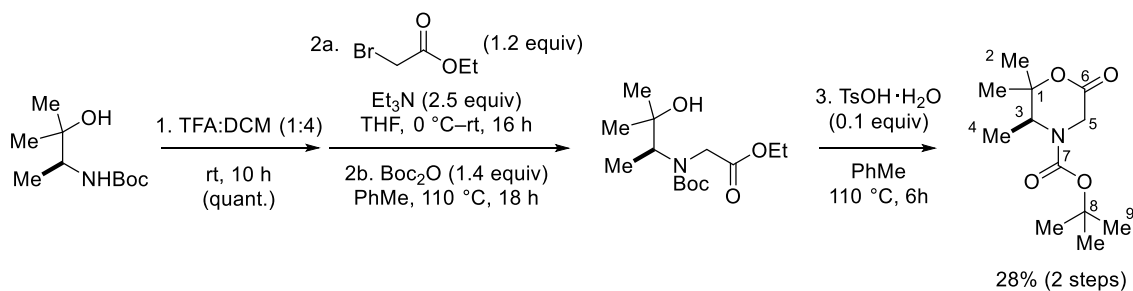
evaporated. The crude material was purified by silica gel flash chromatography (10–20% EtOAc in hexanes) to give the title compound as a colourless oil (10.94 g, 53.8 mmol, 96%). **¹H NMR** (400 MHz, CDCl₃) δ 5.03 (br. s, 1H), 4.39 – 4.24 (m, 1H), 3.74 (s, 3H), 1.44 (s, 9H), 1.38 (d, J = 7.2 Hz, 3H). **¹³C NMR** (101 MHz, CDCl₃) δ 174.0, 155.2, 79.9, 52.4, 49.3, 28.4, 18.8. Spectral data were in accordance with the literature.²⁷⁵

***tert*-Butyl (*S*)-(3-hydroxy-3-methylbutan-2-yl)carbamate**



To a solution of methyl (*tert*-butoxycarbonyl)-L-alaninate (10.94 g, 53.8 mmol, 1 equiv) in THF (250 mL) at 0 °C was added methylmagnesium iodide (3 M in THF, 100 mL, 301 mmol, 5.6 equiv). The reaction was warmed to room temperature and stirred overnight. The reaction was re-cooled to 0 °C and quenched (caution: exothermic) with sat. aq. NH₄Cl (250 mL). The phases were separated and the aqueous phase extracted with diethyl ether (3 x 300 mL) and washed with brine (2 x 200 mL). The combined organics were dried over MgSO₄ and the solvent removed *in vacuo*. The crude product was purified by silica gel flash chromatography (10–30% ethyl acetate in hexanes) to give title compound as a colourless oil (7.55 g, 37.1 mmol, 69% yield). **¹H NMR** (400 MHz, CDCl₃) δ 4.72 (br. s, 1H), 3.68 – 3.47 (m, 1H), 2.17 (br. s, 1H), 1.43 (s, 9H), 1.21 (s, 3H), 1.16 (s, 3H), 1.12 (d, J = 6.8 Hz, 3H). **¹³C NMR** (101 MHz, CDCl₃) δ 156.5, 79.5, 73.1, 54.7, 28.5, 27.5, 25.7, 16.3. Spectral data were in accordance with the literature.²⁷⁶

***tert*-Butyl (*S*)-2,2,3-trimethyl-6-oxomorpholine-4-carboxylate**



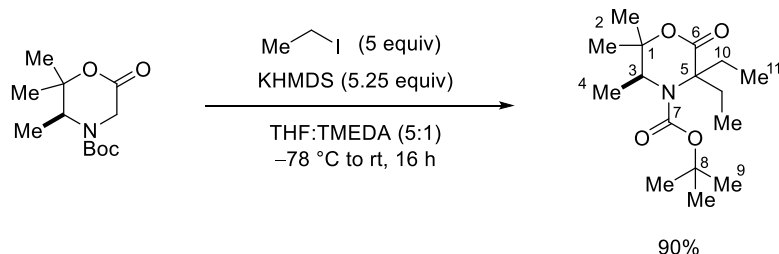
To a solution of *tert*-butyl (*S*)-(3-hydroxy-3-methylbutan-2-yl)carbamate (890 mg, 4.38 mmol, 1 equiv) dichloromethane (4 mL) was added trifluoroacetic acid (1 mL) and the reaction stirred

at room temperature for 10 h. The solvent was evaporated to give the TFA salt of (*S*)-3-amino-2-methylbutan-2-ol as a dark red oil (951 mg, 4.38 mmol, quantitative yield).

To a solution of (*S*)-3-amino-2-methylbutan-2-ol TFA salt (951 mg, 4.38 mmol, 1 equiv) in THF (30 mL) at 0 °C were added triethylamine (1.52 mL, 10.9 mmol, 2.5 equiv) followed by ethyl bromoacetate (877 mg, 5.25 mmol, 1.2 equiv). The reaction was stirred at room temperature for 16 h. Sat. aq. NH₄Cl (10 mL) was added and the aqueous phase extracted with diethyl ether (3 x 50 mL), dried over MgSO₄, filtered and the solvent evaporated to give the crude Boc-protected secondary amine. The crude material was dissolved in toluene (10 mL) and di-*tert*-butyl dicarbonate (1.34 g, 6.12 mmol, 1.4 equiv) added in one portion. The reaction was heated at 110 °C for 18 h.

After cooling to room temperature, *p*-toluenesulfonic acid monohydrate (84 mg, 0.44 mmol, 0.1 equiv) was added and the reaction mixture diluted with toluene (50 mL). The solvent was distilled off (120 °C, atmospheric pressure) and the remaining residue taken up in diethyl ether (50 mL). The solution was washed with water (10 mL) and the organic phase dried over MgSO₄, filtered and the solvent evaporated. The crude material was purified by silica gel flash chromatography (10–30% ethyl acetate in hexanes) to give the title compound as a colourless solid (300 mg, 1.23 mmol, 28% yield over 2 steps). **M.p.** 70–72 °C. $[\alpha]_D^{25.0} +6.2^\circ$ (*c* 1.0, CHCl₃). **¹H NMR** (400 MHz, CDCl₃) δ 4.32 (d, *J* = 19.8 Hz, 1H, **5-H_a**), 4.22 – 3.98 (m, 1H, **3**), 3.90 (d, *J* = 19.8 Hz, 1H, **5-H_b**), 1.46 (s, 9H, **9**), 1.40 (s, 3H, **2**), 1.37 (s, 3H, **2'**), 1.18 (d, *J* = 6.9 Hz, 3H, **4**). **¹³C NMR** (101 MHz, CDCl₃) δ 166.8 (**6**), 153.7 (**7**), 83.2 (**1**), 81.2 (**8**), 50.8 (**3**), 42.3 (**5**), 28.4 (**9**), 27.2 (**2**), 25.3 (**2'**), 13.1 (**4**). **IR** (neat, cm⁻¹) 2975, 2933, 1727, 1697, 1394, 1335, 1289, 1267, 1162, 1113, 1045, 971, 868, 771, 764. **HRMS** *m/z* (ESI) calcd for C₁₂H₂₅N₂O₄ [M+NH₄]⁺ 261.1809, found 261.1816.

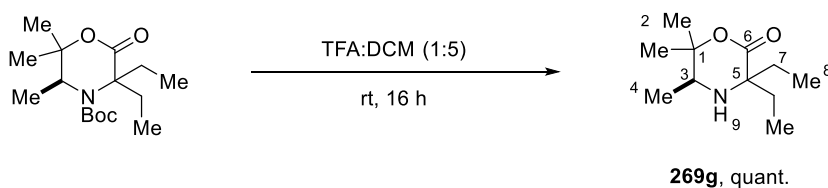
***tert*-Butyl (*S*)-5,5-diethyl-2,2,3-trimethyl-6-oxomorpholine-4-carboxylate**



To a solution of *tert*-butyl (*S*)-2,2,3-trimethyl-6-oxomorpholine-4-carboxylate (235 mg, 0.97 mmol, 1 equiv) and ethyl iodide (753 mg, 4.83 mmol, 5 equiv) in tetrahydrofuran (5 mL) and TMEDA (1 mL) at –78 °C was added KHMDS (0.7 M in toluene, 7.25 mL, 5.07 mmol, 5.25

equiv) dropwise. The reaction was stirred for 1 h at $-78\text{ }^{\circ}\text{C}$ and then at room temperature overnight. The reaction was diluted with ethyl acetate (30 mL) and sat. aq. NH_4Cl (5 mL) added. The organic phase was separated, dried over MgSO_4 , filtered and the solvent evaporated. The crude material was purified by silica gel flash chromatography (10–20% ethyl acetate in hexanes) to give the title compound as a colourless solid (259 mg, 0.87 mmol, 90% yield). **M.p.** $76\text{--}80\text{ }^{\circ}\text{C}$. $[\alpha]_D^{25.0} -22.9^{\circ}$ (c 1.0, CHCl_3). **^1H NMR** (400 MHz, CDCl_3) δ 4.27 (q, $J = 7.1$ Hz, 1H, **3**), 2.56 – 2.41 (m, 1H, **10-H_a**), 2.26 – 2.08 (m, 3H, **10-H_b**, **10'-H_a**, **10'-H_b**), 1.54 (s, 3H, **2**), 1.48 (s, 9H, **9**), 1.33 (s, 3H, **2'**), 1.18 (d, $J = 7.1$ Hz, 3H, **4**), 0.93 – 0.82 (m, 6H, **11**, **11'**). **^{13}C NMR** (101 MHz, CDCl_3) δ 171.0 (**6**), 154.4 (**7**), 81.8 (**1**), 81.0 (**8**), 66.7 (**5**), 53.3 (**3**), 32.3 (**10**), 28.6 (**9**), 28.5 (**10'**), 27.5 (**2**), 27.4 (**2'**), 16.3 (**4**), 10.4 (**11**), 10.0 (**11'**). **IR** (neat, cm^{-1}) 2968, 2880, 1729, 1677, 1457, 1382, 1367, 1324, 1306, 1228, 1166, 1134, 1101, 1045, 1036, 972, 857, 770. **HRMS** m/z (ESI) calcd for $\text{C}_{16}\text{H}_{30}\text{N}_1\text{O}_4$ $[\text{M}+\text{H}]^+$ 300.2169, found 300.2174.

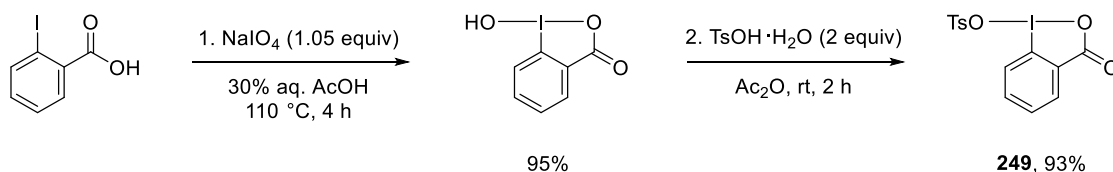
(S)-3,3-Diethyl-5,6,6-trimethylmorpholin-2-one (269g)



tert-Butyl (S)-5,5-diethyl-2,2,3-tri-methyl-6-oxomorpholine-4-carboxylate (205 mg, 0.68 mmol) was dissolved in dichloromethane (4.5 mL) and trifluoroacetic acid (0.9 mL) added. The reaction was stirred at room temperature overnight, concentrated *in vacuo*, sat. aq. NaHCO_3 (5 mL) added and the aqueous phase extracted with dichloromethane. The organics were separated and dried over MgSO_4 , filtered and the solvent removed *in vacuo*. The crude material was purified by silica gel flash chromatography (10–30% ethyl acetate in hexanes) to give the title compound as a pale yellow oil (**269g**, 136 mg, 0.68 mmol, quantitative yield). $[\alpha]_D^{25.0} +7.0^{\circ}$ (c 1.0, CHCl_3). **^1H NMR** (400 MHz, CDCl_3) δ 3.09 (q, $J = 6.6$ Hz, 1H, **3**), 1.94 – 1.76 (m, 2H, **7-H_a**, **7'-H_a**), 1.75 – 1.62 (m, 1H, **7-H_b**), 1.53 – 1.40 (m, 1H, **7'-H_b**), 1.31 (s, 3H, **2**), 1.29 (s, 3H, **2'**), 1.19 (br. s, 1H, **9**), 1.04 (d, $J = 6.6$ Hz, 3H, **4**), 0.94 (t, $J = 7.4$ Hz, 3H, **8'**), 0.88 (t, $J = 7.5$ Hz, 3H, **8**). **^{13}C NMR** (101 MHz, CDCl_3) δ 174.5 (**6**), 86.3 (**1**), 63.2 (**5**), 51.5 (**3**), 30.5 (**7**), 30.4 (**7'**), 26.7 (**2'**), 21.1 (**2**), 17.0 (**4**), 8.9 (**8'**), 7.6 (**8**). **IR** (neat, cm^{-1}) 3334, 2976, 2938, 2880, 1714, 1461, 1374, 1237, 1207, 1192, 1132, 1106, 1088, 974, 808, 732, 707. **HRMS** m/z (ESI) calcd for $\text{C}_{11}\text{H}_{22}\text{N}_1\text{O}_2$ $[\text{M}+\text{H}]^+$ 200.1645, found 200.1644.

Synthesis of Cyclic Iodine(III) Tosylate Oxidant

3-Oxo-1- λ^3 -benzo[*d*][1,2]iodaoxol-1(3*H*)-yl 4-methylbenzenesulfonate (**249**)

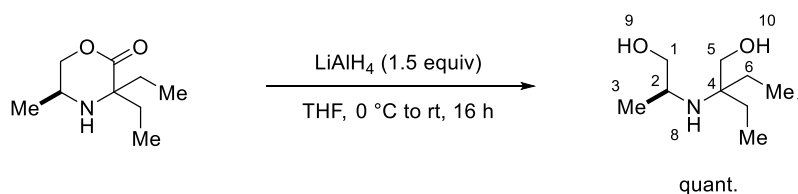


A suspension of 2-iodobenzoic acid (9.92 g, 40 mmol, 1 equiv) and sodium periodate (8.98 g, 42 mmol, 1.05 equiv) in 30% aq. AcOH (60 mL) was heated at reflux for 4 h. The reaction was diluted with cold water and cooled at room temperature in the dark. The precipitate was filtered and the solids washed with ice water and acetone. The product (2-iodosylbenzoic acid) was dried under vacuum and used directly (white powder, 9.99 g, 37.8 mmol, 95% yield).

To a suspension of 2-iodosylbenzoic acid (3.17 g, 12.0 mmol, 1 equiv) in acetic anhydride (6 mL) was added TsOH·H₂O (4.57 g, 24.0 mmol, 2 equiv) portionwise. The reaction was stirred in air at room temperature for 2 h before addition of dry diethyl ether (60 mL). The precipitate was filtered under nitrogen and the solids washed with dry diethyl ether (3 x 60 mL). The product was dried under vacuum overnight to afford the title compound as white powder (**249**, 4.65 g, 11.1 mmol, 93% yield). ¹H NMR (400 MHz, DMSO-*d*₆) δ 8.01 (dd, *J* = 7.6, 1.1 Hz, 1H), 7.98 – 7.92 (m, 1H), 7.84 (d, *J* = 8.1 Hz, 1H), 7.70 (t, *J* = 7.4 Hz, 1H), 7.49 (d, *J* = 8.1 Hz, 2H), 7.13 (d, *J* = 8.1 Hz, 2H), 2.29 (s, 3H). ¹³C NMR (101 MHz, DMSO-*d*₆) δ 167.8, 145.1, 138.1, 134.5, 131.5, 131.1, 130.4, 128.2, 126.4, 125.6, 120.5, 20.8. Spectral data were in accordance with the literature.²⁷⁷

Synthesis of Acyclic Amino-diol Substrates Derived from Morpholinones

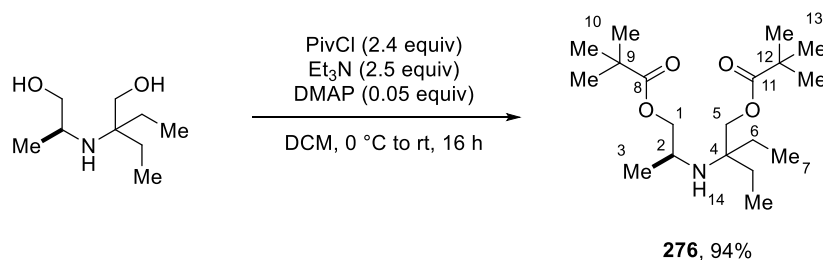
(*S*)-2-Ethyl-2-((1-hydroxypropan-2-yl)amino)butan-1-ol



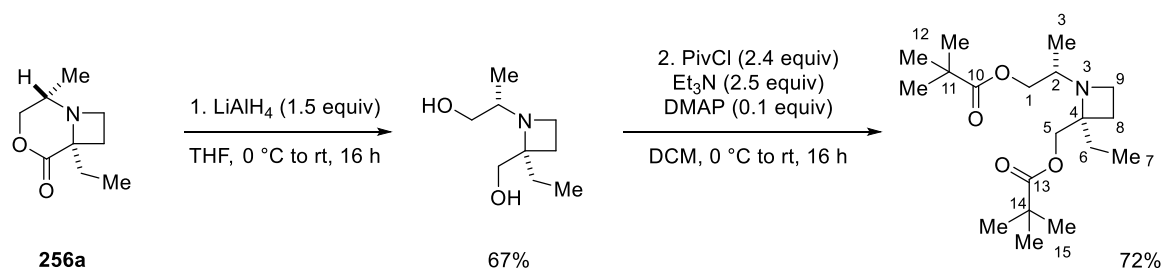
To a solution of (*S*)-3,3-diethyl-5-methylmorpholin-2-one (406 mg, 2.37 mmol, 1 equiv; synthesized by Dr. C. He¹⁵³) in tetrahydrofuran (5 mL) at 0 °C was added LiAlH₄ (2.4 M in THF, 1.5 mL, 3.56 mmol, 1.5 equiv) dropwise. The reaction was warmed to room temperature and stirred overnight. The reaction was re-cooled to 0 °C followed by addition of H₂O (150

μL), 10% aq. NaOH (150 μL) then H_2O (450 μL). The white precipitate was filtered and washed with THF. The filtrate was dried over Na_2SO_4 , filtered and the solvent evaporated to give the title compound as a colourless oil (415 mg, 2.37 mmol, quantitative yield). $[\alpha]_D^{25.0} +34.8^\circ$ (c 1.0, CHCl_3). ^1H NMR (400 MHz, CDCl_3) δ 3.49 (dd, $J = 10.3, 4.3$ Hz, 1H, **1-H_a**), 3.36 (d, $J = 11.4$ Hz, 1H, **5-H_a**), 3.28 (d, $J = 11.4$ Hz, 1H, **5-H_b**), 3.20 (dd, $J = 10.3, 8.0$ Hz, 1H, **1-H_b**), 2.95 – 2.27 (m, 4H, **2, 8, 9, 10**), 1.50 – 1.37 (m, 1H, **6-H_a**), 1.34 – 1.21 (m, 3H, **6-H_b, 6'-H_a, 6'-H_b**), 1.02 (d, $J = 6.5$ Hz, 3H, **3**), 0.86 – 0.78 (m, 6H, **7, 7'**). ^{13}C NMR (101 MHz, CDCl_3) δ 67.7 (**1**), 64.0 (**5**), 59.0 (**4**), 47.3 (**2**), 26.1 (**6**), 24.8 (**6'**), 20.6 (**c**), 7.7 (**7'**), 7.3 (**7**). IR (neat, cm^{-1}) 3295 (br.), 2965, 2934, 2879, 1460, 1378, 1158, 1072, 1051, 930, 889. HRMS m/z (ESI) calcd for $\text{C}_9\text{H}_{22}\text{NO}_2$ $[\text{M}+\text{H}]^+$ 176.1645, found 176.1643.

(S)-2-Ethyl-2-((1-(pivaloyloxy)propan-2-yl)amino)butyl pivalate (276)



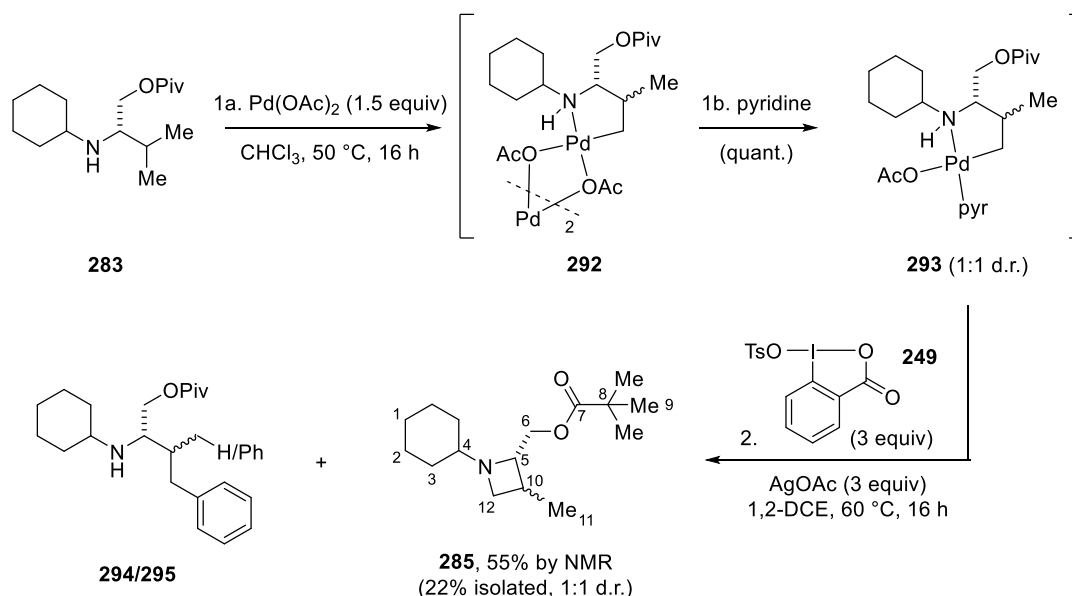
To a solution of (S)-2-ethyl-2-((1-hydroxypropan-2-yl)amino)butan-1-ol (173 mg, 0.99 mmol, 1 equiv) in dichloromethane (5 mL) at 0 °C were added DMAP (6 mg, 0.05 mmol, 0.05 equiv), pivaloyl chloride (286 mg, 2.37 mmol, 2.4 equiv) and triethylamine (344 μL , 2.47 mmol, 2.5 equiv). The reaction was stirred at room temperature overnight, diluted with dichloromethane (20 mL) and water (10 mL) added. The organic phase was separated and the aqueous phase re-extracted with dichloromethane (2 x 20 mL). The combined organic phases were dried over MgSO_4 , filtered and the solvent evaporated. The crude material was purified by silica gel flash chromatography (5–15% ethyl acetate in hexanes) to give the title compound as a colourless oil (**276**, 321 mg, 0.93 mmol, 94% yield). $[\alpha]_D^{25.0} -10.4^\circ$ (c 1.0, CHCl_3). ^1H NMR (400 MHz, CDCl_3) δ 4.00 (dd, $J = 10.5, 4.6$ Hz, 1H, **1-H_a**), 3.93 – 3.83 (m, 2H, **5-H_a, 5-H_b**), 3.64 (dd, $J = 10.5, 7.9$ Hz, 1H, **1-H_b**), 3.07 – 2.95 (m, 1H, **2**), 1.48 – 1.31 (m, 4H, **6-H_a, 6-H_b, 6'-H_a, 14**), 1.26 – 1.13 (m, 19H, **6'-H_b, 10, 13**), 1.06 (d, $J = 6.5$ Hz, 3H, **3**), 0.87 – 0.79 (m, 6H, **7, 7'**). ^{13}C NMR (101 MHz, CDCl_3) δ 178.5 (**8 or 11**), 178.4 (**8 or 11**), 70.0 (**1**), 66.9 (**5**), 57.6 (**4**), 45.0 (**2**), 39.0 (**9 or 12**), 38.9 (**9 or 12**), 27.4 (**10, 13**), 27.1 (**6'**), 26.1 (**6**), 21.1 (**3**), 7.6 (**7 or 7'**), 7.5 (**7 or 7'**). IR (neat, cm^{-1}) 2970, 2876, 1730, 1481, 1461, 1398, 1366, 1283, 1149, 1034, 982, 770. HRMS m/z (ESI) calcd for $\text{C}_{19}\text{H}_{38}\text{NO}_4$ $[\text{M}+\text{H}]^+$ 344.2795, found 344.2798.

Authentic Sample of the Acyclic Piv-protected Azetidine Diol (**277**)**((S)-2-Ethyl-1-((S)-1-(pivaloyloxy)propan-2-yl)azetidin-2-yl)methyl pivalate**

To a solution of (2*S*,6*S*)-6-ethyl-2-methyl-4-oxa-1-azabicyclo[4.2.0]octan-5-one (**256a**, 56 mg, 0.33 mmol, 1 equiv; synthesized by Dr. C. He²²⁶) in tetrahydrofuran (1 mL) at 0 °C was added LiAlH_4 (2 M in THF, 0.25 mL, 0.50 mmol, 1.5 equiv) dropwise. The reaction was warmed to room temperature and stirred overnight. The reaction was re-cooled to 0 °C followed by addition of H_2O (25 μL), 10% aq. NaOH (25 μL) and H_2O (75 μL). The white precipitate was filtered and washed with tetrahydrofuran. The filtrate was dried over Na_2SO_4 , filtered and the solvent evaporated to give the diol intermediate as a colourless oil (38 mg, 0.22 mmol, 67% yield).

The crude diol (38 mg, 0.22 mmol, 1 equiv) was dissolved in dichloromethane (2 mL) at 0 °C and DMAP (2.7 mg, 0.022 mmol, 0.1 equiv), pivaloyl chloride (64 mg, 0.53 mmol, 2.4 equiv) and triethylamine (77 μL , 0.55 mmol, 2.5 equiv) added. The reaction was stirred at room temperature overnight, diluted with dichloromethane (10 mL) and water (5 mL) added. The organic phase was separated and the aqueous phase re-extracted with dichloromethane (2 x 10 mL). The combined organic phases were dried over MgSO_4 , filtered and the solvent evaporated. The crude material was purified by silica gel flash chromatography (5–15% ethyl acetate in hexanes) to give the title compound as a colourless oil (54 mg, 0.16 mmol, 72% yield). $[\alpha]_D^{25.0} +0.8^\circ$ (c 1.0, CHCl_3). $^1\text{H NMR}$ (400 MHz, CDCl_3) δ 4.22 – 4.13 (m, 2H, **5-H_a**, **5-H_b**), 3.99 (dd, J = 10.7, 4.1 Hz, 1H, **1-H_a**), 3.70 (dd, J = 10.7, 7.5 Hz, 1H, **1-H_b**), 3.26 – 3.12 (m, 2H, **9-H_a**, **9-H_b**), 2.96 – 2.85 (m, 1H, **2**), 1.98 – 1.86 (m, 1H, **8-H_a**), 1.77 – 1.59 (m, 3H, **6-H_a**, **6-H_b**, **8-H_b**), 1.19 (s, 9H, **1** or **o**), 1.17 (s, 9H, **12** or **15**), 0.96 (d, J = 6.3 Hz, 3H, **3**), 0.84 (app. t, J = 7.5 Hz, 3H, **7**). $^{13}\text{C NMR}$ (101 MHz, CDCl_3) δ 178.5 (**10** or **13**), 178.4 (**10** or **13**), 68.4 (**4**), 67.5 (**1**), 66.6 (**5**), 52.7 (**2**), 46.6 (**9**), 39.0 (**11** or **14**), 38.9 (**11** or **14**), 28.0 (**6**), 27.3(2) (**12** or **15**), 27.3(0) (**12** or **15**), 23.9 (**8**), 16.1 (**3**), 8.2 (**7**). IR (neat, cm^{-1}) 2970, 2874, 1730, 1481, 1461, 1398, 1367, 1282, 1151, 1035, 983, 770. HRMS m/z (ESI) calcd for $\text{C}_{19}\text{H}_{36}\text{NO}_4$ $[\text{M}+\text{H}]^+$ 342.2639, found 342.2638.

Discovery of Decarboxylative Arylation Reaction

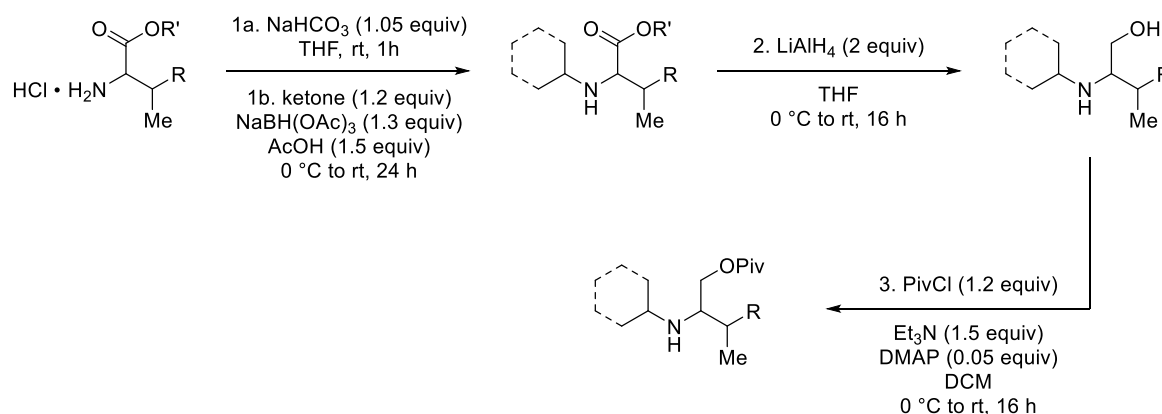
((2*S*,3*R*/*S*)-1-Cyclohexyl-3-methylazetidin-2-yl)methyl pivalate (285**)**

A solution of (*S*)-2-(cyclohexylamino)-3-methylbutyl pivalate (**283**, 81 mg, 0.3 mmol) and $\text{Pd}(\text{OAc})_2$ (101 mg, 0.45 mmol, 1.5 equiv) in chloroform (3 mL) was stirred overnight at 50°C in a sealed microwave vial under air. The reaction was cooled to room temperature and filtered through a plug of Celite. To the filtrate containing palladacycle **292** was added pyridine (50 μL , 0.6 mmol, 2 equiv) and the solution concentrated under reduced pressure to give monomeric palladacycle **293**. Analysis by ^1H NMR indicated quantitative formation to **293** as a 1:1 mixture of diastereomers.

Crude **293** was transferred in 1,2-dichloroethane (4 mL) to a microwave vial containing 3-oxo-1- λ^3 -benzo[d][1,2]iodaoxol-1(3H)-yl 4-methyl-benzenesulfonate (**249**, 376 mg, 0.9 mmol, 3 equiv) and AgOAc (150 mg, 0.9 mmol, 3 equiv). The vial was sealed and the reaction stirred at 60°C overnight. The reaction was cooled to room temperature and filtered through a plug of Celite. The filtrate was diluted with dichloromethane (20 mL) and washed with sat. aq. NaHCO_3 (10 mL). The organic phase was separated, dried over MgSO_4 , filtered and the solvent evaporated. The yield of the azetidine **285** was determined as 55% from analysis of the ^1H NMR spectrum. In addition, analysis of the crude mixture by GC-MS and LC-MS analysis indicated the formation of mono- and di-arylation products (**294** and **295**; characterization provided previously in the Experimental section). The crude residue was purified by silica gel flash chromatography (10–60% ethyl acetate in hexanes) to afford the azetidine product as a pale yellow oil (**285**, 18 mg, 0.067 mmol, 22% yield, 1:1 mixture of diastereomers). ^1H NMR (400

MHz, CDCl₃) δ 4.30 – 4.11 (m, 3H, **6-H_a**, **6*-H_{a,b}**), 4.05 (dd, J = 11.1, 7.2 Hz, 1H, **6-H_b**), 3.61 (app. t, J = 7.1 Hz, 1H, **12-H_a**), 3.45 – 3.34 (m, 1H, **5***), 3.11 – 3.02 (m, 2H, **12*-H_{a,b}**), 2.99 – 2.91 (m, 1H, **5**), 2.56 – 2.41 (m, 2H, **10***, **12-H_b**), 2.29 (app. septet, J = 7.3 Hz, 1H, **10**), 2.16 – 2.01 (m, 2H, **4**, **4***), 1.93 – 1.82 (m, 2H, **3-H_a**, **3*-H_a**), 1.80 – 1.66 (m, 6H, **2-H_a**, **2*-H_a**, **2'-H_a**, **2''-H_a**, **3'-H_a**, **3''-H_a**), 1.65 – 1.55 (m, 2H, **1-H_a**, **1*-H_a**), 1.36 – 0.90 (m, 34H, **1-H_b**, **1*-H_b**, **2-H_b**, **2*-H_b**, **2'-H_b**, **2''-H_b**, **3-H_b**, **3*-H_b**, **3'-H_b**, **3''-H_b**, **9**, **9***, **11**, **11***). ¹³C NMR (101 MHz, CDCl₃) δ 178.3(2) (**7/7***), 178.2(8) (**7/7***), 69.9 (**5**), 68.5 (**6**), 66.6 (**4/4***), 66.2 (**4/4***), 64.2 (**6***), 63.2 (**5***), 57.8 (**12**), 56.7 (**12***), 38.8 (**8/8***), 38.7 (**8/8***), 31.1 (**3/3***), 31.0 (**3/3***), 30.3 (**10**), 29.8 (**3'/3''***), 29.7 (**3'/3''***), 27.2(3) (**9/9***), 27.1(6) (**9/9***), 25.9 (two signals overlapping, **1**, **1***), 25.6 (**10***), 24.6(3) (**2/2***), 24.6(2) (**2/2***), 24.5(7) (**2'/2''***), 24.5(2) (**2'/2''***), 18.9 (**11**), 14.8 (**11***). **IR** (neat, cm⁻¹) 2927, 2854, 1729, 1480, 1368, 1280, 1147, 1033. **HRMS** m/z (ESI) calcd for C₁₆H₃₀N₁O₂ [M+H]⁺ 268.2277, found 268.2265.

Synthesis of Acyclic Piv-protected Amino Alcohol Substrates



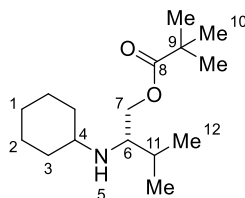
General Procedure D. To a suspension of hydrochloride salt of the 1° amine alkyl ester (1 equiv) in THF (0.3 M) was added NaHCO₃ (1.05 equiv) at room temperature and the reaction stirred for 1 h. The reaction was cooled to 0 °C followed by the addition of ketone (1.2 equiv), NaBH(OAc)₃ (1.3 equiv) and AcOH (1.5 equiv). The reaction was stirred for 24 h at room temperature before quenching with 10% aq. NaOH (2 mL per mmol amino ester). After stirring for 0.5 h, DCM (10 mL per mmol amino ester) was added. The organic phase was separated and the aqueous re-extracted with DCM. The combined organics were washed with brine (2 mL per mmol amino ester), separated, dried over MgSO₄, filtered and the solvent removed *in vacuo*. The crude 2° amino ester product was used directly in the next step.

A solution of the 2° amine alkyl ester (1 equiv) in THF (0.5 M) was cooled to 0 °C and LiAlH₄ (powder, 2 equiv) added portion-wise. The reaction was stirred overnight at room

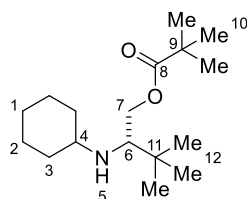
temperature. The reaction was re-cooled to 0 °C before adding water (1 mL per g LiAlH₄), 10% aq. NaOH (1 mL per g LiAlH₄), water (2 mL per g LiAlH₄) and Na₂SO₄ (20 g per g LiAlH₄). The reaction was stirred for 0.5 h at room temperature, filtered through Celite and the solvent removed *in vacuo*. The crude amino alcohol was used directly in the next step.

To a solution of amino alcohol (1 equiv) in DCM (0.5 M) at 0 °C were added DMAP (0.05 equiv), pivaloyl chloride (1.2 equiv) and triethylamine (1.5 equiv). The reaction was warmed to room temperature and stirred overnight. The reaction was diluted with DCM (5 mL per mmol amino alcohol) and water (2 mL per mmol amino alcohol) added. The organic phase was separated, dried over MgSO₄, filtered and the solvent removed *in vacuo*. The crude product was purified by silica gel flash chromatography.

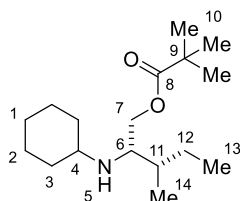
(S)-2-(Cyclohexylamino)-3-methylbutyl pivalate (283)



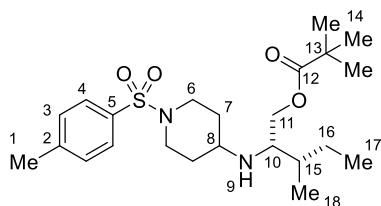
Synthesised using General Procedure D from L-valine ethyl ester hydrochloride (1.817 g, 10.0 mmol) and cyclohexanone. Purification by silica gel flash chromatography (0–20% EtOAc in hexanes) gave the title compound as a colourless oil (**283**, 2.485 g, 9.22 mmol, 92% yield over 3 steps). $[\alpha]_D^{24.2} -11.5^\circ$ (*c* 1.0, CHCl₃). ¹H NMR (400 MHz, CDCl₃) δ 4.08 (dd, *J* = 11.2, 5.2 Hz, 1H, **7-H_a**), 3.96 (dd, *J* = 11.2, 5.8 Hz, 1H, **7-H_b**), 2.64 (app. q, *J* = 5.4 Hz, 1H, **6**), 2.46 (tt, *J* = 10.3 Hz, 3.7 Hz, 1H, **4**), 1.91 – 1.67 (m, 5H, **2-H_a**, **2'-H_a**, **3-H_a**, **3'-H_a**, **11**), 1.63 – 1.54 (m, 1H, **1-H_a**), 1.32 – 0.74 (m, 21H, **1-H_b**, **2-H_b**, **2'-H_b**, **3-H_b**, **3'-H_b**, **5**, **10**, **12**, **12'**). ¹³C NMR (101 MHz, CDCl₃) δ 178.7 (**8**), 65.5 (**7**), 58.5 (**6**), 54.9 (**4**), 39.0 (**9**), 34.7 (**3'**), 34.2 (**3**), 30.2 (**11**), 27.4 (**10**), 26.3 (**1**), 25.3 (**2**), 25.2 (**2'**), 18.9 (**12**), 18.7 (**12'**). IR (film, cm⁻¹) 2956, 2928, 2853, 1730, 1480, 1365, 1283, 1154, 1111, 1034. HRMS *m/z* (ESI) calcd for C₁₆H₃₂N₁O₂ [M+H]⁺ 270.2428, found 270.2427.

(S)-2-(Cyclohexylamino)-3,3-dimethylbutyl pivalate (284)

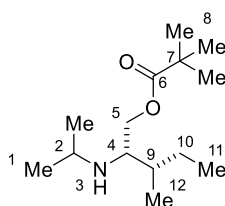
Synthesised using General Procedure D from *L-tert*-leucine methyl ester hydrochloride (5.45 g, 30.0 mmol) and cyclohexanone. Purification by silica gel flash chromatography (0–20% EtOAc in hexanes) gave the title compound as a colourless oil (**284**, 1.99 g, 7.0 mmol, 23% yield over 3 steps). $[\alpha]_D^{24.0} -18.5^\circ$ (*c* 1.0, CHCl₃). ¹H NMR (400 MHz, CDCl₃) δ 4.25 (dd, *J* = 11.5, 4.7 Hz, 1H, **7-H_a**), 3.95 (dd, *J* = 11.5, 5.5 Hz, 1H, **7-H_b**), 2.52 – 2.42 (m, 2H, **4, 6**), 1.93 – 1.84 (m, 1H, **3-H_a**), 1.79 – 1.66 (m, 3H, **2-H_a**, **2'-H_a**, **3'-H_a**), 1.62 – 1.54 (m, 1H, **1-H_a**), 1.32 – 0.88 (m, 23H, **1-H_b**, **2-H_b**, **2'-H_b**, **3-H_b**, **3'-H_b**, **10, 12**), 0.75 (br. s, 1H, **5**). ¹³C NMR (101 MHz, CDCl₃) δ 178.8 (**8**), 65.6 (**7**), 61.7 (**6**), 55.6 (**4**), 38.8 (**9**), 35.0 (**3'**), 34.2 (**3**), 33.7 (**11**), 27.3 (**10**), 27.2 (**12**), 26.2 (**1**), 25.3 (**2**), 24.9 (**2'**). IR (neat, cm⁻¹) 2956, 2927, 2855, 1729, 1479, 1364, 1284, 1154. HRMS *m/z* (ESI) calcd for C₁₇H₃₄N₁O₂ [M+H]⁺ 284.2584, found 284.2580.

(2S,3S)-2-(Cyclohexylamino)-3-methylpentyl pivalate (297)

Synthesised using General Procedure D from *L*-isoleucine methyl ester hydrochloride (3.633 g, 20.0 mmol) and cyclohexanone. Purification by silica gel flash chromatography (0–20% Et₂O in dichloromethane) gave the title compound as a colourless oil (**297**, 3.381 g, 11.9 mmol, 60% yield over 3 steps). $[\alpha]_D^{24.2} -1.7^\circ$ (*c* 1.0, CHCl₃). ¹H NMR (400 MHz, CDCl₃) δ 4.12 (dd, *J* = 11.2, 4.7 Hz, 1H, **7-H_a**), 3.91 (dd, *J* = 11.2, 6.2 Hz, 1H, **7-H_b**), 2.78 – 2.70 (m, 1H, **6**), 2.45 (tt, *J* = 10.3, 3.7 Hz, 1H, **4**), 1.90 – 1.75 (m, 2H, **3-H_a**, **3'-H_a**), 1.74 – 1.65 (m, 2H, **2-H_a**, **2'-H_a**), 1.62 – 1.44 (m, 3H, **1-H_a**, **11, 12-H_a**), 1.31 – 0.95 (m, 16H, **1-H_b**, **2-H_b**, **2'-H_b**, **3-H_b**, **3'-H_b**, **5, 10, 12-H_b**), 0.94 – 0.85 (m, 6H, **13, 14**). ¹³C NMR (101 MHz, CDCl₃) δ 178.7 (**8**), 65.2 (**7**), 57.1 (**6**), 54.5 (**4**), 39.0 (**9**), 37.3 (**11**), 34.5 (**3'**), 34.3 (**3**), 27.4 (**10**), 26.3 (**1**), 26.0 (**12**), 25.3 (**2**), 25.2 (**2'**), 15.0 (**14**), 12.2 (**13**). IR (film, cm⁻¹) 2961, 2927, 2854, 1730, 1480, 1460, 1365, 1283, 1154. HRMS *m/z* (ESI) calcd for C₁₇H₃₄N₁O₂ [M+H]⁺ 284.2584, found 284.2583.

(2S,3S)-3-Methyl-2-((1-tosylpiperidin-4-yl)amino)pentyl pivalate (329f)

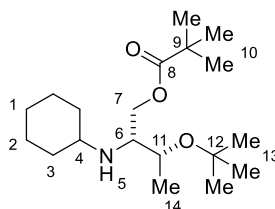
Synthesised using General Procedure D from L-isoleucine methyl ester hydrochloride (1.11 g, 6.09 mmol) and 1-tosylpiperidin-4-one. Purification by silica gel flash chromatography (10–30% EtOAc in hexanes) gave the title compound as a colourless solid (**329f**, 704 mg, 1.60 mmol, 26% yield over 3 steps). **M.p.** 65–69 °C. $[\alpha]_D^{24.2}$ -1.1° (*c* 1.0, CHCl₃). **¹H NMR** (400 MHz, CDCl₃) δ 7.63 (d, *J* = 8.1 Hz, 2H, **4**), 7.31 (d, *J* = 8.1 Hz, 2H, **3**), 4.06 (dd, *J* = 11.2, 4.6 Hz, 1H, **11-H_a**), 3.86 (dd, *J* = 11.2, 6.1 Hz, 1H, **11-H_b**), 3.65 – 3.55 (m, 2H, **6-H_a**, **6'-H_a**), 2.67 – 2.61 (m, 1H, **10**), 2.53 – 2.39 (m, 6H, **1**, **6-H_b**, **6'-H_b**, **8**), 1.92 – 1.80 (m, 2H, **7-H_a**, **7'-H_a**), 1.52 – 1.34 (m, 4H, **7-H_b**, **7'-H_b**, **15**, **16-H_a**), 1.21 – 1.04 (m, 10H, **9**, **14**, **16-H_b**), 0.91 – 0.63 (m, 7H, **9**, **17**, **18**). **¹³C NMR** (101 MHz, CDCl₃) δ 178.7 (**12**), 143.6 (**2**), 133.3 (**5**), 129.7 (**3**), 127.9 (**4**), 64.4 (**11**), 57.1 (**10**), 51.2 (**8**), 45.1 (**6**), 45.0 (**6'**), 38.9 (**13**), 37.0 (**15**), 32.6 (**7**), 32.3 (**7'**), 27.4 (**14**), 25.8 (**16**), 21.6 (**1**), 14.9 (**18**), 12.1 (**17**). **IR** (film, cm⁻¹) 2964, 2932, 2874, 1725, 1463, 1341, 1284, 1164, 1092, 1048, 932, 726. **HRMS** *m/z* (ESI) calcd for C₂₃H₃₉N₂O₄S₁ [M+H]⁺ 439.2625, found 439.2615.

(2S,3S)-2-(Isopropylamino)-3-methylpentyl pivalate (329h)

Synthesised using General Procedure D from L-isoleucine methyl ester hydrochloride (1.817 g, 10.0 mmol) and acetone. Purification by silica gel flash chromatography (0–20% EtOAc in hexanes) gave the title compound as a colourless oil (**329h**, 2.182 g, 8.96 mmol, 90% yield over 3 steps). $[\alpha]_D^{24.2}$ $+2.9^\circ$ (*c* 1.0, CHCl₃). **¹H NMR** (400 MHz, CDCl₃) δ 4.14 (dd, *J* = 11.3, 4.7 Hz, 1H, **5-H_a**), 3.93 (dd, *J* = 11.3, 5.9 Hz, 1H, **5-H_b**), 2.87 (septet, *J* = 6.2 Hz, 1H, **2**), 2.74 – 2.66 (m, 1H, **4**), 1.59 – 1.44 (m, 2H, **9**, **10-H_a**), 1.24 – 1.10 (m, 10H, **8**, **10-H_b**), 1.06 – 0.99 (m, 6H, **1**, **1'**), 0.95 – 0.85 (m, 6H, **11**, **12**). **¹³C NMR** (101 MHz, CDCl₃) δ 178.7 (**6**), 64.9 (**5**), 57.5 (**4**), 46.4 (**2**), 39.0 (**7**), 37.3 (**9**), 27.4 (**8**), 26.1 (**10**), 23.8 (**1**), 23.5 (**1'**), 15.0 (**12**), 12.2 (**11**). **IR**

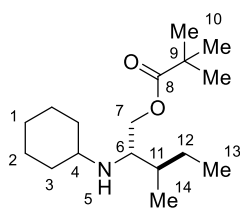
(film, cm^{-1}) 2961, 2931, 2875, 1729, 1480, 1462, 1282, 1151, 1033. **HRMS** m/z (ESI) calcd for $\text{C}_{14}\text{H}_{30}\text{N}_1\text{O}_2$ $[\text{M}+\text{H}]^+$ 244.2271, found 244.2272.

(2*R*,3*R*)-3-(*tert*-Butoxy)-2-(cyclohexylamino)butyl pivalate (329n)



Synthesised using General Procedure D from *O-tert*-butyl-L-threonine methyl ester hydrochloride (2.257 g, 10.0 mmol) and cyclohexanone. Purification by silica gel flash chromatography (10–20% EtOAc in hexanes) gave the title compound as a colourless oil (**329n**, 2.880 g, 8.79 mmol, 88% yield over 3 steps). $[\alpha]_D^{24.2} -9.6^\circ$ (c 1.0, CHCl_3). ^1H NMR (400 MHz, CDCl_3) δ 4.10 – 4.01 (m, 2H, **7-H_{a,b}**), 3.72 – 3.64 (m, 1H, **11**), 2.75 – 2.67 (m, 1H, **6**), 2.53 – 2.44 (m, 1H, **4**), 1.90 – 1.75 (m, 2H, **3-H_a**, **3'-H_a**), 1.75 – 1.66 (m, 2H, **2-H_a**, **2'-H_a**), 1.62 – 1.54 (m, 1H, **1-H_a**), 1.41 – 0.97 (m, 27H, **1-H_b**, **2-H_b**, **2'-H_b**, **3-H_b**, **3'-H_b**, **5**, **10**, **13**, **14**). ^{13}C NMR (101 MHz, CDCl_3) δ 178.6 (**8**), 73.6 (**12**), 67.4 (**11**), 64.7 (**7**), 58.4 (**6**), 55.2 (**4**), 38.9 (**9**), 34.6 (**3'**), 34.0 (**3**), 28.8 (**13**), 27.4 (**10**), 26.3 (**1**), 25.2 (**2**), 25.1 (**2'**), 19.6 (**14**). **IR** (film, cm^{-1}) 2974, 2929, 2853, 1731, 1480, 1365, 1283, 1196, 1152, 1110, 1081. **HRMS** m/z (ESI) calcd for $\text{C}_{19}\text{H}_{38}\text{N}_1\text{O}_3$ $[\text{M}+\text{H}]^+$ 328.2846, found 328.2846.

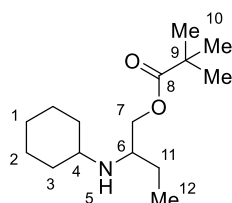
(2*S*,3*R*)-2-(Cyclohexylamino)-3-methylpentyl pivalate (329o)



Synthesised using General Procedure D from L-allo-isoleucine methyl ester hydrochloride (3.633 g, 20.0 mmol) and cyclohexanone. Purification by silica gel flash chromatography (5–20% Et_2O in dichloromethane) gave the title compound as a colourless oil (**329o**, 2.691 g, 9.49 mmol, 47% yield over 3 steps). $[\alpha]_D^{24.2} +12.1^\circ$ (c 1.0, CHCl_3). ^1H NMR (400 MHz, CDCl_3) δ 4.03 (dd, $J = 11.1, 6.0$ Hz, 1H, **7-H_a**), 3.97 (dd, $J = 11.1, 6.0$ Hz, 1H, **7-H_b**), 2.81 – 2.74 (m, 1H, **6**), 2.51 – 2.41 (m, 1H, **4**), 1.91 – 1.75 (m, 2H, **3-H_a**, **3'-H_a**), 1.75 – 1.66 (m, 2H, **2-H_a**, **2'-H_a**), 1.62 – 1.44 (m, 3H, **1-H_a**, **11**, **12-H_a**), 1.33 – 0.93 (m, 15H, **1-H_b**, **2-H_b**, **2'-H_b**, **3-H_b**, **3'-H_b**, **10**,

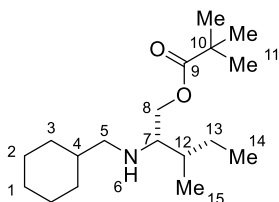
12-H_b), 0.92 – 0.86 (m, 6H, **13**, **14**). ¹³C NMR (101 MHz, CDCl₃) δ 178.7 (**8**), 65.7 (**7**), 56.8 (**6**), 55.0 (**4**), 38.9 (**9**), 36.9 (**11**), 34.8 (**3'**), 34.2 (**3**), 27.4 (**10**), 26.3 (**1**), 25.8 (**12**), 25.3 (**2**), 25.2 (**2'**), 14.8 (**14**), 12.4 (**13**). IR (film, cm⁻¹) 2963, 2927, 2854, 1730, 1480, 1460, 1366, 1282, 1153. HRMS m/z (ESI) calcd for C₁₇H₃₄N₁O₂ [M+H]⁺ 284.2584, found 284.2583.

2-(Cyclohexylamino)butyl pivalate (**331a**)



Synthesised using General Procedure D from methyl 2-aminobutanoate hydrochloride (1.536 g, 10.0 mmol) and cyclohexanone. Purification by silica gel flash chromatography (5–40% EtOAc in hexanes) gave the title compound as a colourless oil (**331a**, 1.548 g, 6.06 mmol, 61% yield over 3 steps). ¹H NMR (400 MHz, CDCl₃) δ 4.02 (dd, *J* = 11.1, 5.1 Hz, 1H, **7-H_a**), 3.94 (dd, *J* = 11.1, 5.7 Hz, 1H, **7-H_b**), 2.78 (quintet, *J* = 5.9 Hz, 1H, **6**), 2.48 (tt, *J* = 10.4, 3.8 Hz, 1H, **4**), 1.91 – 1.76 (m, 2H, **3-H_a**, **3'-H_a**), 1.75 – 1.66 (m, 2H, **2-H_a**, **2'-H_a**), 1.62 – 1.54 (m, 1H, **1-H_a**), 1.52 – 0.86 (m, 20H, **1-H_b**, **2-H_b**, **2'-H_b**, **3-H_b**, **3'-H_b**, **5**, **10**, **11-H_{a,b}**, **12**). ¹³C NMR (101 MHz, CDCl₃) δ 178.6 (**8**), 66.7 (**7**), 54.7 (**4**), 54.2 (**6**), 39.0 (**9**), 34.5 (**3**), 34.3 (**3'**), 27.4 (**10**), 26.2 (**1**), 25.6 (**11**), 25.3 (**2**), 25.2 (**2'**), 10.4 (**12**). IR (film, cm⁻¹) 2926, 2853, 1728, 1480, 1450, 1282, 1147, 1034, 770. HRMS m/z (ESI) calcd for C₁₅H₃₀N₁O₂ [M+H]⁺ 256.2271, found 256.2270.

(2*S*,3*S*)-2-((Cyclohexylmethyl)amino)-3-methylpentyl pivalate (**331c**)

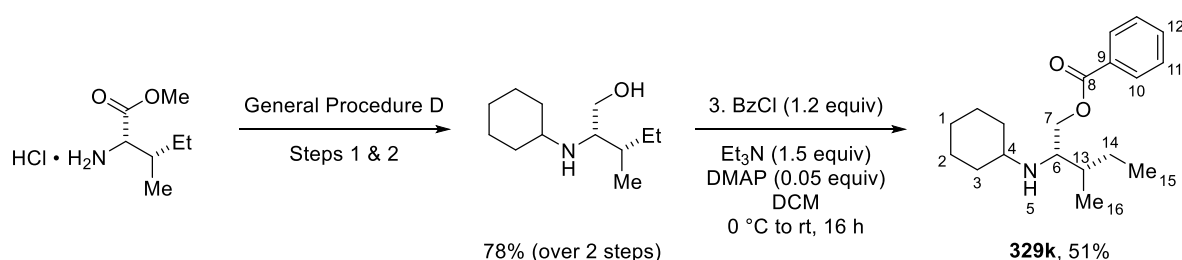


Synthesised using General Procedure D from L-isoleucine methyl ester hydrochloride (1.817 g, 10.0 mmol) and cyclohexanecarbaldehyde. Purification by silica gel flash chromatography (0–20% Et₂O in dichloromethane) gave the title compound as a colourless oil (**331c**, 1.049 g, 3.53 mmol, 35% yield over 3 steps). [α]_D^{24.2} +9.7° (*c* 1.0, CHCl₃). ¹H NMR (400 MHz, CDCl₃) δ 4.19 (dd, *J* = 11.2, 4.2 Hz, 1H, **8-H_a**), 3.95 (dd, *J* = 11.2, 6.7 Hz, 1H, **8-H_b**), 2.65 – 2.59 (m, 1H,

7), 2.50 – 2.39 (m, 2H, **5**), 1.82 – 1.63 (m, 5H, **1-H_a**, **2-H_a**, **2'-H_a**, **3-H_a**, **3'-H_a**), 1.63 – 1.35 (m, 3H, **4**, **12**, **13-H_a**), 1.33 – 1.08 (m, 14H, **1-H_b**, **2-H_b**, **2'-H_b**, **6**, **11**, **13-H_b**), 0.98 – 0.85 (m, 8H, **3-H_b**, **3'-H_b**, **14**, **15**). ¹³C NMR (101 MHz, CDCl₃) δ 178.6 (**9**), 64.6 (**8**), 60.5 (**7**), 54.7 (**5**), 38.8 (**10**), 38.4 (**4**), 36.4 (**12**), 31.5(3) (**3'**), 31.4(9) (**3**), 27.2 (**11**), 26.7 (**1**), 26.1 (**2/2'**), 14.7 (**15**), 12.0 (**14**). IR (film, cm⁻¹) 2965, 2923, 2852, 1731, 1480, 1283, 1154, 1033. HRMS m/z (ESI) calcd for C₁₈H₃₆N₁O₂ [M+H]⁺ 298.2741, found 298.2740.

Miscellaneous Amine Substrates for Pd-catalyzed Decarboxylative Arylation

(2*S*,3*S*)-2-(Cyclohexylamino)-3-methylpentyl benzoate (**329k**)

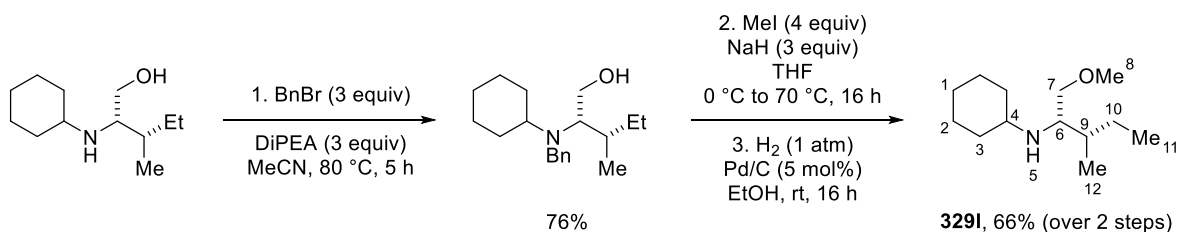


Amino alcohol (2*S*,3*S*)-2-(cyclohexyl-amino)-3-methylpentan-1-ol was synthesised using Steps 1 and 2 from General Procedure D from L-isoleucine methyl ester hydrochloride (1.817 g, 10.0 mmol) and cyclohexanone. The product was isolated as a viscous colourless oil (1.550 g, 7.78 mmol, 78% yield over 2 steps) and used directly in the next step.

To a solution of (2*S*,3*S*)-2-(cyclohexylamino)-3-methylpentan-1-ol (399 mg, 2.0 mmol, 1 equiv) in dichloromethane (10 mL) at 0 °C were added DMAP (12 mg, 0.1 mmol, 0.05 equiv), benzoyl chloride (337 mg, 2.4 mmol, 1.2 equiv) and triethylamine (0.42 mL, 3.0 mmol, 1.5 equiv). The reaction was warmed to room temperature and stirred overnight. The reaction was diluted with dichloromethane (20 mL) and water (10 mL) added. The organic phase was separated, dried over MgSO₄, filtered and the solvent removed *in vacuo*. The crude product was purified by silica gel flash chromatography (5–10% Et₂O in dichloromethane) to give the title compound as a colourless oil (**329k**, 309 mg, 1.02 mmol, 51% yield). [α]_D^{20.0} –10.8° (*c* 1.0, CHCl₃). ¹H NMR (400 MHz, CDCl₃) δ 8.03 (d, *J* = 8.0 Hz, 2H, **10**), 7.56 (app. t, *J* = 7.4 Hz, 1H, **12**), 7.44 (app. t, *J* = 7.8 Hz, 2H, **11**), 4.38 (dd, *J* = 11.2, 4.8 Hz, 1H, **7-H_a**), 4.22 (dd, *J* = 11.2, 6.1 Hz, 1H, **7-H_b**), 2.92 – 2.85 (m, 1H, **6**), 2.53 (tt, *J* = 10.3, 3.7 Hz, 1H, **4**), 1.94 – 1.79 (m, 2H, **3-H_a**, **3'-H_a**), 1.76 – 1.66 (m, 2H, **2-H_a**, **2'-H_a**), 1.65 – 1.52 (m, 3H, **1-H_a**, **13**, **14-H_a**), 1.30 – 0.99 (m, 7H, **1-H_b**, **2-H_b**, **2'-H_b**, **3-H_b**, **3'-H_b**, **5**, **14-H_b**), 0.98 – 0.91 (m, 6H, **15**, **16**). ¹³C NMR (101 MHz, CDCl₃) δ 166.8 (**8**), 133.0 (**12**), 130.5 (**9**), 129.7 (**10**), 128.5 (**11**), 65.9 (**7**), 57.4 (**6**), 54.8 (**4**), 37.5 (**13**), 34.6 (**3'**), 34.3 (**3**), 26.3 (**1**), 26.0 (**14**), 25.3 (**2**), 25.2 (**2'**), 15.2

(16), 12.2 (15). IR (film, cm^{-1}) 2928, 2854, 1720, 1451, 1272, 1113, 711. HRMS m/z (ESI) calcd for $\text{C}_{19}\text{H}_{30}\text{N}_1\text{O}_2$ $[\text{M}+\text{H}]^+$ 304.2271, found 304.2272.

***N*-((2*S*,3*S*)-1-Methoxy-3-methylpentan-2-yl)cyclohexanamine (329I)**



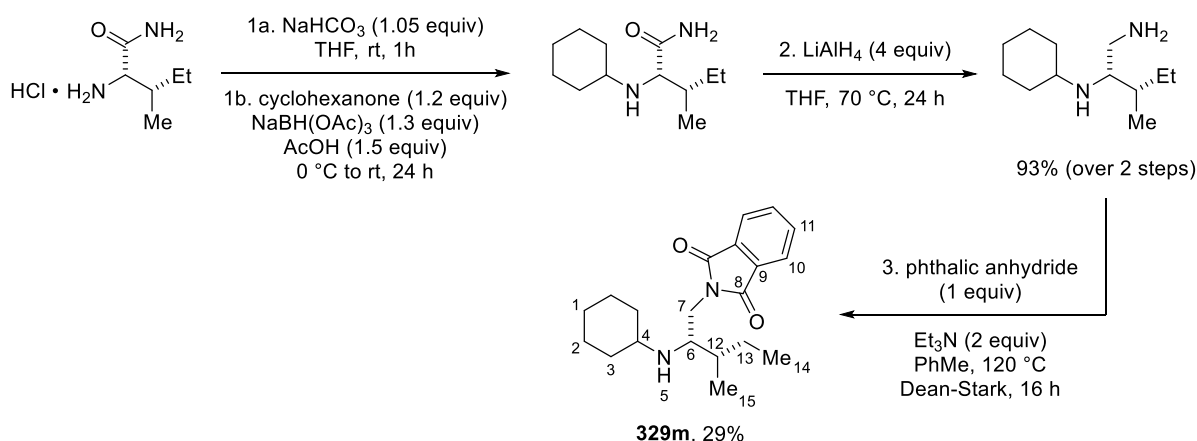
To a solution of (2*S*,3*S*)-2-(cyclohexyl-amino)-3-methylpentan-1-ol (551 mg, 2.76 mmol, 1 equiv) at room temperature were added benzyl bromide (990 μL , 8.29 mmol, 3 equiv) and Hünig's base (1.44 mL, 8.29 mmol, 3 equiv). The reaction was stirred at 80 °C for 5 h before cooling to room temperature and removing the solvent *in vacuo*. The crude material was purified by silica gel flash chromatography (5–10% EtOAc in hexanes) to give protected amino alcohol (2*S*,3*S*)-2-(benzyl(cyclohexyl)amino)-3-methylpentan-1-ol as a pale yellow oil (610 mg, 2.11 mmol, 76% yield).

A solution of (2*S*,3*S*)-2-(benzyl(cyclohexyl)amino)-3-methylpentan-1-ol (289 mg, 1.0 mmol, 1 equiv) in THF (5 mL) was added dropwise to a suspension of sodium hydride (60 wt%, 120 mg, 3.0 mmol, 3 equiv) in THF (5 mL) at 0 °C. After stirring for 0.5 h at room temperature, methyl iodide (250 μL , 4.0 mmol, 4 equiv) was added and the reaction heated at reflux overnight. The reaction was cooled to room temperature and water (10 mL) added. The reaction was diluted with Et_2O (50 mL) and the organic phase separated, dried over MgSO_4 , filtered and the solvent removed *in vacuo*.

The crude product was re-dissolved in EtOH (10 mL) under an atmosphere of nitrogen. Palladium on carbon (10 wt%, 53 mg, 0.05 mmol, 5 mol%) was added, and the atmosphere exchanged for hydrogen (1 atm, balloon). The reaction was stirred at room temperature overnight, filtered through Celite and the solvent removed *in vacuo*. The crude material was purified by silica gel flash chromatography (10–30% EtOAc in hexanes) to give the title compound as a colourless oil (**329I**, 141 mg, 0.66 mmol, 66% yield over 2 steps). $[\alpha]_D^{24.2} -1.8^\circ$ (*c* 1.0, CHCl_3). $^1\text{H NMR}$ (400 MHz, CDCl_3) δ 3.37 (dd, $J = 9.4, 4.4$ Hz, 1H, **7-H_a**), 3.31 (s, 3H, **8**), 3.24 (dd, $J = 9.4, 6.6$ Hz, 1H, **7-H_b**), 2.73 – 2.67 (m, 1H, **6**), 2.42 (tt, $J = 10.4, 3.8$ Hz, 1H, **4**), 1.91 – 1.79 (m, 2H, **3-H_a**, **3'-H_a**), 1.75 – 1.66 (m, 2H, **2-H_a**, **2'-H_a**), 1.62 – 0.95 (m, 10H, **1-H_{a,b}**, **2-H_b**, **2'-H_b**, **3-H_b**, **3'-H_b**, **5**, **9**, **10-H_{a,b}**), 0.90 (t, $J = 7.3$ Hz, 3H, **11**), 0.85 (d, $J = 6.9$ Hz,

3H, **12**). ^{13}C NMR (101 MHz, CDCl_3) δ 73.4 (**7**), 59.0 (**8**), 57.9 (**6**), 54.3 (**4**), 36.4 (**9**), 34.7 (**3'**), 34.1 (**3**), 26.3 (**1**), 26.2 (**10**), 25.5 (**2**), 25.4 (**2'**), 14.7 (**12**), 12.4 (**11**). IR (film, cm^{-1}) 2959, 2926, 2853, 1449, 1372, 1196, 1111. HRMS m/z (ESI) calcd for $\text{C}_{13}\text{H}_{28}\text{N}_1\text{O}_1$ $[\text{M}+\text{H}]^+$ 214.2165, found 214.2166.

2-((2*S*,3*S*)-2-(Cyclohexylamino)-3-methylpentyl)isoindoline-1,3-dione (**329m**)



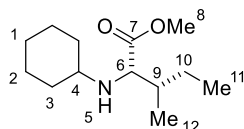
To a suspension of L-isoleucinamide hydrochloride (1.667g, 10.0 mmol, 1 equiv) in THF (50 mL) was added NaHCO_3 (882 mg, 10.05 mmol, 1.05 equiv) at room temperature and the reaction stirred for 1 h. The reaction was cooled to 0°C followed by addition of cyclohexanone (1.178 g, 12.0 mmol, 1.2 equiv), $\text{NaBH}(\text{OAc})_3$ (2.755 g, 13.0 mmol, 1.3 equiv) and AcOH (0.86 mL, 15.0 mmol, 1.5 equiv). The reaction was stirred for 24 h at room temperature before quenching with 10% aq. NaOH (30 mL). After stirring for 0.5 h, dichloromethane (200 mL) was added. The organic phase was separated, and the aqueous phase re-extracted with dichloromethane. The combined organics were washed with brine (30 mL), separated, dried over MgSO_4 , filtered and the solvent removed *in vacuo*.

The crude material was re-dissolved in tetrahydrofuran (30 mL) and cooled to 0°C . LiAlH_4 (powder, 1.518 g, 40.0 mmol, 4 equiv) was added portionwise and the reaction stirred under reflux for 24 h. The reaction was cooled to 0°C followed by addition of water (1.5 mL), 10% aq. NaOH (1.5 mL), water (3 mL) and Na_2SO_4 (30 g). The reaction was stirred for 0.5 h at room temperature, filtered through Celite and the solvent removed *in vacuo* to give (2*S*,3*S*)- N^2 -cyclohexyl-3-methylpentane-1,2-diamine as a colourless oil (1.842 g, 9.29 mmol, 93% yield over 2 steps).

A solution of (2*S*,3*S*)- N^2 -cyclohexyl-3-methylpentane-1,2-diamine (595 mg, 3.00 mmol, 1 equiv), phthalic anhydride (444 mg, 3.00 mmol, 1 equiv) and triethylamine (0.84 mL, 6.00

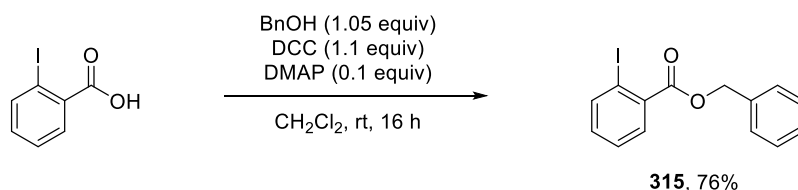
mmol, 2 equiv) in toluene (20 mL) was heated under reflux using Dean-Stark apparatus overnight. The reaction was cooled to room temperature, concentrated *in vacuo*, dichloromethane added (50 mL) and washed with 10% aq. K₂CO₃ (20 mL). The organic phase was separated and washed with brine (20 mL), dried over MgSO₄, filtered and the solvent removed *in vacuo*. The crude material was purified by silica gel flash chromatography (10–20% EtOAc in hexanes) to give the title compound as a pale yellow oil (**329m**, 283 mg, 0.86 mmol, 29% yield). $[\alpha]_D^{20.0} +39.5^\circ$ (*c* 1.0, CHCl₃). **¹H NMR** (400 MHz, CDCl₃) δ 7.87 – 7.81 (m, 2H, **10**), 7.73 – 7.68 (m, 2H, **11**), 3.66 (dd, *J* = 13.7, 5.4 Hz, 1H, **7-H_a**), 3.56 (dd, *J* = 13.7, 8.6 Hz, 1H, **7-H_b**), 2.96 – 2.89 (m, 1H, **6**), 2.35 (tt, *J* = 10.0, 3.7 Hz, 1H, **4**), 1.78 – 1.70 (m, 1H, **3-H_a**), 1.69 – 1.43 (m, 6H, **1-H_a**, **2-H_a**, **2'-H_a**, **3'-H_a**, **12**, **13-H_a**), 1.37 – 0.89 (m, 12H, **1-H_b**, **2-H_b**, **2'-H_b**, **3-H_b**, **5**, **13-H_b**, **14**, **15**), 0.85 – 0.73 (m, 1H, **3'-H_b**). **¹³C NMR** (101 MHz, CDCl₃) δ 169.0 (**8**), 134.0 (**11**), 132.3 (**9**), 123.3 (**10**), 57.4 (**6**), 55.0 (**4**), 40.1 (**7**), 37.4 (**12**), 34.5 (**3**), 34.0 (**3'**), 26.2 (**1**), 25.5 (**13**), 25.1 (**2**), 24.9 (**2'**), 14.7 (**15**), 12.5 (**14**). **IR** (film, cm⁻¹) 2927, 2852, 1773, 1712, 1434, 1397, 1062, 724. **HRMS** *m/z* (ESI) calcd for C₂₀H₂₉N₂O₂ [M+H]⁺ 329.2224, found 329.2225.

Methyl cyclohexyl-L-isoleucinate (**331b**)

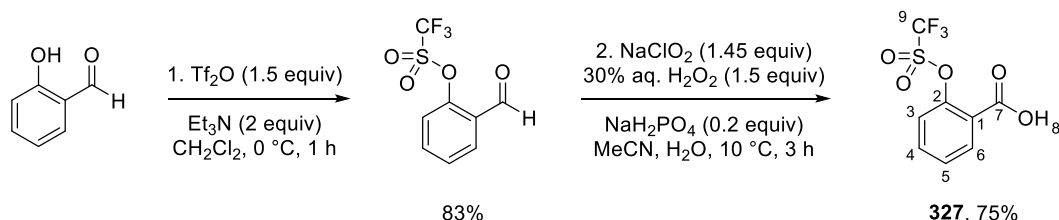


En route to substrate **297**, a portion of the intermediate formed after Step 1 of General Procedure D was purified by silica gel flash chromatography (0–10% ethyl acetate in hexanes) to provide the title compound (**331b**). $[\alpha]_D^{24.2} -22.5^\circ$ (*c* 1.0, CHCl₃). **¹H NMR** (400 MHz, CDCl₃) δ 3.72 (s, 3H, **8**), 3.20 (d, *J* = 6.1 Hz, 1H, **6**), 2.28 (tt, *J* = 10.1, 3.4 Hz, 1H, **4**), 1.90 – 1.81 (m, 1H, **3-H_a**), 1.77 – 1.48 (m, 6H, **1-H_a**, **2-H_a**, **2'-H_a**, **3'-H_a**, **5**, **9**), 1.33 – 1.09 (m, 6H, **1-H_b**, **2-H_b**, **2'-H_b**, **3'-H_b**, **10-H_{a,b}**), 1.08 – 0.96 (m, 1H, **3-H_b**), 0.93 – 0.85 (m, 6H, **11**, **12**). **¹³C NMR** (101 MHz, CDCl₃) δ 176.4 (**7**), 63.0 (**6**), 55.5 (**4**), 51.3 (**8**), 38.6 (**9**), 34.3 (**3'**), 32.8 (**3**), 26.1 (**1**), 25.7 (**10**), 25.0 (**2**), 24.6 (**2'**), 15.5 (**12**), 11.4 (**11**). **IR** (film, cm⁻¹) 2926, 2854, 1736, 1450, 1193, 1172, 1150. **HRMS** *m/z* (ESI) calcd for C₁₃H₂₆N₁O₂ [M+H]⁺ 228.1958, found 228.1958.

Synthesis of Aryl Halide or Triflate Reagents

Benzyl 2-iodobenzoate (**315**)

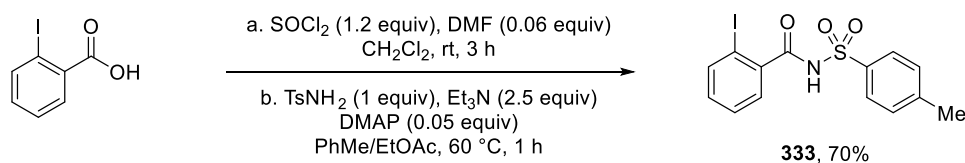
To a solution of 2-iodobenzoic acid (12.40 g, 50.0 mmol, 1 equiv) in dichloromethane (30 mL) at room temperature were added benzyl alcohol (5.68 g, 52.5 mmol, 1.05 equiv), DCC (11.35 g, 55.0 mmol, 1.1 equiv) and DMAP (611 mg, 5.0 mmol, 0.1 equiv). The reaction was stirred at room temperature overnight before filtering through a pad of Celite and removing the solvent *in vacuo*. The crude material was purified by silica gel flash chromatography (5–10% EtOAc in hexanes) to give the title compound as a colourless oil (**315**, 12.84 g, 38.0 mmol, 76% yield). ¹H NMR (400 MHz, CDCl₃) δ 7.99 (dd, J = 8.0, 0.7 Hz, 1H), 7.82 (dd, J = 7.8, 1.6 Hz, 1H), 7.50 – 7.45 (m, 2H), 7.43 – 7.32 (m, 4H), 7.15 (td, J = 7.7, 1.6 Hz, 1H), 5.38 (s, 2H). ¹³C NMR (101 MHz, CDCl₃) δ 166.4, 141.5, 135.6, 135.1, 132.8, 131.2, 128.8, 128.7, 128.6, 128.0, 94.3, 67.5. Spectral data were in accordance with the literature.²⁷⁸

2-(((Trifluoromethyl)sulfonyl)oxy)benzoic acid (**327**)

To a solution of salicylaldehyde (1.221 g, 10 mmol, 1 equiv) and triethylamine (2.8 mL, 20 mmol, 2 equiv) in dichloromethane (60 mL) at 0 °C was added triflic anhydride (2.5 mL, 15 mmol, 1.5 equiv) in dichloromethane (10 mL) dropwise. After stirring at 0 °C for 1 h, the reaction was diluted with DCM (300 mL) and washed with 1 M aq. HCl, sat. aq. NaHCO₃ and brine (100 mL each). The organic phase was dried over MgSO₄, filtered and the solvent removed *in vacuo*. Purification by silica gel flash chromatography (10% EtOAc in hexanes) gave 2-formylphenyl trifluoromethanesulfonate as a pale yellow oil (2.106 g, 8.29 mmol, 83% yield).

To a solution of 2-formylphenyl trifluoromethanesulfonate (755 mg, 2.97 mmol, 1 equiv), NaH₂PO₄ (71 mg, 0.59 mmol, 0.2 equiv) and 30% aq. H₂O₂ (505 μ L, 4.46 mmol, 1.5 equiv) in MeCN (30 mL) / water (3 mL) at 10 °C was added NaClO₂ (390 mg, 4.31 mmol, 1.45 equiv) in water (3 mL). The reaction was stirred at 10 °C for 3 h before adding sat. aq. NaHSO₃ (20 mL). The resulting mixture was poured into water (100 mL), extracted with ethyl acetate (300 mL) and the organic phase dried over MgSO₄, filtered and the solvent removed *in vacuo*. Purification by silica gel flash chromatography (10–50% ethyl acetate in hexanes, plus drops of AcOH) gave the title compound as a colourless solid (**327**, 600 mg, 2.22 mmol, 75% yield). **M.p.** 114–116 °C. **¹H NMR** (400 MHz, CDCl₃) δ 10.00 (br. s, 1H, **8**), 8.21 (dd, *J* = 7.8, 1.8 Hz, 1H, **6**), 7.70 (app. td, *J* = 8.0, 1.8 Hz, 1H, **5**), 7.53 (app. td, *J* = 7.8, 1.1 Hz, 1H, **4**), 7.38 (d, *J* = 8.2 Hz, 1H, **3**). **¹³C NMR** (101 MHz, CDCl₃) δ 168.8 (**7**), 149.0 (**2**), 135.4 (**4**), 133.5 (**6**), 128.7 (**5**), 123.2(9) (**3**), 123.2(5) (**1**), 118.9 (q, ¹*J*_{CF} = 321 Hz, **9**). **¹⁹F NMR** (376 MHz, CDCl₃) δ –73.2. **IR** (neat, cm^{–1}) 3028, 2871, 1700, 1609, 1492, 1415, 1283, 1269, 1201, 1134, 1076, 884, 799, 768. **HRMS** *m/z* (ESI) calcd for C₈H₄F₃O₅S₁ [M–H][–] 268.9737, found 268.9738.

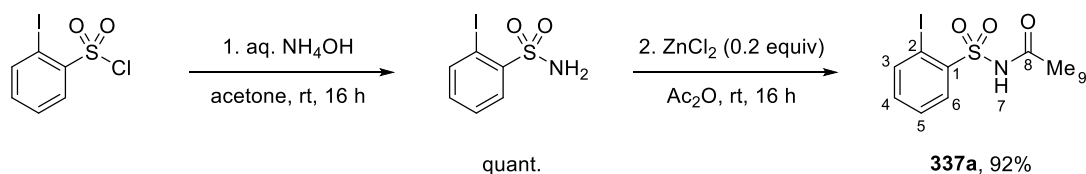
2-Iodo-*N*-tosylbenzamide (**333**)



To a solution of 2-iodobenzoic acid (4.960, 20.0 mmol, 1 equiv) in dichloromethane (100 mL) at 0 °C were added thionyl chloride (1.75 mL, 24.0 mmol, 1.2 equiv) and DMF (93 μ L, 1.2 mmol, 0.06 equiv). After stirring for 3 h at room temperature, the solvent was removed *in vacuo* and the residue dissolved in toluene (15 mL) and ethyl acetate (40 mL). *p*-Toluenesulfonamide (3.424 g, 20.0 mmol, 1 equiv), triethylamine (7.0 mL, 50 mmol, 2.5 equiv) and DMAP (122 mg, 1.0 mmol, 0.05 mmol) were added and the reaction was heated to 60 °C for 1 h. After cooling to room temperature, the reaction was quenched with 1 M aq. HCl (25 mL). The organic phase was separated and the aqueous phase extracted with EtOAc (2 x 100 mL). The combined organics were dried over MgSO₄, filtered and the solvent evaporated. The crude material was purified by silica gel flash chromatography (20–50% ethyl acetate in hexanes) to give the title compound as a viscous yellow oil (**333**, 5.656 g, 14.1 mmol, 70% yield). **¹H NMR** (400 MHz, CDCl₃) δ 8.63 (br. s, 1H), 8.05 (d, *J* = 8.4 Hz, 2H), 7.84 (d, *J* = 8.0 Hz, 1H), 7.45 – 7.35 (m, 4H), 7.17 – 7.12 (m, 1H), 2.47 (s, 3H). **¹³C NMR** (126 MHz, CDCl₃) δ 165.9, 145.5, 140.4,

138.7, 135.2, 132.6, 129.7, 129.0, 128.9, 128.4, 91.7, 21.9. Spectral data were in accordance with the literature.²⁷⁹

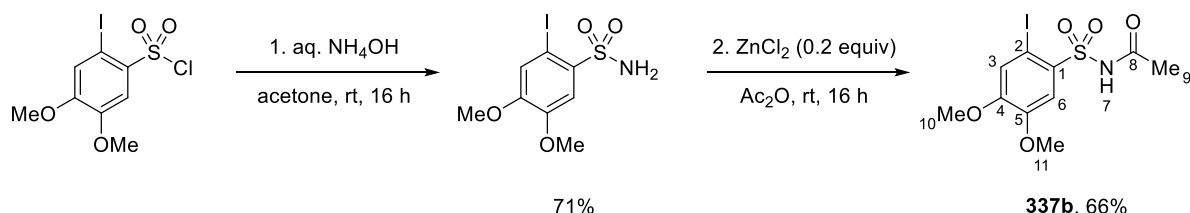
N-((2-Iodophenyl)sulfonyl)acetamide (**337a**)



2-Iodobenzenesulfonyl chloride (1.00 g, 3.31 mmol, 1 equiv) in acetone (5 mL) and aqueous ammonia (35% solution, 15 mL) were stirred at room temperature overnight. The volume of solvent was reduced by half *in vacuo* and the precipitate filtered. The solid material was washed with water and dried in a vacuum desiccator to give 2-iodobenzenesulfonamide as a colourless crystalline solid (937 mg, 3.31 mmol, quantitative yield).

2-Iodobenzenesulfonamide (937 mg, 3.31 mmol, 1 equiv) in acetic anhydride (4 mL) with added zinc chloride (90 mg, 0.66 mmol, 0.2 equiv) was stirred at room temperature overnight. The reaction was diluted with ethyl acetate (100 mL) and water (50 mL) added. The organic phase was separated, dried over MgSO_4 , filtered and the solvent evaporated. The material was triturated in dichloromethane then Et_2O to give the title compound as a colourless solid powder (**337a**, 992 mg, 3.05 mmol, 92% yield). **M.p.** 191–195 °C. **^1H NMR** (400 MHz, DMSO-d_6) δ 12.45 (s, 1H, **7**), 8.17 – 8.10 (m, 2H, **3**, **6**), 7.63 (td, $J = 7.6, 1.1$ Hz, 1H, **5**), 7.36 (td, $J = 7.6, 1.5$ Hz, 1H, **4**), 1.98 (s, 3H, **9**). **^{13}C NMR** (101 MHz, DMSO-d_6) δ 169.0 (**8**), 142.8 (**3**), 141.6 (**1**), 134.9 (**4**), 132.4 (**6**), 128.9 (**5**), 93.6 (**2**), 23.5 (**9**). **IR** (neat, cm^{-1}) 3231, 3058, 1721, 1421, 1334, 1219, 1153, 1017, 947, 864. **HRMS** m/z (ESI) calcd for $\text{C}_8\text{H}_9\text{I}_1\text{N}_1\text{O}_3\text{S}_1$ $[\text{M}+\text{H}]^+$ 325.9348, found 325.9340.

N-((2-Iodo-4,5-dimethoxyphenyl)sulfonyl)acetamide (**337b**)

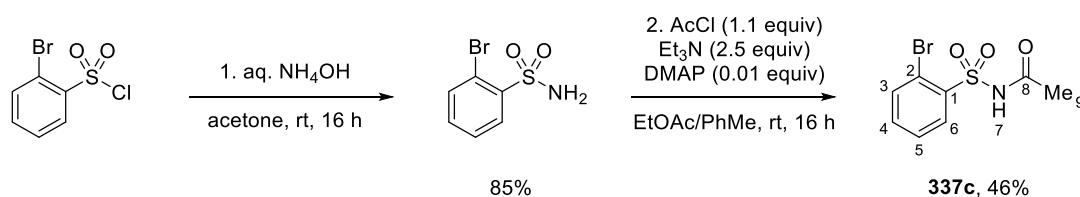


2-Iodo-4,5-dimethoxybenzenesulfonyl chloride (662 mg, 1.83 mmol, 1 equiv) in acetone (5 mL) and aqueous ammonia (35% solution, 10 mL) were stirred at room temperature overnight.

The volume of solvent was reduced by half *in vacuo* and the precipitate filtered. The solid material was washed with water and dried in a vacuum desiccator to give 2-iodo-4,5-dimethoxybenzenesulfonamide as a colourless solid powder (445 mg, 1.30 mmol, 71% yield).

2-Iodo-4,5-dimethoxybenzenesulfonamide (445 mg, 1.30 mmol, 1 equiv) in acetic anhydride (1.5 mL) with added zinc chloride (35 mg, 0.26 mmol, 0.2 equiv) was stirred at room temperature overnight. The reaction was diluted with ethyl acetate (100 mL) and water (50 mL) added. The organic phase was separated, dried over MgSO_4 , filtered and the solvent evaporated. The material was triturated in dichloromethane and Et_2O to give the title compound as a colourless solid powder (**337b**, 330 mg, 0.86 mmol, 66% yield). **M.p.** 178–182 °C. ^1H NMR (400 MHz, DMSO-d_6) δ 12.32 (s, 1H, **7**), 7.59 (s, 1H, **3**), 7.54 (s, 1H, **6**), 3.87 (s, 3H, **10**), 3.81 (s, 3H, **11**), 1.96 (s, 3H, **9**). ^{13}C NMR (101 MHz, DMSO-d_6) δ 168.8 (**8**), 152.7 (**4**), 148.3 (**5**), 133.4 (**1**), 124.5 (**6**), 115.3 (**3**), 84.1 (**2**), 56.7 (**10**), 56.3 (**11**), 23.5 (**9**). **IR** (neat, cm^{-1}) 3237, 3012, 2960, 1722, 1435, 1353, 1262, 1153, 996, 841. **HRMS** m/z (ESI) calcd for $\text{C}_{10}\text{H}_{13}\text{I}_1\text{N}_1\text{O}_5\text{S}_1$ $[\text{M}+\text{H}]^+$ 385.9559, found 385.9575.

N-((2-Bromophenyl)sulfonyl)acetamide (**337c**)

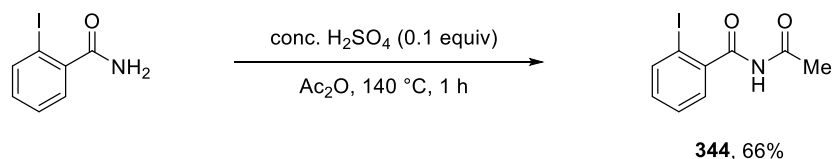


2-Bromobenzenesulfonyl chloride (5.11 g, 20.0 mmol, 1 equiv) in acetone (30 mL) and aqueous ammonia (35% solution, 100 mL) were stirred at room temperature overnight. The volume of solvent was reduced by half *in vacuo* and the precipitate filtered. The solid material was washed with water and dried in a vacuum desiccator to give 2-bromobenzenesulfonamide as a colourless crystalline solid (4.032 g, 17.1 mmol, 85% yield).

Acetyl chloride (785 μL , 11.0 mmol, 1.1 equiv) in toluene (8 mL) was added to a suspension of 2-bromobenzenesulfonamide (2.361 g, 10.0 mmol, 1 equiv), triethylamine (3.5 mL, 25.0 mmol, 2.5 equiv) and DMAP (12 mg, 0.1 mmol, 0.01 equiv) in ethyl acetate (20 mL) at 0 °C. The reaction was stirred at room temperature overnight. Water (20 mL) and ethyl acetate (100 mL) were added to the reaction and the aqueous phase separated. The aqueous phase was acidified and the product extracted with ethyl acetate (2 x 100 mL). The combined organic phases were dried over MgSO_4 , filtered and the solvent evaporated. The material was triturated in dichloromethane and to provide the title compound as a colourless solid powder (**337c**, 1.267

g, 4.56 mmol, 46% yield). **M.p.** 137–139 °C. **¹H NMR** (400 MHz, acetone-*d*₆) δ 10.99 (br. s, 7), 8.26 (dd, *J* = 7.7, 2.0 Hz, 1H, 6), 7.86 (dd, *J* = 7.5, 1.4 Hz, 1H, 3), 7.69 – 7.59 (m, 2H, 4, 5), 2.10 (s, 3H, 9). **¹³C NMR** (126 MHz, acetone-*d*₆) δ 168.7 (8), 139.5 (1), 136.1 (3), 135.7 (4), 133.9 (6), 128.7 (5), 120.3 (2), 23.4 (9). **IR** (neat, cm⁻¹) 3234, 1726, 1425, 1336, 1153, 1030, 946, 870, 750. **HRMS** *m/z* (ESI) calcd for C₈H₉BrN₁O₃S₁ [M+H]⁺ 277.9487, found 277.9492.

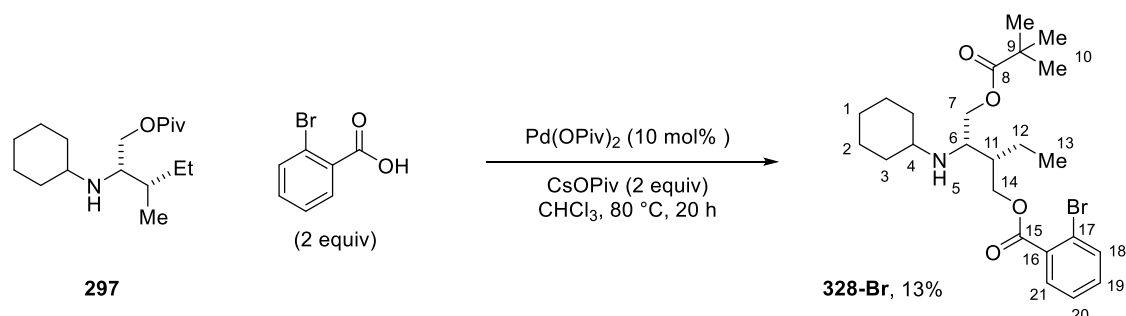
N-Acetyl-2-iodobenzamide (344)



To a solution of 2-iodobenzamide (2.470, 10.0 mmol, 1 equiv) in acetic anhydride (5 mL) was added concentrated sulfuric acid (50 μ L, 1 mmol, 0.1 equiv). The reaction was heated in a sealed tube for 1 h at 140 °C. The reaction was cooled to room temperature and sat. aq. NaHCO₃ (50 mL) and dichloromethane (100 mL) added. The organic phase was separated, dried over MgSO₄, filtered and the solvent evaporated. The crude material was purified by silica gel flash chromatography (20 – 40% ethyl acetate in hexanes) to give the title compound as an off-white solid powder (**344**, 1.899 g, 6.57 mmol, 66% yield). **¹H NMR** (400 MHz, CDCl₃) δ 8.43 (br. s, 1H), 7.94 (d, *J* = 8.0 Hz, 1H), 7.48 – 7.44 (m, 2H), 7.24 – 7.16 (m, 1H), 2.59 (s, 3H). **¹³C NMR** (126 MHz, CDCl₃) δ 172.4, 167.6, 140.3, 140.0, 132.2, 128.3, 128.2, 91.9, 25.3. Spectral data were in accordance with the literature.²⁸⁰

Pd-catalyzed Acyloxylation Reaction with 2-Bromobenzoic acid

(2*S*,3*S*)-3-(Cyclohexylamino)-2-ethyl-4-(pivaloyloxy)butyl 2-bromobenzoate (328-Br)

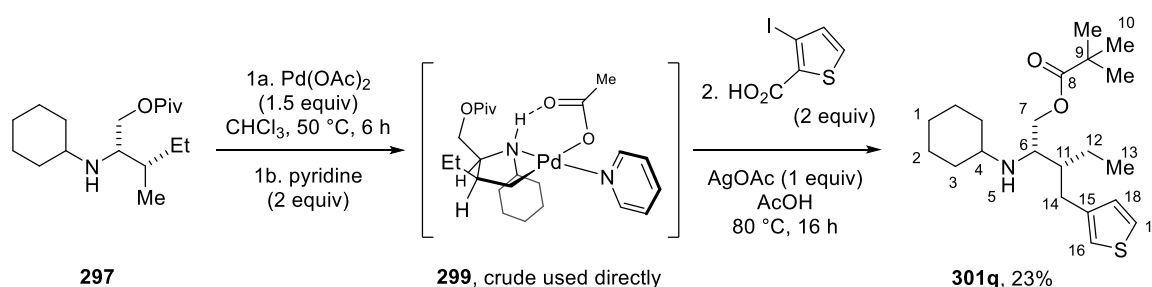


To a 2–5 mL microwave vial containing a 10 mm magnetic stirrer bar were added Pd(OPiv)₂ (6.2 mg, 0.02 mmol, 10 mol%), CsOPiv (93.6 mg, 0.4 mmol, 2 equiv) and 2-bromobenzoic acid

(80.4 mg, 0.4 mmol, 2 equiv). Under air, a solution of amine **297** (56.7 mg, 0.2 mmol, 1 equiv) in CHCl_3 (2 mL) was added via syringe and the vial sealed with a crimp cap with silicone/PTFE septum. The vial was placed in an oil bath pre-heated to 80 °C, and the reaction stirred at this temperature for 20 h. After cooling to room temperature, the reaction was filtered through a short plug of Celite and the filtrate concentrated *in vacuo*. The crude residue was purified by silica gel flash chromatography (5–10% Et_2O in toluene) to give the title compound as a colourless oil (**328-Br**, 12.5 mg, 0.026 mmol, 13% yield). $[\alpha]_D^{25.0} +2.4^\circ$ (*c* 1.0, CHCl_3). ^1H NMR (400 MHz, CDCl_3) δ 7.77 (dd, *J* = 7.6, 2.0 Hz, 1H, **21**), 7.66 (dd, *J* = 7.4, 1.3 Hz, 1H, **18**), 7.37 (td, *J* = 7.6, 1.3 Hz, 1H, **20**), 7.32 (td, *J* = 7.4, 2.0 Hz, 1H, **19**), 4.44 (dd, *J* = 11.1, 6.7 Hz, 1H, **14-H_a**), 4.37 (dd, *J* = 11.1, 4.7 Hz, 1H, **14-H_b**), 4.15 (dd, *J* = 11.3, 5.8 Hz, 1H, **7-H_a**), 4.03 (dd, *J* = 11.3, 5.8 Hz, 1H, **7-H_b**), 3.13 – 3.07 (m, 1H, **6**), 2.49 (tt, *J* = 10.1, 3.6 Hz, 1H, **4**), 1.90 – 1.64 (m, 5H, **2-H_a**, **2'-H_a**, **3-H_a**, **3'-H_a**, **11**), 1.63 – 1.51 (m, 2H, **1-H_a**, **12-H_a**), 1.47 – 0.97 (m, 19H, **1-H_b**, **2-H_b**, **2'-H_b**, **3-H_b**, **3'-H_b**, **5**, **10**, **12-H_b**, **13**). ^{13}C NMR (101 MHz, CDCl_3) δ 178.6 (**8**), 166.4 (**15**), 134.5 (**18**), 132.6(2) (**19**), 132.6(0) (**16**), 131.4 (**21**), 127.3 (**20**), 121.7 (**17**), 65.6 (**14**), 64.9 (**7**), 54.6 (**4**), 53.9 (**6**), 41.9 (**11**), 39.0 (**9**), 34.6 (**3'**), 34.1 (**3**), 27.4 (**10**), 26.2 (**1**), 25.2 (**2**), 25.0 (**2'**), 20.0 (**12**), 12.5 (**13**). IR (neat, cm^{-1}) 2964, 2927, 2854, 1729, 1479, 1287, 1248, 1152, 1030, 745. HRMS *m/z* (ESI) calcd for $\text{C}_{24}\text{H}_{37}\text{Br}_1\text{N}_1\text{O}_4$ $[\text{M}+\text{H}]^+$ 482.1900, found 482.1894.

Isolation of Thiophenyl Decarboxylative Arylation Product

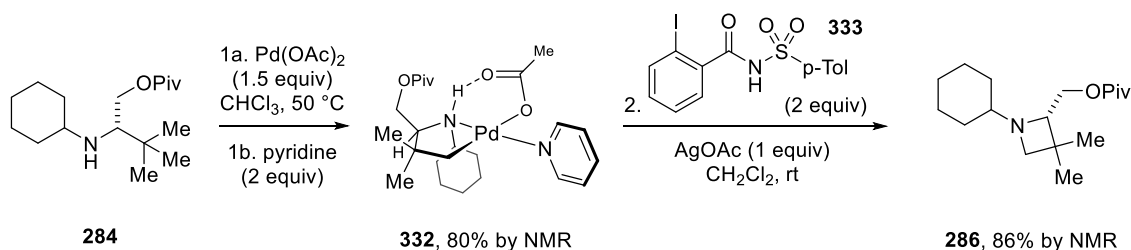
(2*S*,3*R*)-2-(Cyclohexylamino)-3-(thiophen-3-ylmethyl)pentyl pivalate (**301q**)



A solution of (2*S*,3*S*)-2-(cyclohexylamino)-3-methylpentyl pivalate (**297**, 28.3 mg, 0.10 mmol, 1 equiv) and $\text{Pd}(\text{OAc})_2$ (33.7 mg, 0.15 mmol, 1.5 equiv) in CHCl_3 (1 mL) was stirred in a sealed vial at 50 °C for 6 h. The reaction was cooled to room temperature, passed through a Celite plug and pyridine (16 μL , 0.20 mmol, 2 equiv) added. The reaction was concentrated *in vacuo* to give the crude pyridine-ligated palladacycle (**299**), which was used directly in the next step.

The crude palladacycle **299** was re-dissolved in AcOH (1 mL), followed by addition of 3-iodothiophene-2-carboxylic acid (50.8 mg, 0.20 mmol, 2 equiv) and AgOAc (16.7 mg, 0.10 mmol, 1 equiv). The reaction was stirred at 80 °C overnight, passed through a Celite plug and concentrated *in vacuo*. Dichloromethane (20 mL) was added followed by washing with sat. aq. NaHCO₃ (10 mL). The organic phase was separated, dried over MgSO₄, filtered and the solvent evaporated. Purification by silica gel flash chromatography (10% ethyl acetate in hexanes) gave title compound as a pale yellow oil (**301q**, 8.5 mg, 0.023 mmol, 23% yield). ¹H NMR (400 MHz, CDCl₃) δ 7.24 (dd, *J* = 4.7, 3.0 Hz, 1H, **17**), 6.94 – 6.89 (m, 2H, **16**, **18**), 4.09 (dd, *J* = 11.1, 6.1 Hz, 1H, **7-H_a**), 3.97 (dd, *J* = 11.1, 6.0 Hz, 1H, **7-H_b**), 2.92 (td, *J* = 5.7, 3.5 Hz, 1H, **6**), 2.83 (dd, *J* = 14.3, 6.9 Hz, 1H, **14-H_a**), 2.55 – 2.41 (m, 2H, **4**, **14-H_b**), 1.85 – 1.65 (m, 5H, **2-H_a**, **2'-H_a**, **3-H_a**, **3'-H_a**, **11**), 1.63 – 1.54 (m, 1H, **1-H_a**), 1.47 – 0.87 (m, 20H, **1-H_b**, **2-H_b**, **2'-H_b**, **3-H_b**, **3'-H_b**, **5**, **10**, **12-H_{a,b}**, **13**). ¹³C NMR (101 MHz, CDCl₃) δ 178.7 (**8**), 142.2 (**15**), 128.6 (**18**), 125.4 (**17**), 120.9 (**16**), 65.1 (**7**), 54.4 (**4**), 54.1 (**6**), 43.5 (**11**), 38.9 (**9**), 34.6 (**3'**), 34.3 (**3**), 30.7 (**14**), 27.4 (**10**), 26.3 (**1**), 25.3 (**2**), 25.1 (**2'**), 22.4 (**12**), 12.5 (**13**). IR (neat, cm⁻¹) 2958, 2926, 2852, 1727, 1479, 1282, 1152, 765. HRMS *m/z* (ESI) calcd for C₂₁H₃₆N₁O₂S₁ [M+H]⁺ 366.2467, found 366.2463.

Reaction of Palladacycle **332** with Aryl Iodide **333**

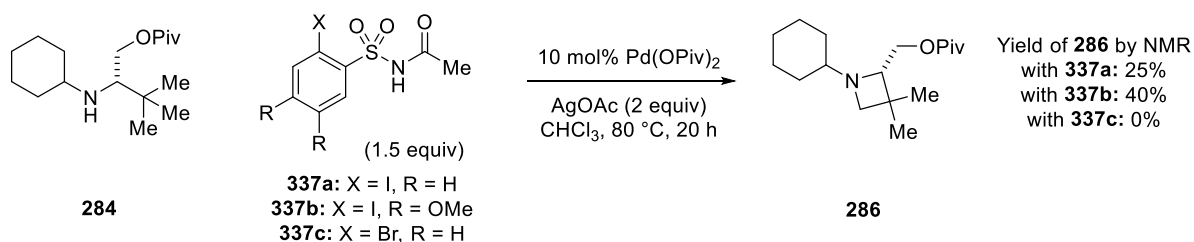


A solution of (*S*)-2-(cyclohexylamino)-3,3-dimethylbutyl pivalate (**284**, 28.3 mg, 0.10 mmol, 1 equiv) and Pd(OAc)₂ (33.7 mg, 0.15 mmol, 1.5 equiv) in CHCl₃ (1 mL) was stirred in a sealed vial at 50 °C for 6 h under air. The reaction was cooled to room temperature, passed through a Celite plug and pyridine (16 μ L, 0.20 mmol, 2 equiv) added. The solvent was removed *in vacuo*, and Et₂O (10 mL) added. The resulting suspension was filtered through Celite and the filtrate concentrated *in vacuo*. Hexane (10 mL) was added followed by filtration again through Celite. Removal of the solvent and drying under high vacuum gave palladacycle **332** (80% yield by NMR; spectral data presented in the Experimental Section).

Palladacycle **332** was re-dissolved in dichloromethane (2 mL), followed by addition of 2-iodo-*N*-tosylbenzamide (**333**, 80.2 mg, 0.20 mmol, 2 equiv) and AgOAc (16.7 mg, 0.10

mmol, 1 equiv). The reaction was stirred under air at room temperature overnight, passed through a Celite plug and concentrated *in vacuo*. Analysis of the reaction mixture by NMR indicated formation of the azetidine product (**286**, 86% yield against internal standard). Spectral data for **286** were presented previously in the Experimental Section.

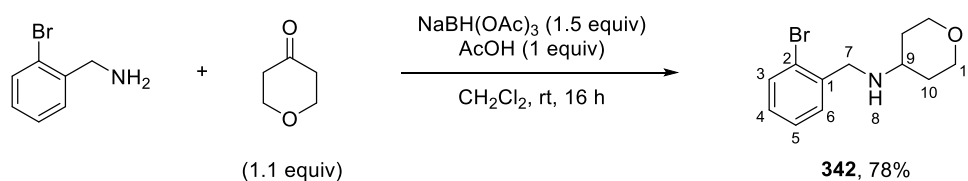
Pd-catalyzed Azetidine Formation using N-Acetylbenzenesulfonamide Reagents



To a 2–5 mL microwave vial containing a 10 mm magnetic stirrer bar were added Pd(OPiv)₂ (3.1 mg, 0.01 mmol, 10 mol%), AgOAc (33.4 mg, 0.2 mmol, 2 equiv) and aryl halide (0.15 mmol, 1.5 equiv). Under air, a solution of amine **284** (28.3 mg, 0.1 mmol, 1 equiv) in CHCl₃ (1 mL) was added via syringe and the vial sealed with a crimp cap with silicone/PTFE septum. The vial was placed in an oil bath pre-heated to 80 °C, and the reaction stirred at this temperature for 20 h. After cooling to room temperature, the reaction was filtered through a short plug of Celite and the filtrate concentrated *in vacuo*. The crude residue was analysed by ¹H NMR in CDCl₃ against an internal standard. The azetidine product (**286**; spectral data presented in Experimental Section) was observed in 25%, 40% and 0% yield using aryl halide **337a**, **337b** and **337c**, respectively.

Synthesis of Benzylamine Substrates

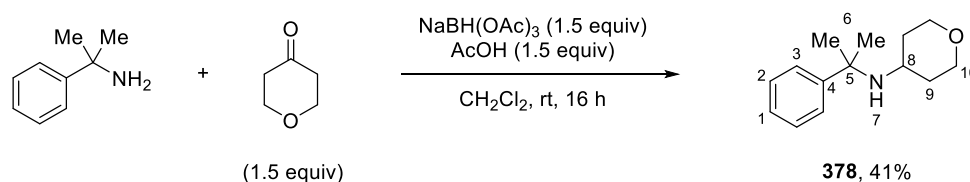
N-(2-Bromobenzyl)tetrahydro-2H-pyran-4-amine (**342**)



To a solution (2-bromophenyl)methanamine (1.861 g, 10.0 mmol, 1 equiv) in dichloromethane (30 mL) at 0 °C were added tetrahydro-4H-pyran-4-one (1.101 g, 11.0 mmol, 1.1 equiv), NaBH(OAc)₃ (3.179 g, 15.0 mmol, 1.5 equiv) and AcOH (0.57 mL, 10.0 mmol, 1 equiv). The reaction was stirred for 16 h at room temperature before quenching with 10% aq. NaOH (50

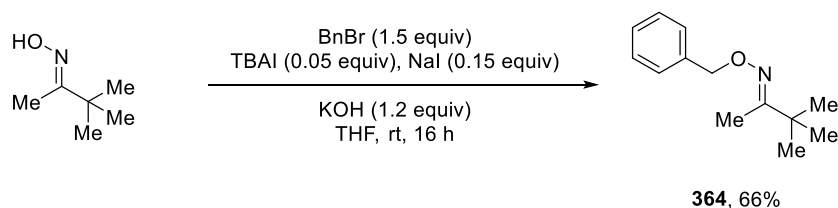
mL). After stirring for 0.5 h, dichloromethane (100 mL) was added. The organic phase was separated and the aqueous re-extracted with dichloromethane (100 mL). The combined organics were washed with brine (50 mL), separated, dried over MgSO_4 , filtered and the solvent removed *in vacuo*. The crude material was purified by silica gel flash chromatography (10–50% ethyl acetate in hexanes) to give the title compound as a pale yellow oil (**342**, 2.109 g, 7.81 mmol, 78%). ^1H NMR (400 MHz, CDCl_3) δ 7.54 (d, J = 7.8 Hz, 1H, **3**), 7.40 (d, J = 7.5 Hz, 1H, **6**), 7.28 (t, J = 7.5 Hz, 1H, **5**), 7.12 (t, J = 7.8 Hz, 1H, **4**), 4.01 – 3.94 (m, 2H, **11-H_a**), 3.89 (s, 2H, **7**), 3.40 (t, J = 11.4 Hz, 2H, **11-H_b**), 2.72 (tt, J = 10.5, 4.0 Hz, 1H, **9**), 1.91 – 1.82 (m, 2H, **10-H_a**), 1.57 – 1.41 (m, 3H, **8**, **10-H_b**). ^{13}C NMR (101 MHz, CDCl_3) δ 139.4 (**1**), 132.8 (**3**), 130.3 (**6**), 128.6 (**4**), 127.5 (**5**), 123.9 (**2**), 66.7 (**11**), 53.2 (**9**), 50.5 (**7**), 33.7 (**10**). IR (neat, cm^{-1}) 2934, 2840, 1439, 1362, 1234, 1139, 1088, 1023, 748. HRMS m/z (ESI) calcd for $\text{C}_{12}\text{H}_{17}\text{Br}_1\text{N}_1\text{O}_1$ $[\text{M}+\text{H}]^+$ 270.0494, found 270.0499.

N-(2-Phenylpropan-2-yl)tetrahydro-2H-pyran-4-amine (**378**)

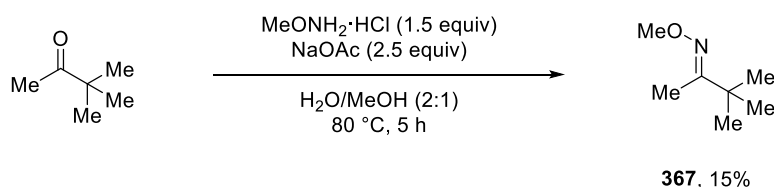


To a solution cumylamine (2.88 mL, 20.0 mmol, 1 equiv) in dichloromethane (60 mL) at 0 °C were added tetrahydro-4H-pyran-4-one (2.8 mL, 30.0 mmol, 1.5 equiv), $\text{NaBH}(\text{OAc})_3$ (6.358 g, 30.0 mmol, 1.5 equiv) and AcOH (1.8 mL, 30.0 mmol, 1.5 equiv). The reaction was stirred for 16 h at room temperature before quenching with 10% aq. NaOH (100 mL). After stirring for 0.5 h, dichloromethane (100 mL) was added. The organic phase was separated and the aqueous re-extracted with dichloromethane (200 mL). The combined organics were washed with brine (50 mL), separated, dried over MgSO_4 , filtered and the solvent removed *in vacuo*. The crude material was purified by silica gel flash chromatography (5–50% ethyl acetate in hexanes) to give the title compound as a colourless solid (**378**, 1.794 g, 8.18 mmol, 41% yield). ^1H NMR (400 MHz, CDCl_3) δ 7.49 (d, J = 7.5 Hz, 2H, **3**), 7.34 (t, J = 7.5 Hz, 2H, **2**), 7.24 (t, J = 7.5 Hz, 1H, **1**), 3.87 – 3.79 (m, 2H, **10-H_a**), 3.26 (td, J = 11.7, 2.2 Hz, 2H, **10-H_b**), 2.50 (tt, J = 10.6, 4.1 Hz, 1H, **8**), 1.63 – 1.31 (m, 11H, **6**, **7**, **9-H_{a,b}**). ^{13}C NMR (101 MHz, CDCl_3) δ 148.8 (**4**), 128.1 (**2**), 126.4 (**1**), 126.0 (**3**), 67.3 (**10**), 56.2 (**5**), 49.5 (**8**), 36.6 (**9**), 30.7 (**6**). IR (neat, cm^{-1}) 2938, 2843, 1467, 1379, 1236, 1139, 1083, 976, 771, 701. HRMS m/z (ESI) calcd for $\text{C}_{14}\text{H}_{22}\text{N}_1\text{O}_1$ $[\text{M}+\text{H}]^+$ 220.1701, found 220.1706.

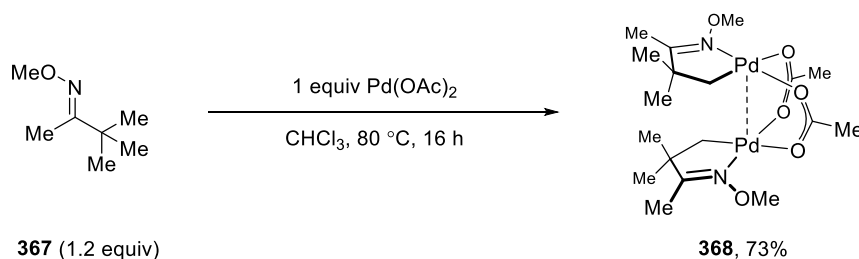
Synthesis of Oxime Substrates

(E)-3,3-Dimethylbutan-2-one O-benzyl oxime (364)

Pinacolone oxime (576 mg, 5.00 mmol, 1 equiv), benzyl bromide (0.89 mL, 7.50 mmol, 1.5 equiv), TBAI (81 mg, 0.25 mmol, 0.05 equiv), NaI (112 mg, 0.75 mmol, 0.15 equiv) and KOH (337 mg, 6.00 mmol, 1.2 equiv) in tetrahydrofuran (30 mL) were stirred at room temperature for 16 h. The reaction was concentrated *in vacuo* and ethyl acetate (100 mL) and sat. aq. NaHCO₃ added (100 mL). The organic phase was washed, separated, dried over MgSO₄, filtered and the solvent evaporated. The crude material was purified by silica gel flash chromatography (0–5% Et₂O in hexanes) to give the title compound as a colourless oil (**364**, 682 mg, 3.32 mmol, 66% yield). ¹H NMR (400 MHz, CDCl₃) δ 7.42 – 7.26 (m, 5H), 5.10 (s, 2H), 1.85 (s, 3H), 1.13 (s, 9H). ¹³C NMR (101 MHz, CDCl₃) δ 163.7, 138.6, 128.2, 128.1, 127.5, 75.3, 37.1, 27.7, 10.7. Spectral data were in accordance with the literature.²⁸¹

(E)-3,3-Dimethylbutan-2-one O-methyl oxime (367)

A solution of pinacolone (1.002 g, 10.0 mmol, 1 equiv), methoxyamine hydrochloride (1.253 g, 15.0 mmol, 1.5 equiv) and NaOAc (2.051 g, 25.0 mmol, 2.5 equiv) in water (20 mL) and methanol (10 mL) was heated at 80 °C for 5 h. After cooling to room temperature, dichloromethane (200 mL) and water (100 mL) were added. The organic phase was separated, dried over MgSO₄, filtered and the solvent removed under reduce pressure (note: oxime is volatile!) to give the title compound as a colourless oil (**367**, 200 mg, 1.55 mmol, 15% yield). ¹H NMR (400 MHz, CDCl₃) δ 3.85 (s, 3H), 1.81 (s, 3H), 1.13 (s, 9H). ¹³C NMR (101 MHz, CDCl₃) δ 163.5, 61.2, 37.1, 27.8, 10.5. Spectral data were in accordance with the literature.²⁸²

*Synthesis of Cyclopalladated Oxime Dimer***Oxime-derived palladacycle dimer **368****

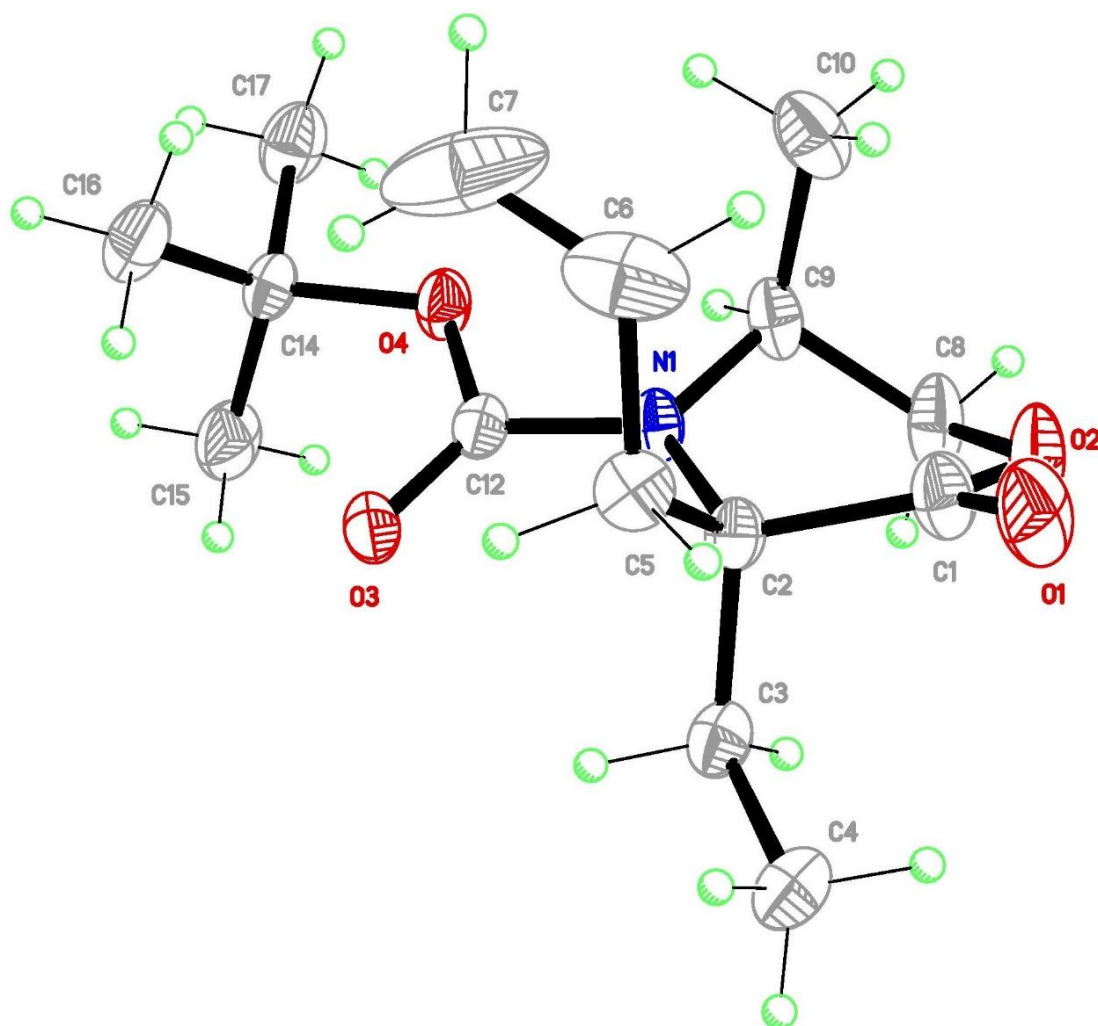
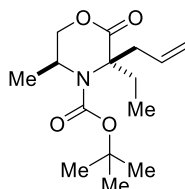
A solution of (*E*)-3,3-dimethylbutan-2-one O-methyl oxime (**367**, 77.5 mg, 0.60 mmol, 1.2 equiv) and Pd(OAc)₂ (112 mg, 0.50 mmol, 1 equiv) in chloroform (5 mL) was heated at 80 °C under air in a sealed tube for 16 h. After cooling to room temperature, the reaction was filtered through Celite and the filtrate concentrated *in vacuo*. The residue was triturated in hexanes to obtain a free-flowing brown powder (**368**, 108 mg, 0.37 mmol, 73% yield). The complex was characterized by X-ray crystallography (see Appendix II).

Appendix II: Supplementary Data

X-ray Crystallography

***tert*-Butyl (3*R*,5*S*)-3-allyl-3-ethyl-5-methyl-2-oxomorpholine-4-carboxylate (268a).**

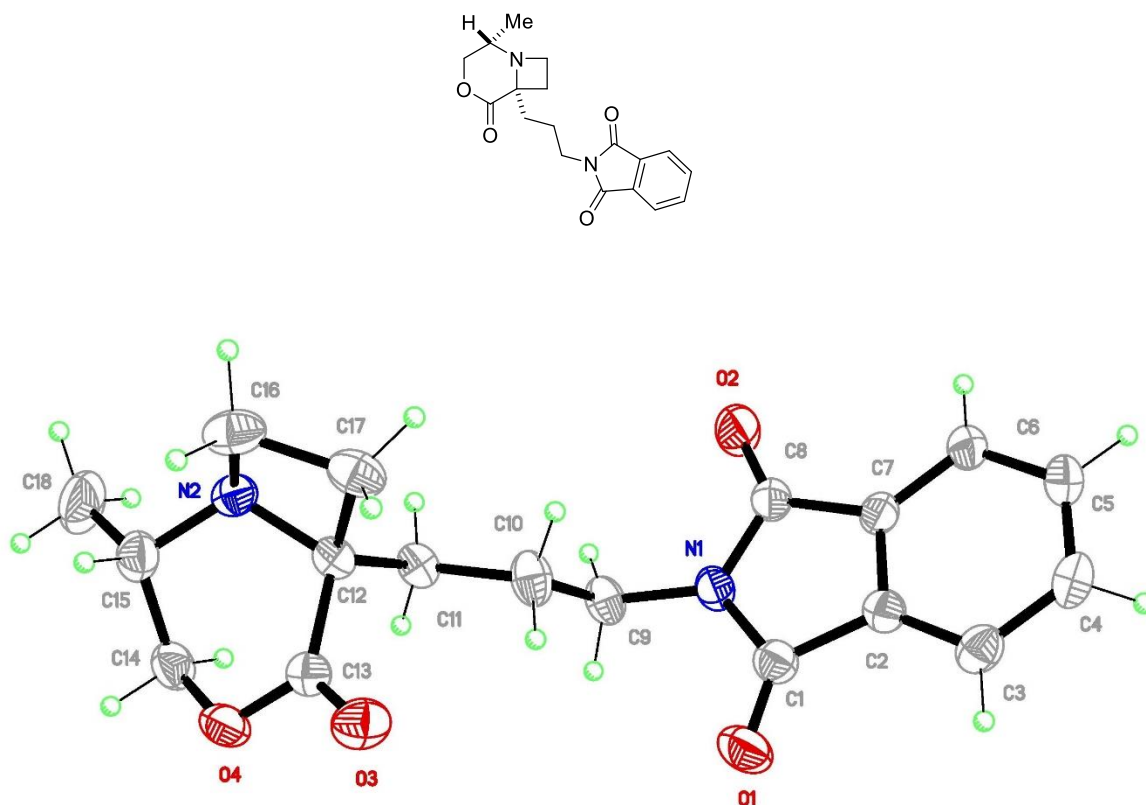
Crystals suitable for single crystal X-ray crystallography were grown by slow evaporation from a saturated solution of the title compound in ethyl acetate.



Crystal Data and Structure Refinement for 268a

Identification code	MG_K3_0045
Formula	C ₁₅ H ₂₅ N O ₄
Formula weight	283.36
Temperature	180 K
Diffractionmeter, wavelength	Nonius KappaCCD, 0.71073 Å
Crystal system, space group	Orthorhombic, P 2 ₁ c 2 ₁ b
Unit cell dimensions	a = 7.8793(3) Å α = 90° b = 9.5453(3) Å β = 90° c = 21.5608(10) Å γ = 90°
Volume, Z	1621.59(11) Å ³ , 4
Density (calculated)	1.161 Mg/m ³
Absorption coefficient	0.083 mm ⁻¹
F(000)	616
Crystal colour / morphology	Colourless blocks
Crystal size	0.28 x 0.28 x 0.20 mm ³
θ range for data collection	3.549 to 29.477°
Index ranges	-8 ≤ h ≤ 10, -11 ≤ k ≤ 12, -29 ≤ l ≤ 29
Reflns collected / unique	10109 / 3728
Reflns observed [F > 4σ(F)]	2404
Absorption correction	Multi-scan
Min. and max. transmission	0.977 and 0.984
Refinement method	Full-matrix least-squares on F ²
Data / restraints / parameters	3728 / 0 / 186
Goodness-of-fit on F ²	1.031
Final R indices [F > 4σ(F)]	R ₁ = 0.0510, wR ₂ = 0.0998
R indices (all data)	R ₁ = 0.0963, wR ₂ = 0.1160
Largest diff. peak, hole	0.138, -0.172 eÅ ⁻³
Mean and maximum shift/error	0.000 and 0.000

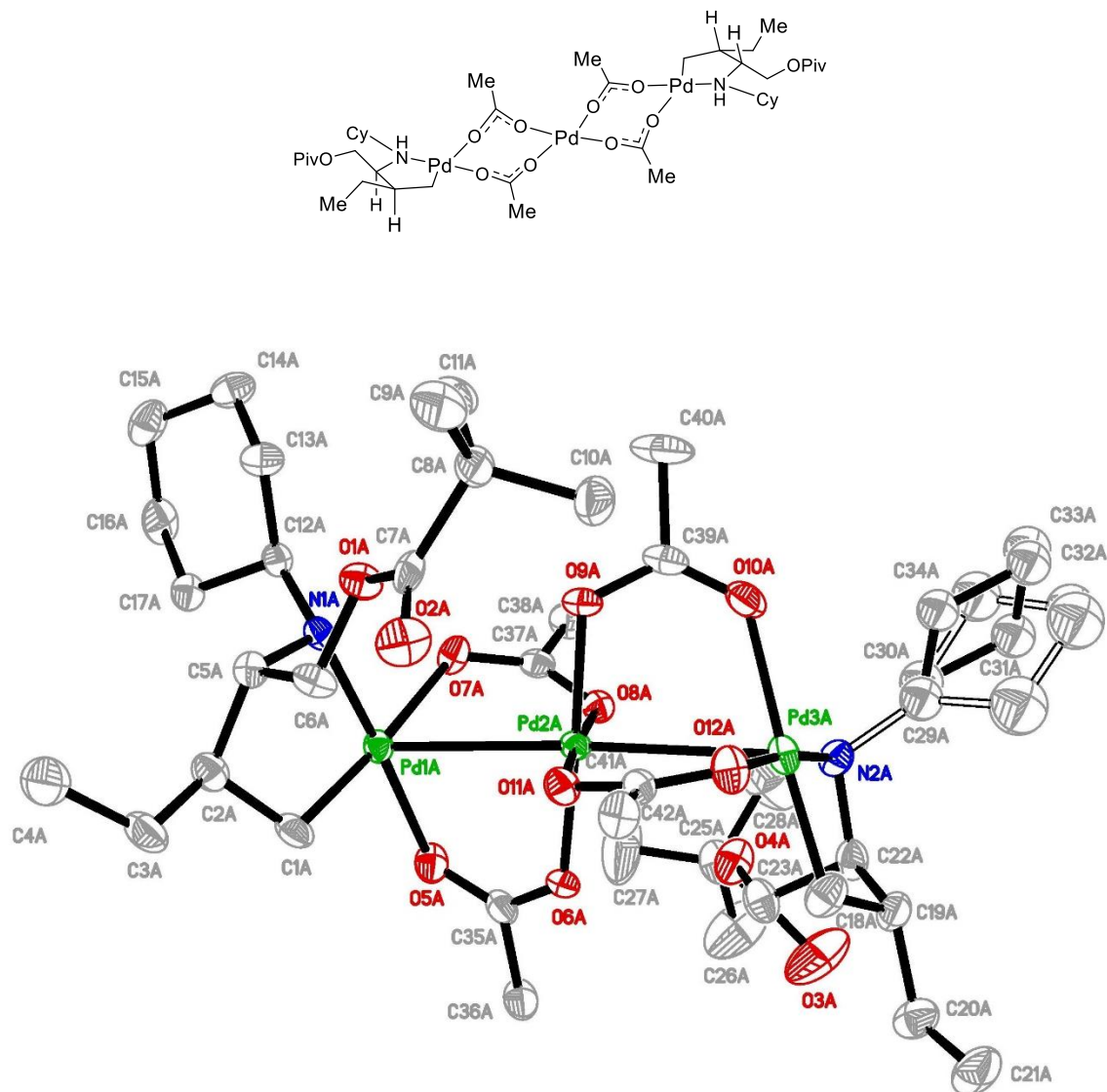
2-(3-((2*S*,6*S*)-2-Methyl-5-oxo-4-oxa-1-azabicyclo[4.2.0]octan-6-yl)propyl)isoindoline-1,3-dione (273f). Crystals suitable for single crystal X-ray crystallography were grown by slow evaporation from a saturated solution of the title compound in ethyl acetate. The crystal structure is deposited in the Cambridge Crystallographic Data Centre CCDC 1537951.



Crystal Data and Structure Refinement for 273f

Identification code	MG_B2_0032
Formula	C ₁₈ H ₂₀ N ₂ O ₄
Formula weight	328.36
Temperature	180 K
Diffractionmeter, wavelength	Bruker D8-QUEST PHOTON-100, 1.54178 Å
Crystal system, space group	Monoclinic, P 2 ₁
Unit cell dimensions	a = 8.7257(2) Å α = 90° b = 7.4065(2) Å β = 90.4860(10)° c = 12.7010(3) Å γ = 90°
Volume, Z	820.80(3) Å ³ , 2
Density (calculated)	1.329 Mg/m ³
Absorption coefficient	0.778 mm ⁻¹
F(000)	348
Crystal colour / morphology	Colourless blocks
Crystal size	0.30 x 0.26 x 0.20 mm ³
θ range for data collection	3.480 to 69.969°
Index ranges	-10 ≤ h ≤ 10, -9 ≤ k ≤ 9, -15 ≤ l ≤ 15
Reflns collected / unique	10408 / 3070
Reflns observed [F > 4σ(F)]	2975
Absorption correction	Multi-scan
Min. and max. transmission	0.6627 and 0.7533
Refinement method	Full-matrix least-squares on F ²
Data / restraints / parameters	3070 / 1 / 218
Goodness-of-fit on F ²	1.056
Final R indices [F > 4σ(F)]	R ₁ = 0.0311, wR ₂ = 0.0787
R indices (all data)	R ₁ = 0.0302, wR ₂ = 0.0778
Largest diff. peak, hole	0.158, -0.178 eÅ ⁻³
Mean and maximum shift/error	0.000 and 0.000

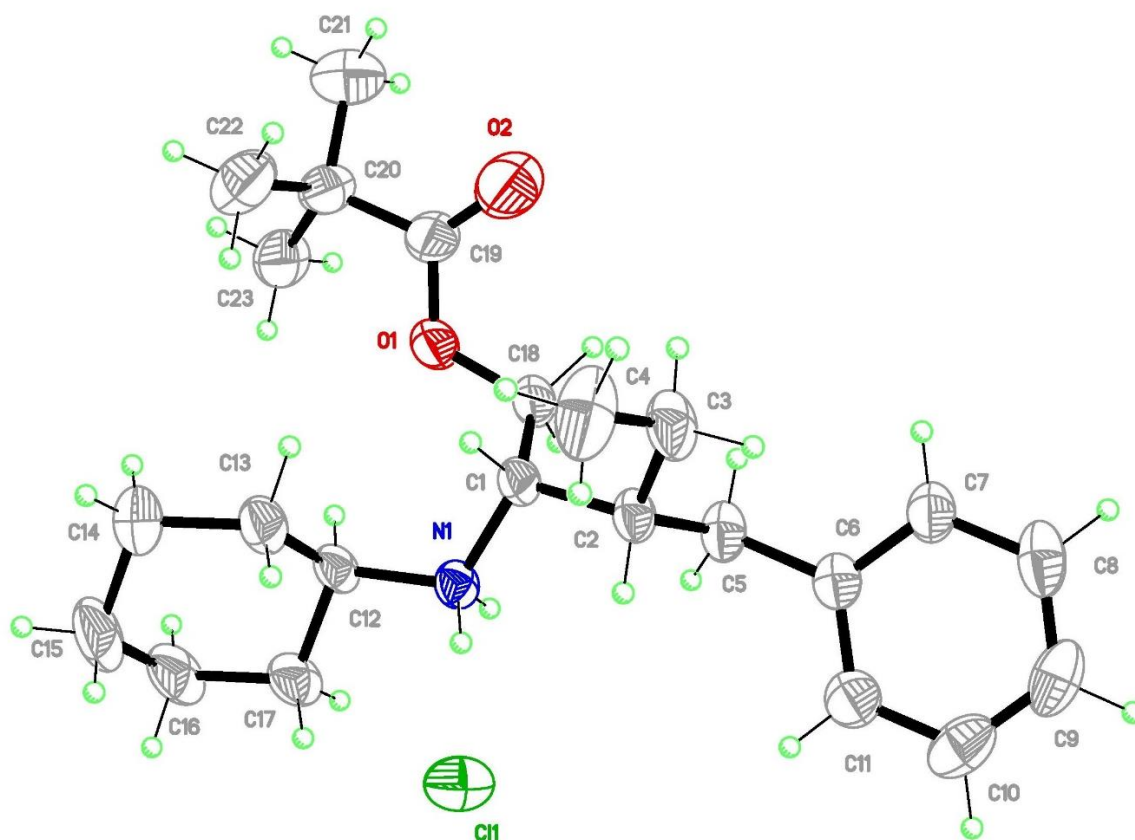
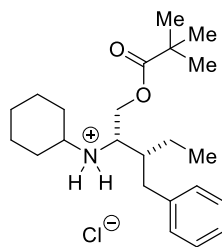
Trinuclear palladacycle 298. Crystals suitable for single crystal X-ray crystallography were grown by slow evaporation from a saturated solution of the title compound in hexane. The crystal structure is deposited in the Cambridge Crystallographic Data Centre CCDC 1850704.



Crystal Data and Structure Refinement for 298

Identification code	MG_B1_0029
Formula	C42 H76 N2 O12 Pd3
Formula weight	1120.24
Temperature	180 K
Diffractionmeter, wavelength	Bruker D8-QUEST PHOTON-100, 1.54178 Å
Crystal system, space group	Monoclinic, P 2 ₁
Unit cell dimensions	a = 16.8682(5) Å α = 90° b = 10.9641(3) Å β = 105.339(2)° c = 28.1073(8) Å γ = 90°
Volume, Z	5013.1(3) Å ³ , 4
Density (calculated)	1.484 Mg/m ³
Absorption coefficient	9.050 mm ⁻¹
F(000)	2304
Crystal colour / morphology	Green blocks
Crystal size	0.120 x 0.120 x 0.080 mm ³
θ range for data collection	2.716 to 67.007°
Index ranges	-20 ≤ h ≤ 18, -13 ≤ k ≤ 12, -33 ≤ l ≤ 33
Reflns collected / unique	77299 / 17729
Reflns observed [F > 4σ(F)]	15391
Absorption correction	Multi-scan
Min. and max. transmission	0.5400 and 0.7528
Refinement method	Full-matrix least-squares on F ²
Data / restraints / parameters	17729 / 100 / 1069
Goodness-of-fit on F ²	1.027
Final R indices [F > 4σ(F)]	R1 = 0.0472, wR2 = 0.1033
R indices (all data)	R1 = 0.0597, wR2 = 0.1093
Largest diff. peak, hole	0.690, -0.895 eÅ ⁻³
Mean and maximum shift/error	0.000 and 0.000

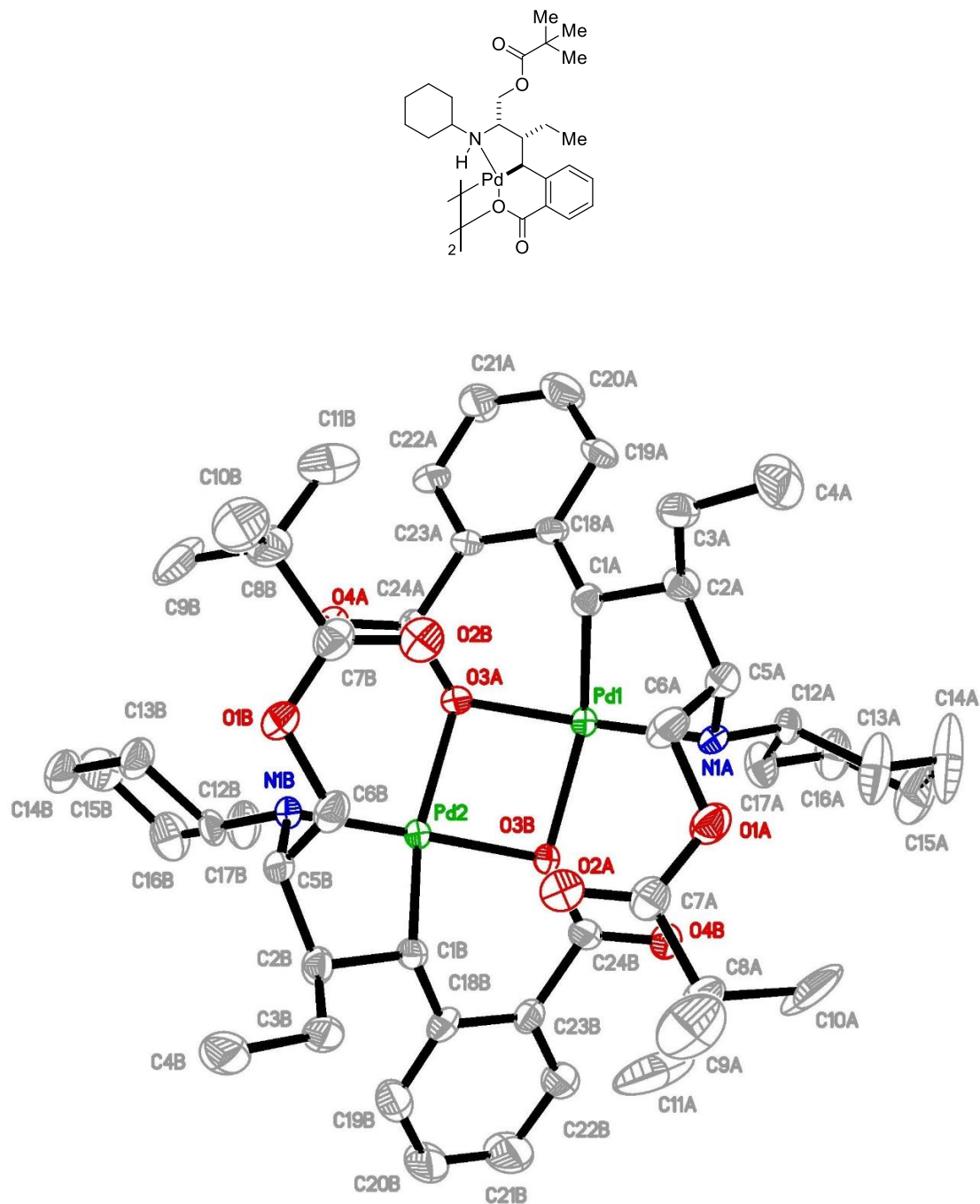
(2*S*,3*R*)-3-Benzyl-2-(cyclohexylamino)pentyl pivalate hydrochloride salt (301a•HCl). **301a** (72 mg, 0.2 mmol) was dissolved in methanolic HCl (1 M, 3 mL) at 0 °C and the resulting mixture stirred at room temperature for 0.5 h. The solvent was removed *in vacuo* to give the hydrochloride salt **301a•HCl** as a colourless solid (79 mg, 0.2 mmol, quantitative). Crystals suitable for single crystal X-ray crystallography were grown by slow evaporation from a saturated solution of **301a•HCl** in MeOH. The crystal structure is deposited in the Cambridge Crystallographic Data Centre CCDC 1850703.



Crystal Data and Structure Refinement for 301a•HCl

Identification code	MG_B1_0033
Formula	C ₂₃ H ₃₈ Cl N O ₂
Formula weight	395.99
Temperature	180 K
Diffractionmeter, wavelength	Bruker D8-QUEST PHOTON-100, 1.54178 Å
Crystal system, space group	Orthorhombic, P 2 ₁ c 2 ₁ b
Unit cell dimensions	a = 8.4516(3) Å α = 90° b = 11.1098(3) Å β = 90° c = 24.9575(8) Å γ = 90°
Volume, Z	2343.40(13) Å ³ , 4
Density (calculated)	1.122 Mg/m ³
Absorption coefficient	1.556 mm ⁻¹
F(000)	864
Crystal colour / morphology	Colourless plates
Crystal size	0.250 x 0.120 x 0.040 mm ³
θ range for data collection	3.542 to 66.671°
Index ranges	-10 ≤ h ≤ 9, -11 ≤ k ≤ 13, -29 ≤ l ≤ 29
Reflns collected / unique	17448 / 4136
Reflns observed [F > 4σ(F)]	3425
Absorption correction	Multi-scan
Min. and max. transmission	0.6042 and 0.7528
Refinement method	Full-matrix least-squares on F ²
Data / restraints / parameters	4136 / 0 / 252
Goodness-of-fit on F ²	1.037
Final R indices [F > 4σ(F)]	R1 = 0.0506, wR2 = 0.1142
R indices (all data)	R1 = 0.0658, wR2 = 0.1224
Largest diff. peak, hole	0.305, -0.256 eÅ ⁻³
Mean and maximum shift/error	0.000 and 0.000

Bicyclic palladacycle dimer 319. Crystals suitable for single crystal X-ray crystallography were grown by slow evaporation from a saturated solution of the title compound in hexane. The crystal structure is deposited in the Cambridge Crystallographic Data Centre CCDC 1858105.

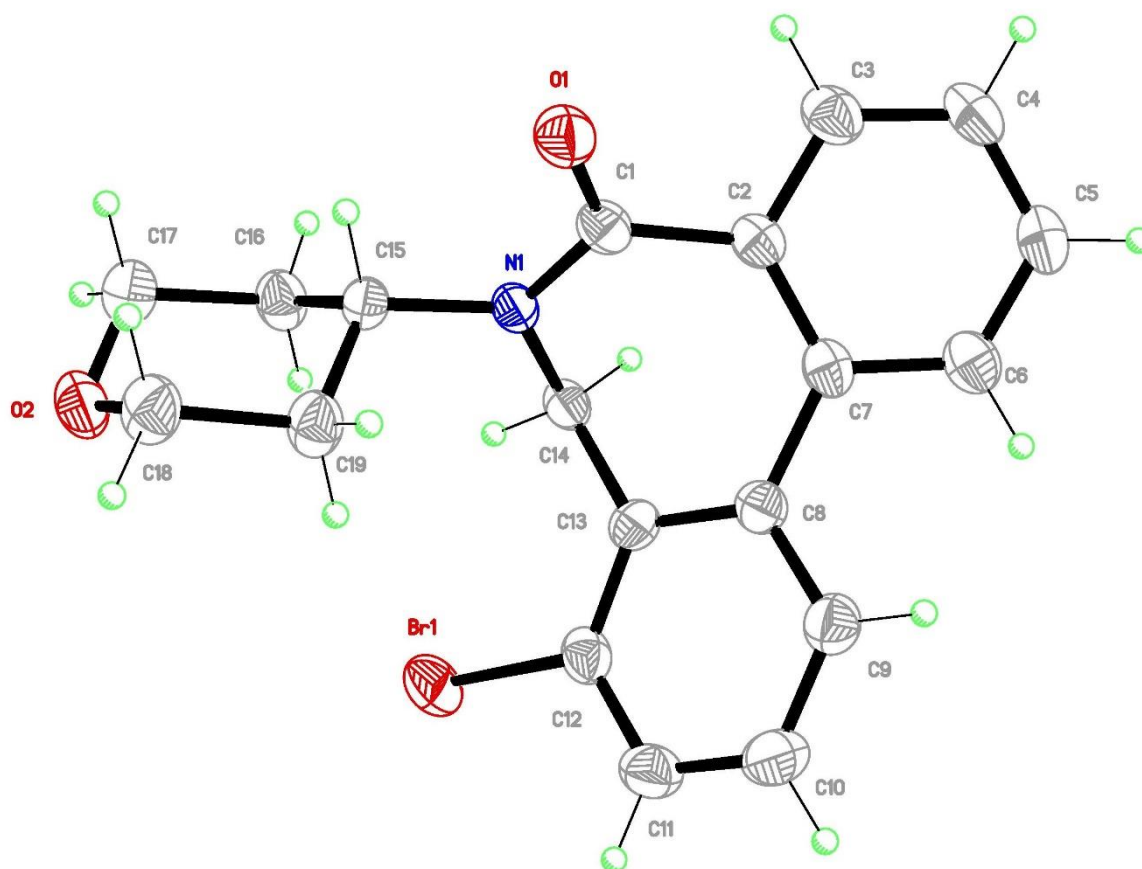
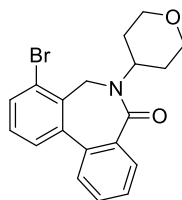


Crystal Data and Structure Refinement for 319

Identification code	MG_B1_0042
Formula	C ₄₈ H ₇₀ N ₂ O ₈ Pd ₂
Formula weight	1015.86
Temperature	180 K
Diffractionmeter, wavelength	Bruker D8-QUEST PHOTON-100, 1.54178 Å
Crystal system, space group	Orthorhombic, P 2 ₁ c 2 ₁ b
Unit cell dimensions	a = 11.4868(2) Å α = 90° b = 17.2747(4) Å β = 90° c = 24.2881(5) Å γ = 90°
Volume, Z	4819.51(17) Å ³ , 4
Density (calculated)	1.400 Mg/m ³
Absorption coefficient	6.435 mm ⁻¹
F(000)	2112
Crystal colour / morphology	Yellow blocks
Crystal size	0.100 x 0.100 x 0.030 mm ³
θ range for data collection	3.139 to 66.803°
Index ranges	-12 ≤ h ≤ 13, -20 ≤ k ≤ 19, -27 ≤ l ≤ 28
Reflns collected / unique	30914 / 8513
Reflns observed [F > 4σ(F)]	7250
Absorption correction	Multi-scan
Min. and max. transmission	0.6185 and 0.7528
Refinement method	Full-matrix least-squares on F ²
Data / restraints / parameters	8513 / 0 / 549
Goodness-of-fit on F ²	1.054
Final R indices [F > 4σ(F)]	R ₁ = 0.0424, wR ₂ = 0.0734
R indices (all data)	R ₁ = 0.0571, wR ₂ = 0.0780
Largest diff. peak, hole	0.428, -0.509 eÅ ⁻³
Mean and maximum shift/error	0.000 and 0.001

8-Bromo-6-(tetrahydro-2H-pyran-4-yl)-6,7-dihydro-5H-dibenzo[*c,e*]azepin-5-one (347).

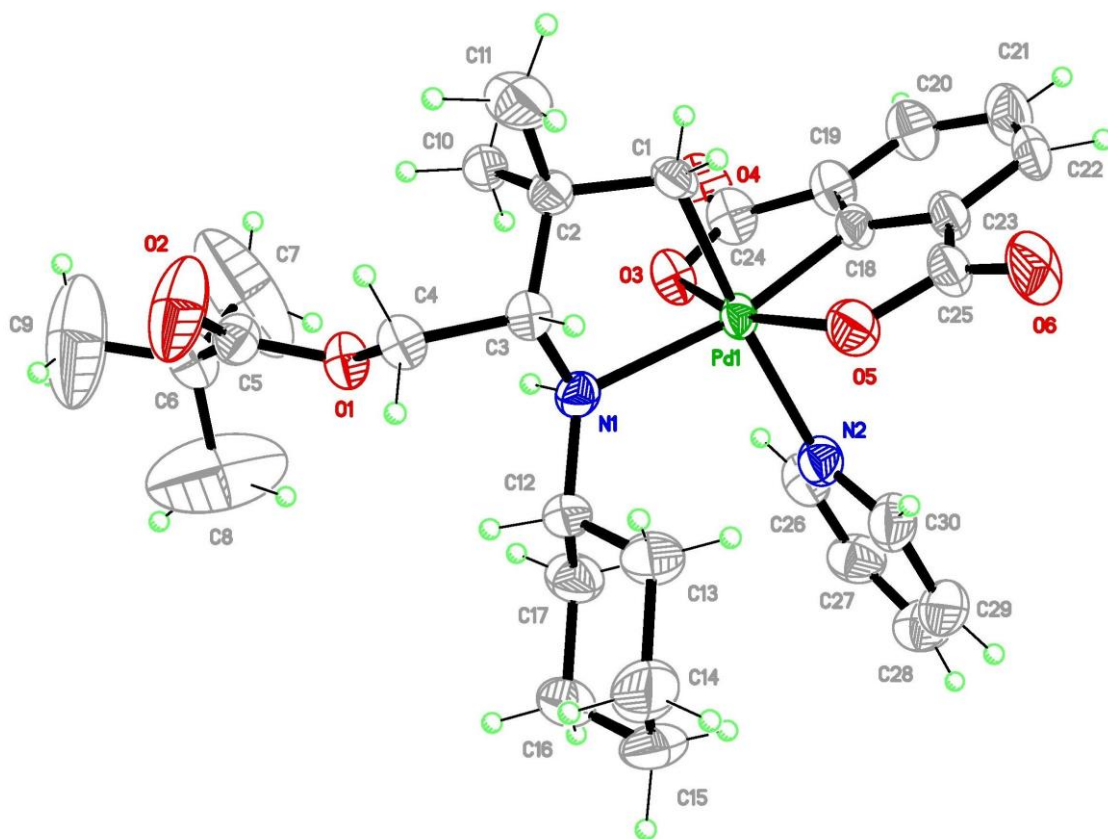
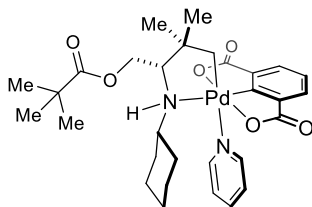
Crystals suitable for single crystal X-ray crystallography were grown by slow evaporation from a saturated solution of the title compound in ethyl acetate.



Crystal Data and Structure Refinement for 347

Identification code	MG_K1_0005
Formula	C ₁₉ H ₁₈ BrN ₂ O ₂
Formula weight	372.25
Temperature	180 K
Diffraction, wavelength	Nonius KappaCCD, 0.71073 Å
Crystal system, space group	Monoclinic, -P 2 ₁ /c
Unit cell dimensions	a = 9.3078(3) Å α = 90° b = 10.3678(4) Å β = 101.8543(14)° c = 16.7352(7) Å γ = 90°
Volume, Z	1580.53(10) Å ³ , 4
Density (calculated)	1.564 Mg/m ³
Absorption coefficient	2.610 mm ⁻¹
F(000)	760
Crystal colour / morphology	Colourless blocks
Crystal size	0.200 x 0.160 x 0.120 mm ³
θ range for data collection	3.573 to 25.024°
Index ranges	-11 ≤ h ≤ 11, -11 ≤ k ≤ 12, -19 ≤ l ≤ 19
Reflns collected / unique	8393 / 2781
Reflns observed [F > 4σ(F)]	1688
Absorption correction	Multi-scan
Min. and max. transmission	0.610 and 0.736
Refinement method	Full-matrix least-squares on F ²
Data / restraints / parameters	2781 / 0 / 208
Goodness-of-fit on F ²	0.826
Final R indices [F > 4σ(F)]	R ₁ = 0.0322, wR ₂ = 0.0570
R indices (all data)	R ₁ = 0.0644, wR ₂ = 0.0603
Largest diff. peak, hole	0.340, -0.373 eÅ ⁻³
Mean and maximum shift/error	0.000 and 0.001

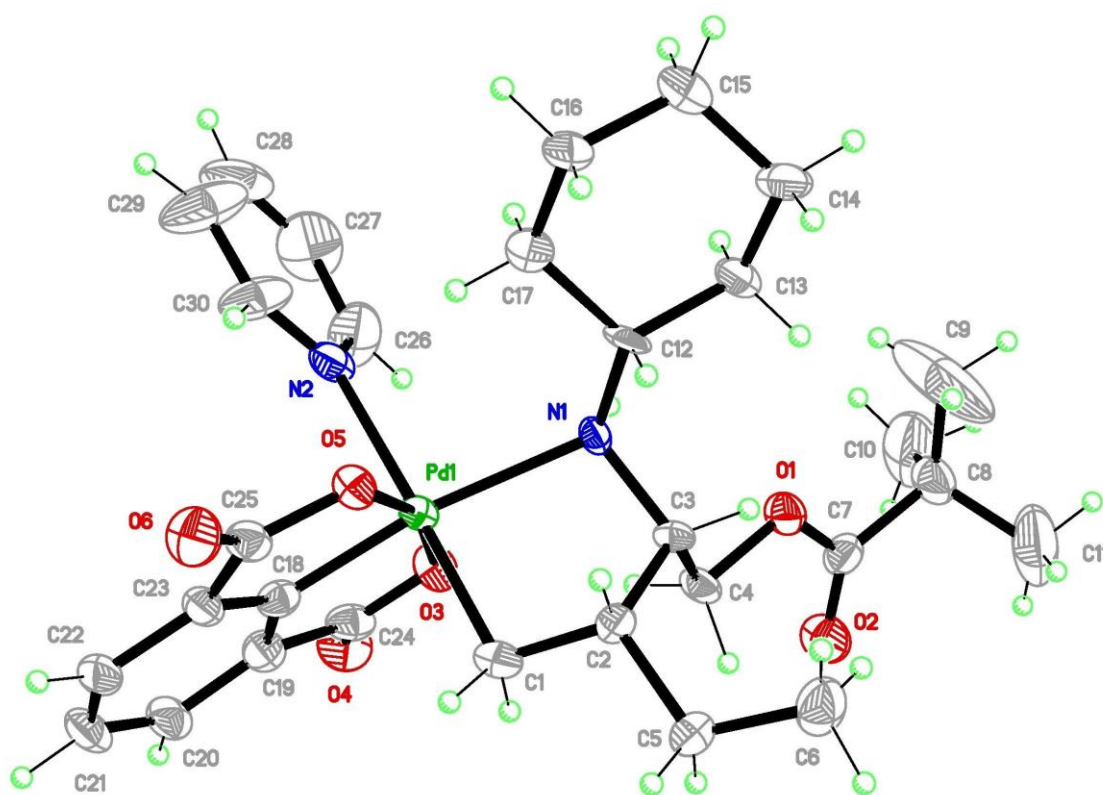
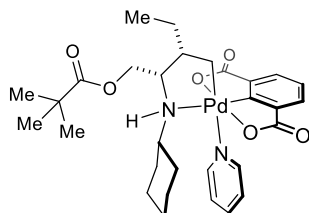
Amine-derived Pd^{IV} complex 352. Crystals suitable for single crystal X-ray crystallography were grown by slow evaporation from a saturated solution of the title compound in dichloromethane. The crystal structure is deposited in the Cambridge Crystallographic Data Centre CCDC 1991535.



Crystal Data and Structure Refinement for 352

Identification code	MG_B1_0054
Formula	C30 H40 N2 O6 Pd
Formula weight	631.04
Temperature	180 K
Diffractionmeter, wavelength	Bruker D8-QUEST PHOTON-100, 1.54178 Å
Crystal system, space group	Monoclinic, P 2 ₁
Unit cell dimensions	a = 9.6524(3) Å α = 90° b = 9.3271(3) Å β = 105.943(2)° c = 17.0545(5) Å γ = 90°
Volume, Z	1476.34(8) Å ³ , 2
Density (calculated)	1.420 Mg/m ³
Absorption coefficient	5.431 mm ⁻¹
F(000)	656
Crystal colour / morphology	Colourless blocks
Crystal size	0.160 x 0.080 x 0.020 mm ³
θ range for data collection	2.694 to 66.843°
Index ranges	-11 ≤ h ≤ 11, -11 ≤ k ≤ 11, -20 ≤ l ≤ 20
Reflns collected / unique	16009 / 5187
Reflns observed [F > 4σ(F)]	4759
Absorption correction	Multi-scan
Min. and max. transmission	0.5321 and 0.7528
Refinement method	Full-matrix least-squares on F ²
Data / restraints / parameters	5187 / 1 / 357
Goodness-of-fit on F ²	1.116
Final R indices [F > 4σ(F)]	R1 = 0.0485, wR2 = 0.1048
R indices (all data)	R1 = 0.0544, wR2 = 0.1073
Largest diff. peak, hole	1.492, -1.179 eÅ ⁻³
Mean and maximum shift/error	0.000 and 0.000

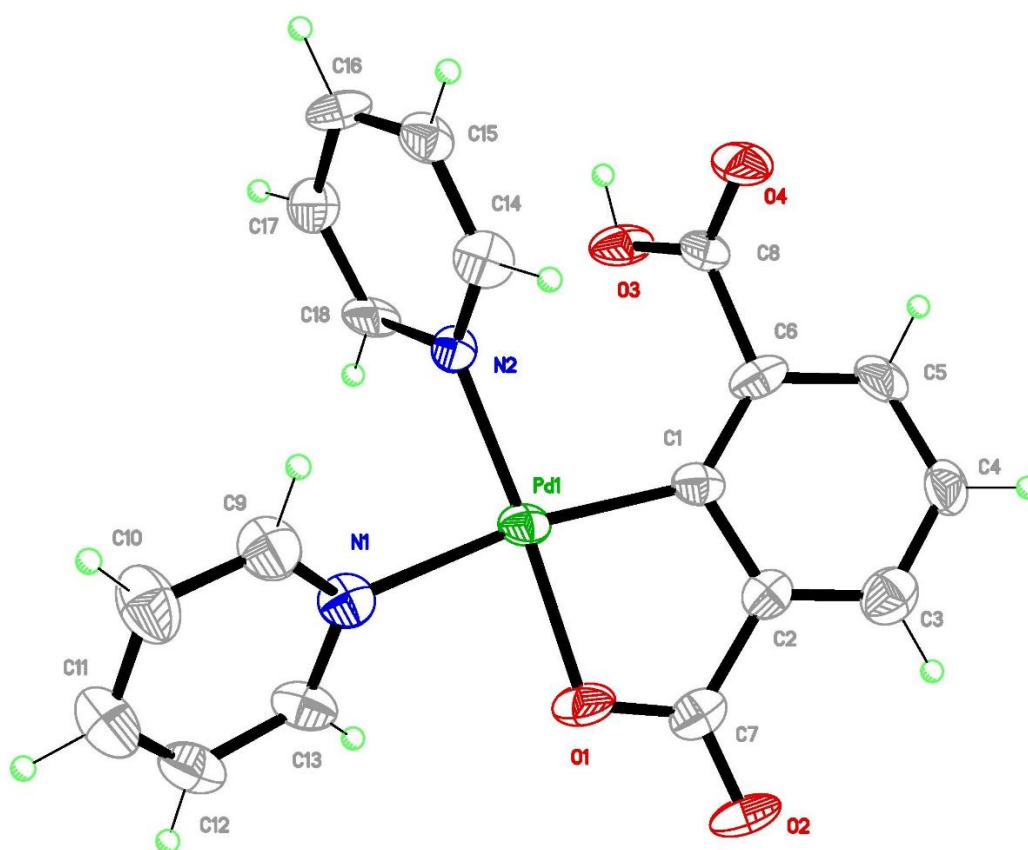
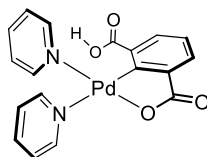
Amine-derived Pd^{IV} complex 353. Crystals suitable for single crystal X-ray crystallography were grown by layer diffusion of hexane into a concentrated solution of the title compound in dichloromethane at $-20\text{ }^{\circ}\text{C}$. The crystal structure is deposited in the Cambridge Crystallographic Data Centre CCDC 1991533.



Crystal Data and Structure Refinement for 353

Identification code	MG_B1_0072
Formula	C31 H42 Cl2 N2 O6 Pd
Formula weight	715.96
Temperature	180 K
Diffractionmeter, wavelength	Bruker D8-QUEST PHOTON-100, 1.54178 Å
Crystal system, space group	Monoclinic, P 2 ₁
Unit cell dimensions	a = 12.8922(4) Å α = 90° b = 10.0897(4) Å β = 108.728(2)° c = 13.3787(5) Å γ = 90°
Volume, Z	1648.14(10) Å ³ , 2
Density (calculated)	1.443 Mg/m ³
Absorption coefficient	6.391 mm ⁻¹
F(000)	740
Crystal colour / morphology	Colourless blocks
Crystal size	0.100 x 0.050 x 0.020 mm ³
θ range for data collection	3.488 to 66.728°
Index ranges	-15 ≤ h ≤ 15, -11 ≤ k ≤ 12, -15 ≤ l ≤ 15
Reflns collected / unique	15968 / 5792
Reflns observed [F > 4σ(F)]	5006
Absorption correction	Multi-scan
Min. and max. transmission	0.5981 and 0.7528
Refinement method	Full-matrix least-squares on F ²
Data / restraints / parameters	5792 / 1 / 383
Goodness-of-fit on F ²	1.034
Final R indices [F > 4σ(F)]	R1 = 0.0453, wR2 = 0.1005
R indices (all data)	R1 = 0.0601, wR2 = 0.1077
Largest diff. peak, hole	0.585, -0.457 eÅ ⁻³
Mean and maximum shift/error	0.000 and 0.001

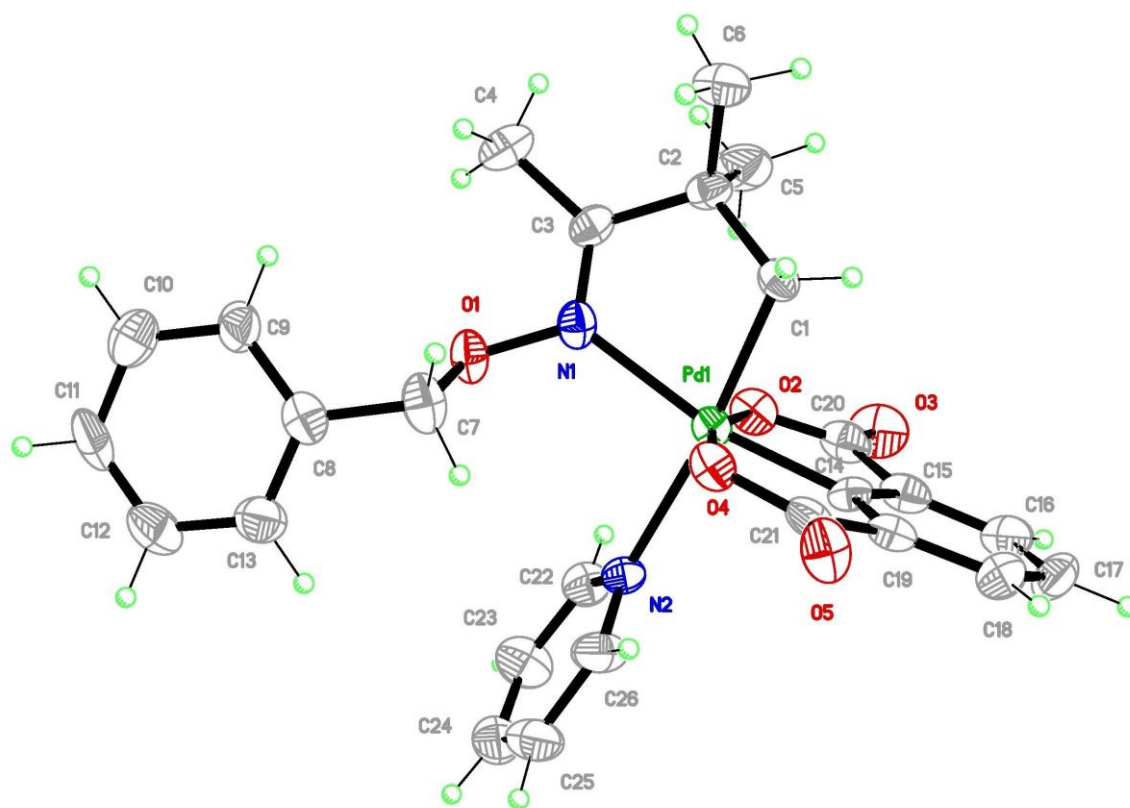
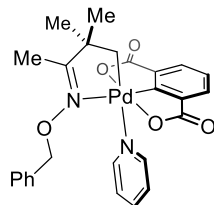
Bis(pyridyl)-Pd^{II} complex 358. Crystals suitable for single crystal X-ray crystallography were obtained by recrystallization of the title compound from boiling methanol. The crystal structure is deposited in the Cambridge Crystallographic Data Centre CCDC 1991534.



Crystal Data and Structure Refinement for 358

Identification code	MG_B1_0074
Formula	C ₁₈ H ₁₄ N ₂ O ₄ Pd
Formula weight	428.71
Temperature	180 K
Diffractometer, wavelength	Bruker D8-QUEST PHOTON-100, 1.54178 Å
Crystal system, space group	Triclinic, $\bar{P}1$
Unit cell dimensions	$a = 9.1222(4)$ Å $\alpha = 104.921(3)^\circ$ $b = 9.4681(5)$ Å $\beta = 104.897(3)^\circ$ $c = 10.7015(6)$ Å $\gamma = 105.987(3)^\circ$
Volume, Z	803.27(7) Å ³ , 2
Density (calculated)	1.772 Mg/m ³
Absorption coefficient	9.558 mm ⁻¹
F(000)	428
Crystal colour / morphology	Colourless plates
Crystal size	0.160 x 0.100 x 0.030 mm ³
θ range for data collection	4.570 to 66.678°
Index ranges	-10 ≤ h ≤ 10, -11 ≤ k ≤ 10, 0 ≤ l ≤ 12
Reflns collected / unique	12801 / 2770
Reflns observed [$F > 4\sigma(F)$]	2232
Absorption correction	Multi-scan
Min. and max. transmission	0.354 and 0.753
Refinement method	Full-matrix least-squares on F^2
Data / restraints / parameters	2770 / 0 / 227
Goodness-of-fit on F^2	1.113
Final R indices [$F > 4\sigma(F)$]	R1 = 0.0693, wR2 = 0.1474
R indices (all data)	R1 = 0.1030, wR2 = 0.1656
Largest diff. peak, hole	1.123, -1.431 eÅ ⁻³
Mean and maximum shift/error	0.000 and 0.000

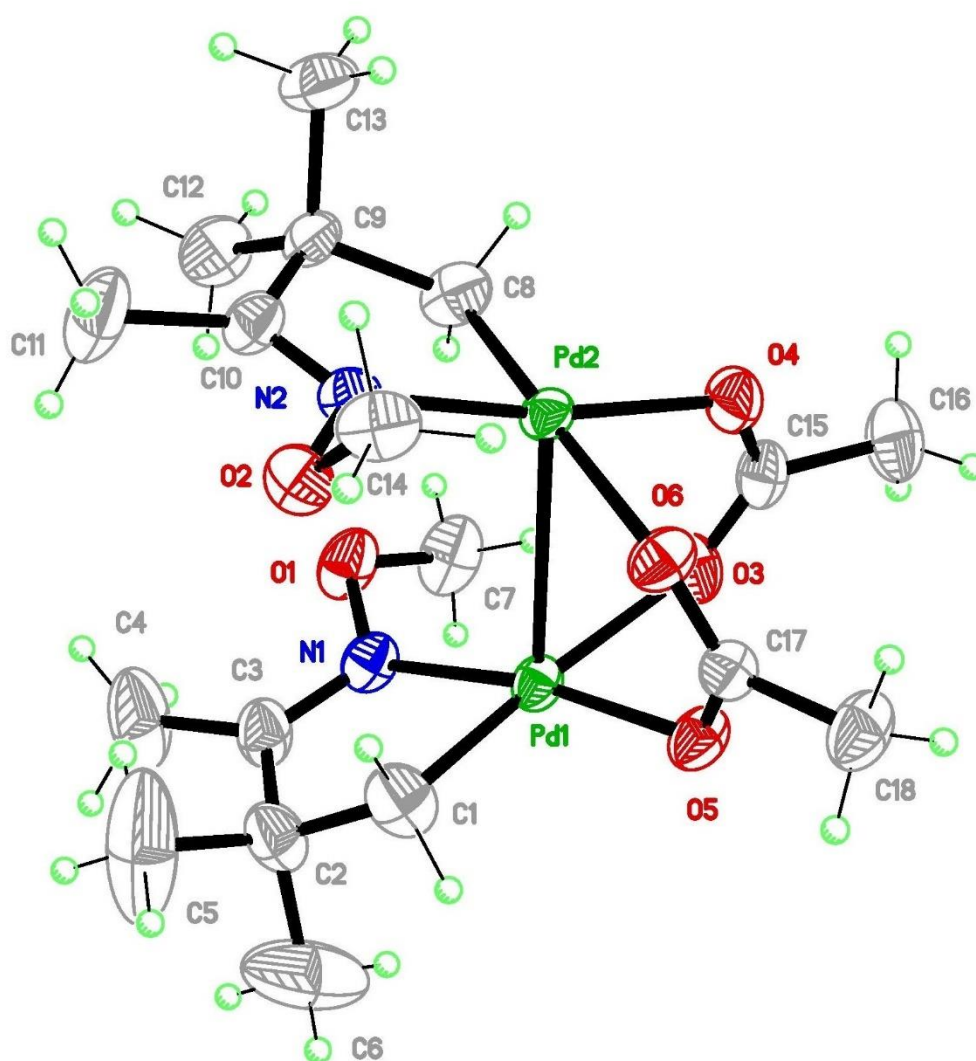
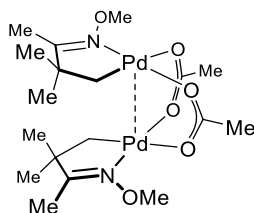
Oxime-derived Pd^{IV} complex 366c. A sample of **366b** (ca. 10 mg) was dissolved in acetone (10 mL) with several drops of pyridine added (**366b** immediately converts to a pyridine-ligated Pd^{IV} complex, **366c**). Slow evaporation of the solution at room temperature in air afforded crystals that were suitable for analysis by single crystal X-ray crystallography. The crystal structure is deposited in the Cambridge Crystallographic Data Centre CCDC 1991532.



Crystal Data and Structure Refinement for 366c

Identification code	MG_B1_0068
Formula	C ₂₆ H ₂₆ N ₂ O ₅ Pd
Formula weight	552.89
Temperature	180 K
Diffractionmeter, wavelength	Bruker D8-QUEST PHOTON-100, 1.54178 Å
Crystal system, space group	Monoclinic, -P 2 ₁ n
Unit cell dimensions	a = 15.8133(4) Å α = 90° b = 8.2009(2) Å β = 98.653(2)° c = 18.7485(5) Å γ = 90°
Volume, Z	2403.69(11) Å ³ , 4
Density (calculated)	1.528 Mg/m ³
Absorption coefficient	6.560 mm ⁻¹
F(000)	1128
Crystal colour / morphology	Yellow blocks
Crystal size	0.130 x 0.080 x 0.080 mm ³
θ range for data collection	3.413 to 66.748°
Index ranges	-18 ≤ h ≤ 18, 0 ≤ k ≤ 9, 0 ≤ l ≤ 22
Reflns collected / unique	4453 / 4453
Reflns observed [F > 4σ(F)]	3509
Absorption correction	Multi-scan
Min. and max. transmission	0.544 and 0.753
Refinement method	Full-matrix least-squares on F ²
Data / restraints / parameters	4453 / 0 / 311
Goodness-of-fit on F ²	1.066
Final R indices [F > 4σ(F)]	R ₁ = 0.0657, wR ₂ = 0.1287
R indices (all data)	R ₁ = 0.0984, wR ₂ = 0.1483
Largest diff. peak, hole	0.852, -0.932 eÅ ⁻³
Mean and maximum shift/error	0.000 and 0.001

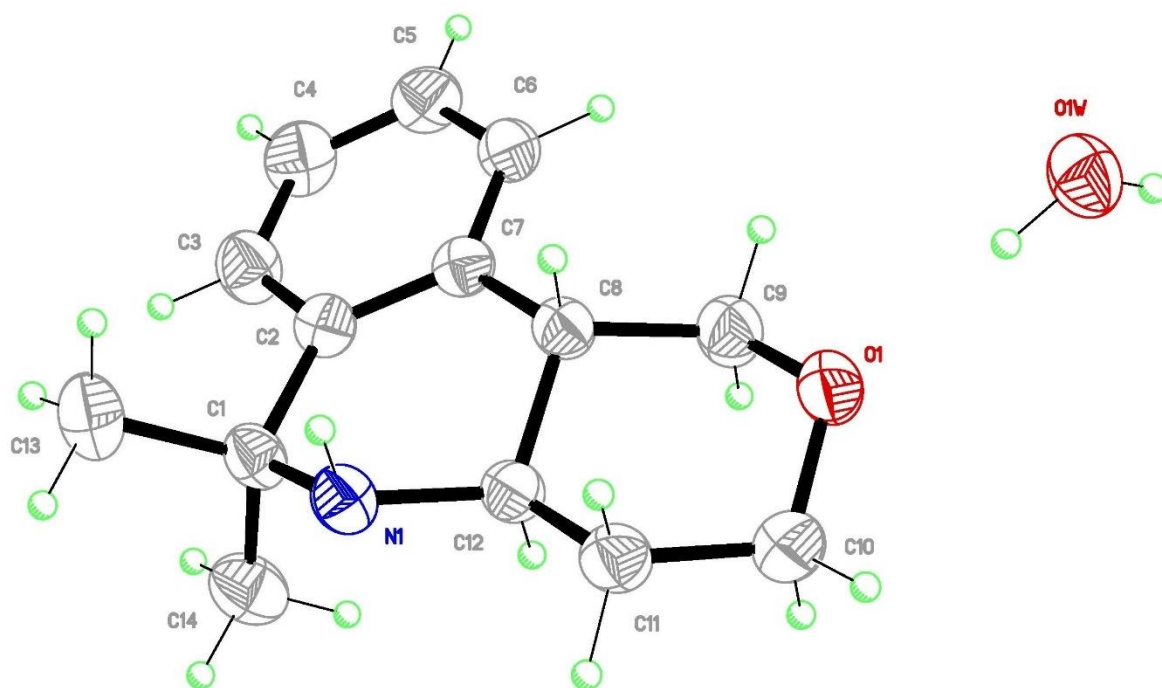
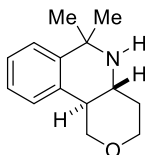
Oxime-derived palladacycle dimer 368. Crystals suitable for single crystal X-ray crystallography were grown by slow evaporation from a saturated solution of the title compound in hexane.



Crystal Data and Structure Refinement for 368

Identification code	MG_B1_0066
Formula	C ₁₈ H ₃₄ N ₂ O ₆ Pd ₂
Formula weight	587.27
Temperature	180 K
Diffractionmeter, wavelength	Bruker D8-QUEST PHOTON-100, 1.54178 Å
Crystal system, space group	Monoclinic, -P 2 ₁ /n
Unit cell dimensions	a = 9.8120(2) Å α = 90° b = 17.3087(5) Å β = 98.8520(10)° c = 14.2761(4) Å γ = 90°
Volume, Z	2395.67(11) Å ³ , 4
Density (calculated)	1.628 Mg/m ³
Absorption coefficient	12.391 mm ⁻¹
F(000)	1184
Crystal colour / morphology	Colourless blocks
Crystal size	0.080 x 0.080 x 0.060 mm ³
θ range for data collection	4.043 to 67.353°
Index ranges	-11 ≤ h ≤ 11, -20 ≤ k ≤ 20, -17 ≤ l ≤ 17
Reflns collected / unique	20108 / 4274
Reflns observed [F > 4σ(F)]	3550
Absorption correction	Multi-scan
Min. and max. transmission	0.5338 and 0.7528
Refinement method	Full-matrix least-squares on F ²
Data / restraints / parameters	4274 / 0 / 263
Goodness-of-fit on F ²	1.082
Final R indices [F > 4σ(F)]	R ₁ = 0.0310, wR ₂ = 0.0591
R indices (all data)	R ₁ = 0.0436, wR ₂ = 0.0626
Largest diff. peak, hole	0.646, -0.439 eÅ ⁻³
Mean and maximum shift/error	0.000 and 0.001

6,6-Dimethyl-3,4,4a,5,6,10b-hexahydro-1*H*-pyrano[4,3-*c*]isoquinoline (388). Crystals suitable for single crystal X-ray crystallography were grown by slow evaporation from a saturated solution of the title compound in methanol.

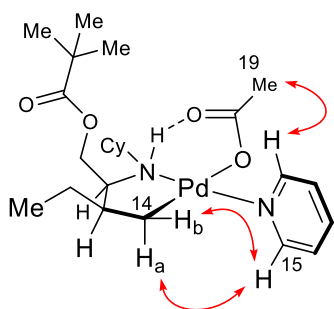


Crystal Data and Structure Refinement for 388

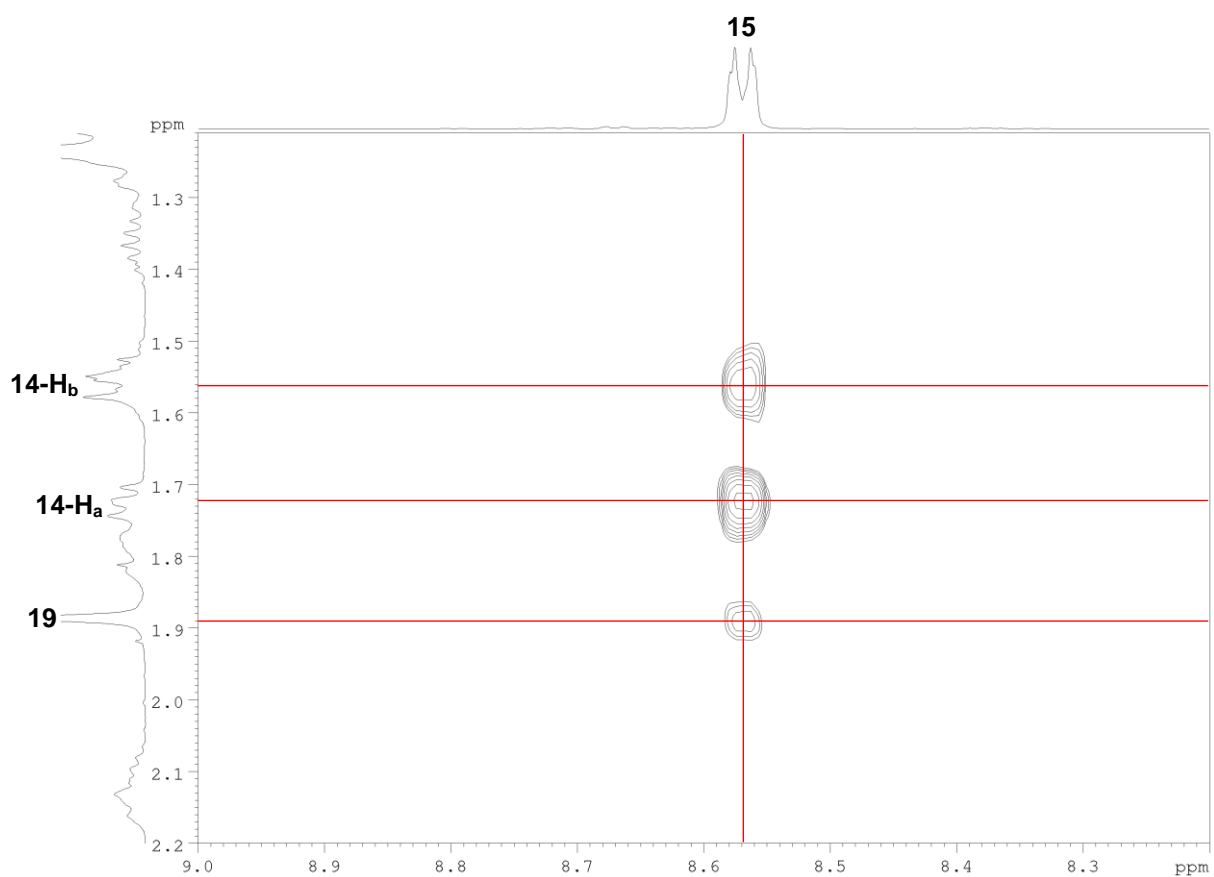
Identification code	MG_K1_0007
Formula	C ₁₄ H ₂₁ N O ₂
Formula weight	235.32
Temperature	180 K
Diffractionmeter, wavelength	Nonius KappaCCD, 0.71073 Å
Crystal system, space group	Monoclinic, -P 2 ₁ /c
Unit cell dimensions	a = 12.4051(3) Å α = 90° b = 6.3095(2) Å β = 90.450(2)° c = 16.6652(5) Å γ = 90°
Volume, Z	1304.34(7) Å ³ , 4
Density (calculated)	1.198 Mg/m ³
Absorption coefficient	0.079 mm ⁻¹
F(000)	512
Crystal colour / morphology	Colourless blocks
Crystal size	0.220 x 0.220 x 0.120 mm ³
θ range for data collection	3.623 to 27.499°
Index ranges	-16 ≤ h ≤ 16, -8 ≤ k ≤ 8, -21 ≤ l ≤ 21
Reflns collected / unique	13109 / 2962
Reflns observed [F > 4σ(F)]	1651
Absorption correction	Multi-scan
Min. and max. transmission	0.871 and 0.993
Refinement method	Full-matrix least-squares on F ²
Data / restraints / parameters	2962 / 0 / 168
Goodness-of-fit on F ²	0.864
Final R indices [F > 4σ(F)]	R ₁ = 0.0383, wR ₂ = 0.0886
R indices (all data)	R ₁ = 0.0771, wR ₂ = 0.0945
Largest diff. peak, hole	0.130, -0.180 eÅ ⁻³
Mean and maximum shift/error	0.000 and 0.000

2D NMR Data for Palladium Complexes

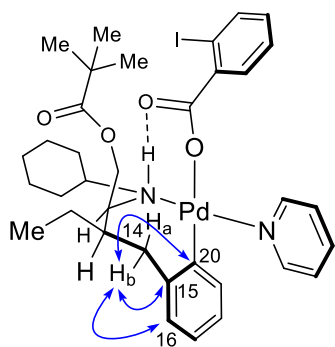
Pyridine-ligated palladacycle 299



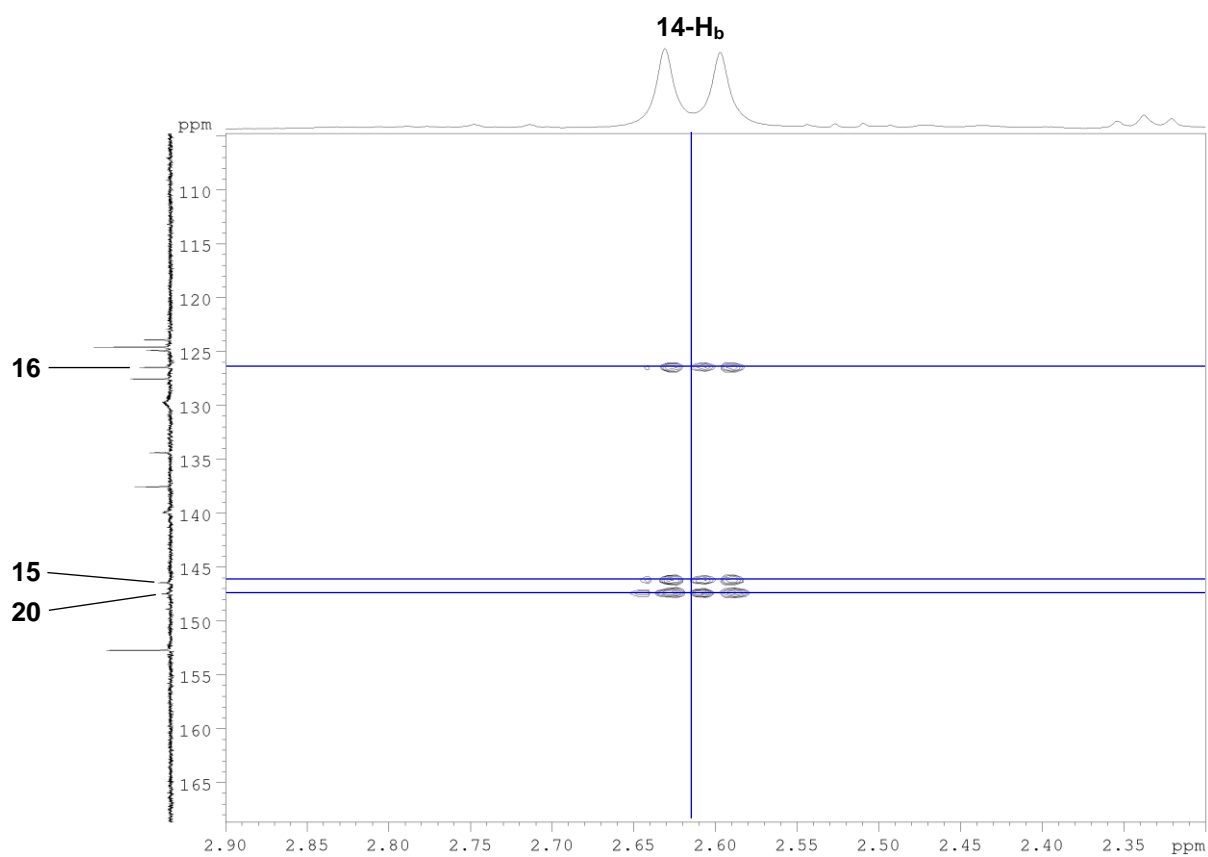
^1H - ^1H NOESY NMR spectrum (298 K, mixing time = 0.6 s)

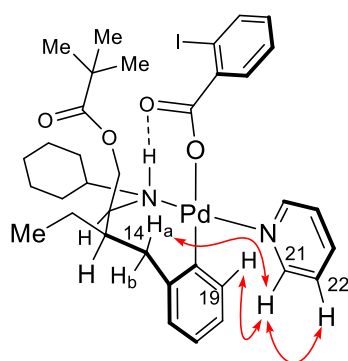


Pyridine-ligated 7-membered ring palladacycle 300

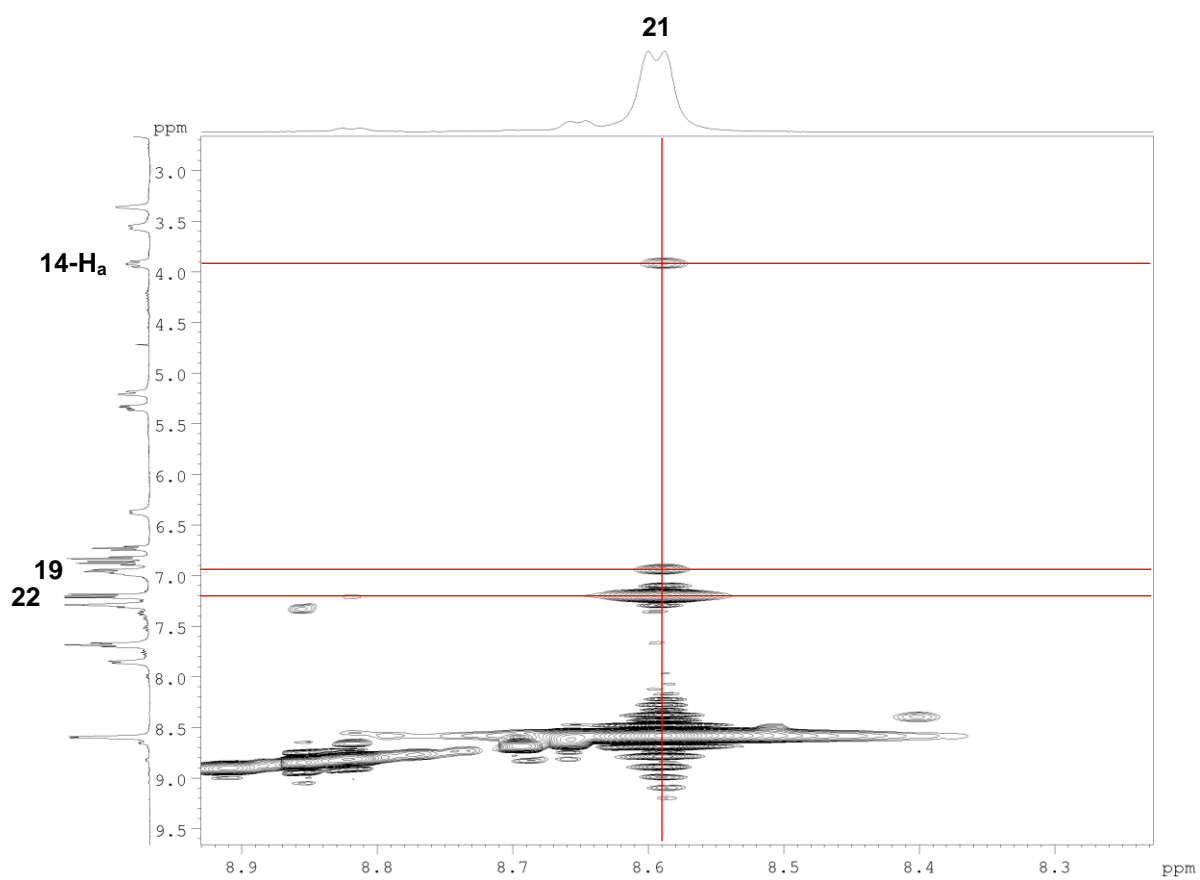


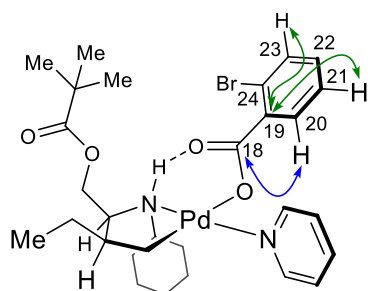
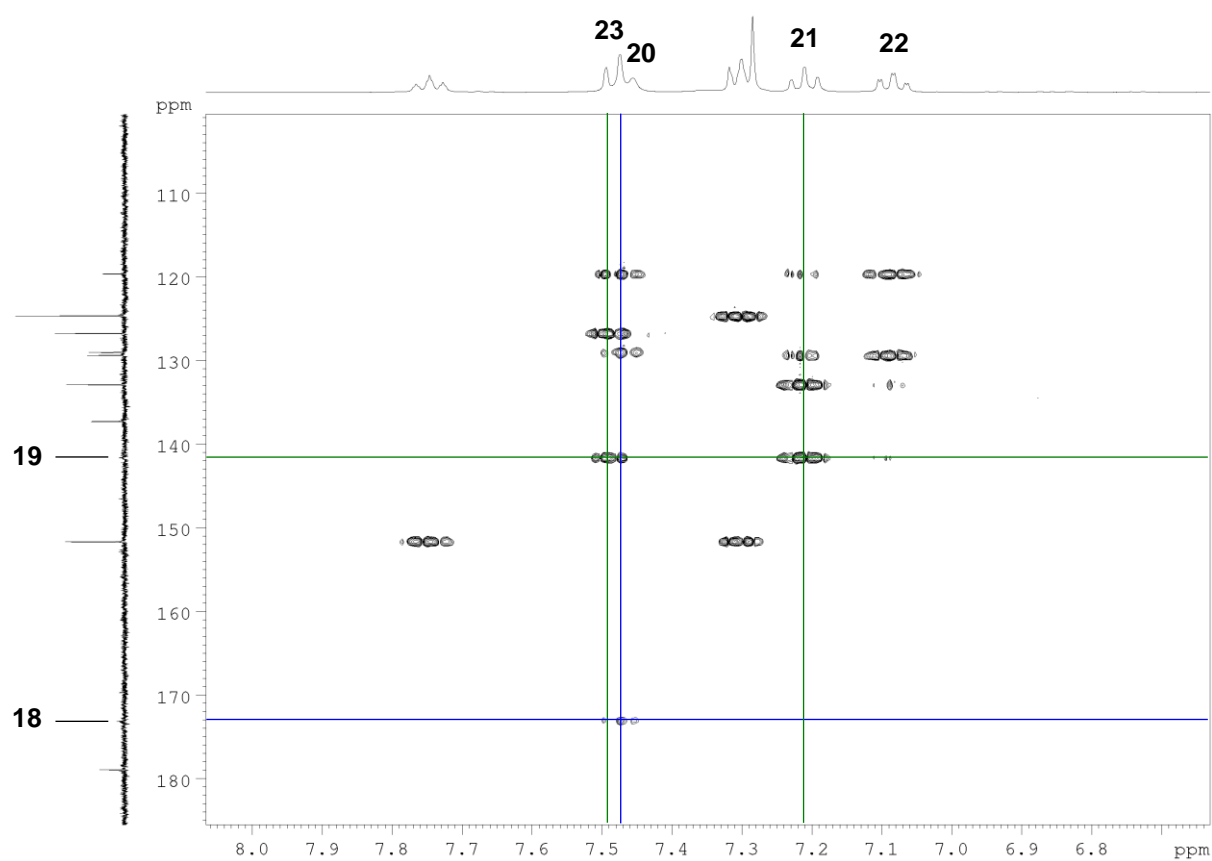
^1H - ^{13}C HMBC NMR spectrum

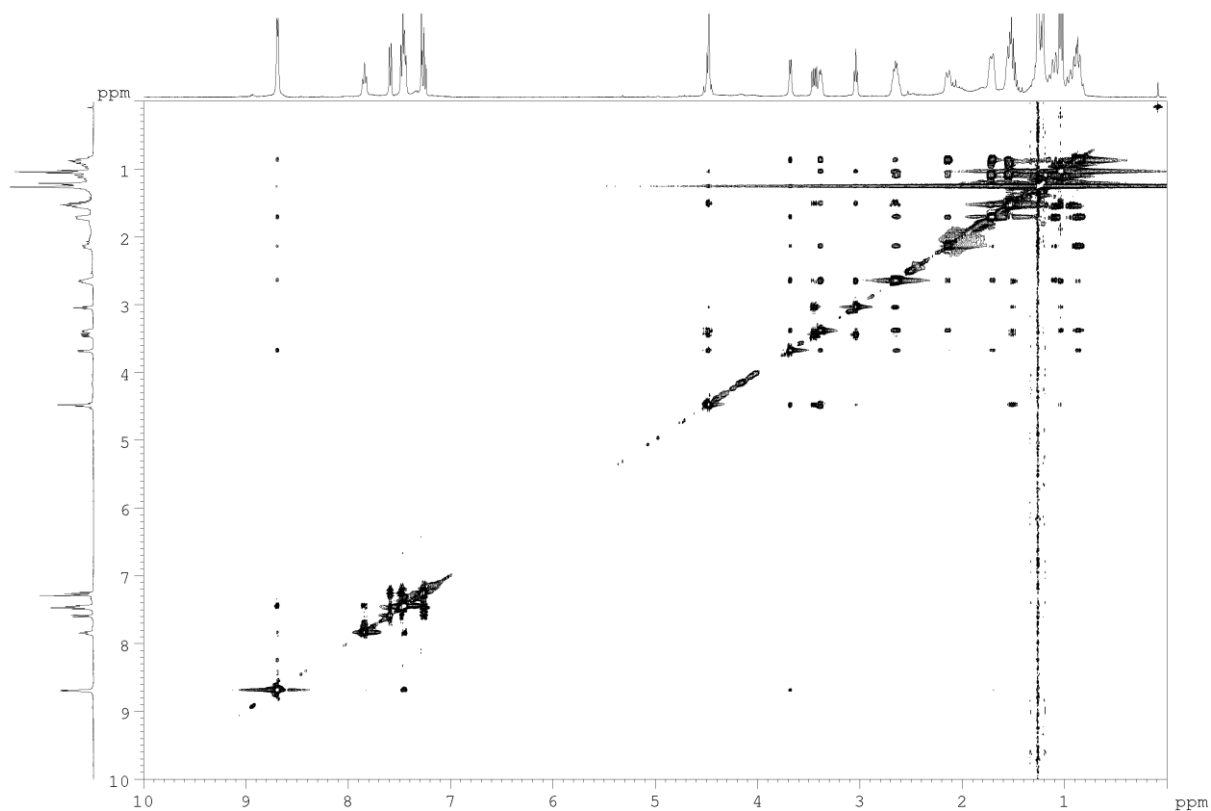
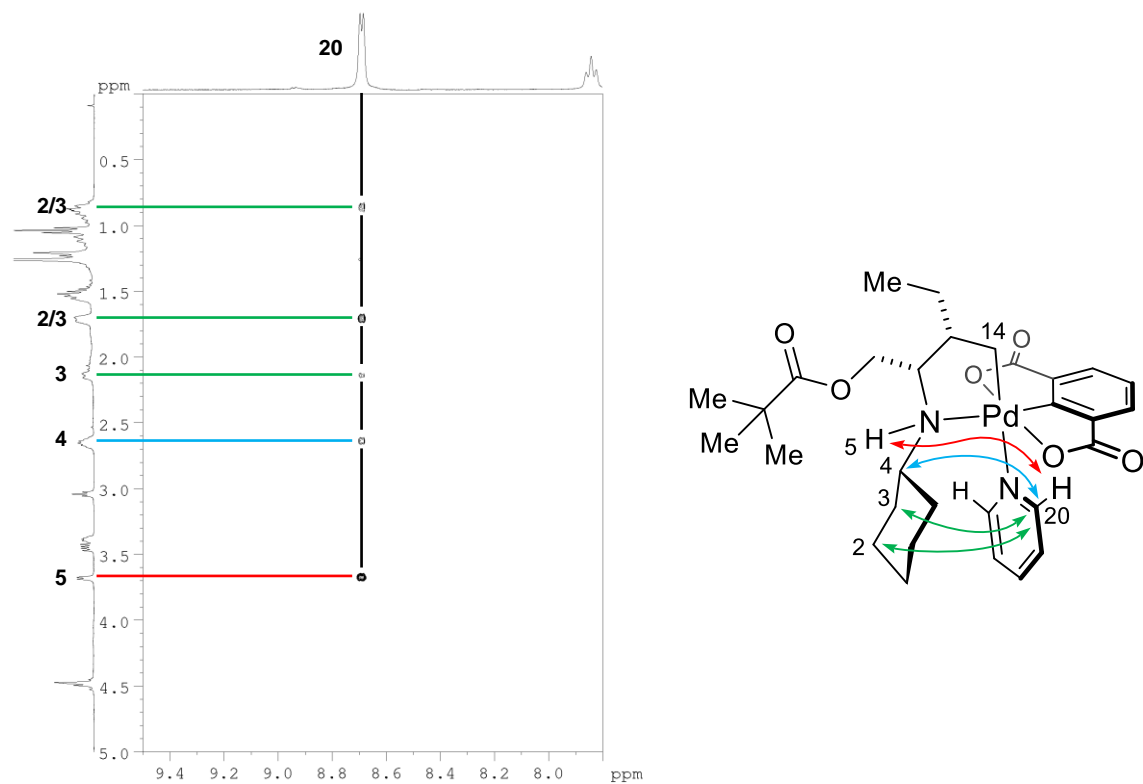


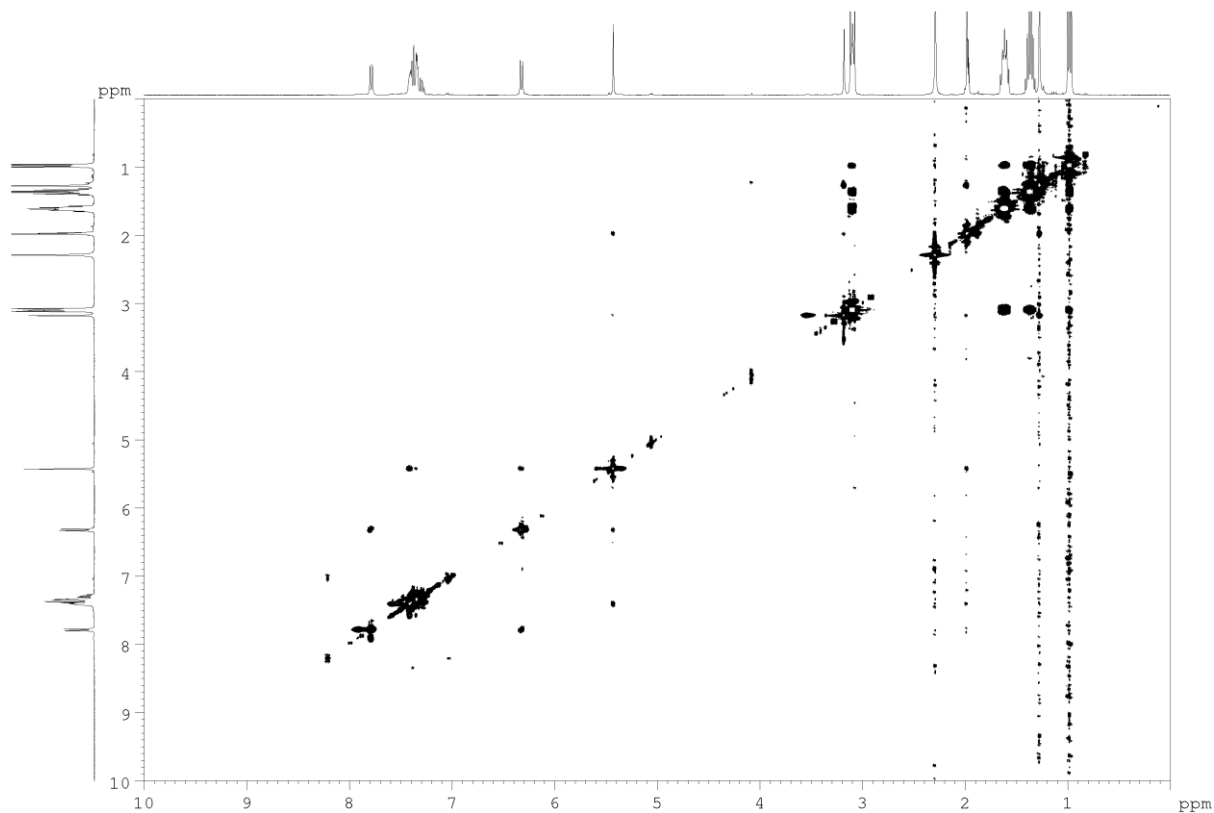
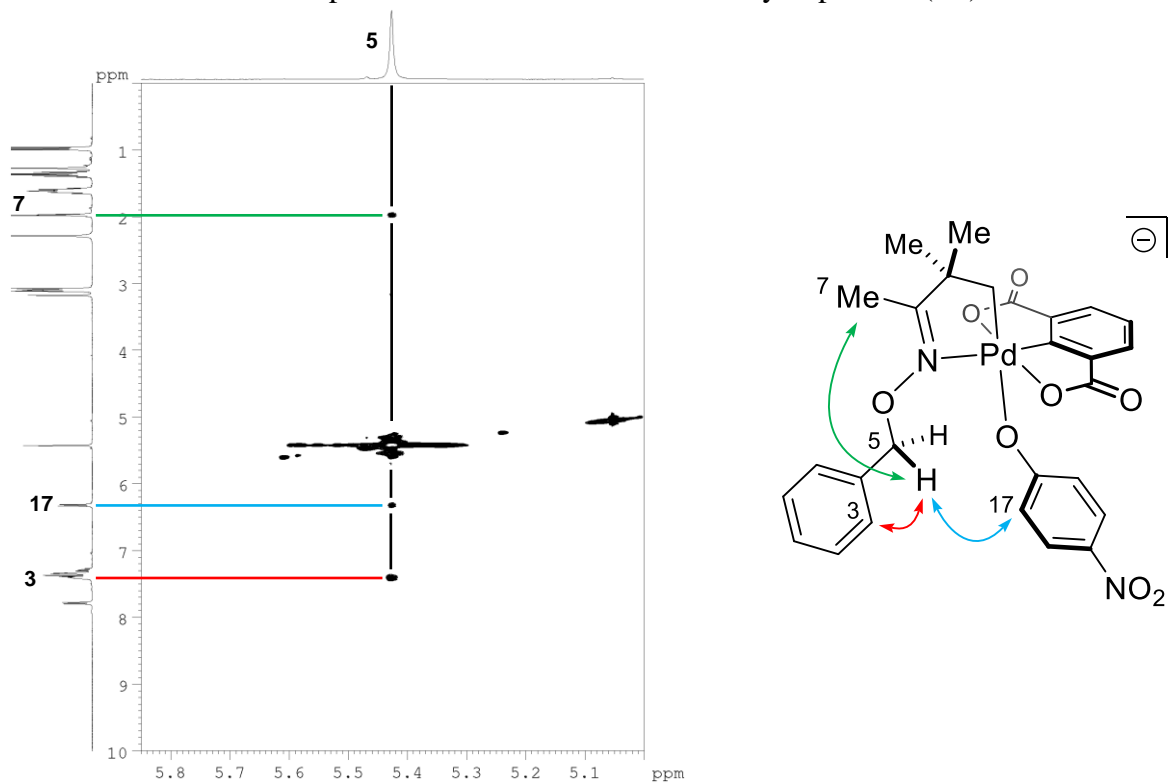


^1H - ^1H NOESY NMR spectrum (298 K, mixing time = 0.6 s)



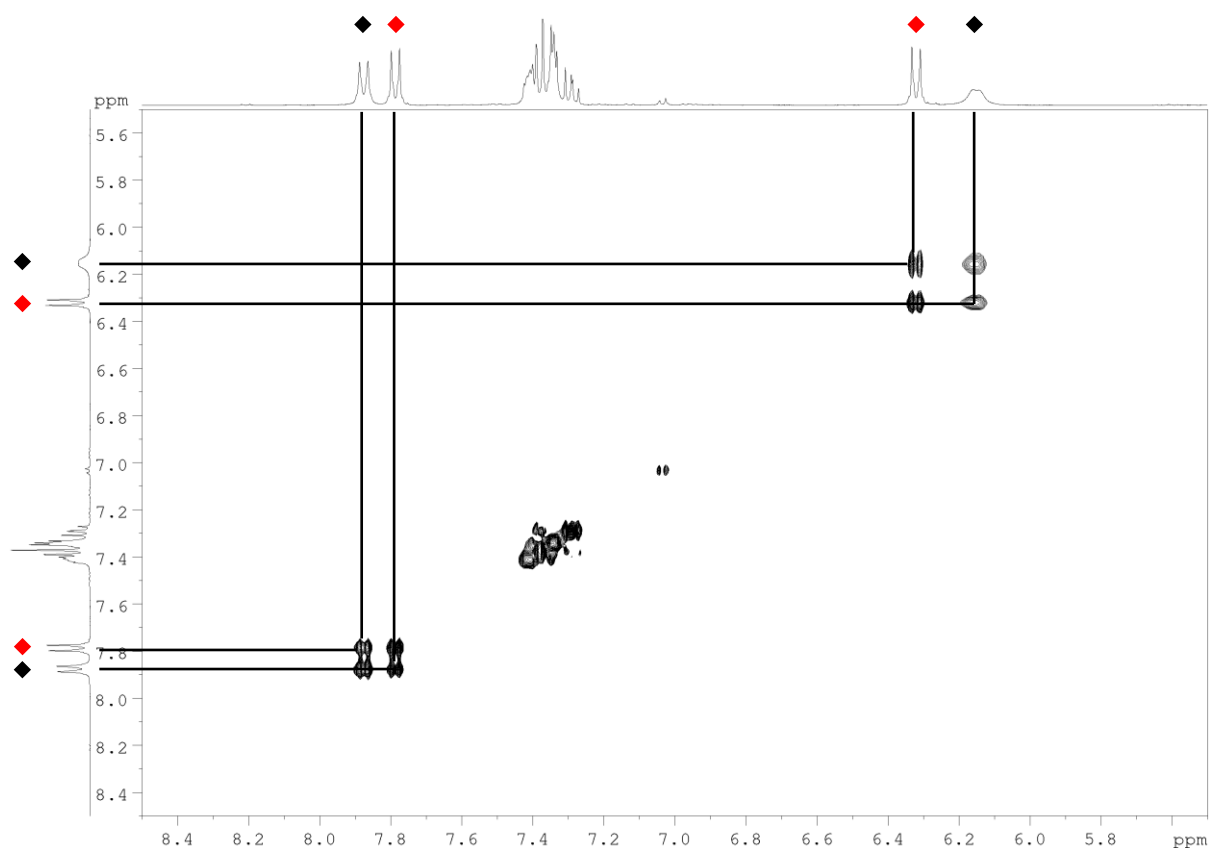
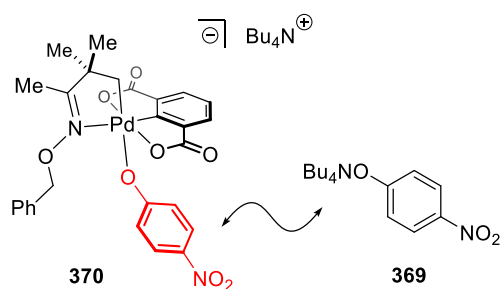
Pyridine-ligated palladacycle with 2-bromobenzoate ligand (305) ^1H - ^{13}C HMBC NMR spectrum

Amine-derived Pd^{IV} complex 353¹H-¹H NOESY NMR spectrum (298 K, mixing time = 0.6 s)Zoom-in: NOESY cross-peaks associated with pyridine *ortho* protons (**H**₂₀):

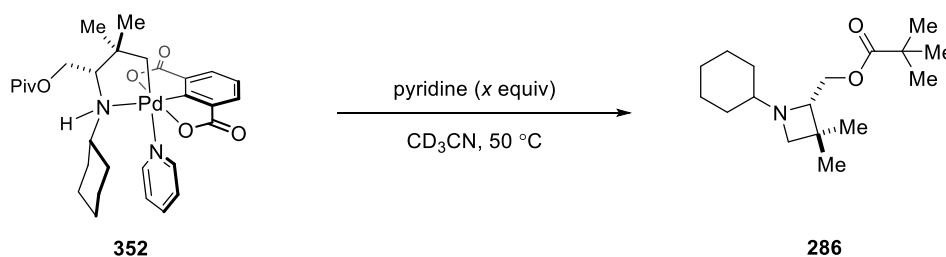
Anionic alkyl Pd^{IV} complex 370¹H-¹H NOESY NMR spectrum (298 K, mixing time = 0.6 s)Zoom-in: NOESY cross-peaks associated with oxime benzylic protons (**H**₅):

^1H - ^1H EXSY NMR spectrum: A solution of phenoxide-ligated oxime-Pd^{IV} complex **370** (0.04 M) with 1 equivalent of added (unbound) tetrabutylammonium *p*-nitrophenoxide **369** (0.04 M) in acetonitrile- d_3 was analysed by 2D EXSY NMR spectroscopy (NOESY protocol, T = 298 K, mixing time = 0.6 s). Over the course of the NMR experiment, <1% conversion of Pd^{IV} complex **370** (by reductive elimination) took place.

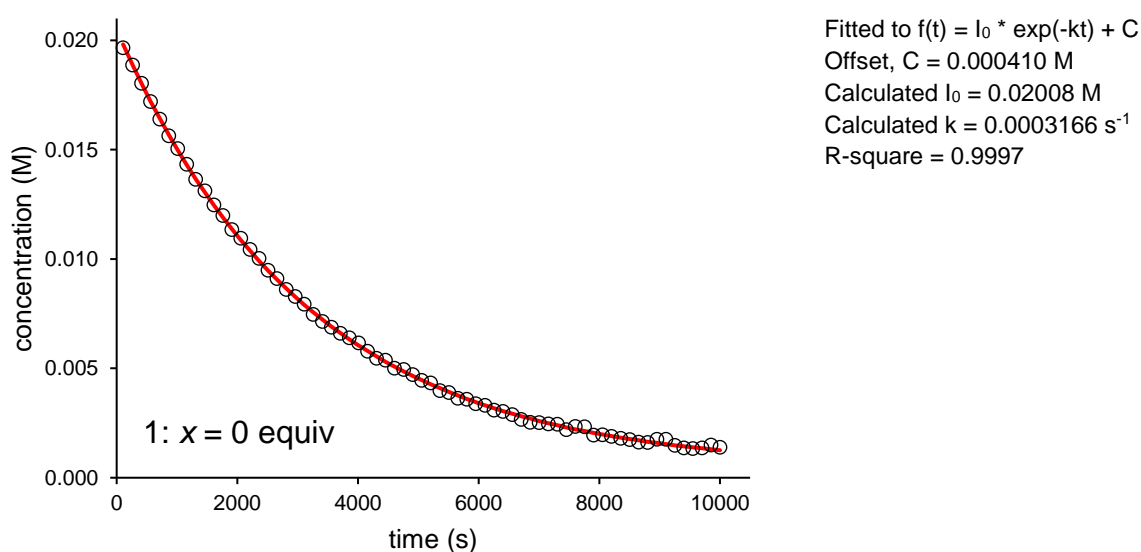
Note: red diamonds = bound phenoxide; black diamonds = unbound phenoxide.



Data for Kinetic Studies

Kinetics of Thermal Decomposition of **352** (with Added Pyridine)

To a solution of Pd^{IV} complex **352** (6.3 mg, 0.01 mmol, 1 equiv) in CD_3CN (0.5 mL) were added pyridine (x equiv) and 1,1,2,2-tetrachloroethane ($1 \mu\text{L}$, internal standard). The solution was transferred to a screw-top NMR tube and inserted into a pre-heated NMR spectrometer at $50 \text{ } ^\circ\text{C}$. ^1H NMR spectra were recorded at fixed time intervals. The disappearance of **352** was monitored by integrating peaks in the region 4.60–4.20 ppm (RCH_2OPiv), relative to the internal standard. The reactions were monitored for a period of greater than three half-lives. **286** was obtained as the sole amine product in all cases and was obtained in >90% yield by the final time point. Plots of concentration versus time showed first order kinetic behaviour. To obtain rate constants, decay of **352** was fitted by non-linear least squares analysis to $f(t) = I_0 * \exp(-kt) + C$ (error estimation by weighted fit, 95% confidence level). Concentration-time plots with fitted curves are shown for each experiment (black circles = experimental data; red line = calculated trendline). The kinetic data are summarised in Table S-1.



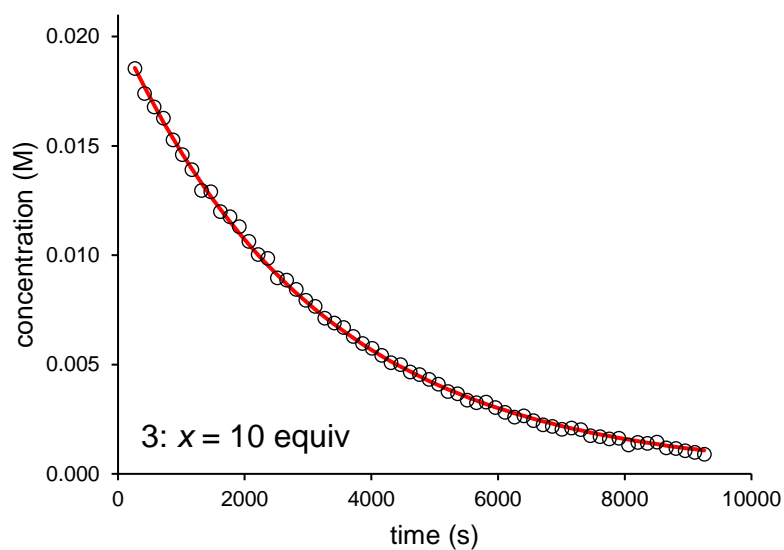
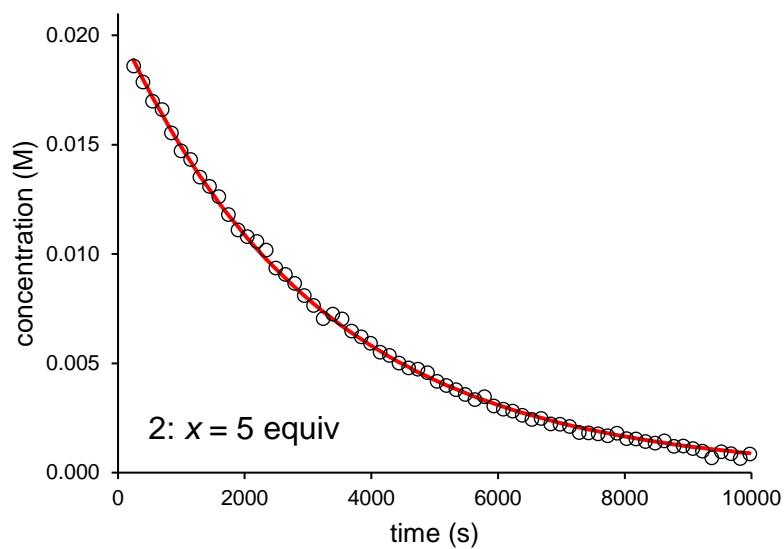
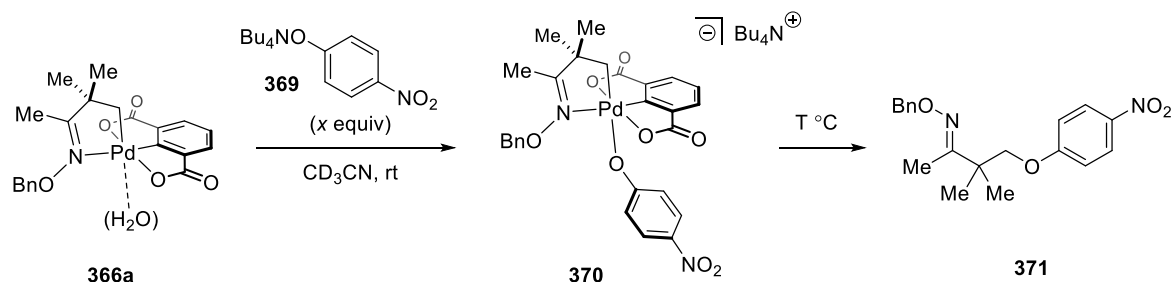
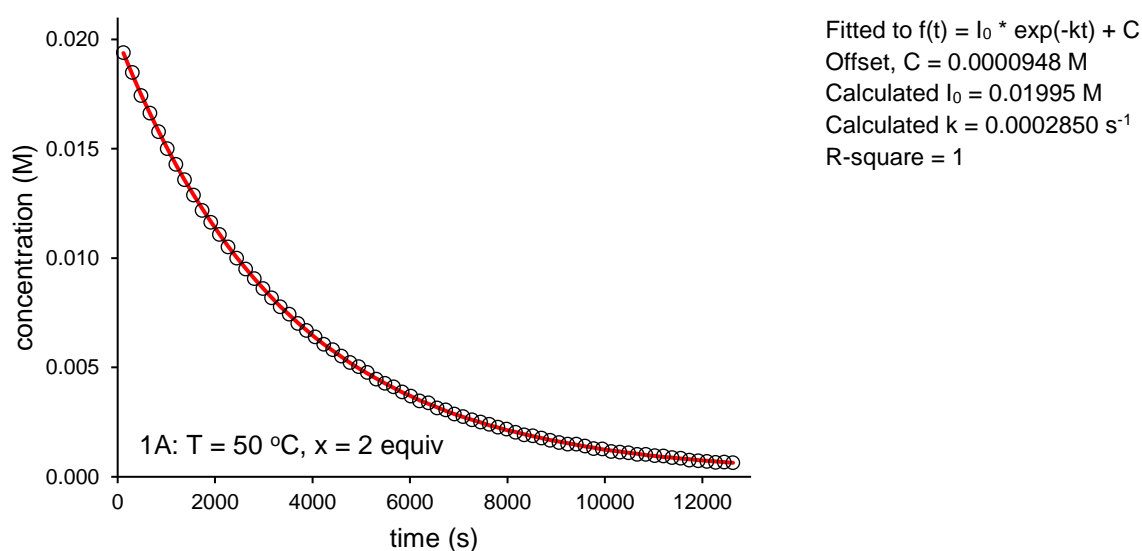


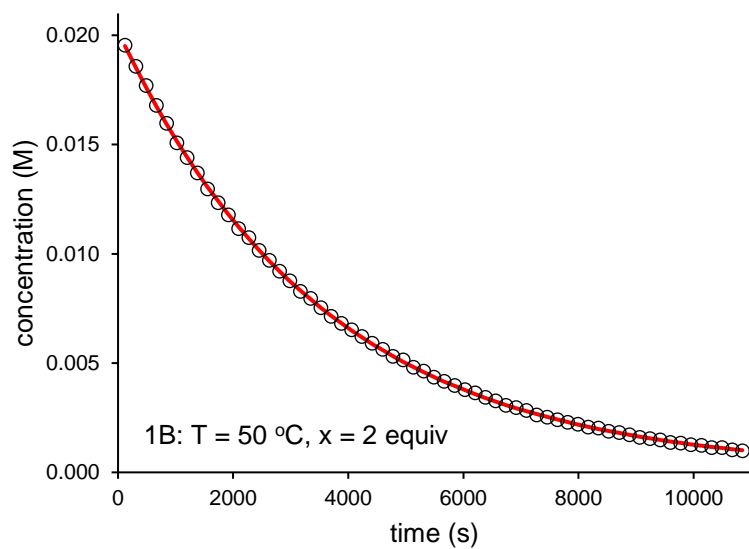
Table S-1. Rate of reductive elimination from **352**: varying equivalents of pyridine.

Entry	pyridine (x , equiv)	k_{obs} (s ⁻¹)
1	0	0.0003166
2	5	0.0003142
3	10	0.0003173

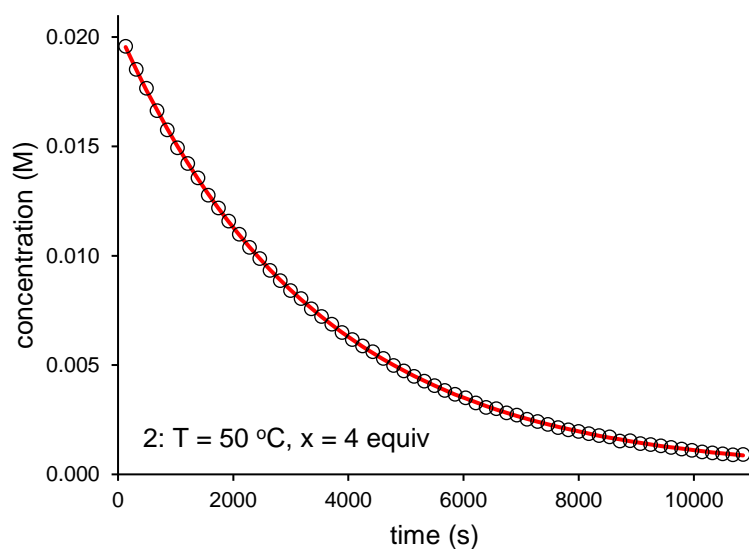
Kinetics of Thermal Decomposition of **370** in CD₃CN

To a vial containing Pd^{IV} complex **366b** (4.9 mg, 0.01 mmol, 1 equiv) and tetrabutylammonium *p*-nitrophenoxide **369** (x equiv) were added CD₃CN (0.5 mL) and anisole (ca. 1 μ L, internal standard). The solution was transferred to a screw-top NMR tube and inserted into a pre-heated NMR spectrometer at the specified temperature (T °C). ¹H NMR spectra were recorded at fixed time intervals. The disappearance of **370** and the formation of **371** were monitored by integrating peaks at 5.46 ppm and 4.09 ppm, respectively, relative to the internal standard. The reactions were monitored for a period of greater than three half-lives. **371** was obtained as the sole product in all cases and in >90% yield by the final time point. Plots of concentration versus time showed first order kinetic behaviour. To obtain rate constants, decay of **370** was fitted by non-linear least squares analysis to $f(t) = I_0 * \exp(-kt) + C$ (error estimation by weighted fit, 95% confidence level). Concentration-time plots with fitted curves are shown for each experiment (black circles = experimental data; red line = calculated trendline). The kinetic data are summarised in Table S-2.

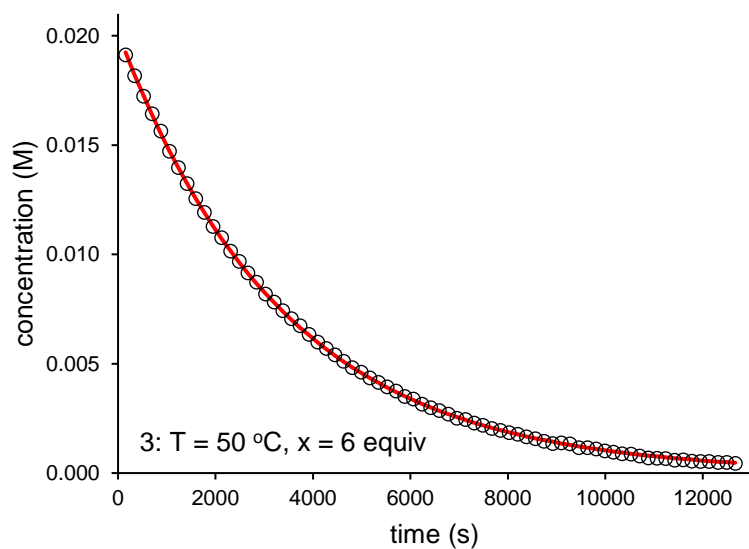




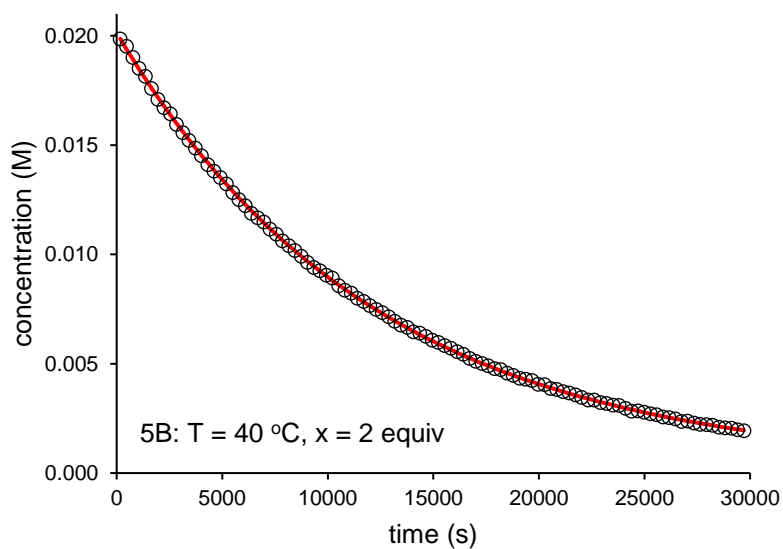
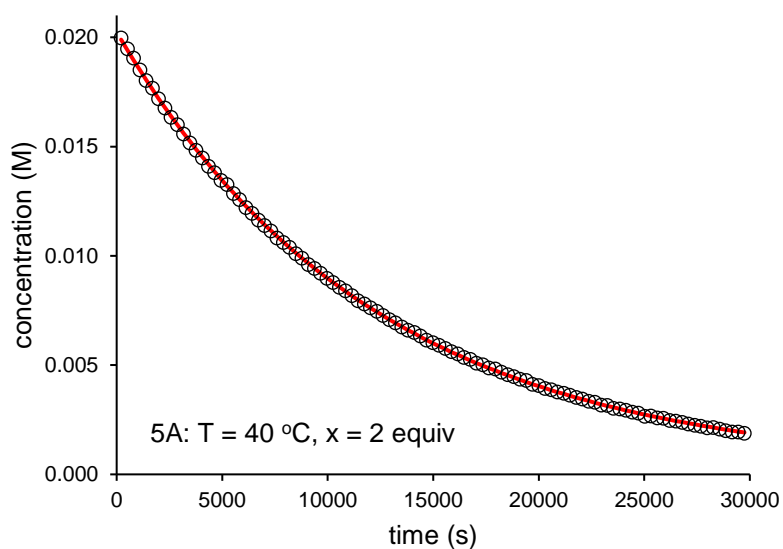
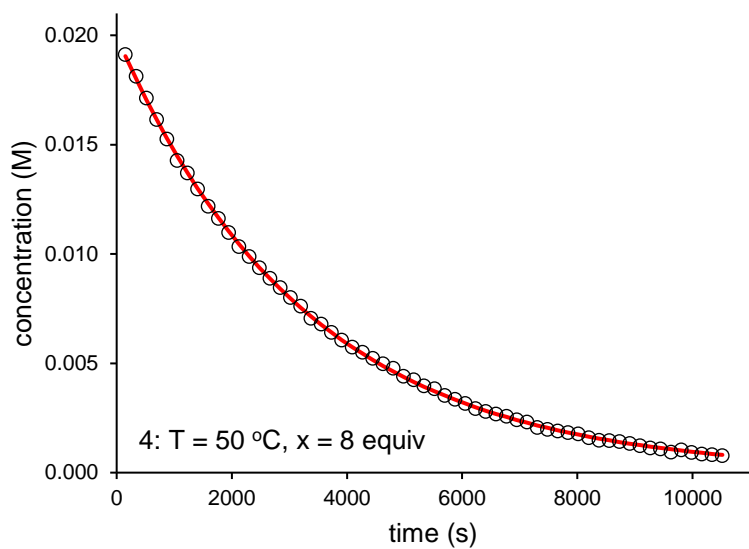
Fitted to $f(t) = I_0 * \exp(-kt) + C$
 Offset, C = 0.0000568 M
 Calculated $I_0 = 0.02012$ M
 Calculated $k = 0.0002810$ s⁻¹
 R-square = 0.9999

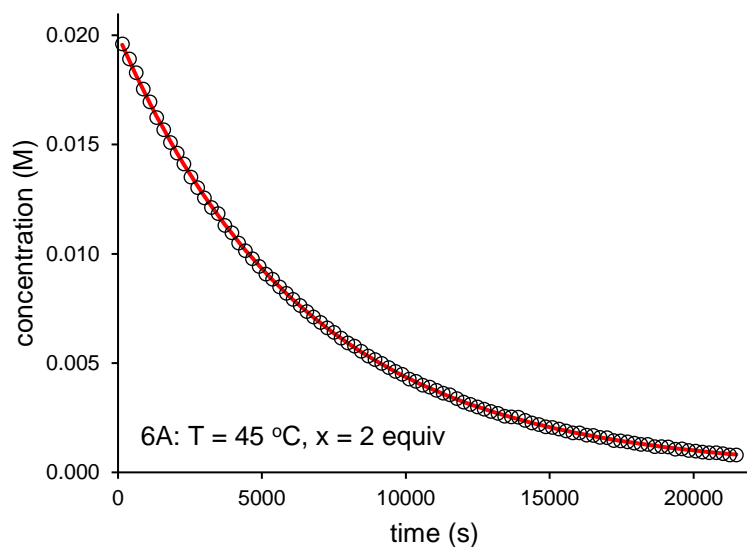


Fitted to $f(t) = I_0 * \exp(-kt) + C$
 Offset, C = 0.0000354 M
 Calculated $I_0 = 0.02028$ M
 Calculated $k = 0.0002942$ s⁻¹
 R-square = 1

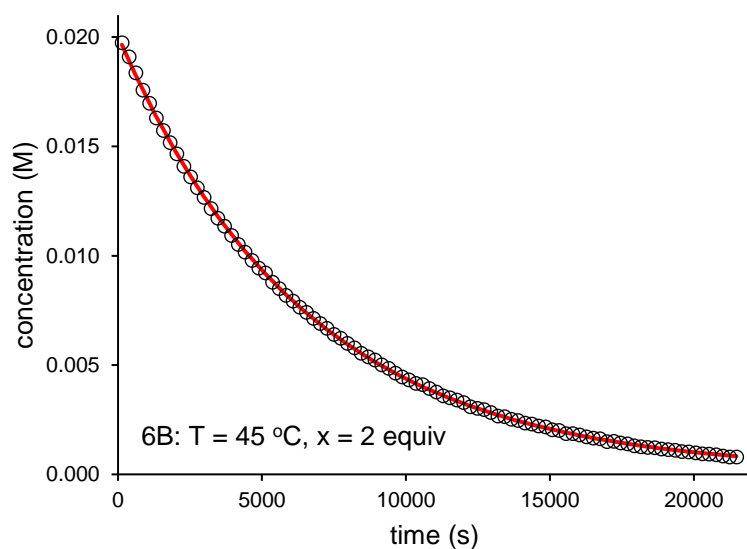


Fitted to $f(t) = I_0 * \exp(-kt)$
 Calculated $I_0 = 0.02014$ M
 Calculated $k = 0.0002966$ s⁻¹
 R-square = 0.9999

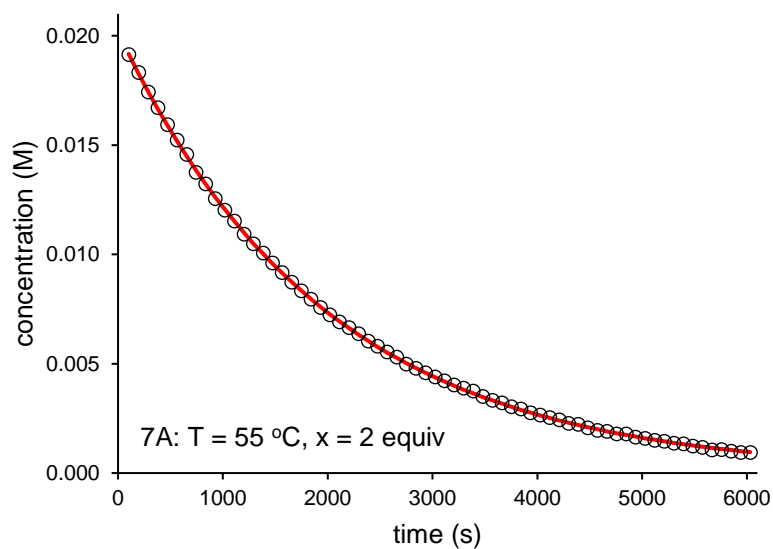




Fitted to $f(t) = I_0 * \exp(-kt) + C$
 Offset, C = 0.0000838 M
 Calculated $I_0 = 0.01992$ M
 Calculated $k = 0.0001538$ s⁻¹
 R-square = 0.9999



Fitted to $f(t) = I_0 * \exp(-kt) + C$
 Offset, C = 0.0000954 M
 Calculated $I_0 = 0.01997$ M
 Calculated $k = 0.0001540$ s⁻¹
 R-square = 0.9999



Fitted to $f(t) = I_0 * \exp(-kt)$
 Calculated $I_0 = 0.02018$ M
 Calculated $k = 0.0005052$ s⁻¹
 R-square = 0.9999

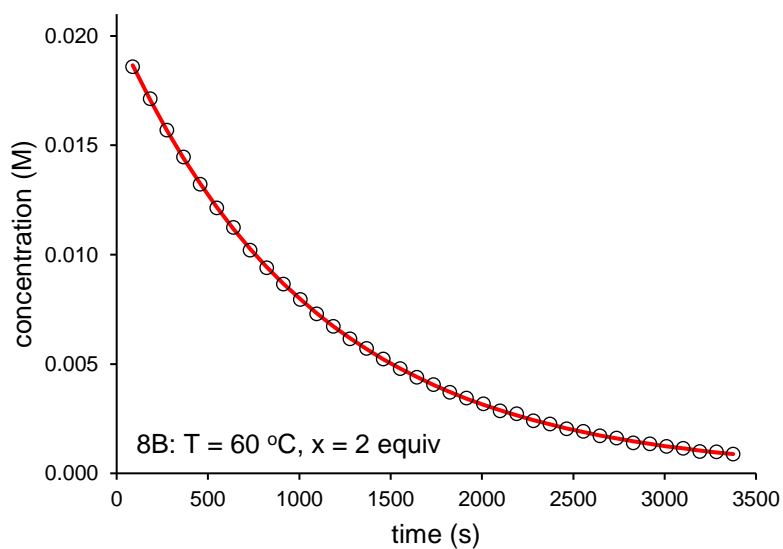
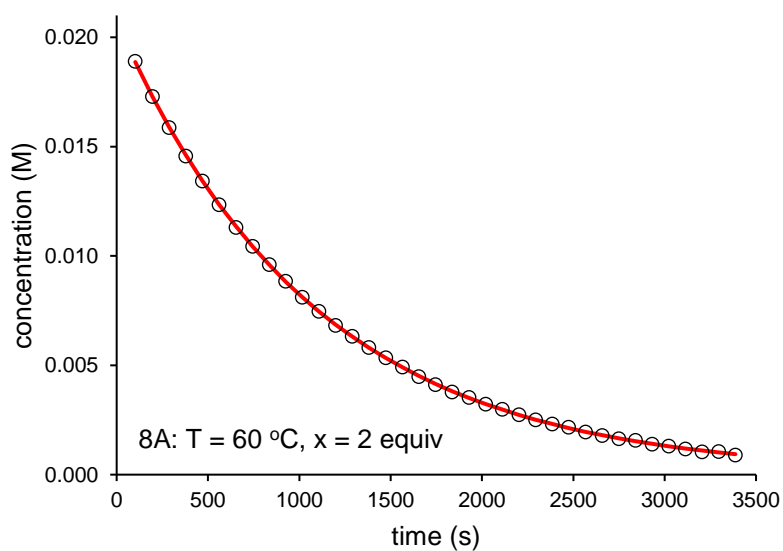
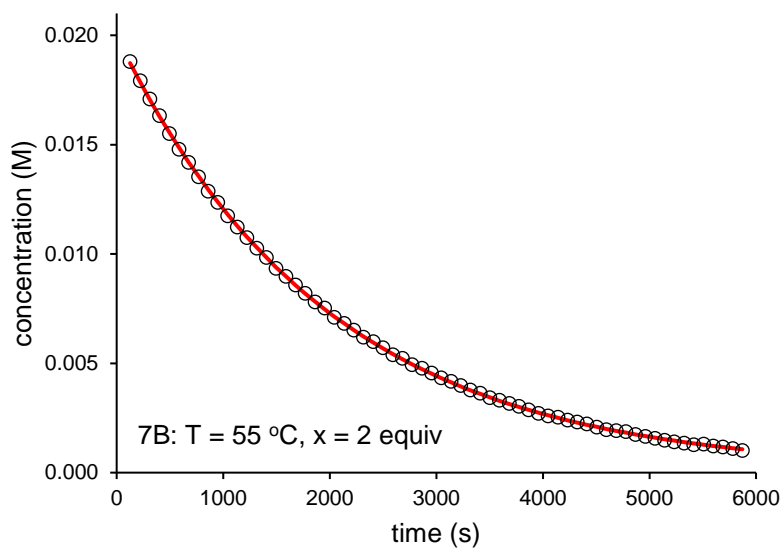


Table S-2. Rate of decay of Pd^{IV} complex **370**: varying T and nucleophile **369** equivalency.

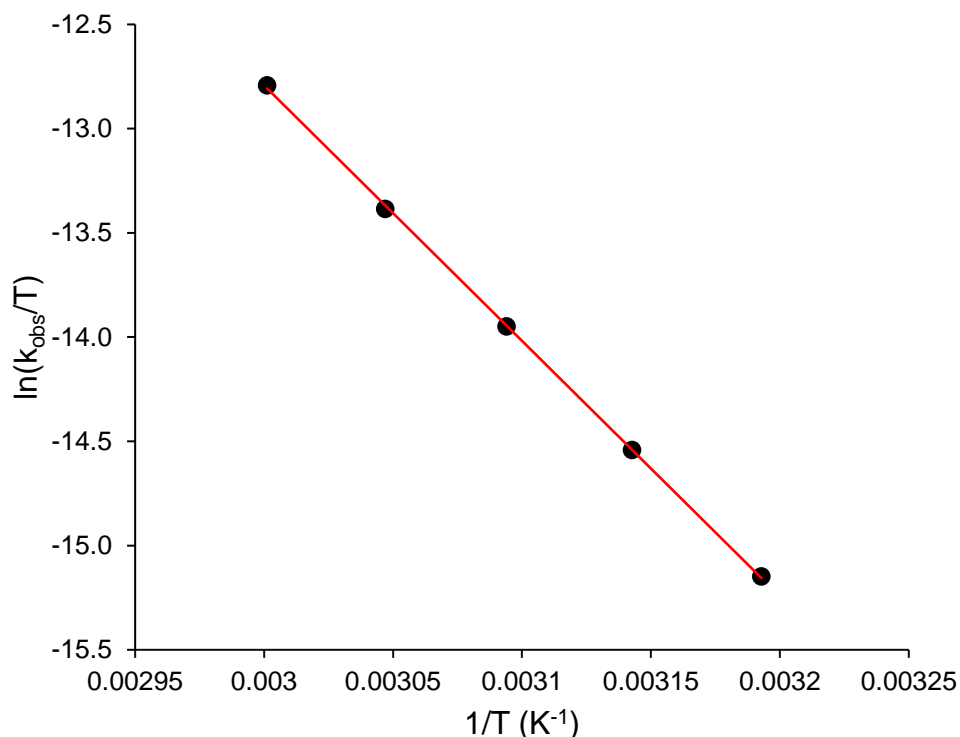
Entry	Temperature (T, °C)	369 (x, equiv)	k _{obs} (s ⁻¹)
1A	50	2	0.0002850
1B	50	2	0.0002810
2	50	4	0.0002942
3	50	6	0.0002966
4	50	8	0.0003044
5A	40	2	0.00008276
5B	40	2	0.00008242
6A	45	2	0.0001538
6B	45	2	0.0001540
7A	55	2	0.0005052
7B	55	2	0.0005049
8A	60	2	0.0009249
8B	60	2	0.0009291

Temperature Dependence and Determination of Activation Parameters

Reactions employing 2 equivalents of tetrabutylammonium *p*-nitrophenoxide **369** at 40–60 °C (5 °C intervals) were run in duplicate (Entries 1 & 5–8, Table S-2). The average k_{obs} values were calculated, and a plot of ln(k_{obs}/T) versus 1/T generated (Table S-3).

Table S-3. Temperature dependence of reaction rate.

T (°C)	T (K)	Mean k _{obs} (s ⁻¹)	1/T (K ⁻¹)	ln(k _{obs} /T)
40	313.2	0.00008259	0.003193	−15.15
45	318.2	0.0001539	0.003143	−14.54
50	323.2	0.0002830	0.003094	−13.95
55	328.2	0.00050505	0.003047	−13.38
60	333.2	0.0009270	0.003001	−12.79



Slope = $-12250.67954 (\pm 91.92440092)$

y-Intercept = $23.95939579 (\pm 0.282603919)$

$R^2 = 0.9998$.

Calculated activation parameters:

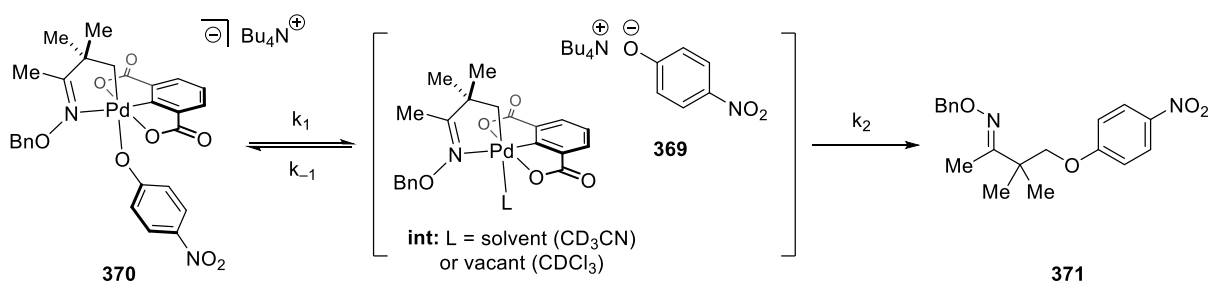
$\Delta H^\ddagger = -(\text{slope}) * R = +24.3 \pm 0.2 \text{ kcal mol}^{-1}$

$\Delta S^\ddagger = R * [\text{y-intercept} - \ln(k_b/h)] = +0.4 \pm 0.6 \text{ cal K}^{-1} \text{ mol}^{-1}$

Kinetics of Thermal Decomposition of **370** in CDCl_3

To a vial containing Pd^{IV} complex **366b** (4.9 mg, 0.01 mmol 1 equiv) and tetrabutylammonium *p*-nitrophenoxide **369** (7.6 mg, 0.02 mmol, 2 equiv) were added CDCl_3 (1 mL), anisole (ca. 1 μL , internal standard) and pyridine (0, 1, or 3 equiv). The solution was transferred to a screw-top NMR tube and inserted into a pre-heated NMR spectrometer (50 °C). ^1H NMR spectra were recorded at fixed time intervals over 8000 s. The formation of **371** was monitored by integrating the peak at 4.01 ppm relative to the internal standard. Plots of concentration versus time showed that increasing equivalency of pyridine reduces the rate of reductive elimination (see Section 4.2.3. Figure 11).

Derivation of Rate Law for C–O Reductive Elimination from 370



$$\text{rate} = \frac{d[\mathbf{371}]}{dt} = k_2[\text{int}][\mathbf{369}]$$

$$\frac{d[\text{int}]}{dt} = k_1[\mathbf{370}] - k_{-1}[\text{int}][\mathbf{369}] - k_2[\text{int}][\mathbf{369}] \approx 0 \quad (\text{steady-state approx.})$$

$$[\text{int}] = \frac{k_1[\mathbf{370}]}{(k_{-1} + k_2)[\mathbf{369}]}$$

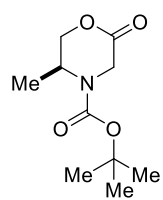
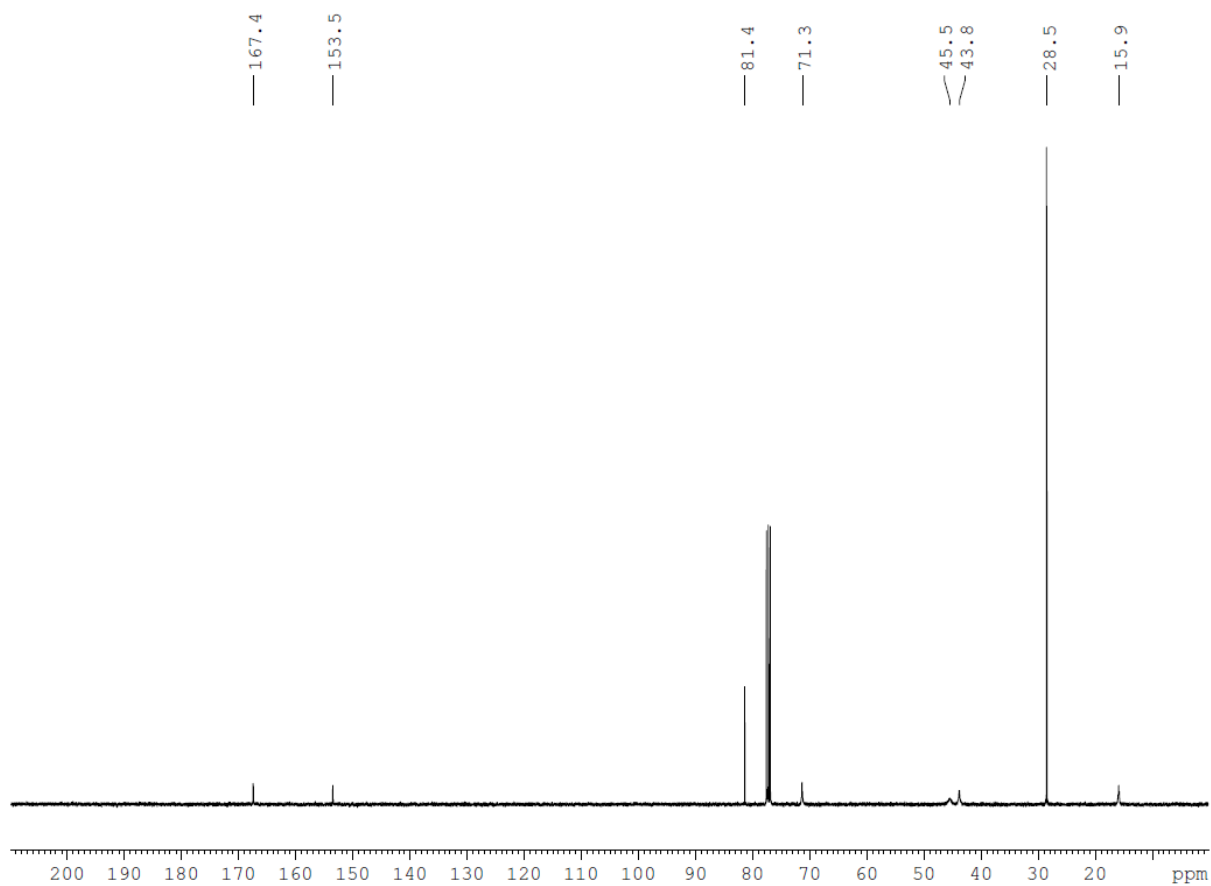
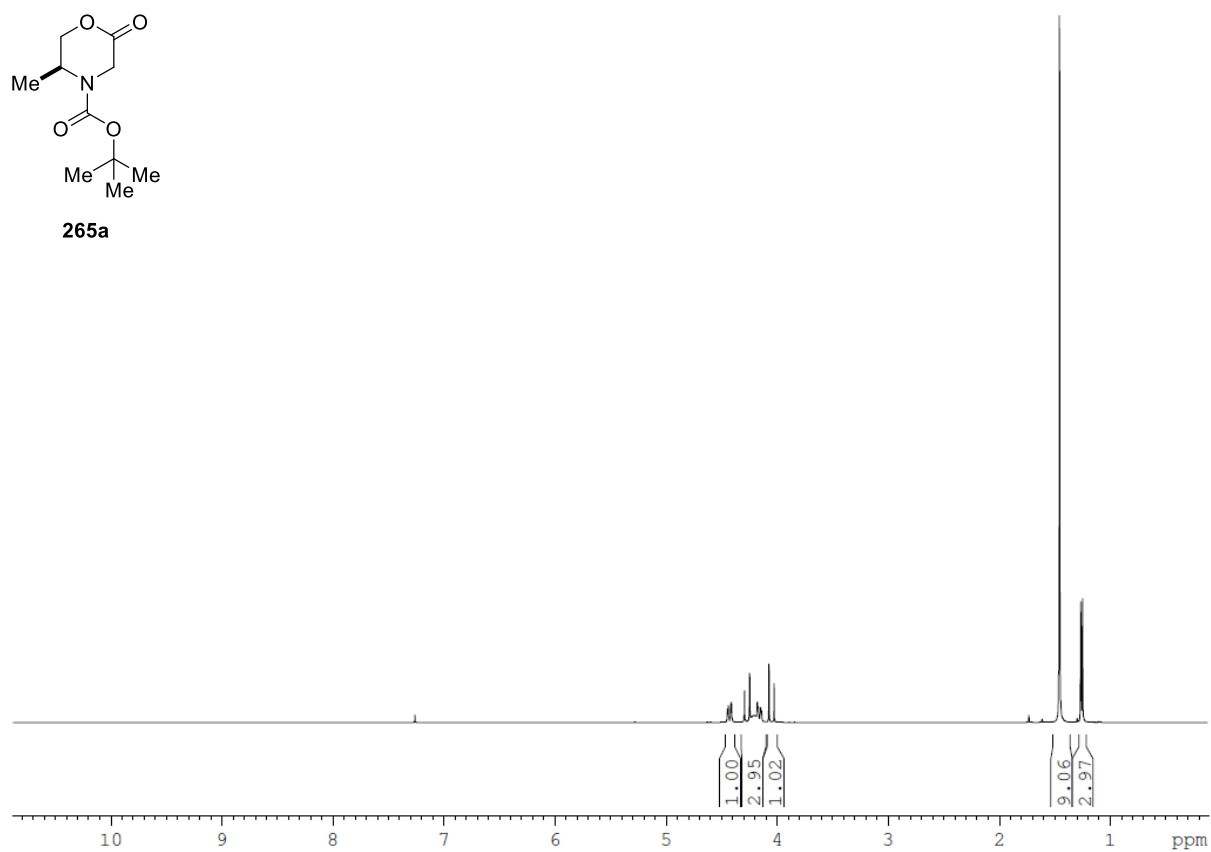
$$\therefore \text{rate} = \frac{k_1 k_2 [\mathbf{370}][\mathbf{369}]}{(k_{-1} + k_2)[\mathbf{369}]} = \frac{k_1 k_2 [\mathbf{370}]}{(k_{-1} + k_2)}$$

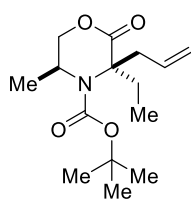
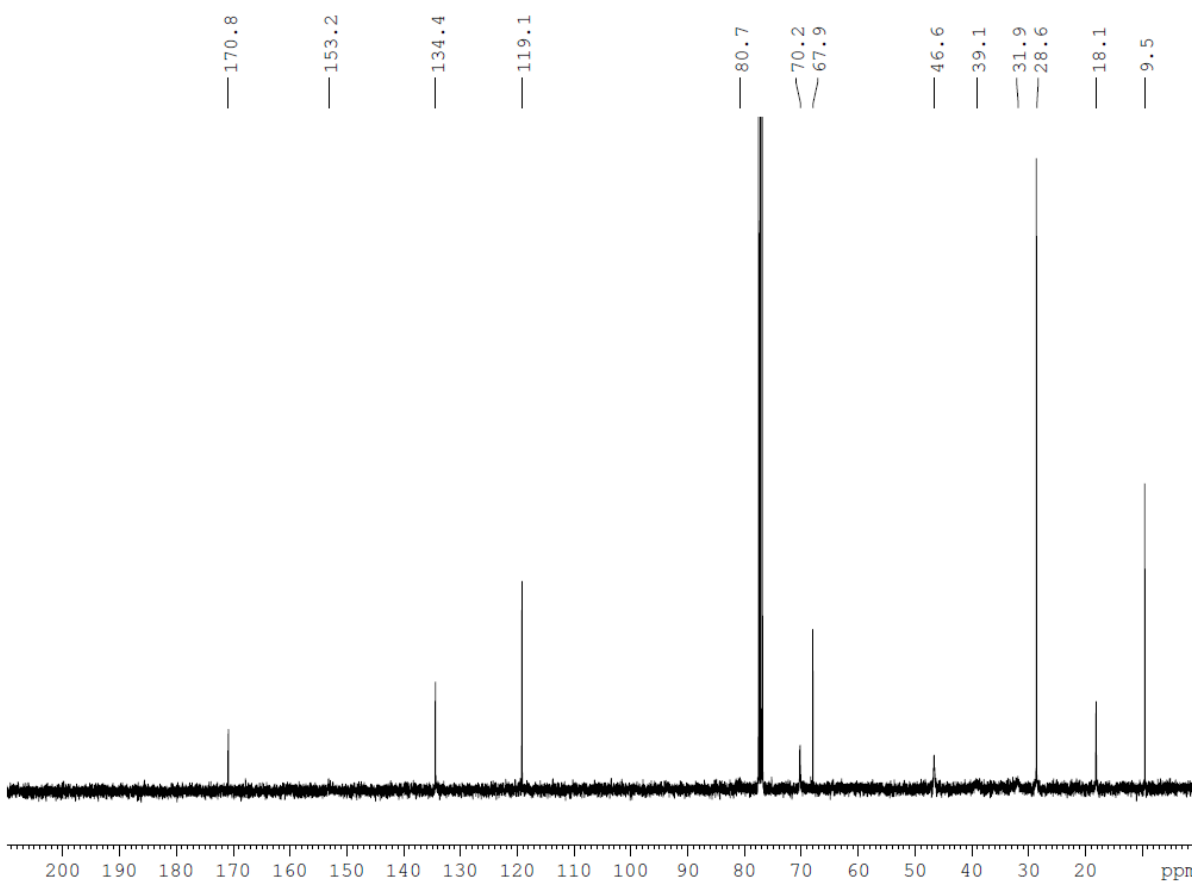
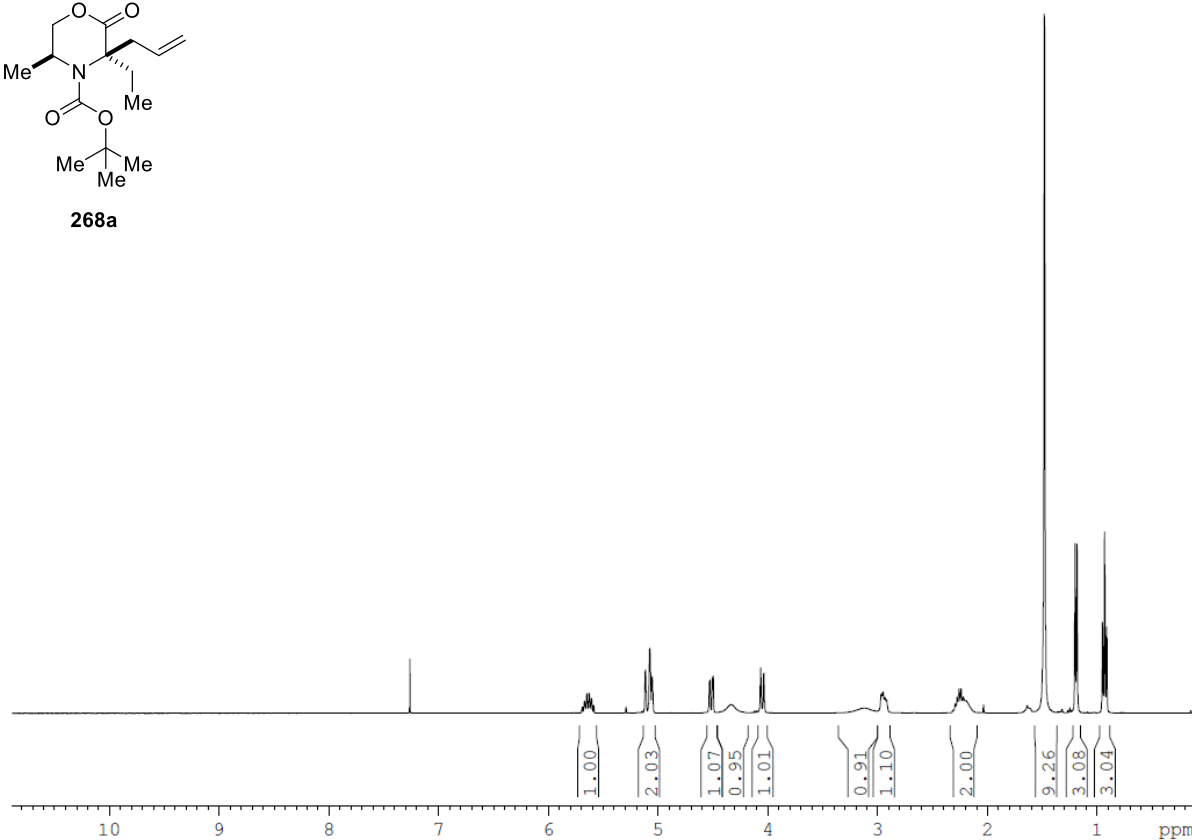
Assuming that $k_{-1} \gg k_2$, then:

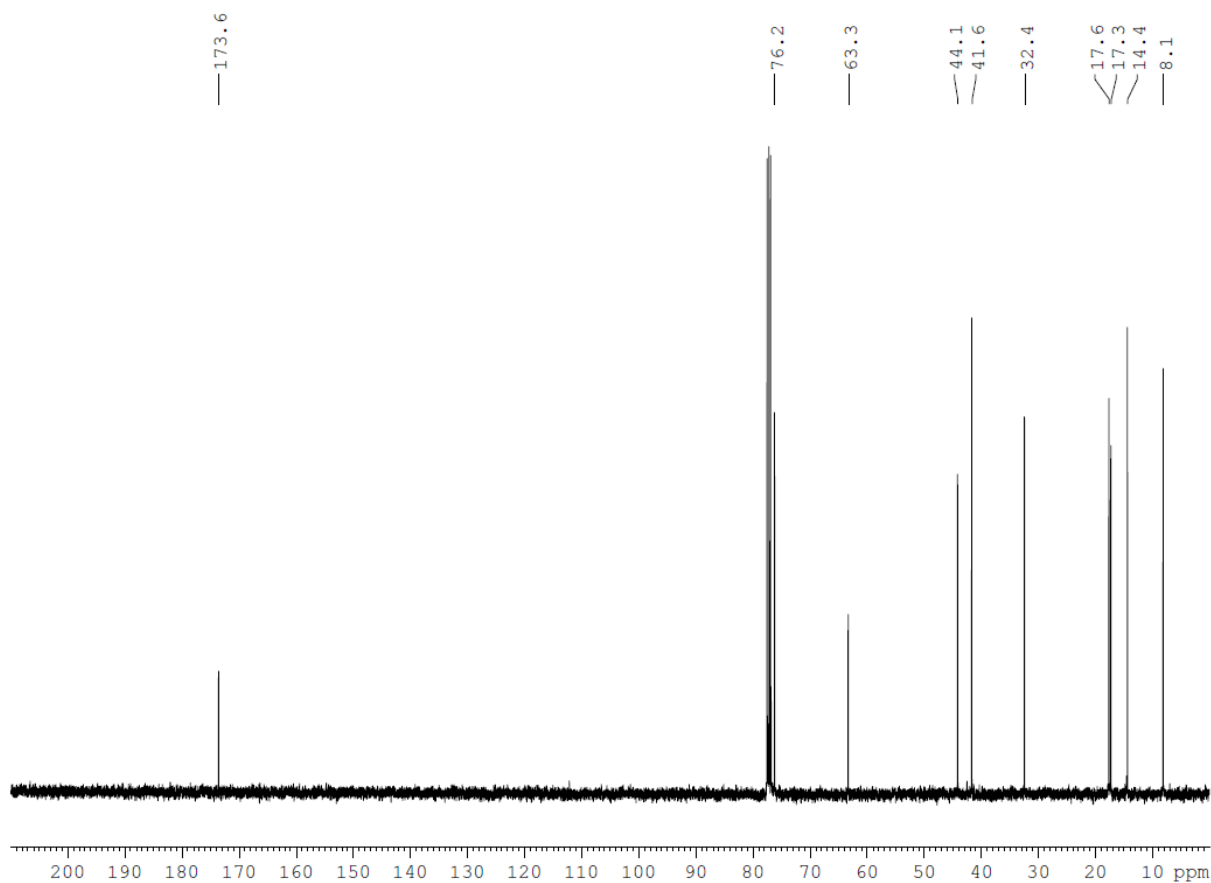
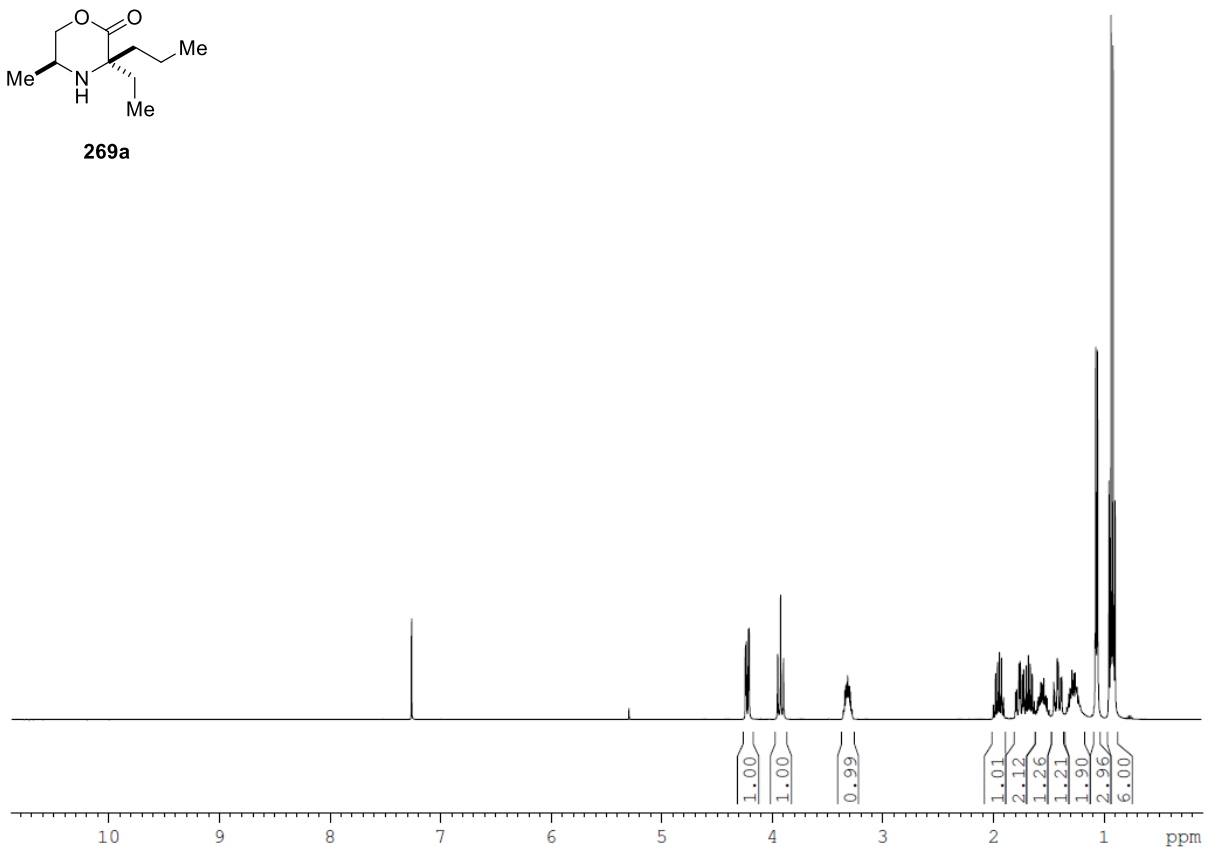
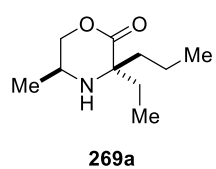
$$\text{rate} = \frac{k_1 k_2 [\mathbf{370}]}{k_{-1}} = K_{eq} k_2 [\mathbf{370}]$$

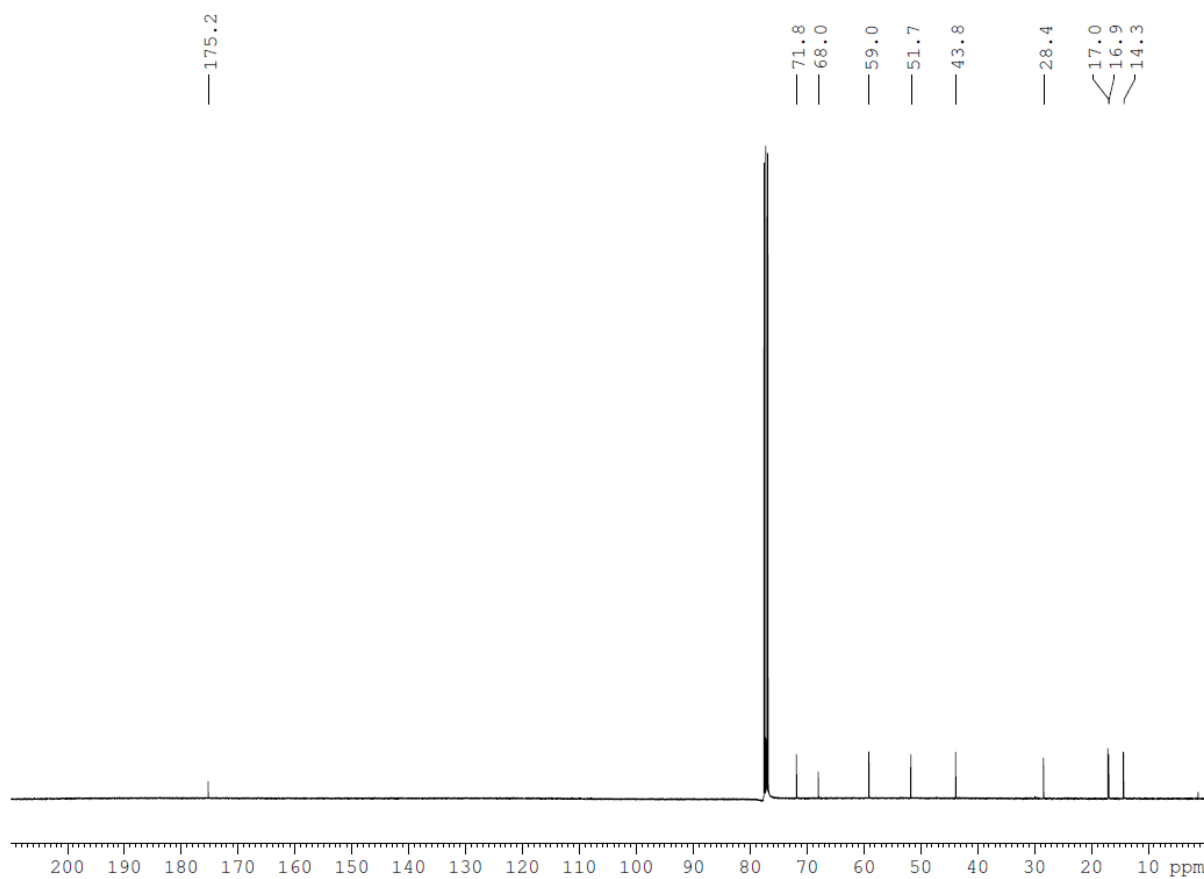
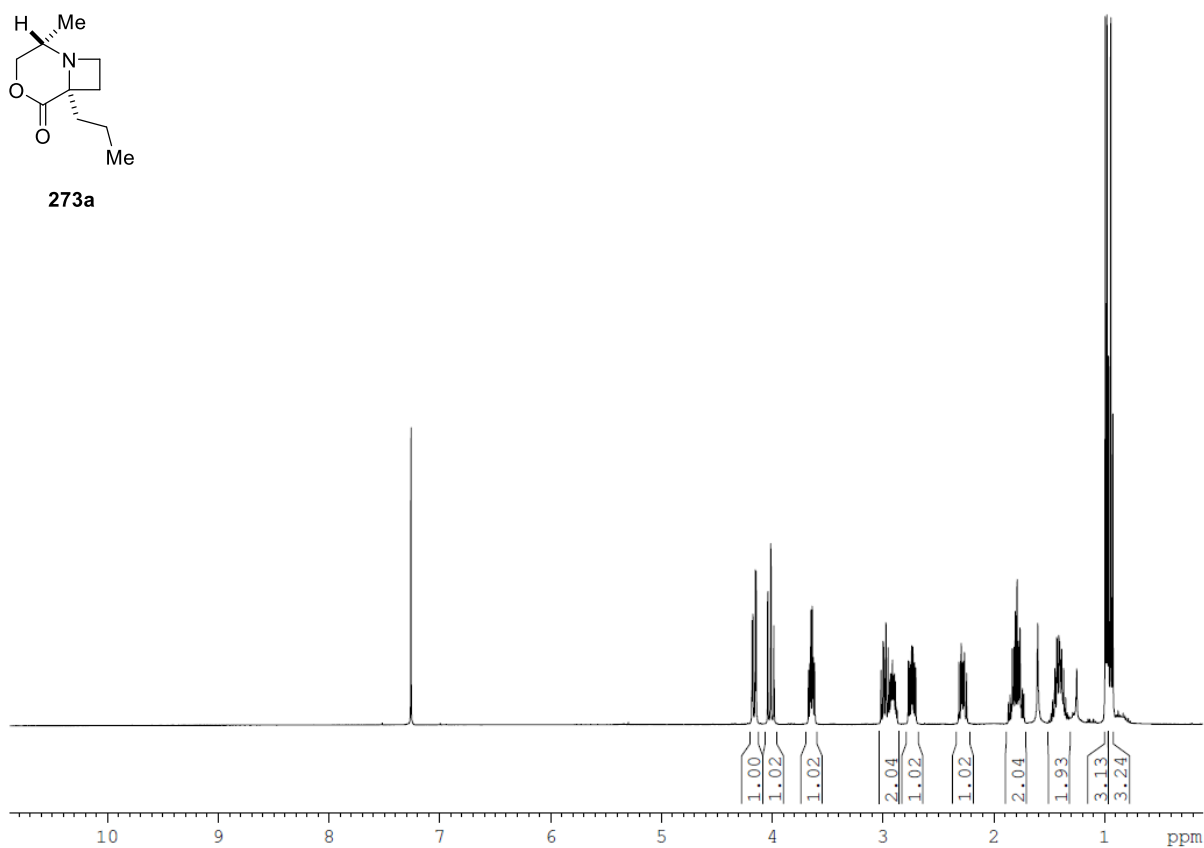
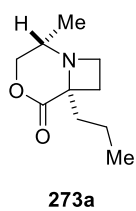
Appendix III: ^1H , ^{13}C and ^{19}F NMR Spectra

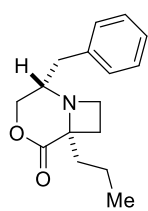
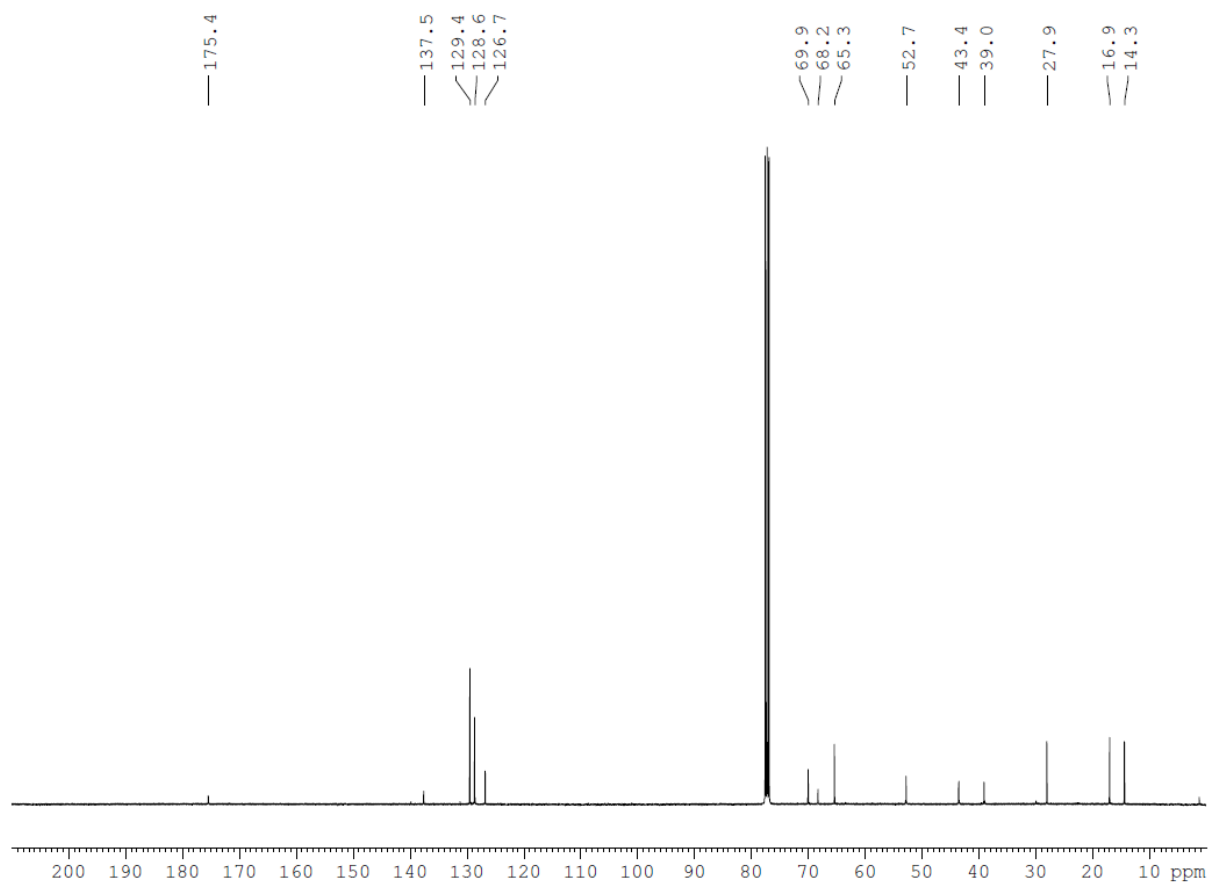
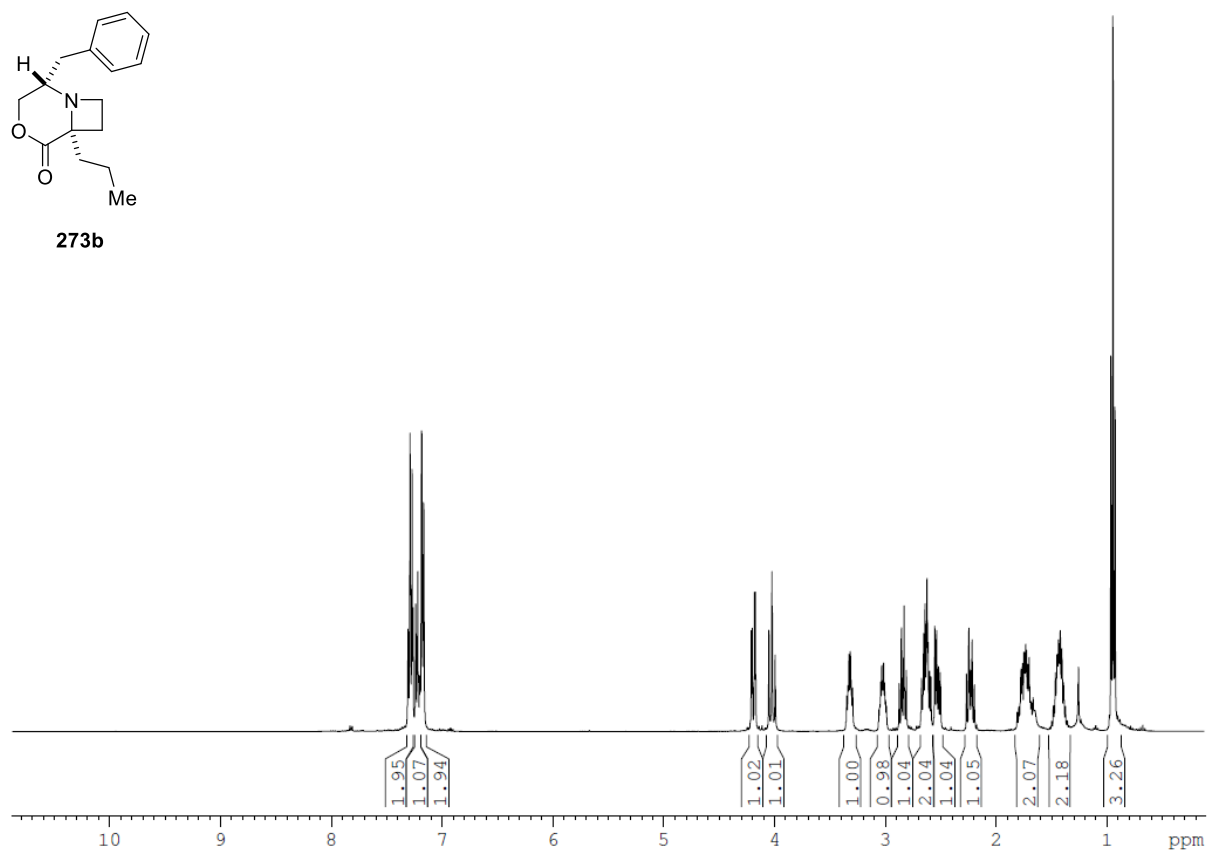
Synthesized Compounds from the Experimental Section

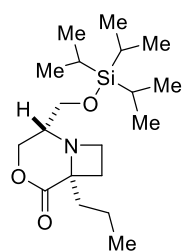
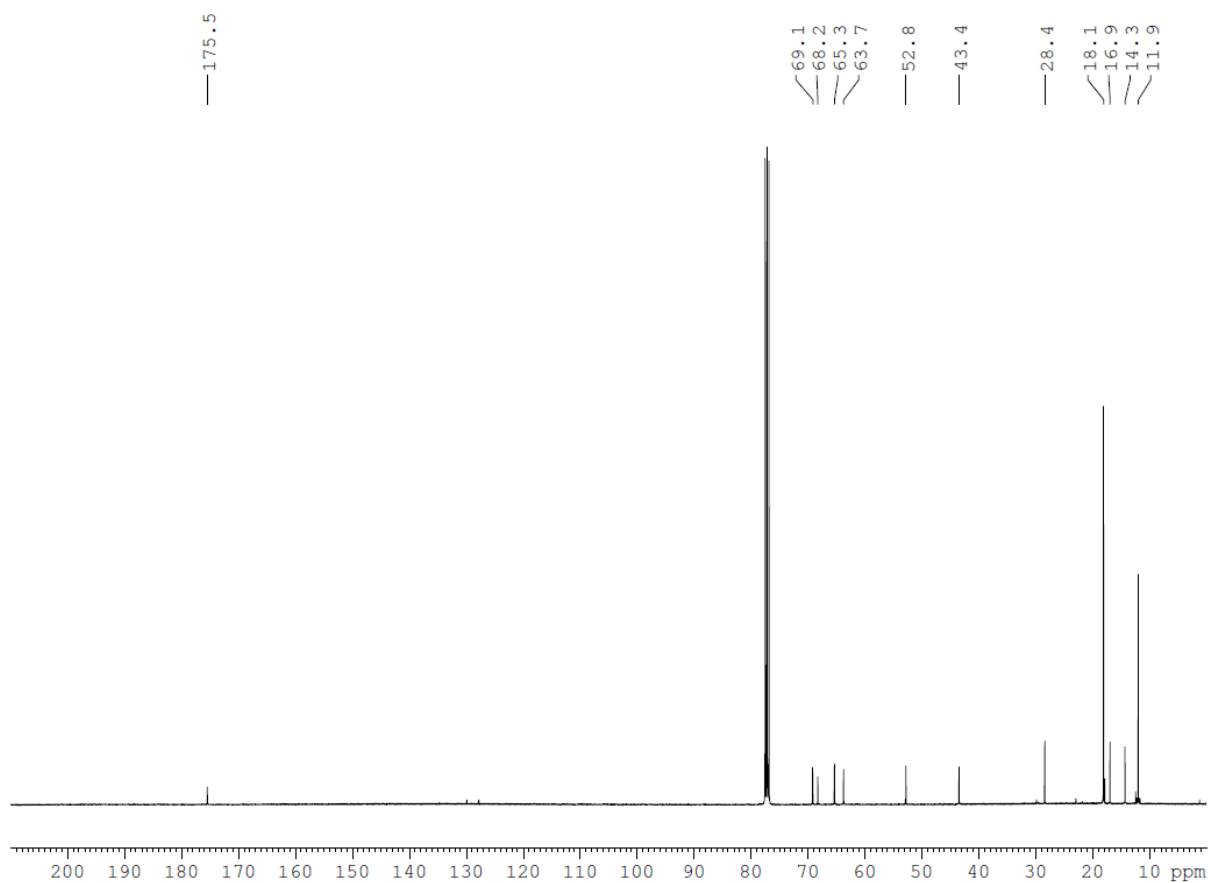
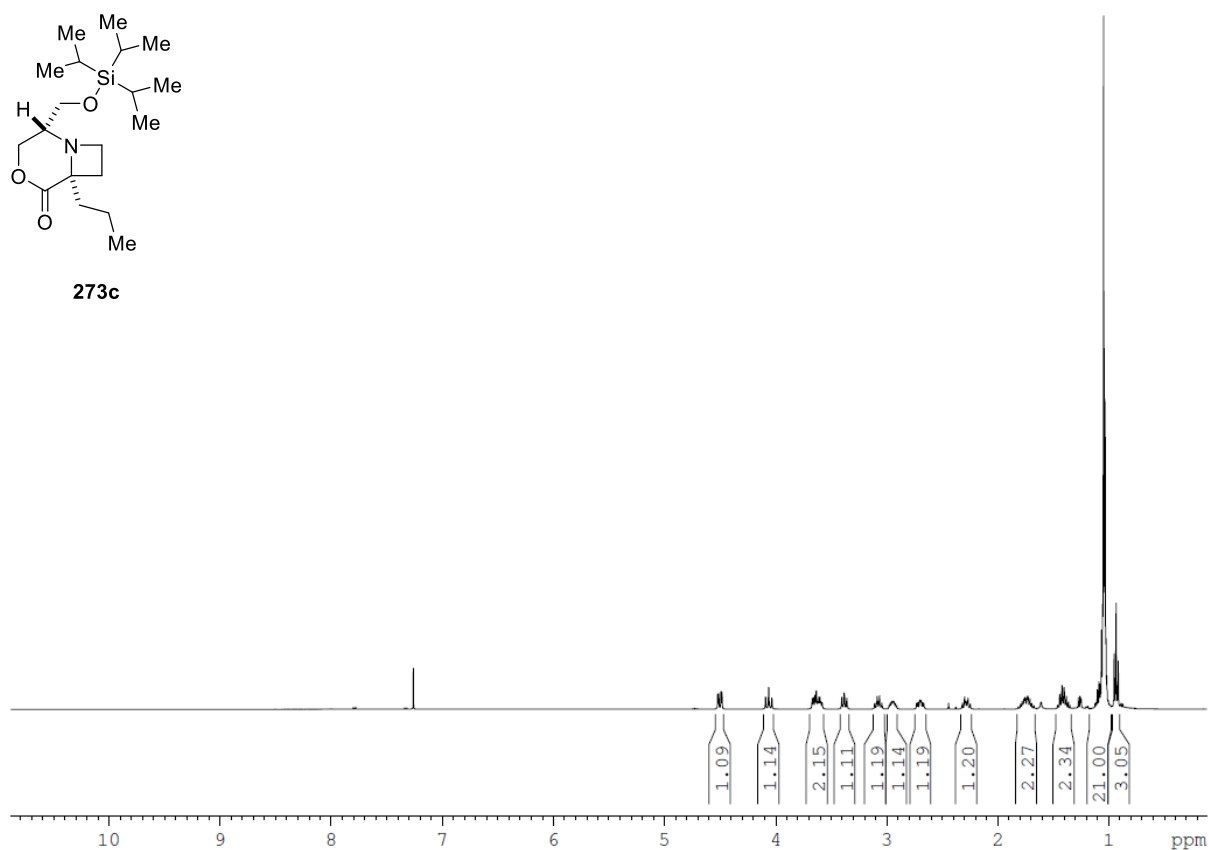
**265a**

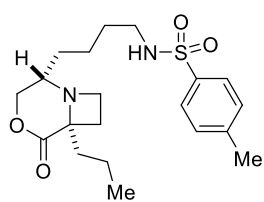
**268a**



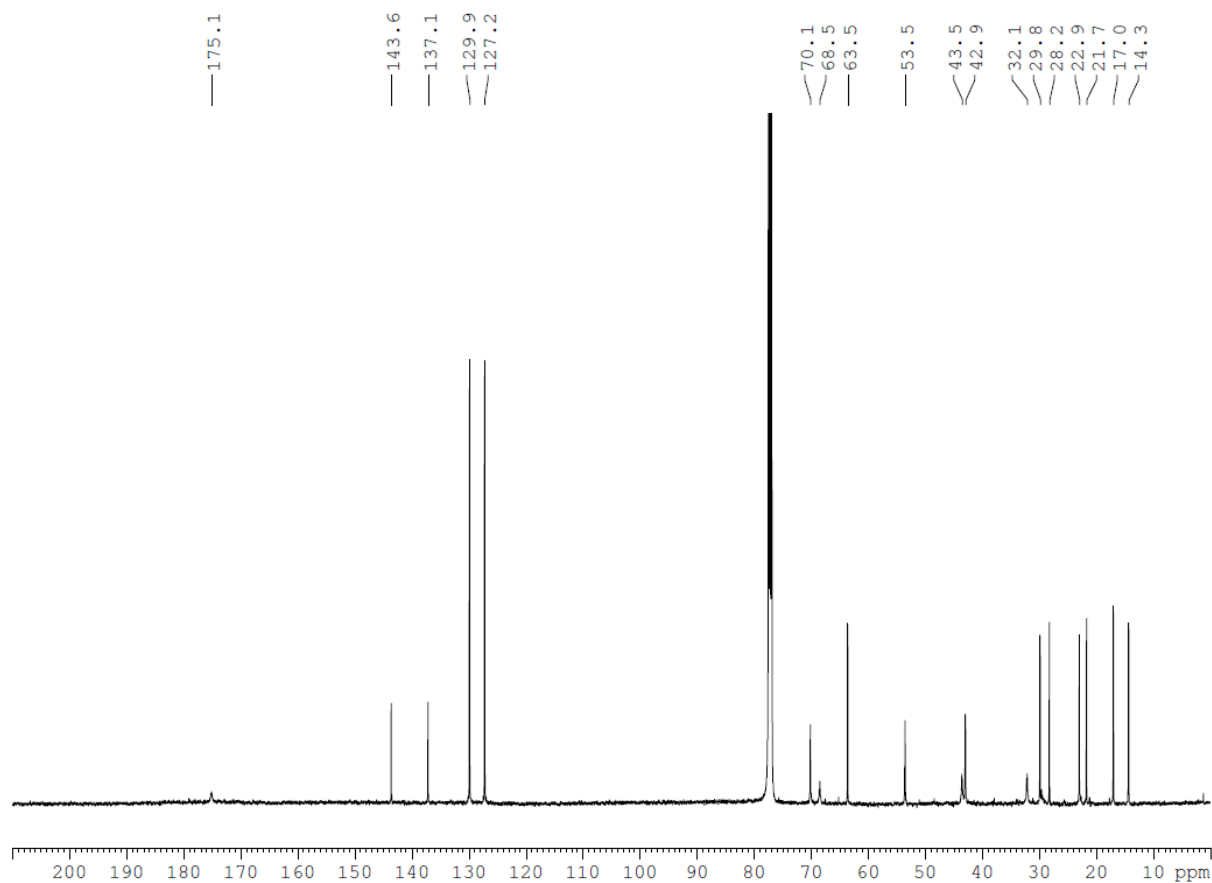
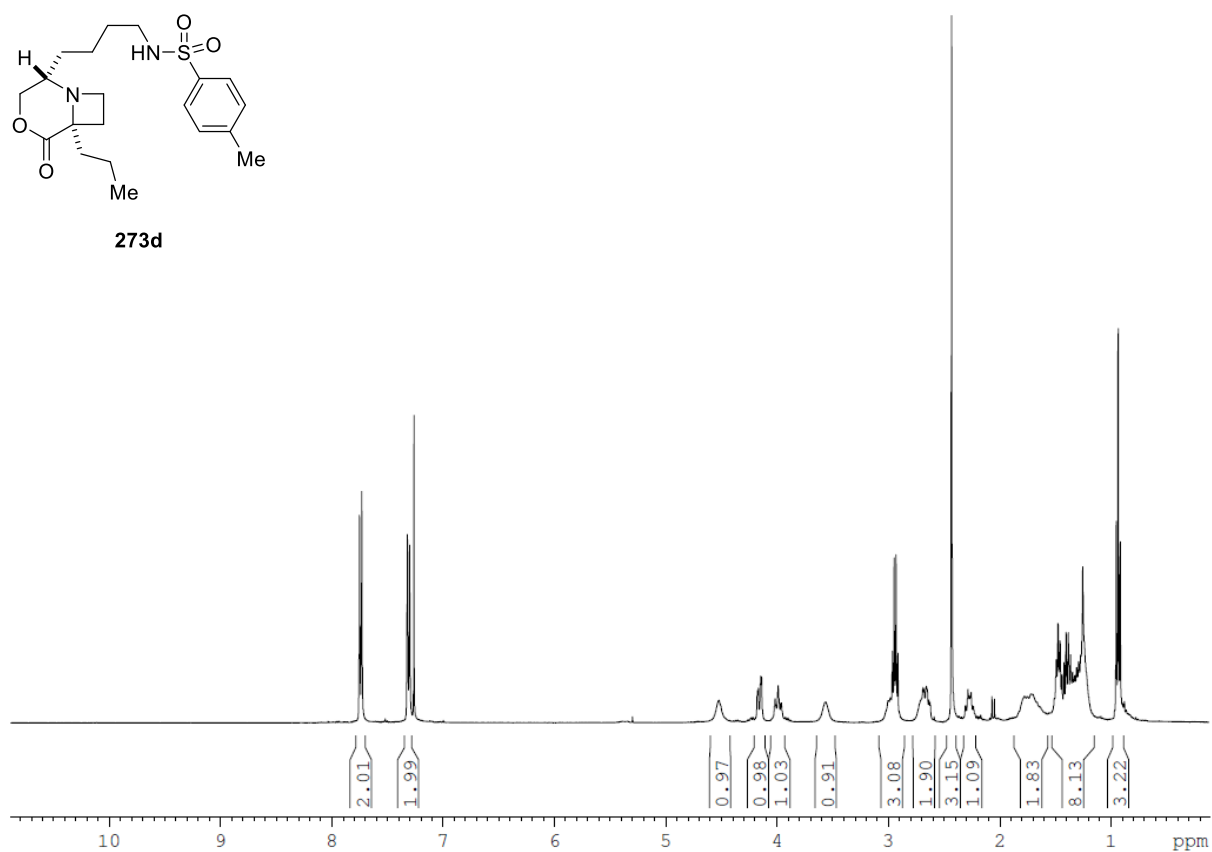


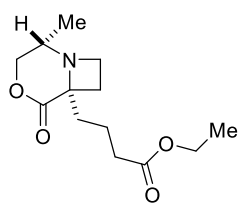
**273b**

**273c**

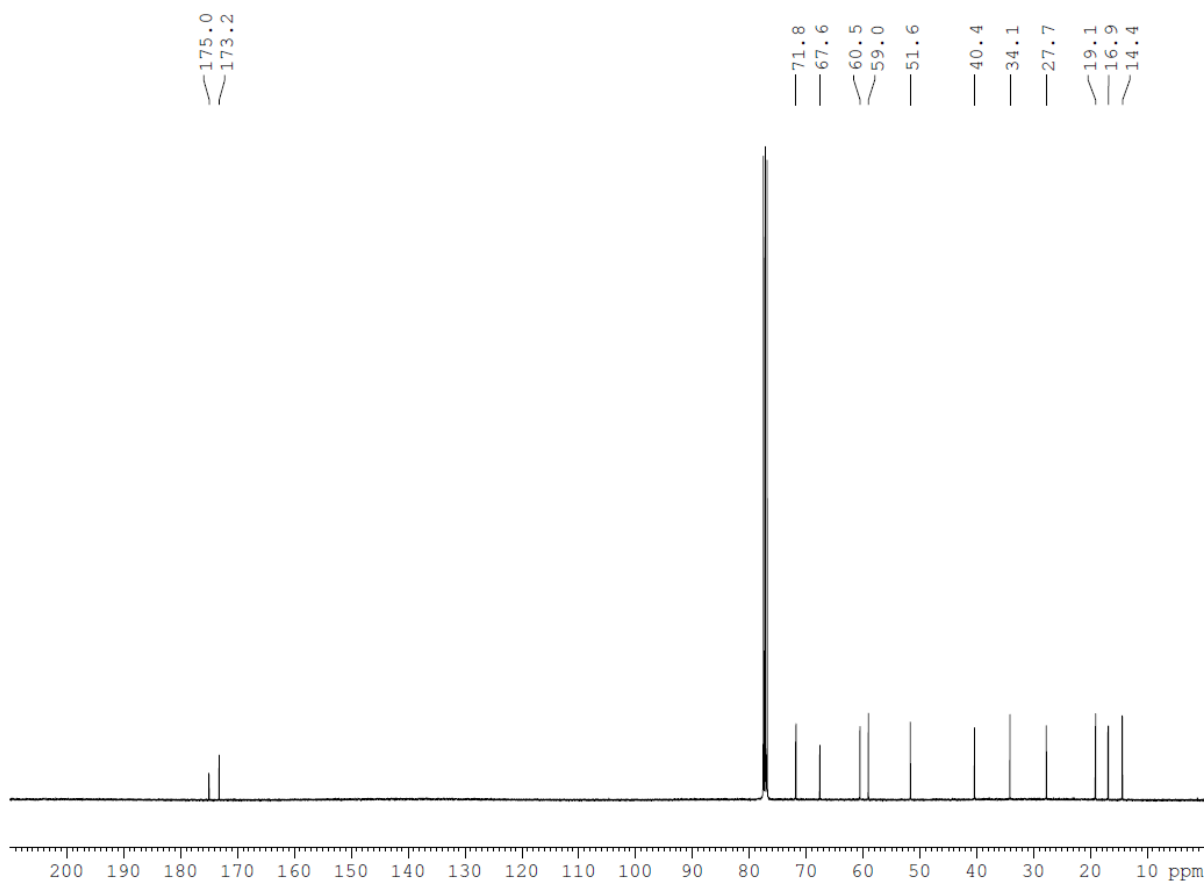
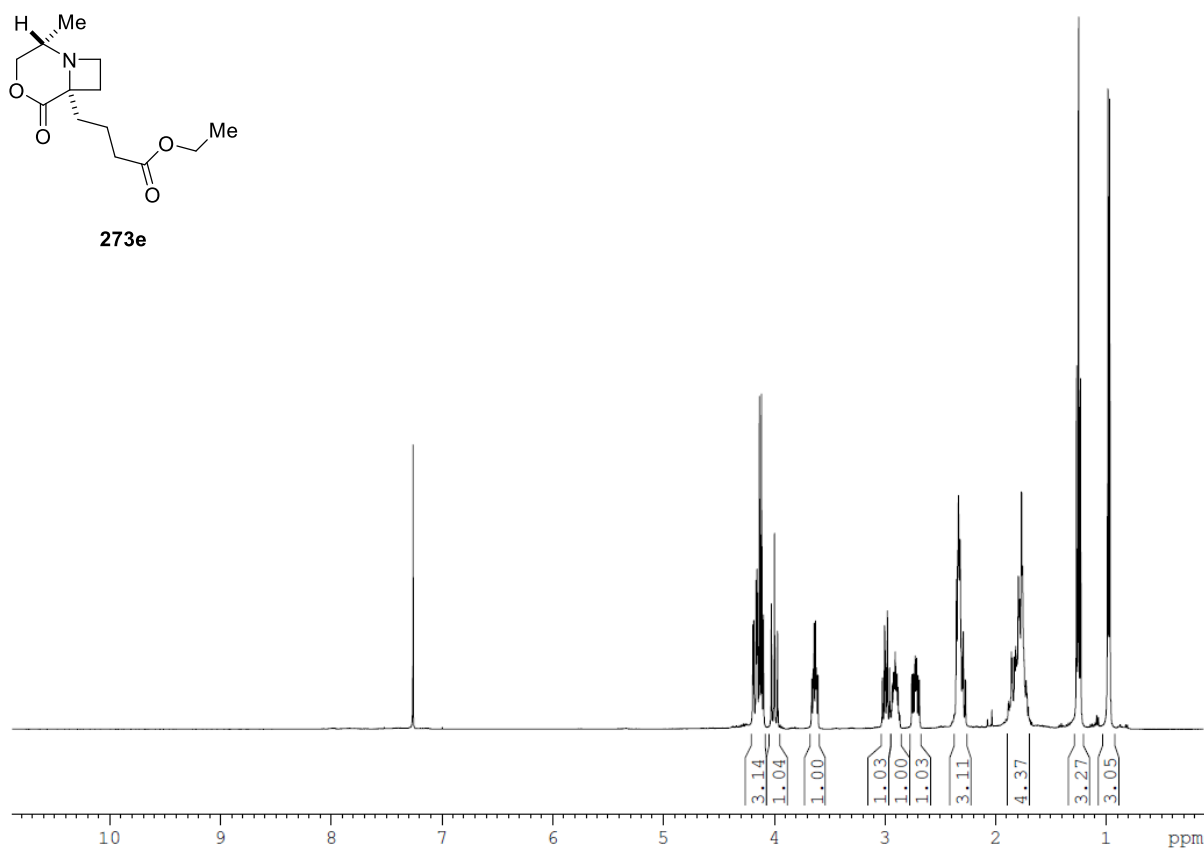


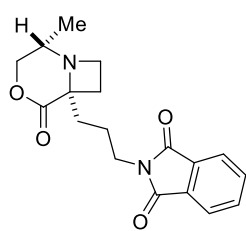
273d



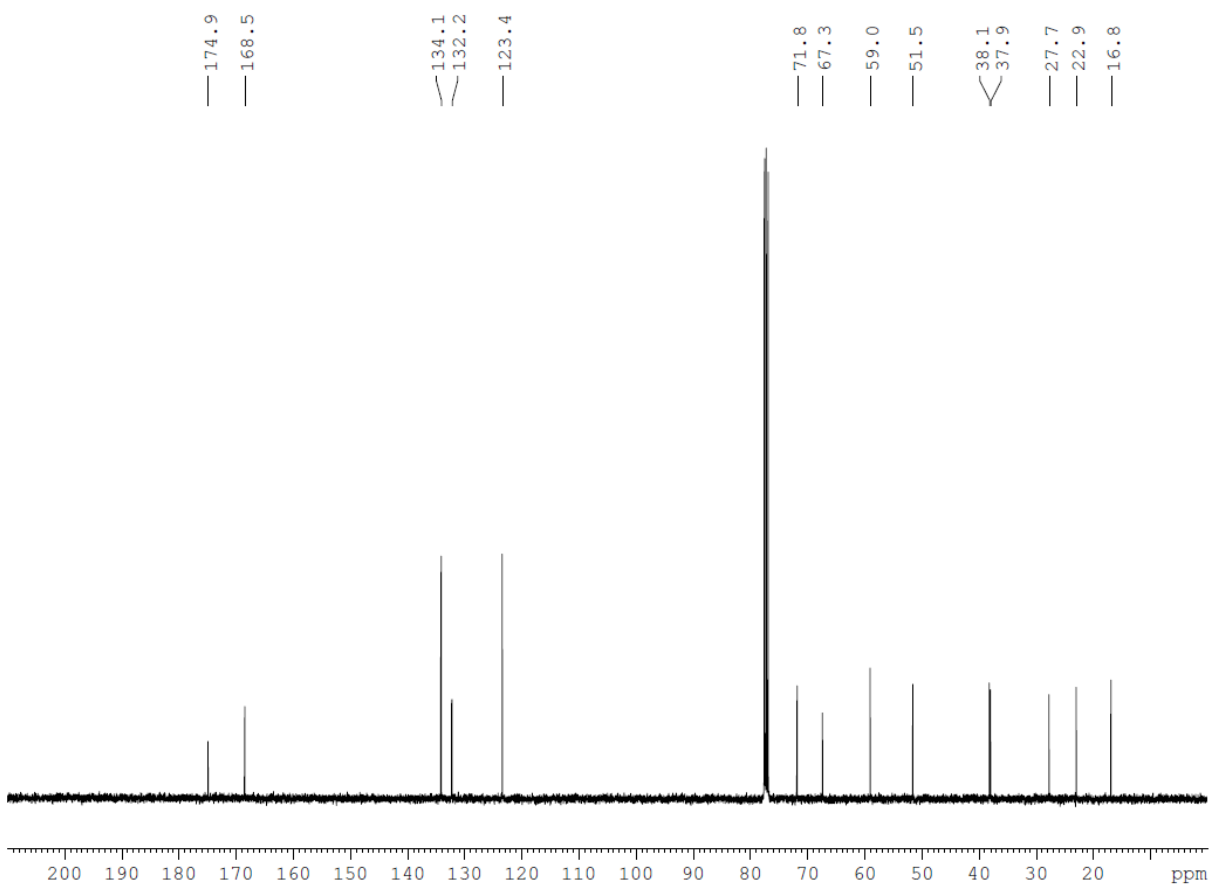
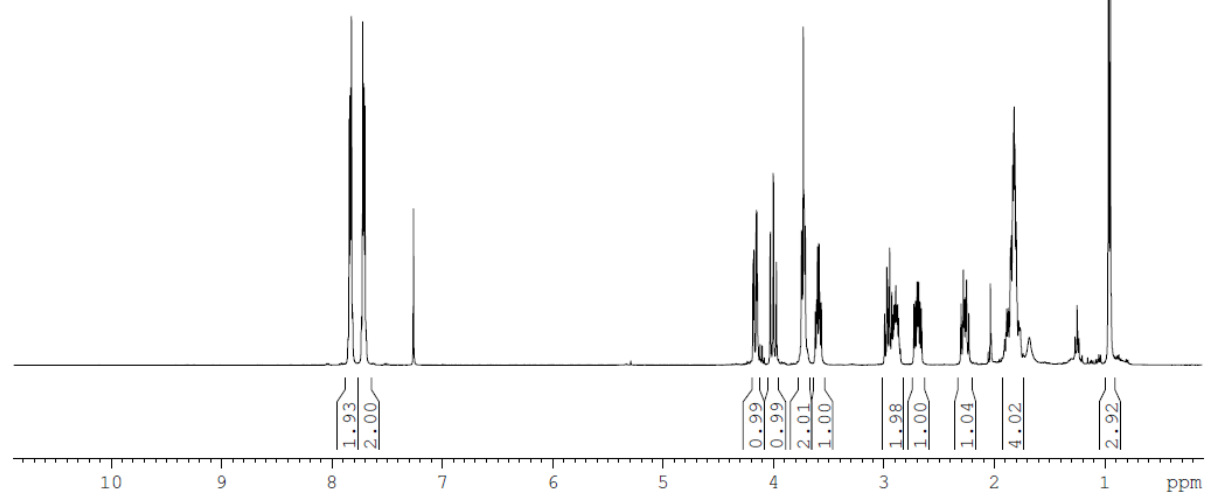


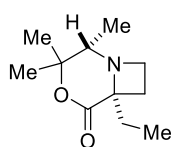
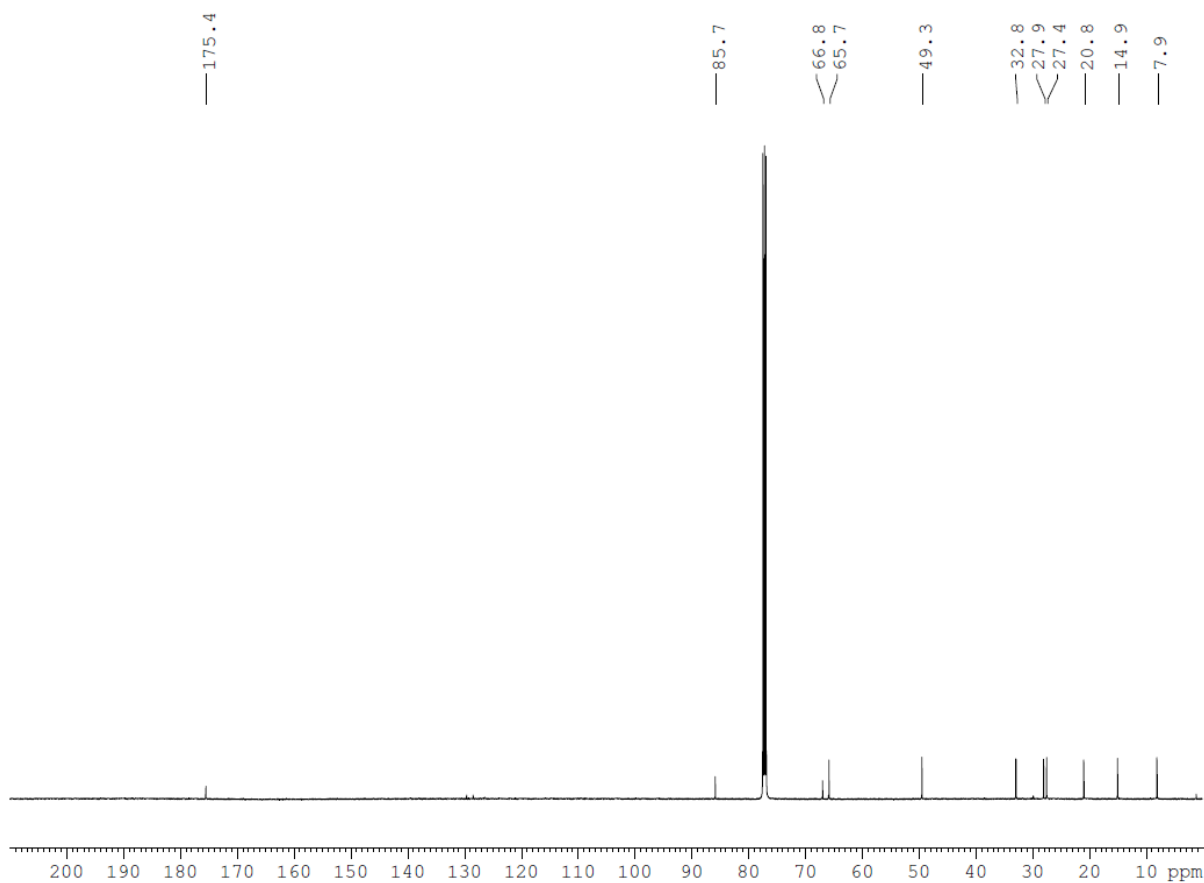
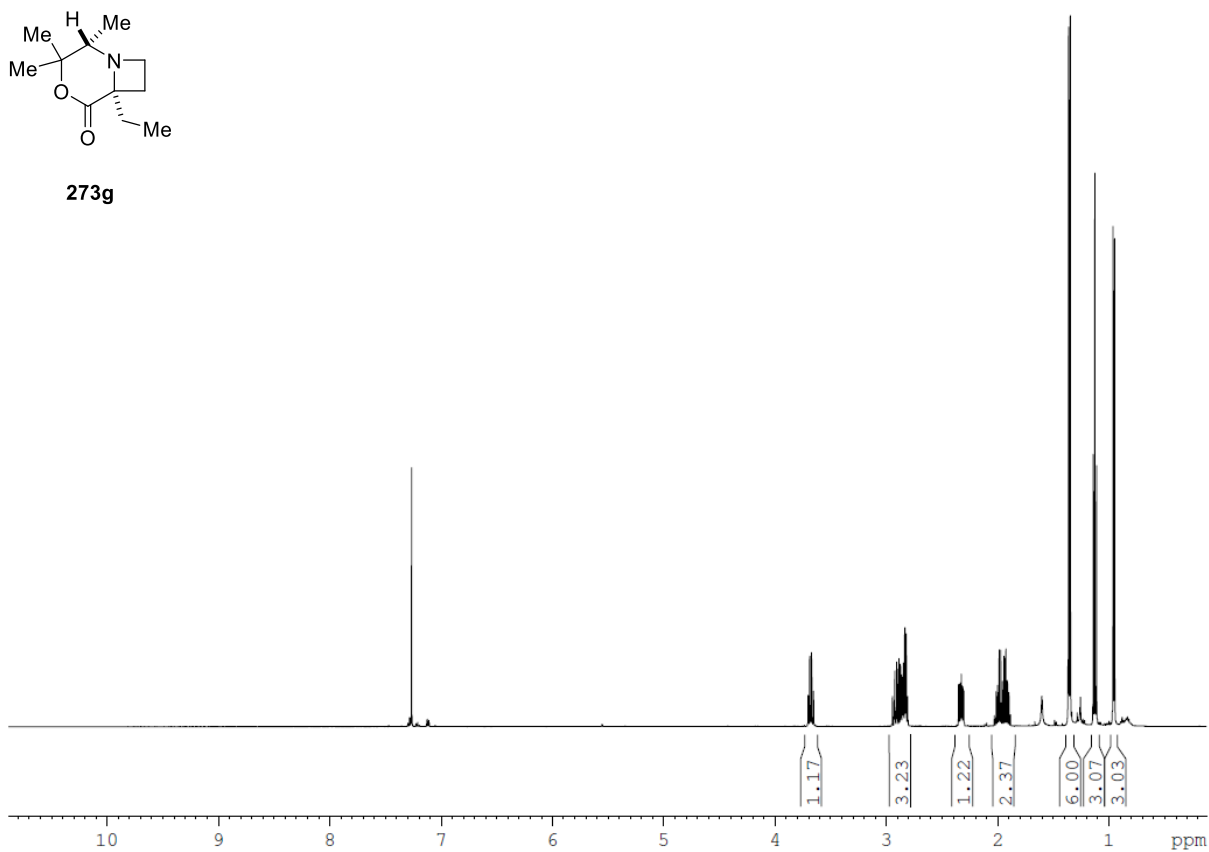
273e

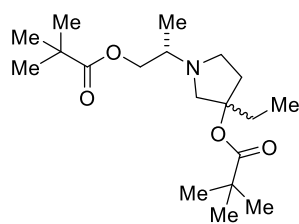




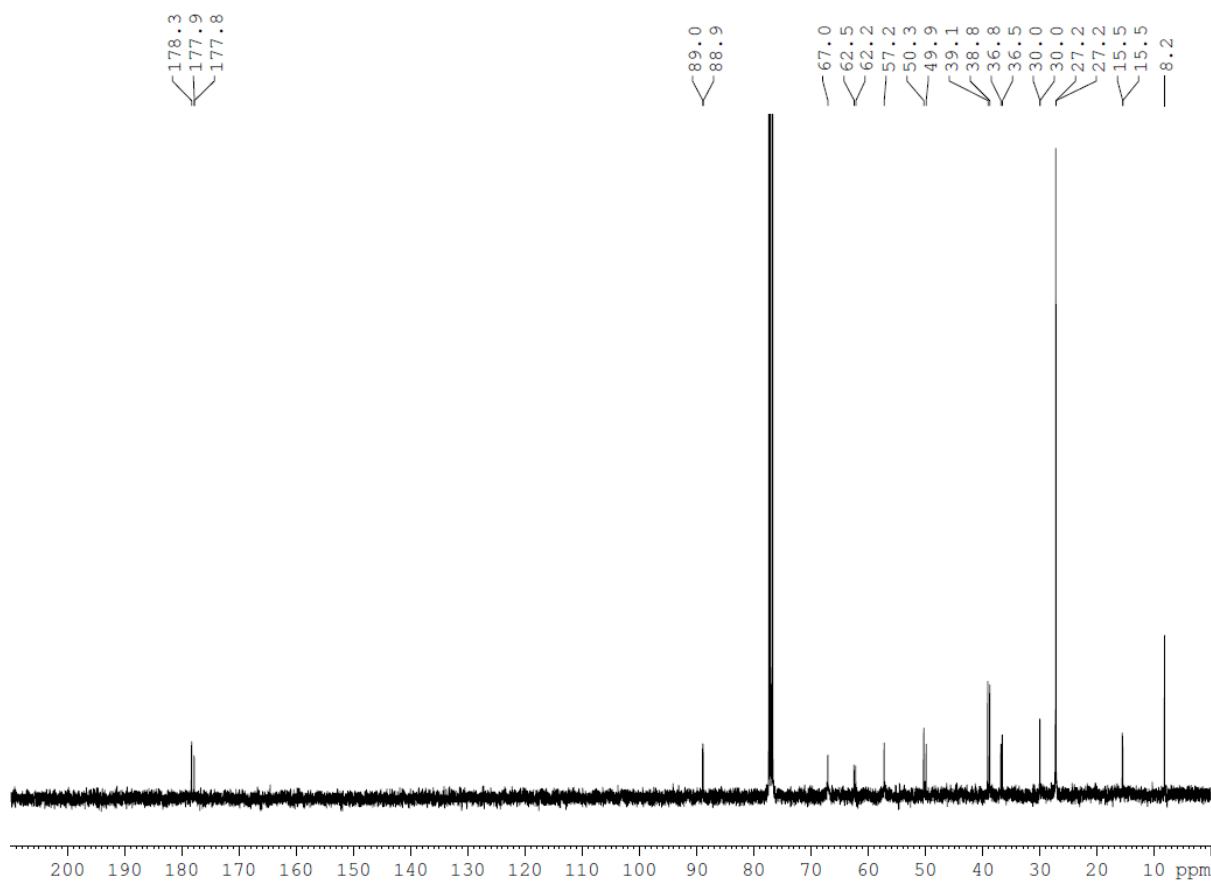
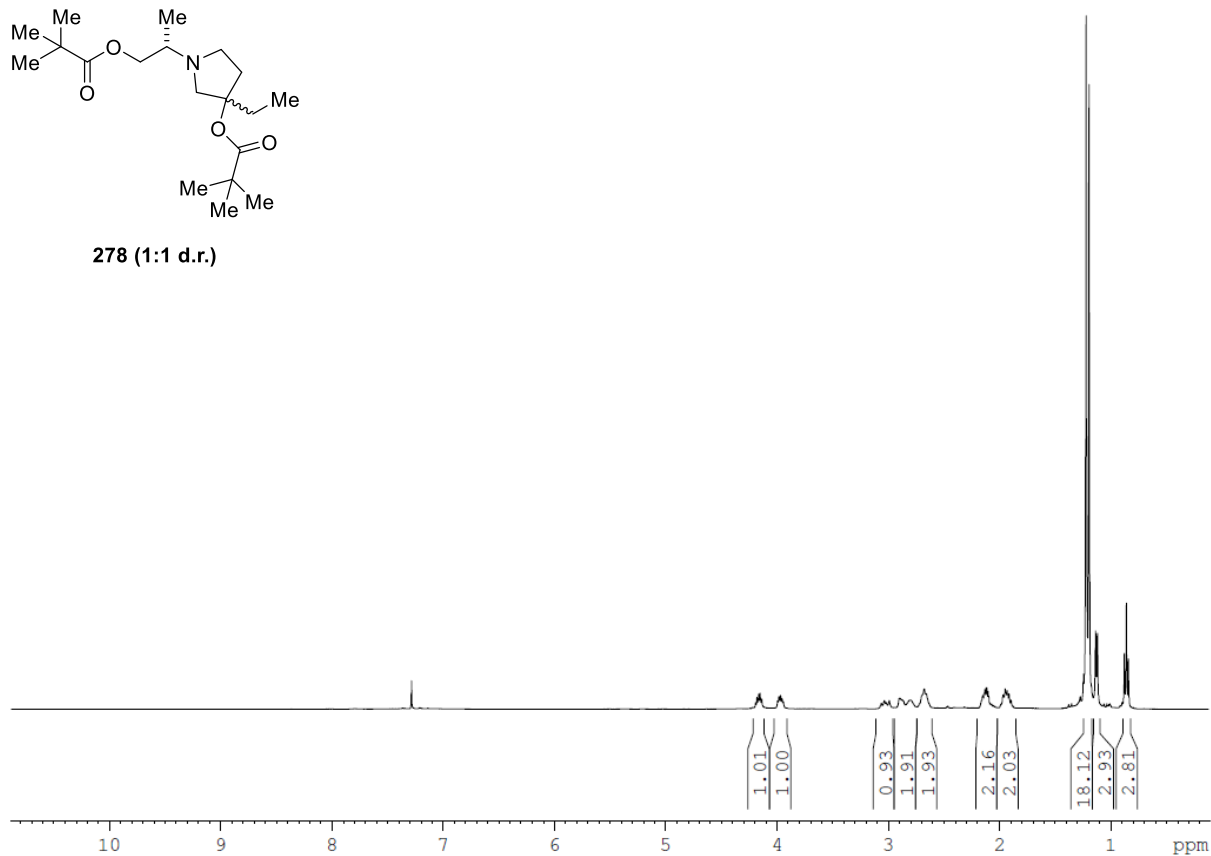
273f

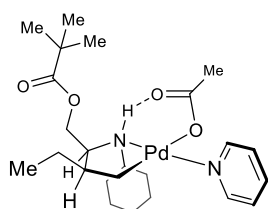
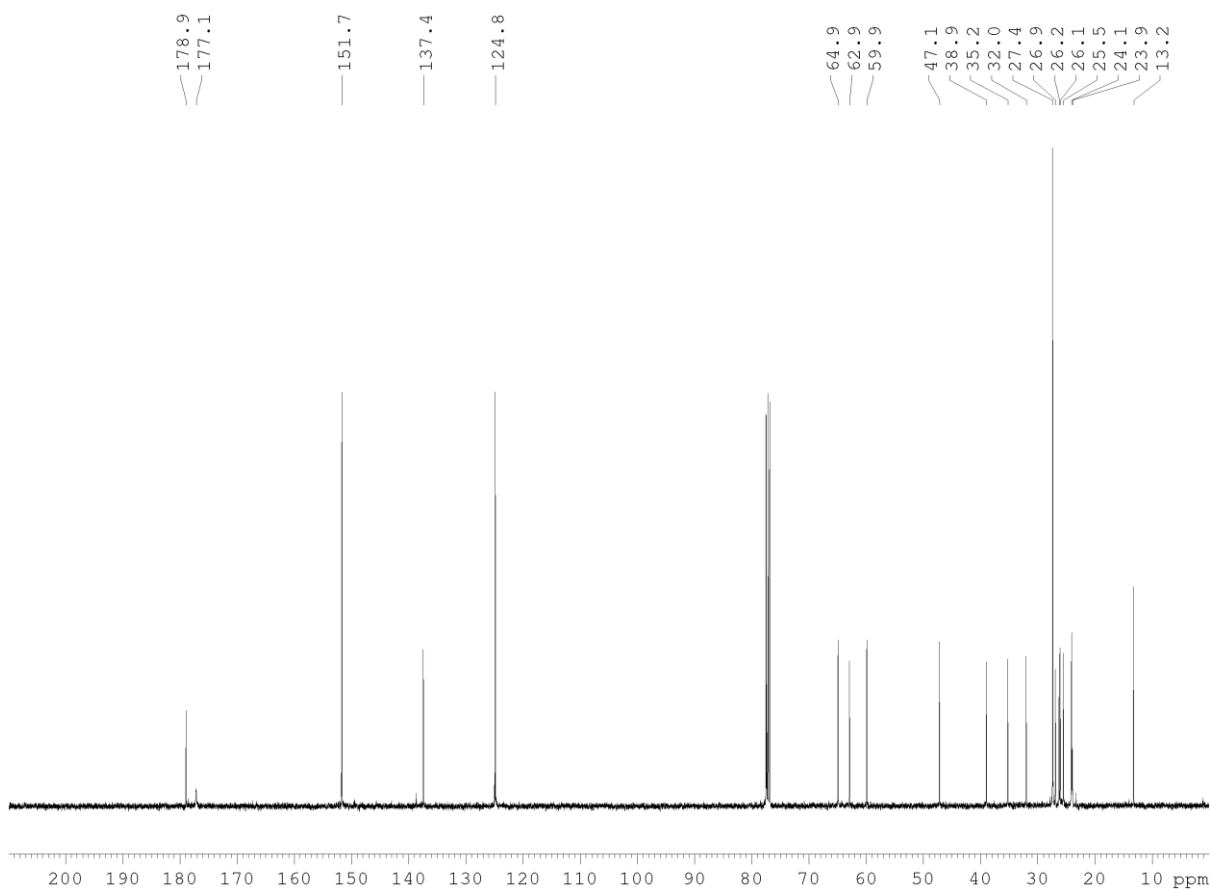
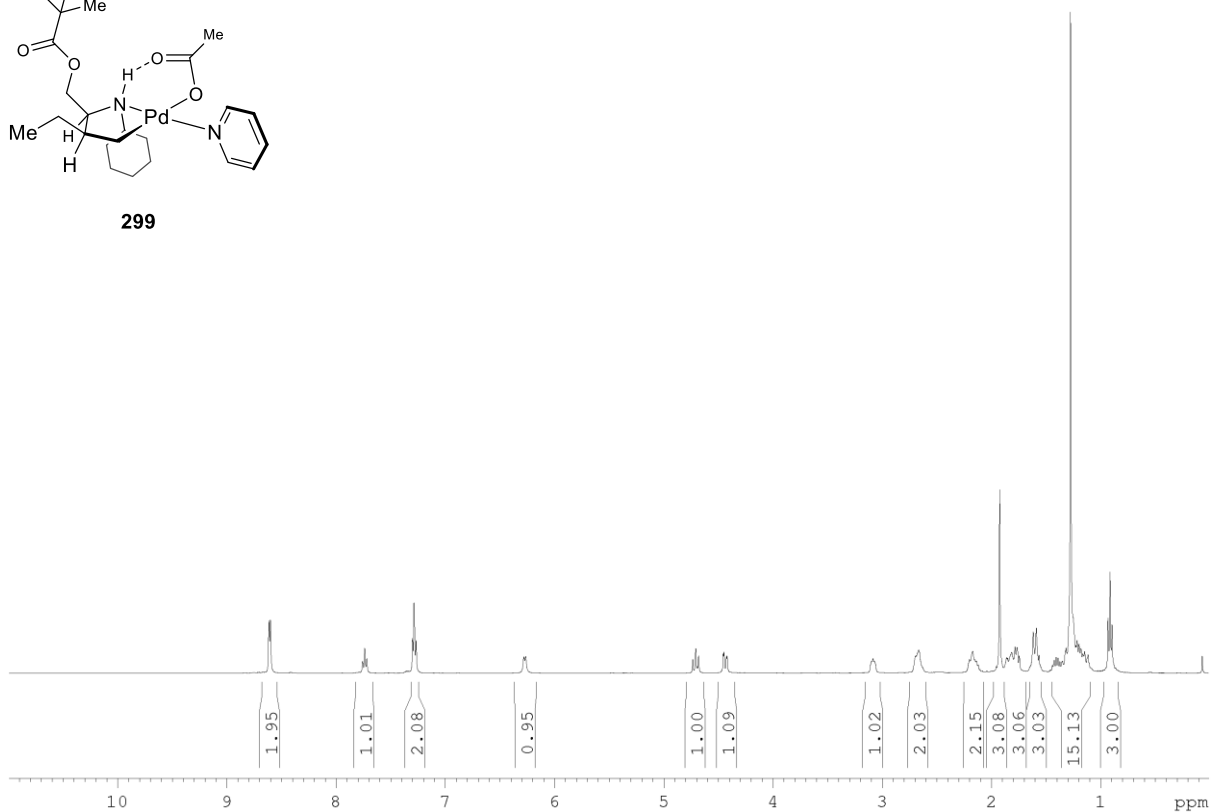


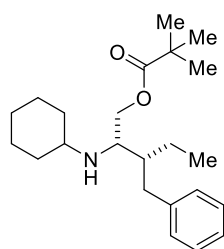
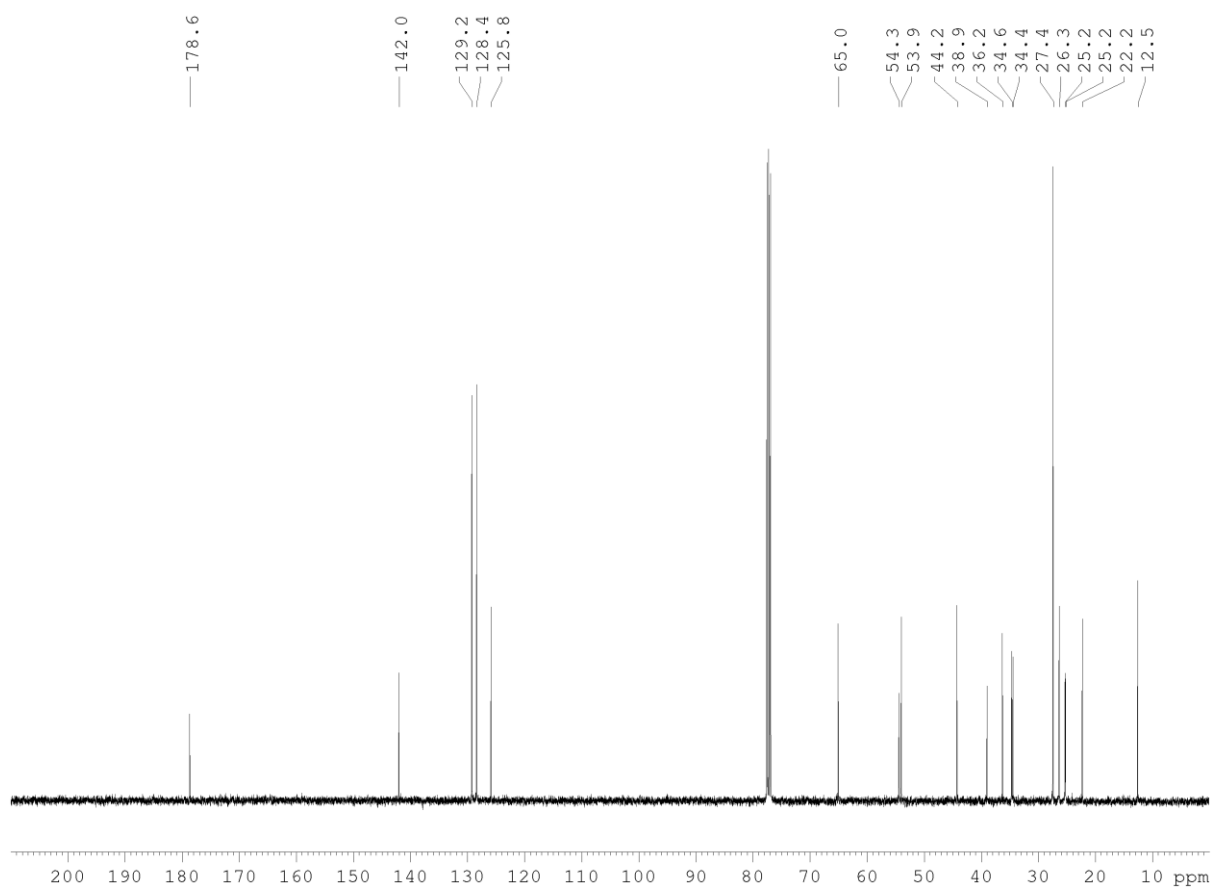
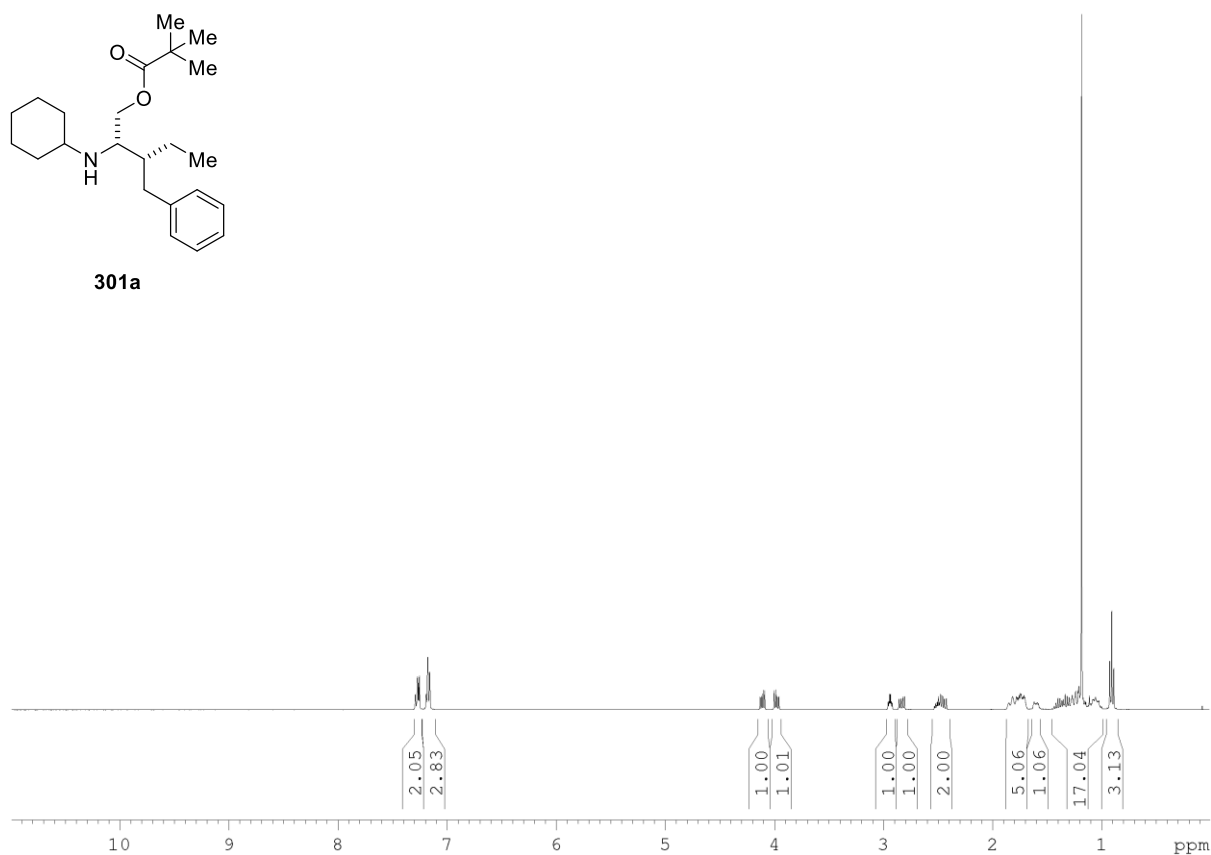
**273g**

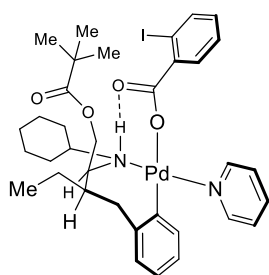


278 (1:1 d.r.)

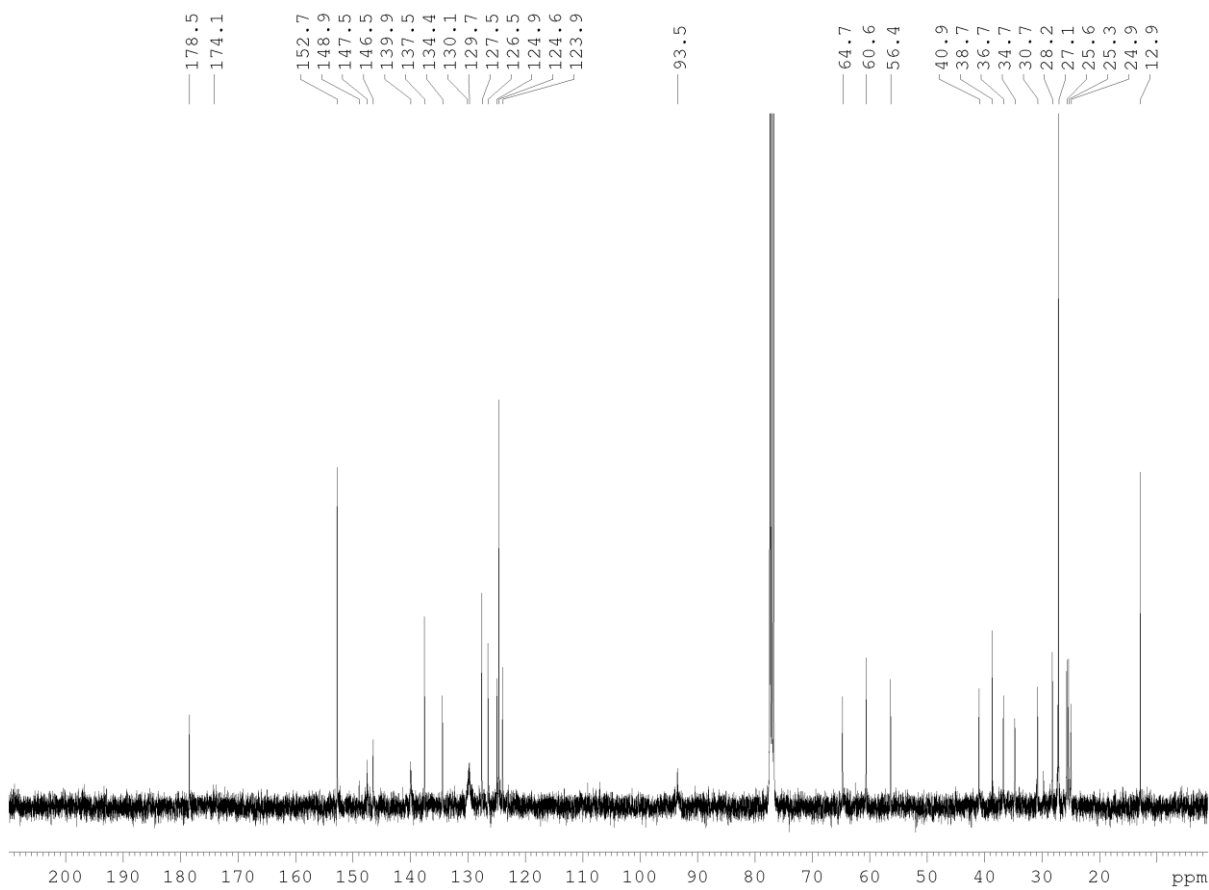
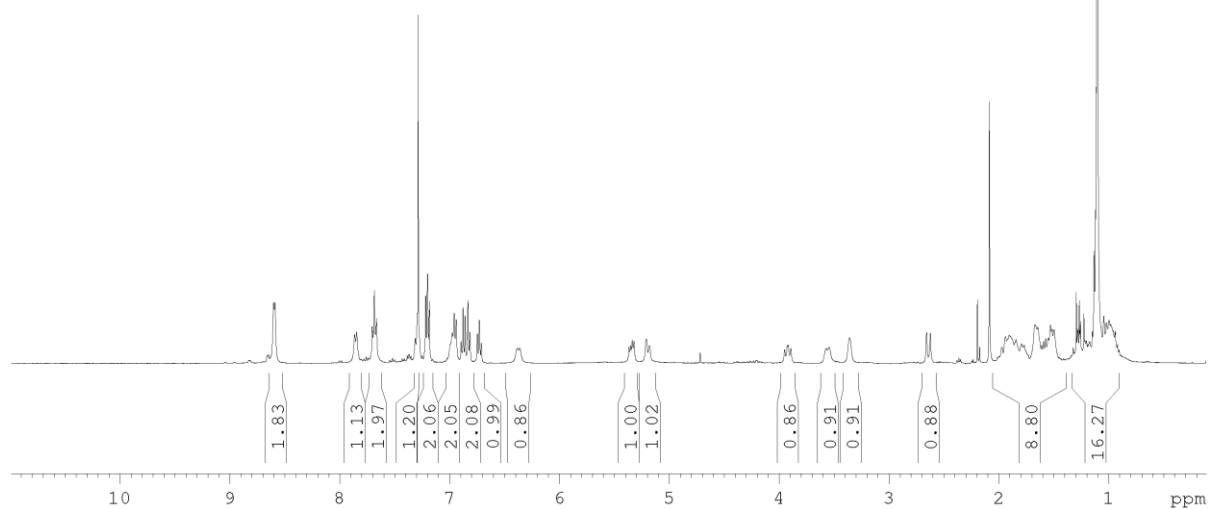


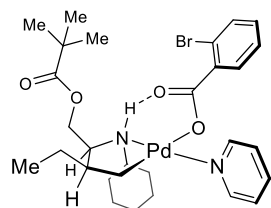
**299**

**301a**

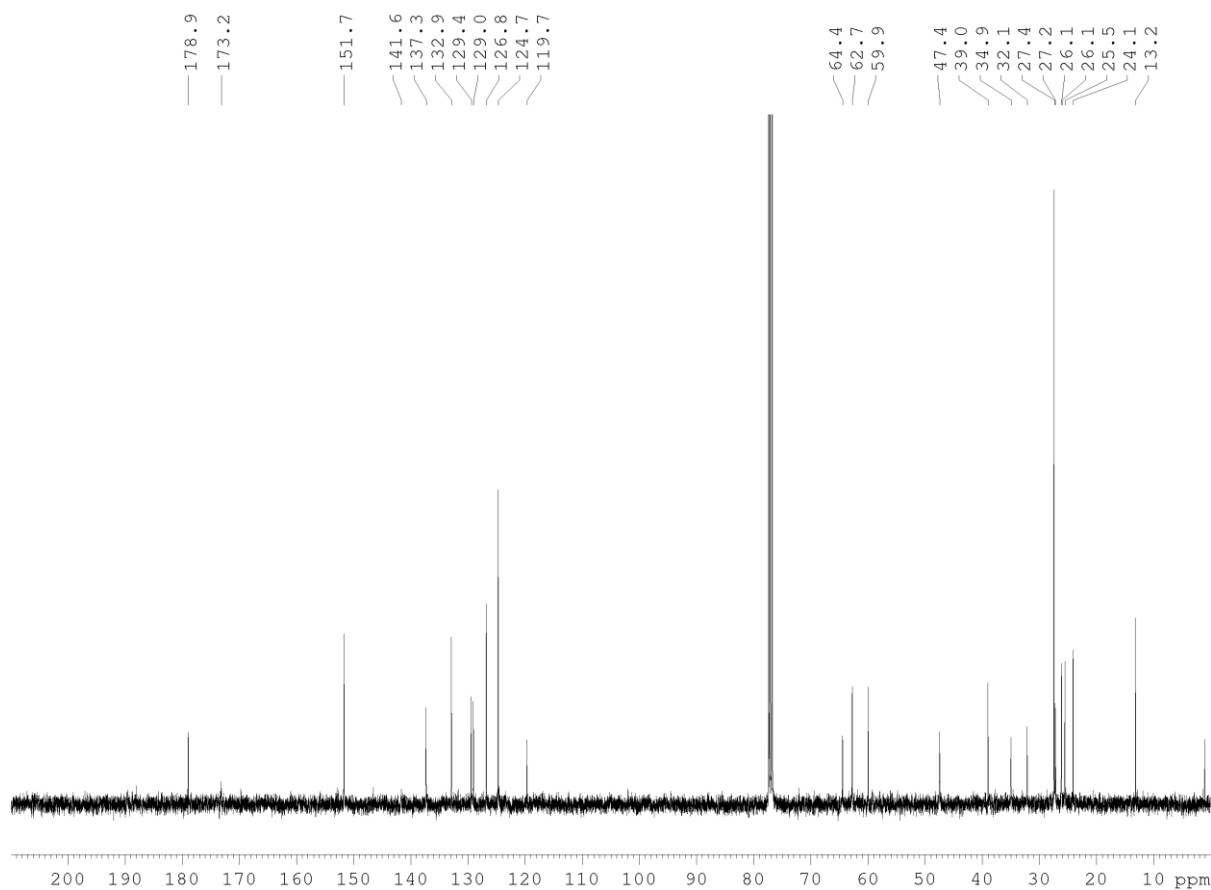
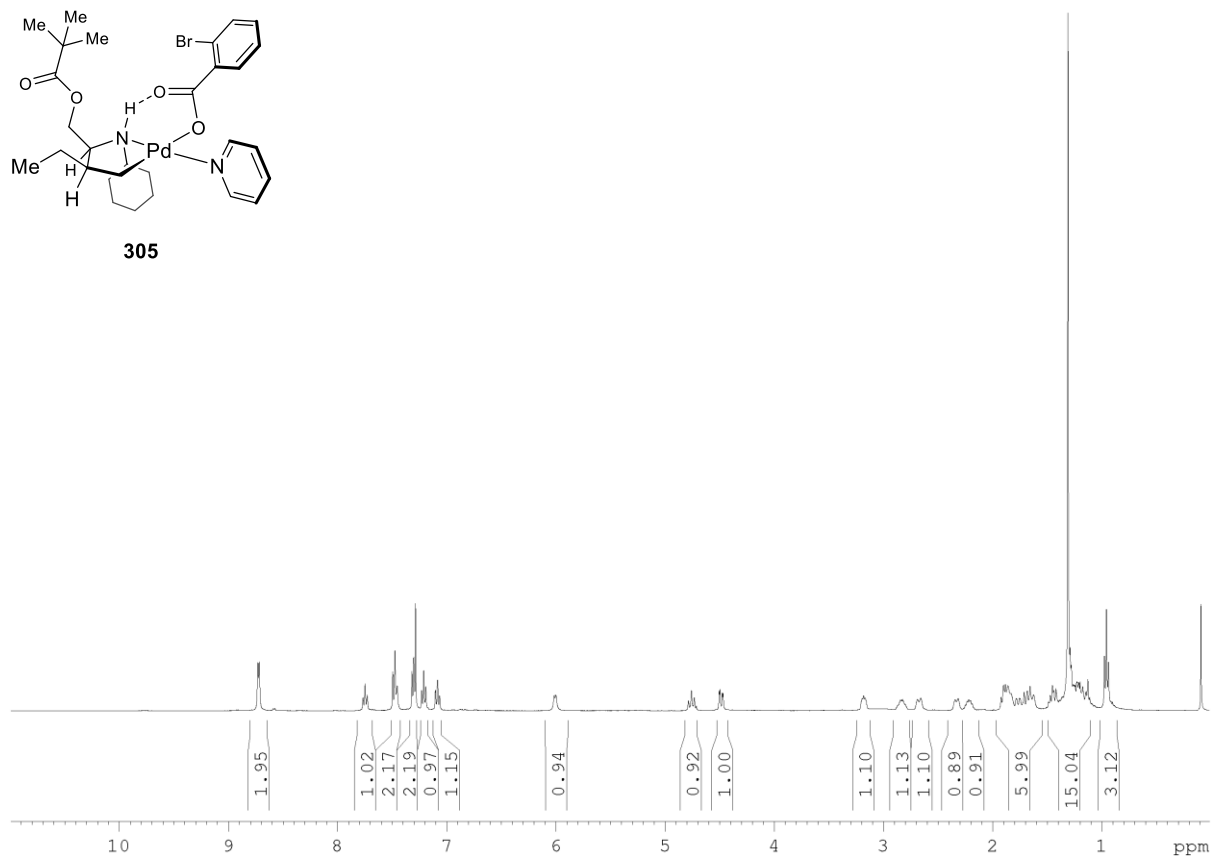


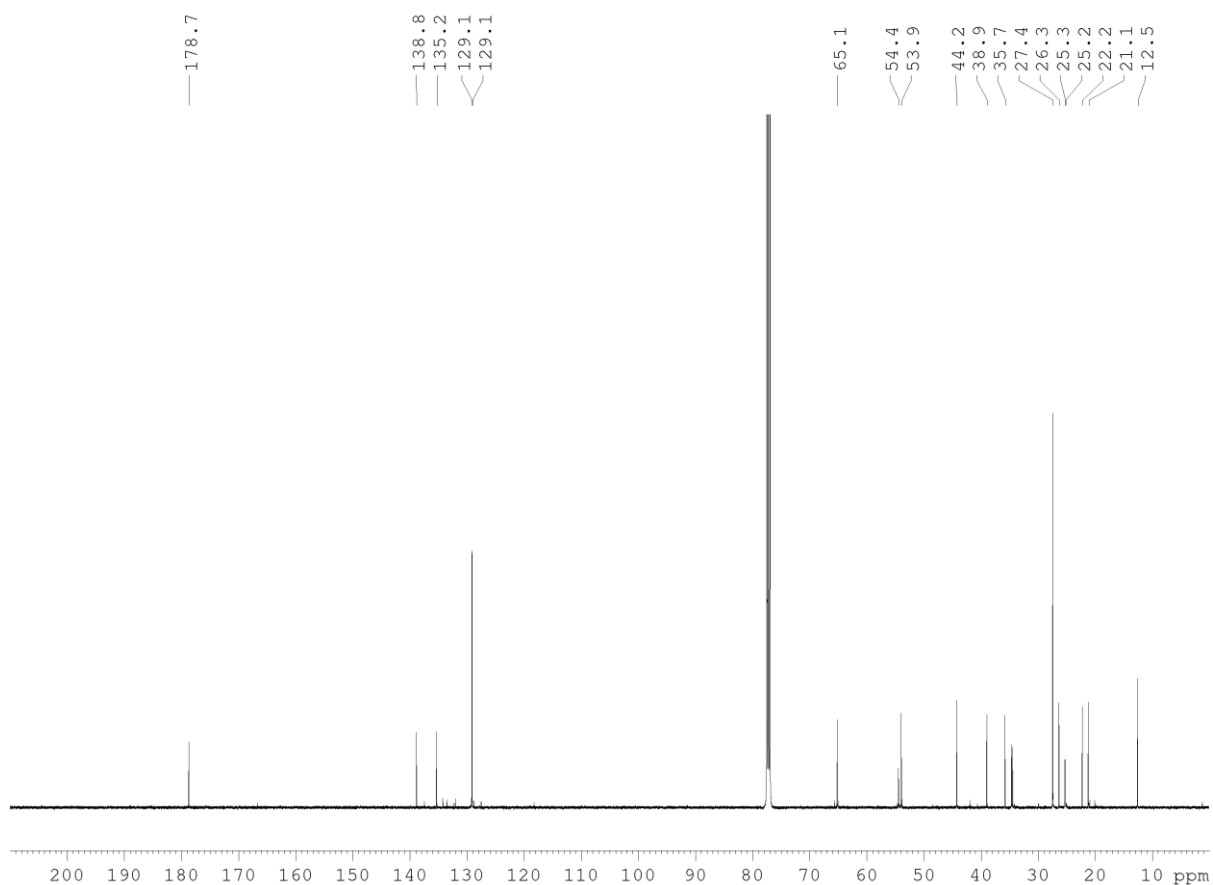
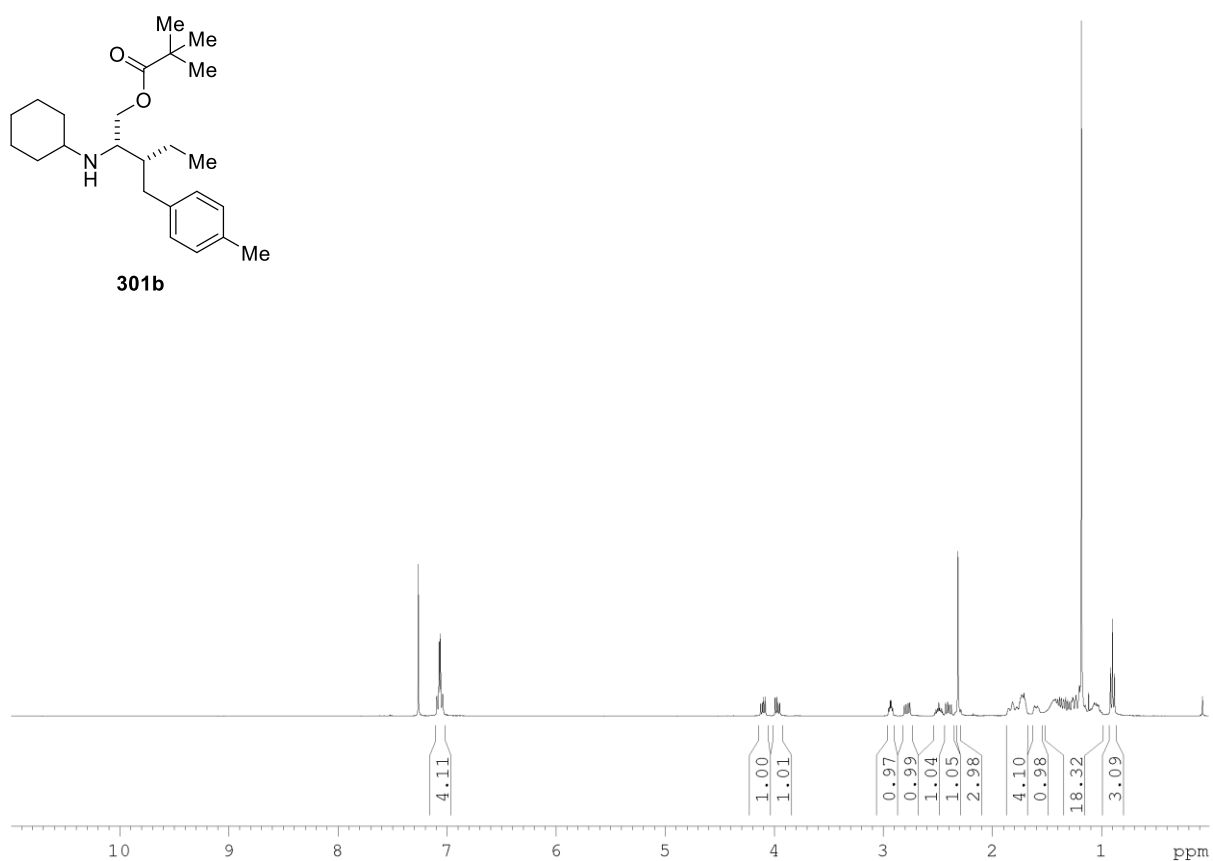
300

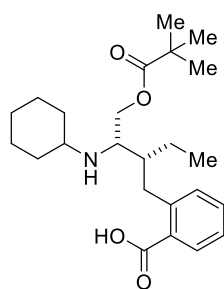




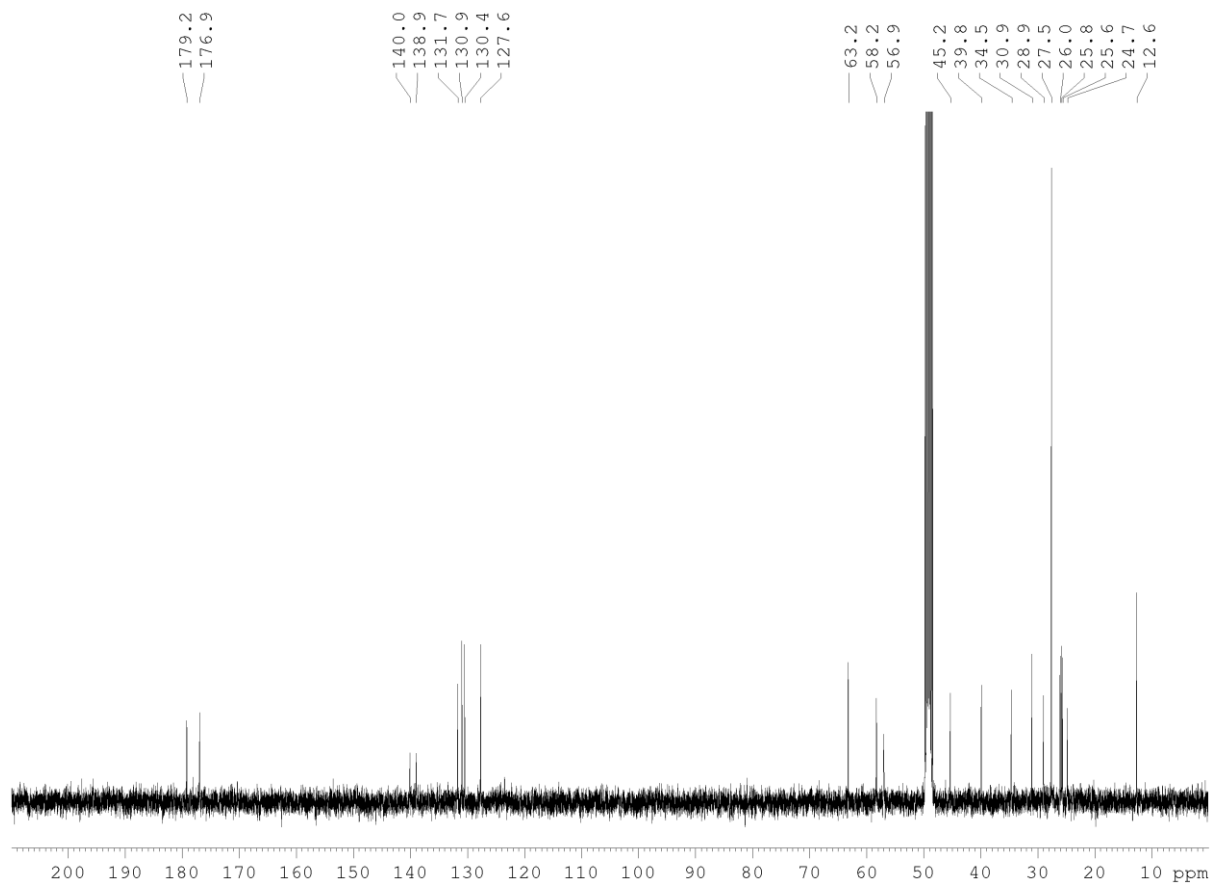
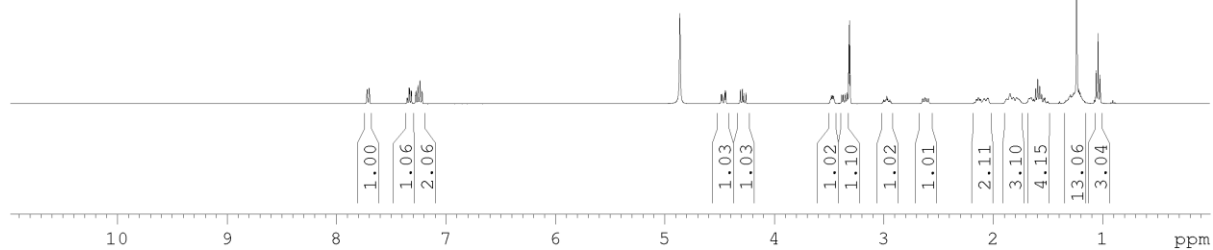
305

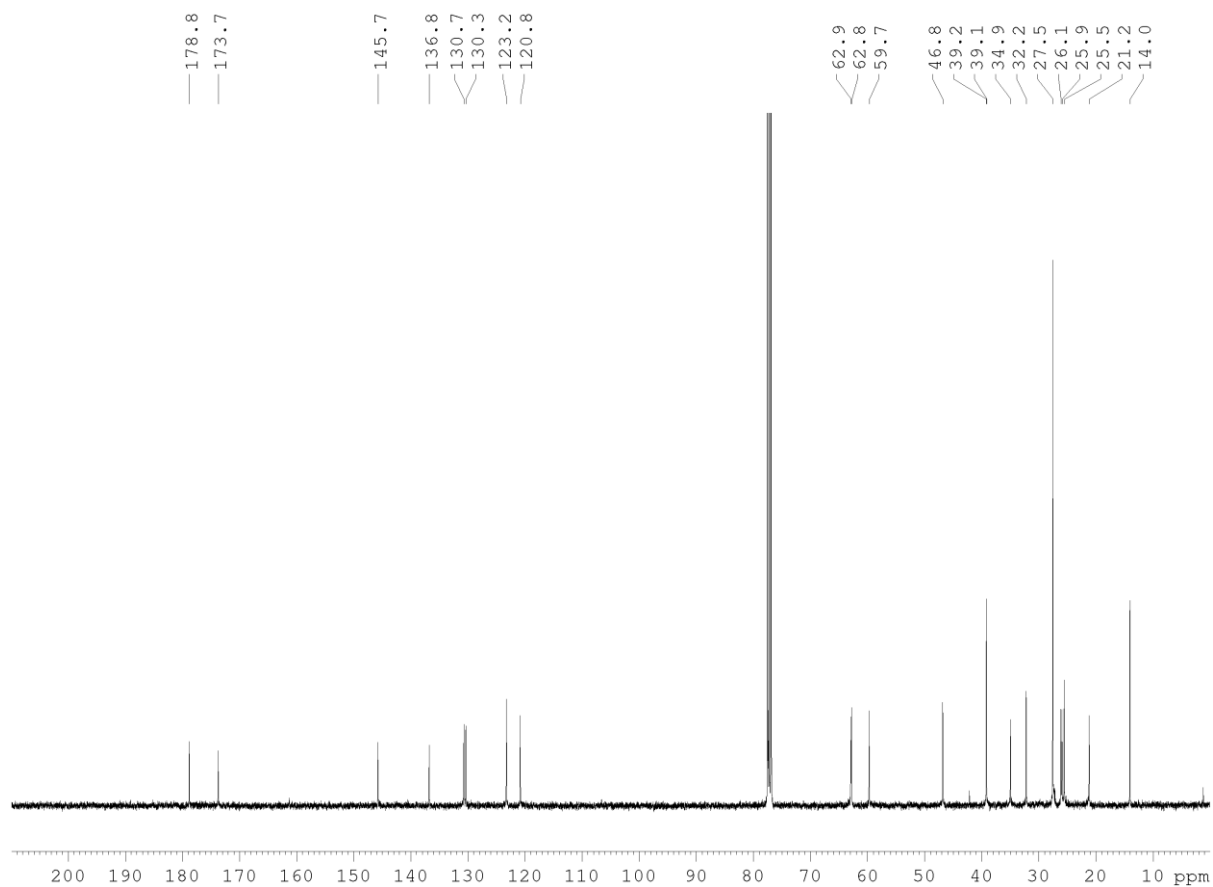
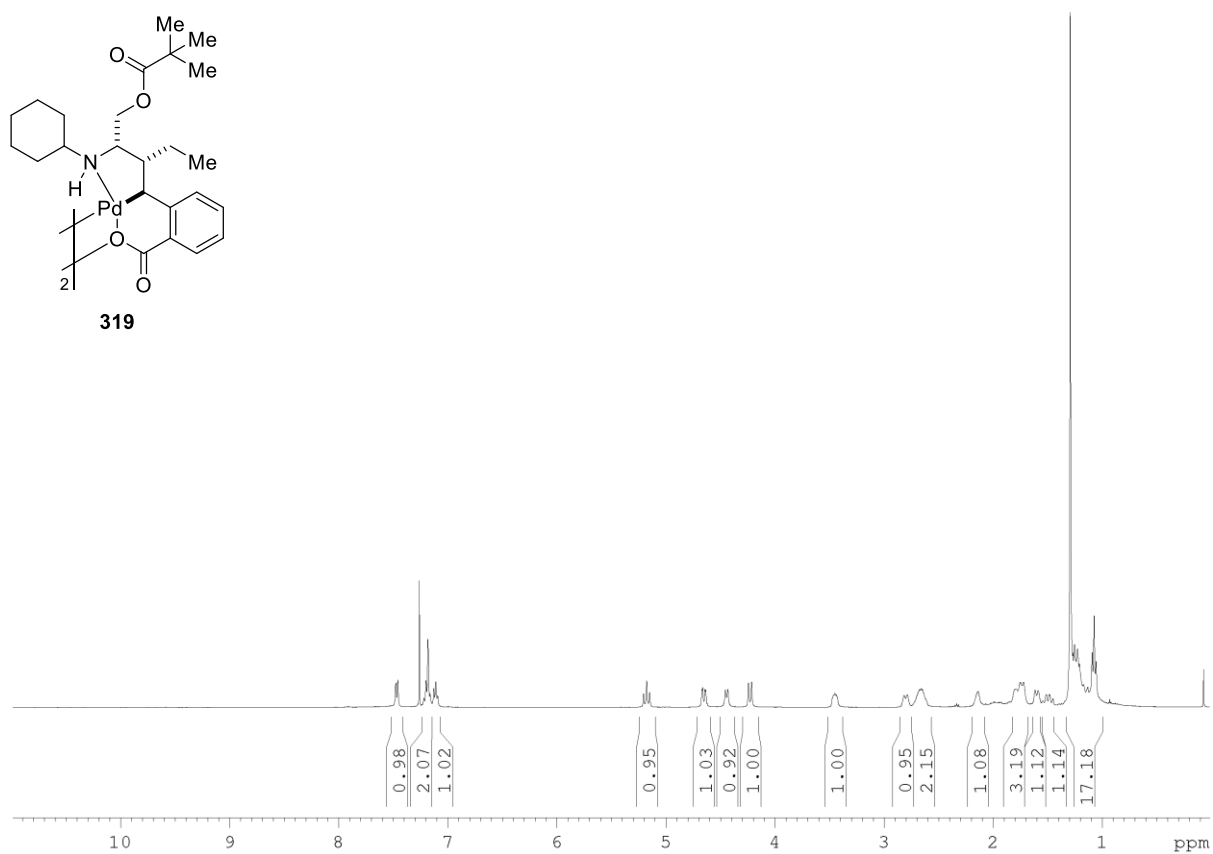


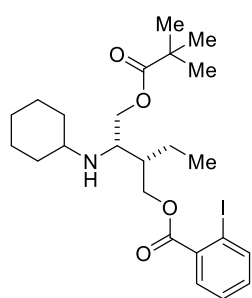




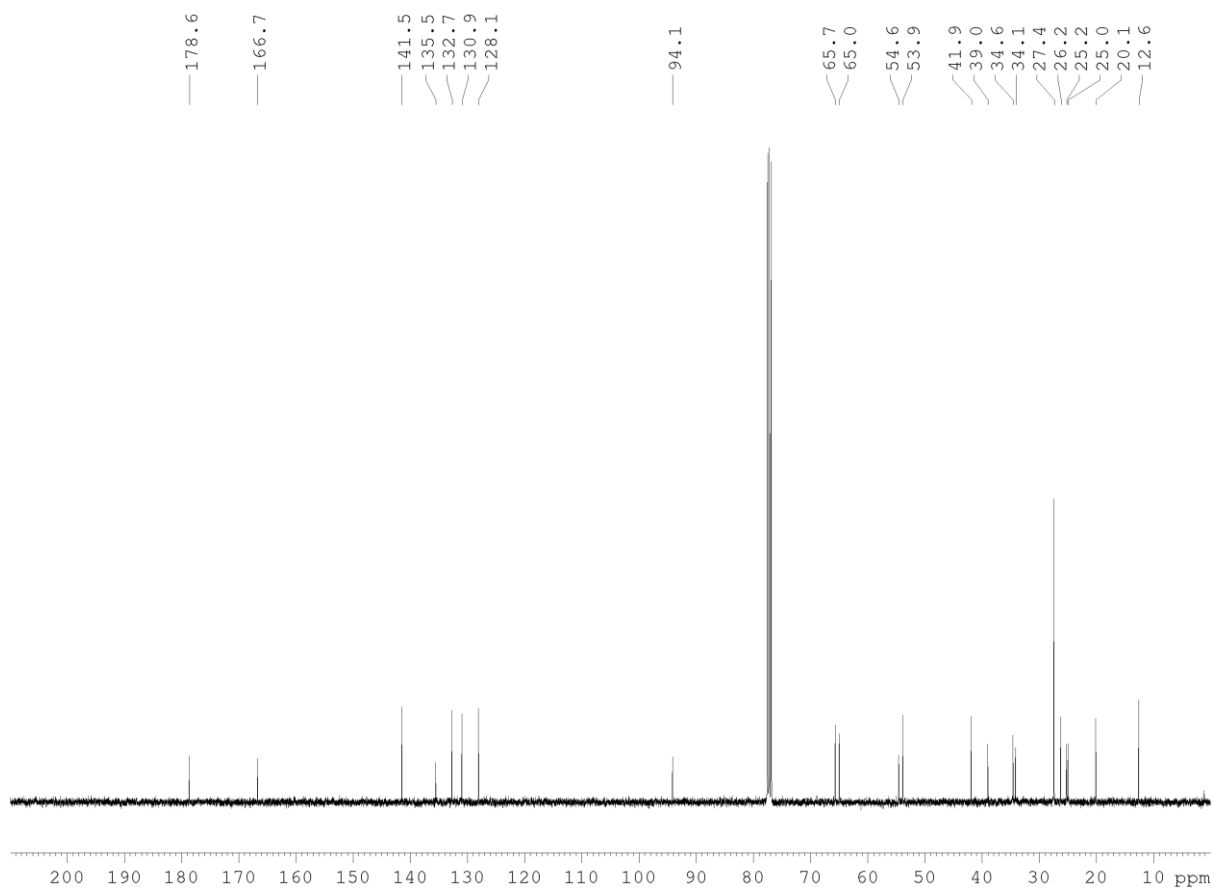
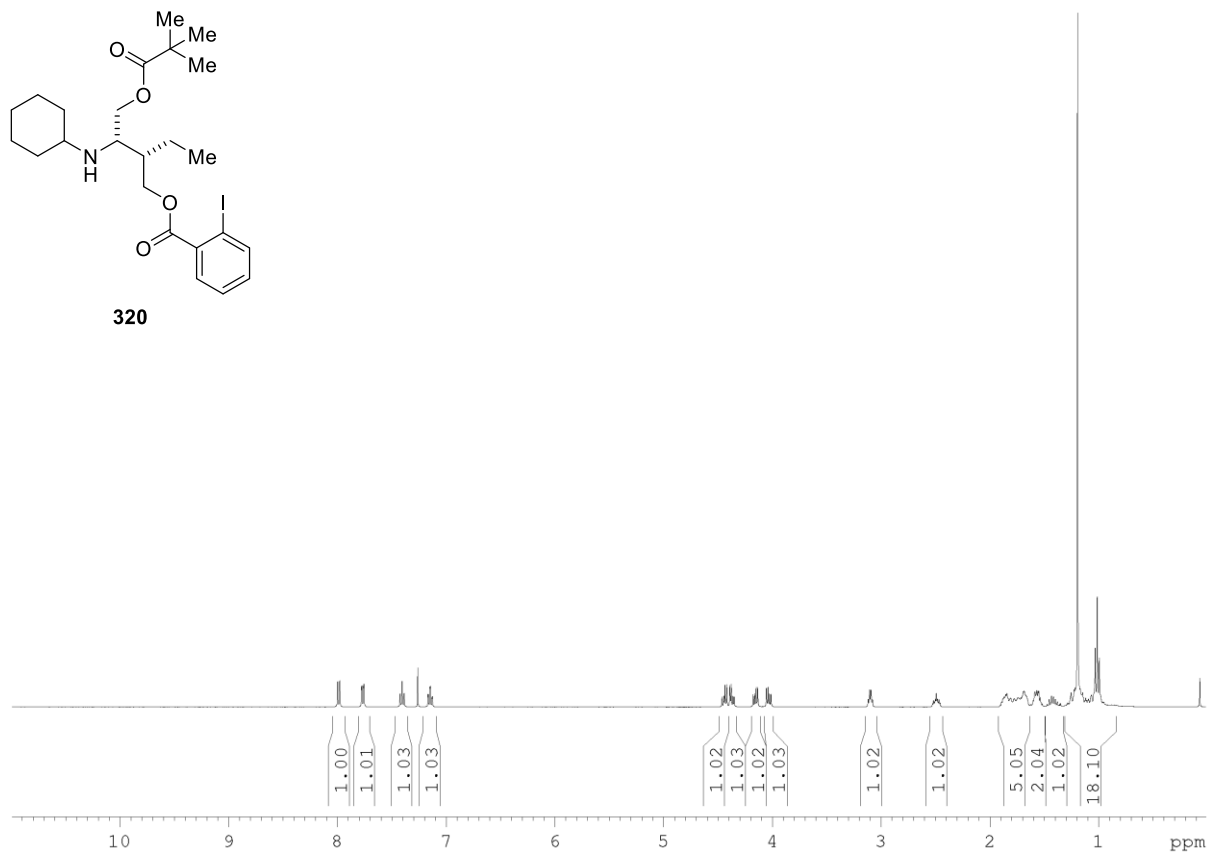
318

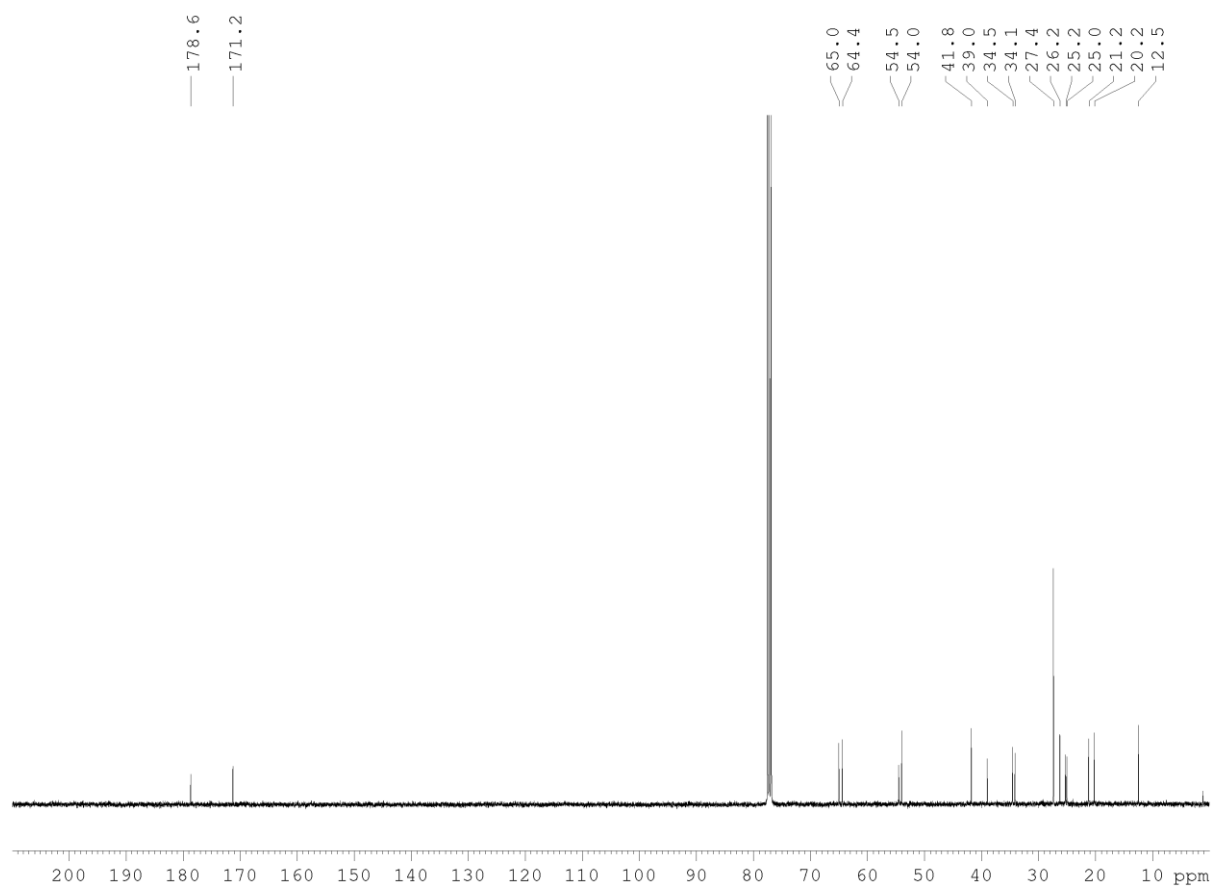
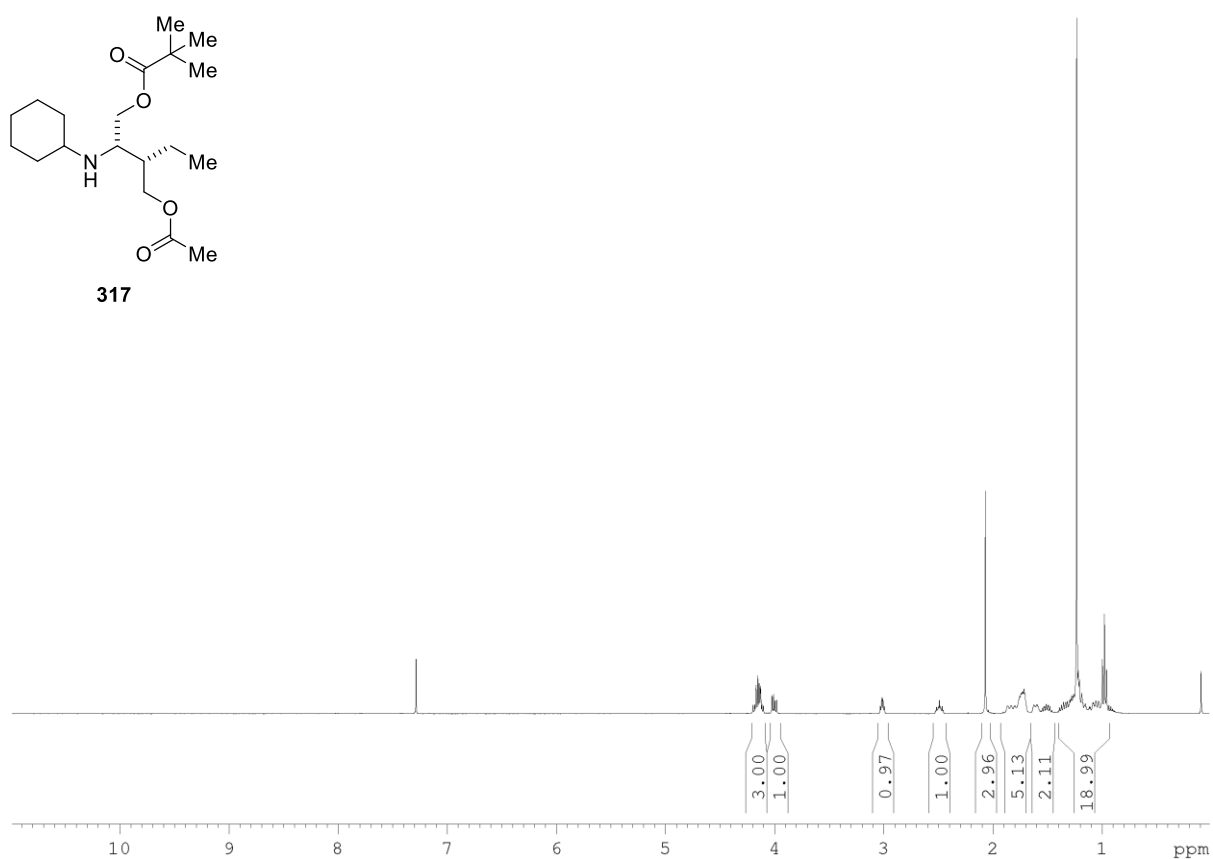


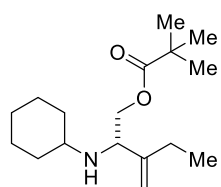




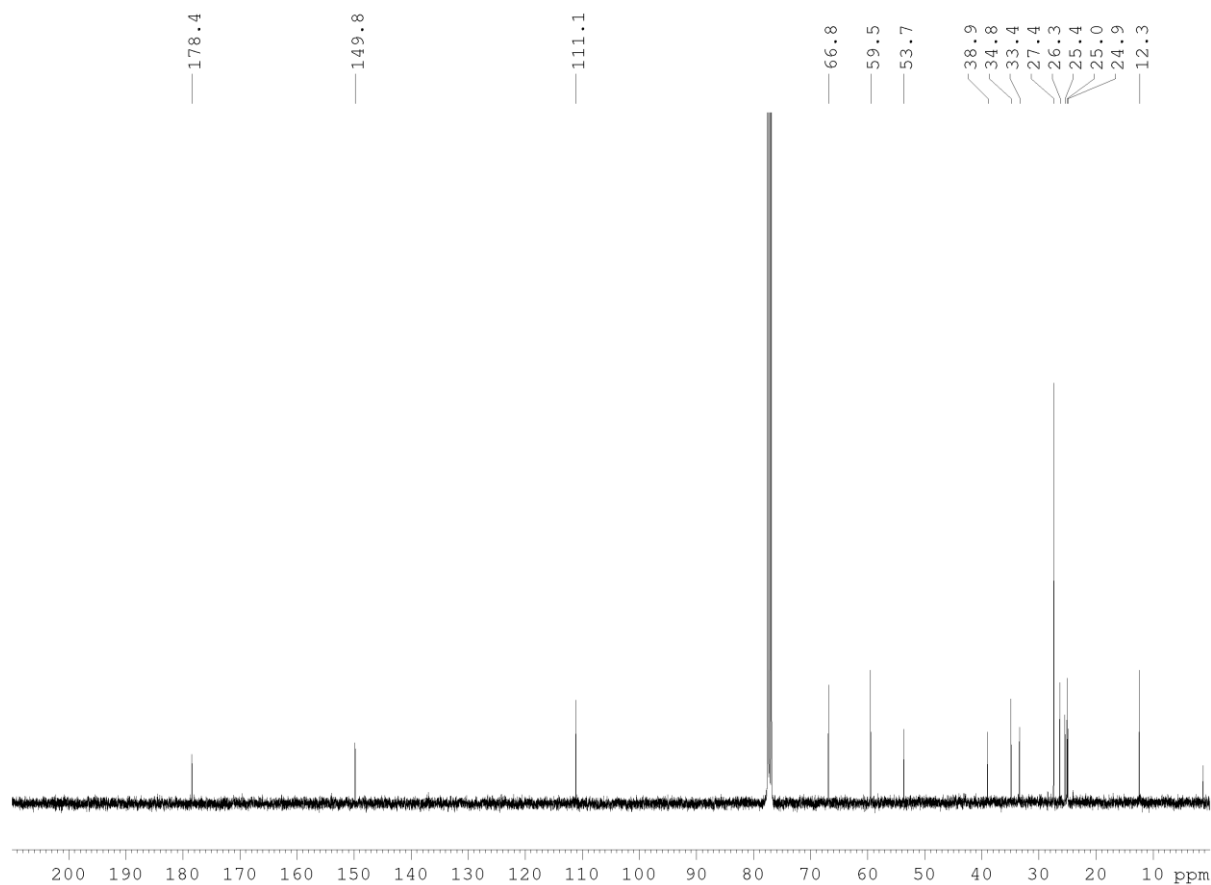
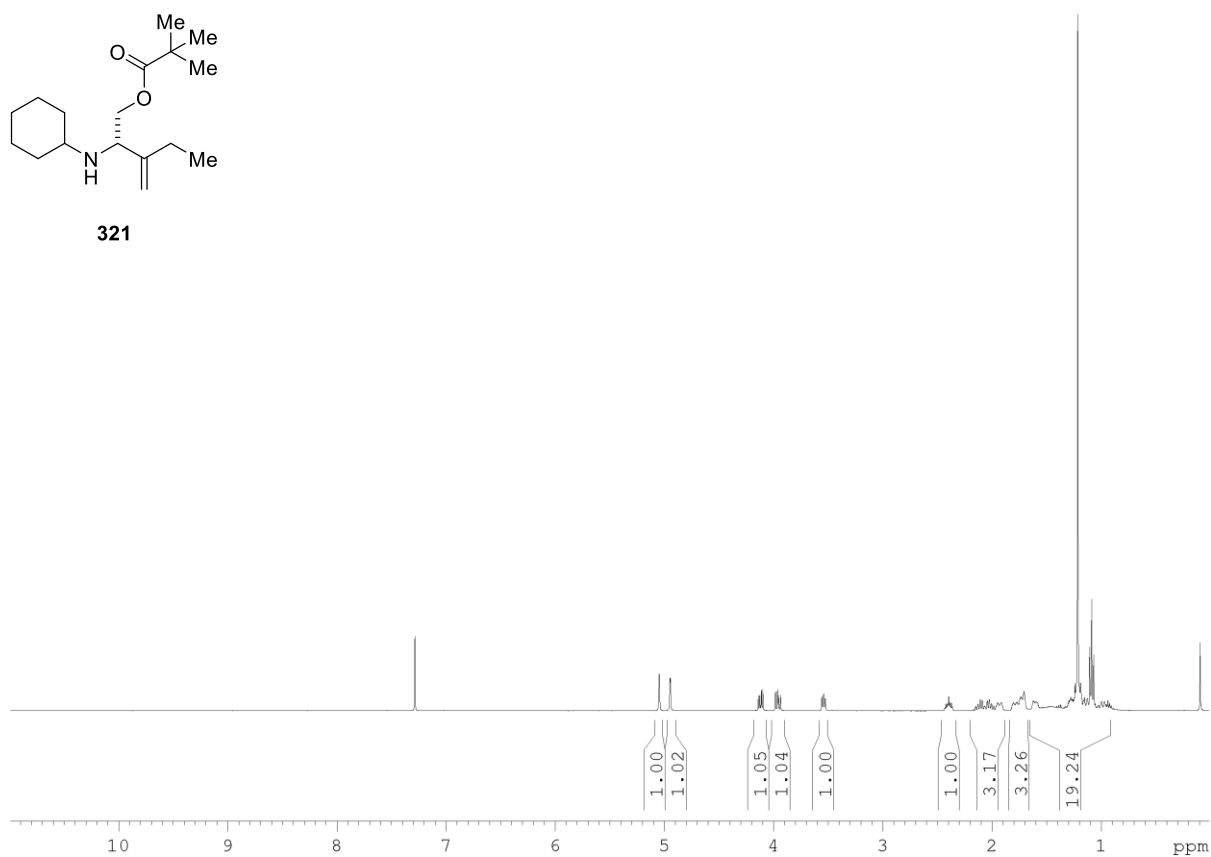
320

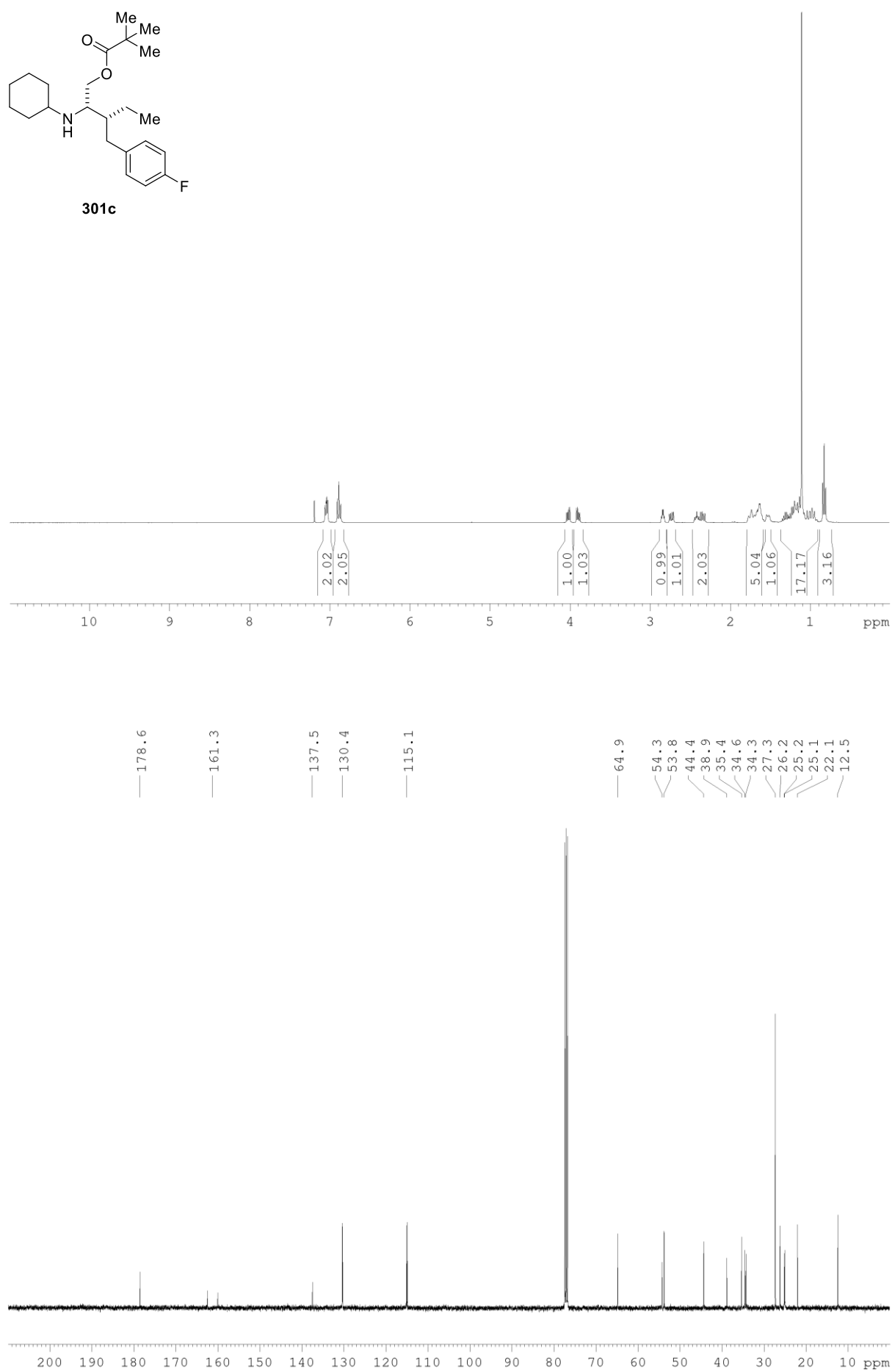


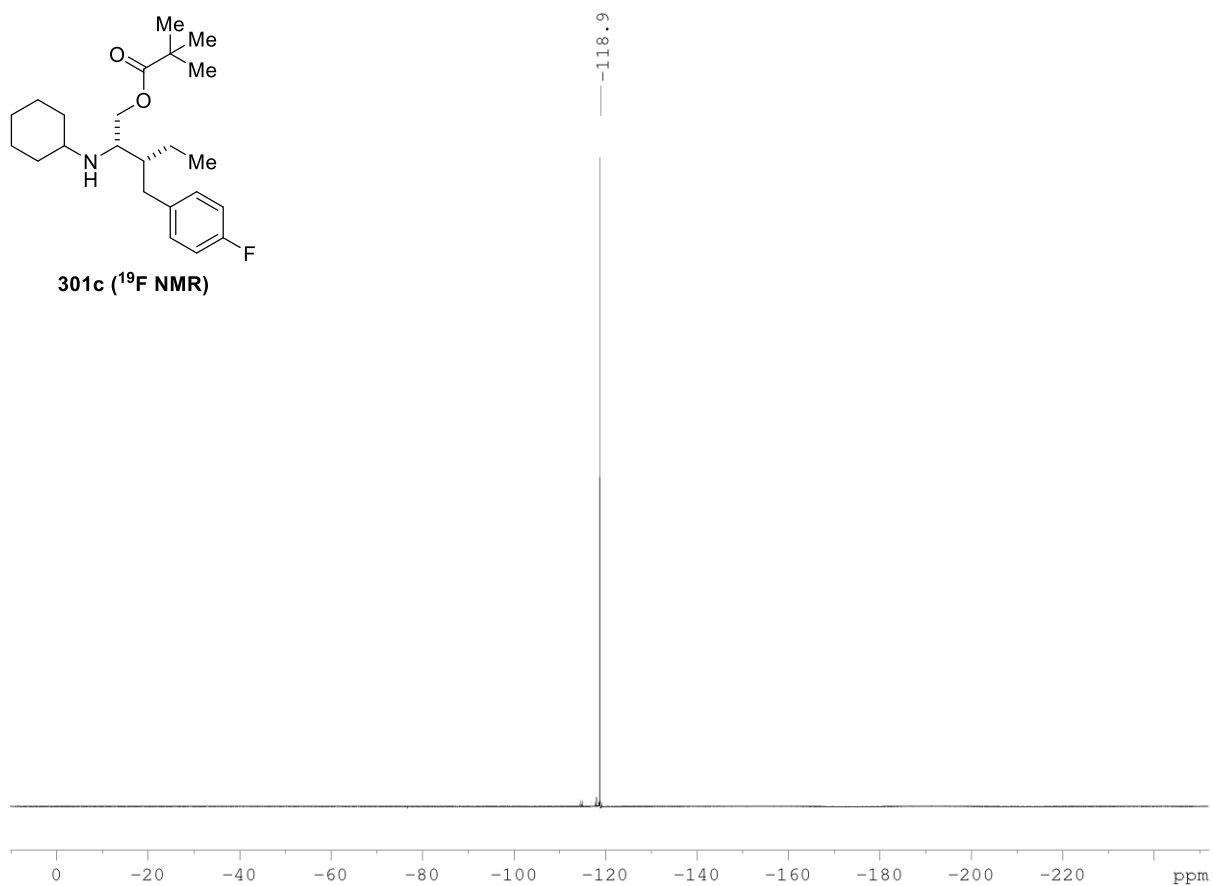


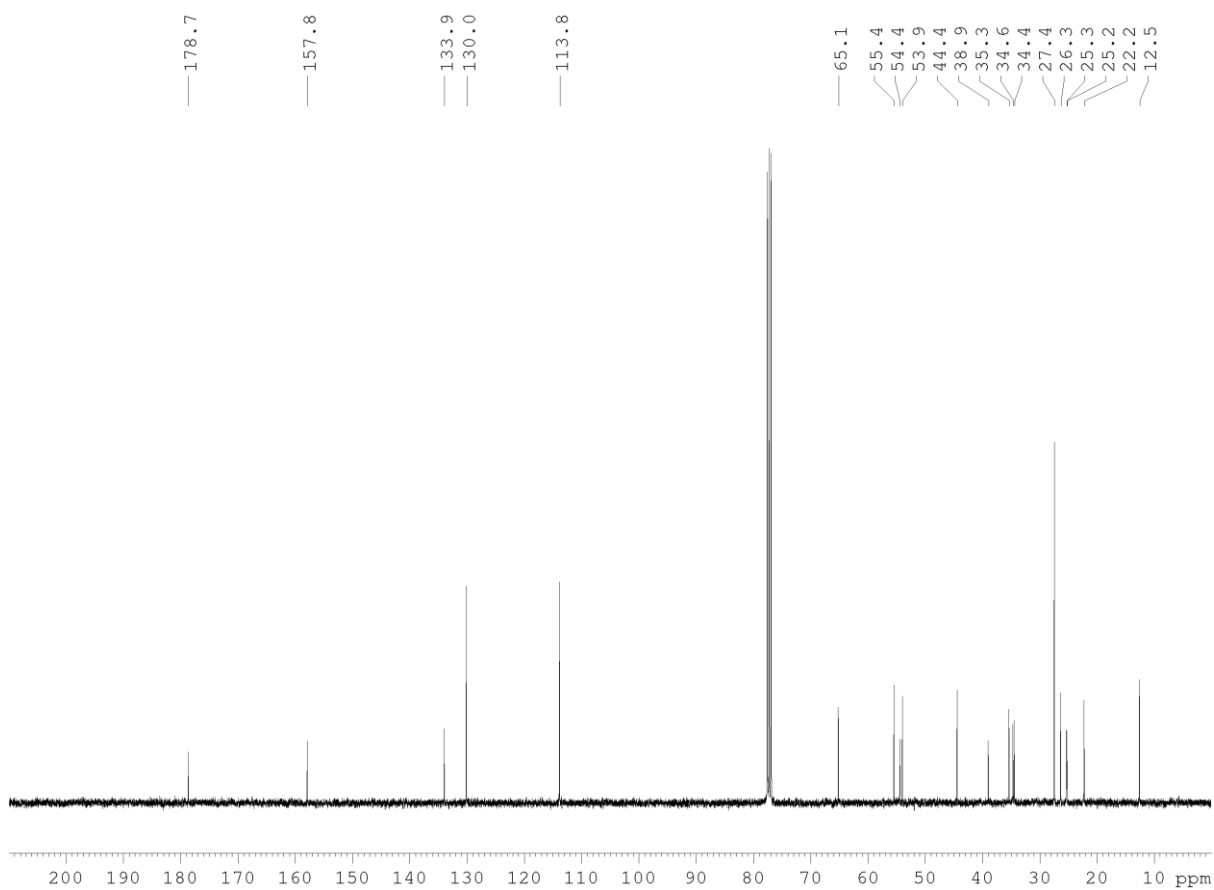
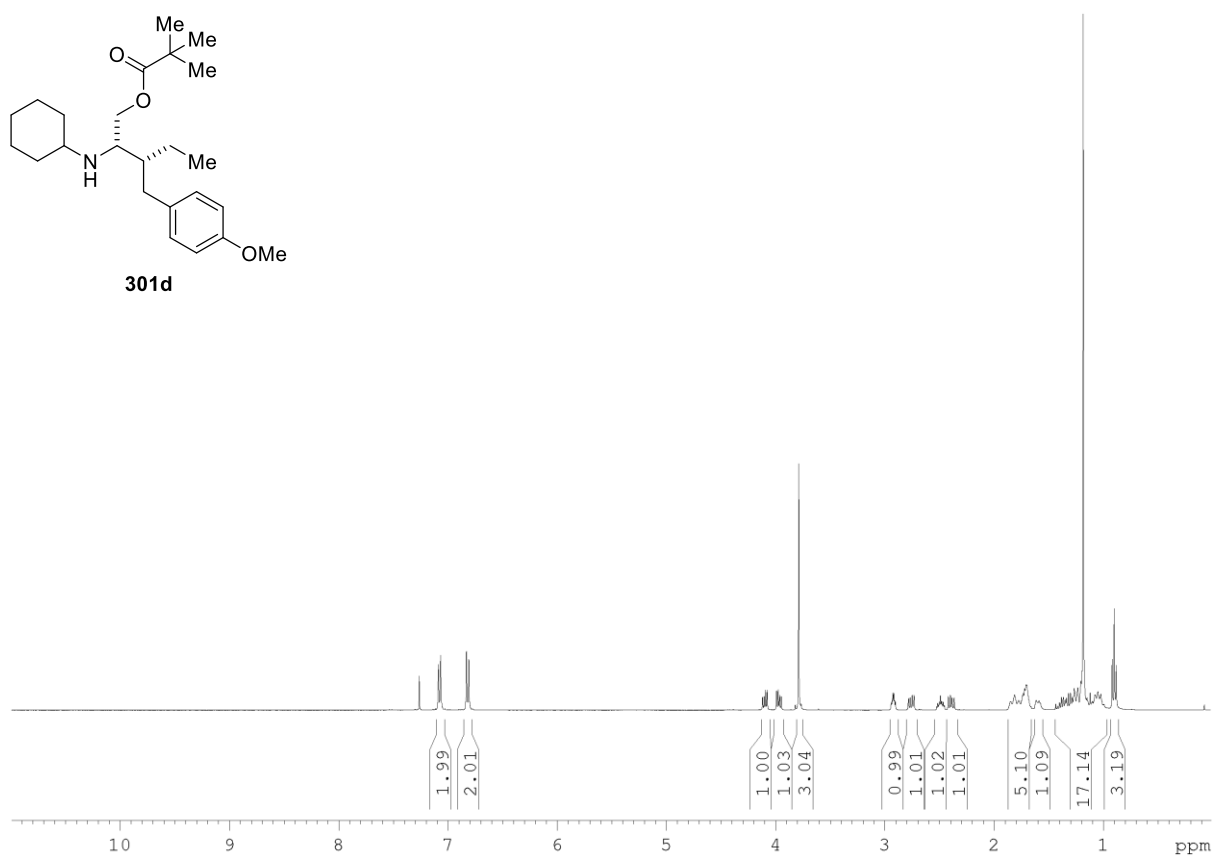
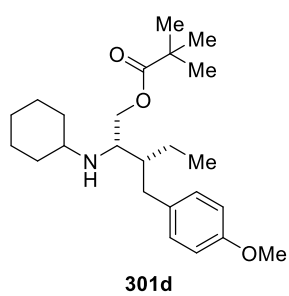


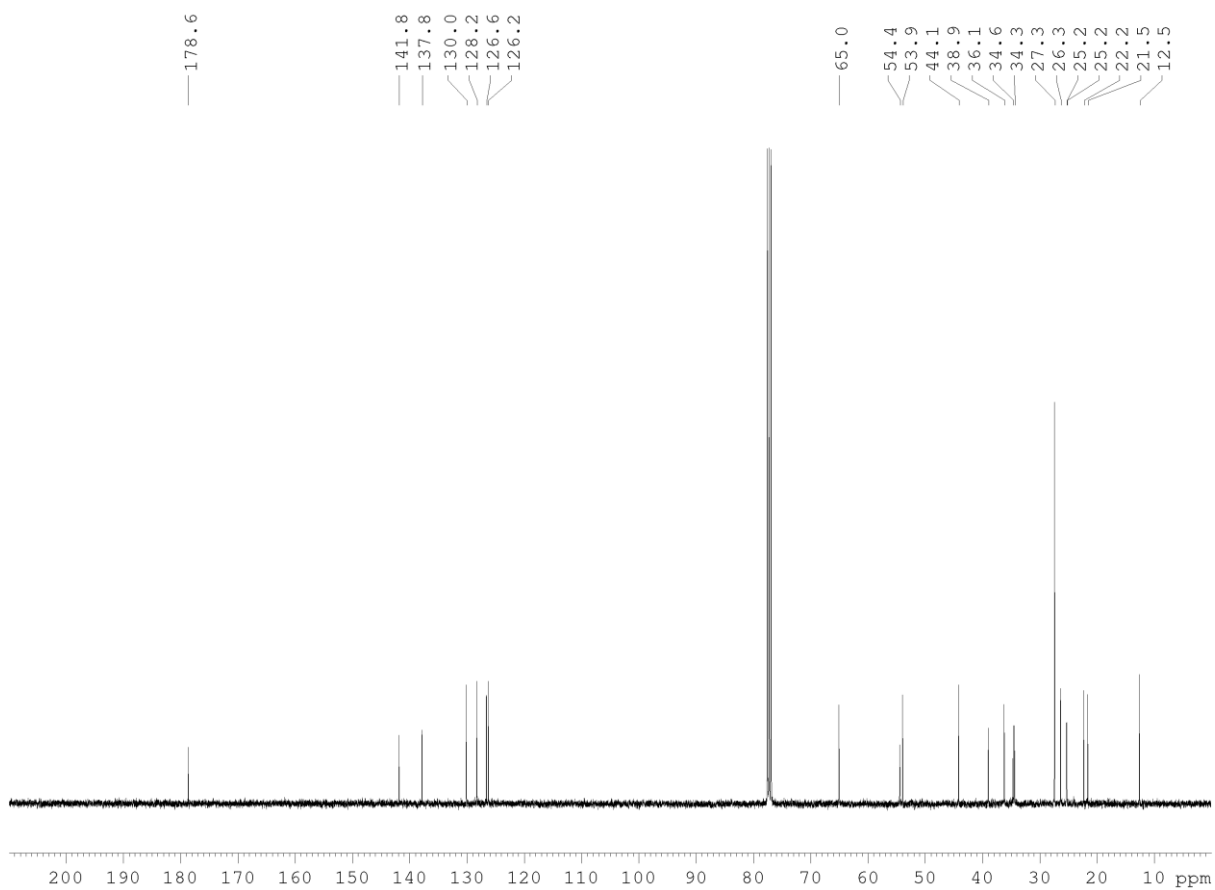
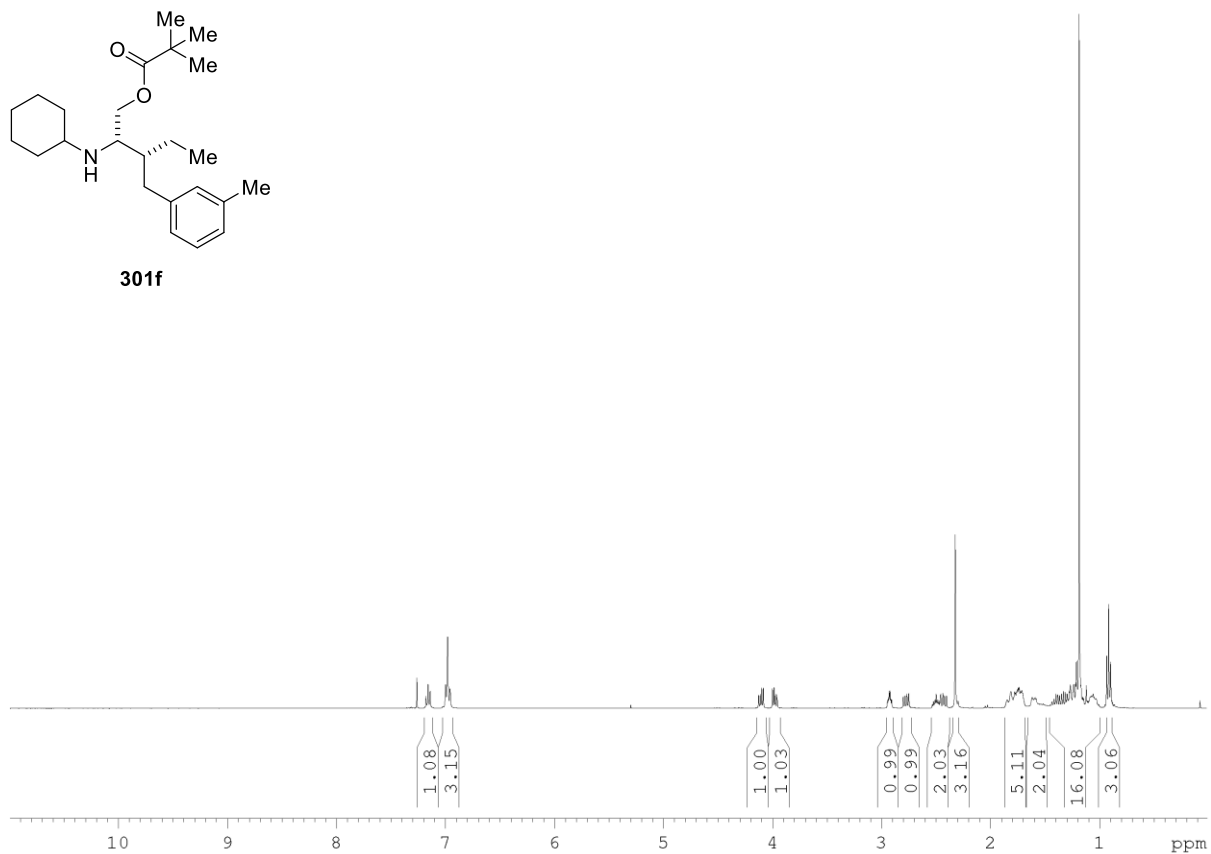
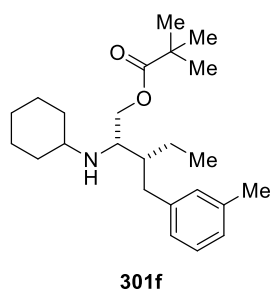
321

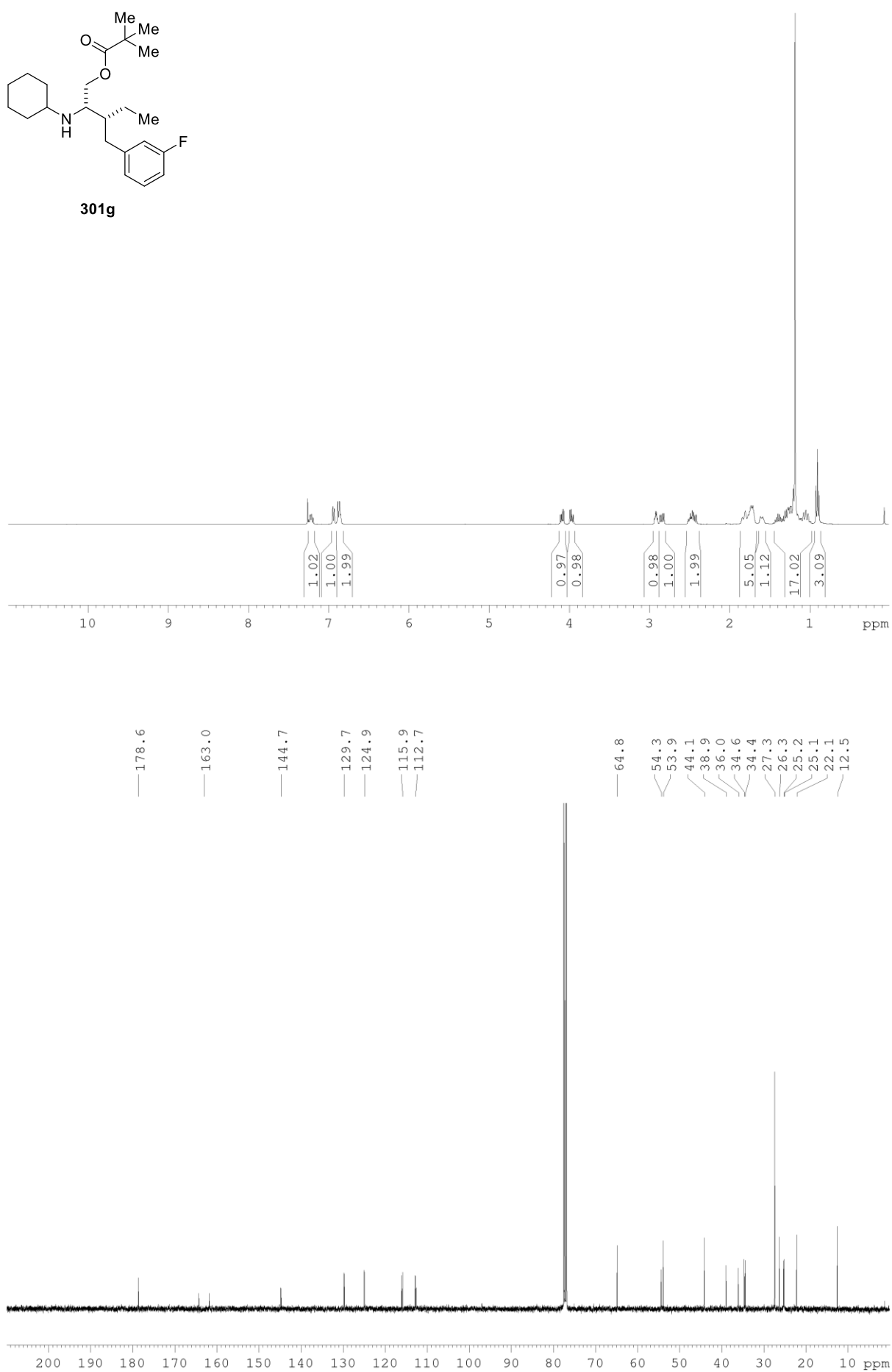


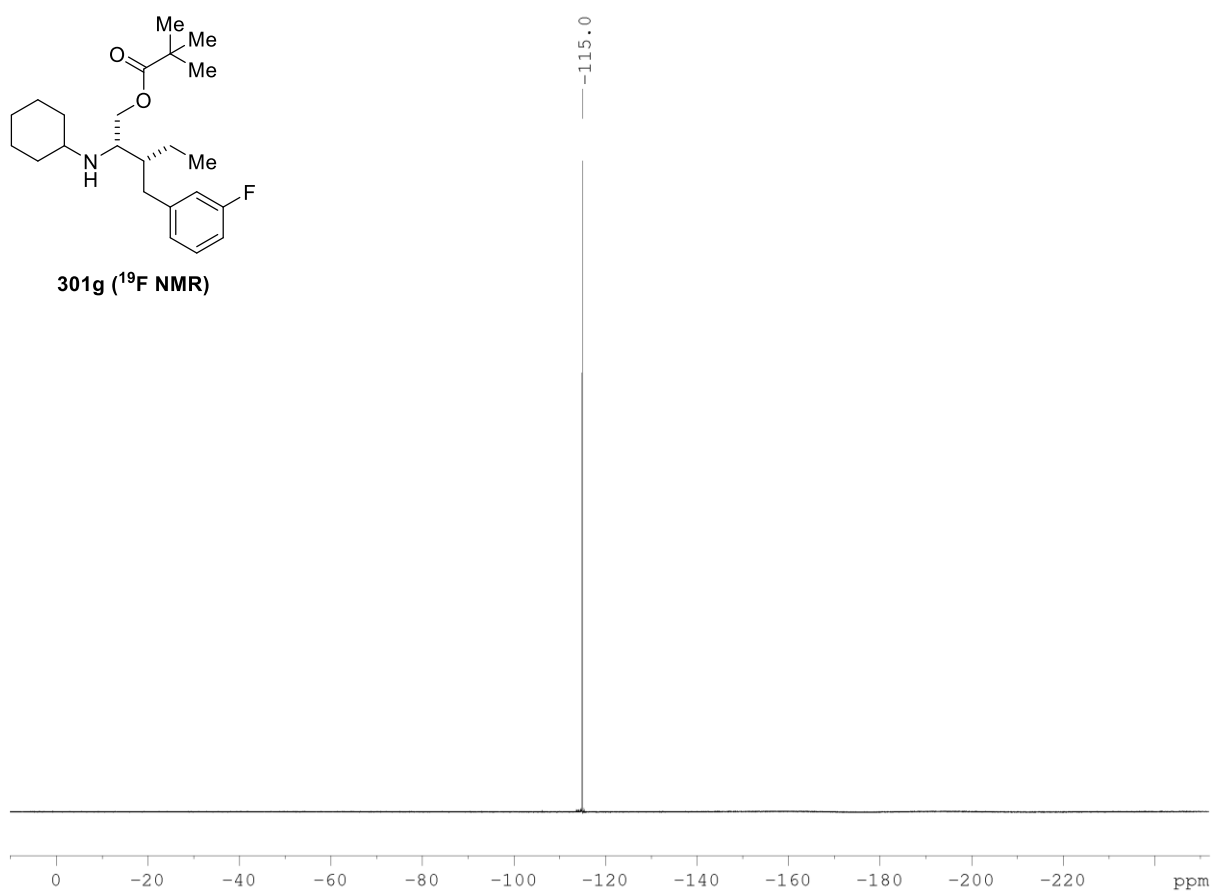


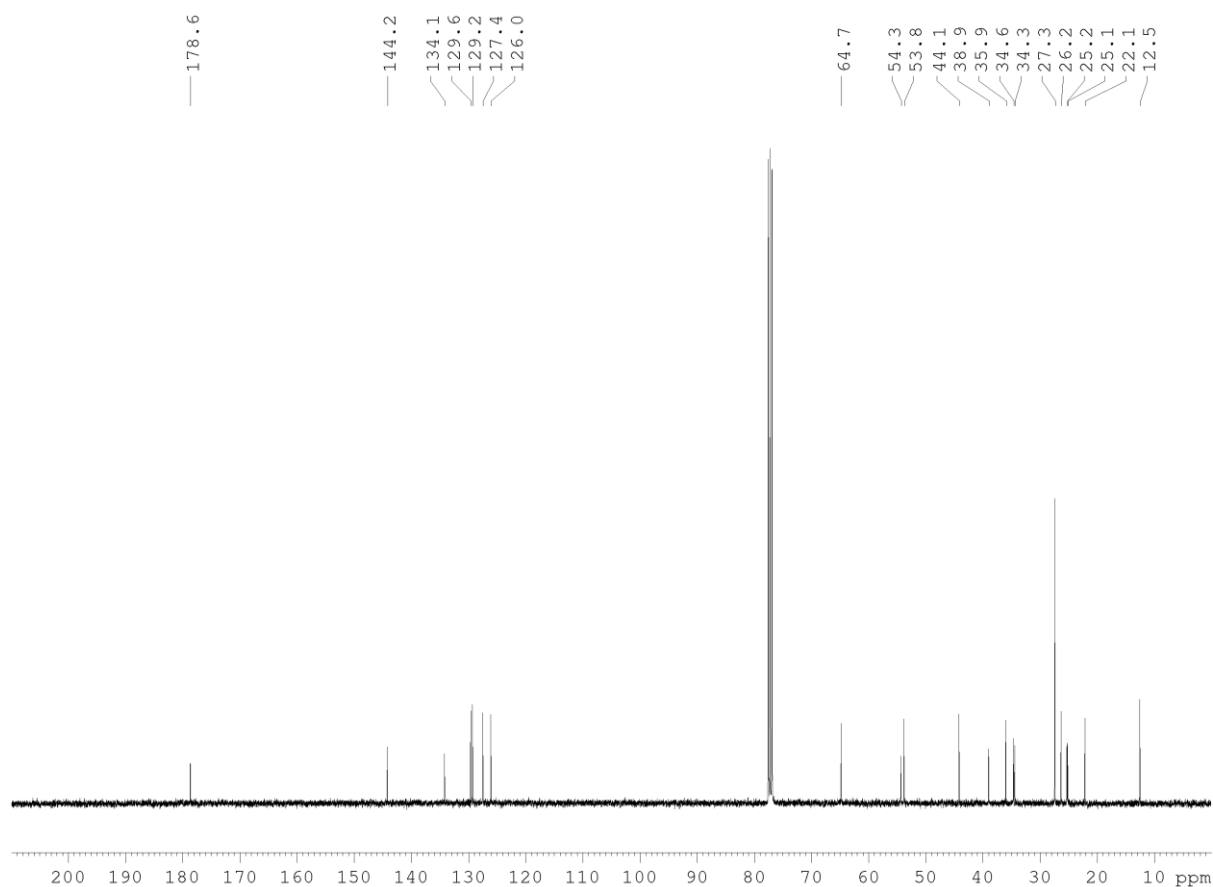
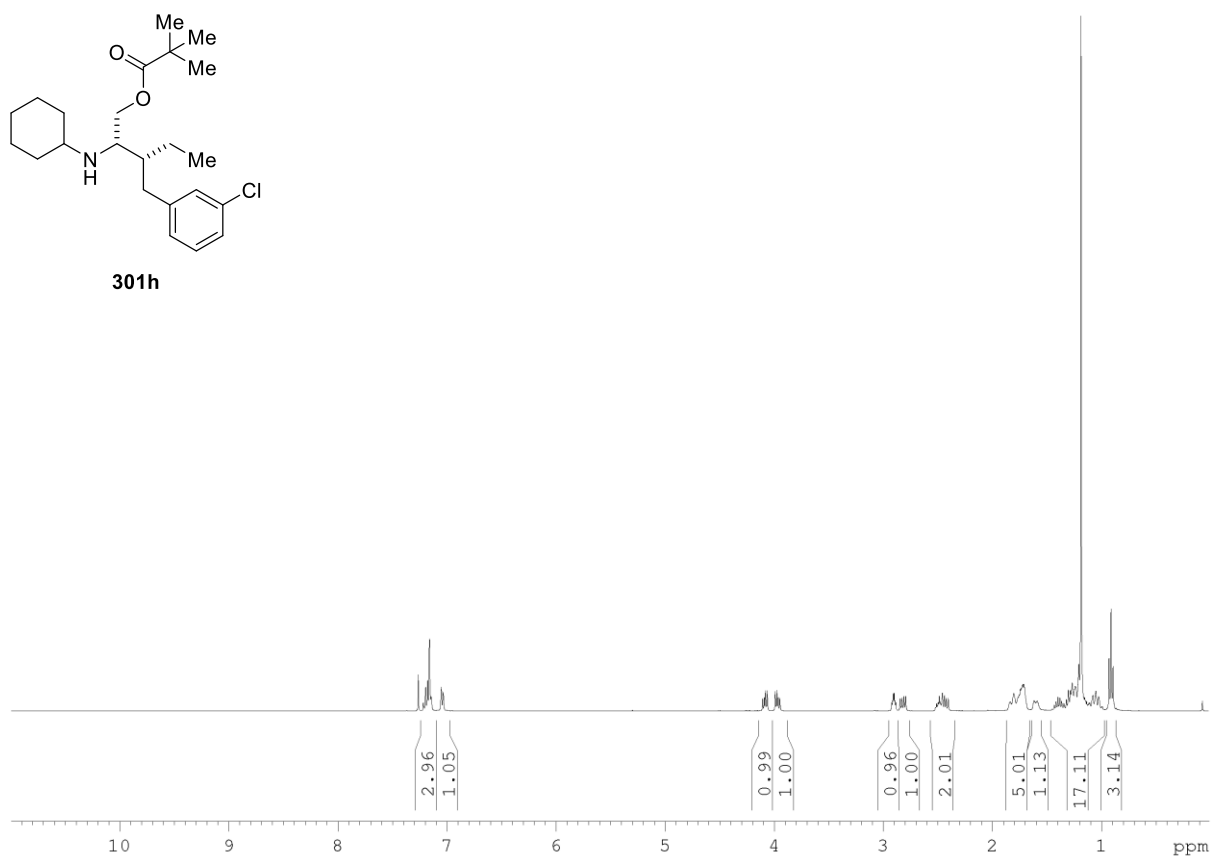
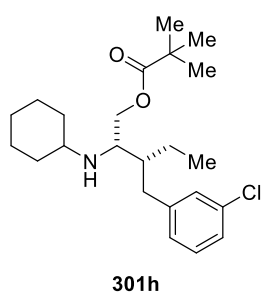


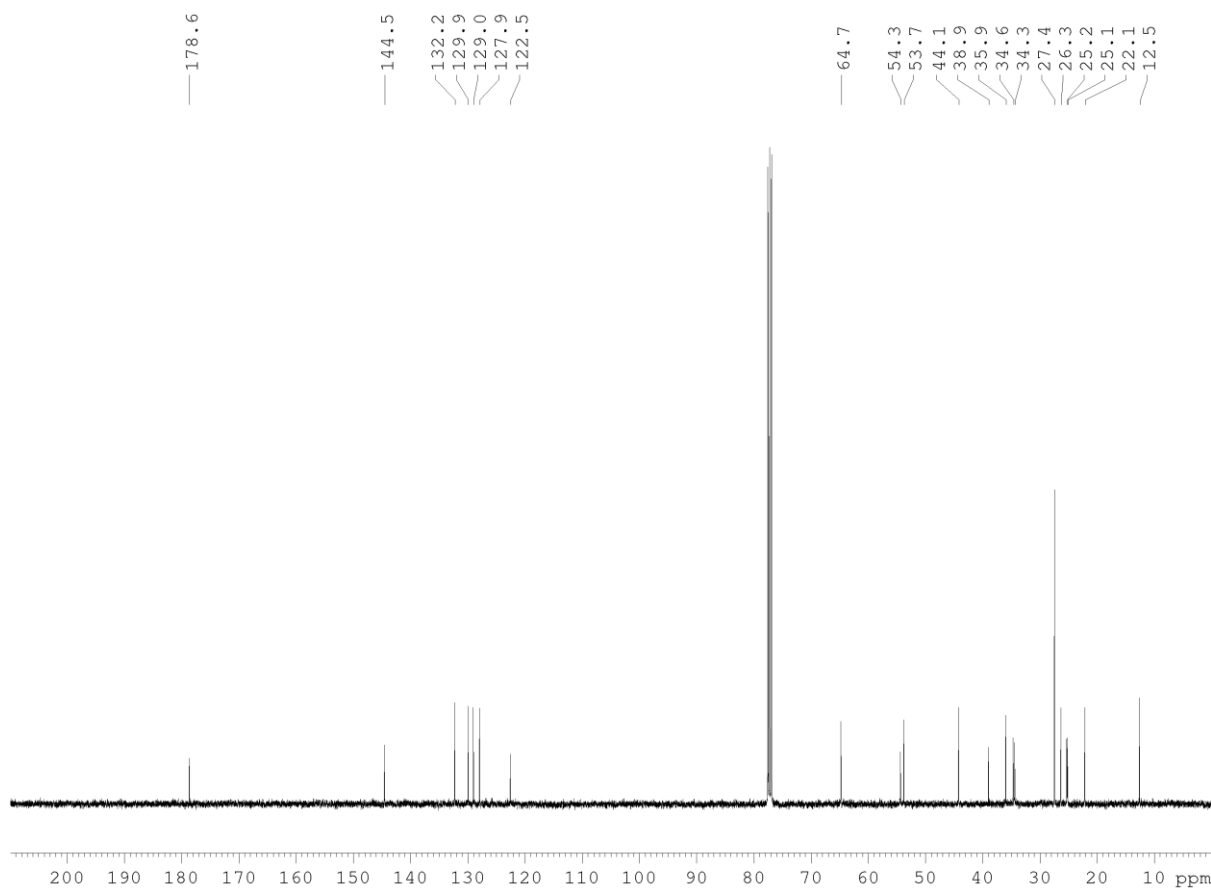
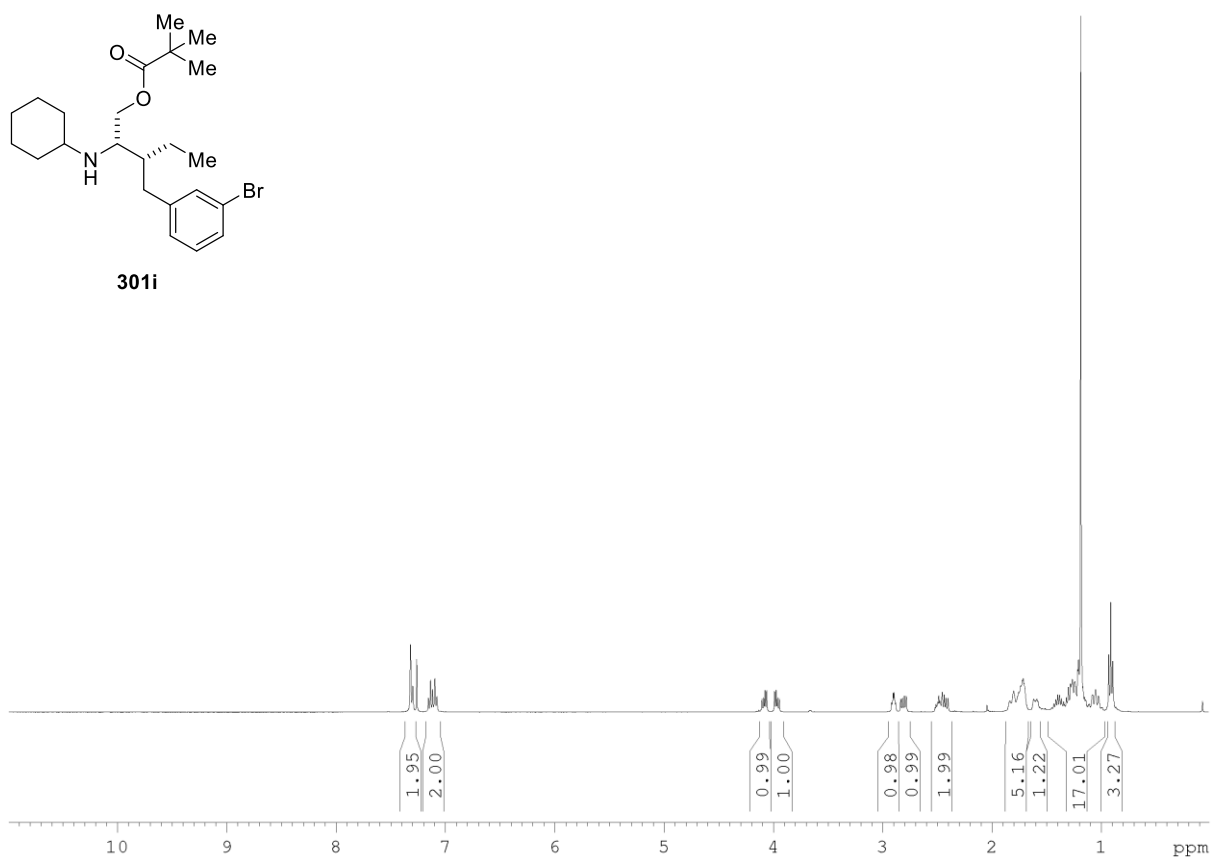
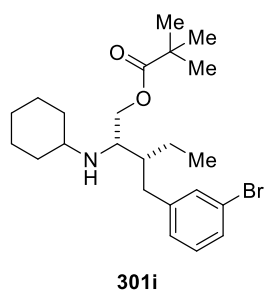


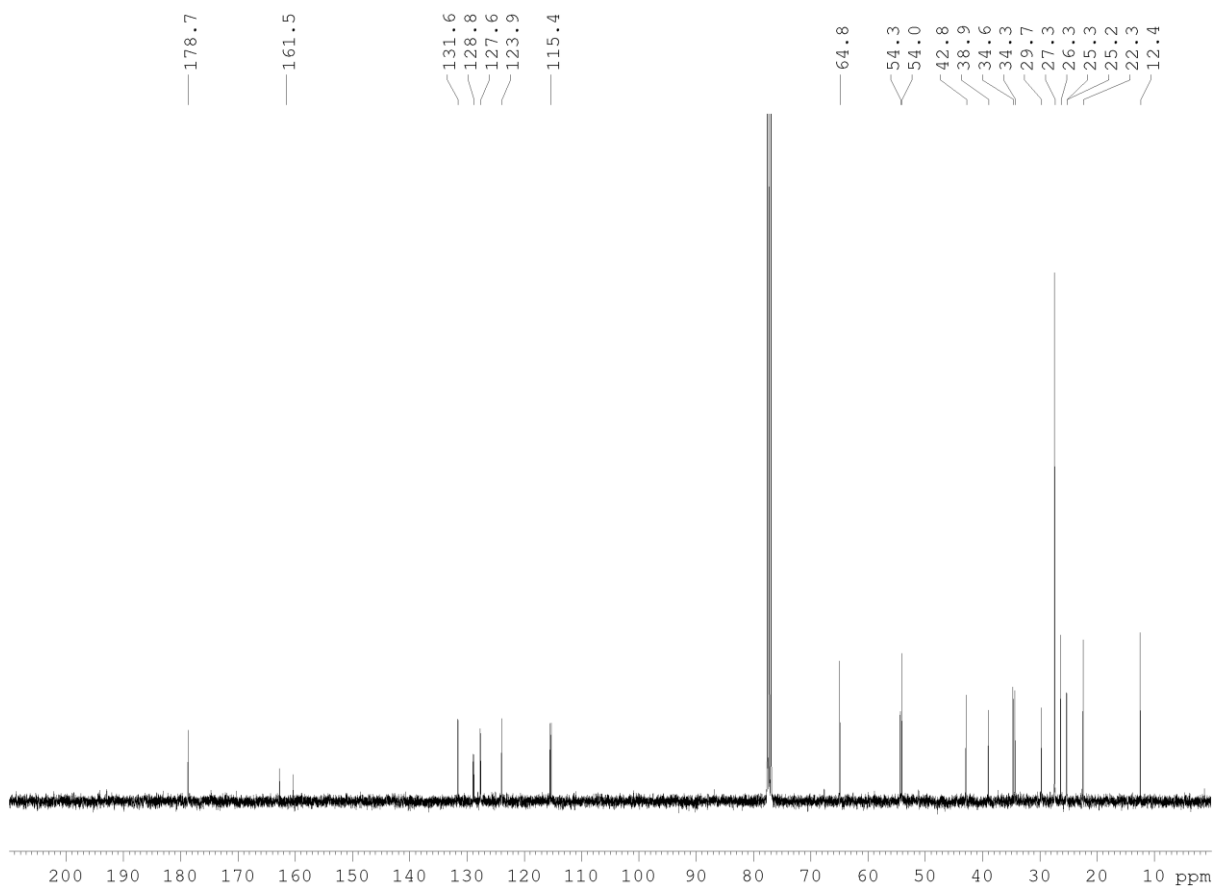
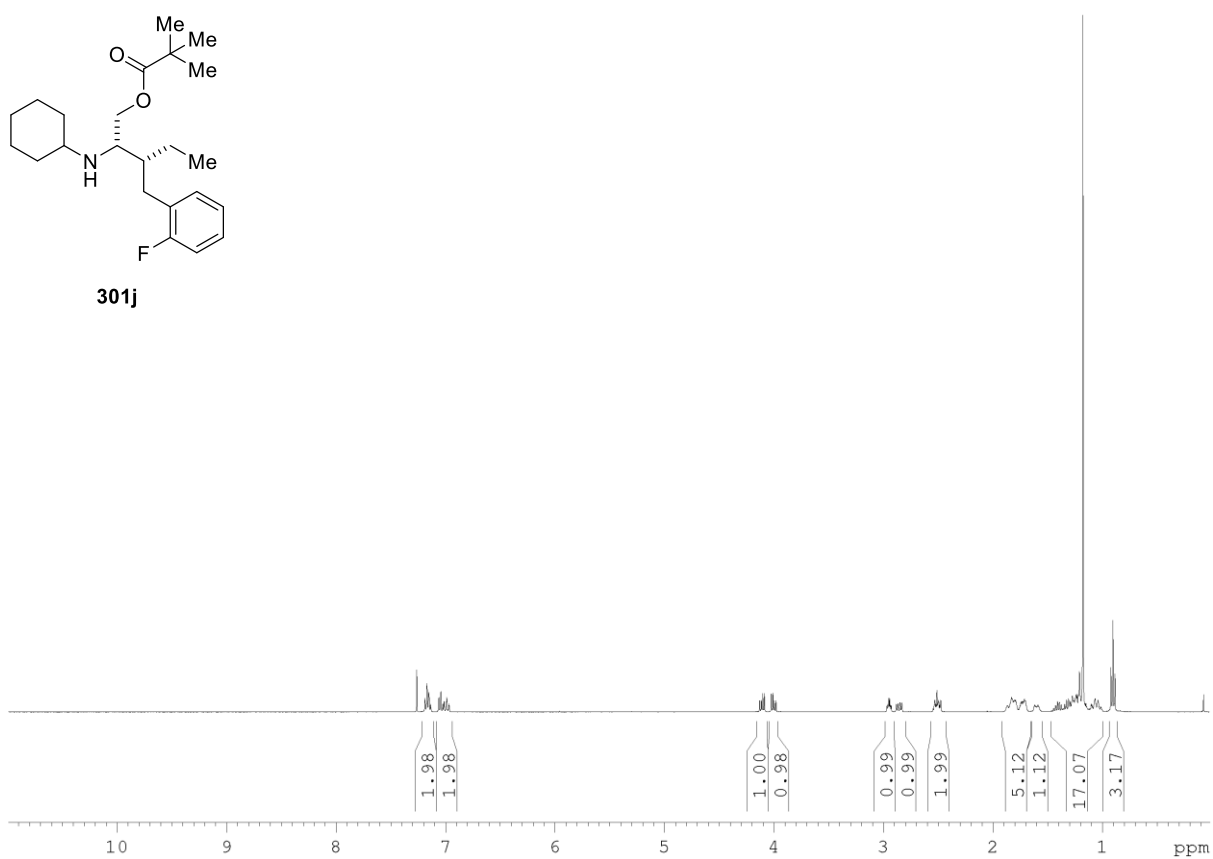


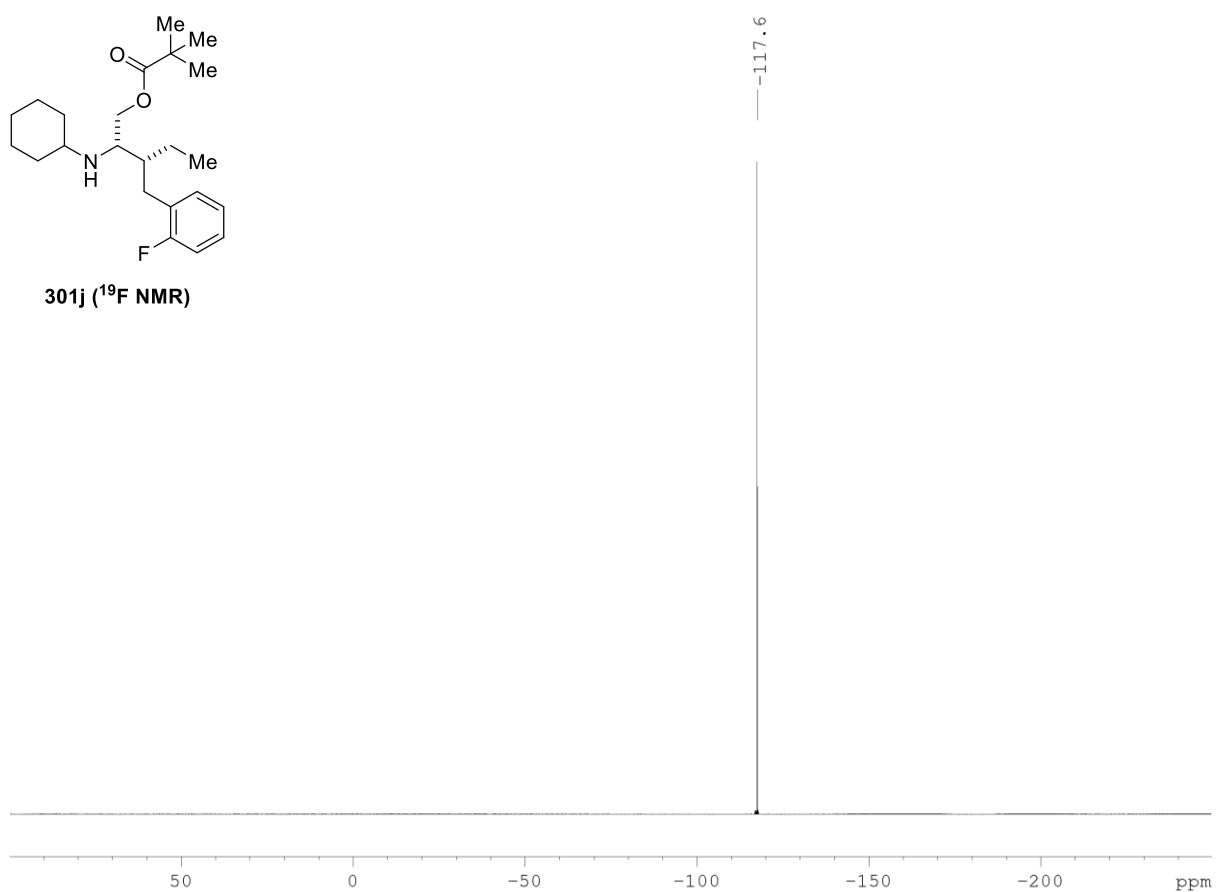


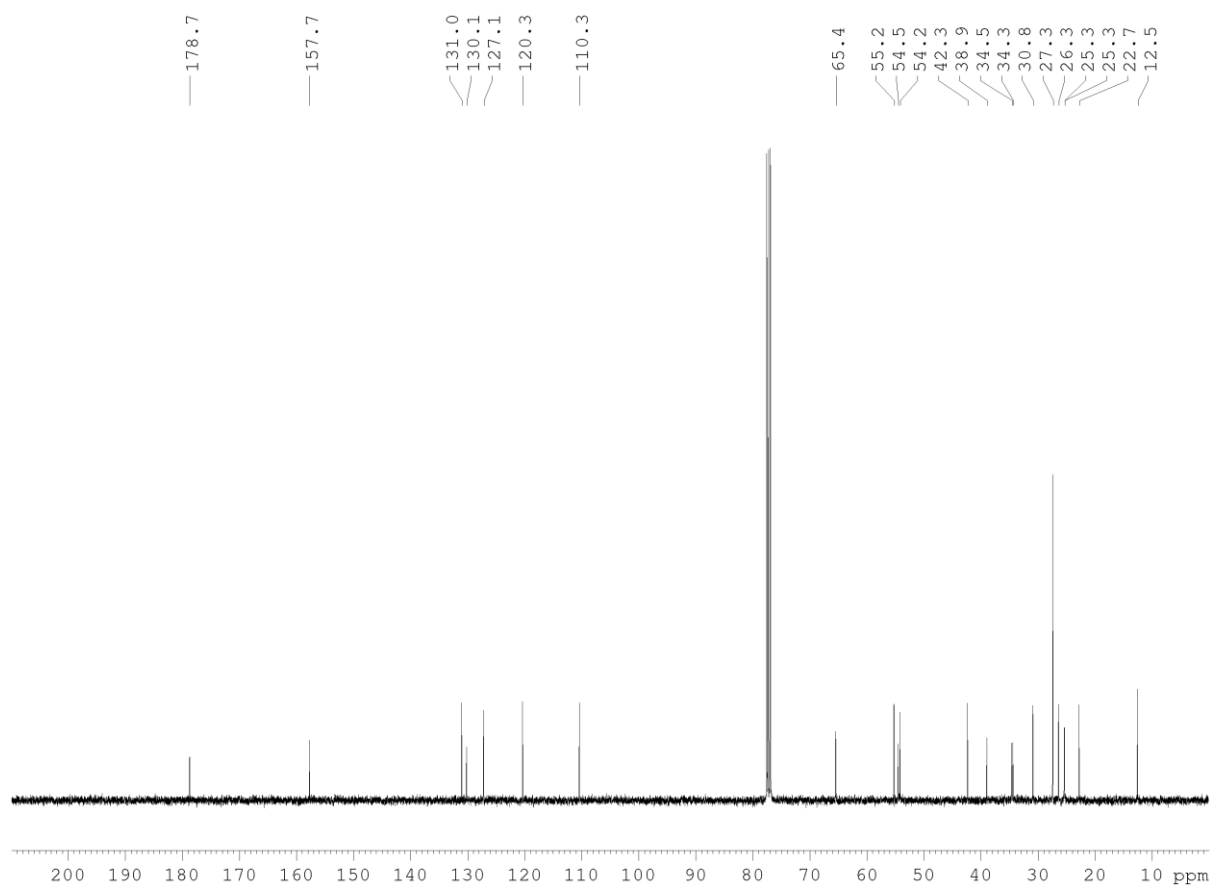
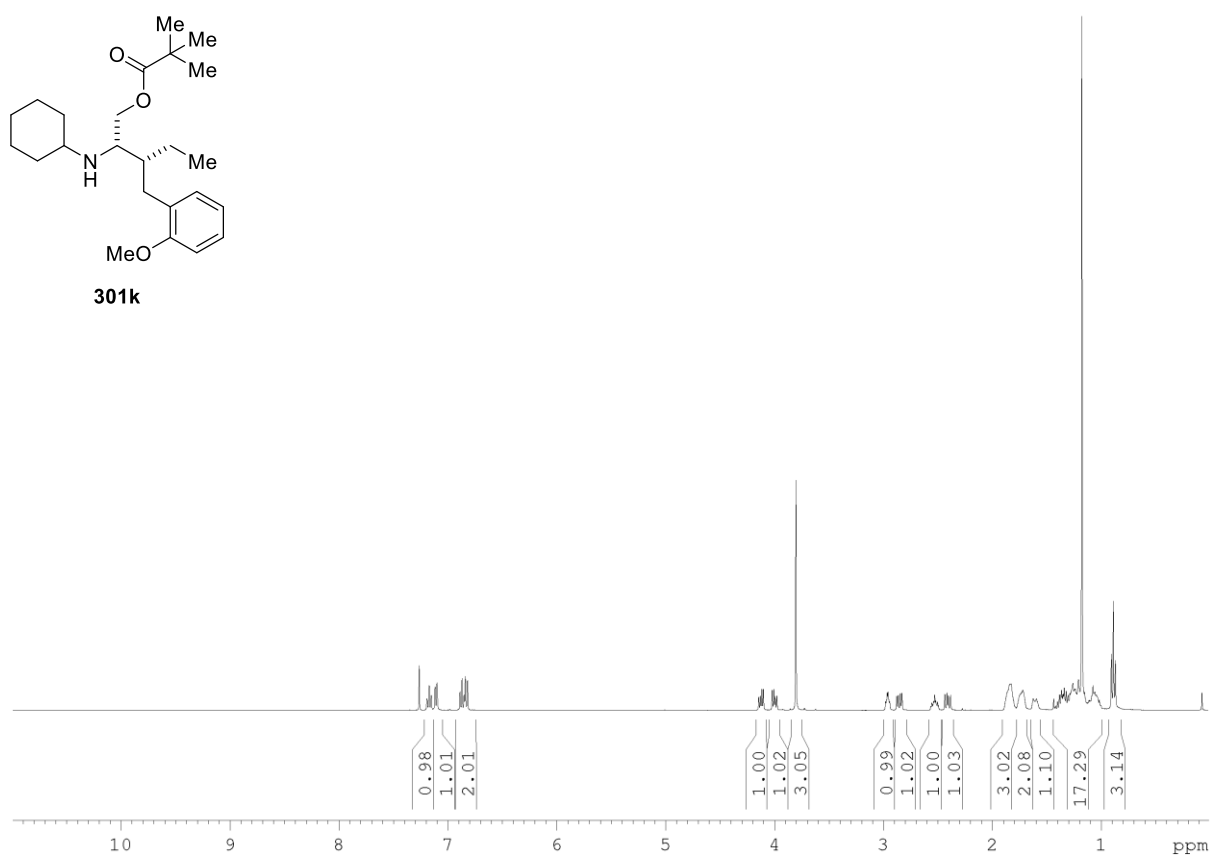


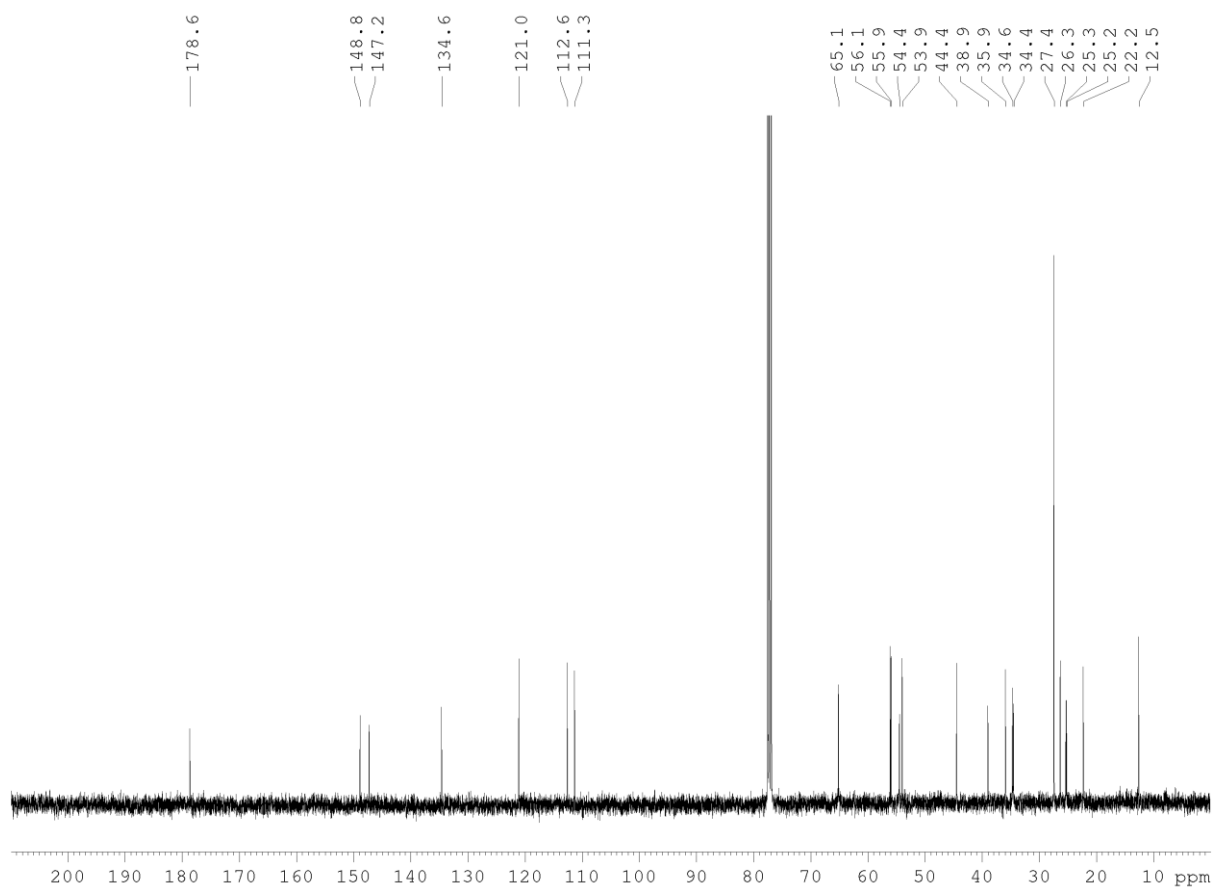
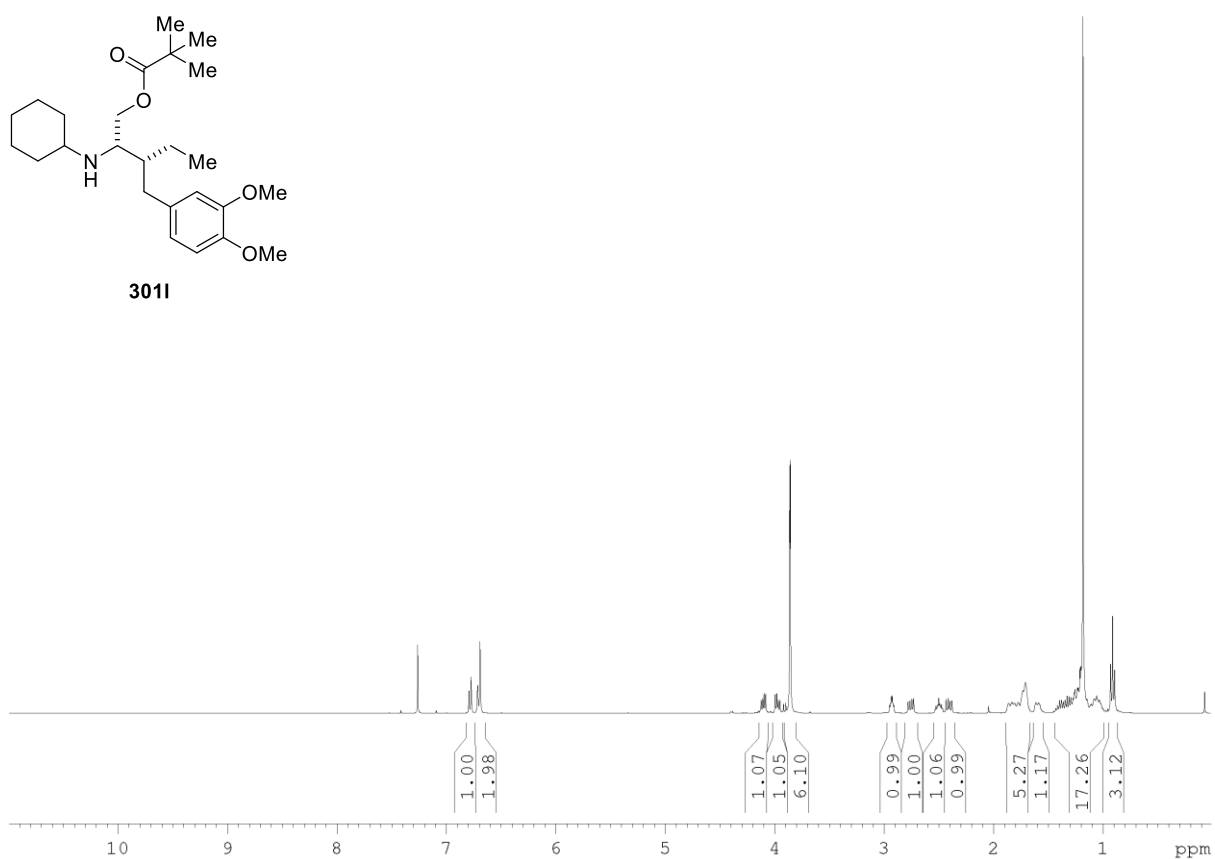
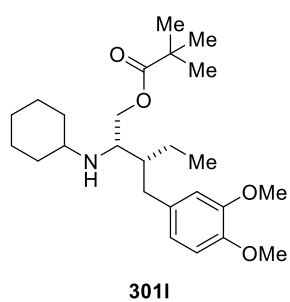


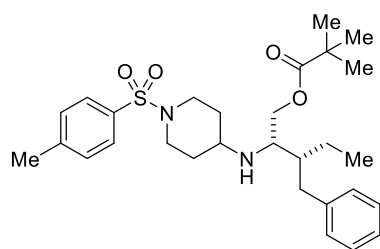




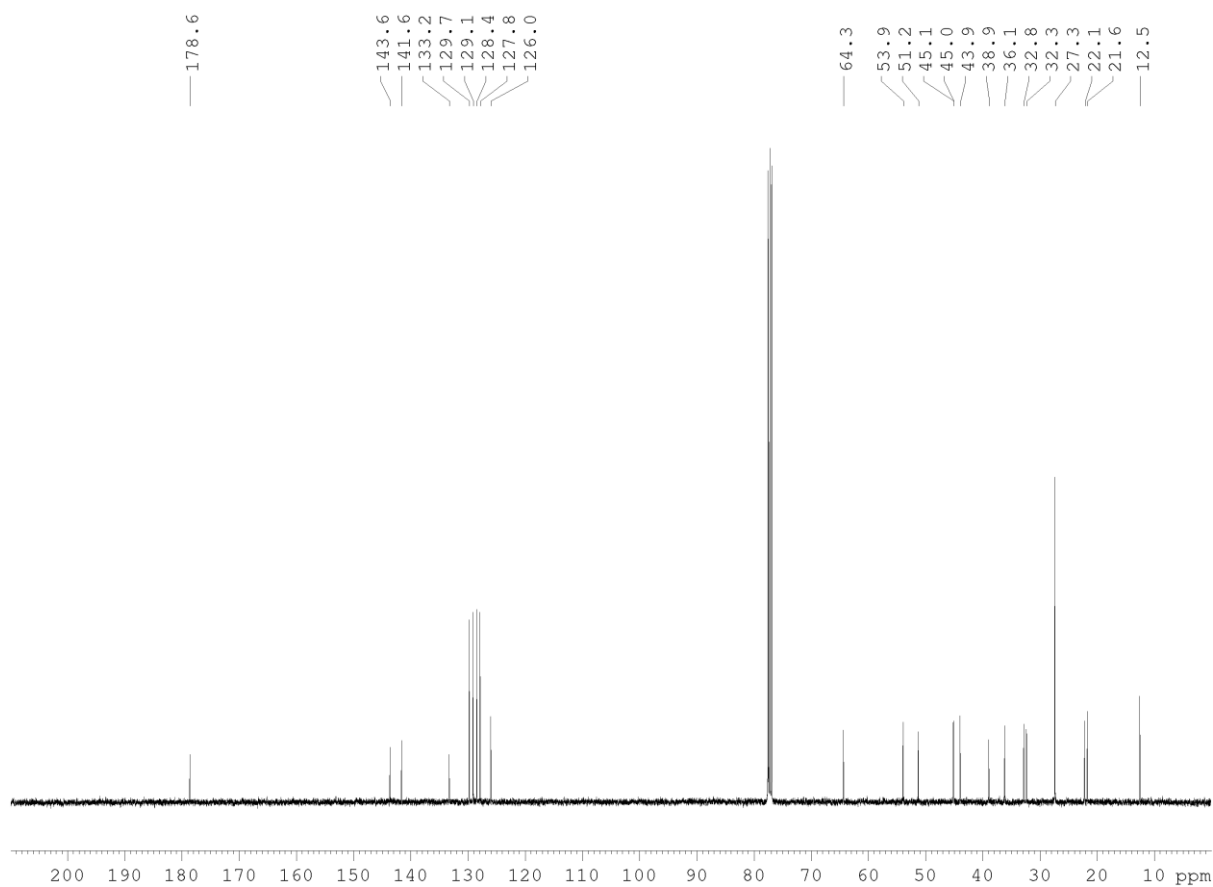
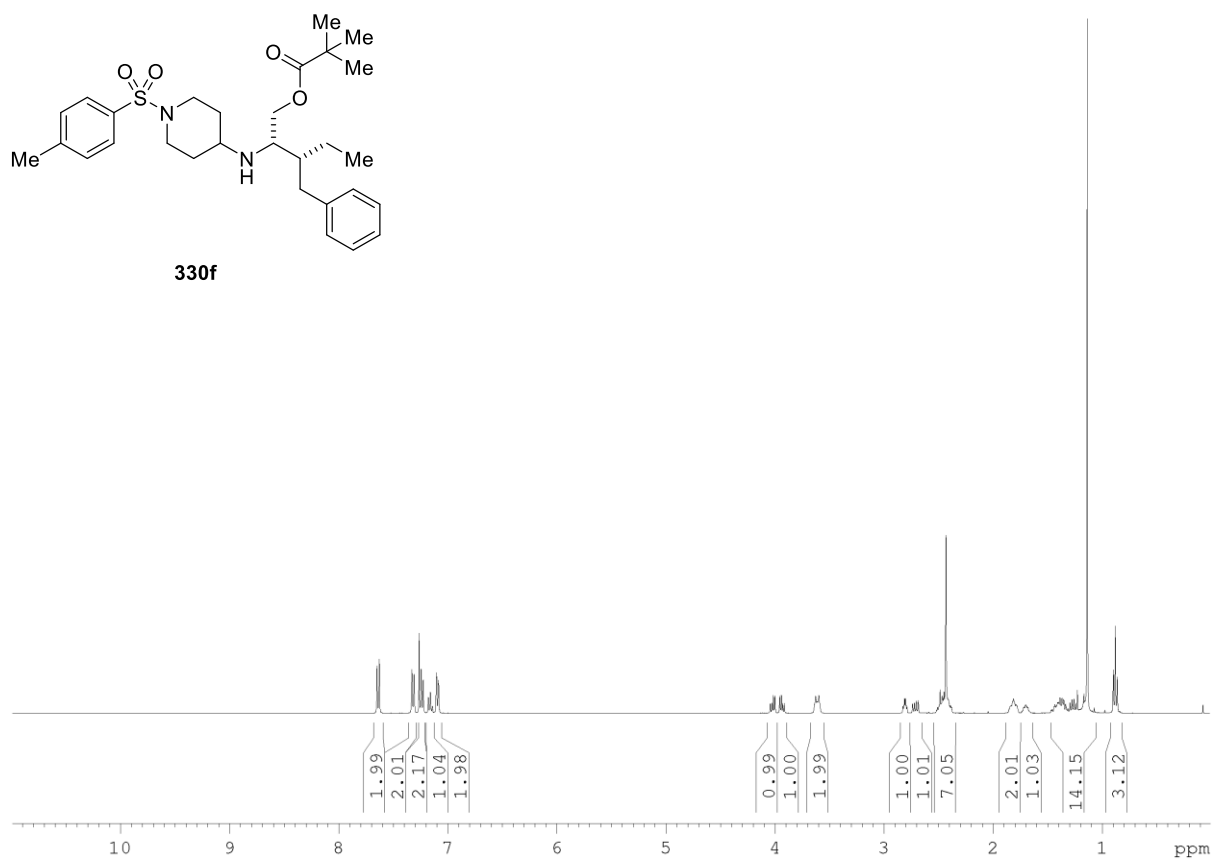


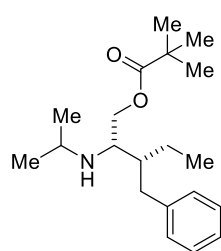




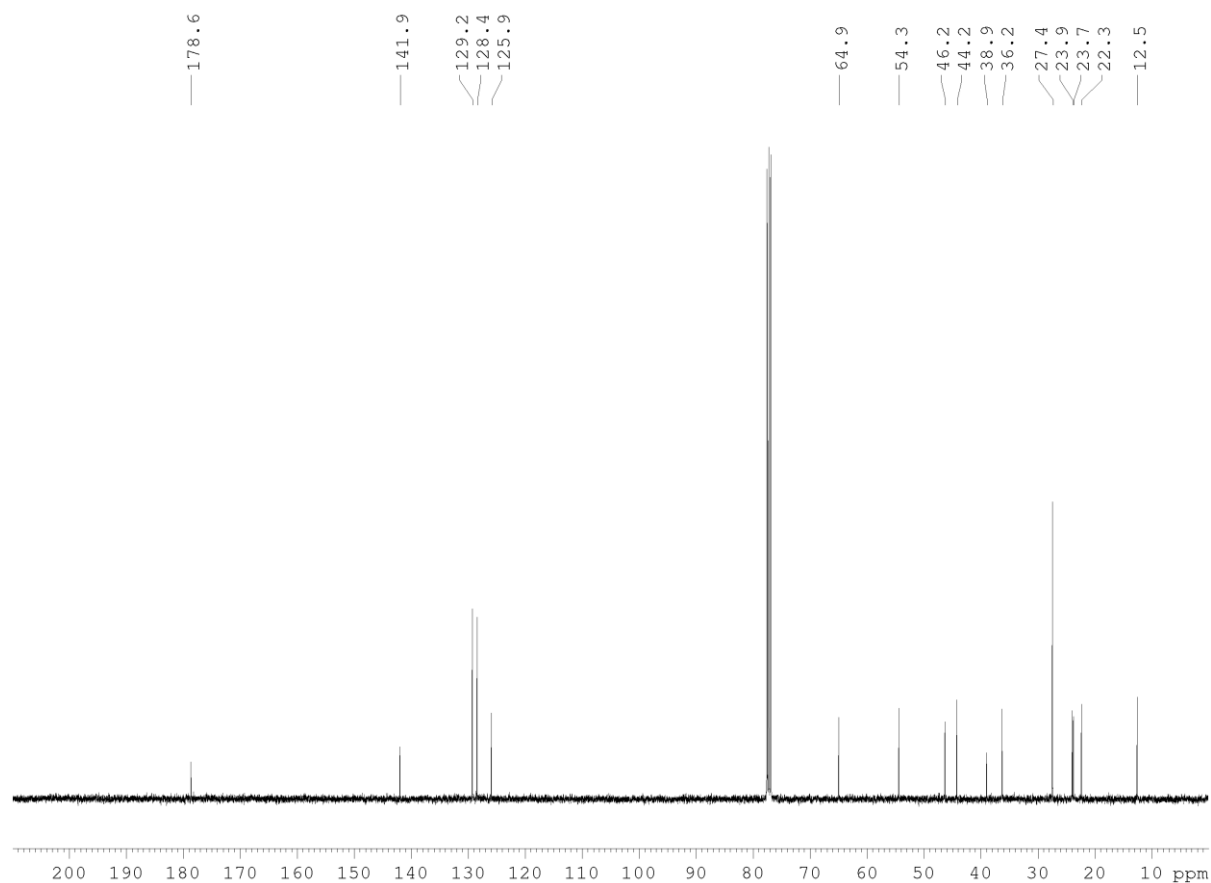
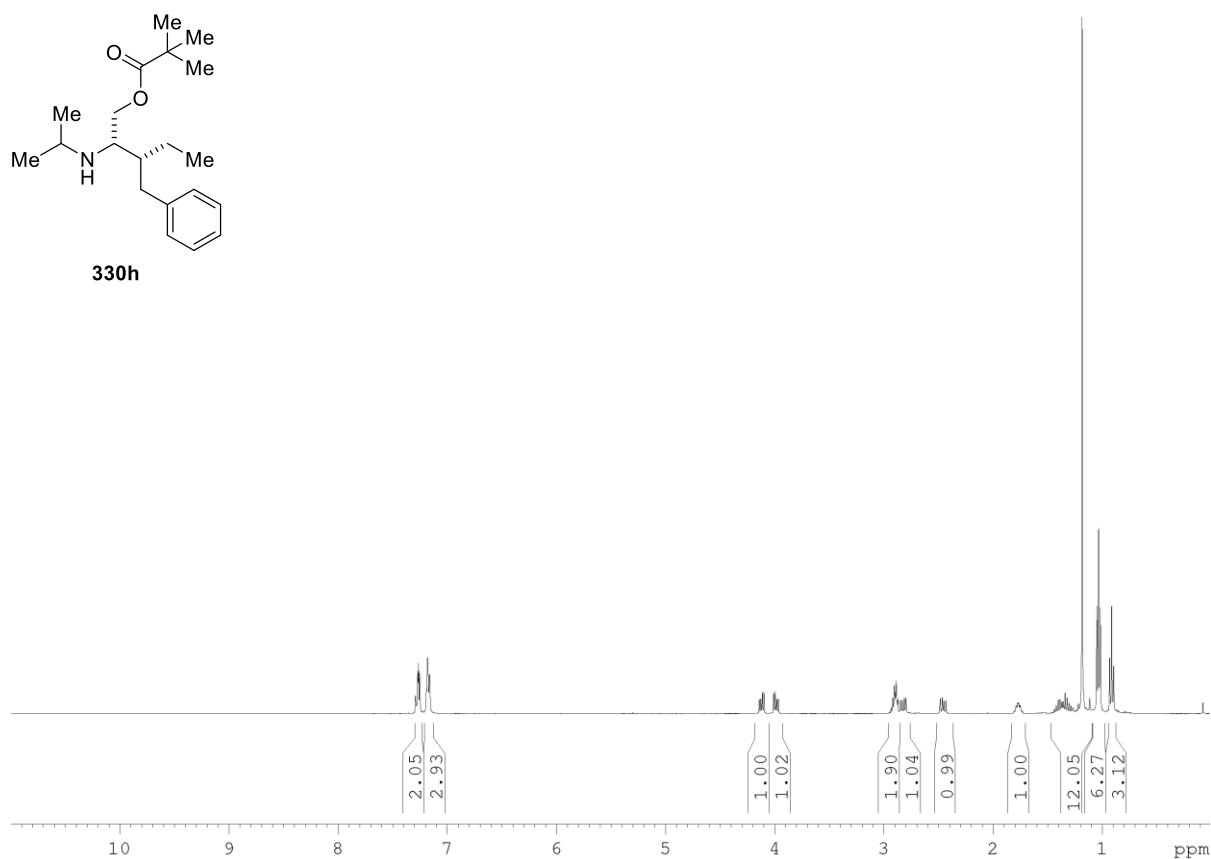


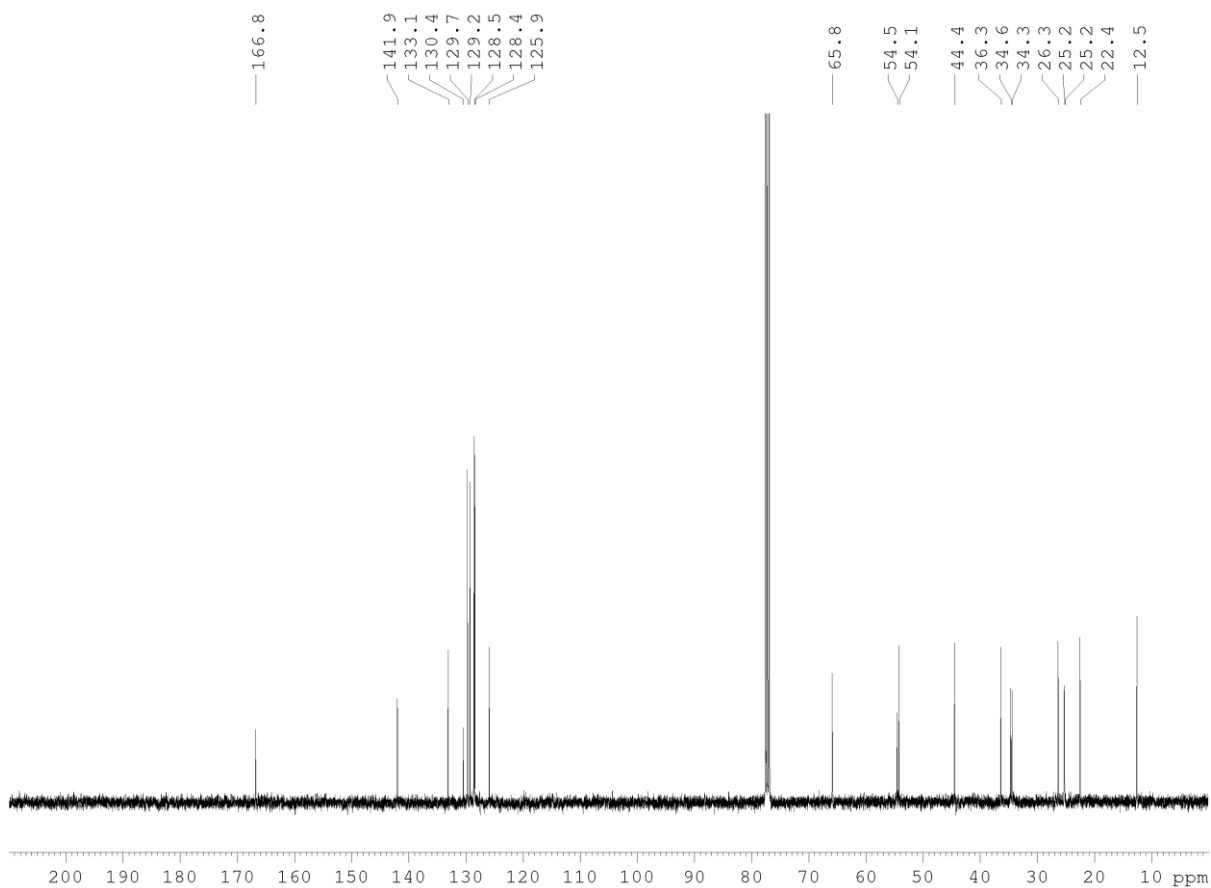
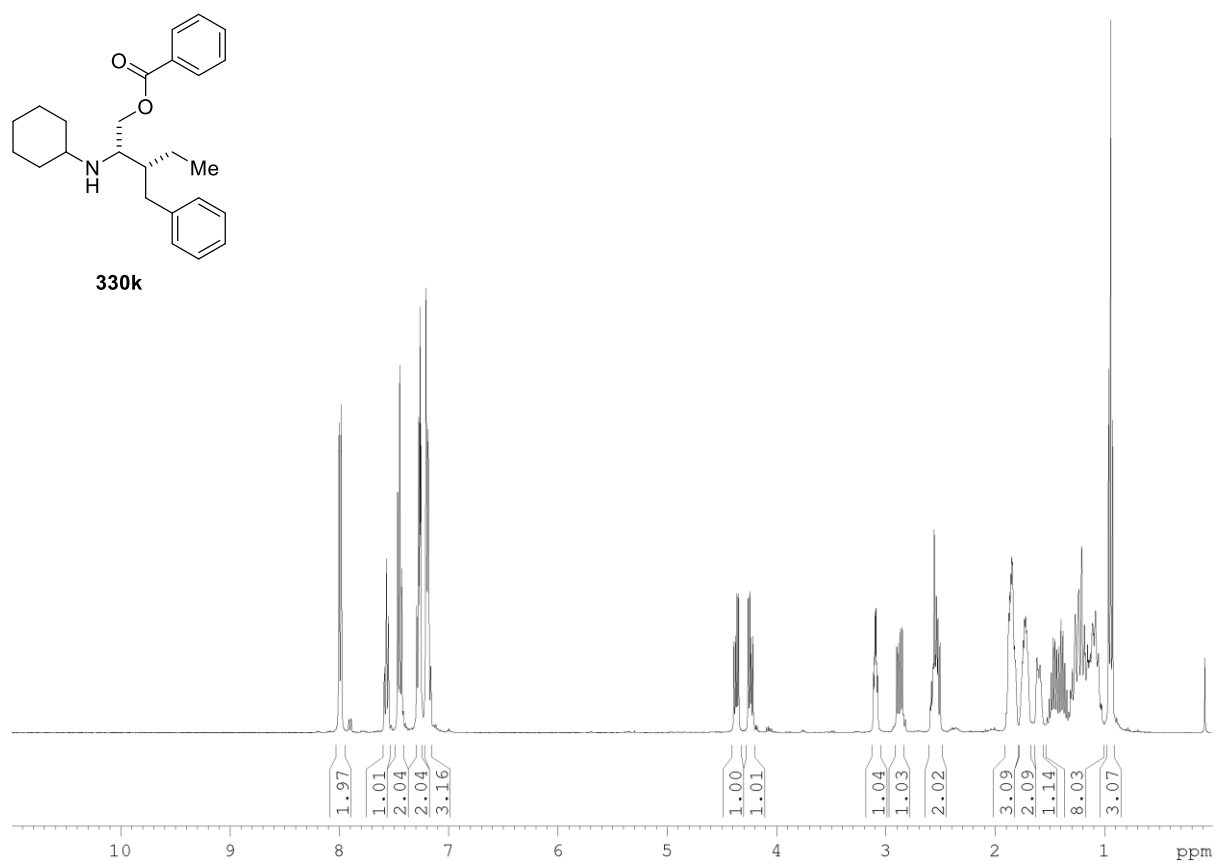
330f

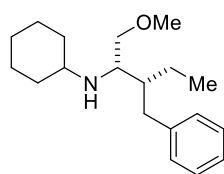




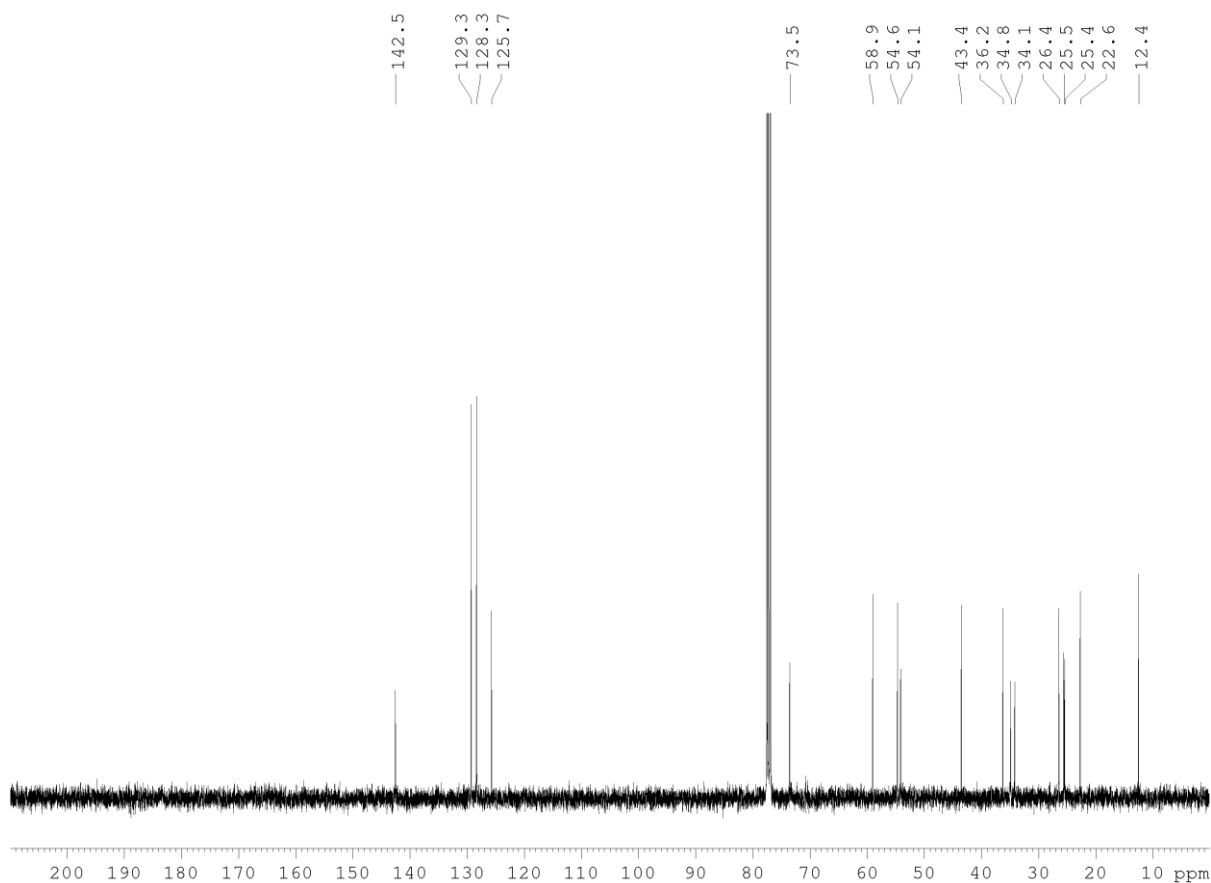
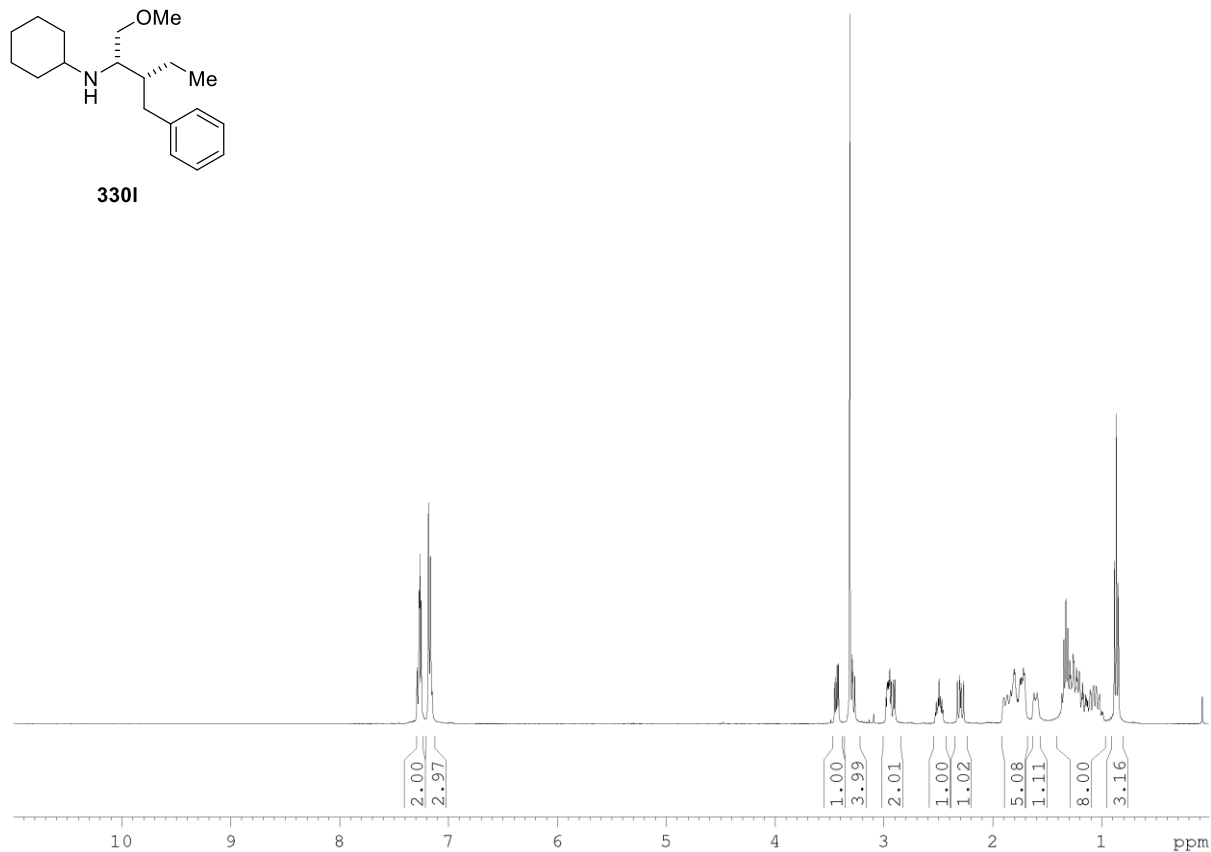
330h

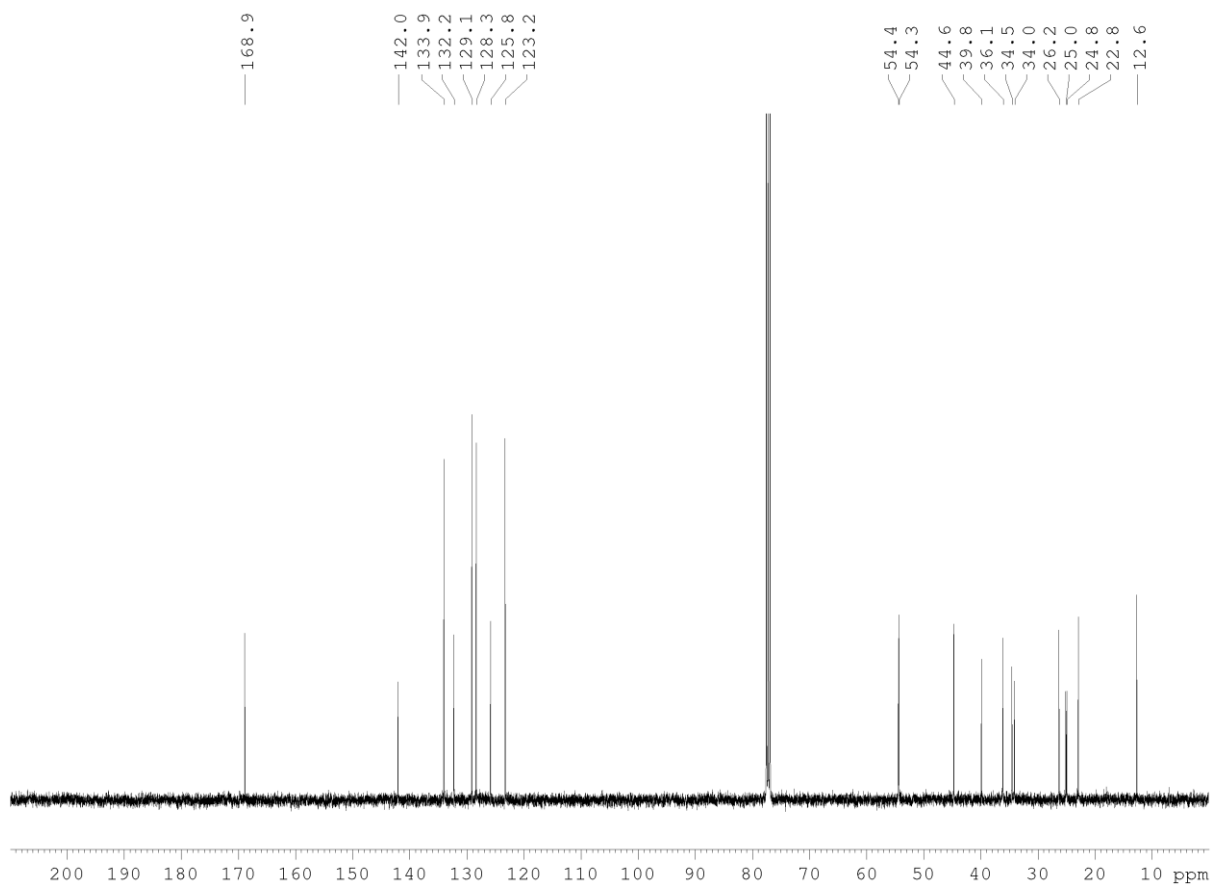
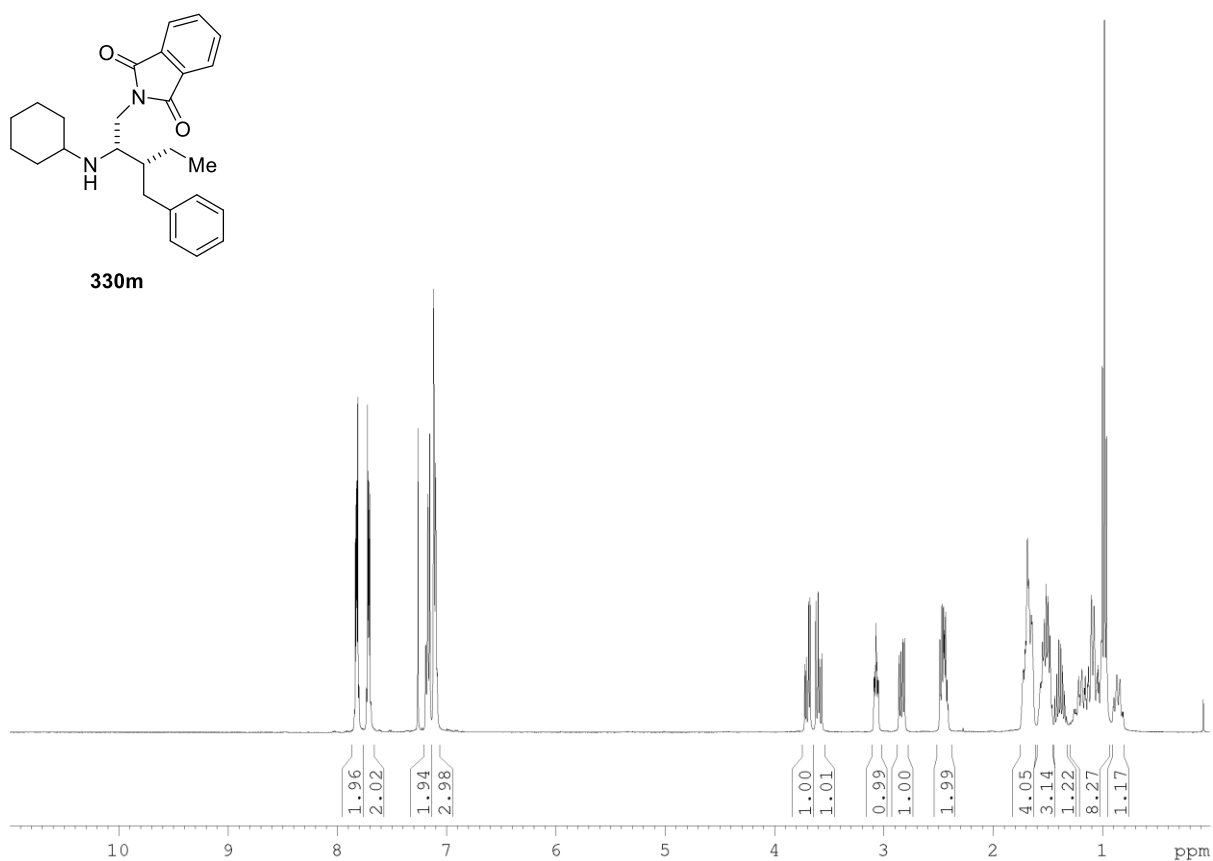


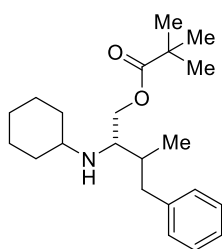
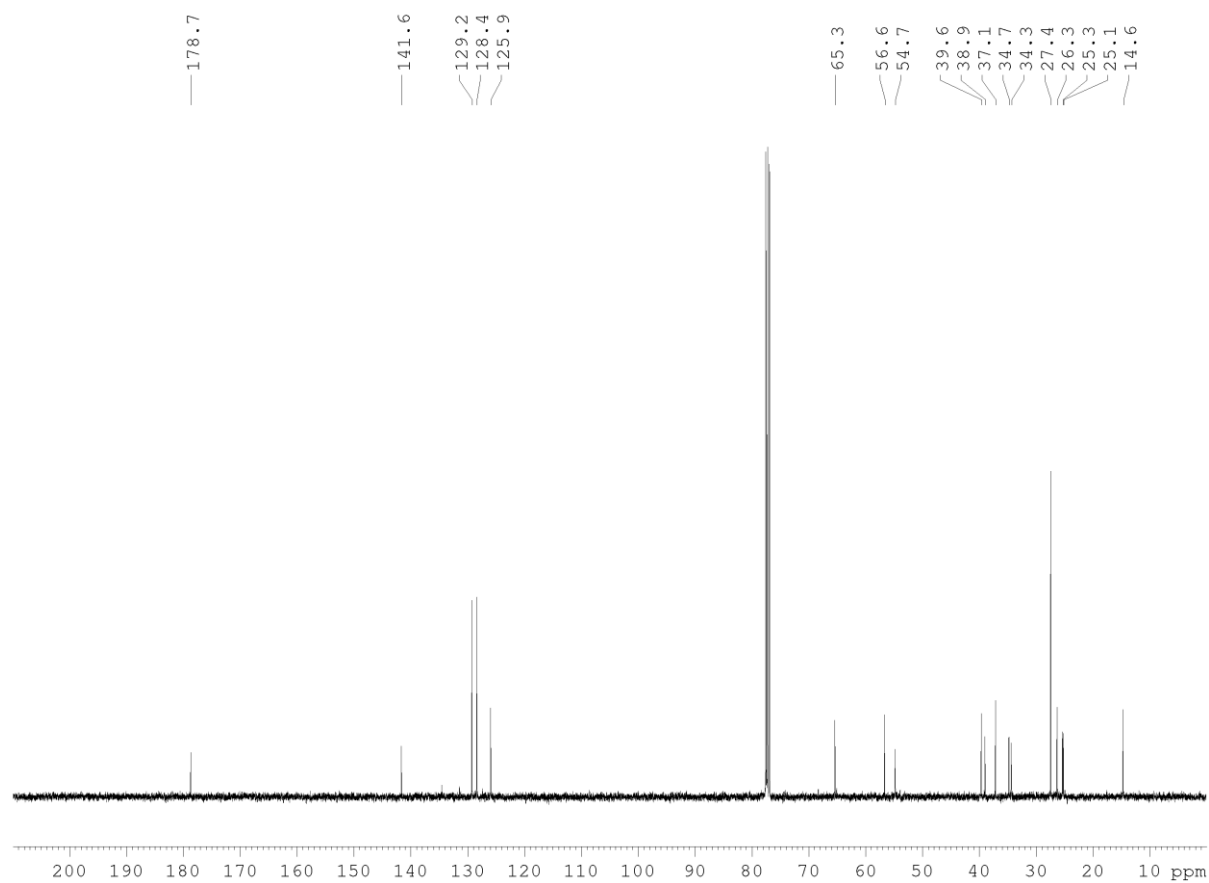
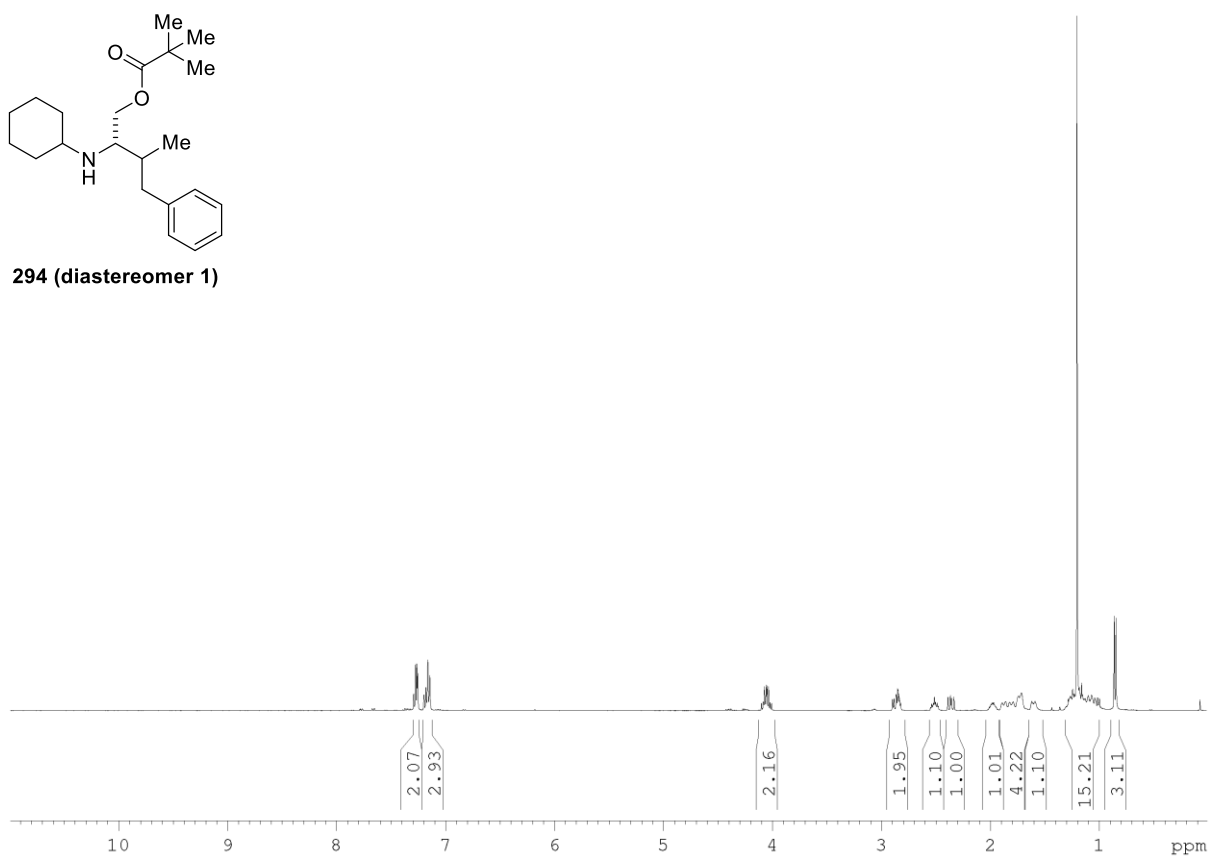


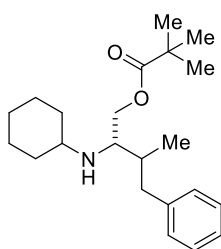
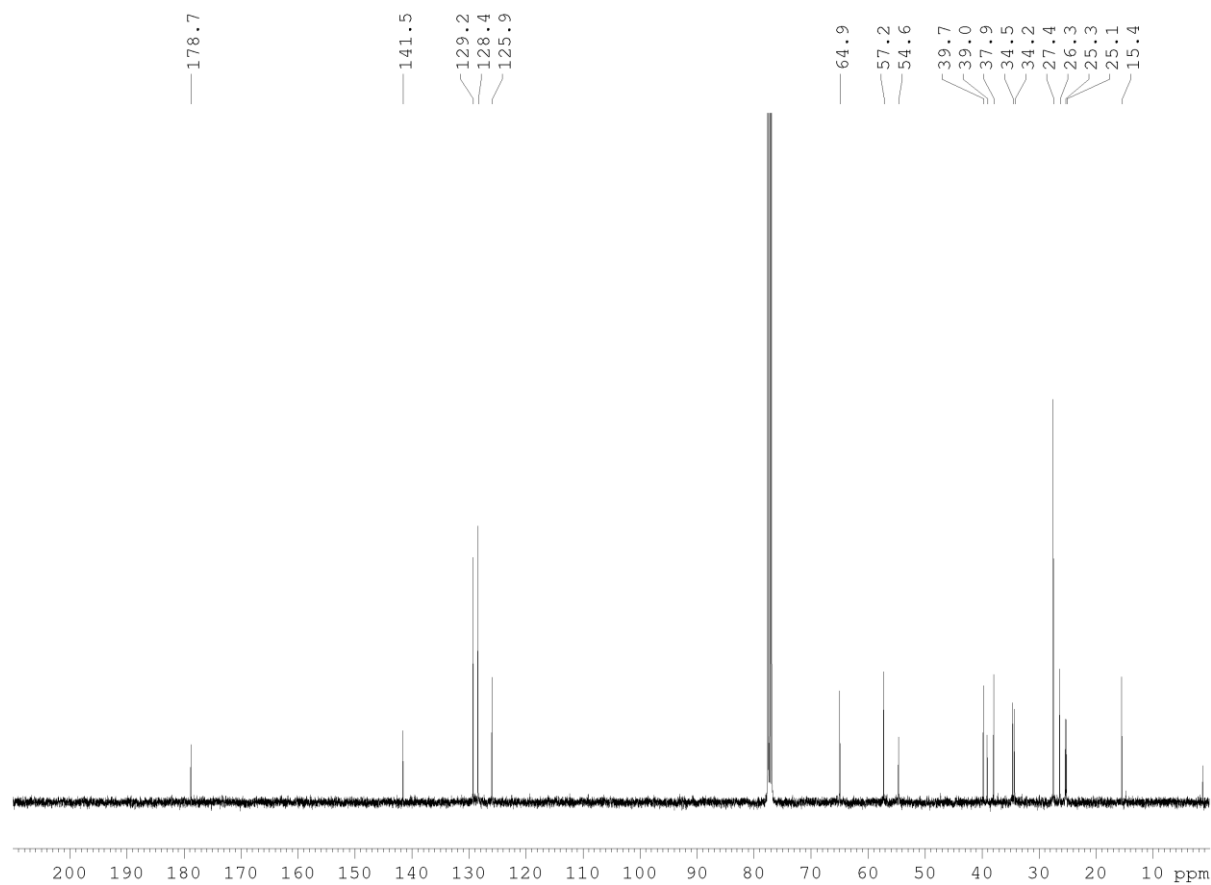
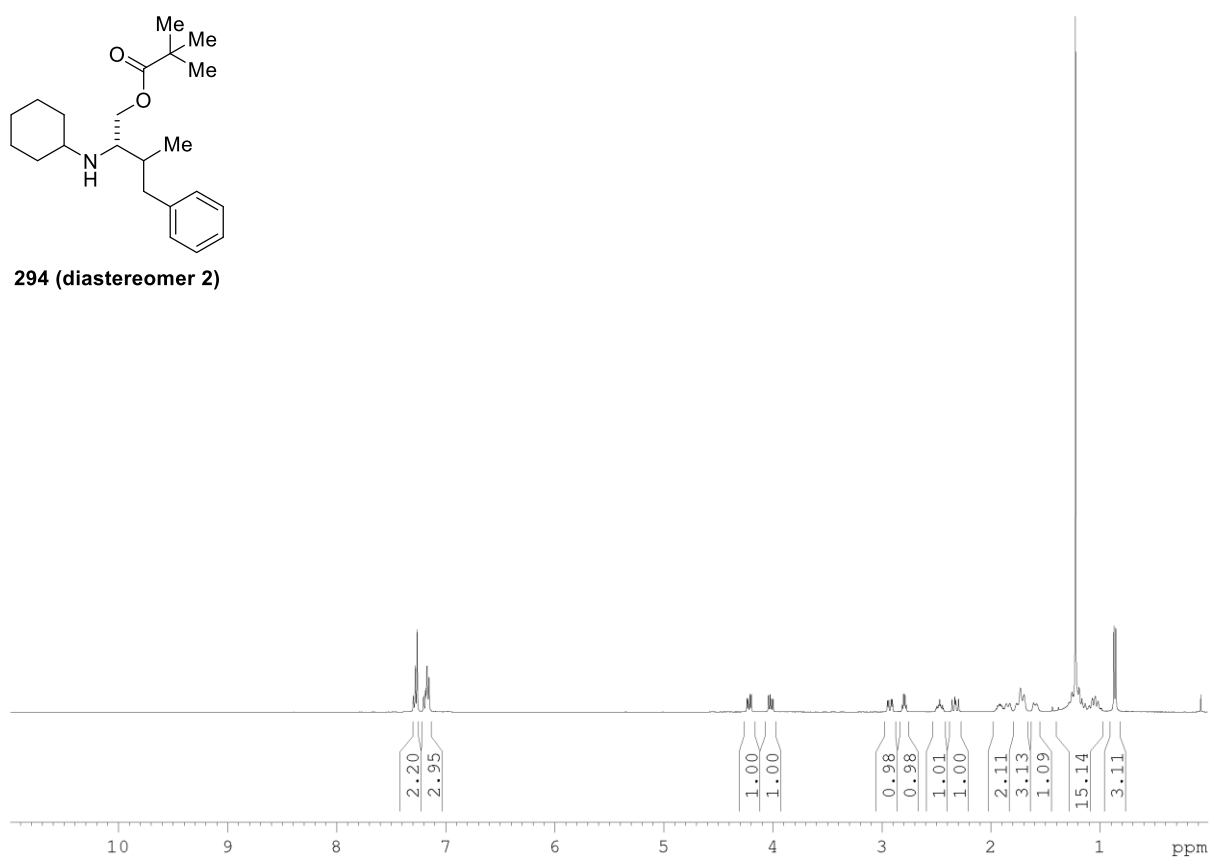


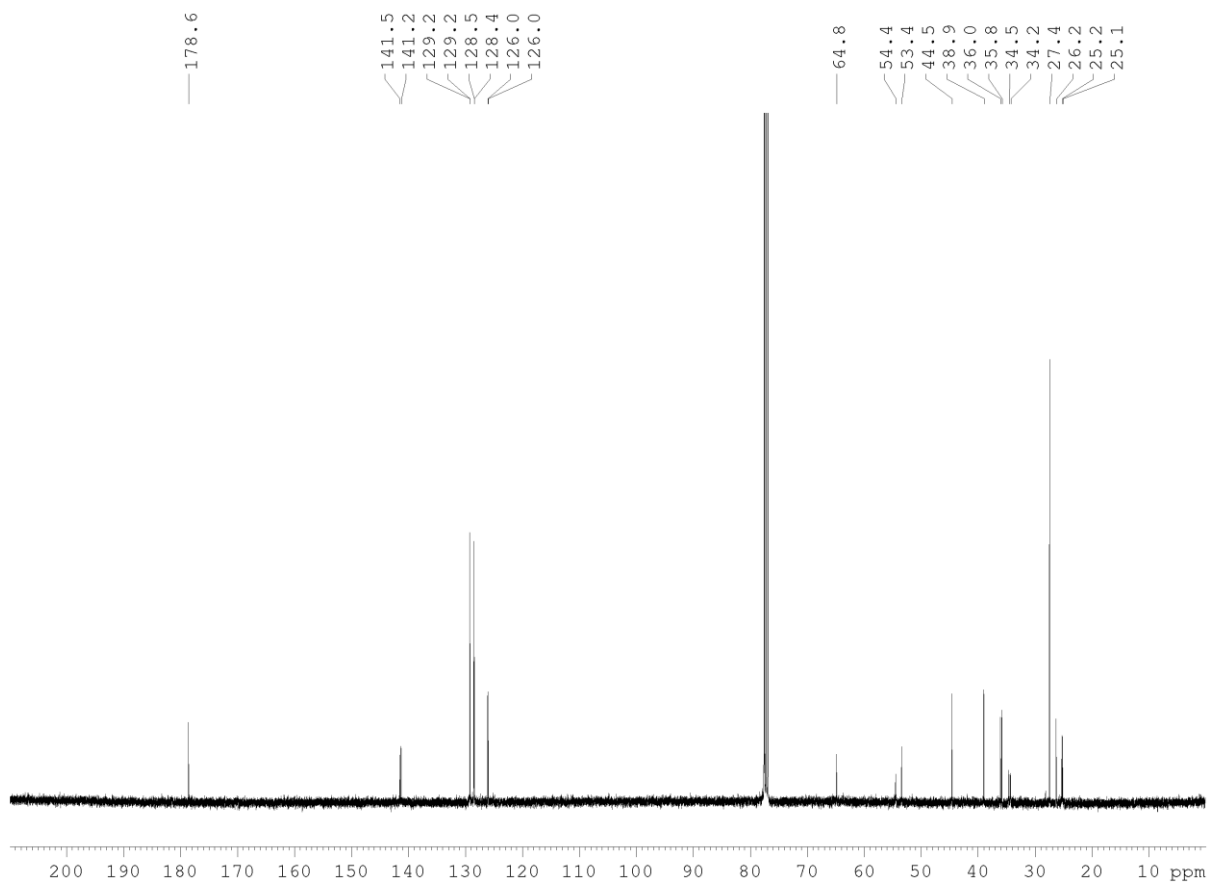
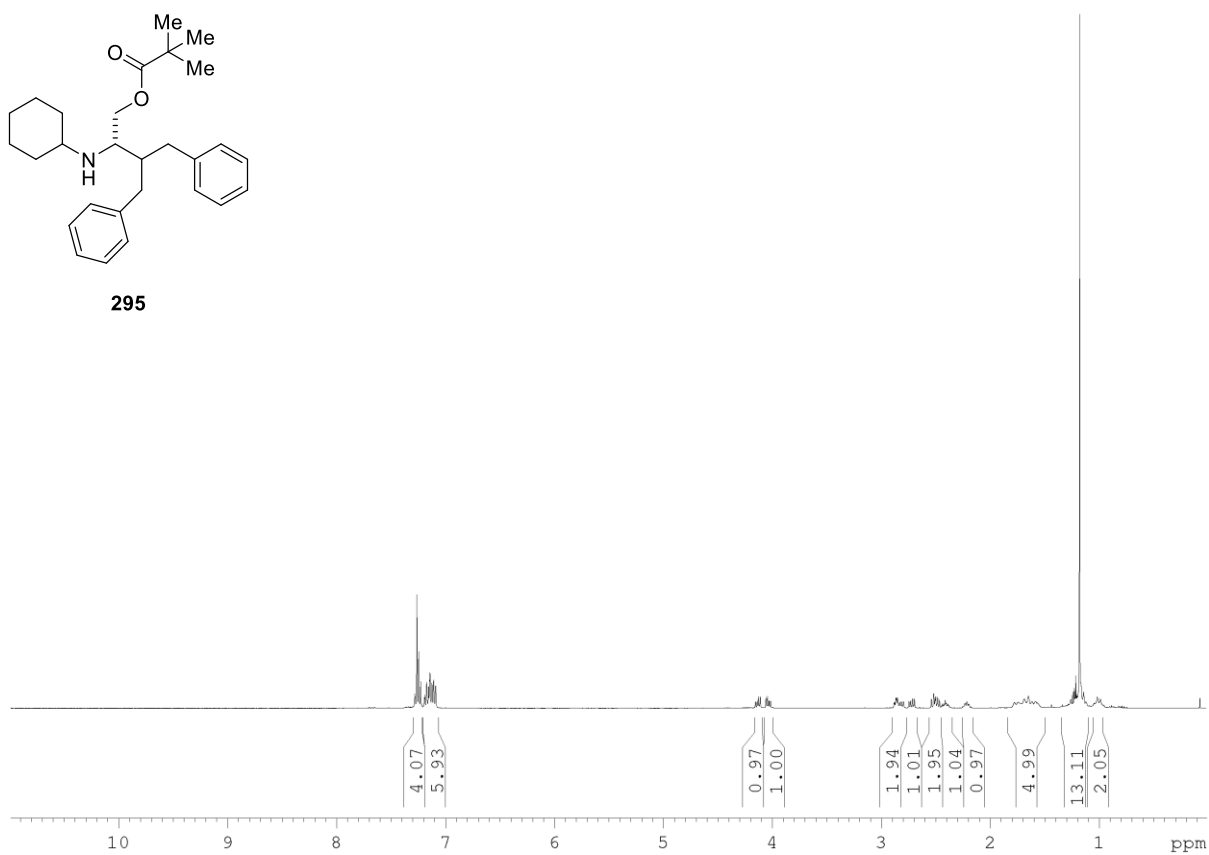
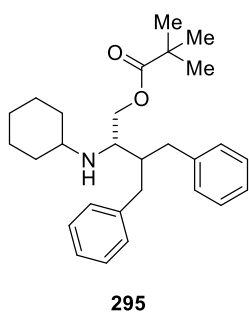
330I

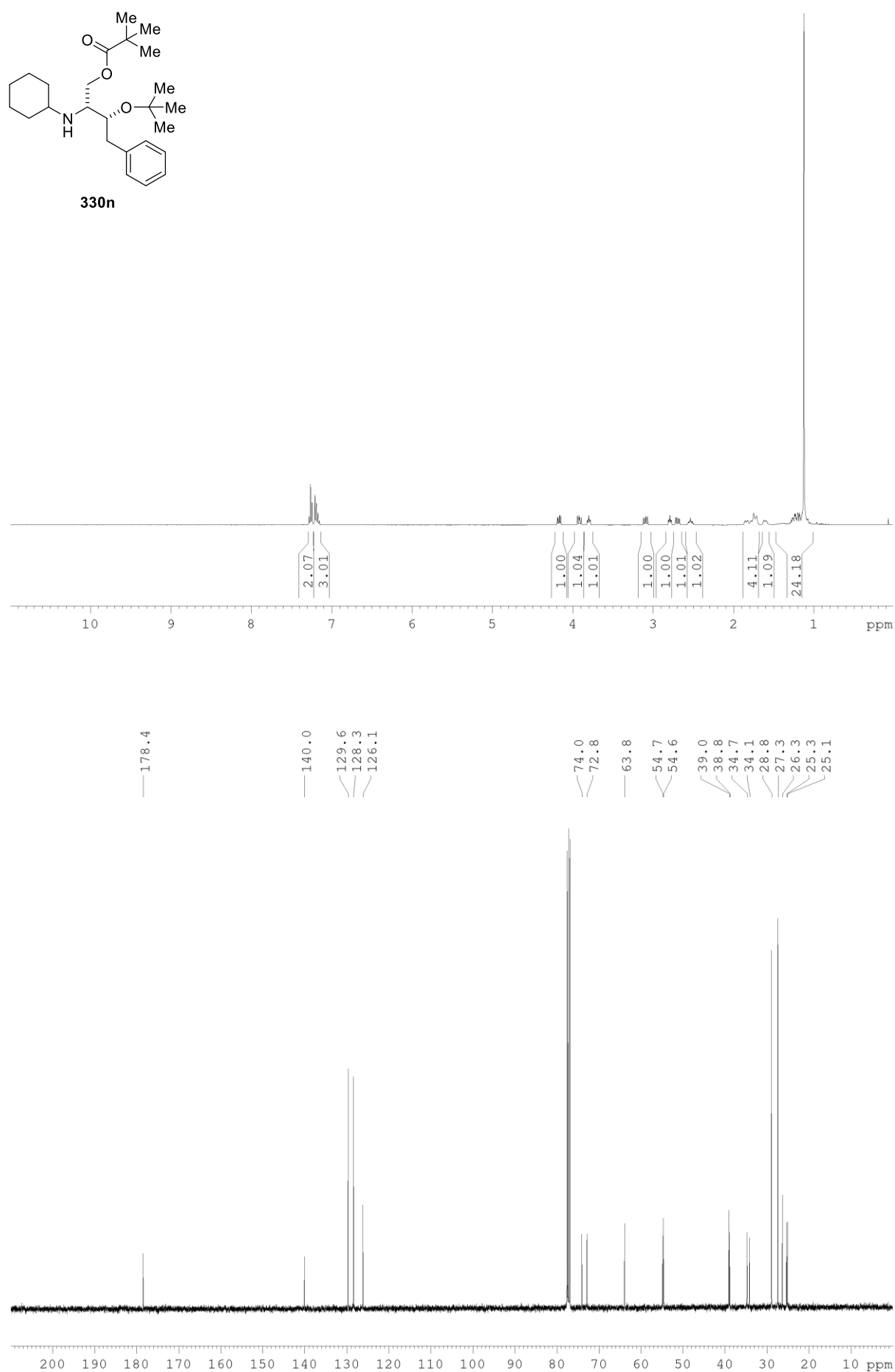


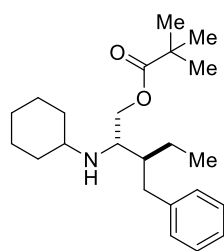
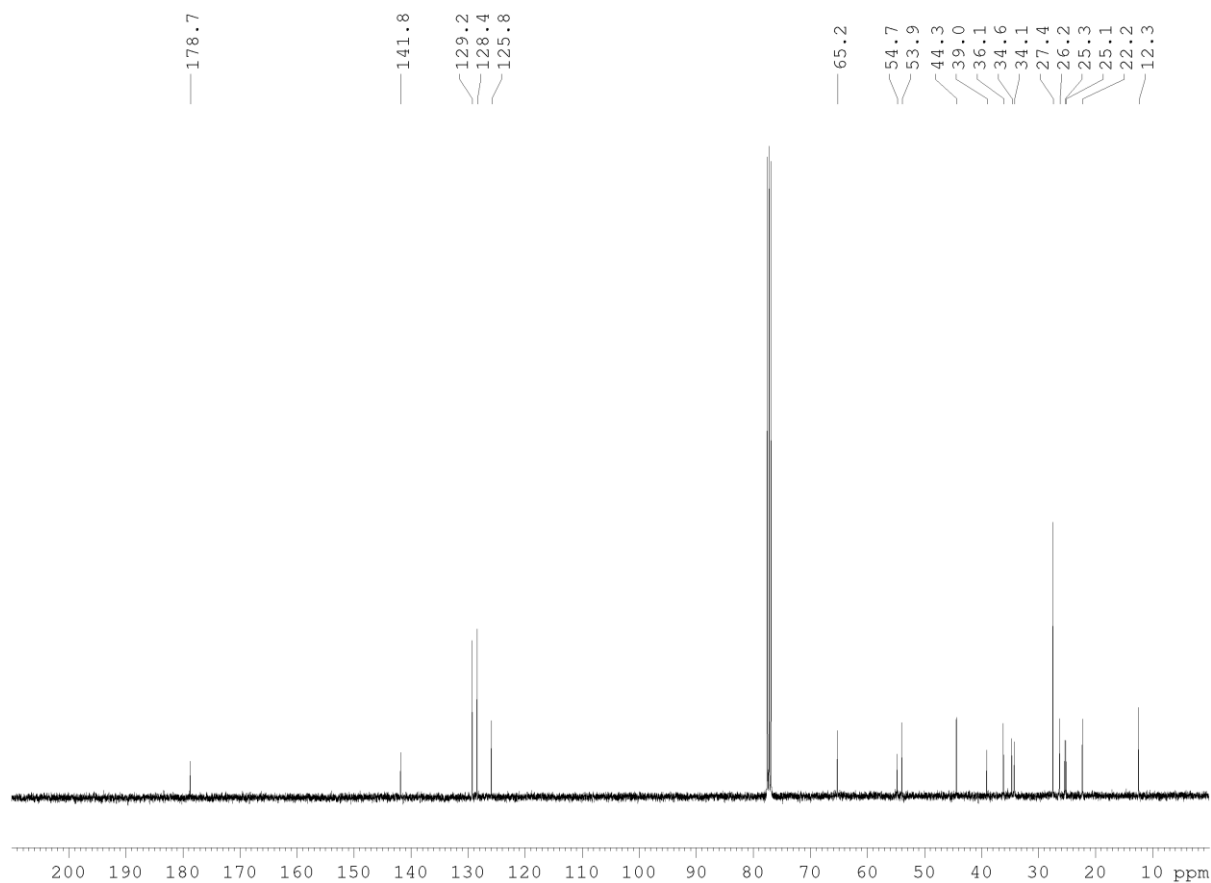
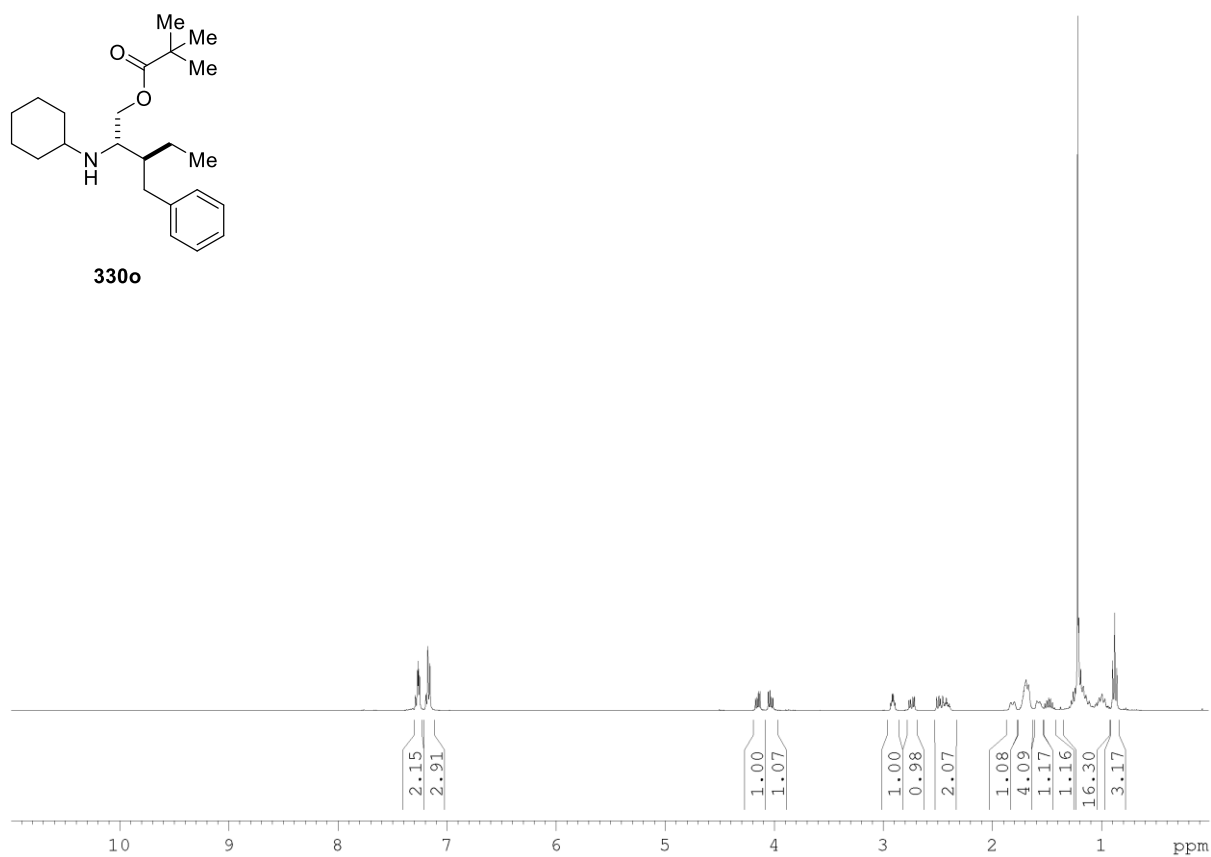


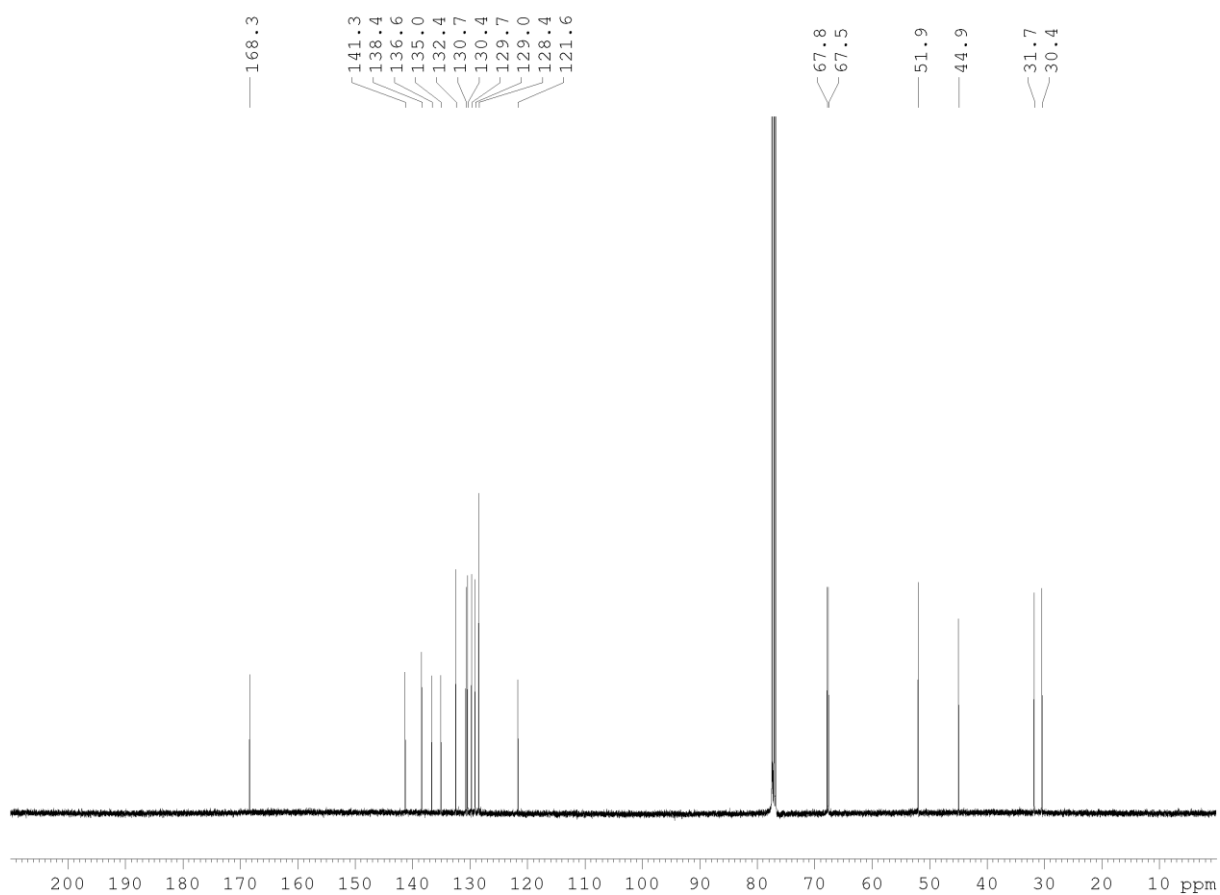
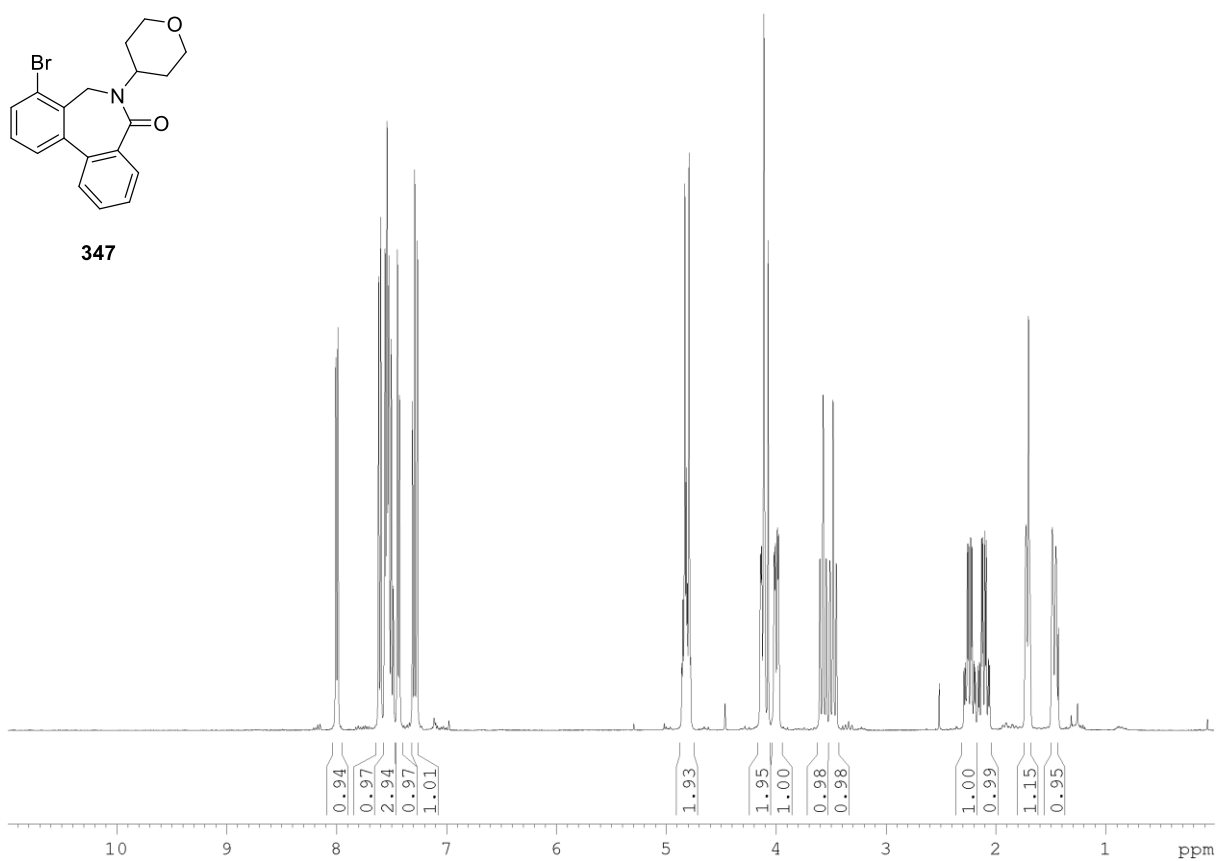
**294 (diastereomer 1)**

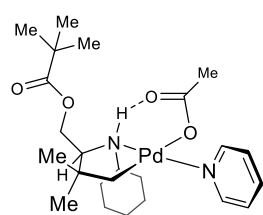
**294 (diastereomer 2)**



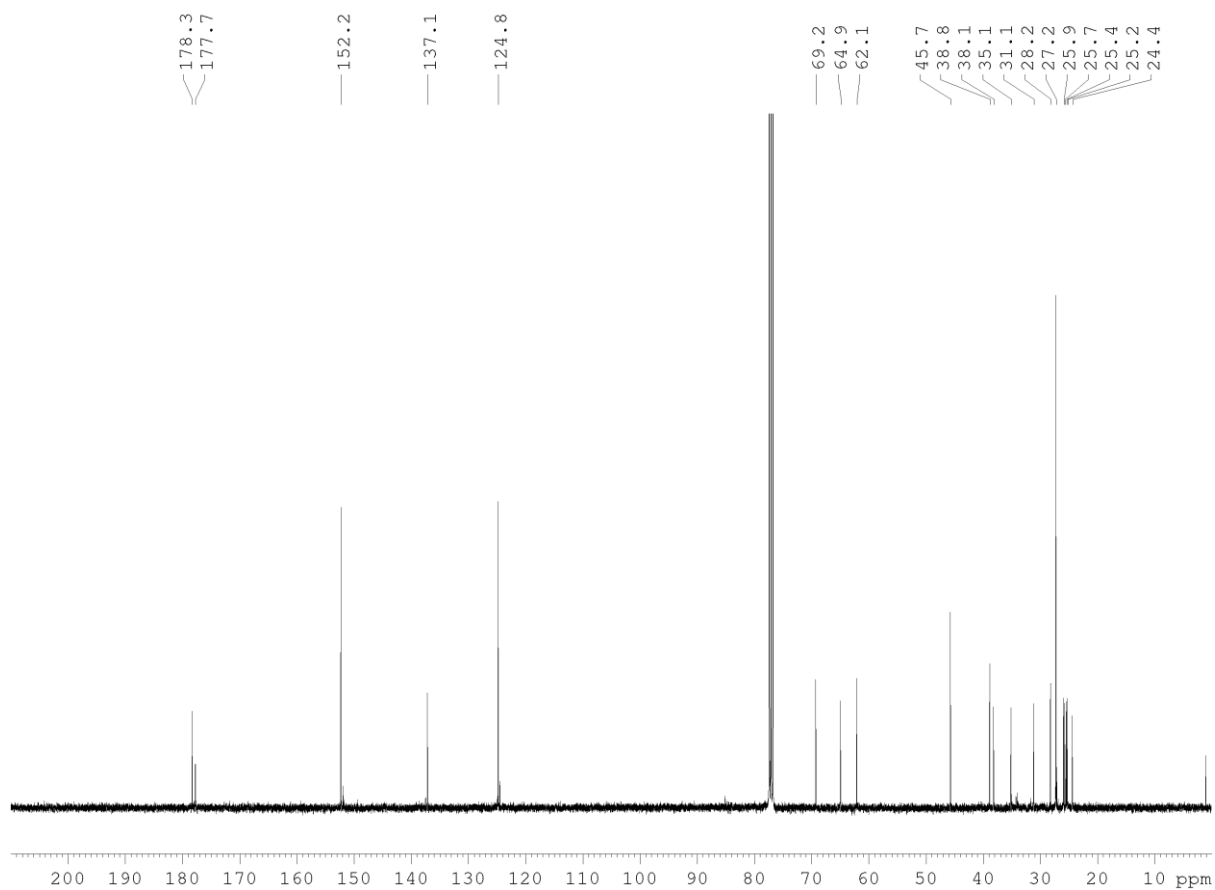
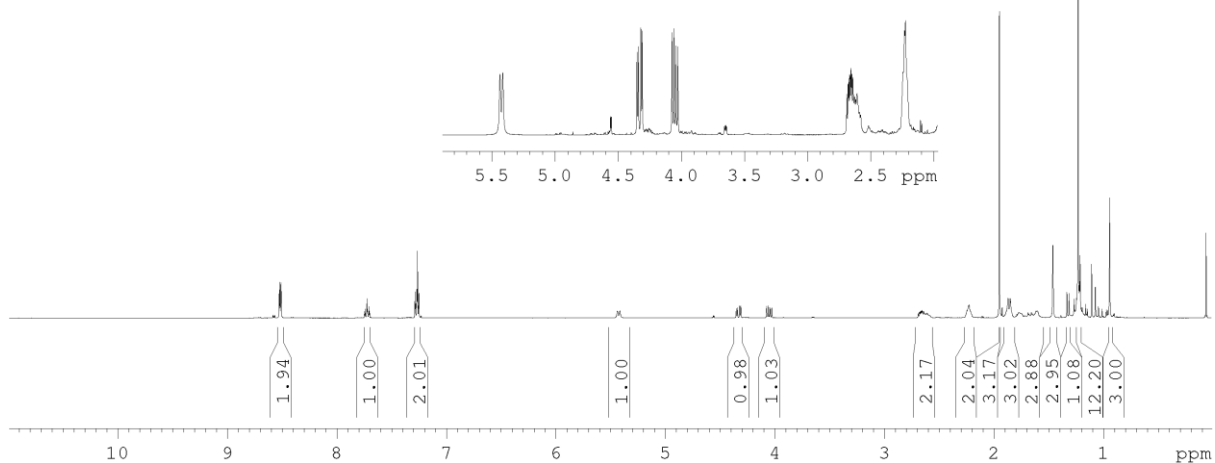


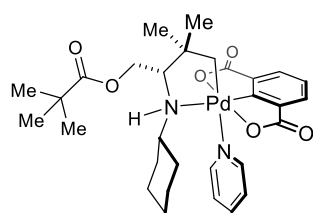
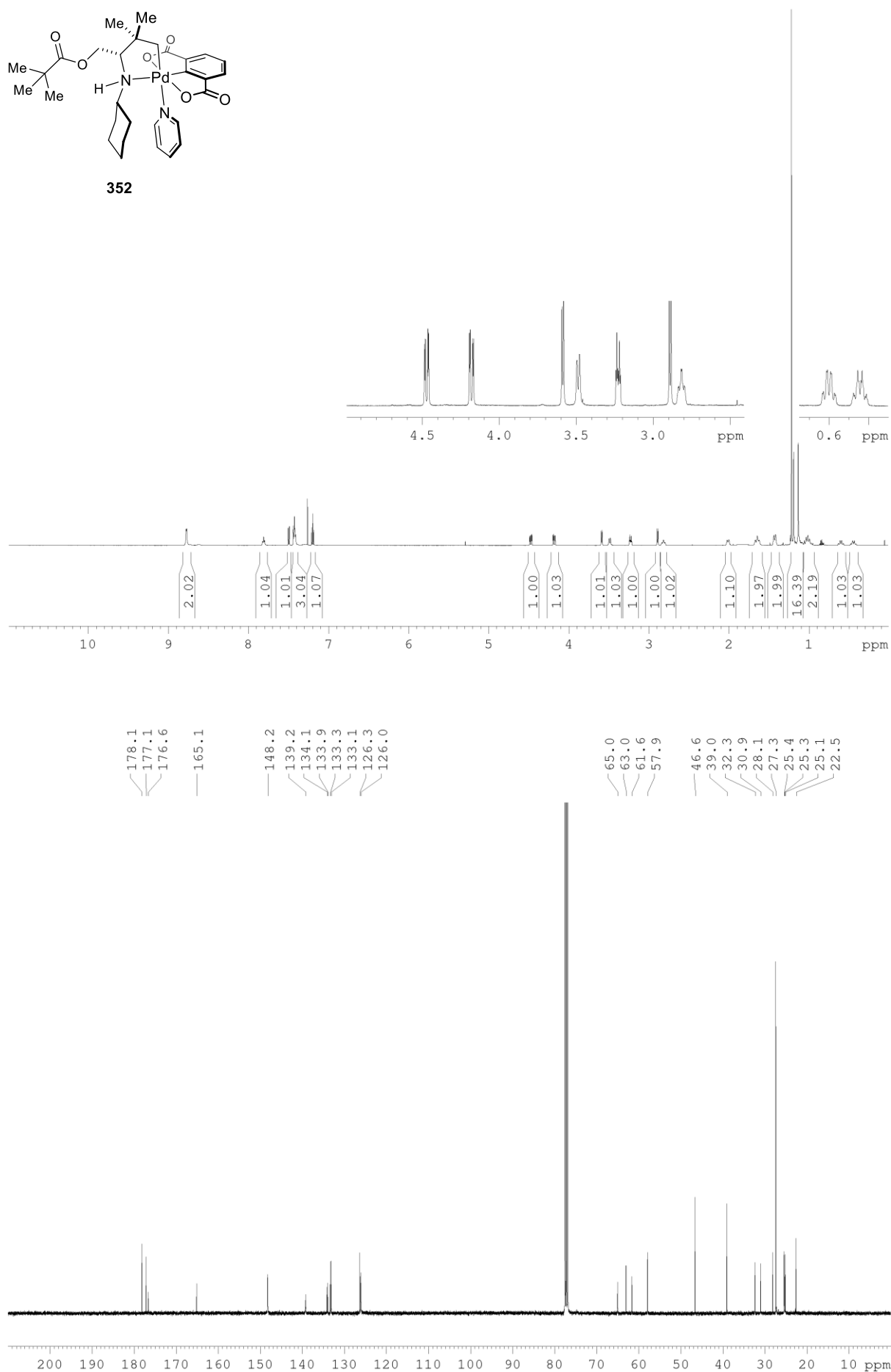
**330o**

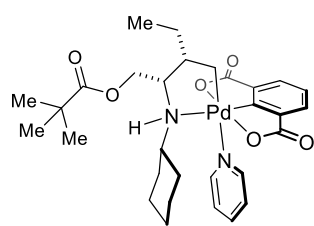




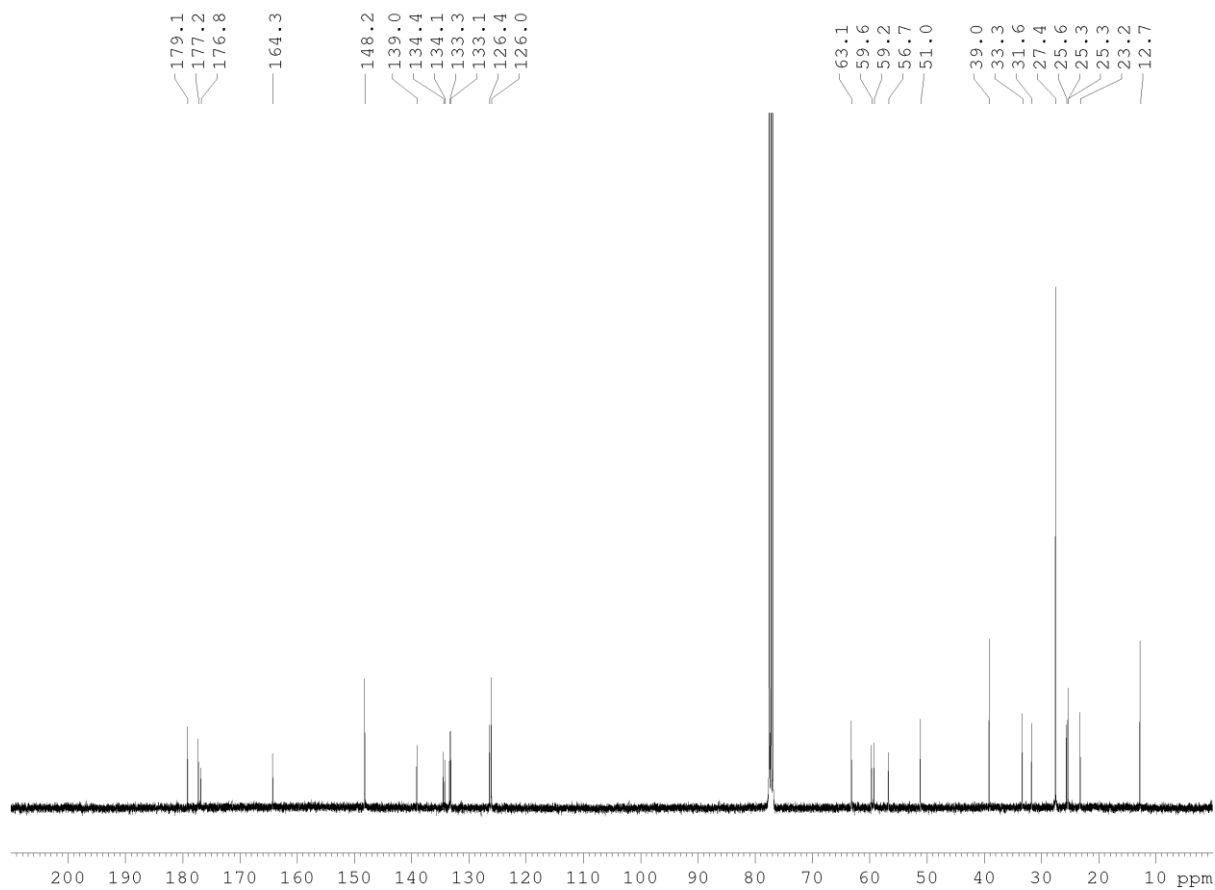
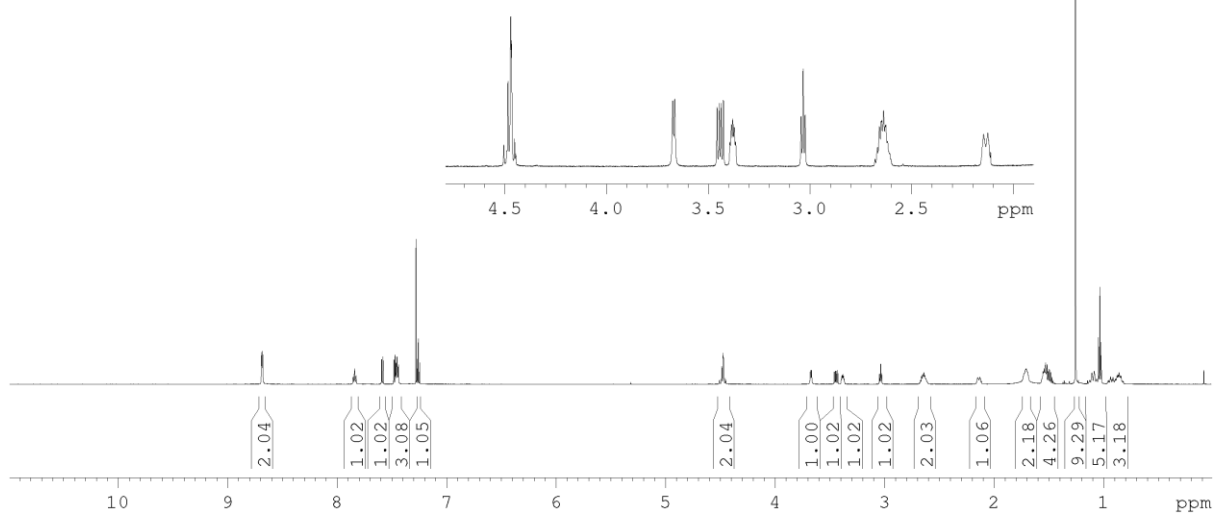
332

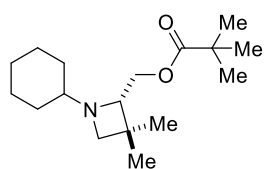


**352**

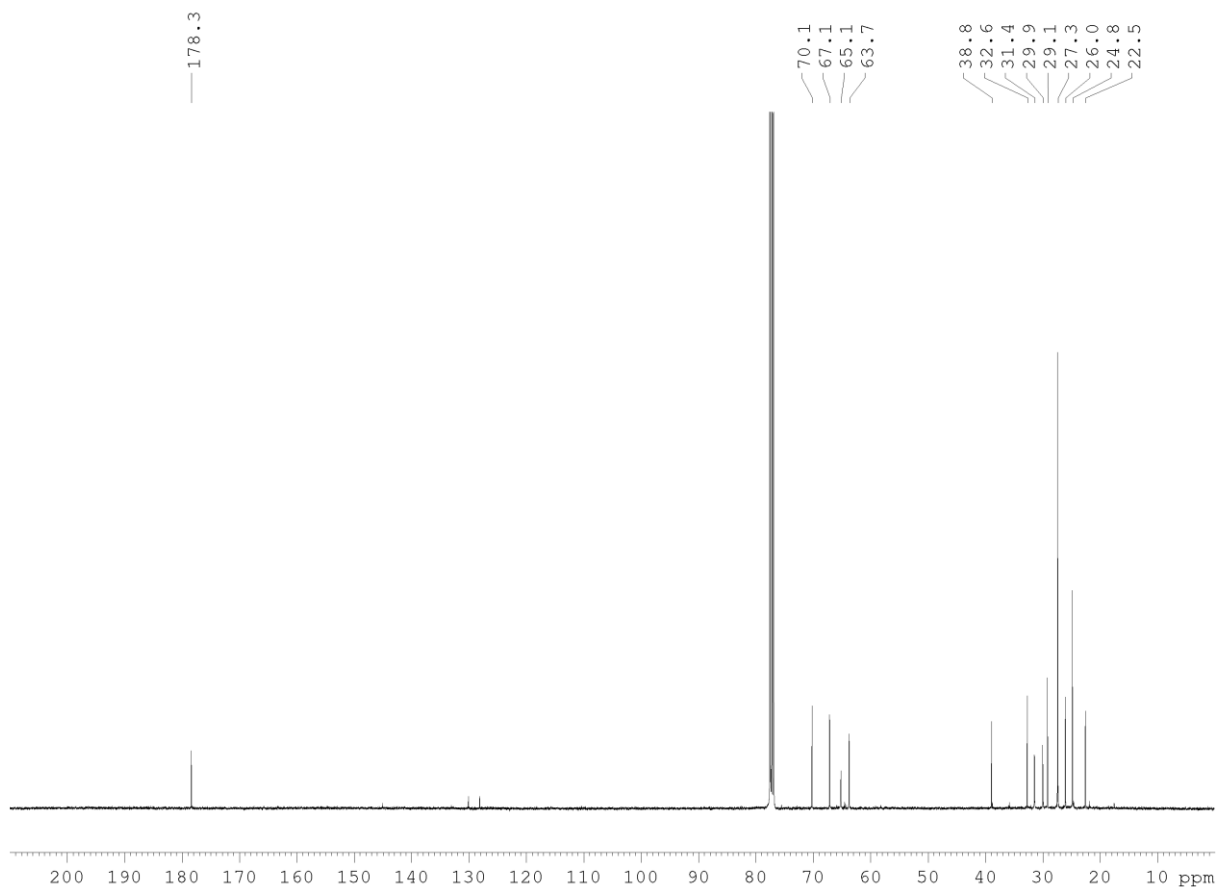
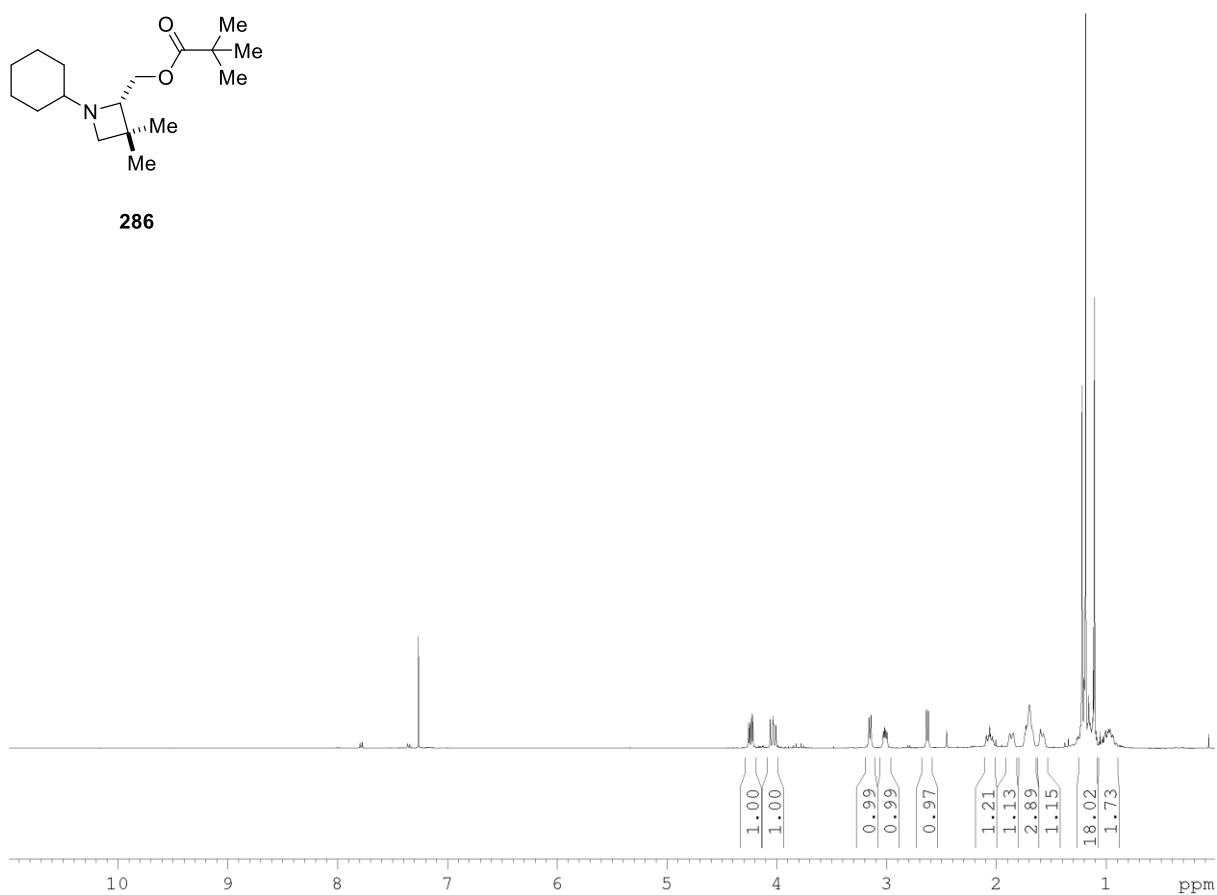


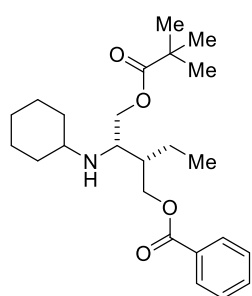
353



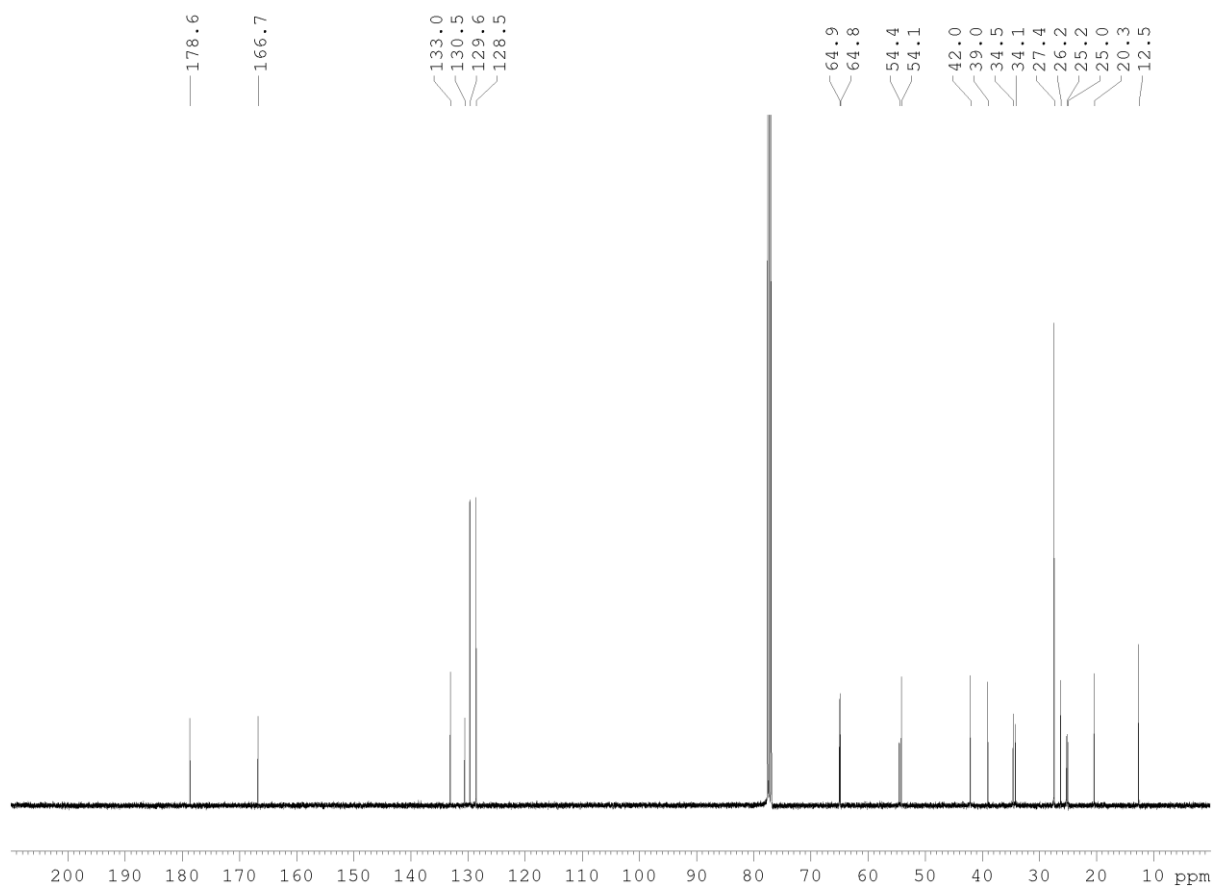
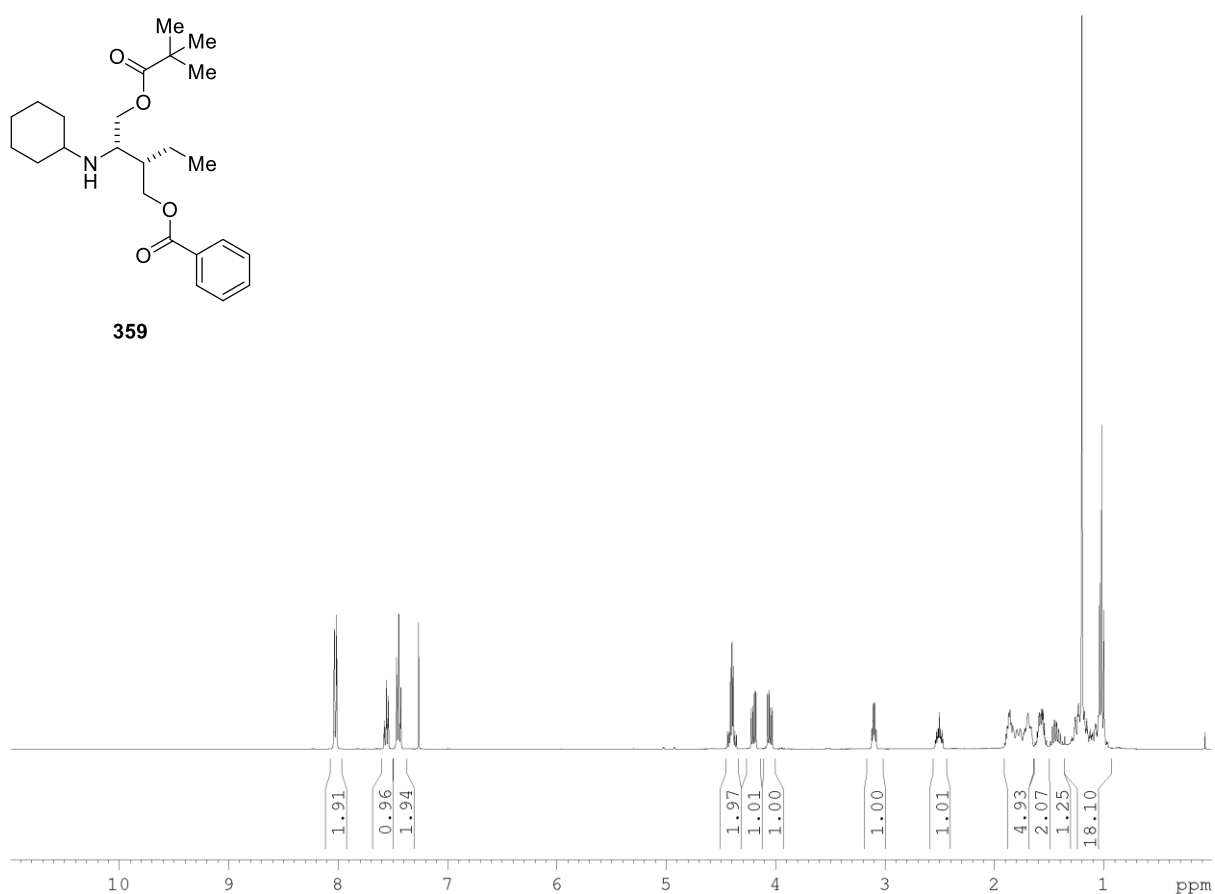


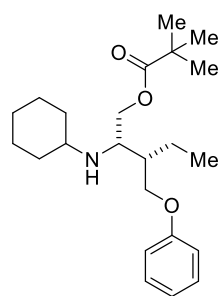
286



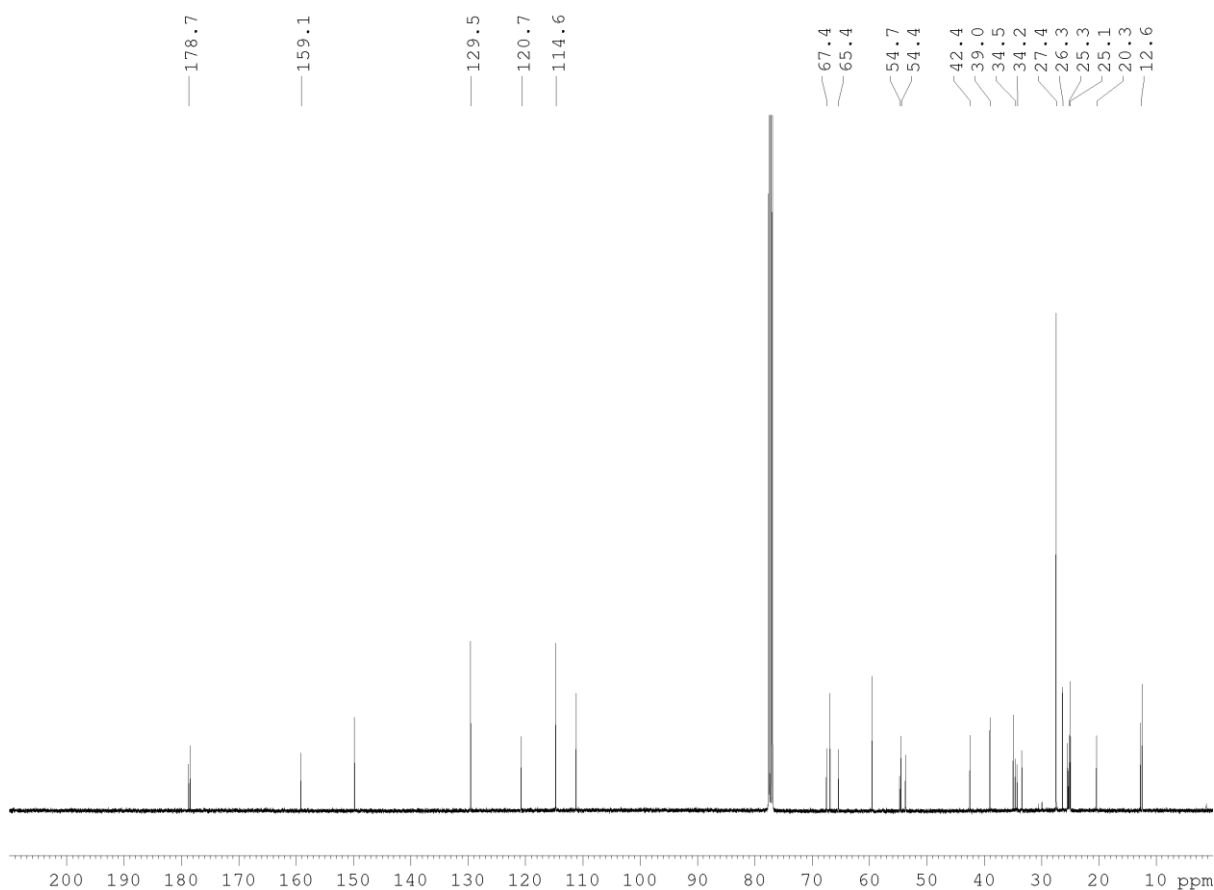
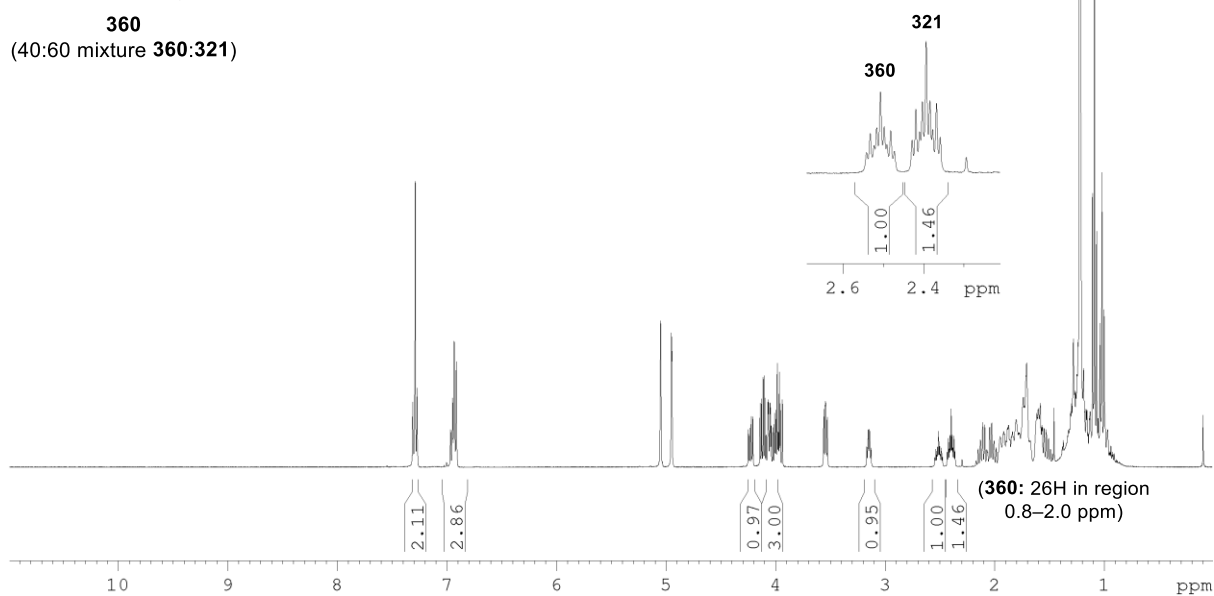


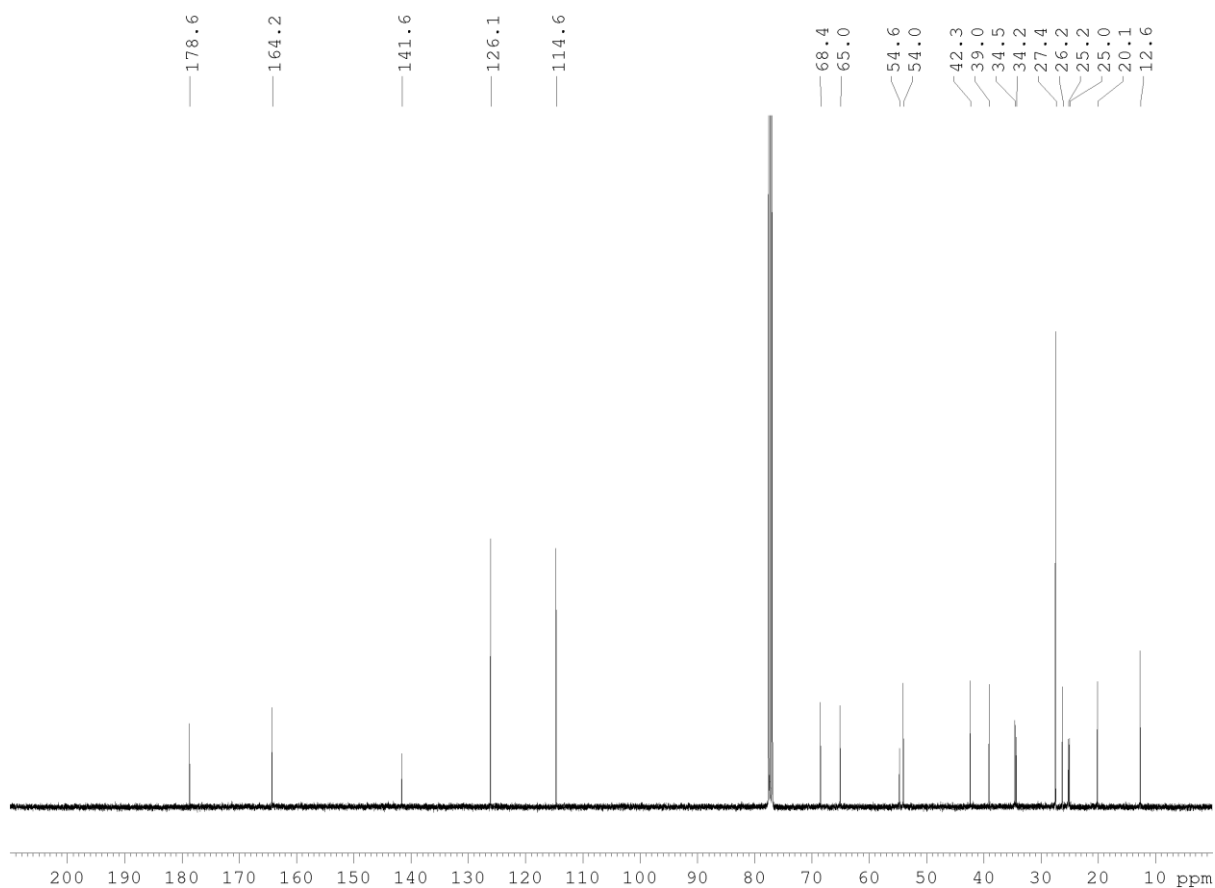
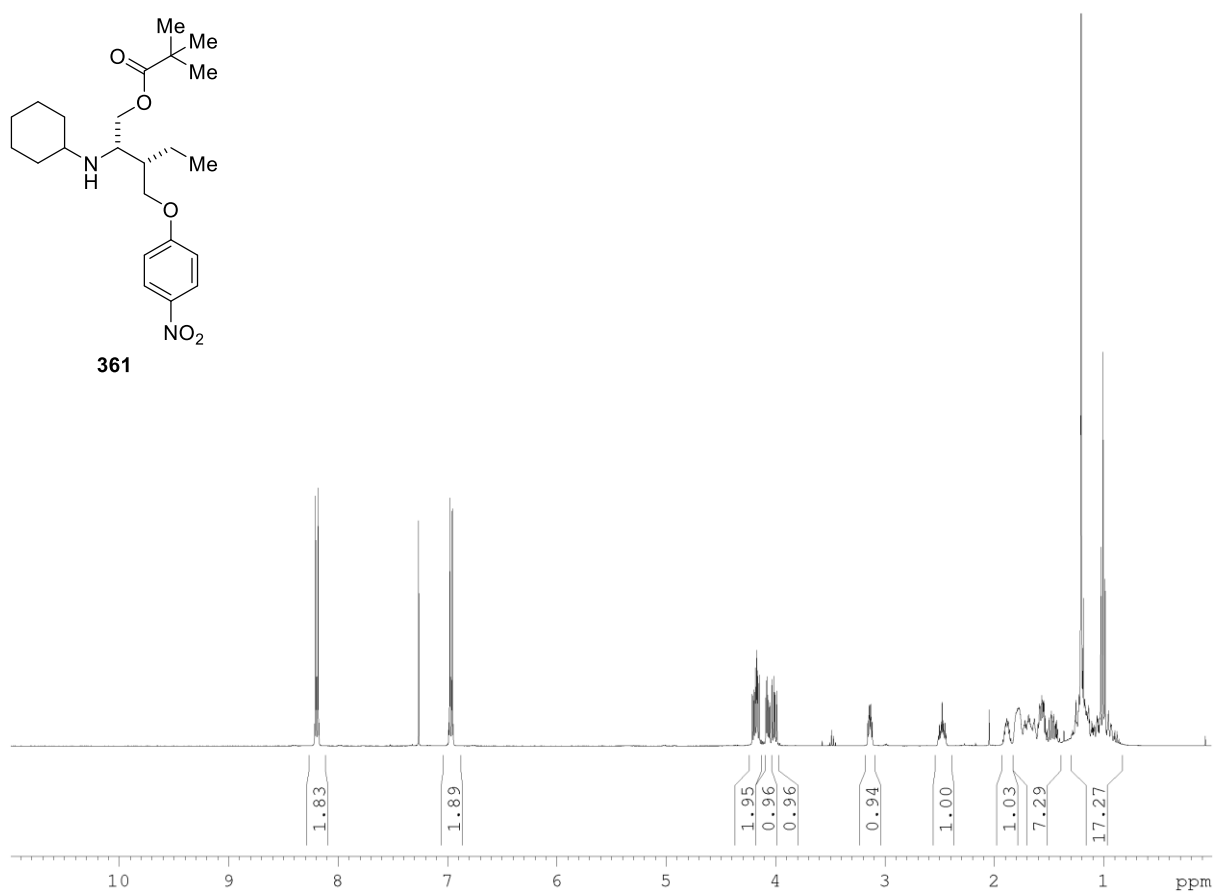
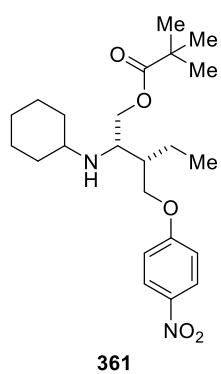
359

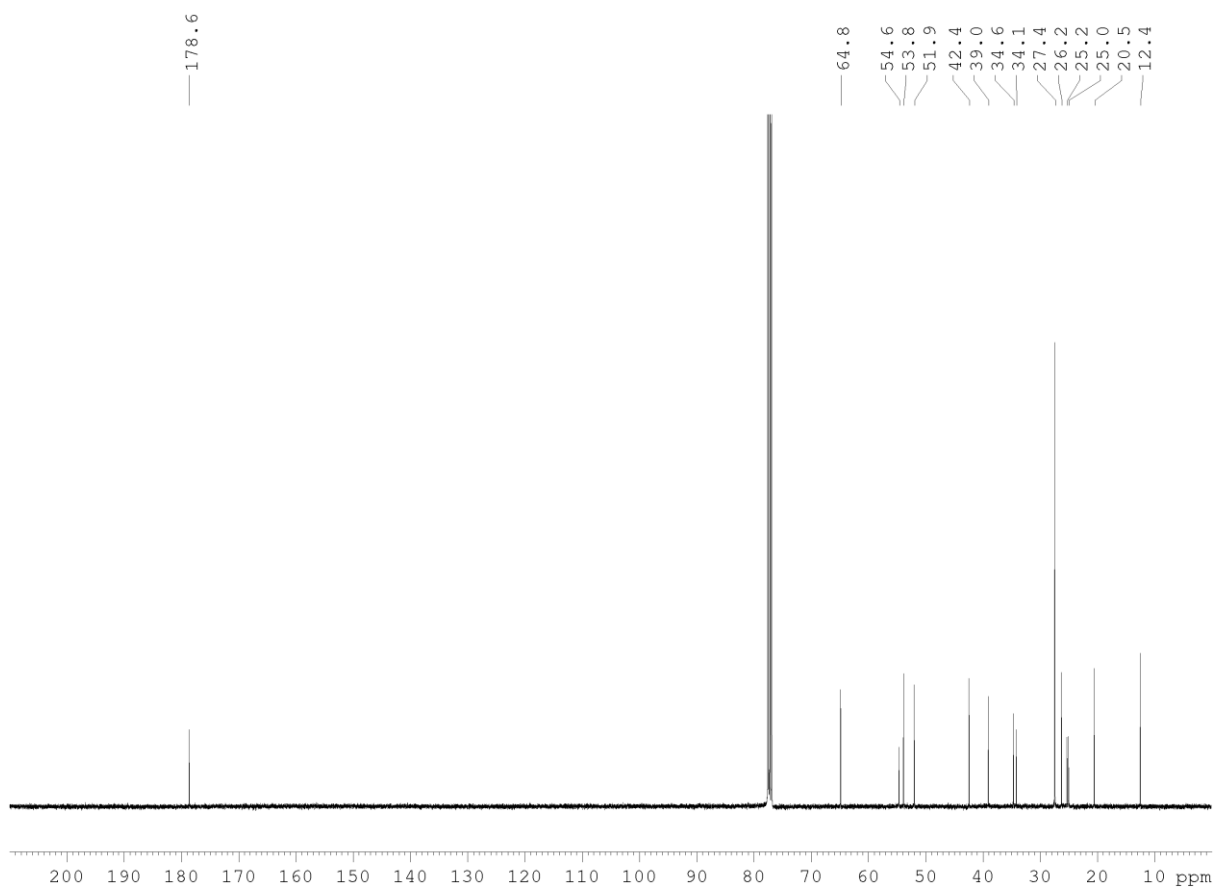
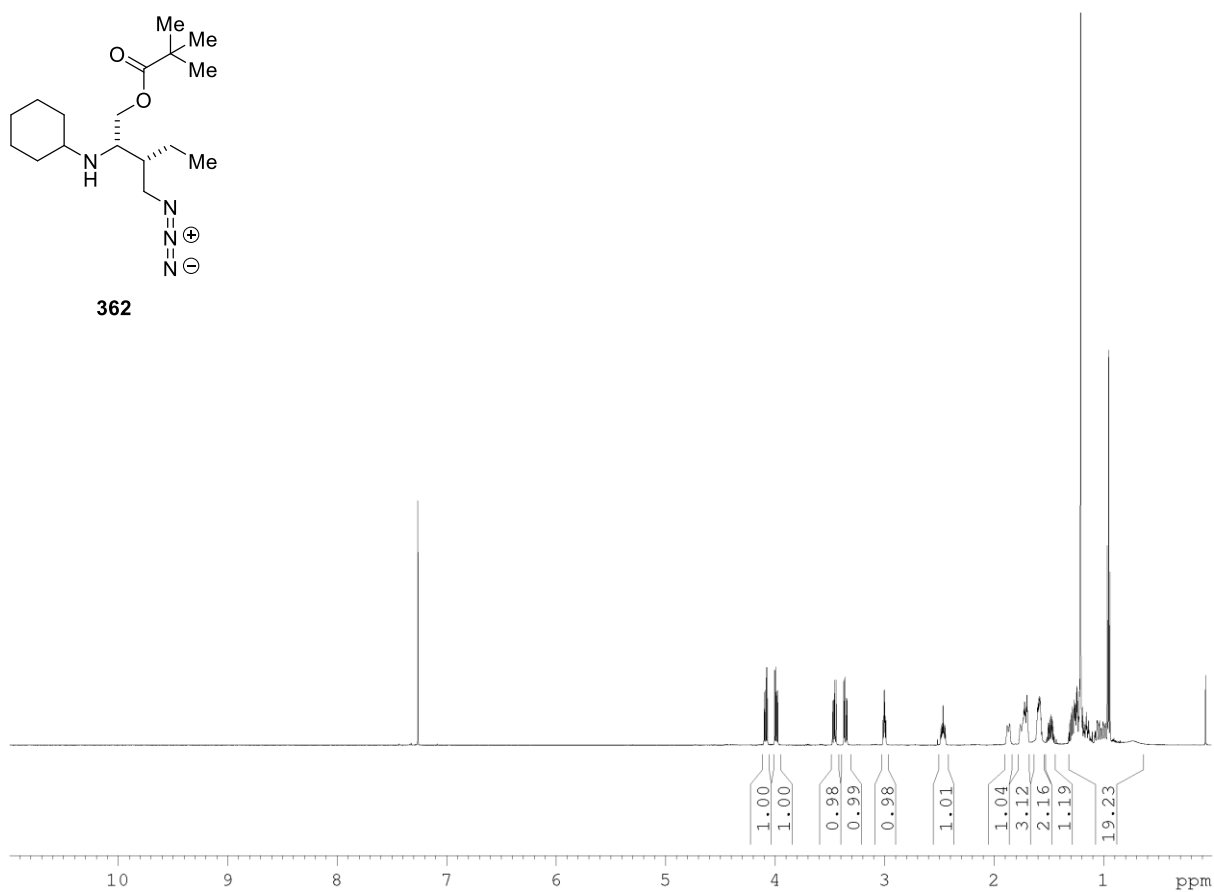


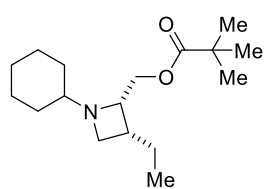


360
(40:60 mixture **360:321**)

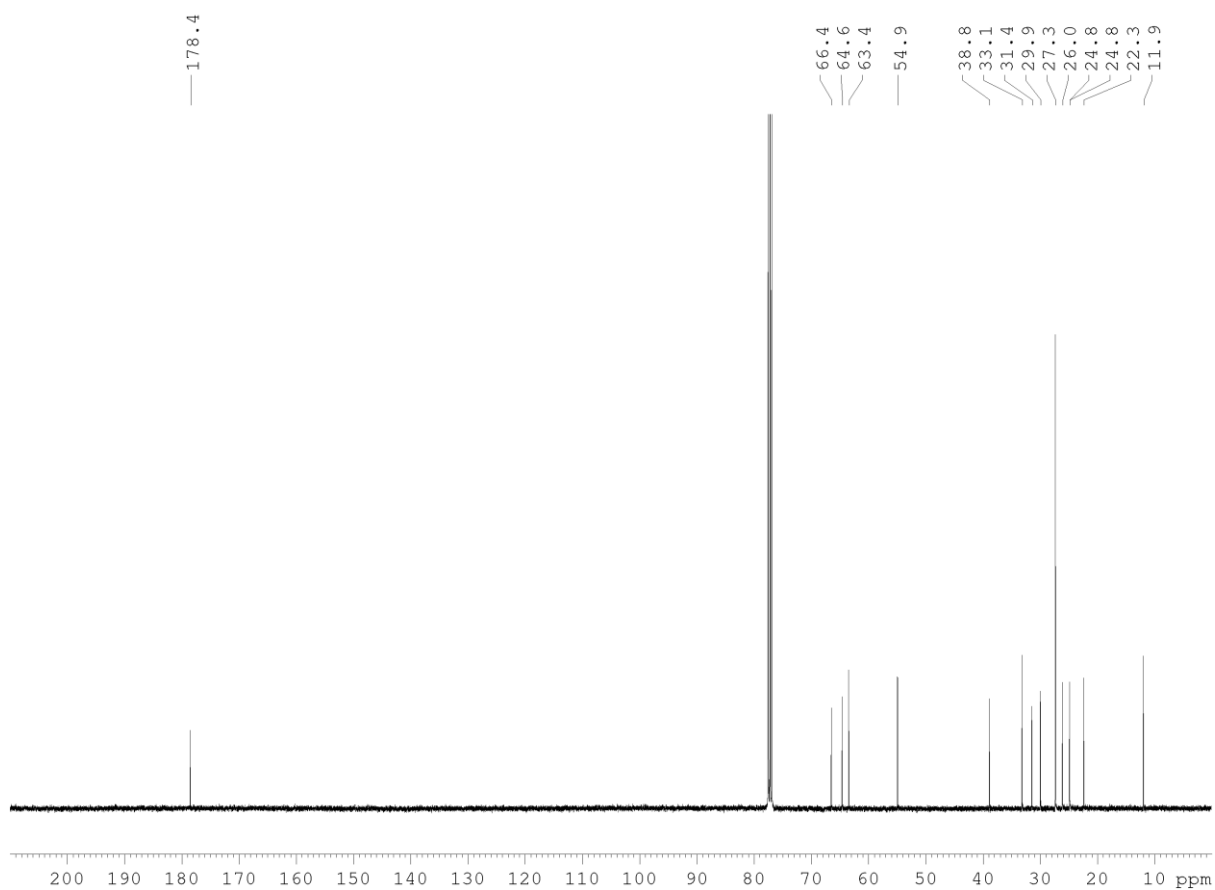
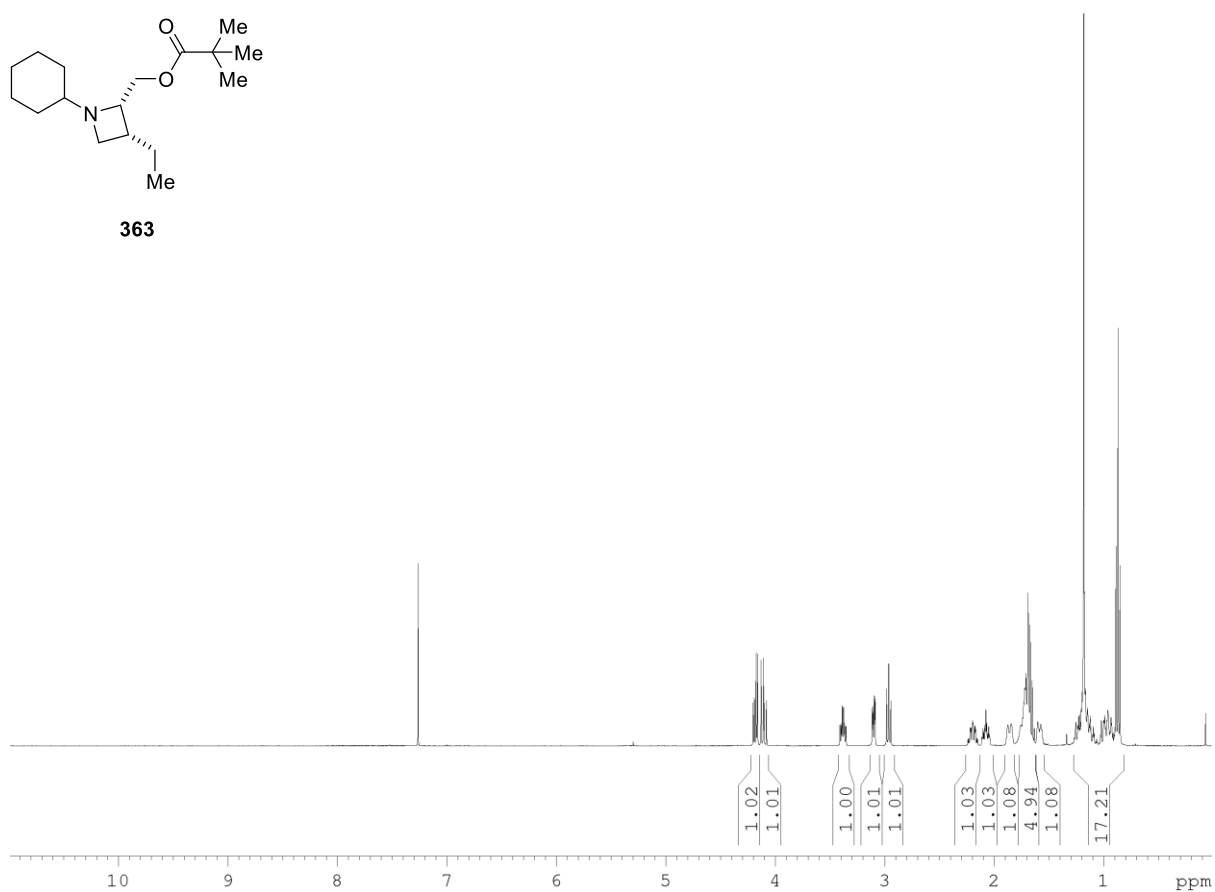


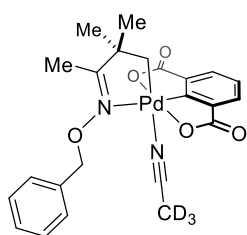




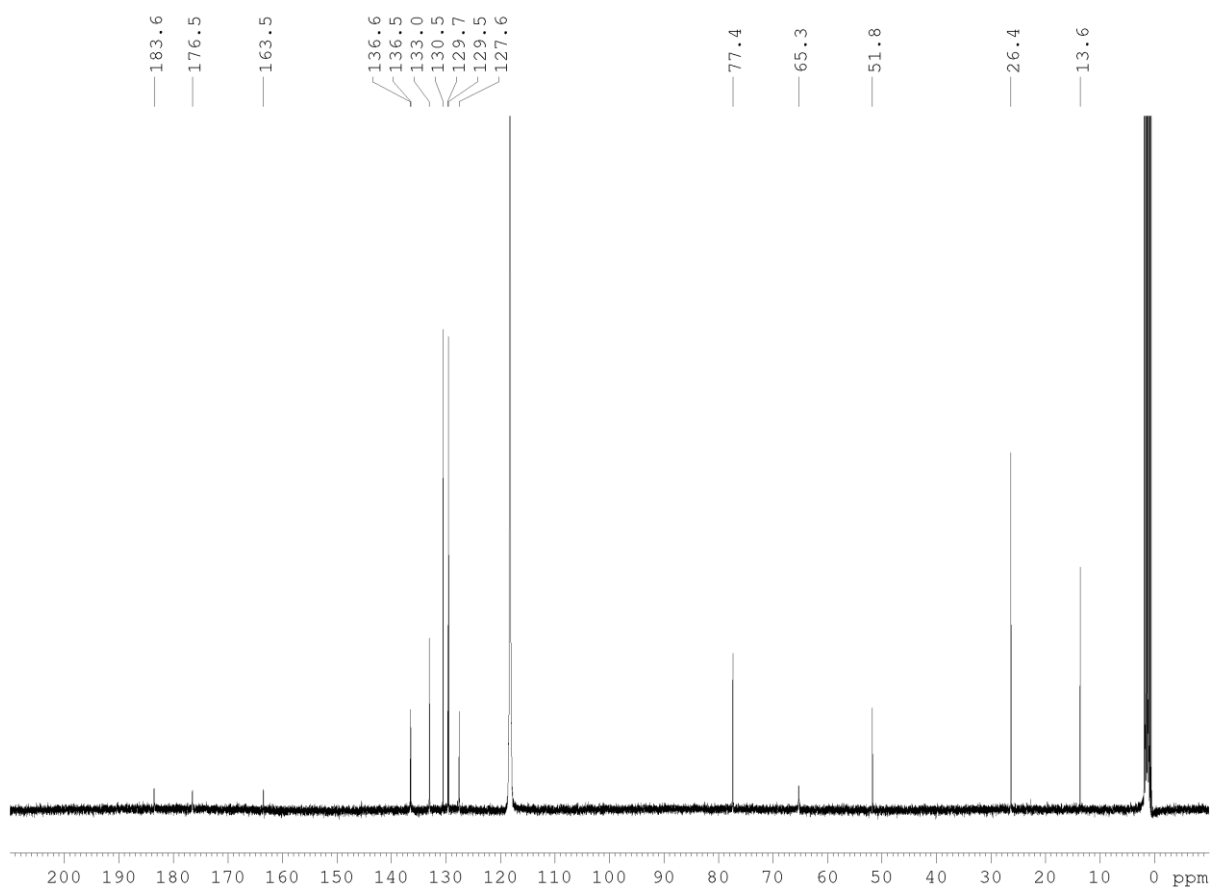
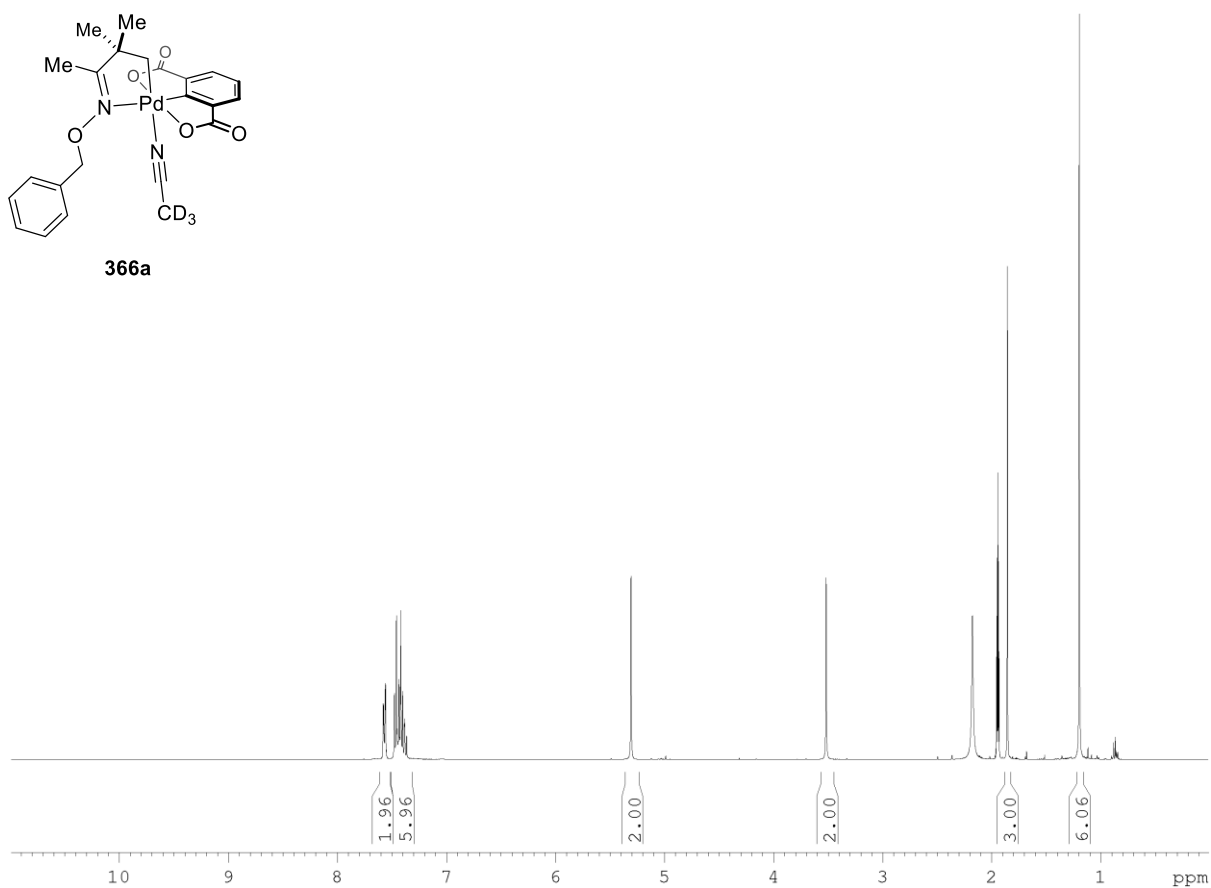


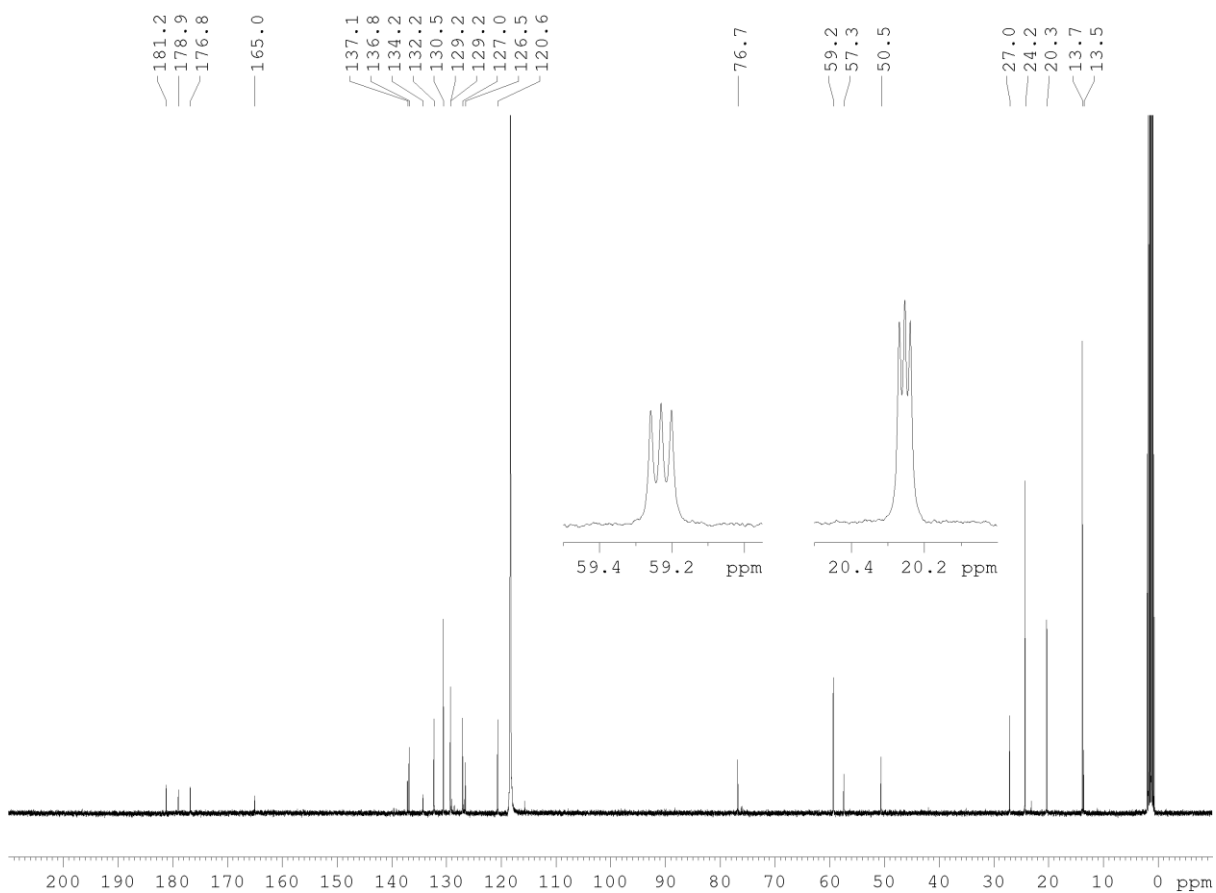
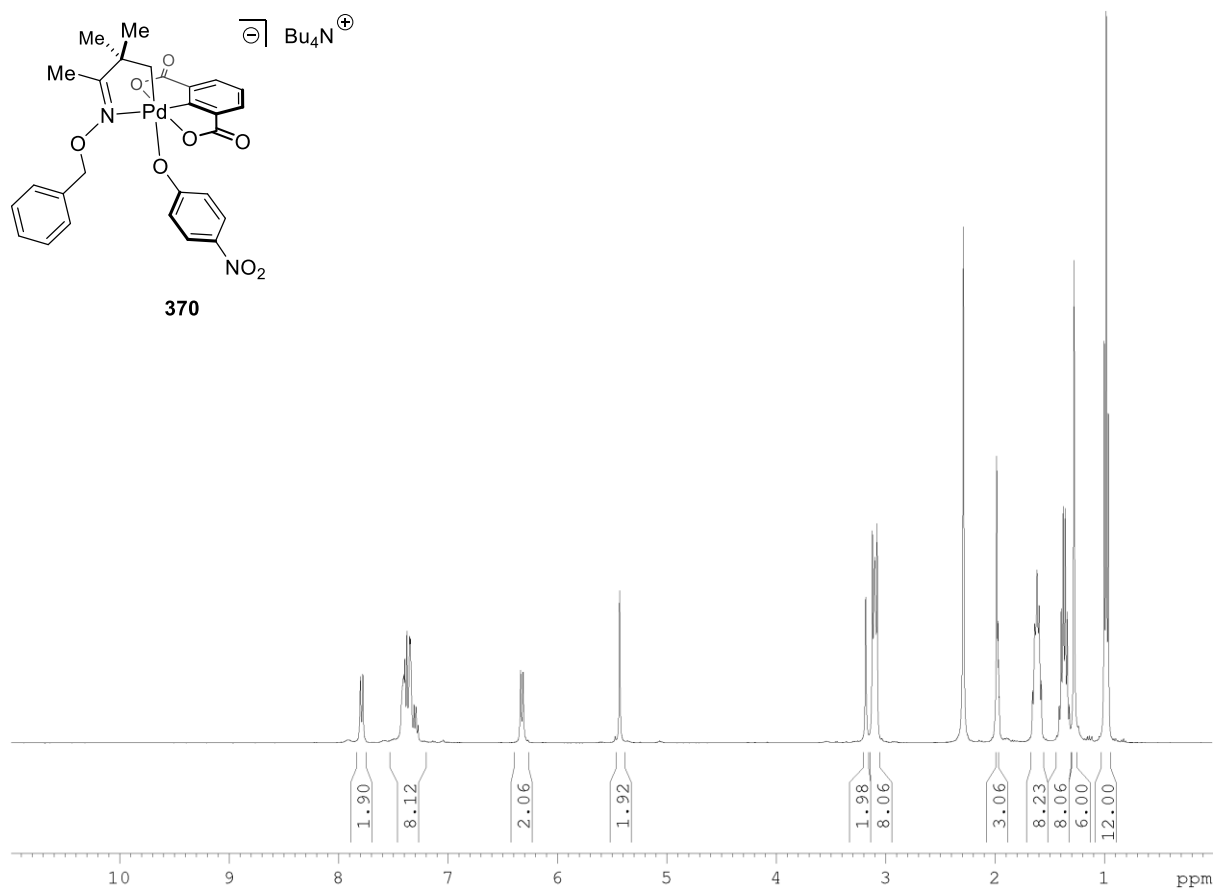
363

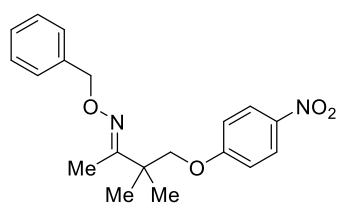




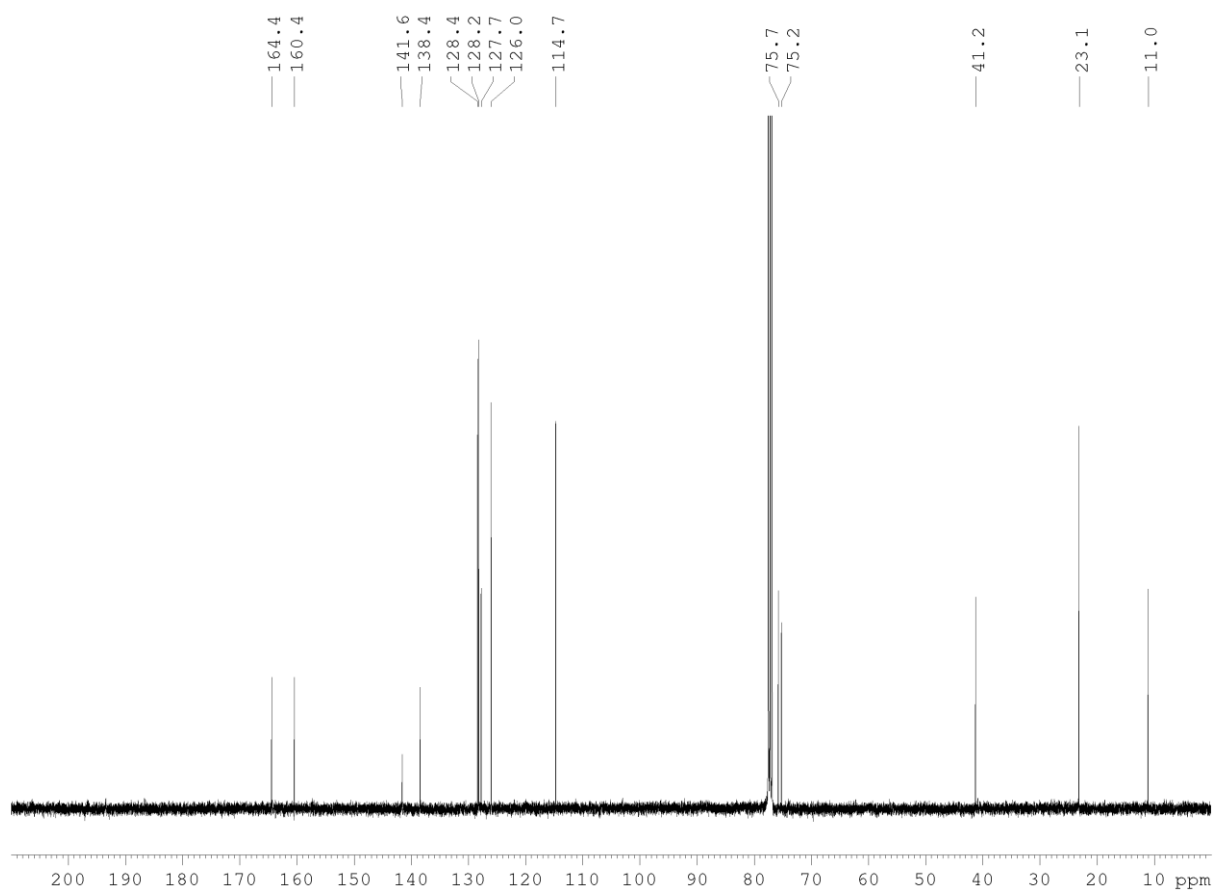
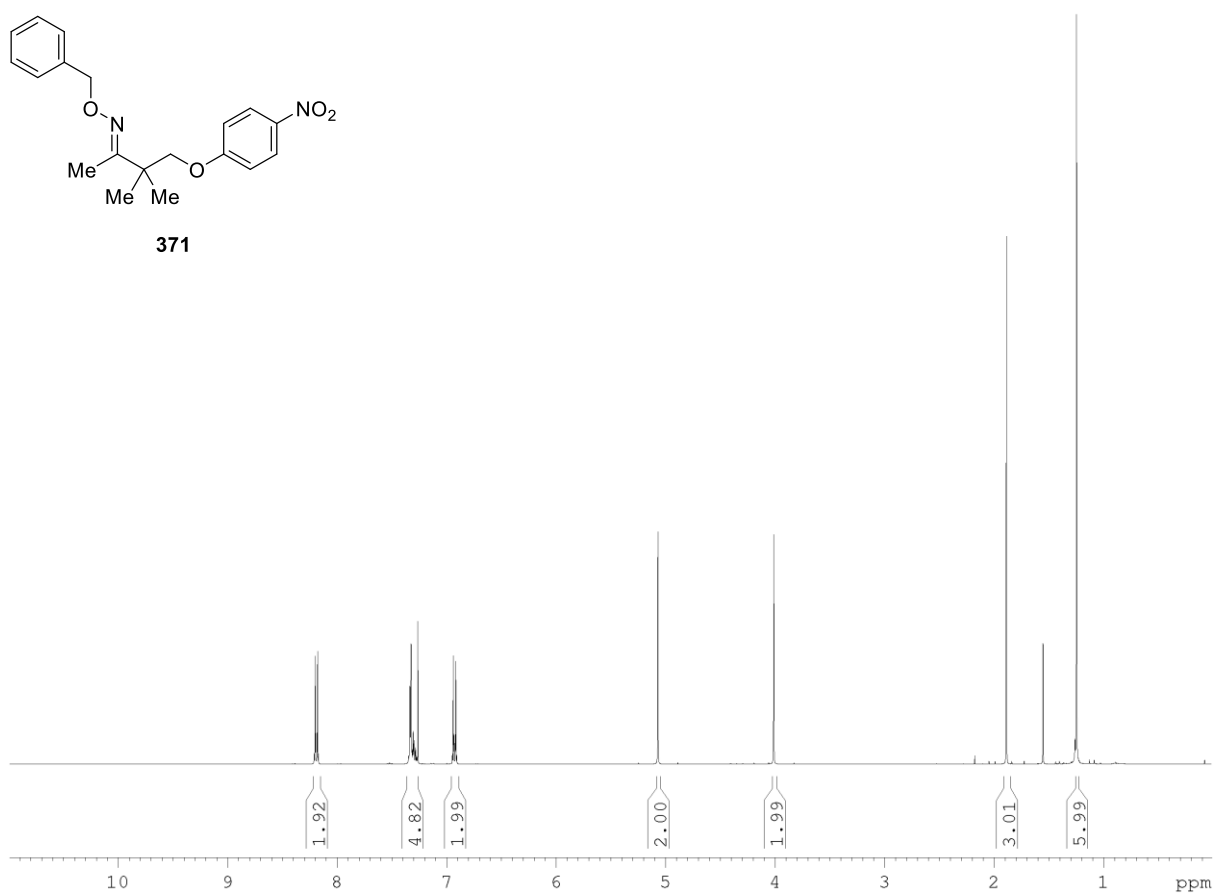
366a

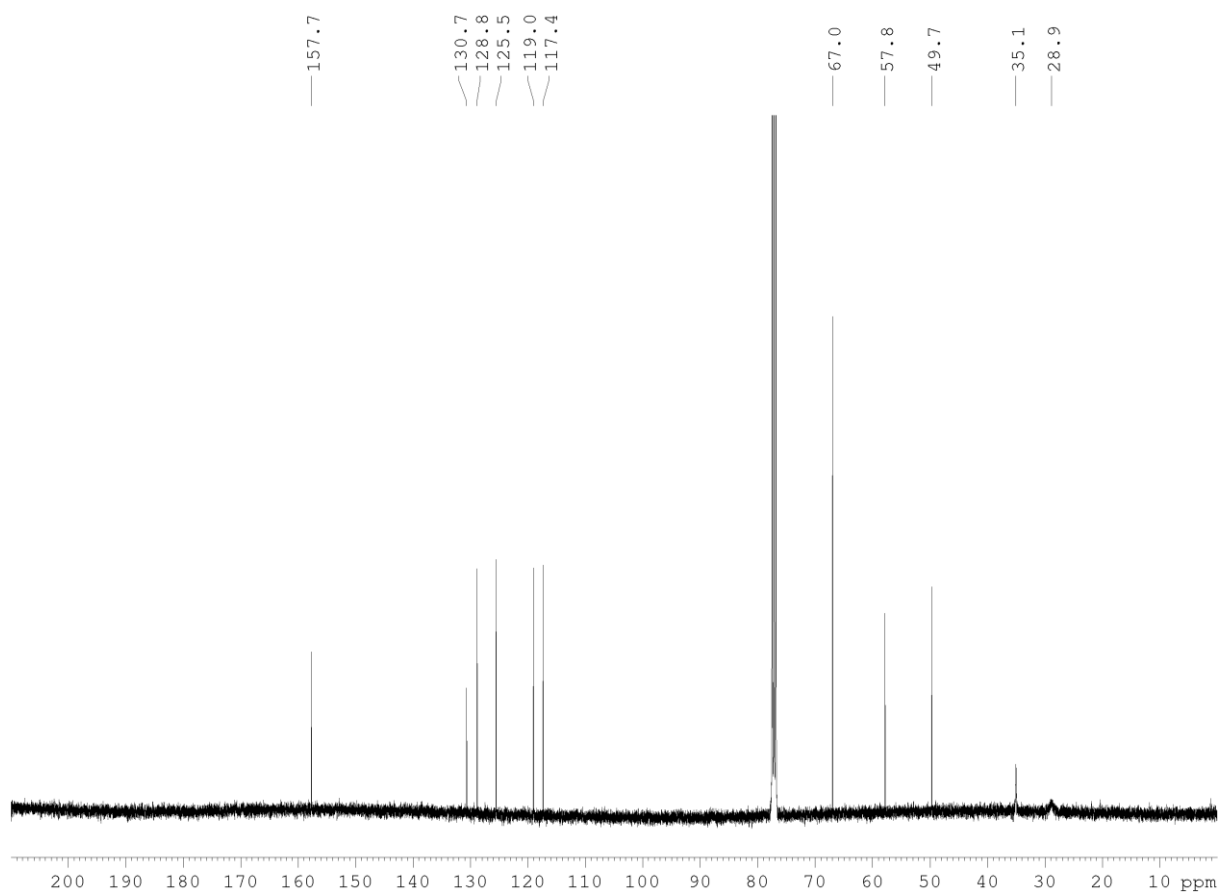
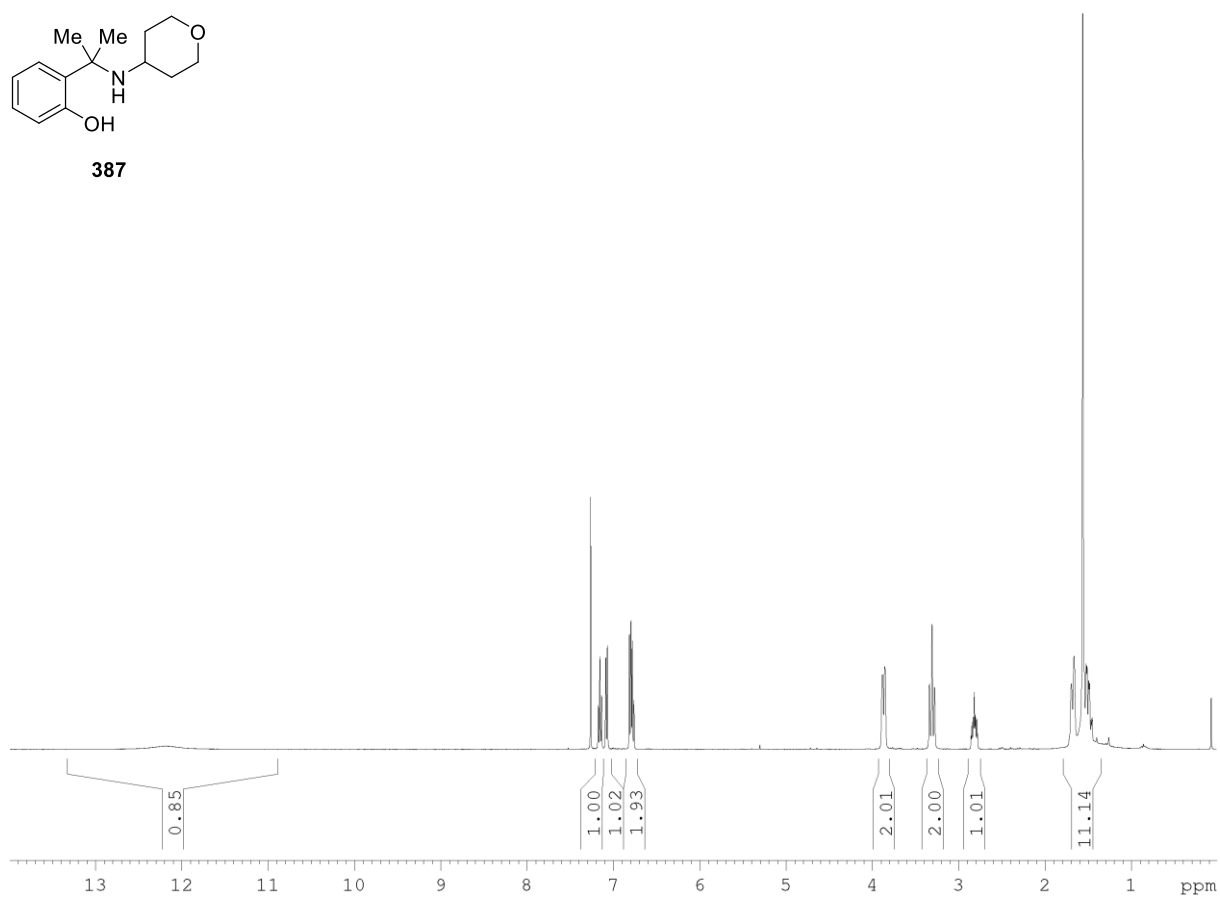
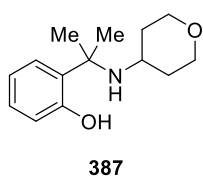


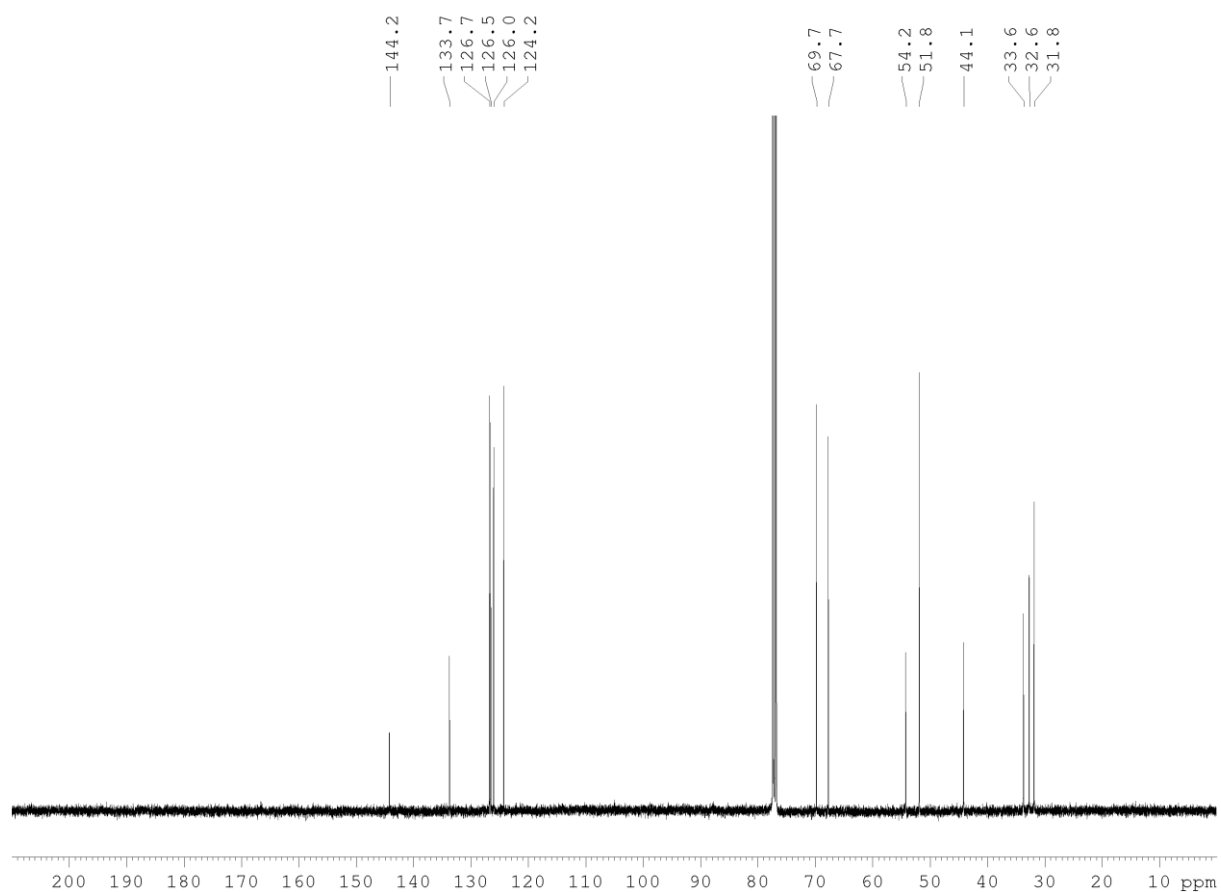
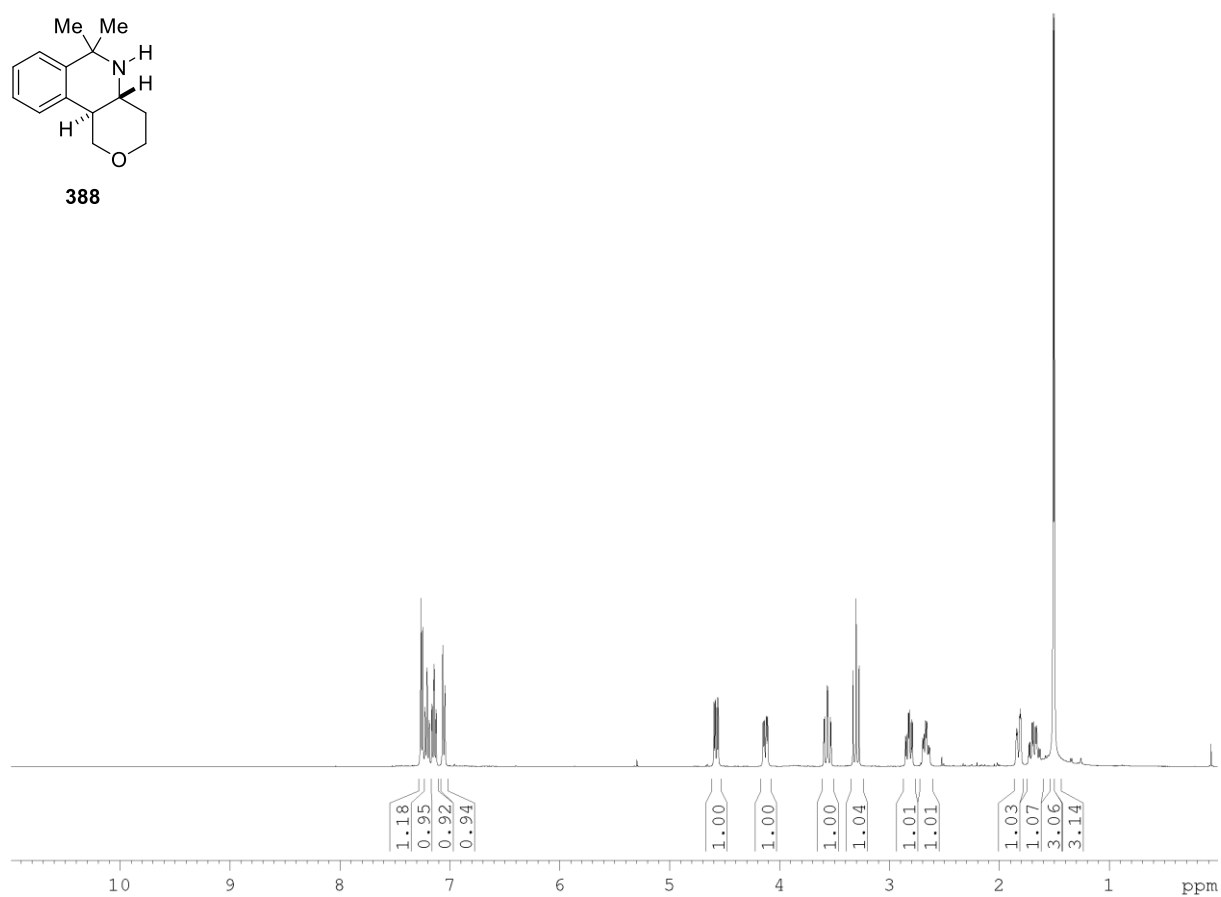


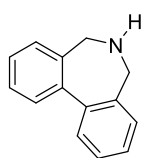


371

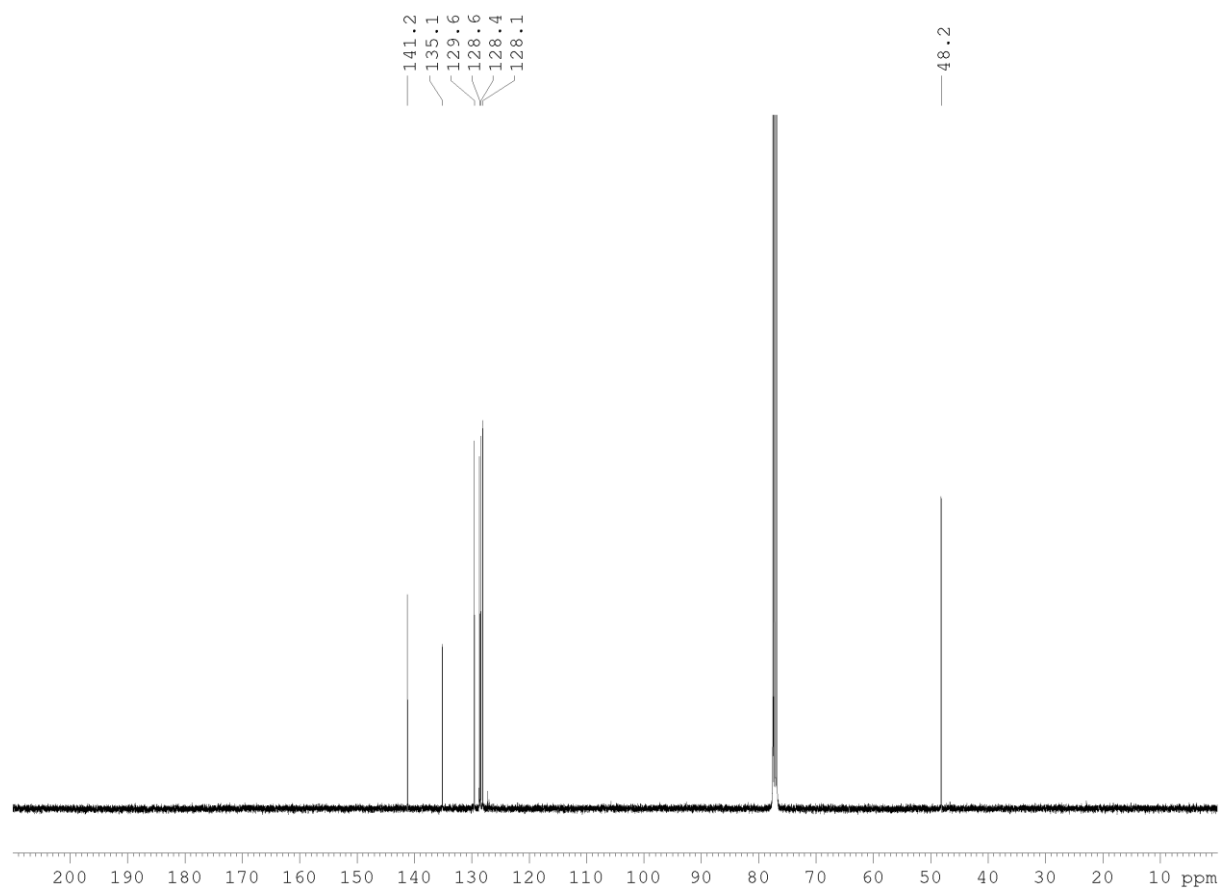
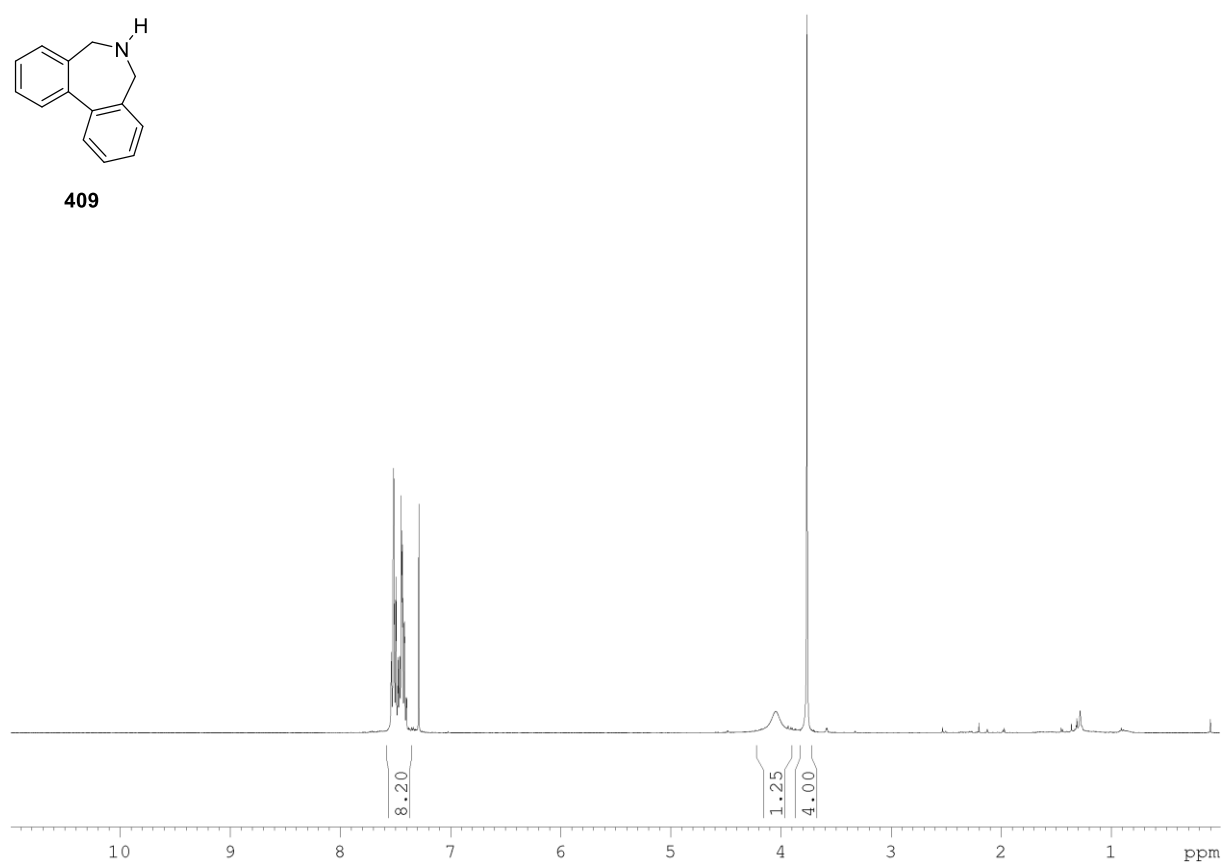




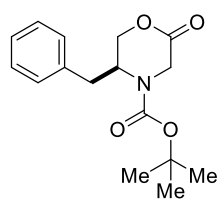
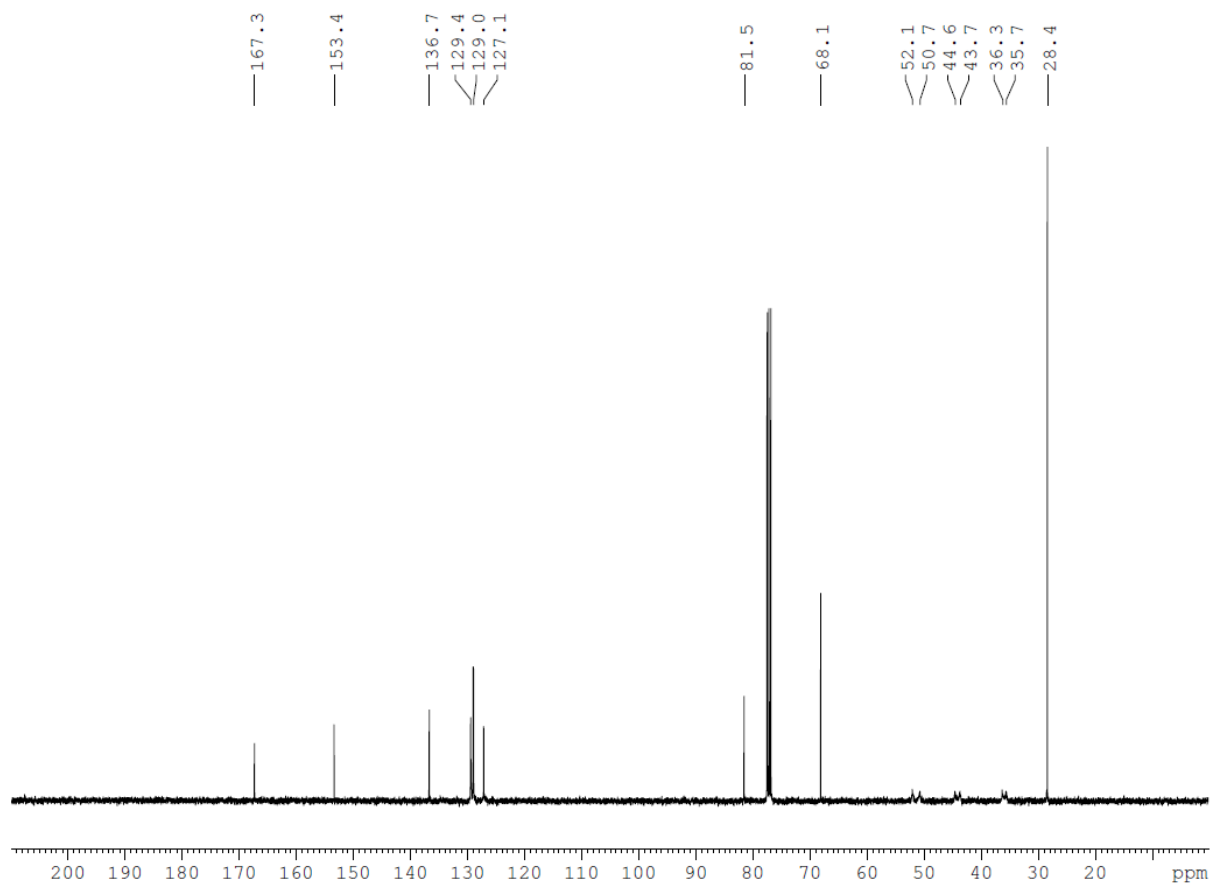
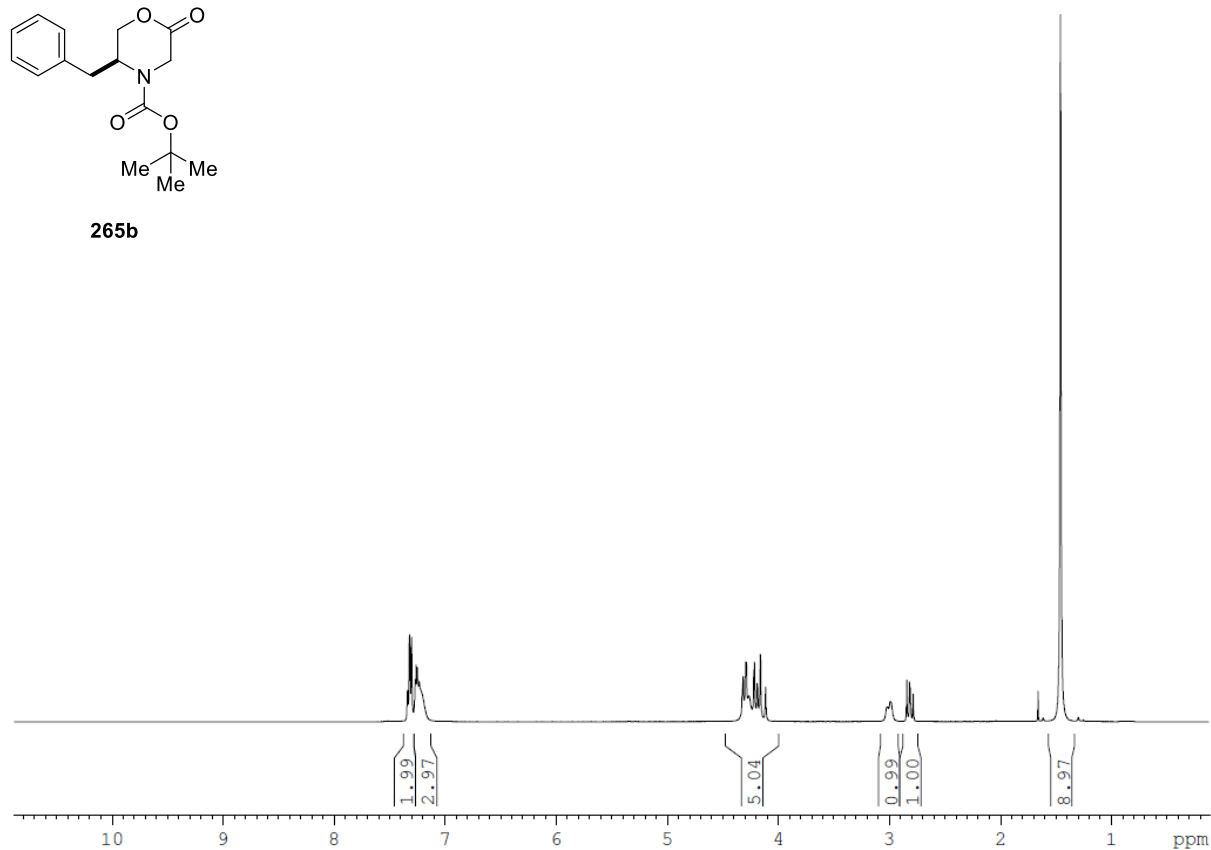


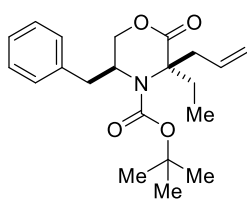
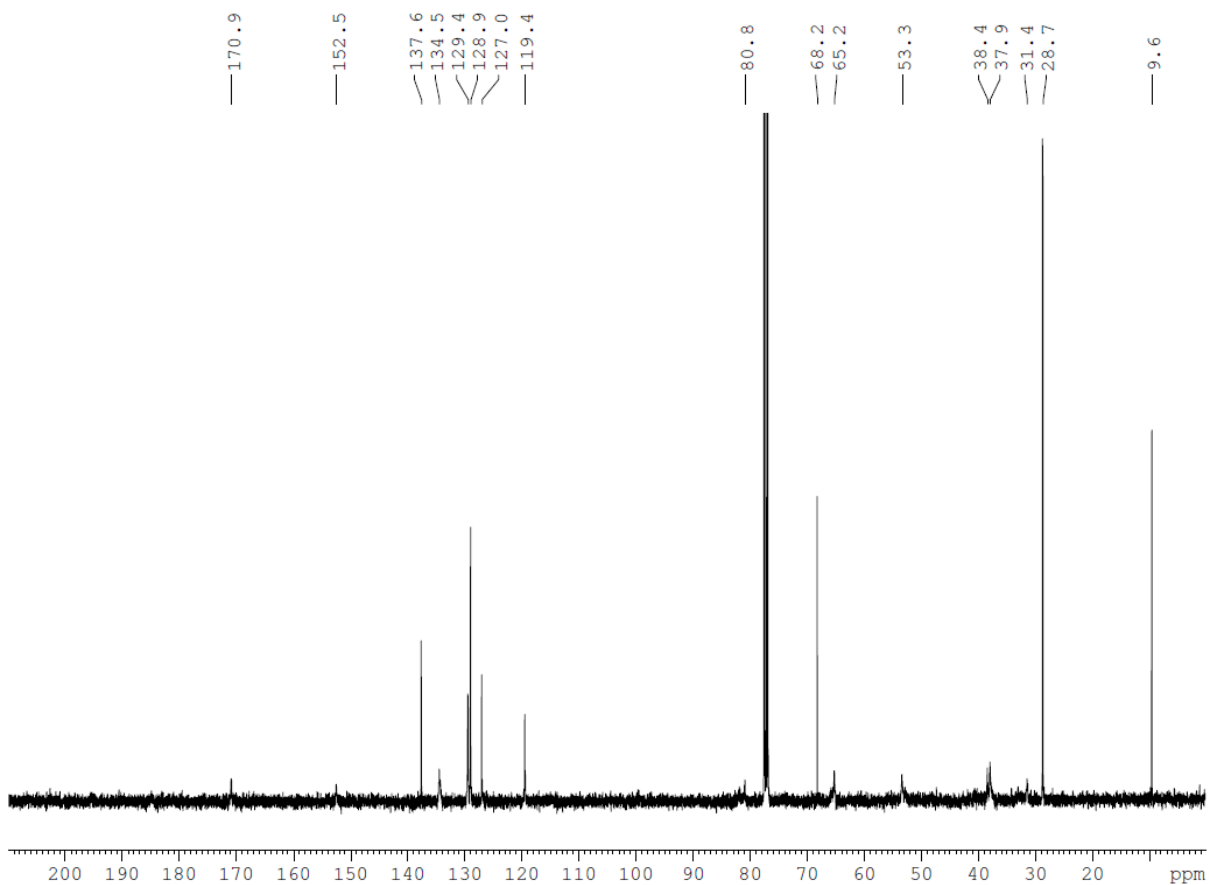
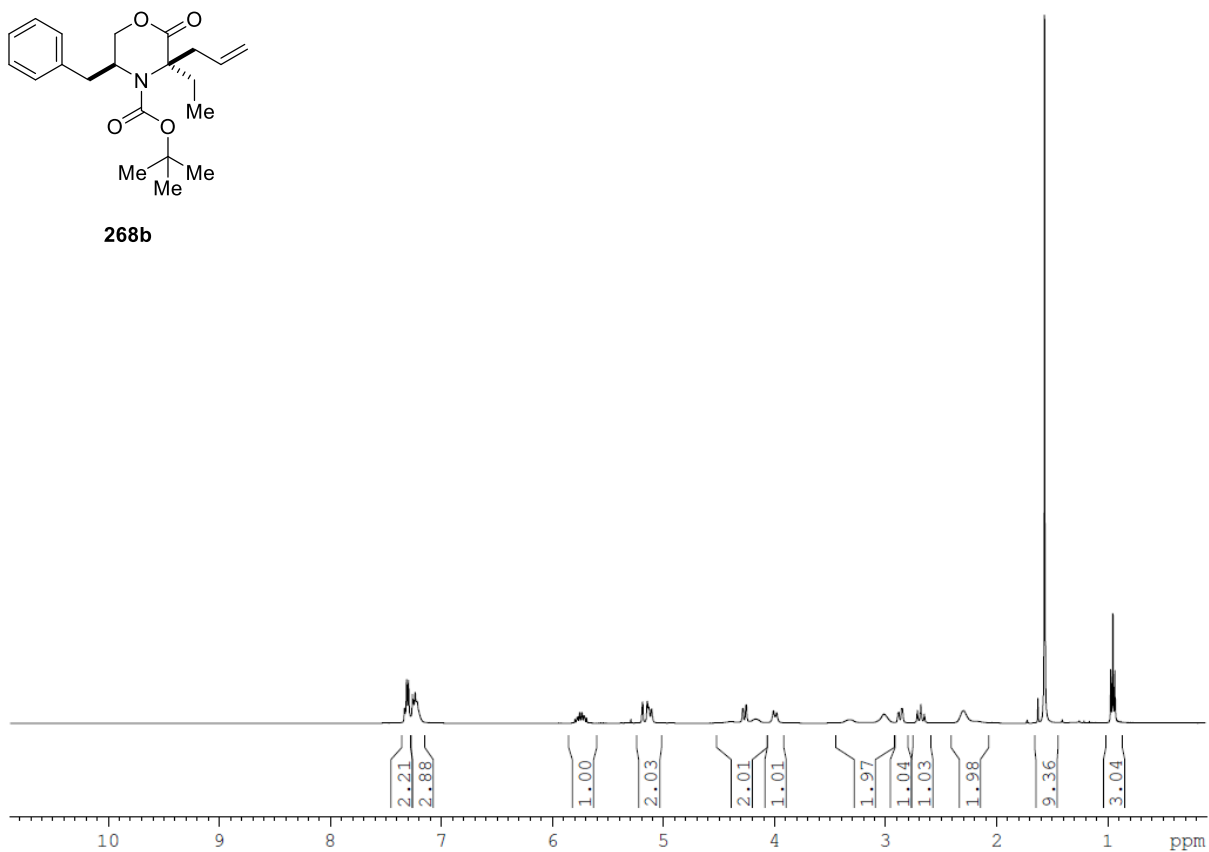


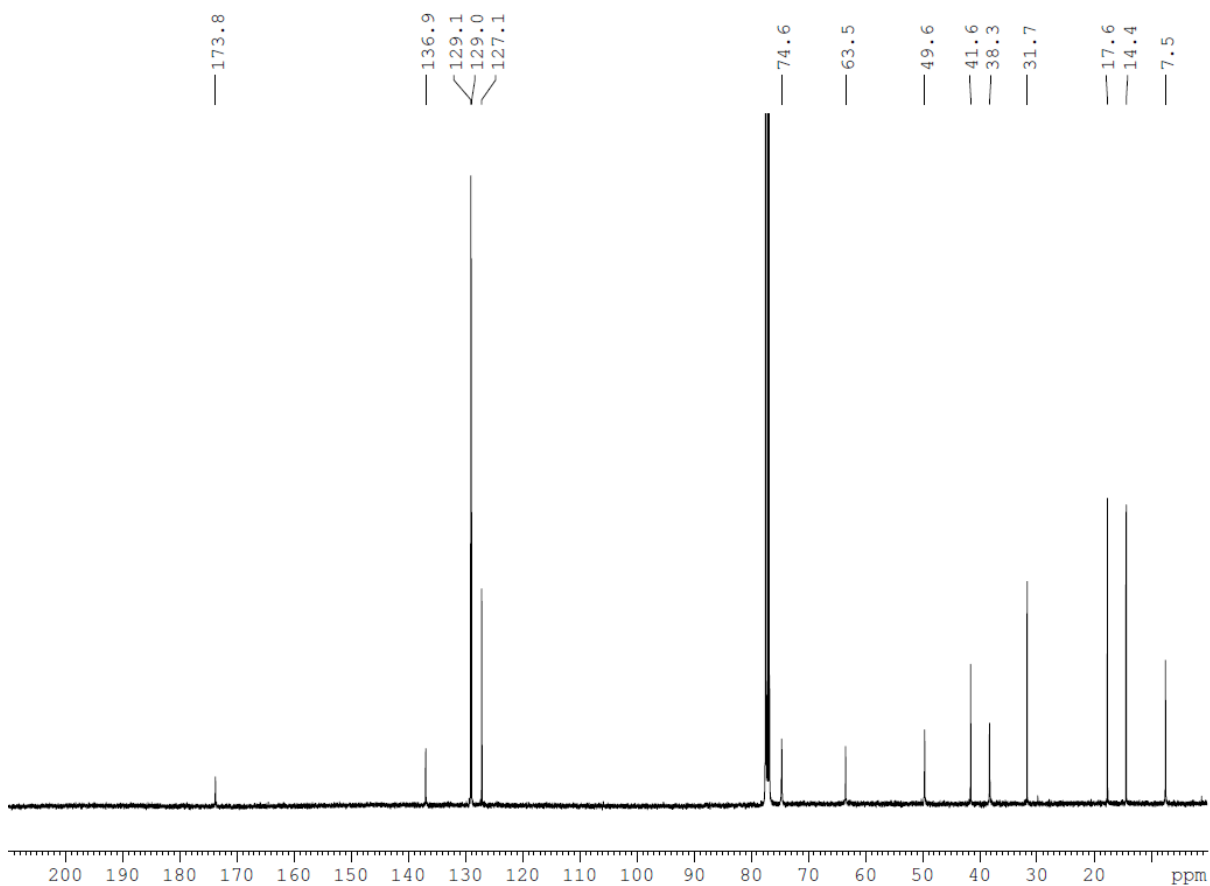
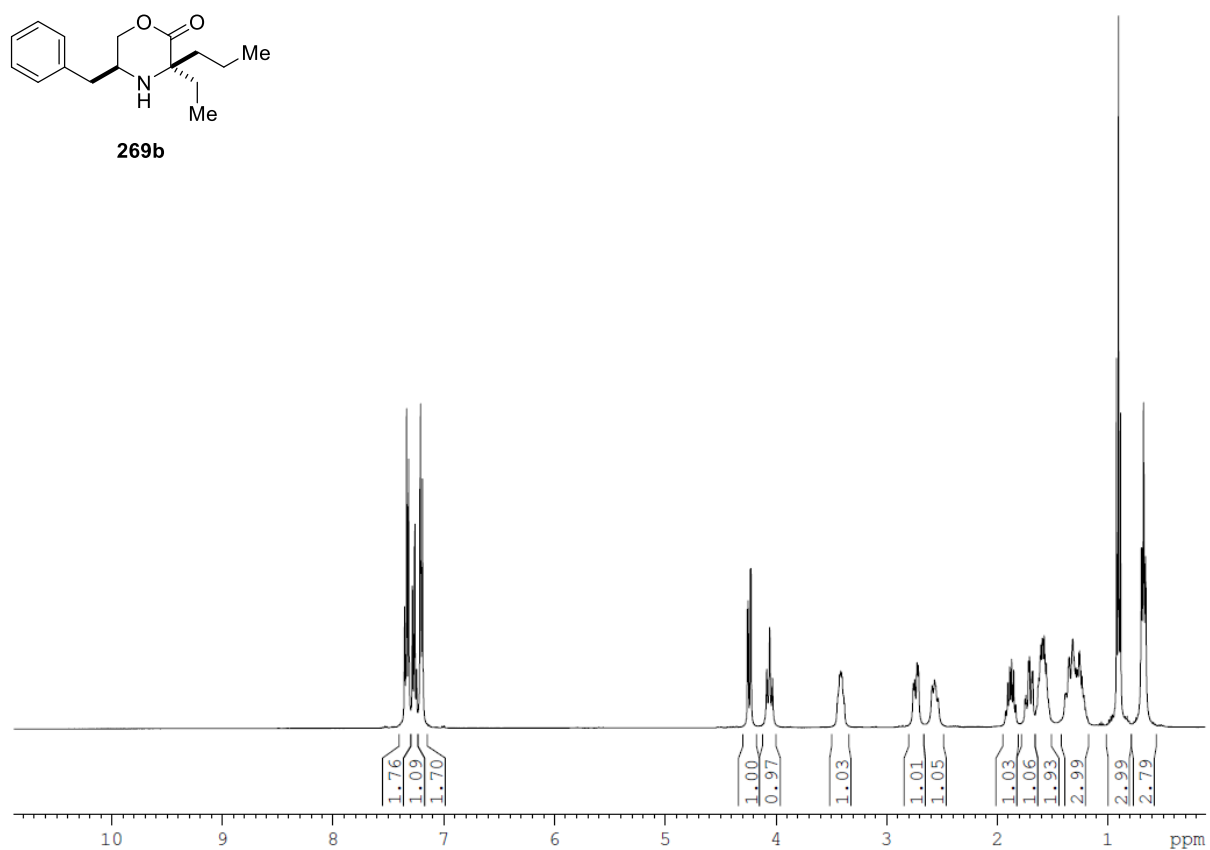
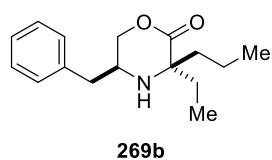
409

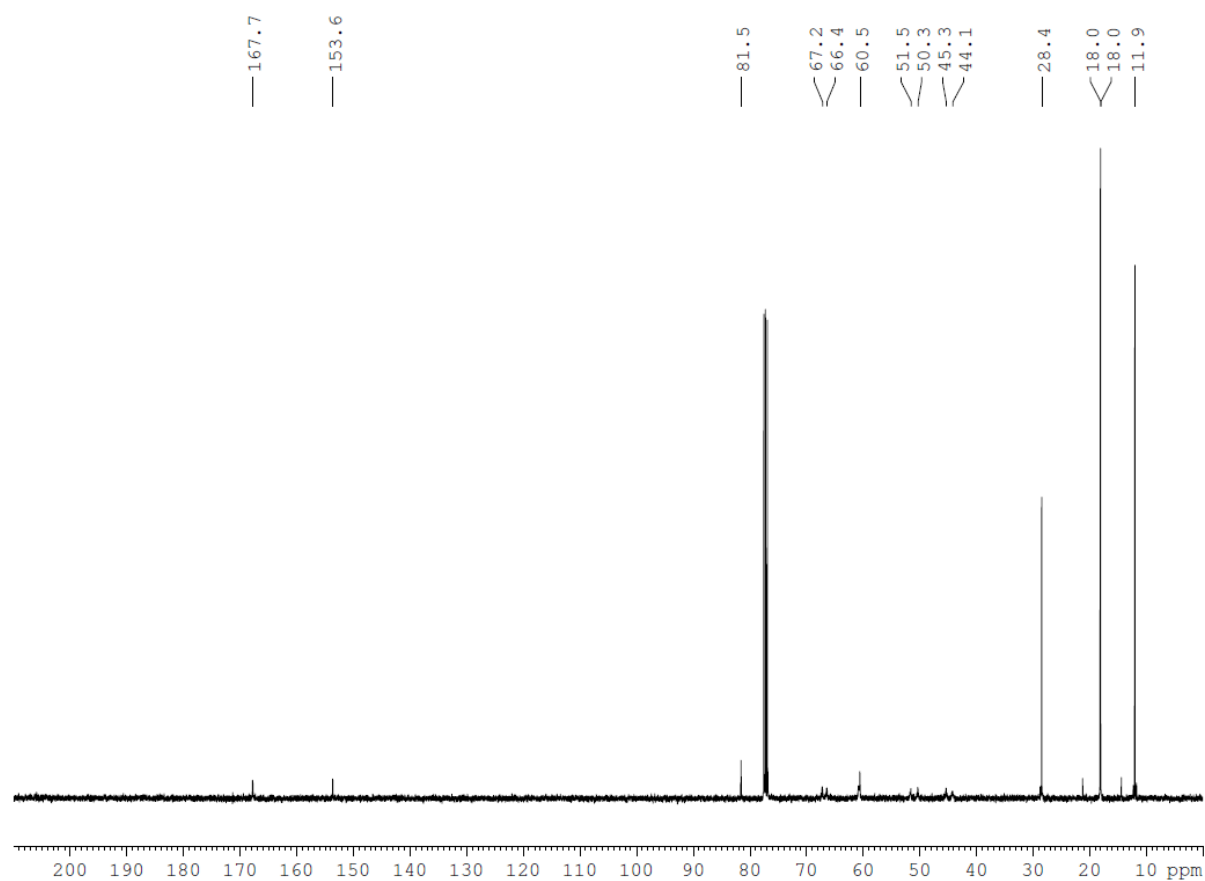
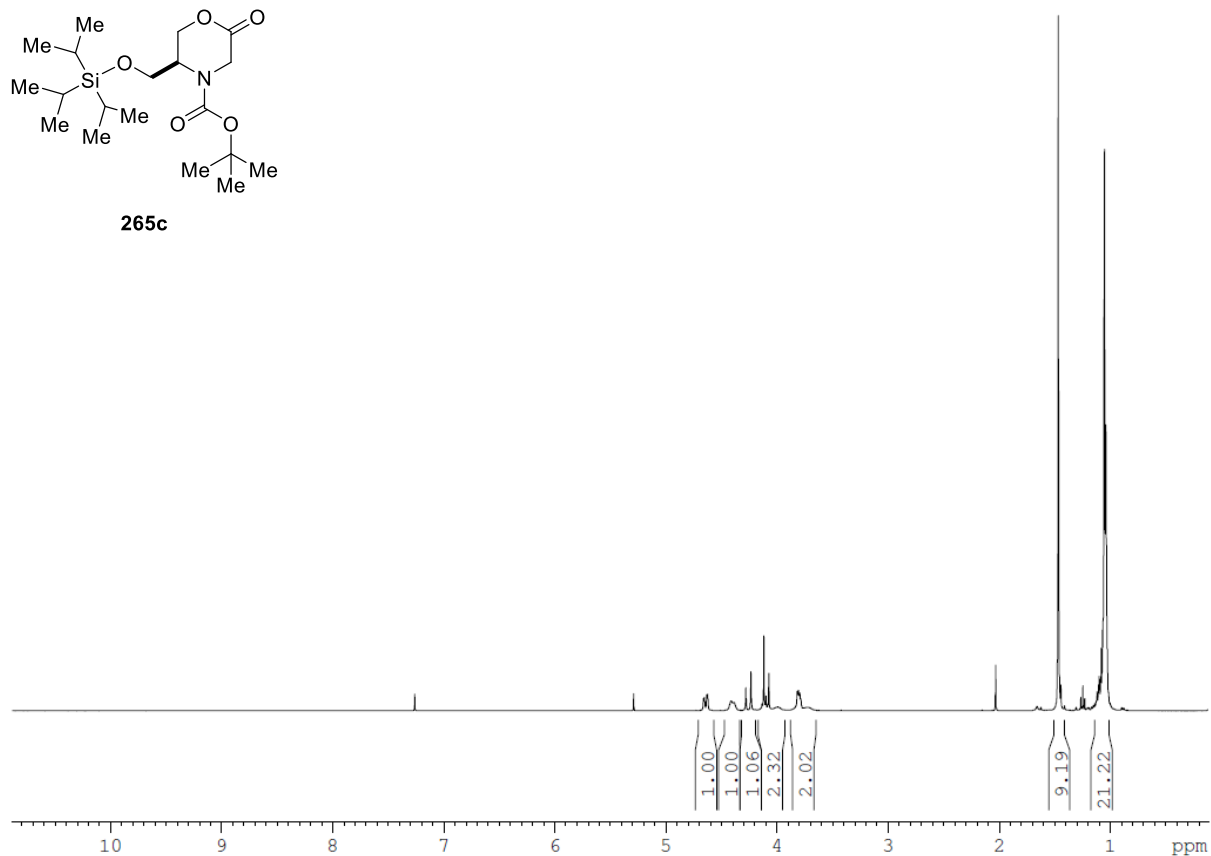
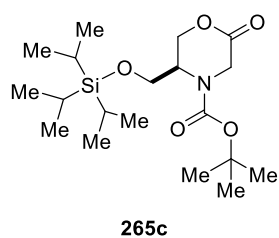


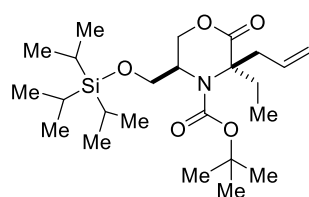
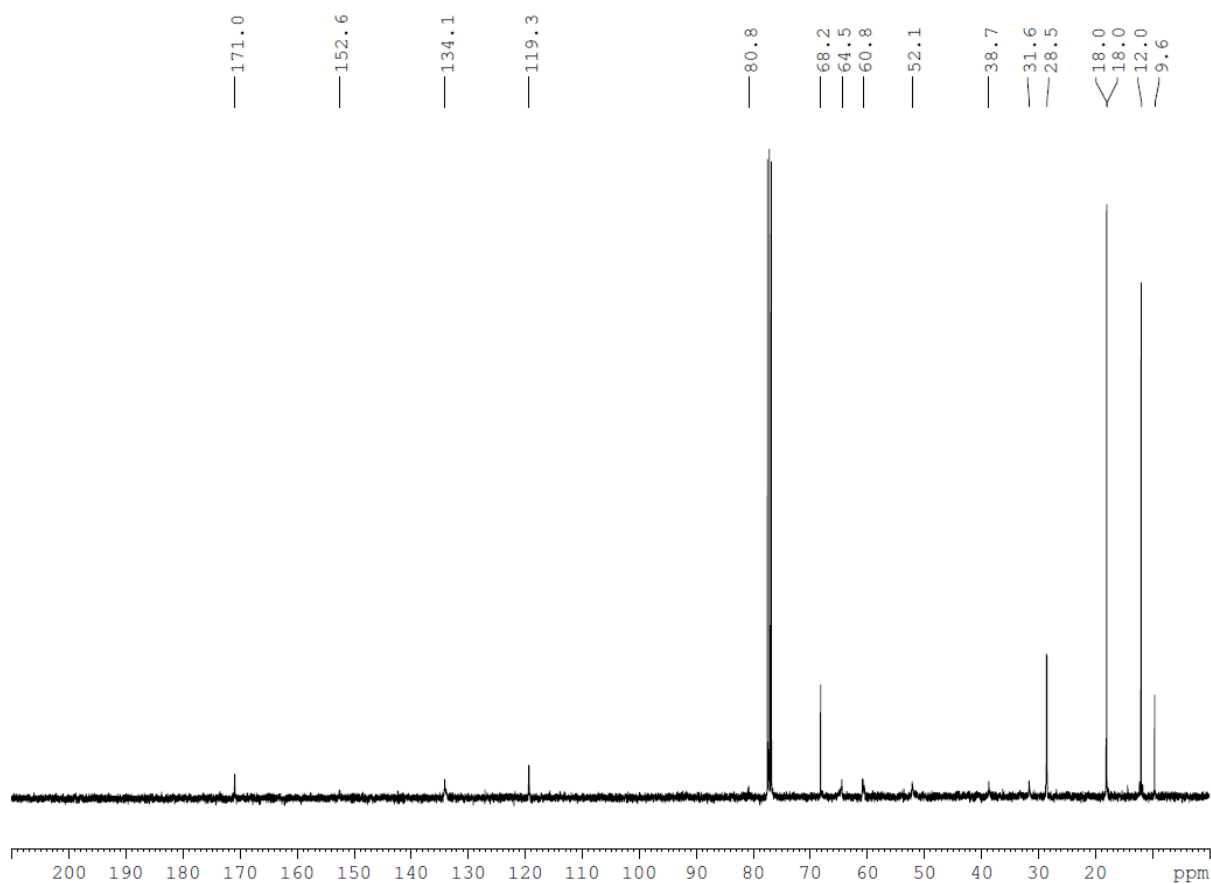
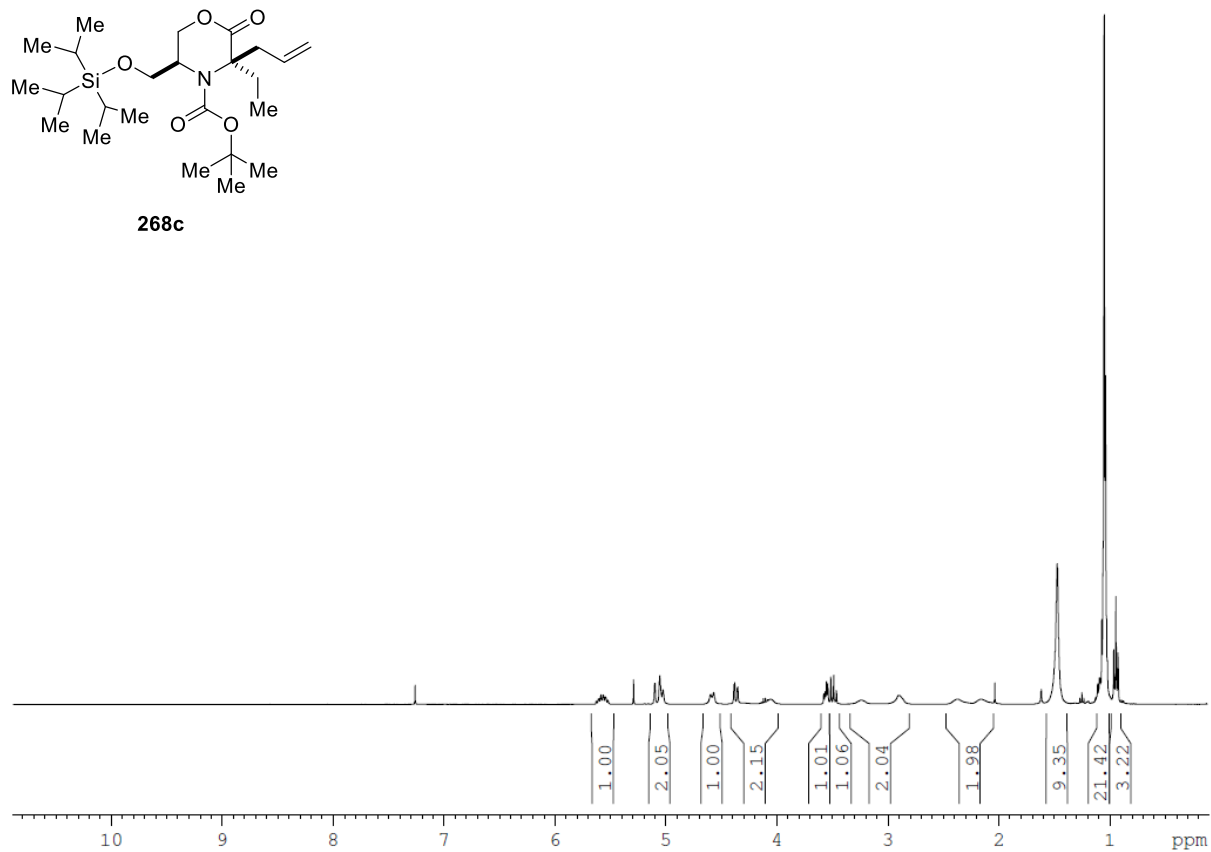
Synthesized (Novel) Compounds from Appendix I

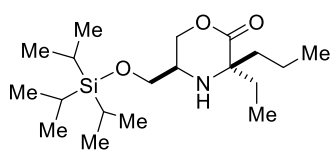
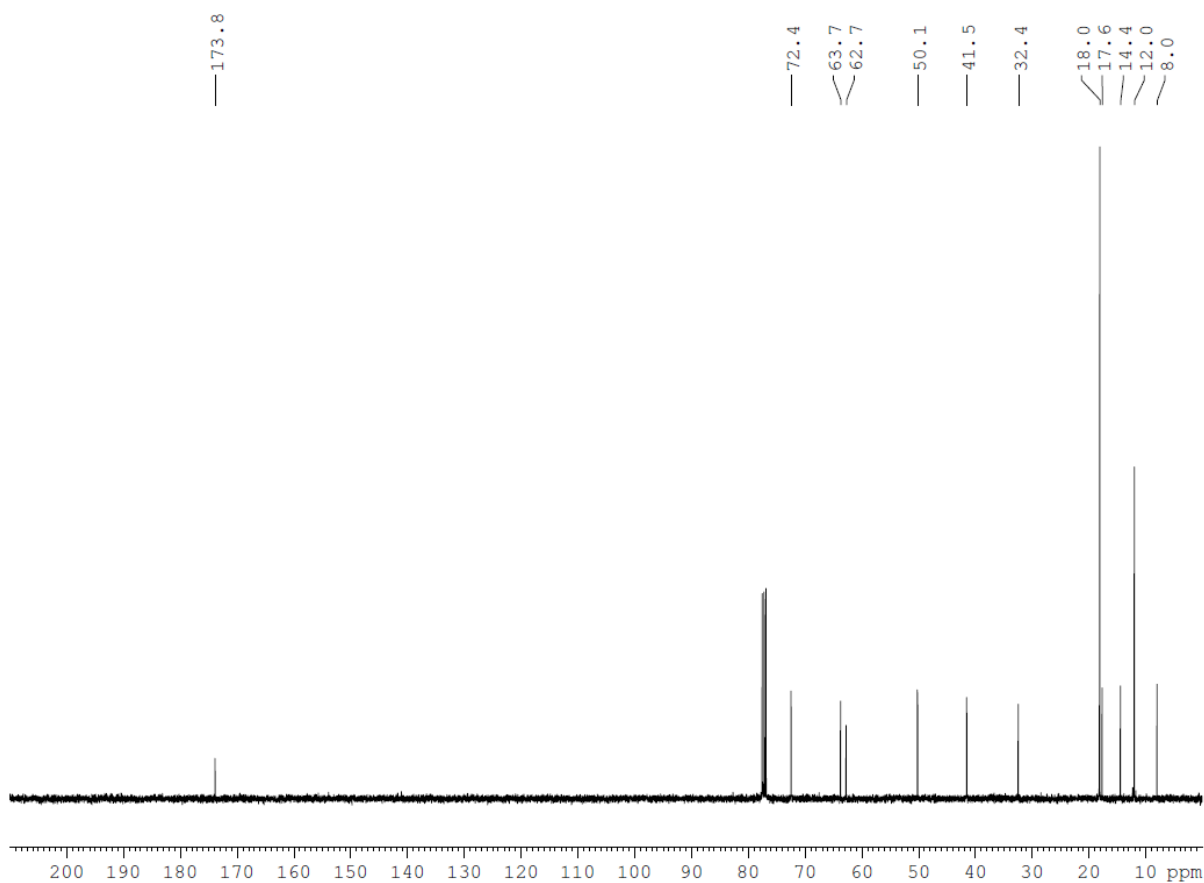
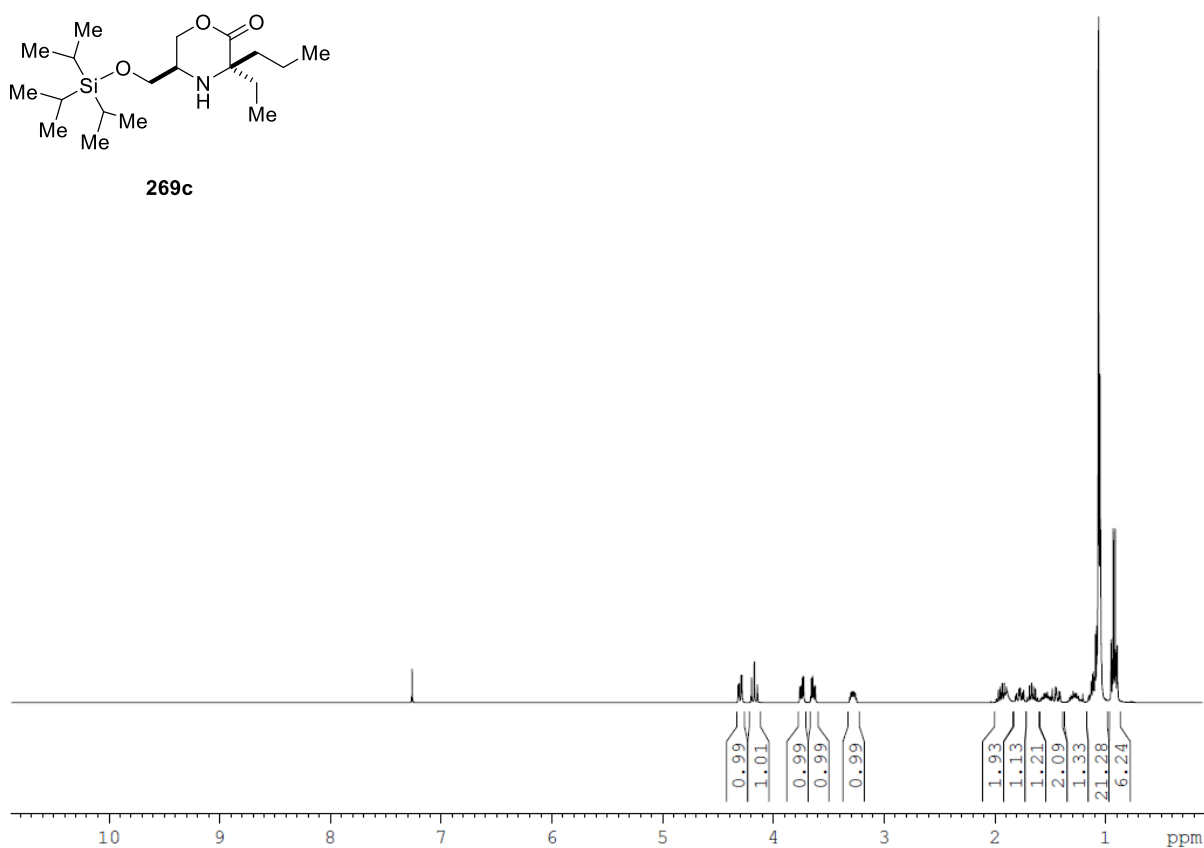
**265b**

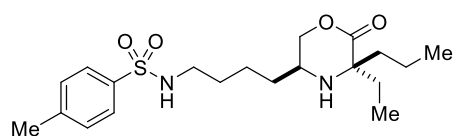
**268b**



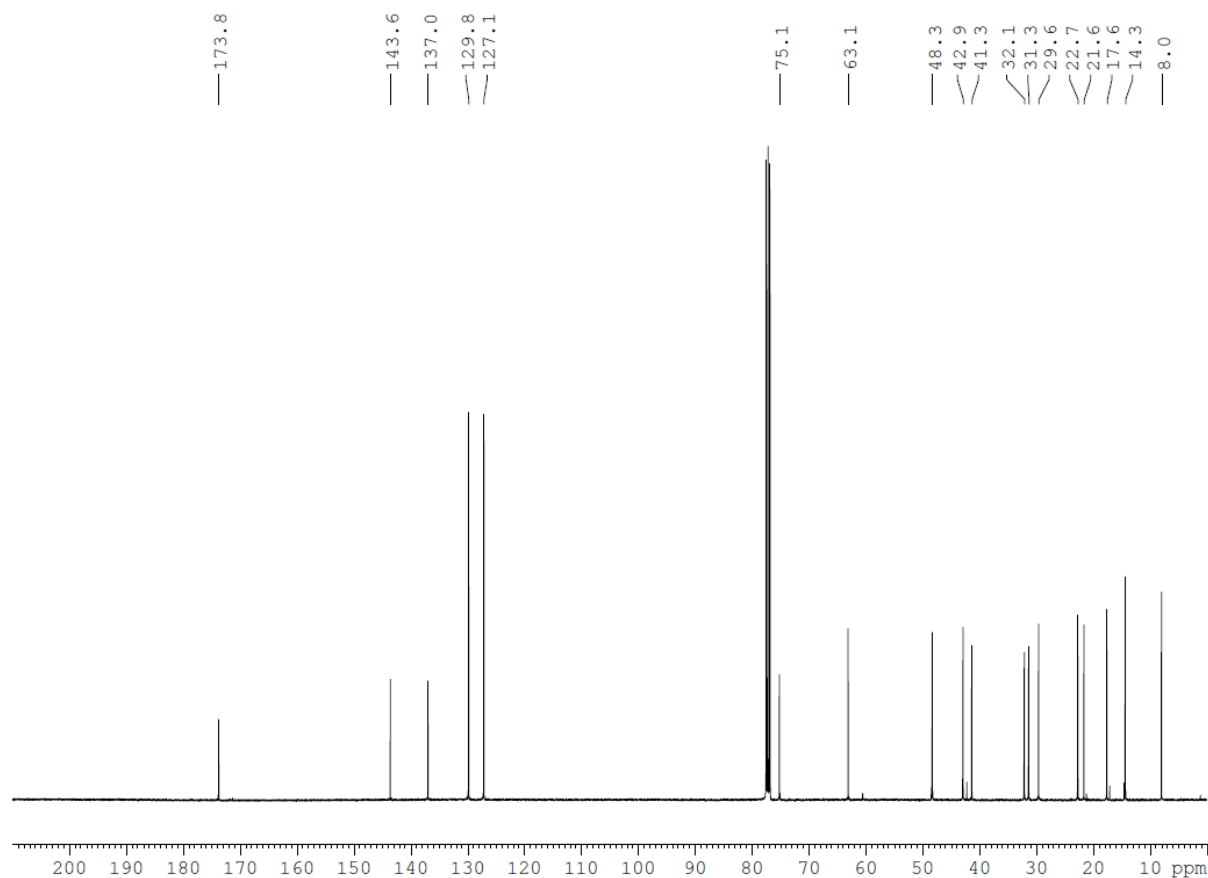
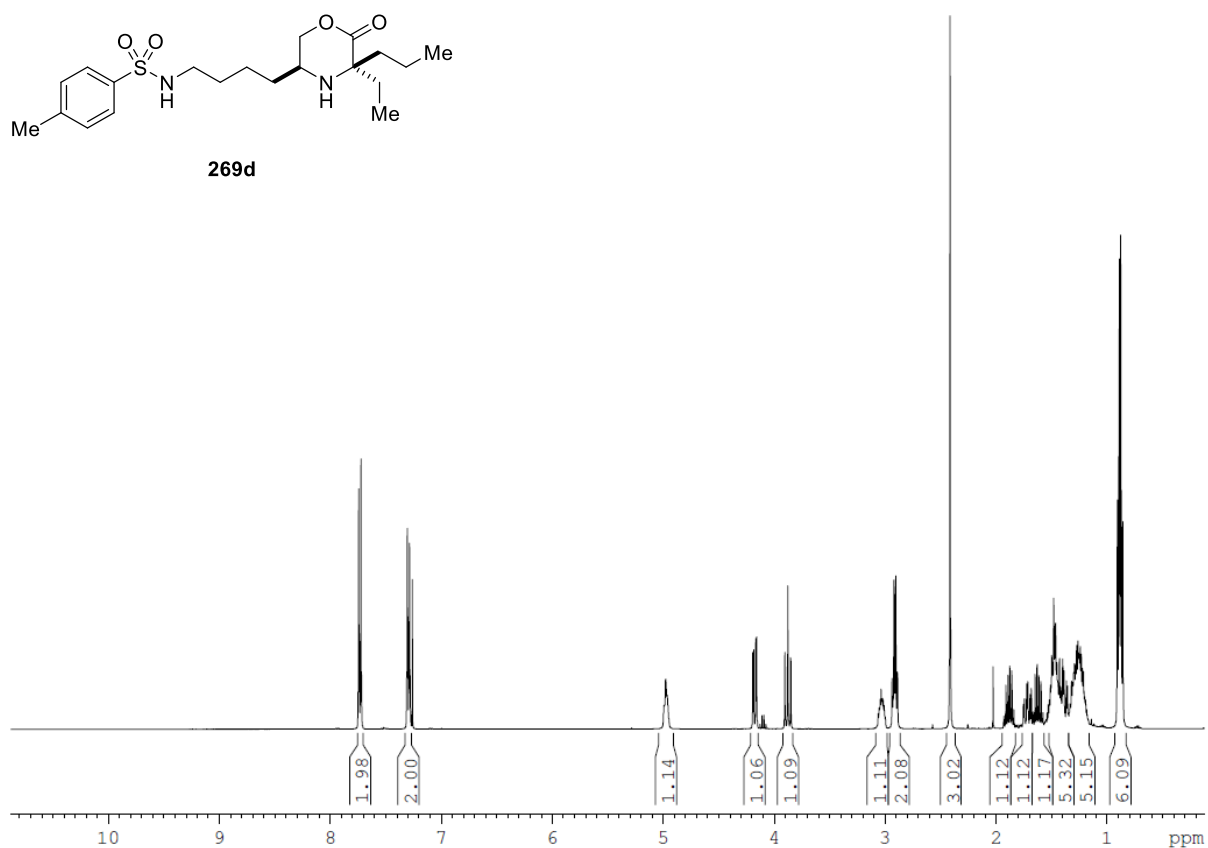


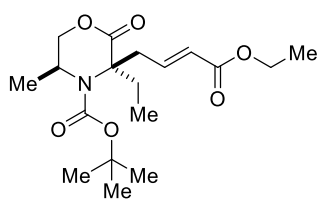
**268c**

**269c**

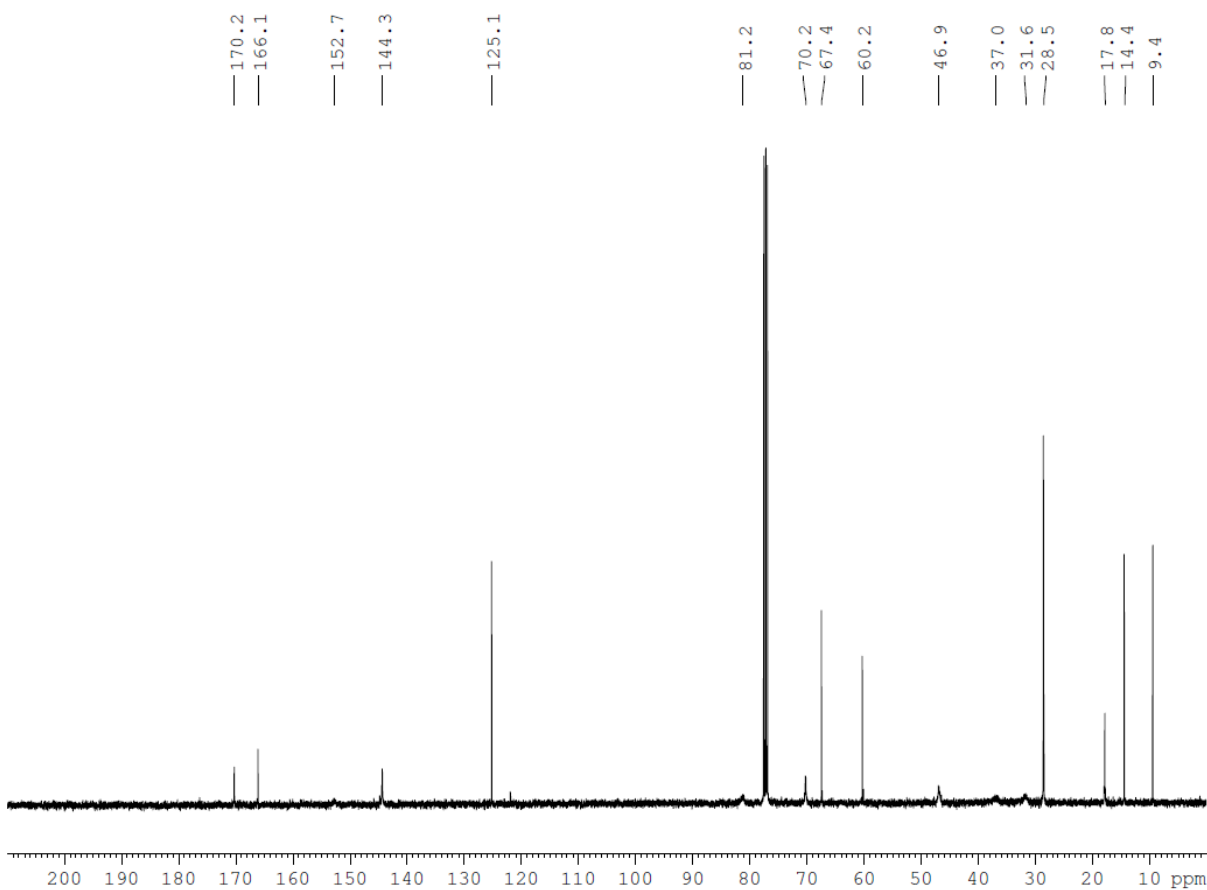


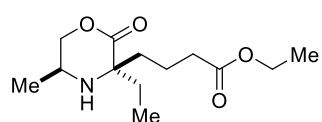
269d



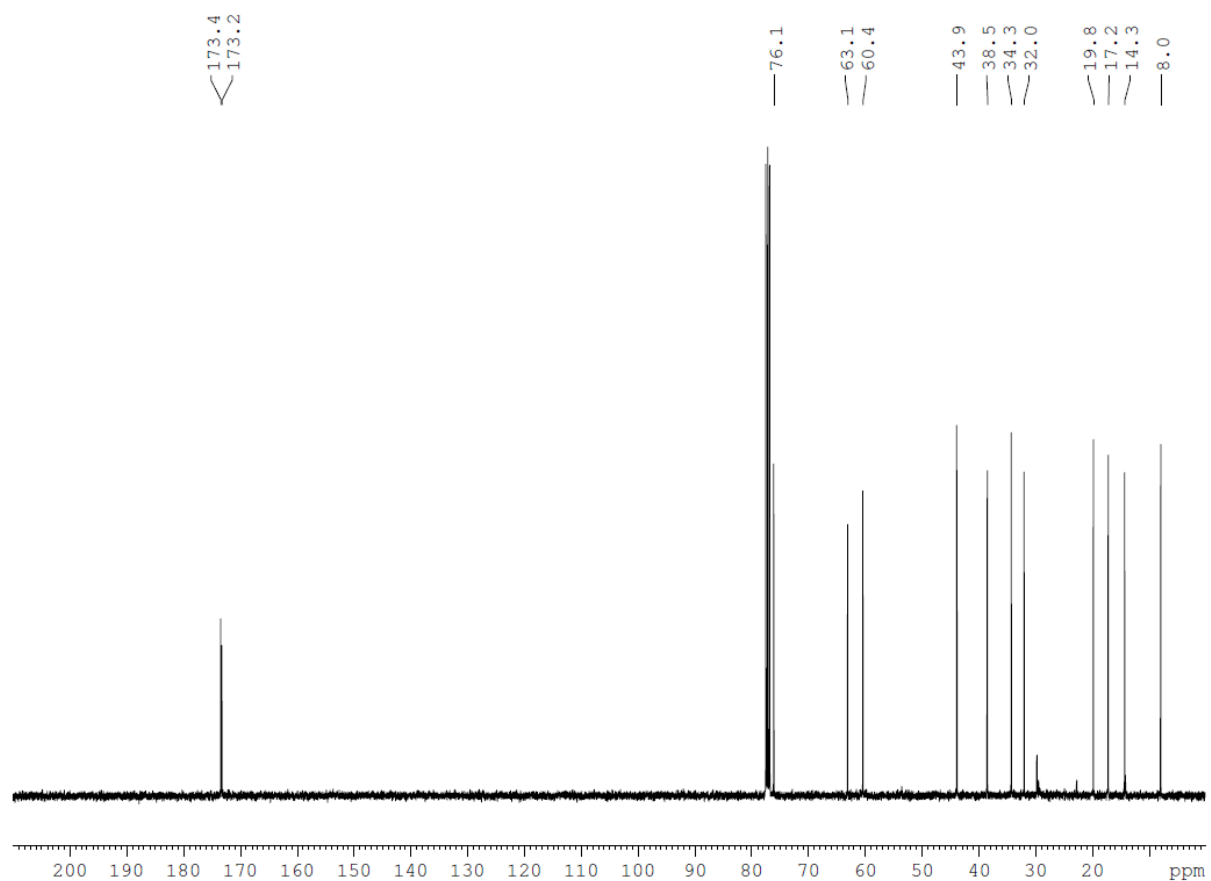
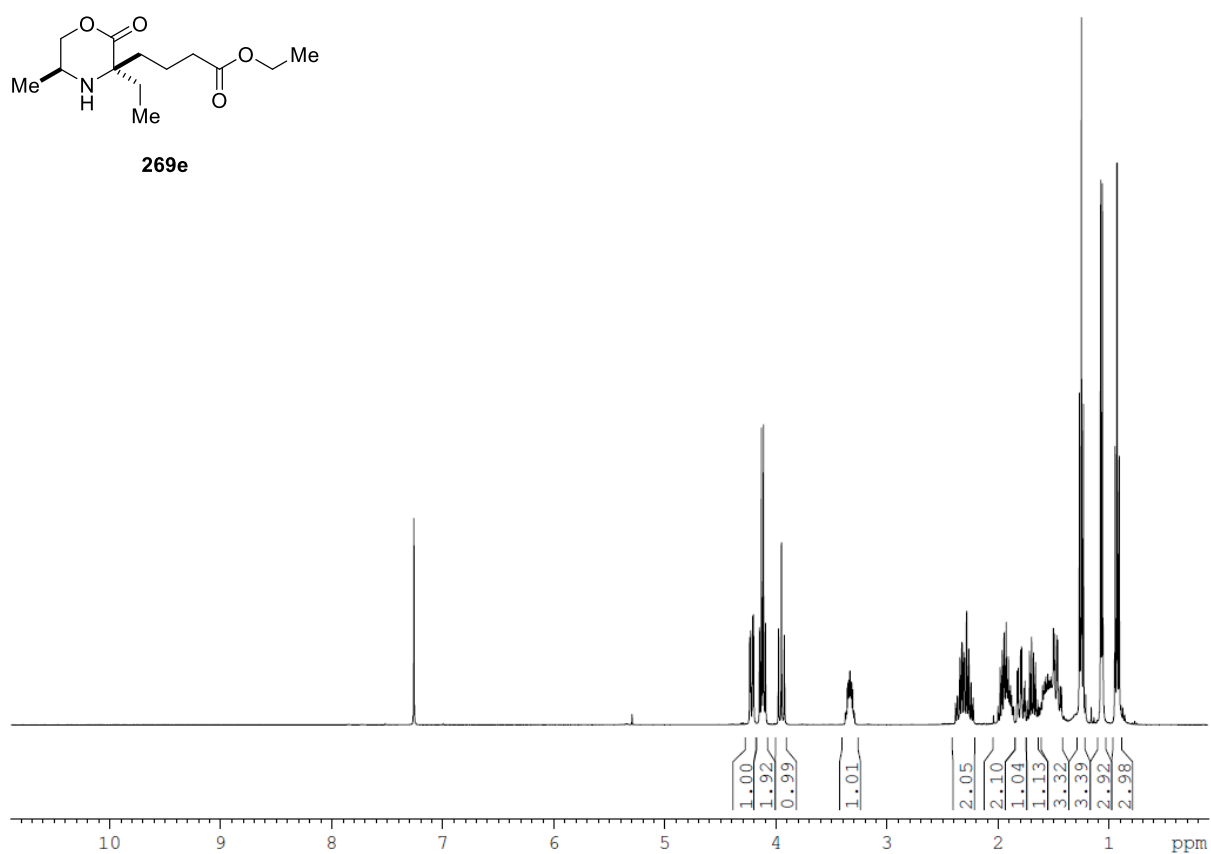


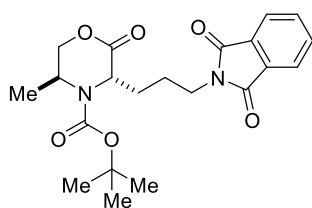
270



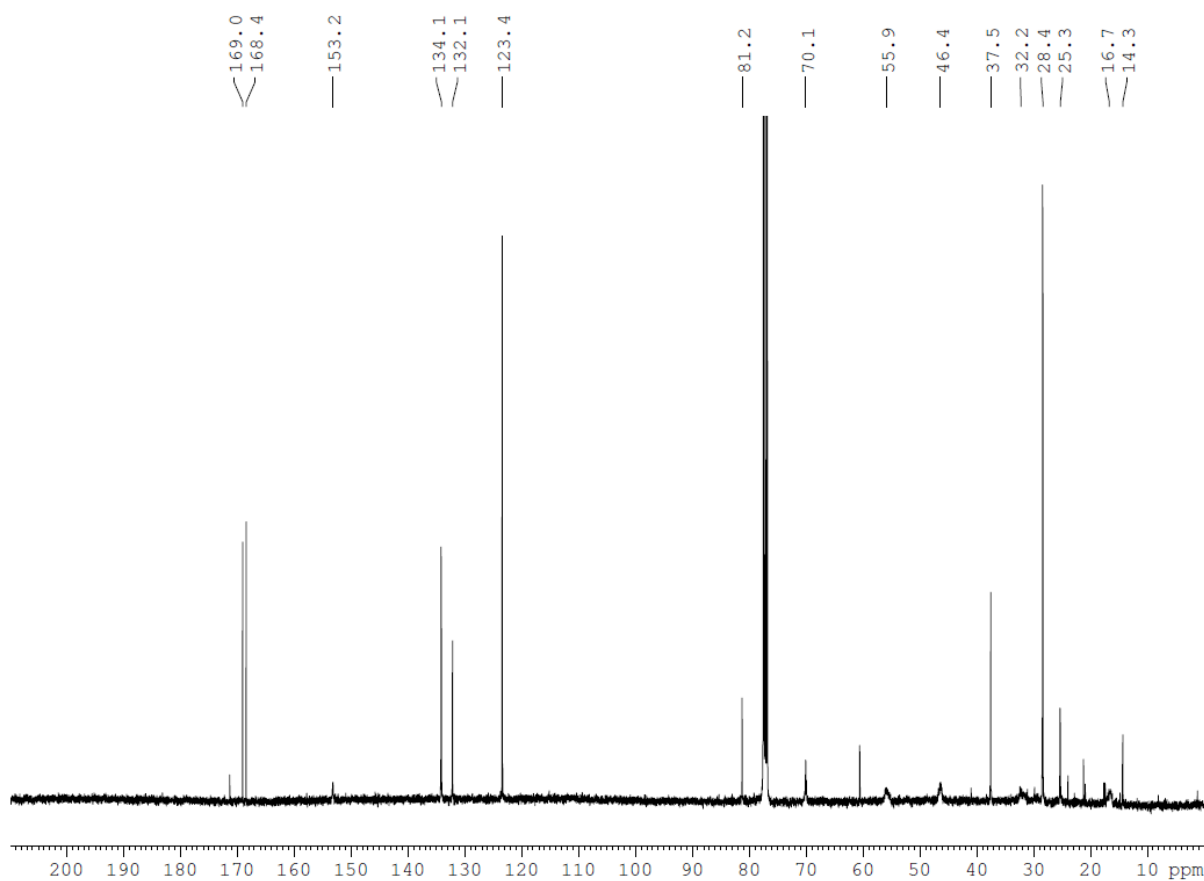
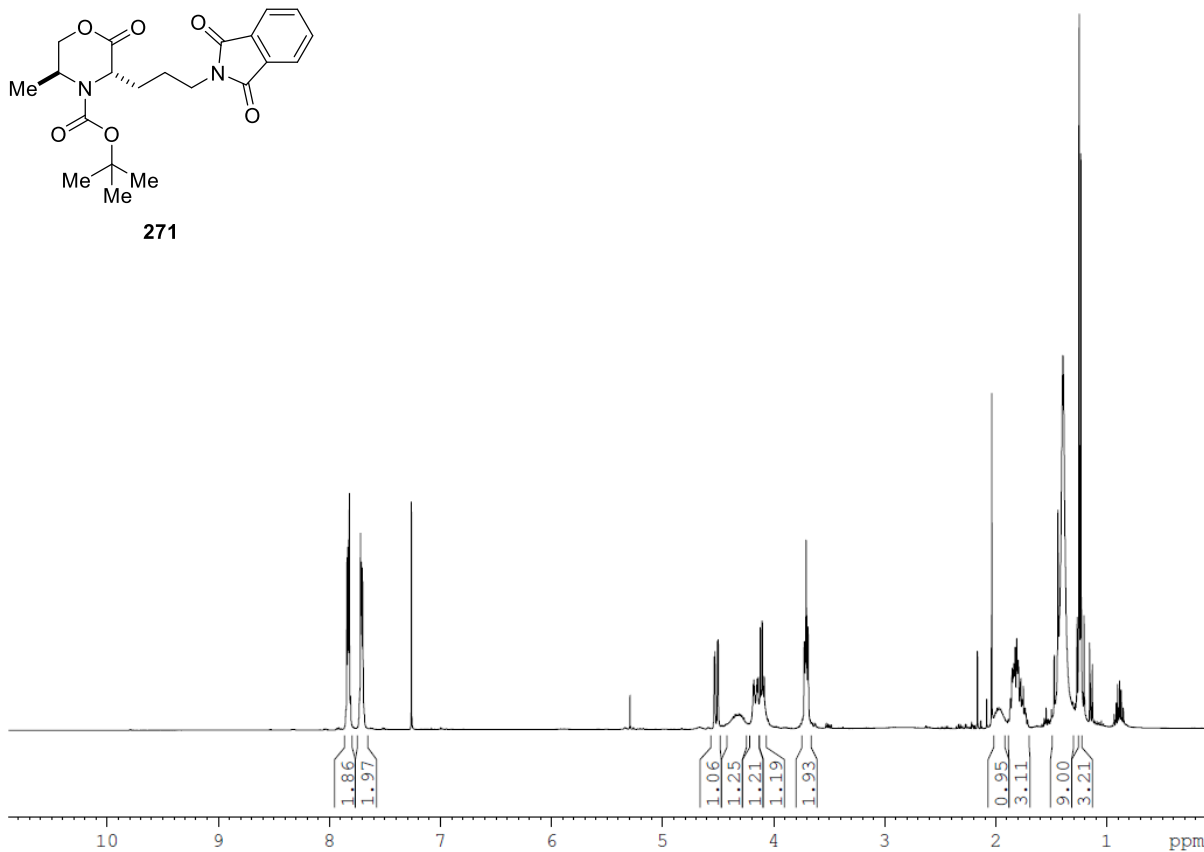


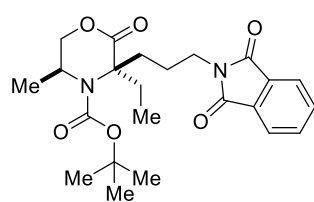
269e



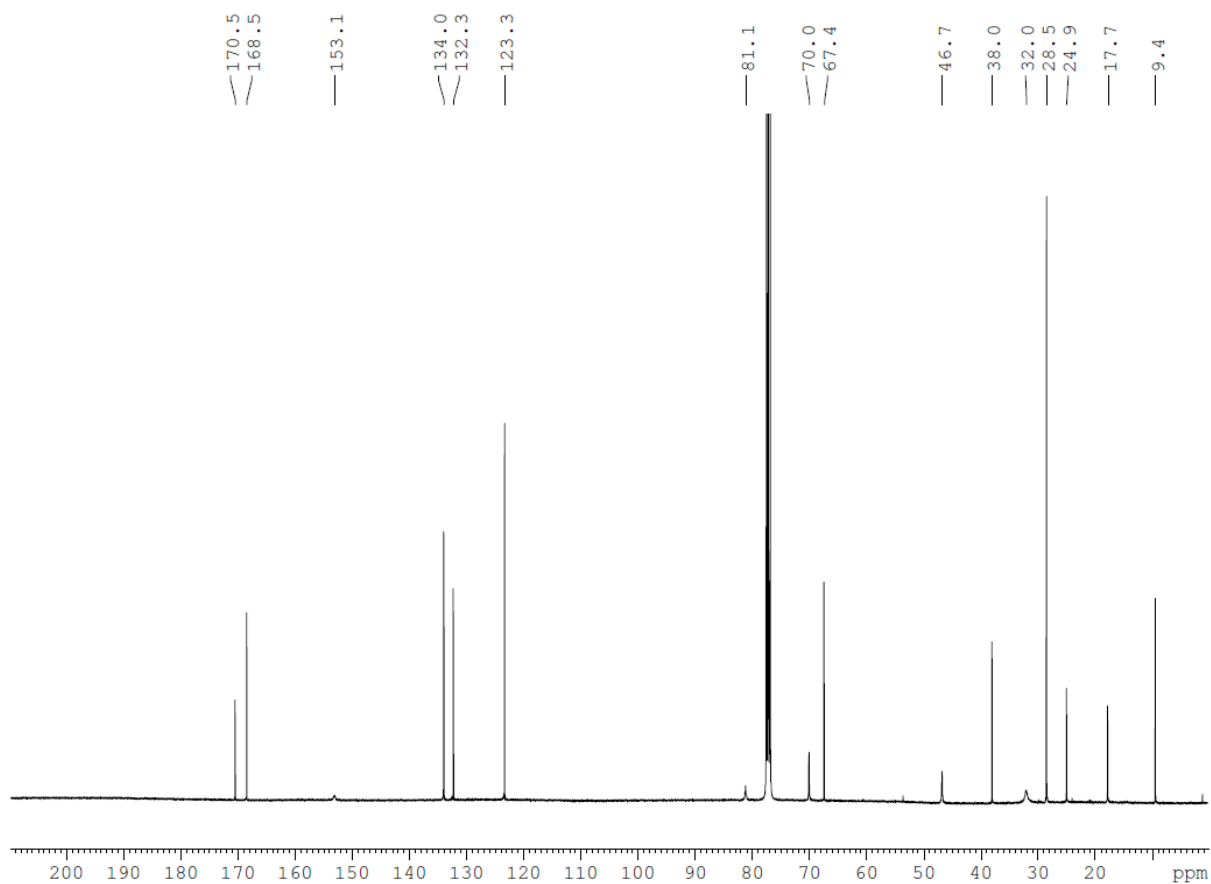
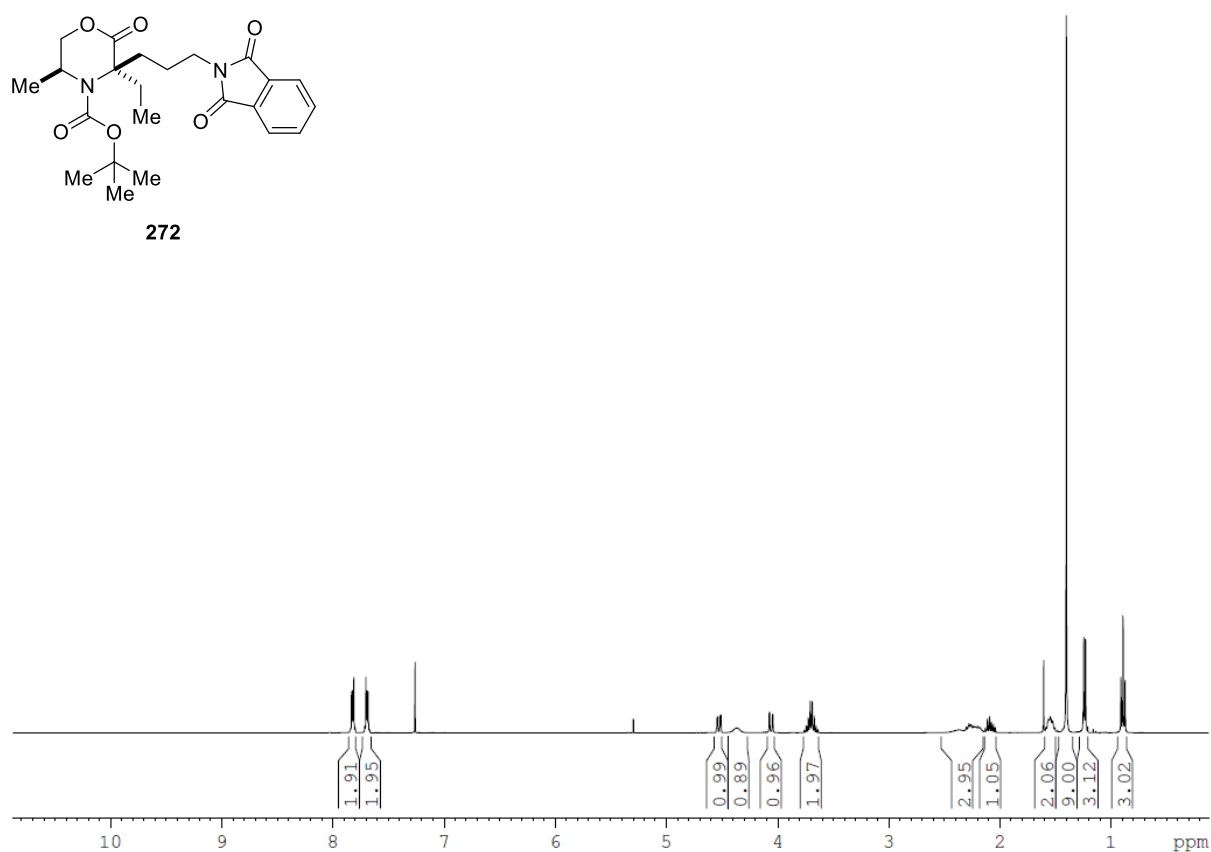


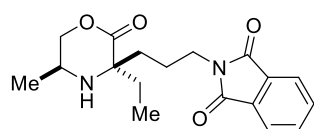
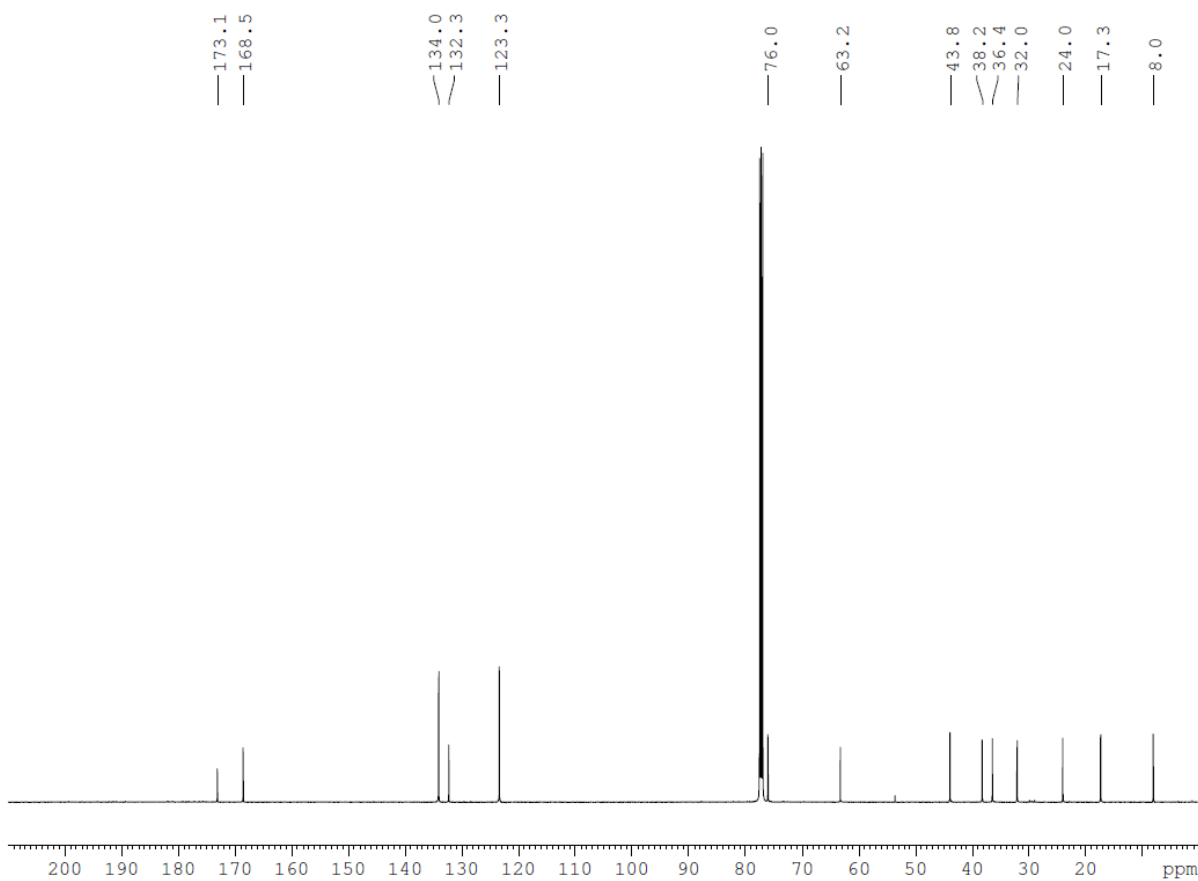
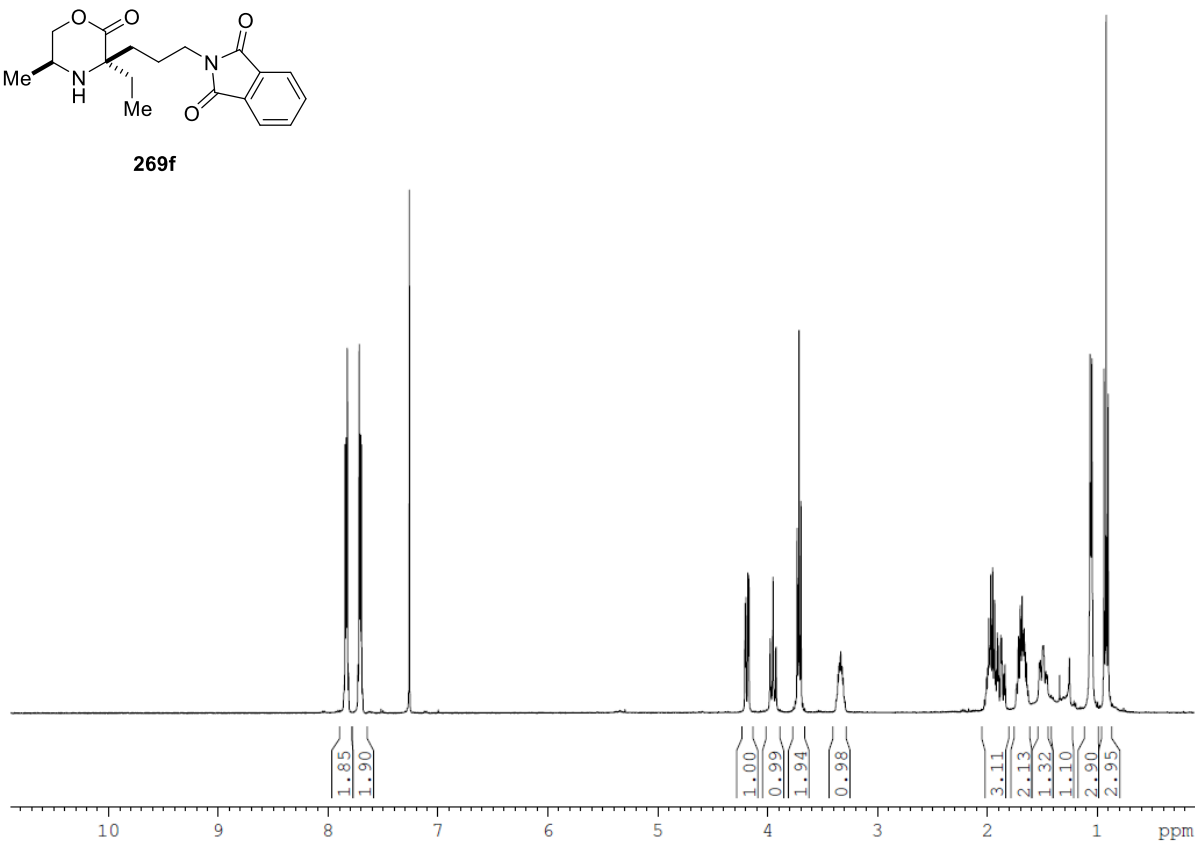
271

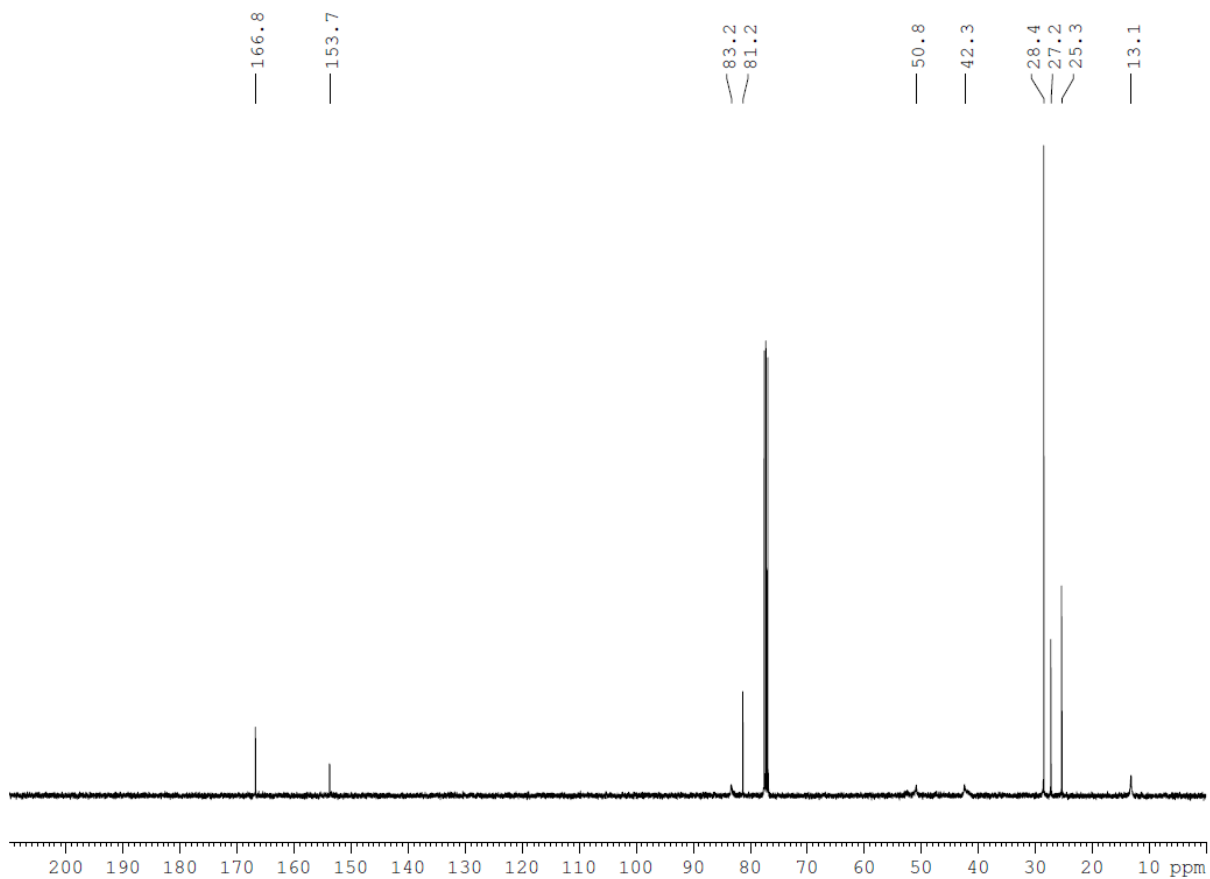
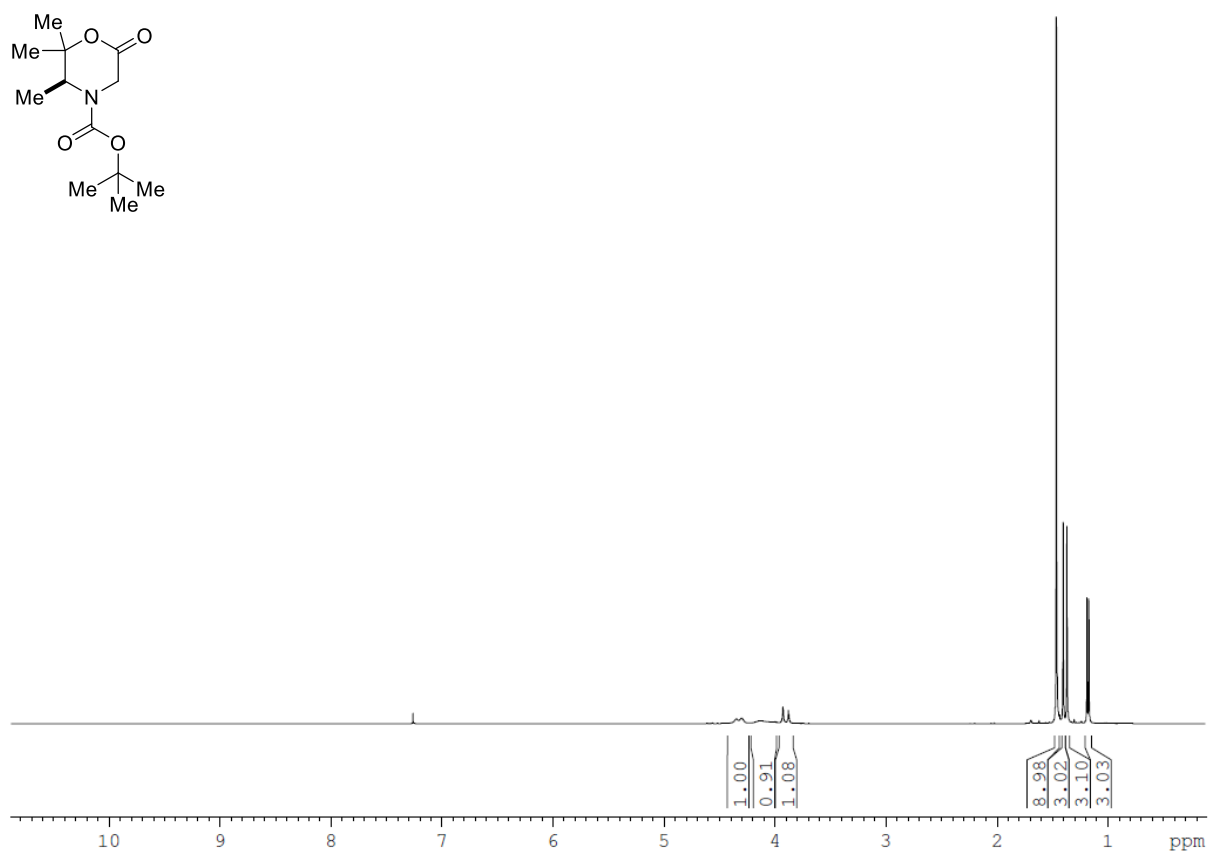


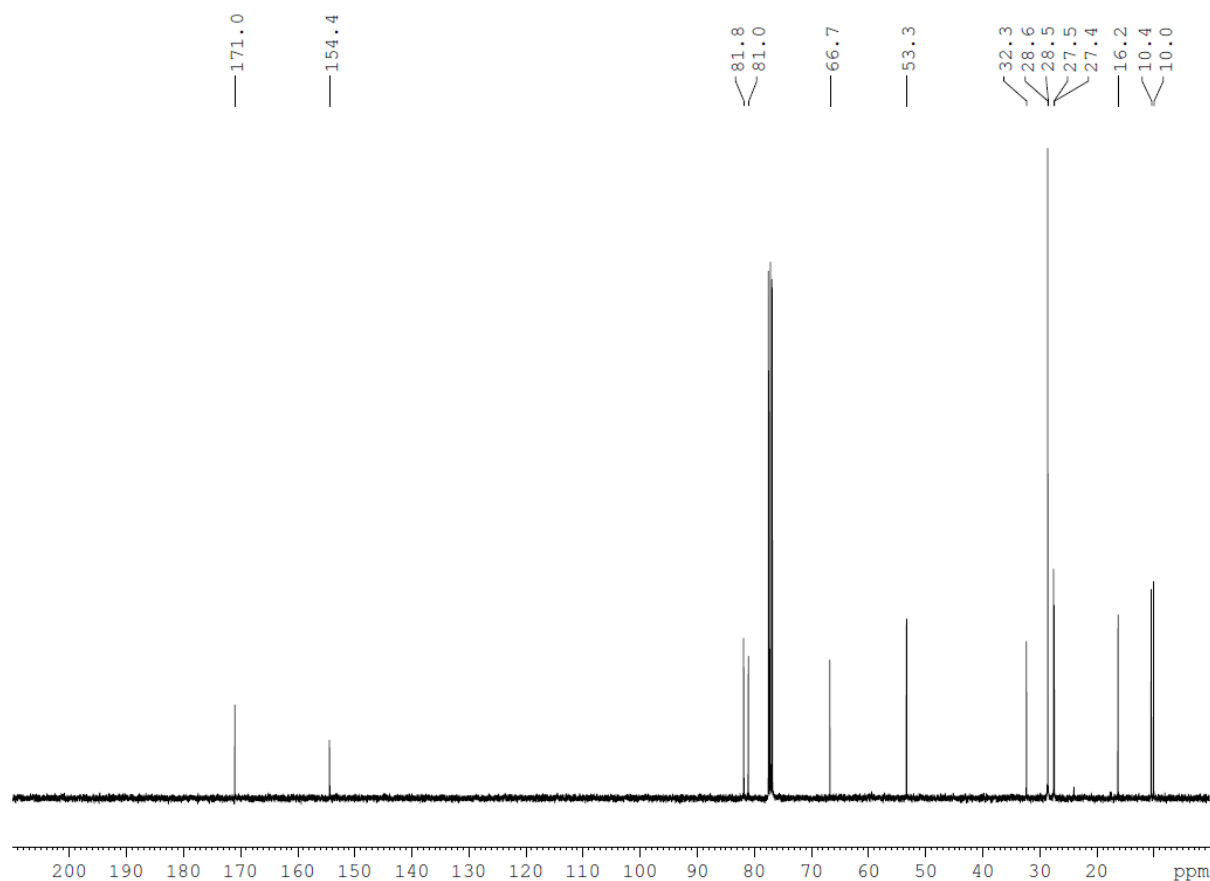
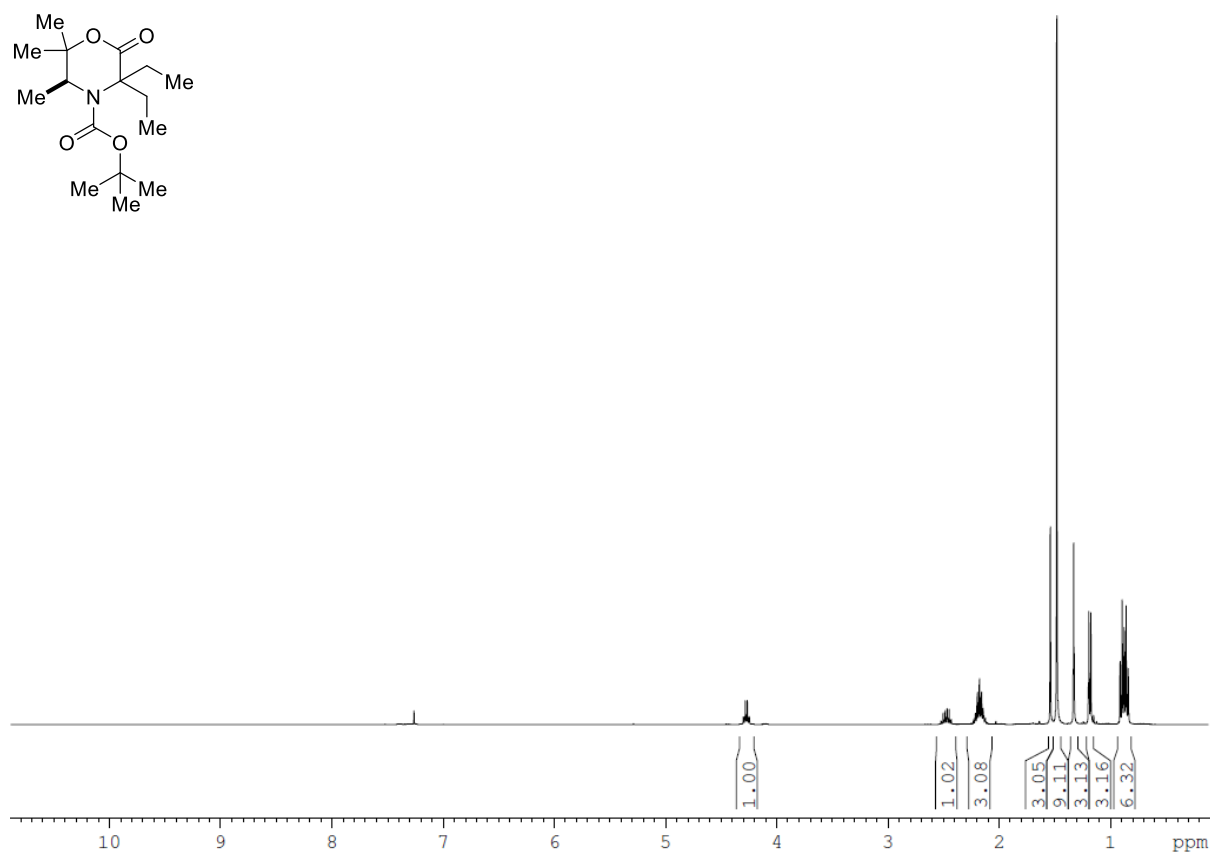
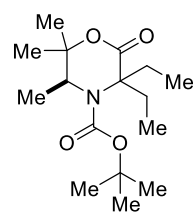


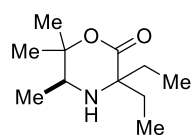
272



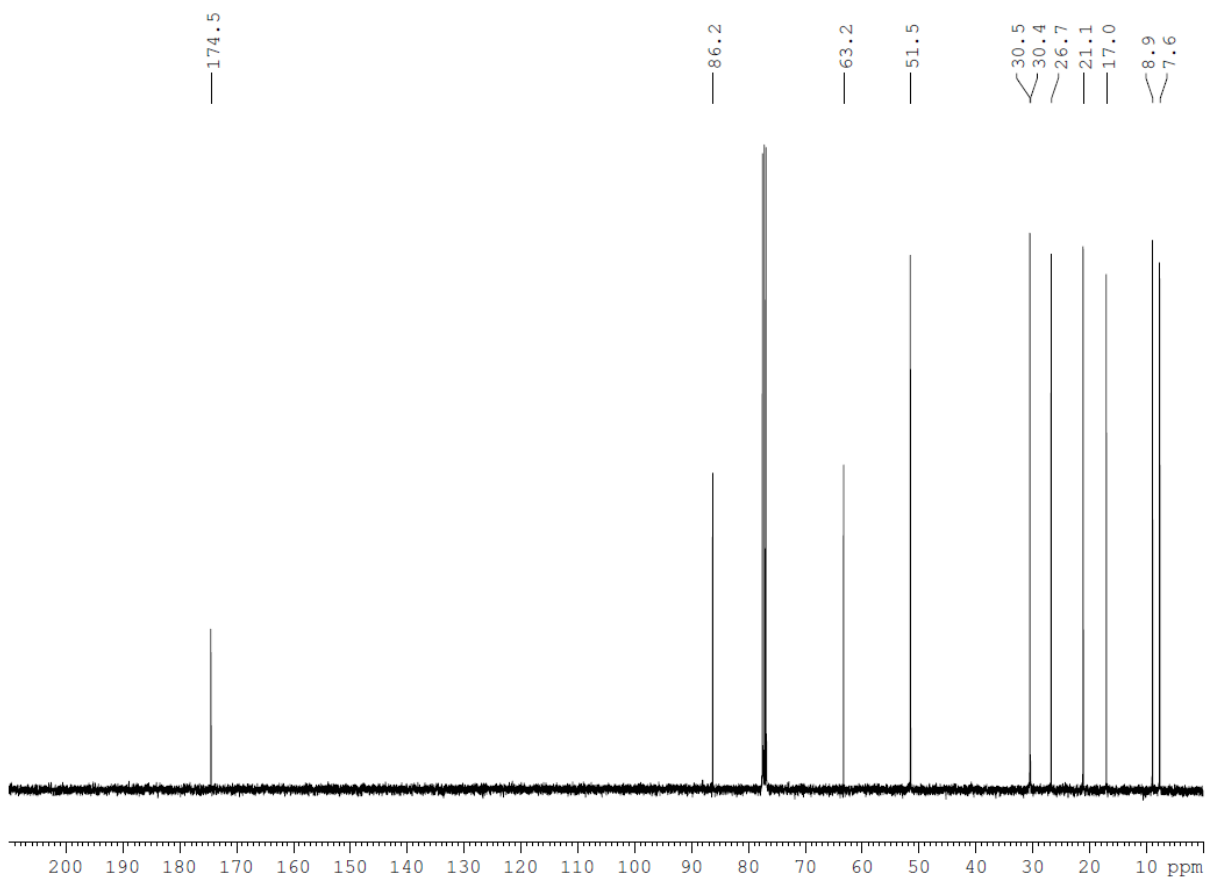
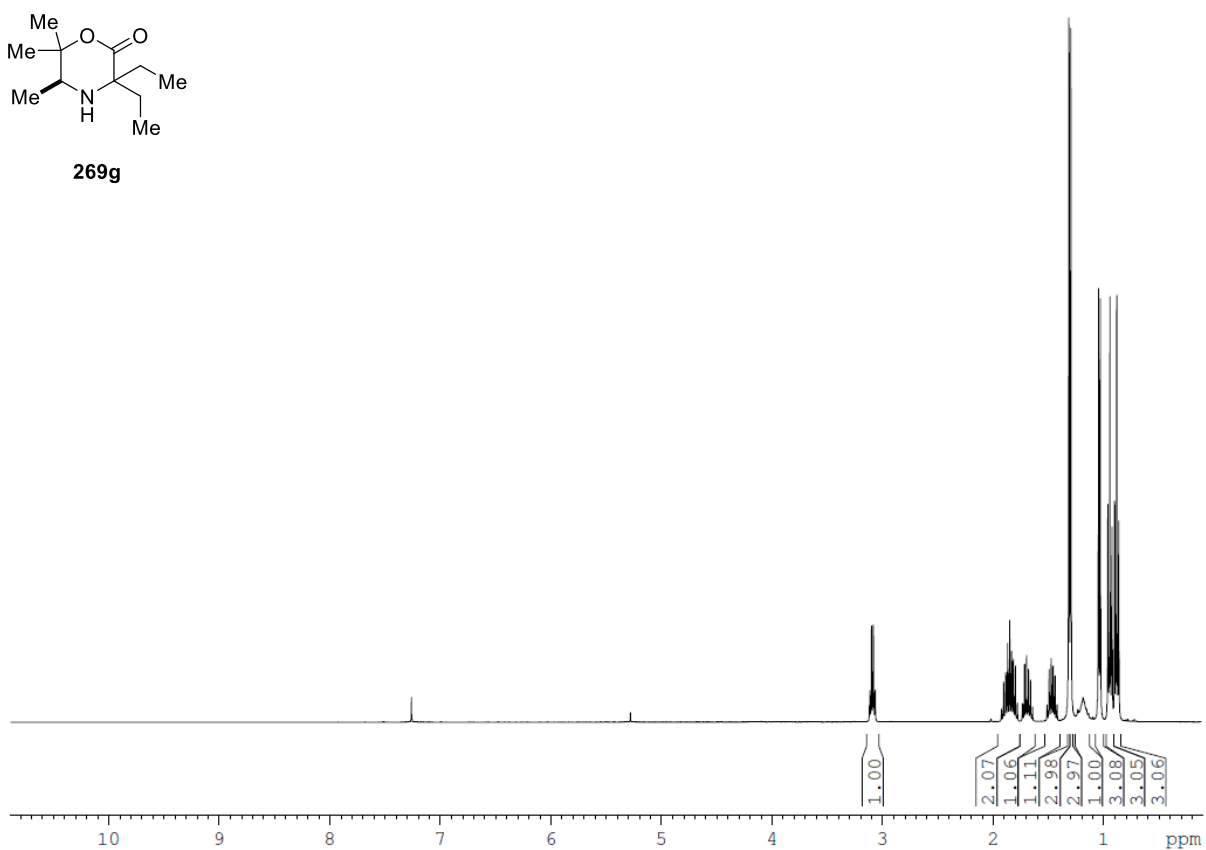
**269f**

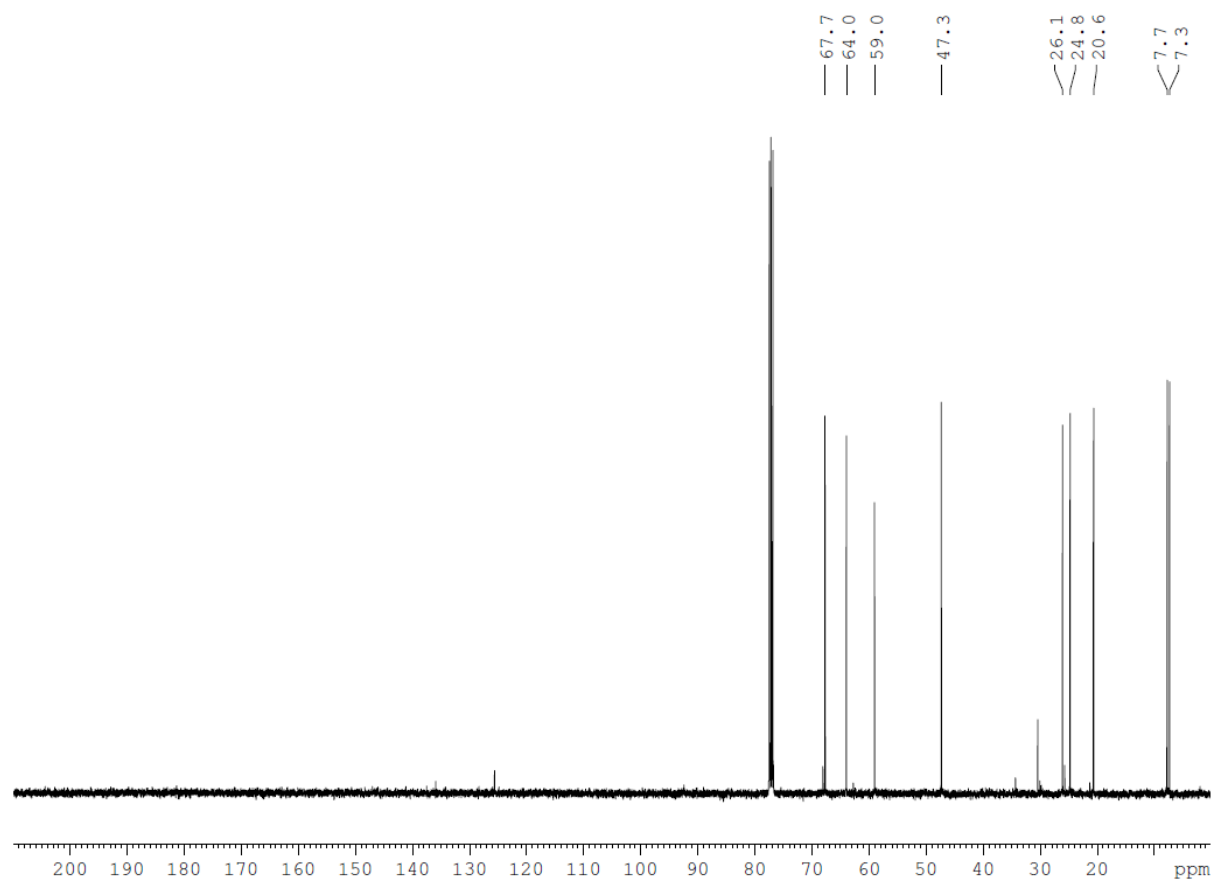
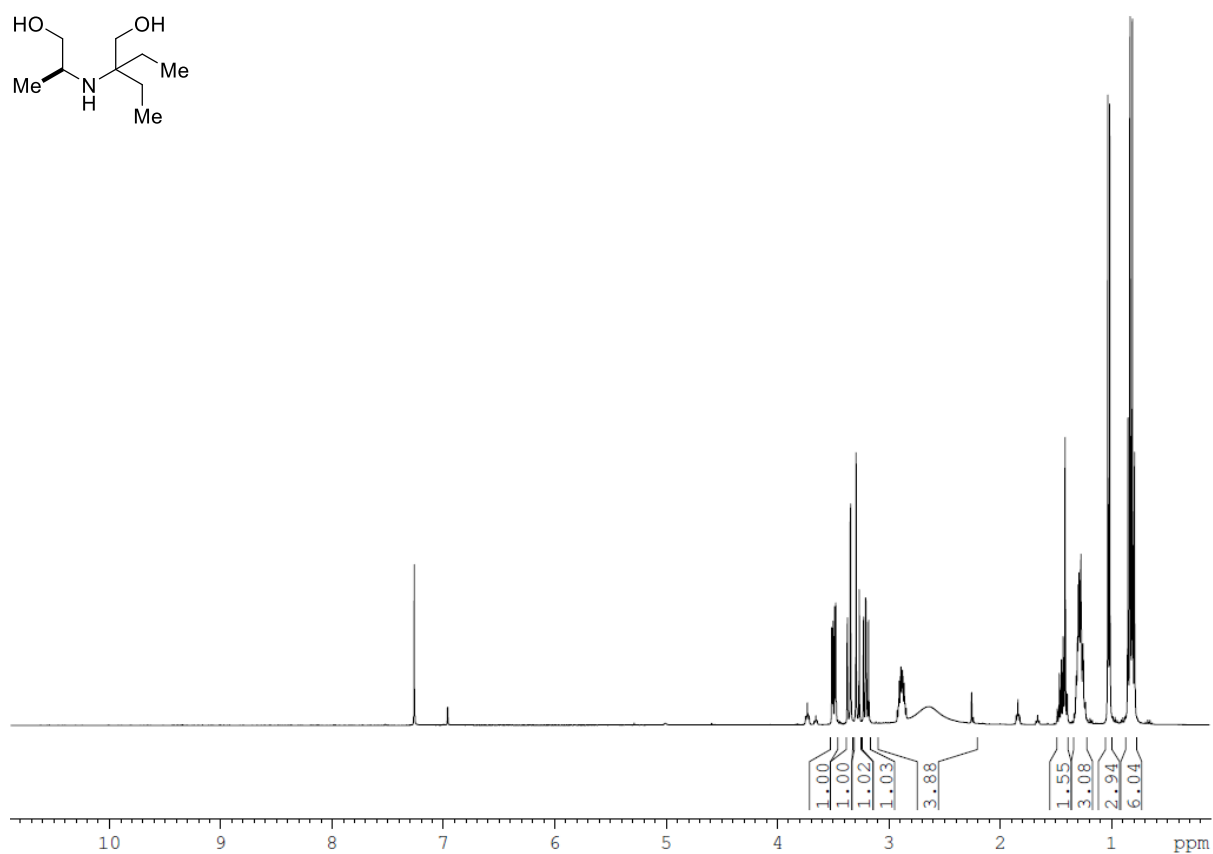
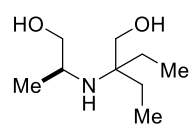


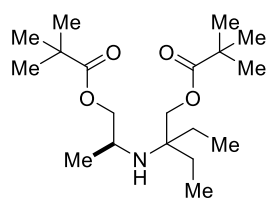




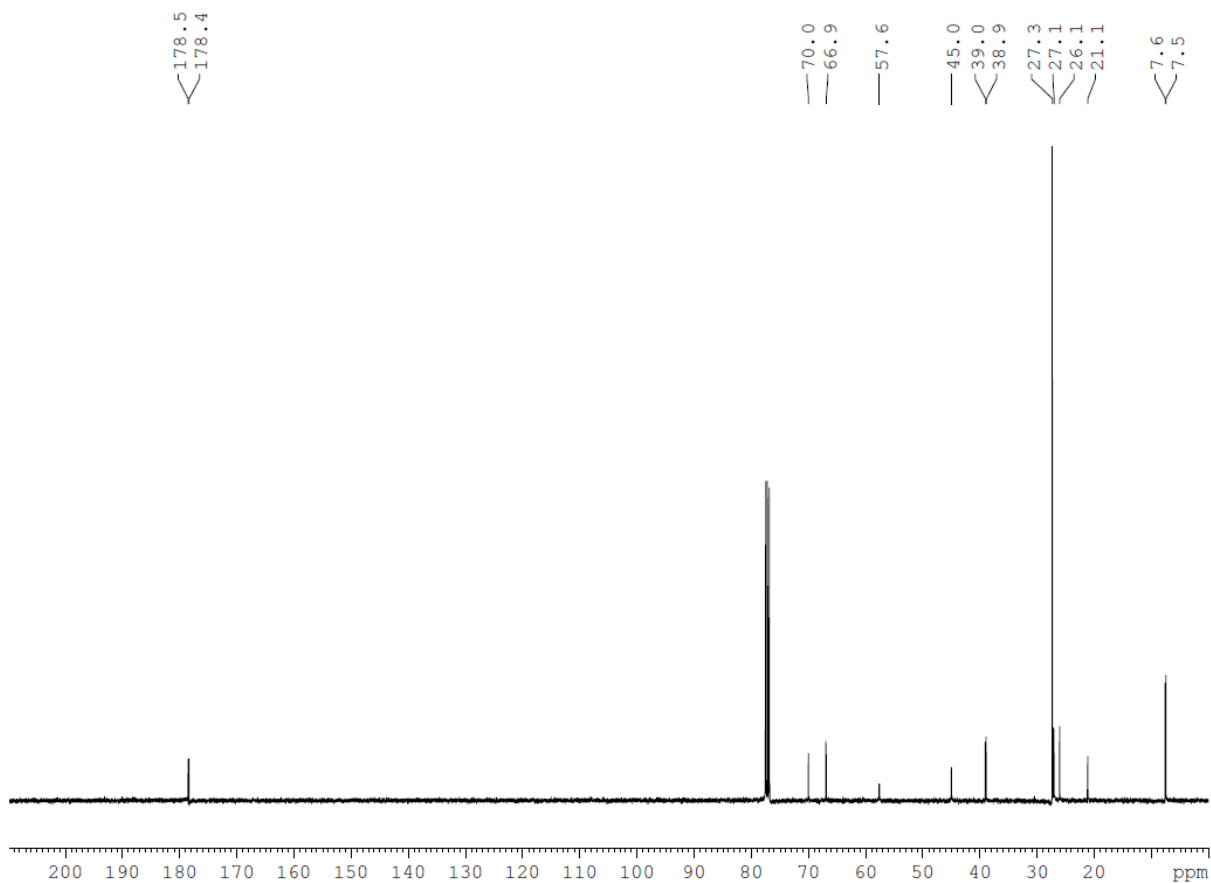
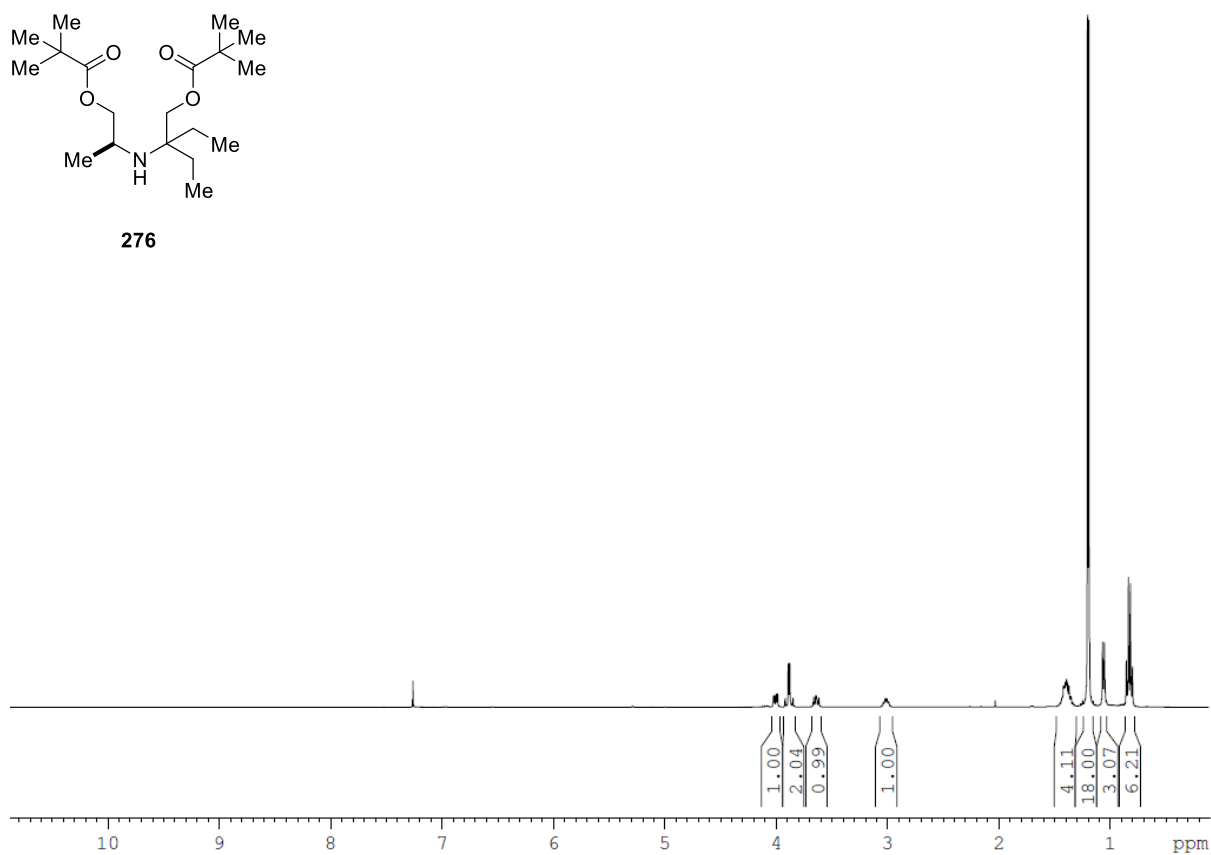
269g

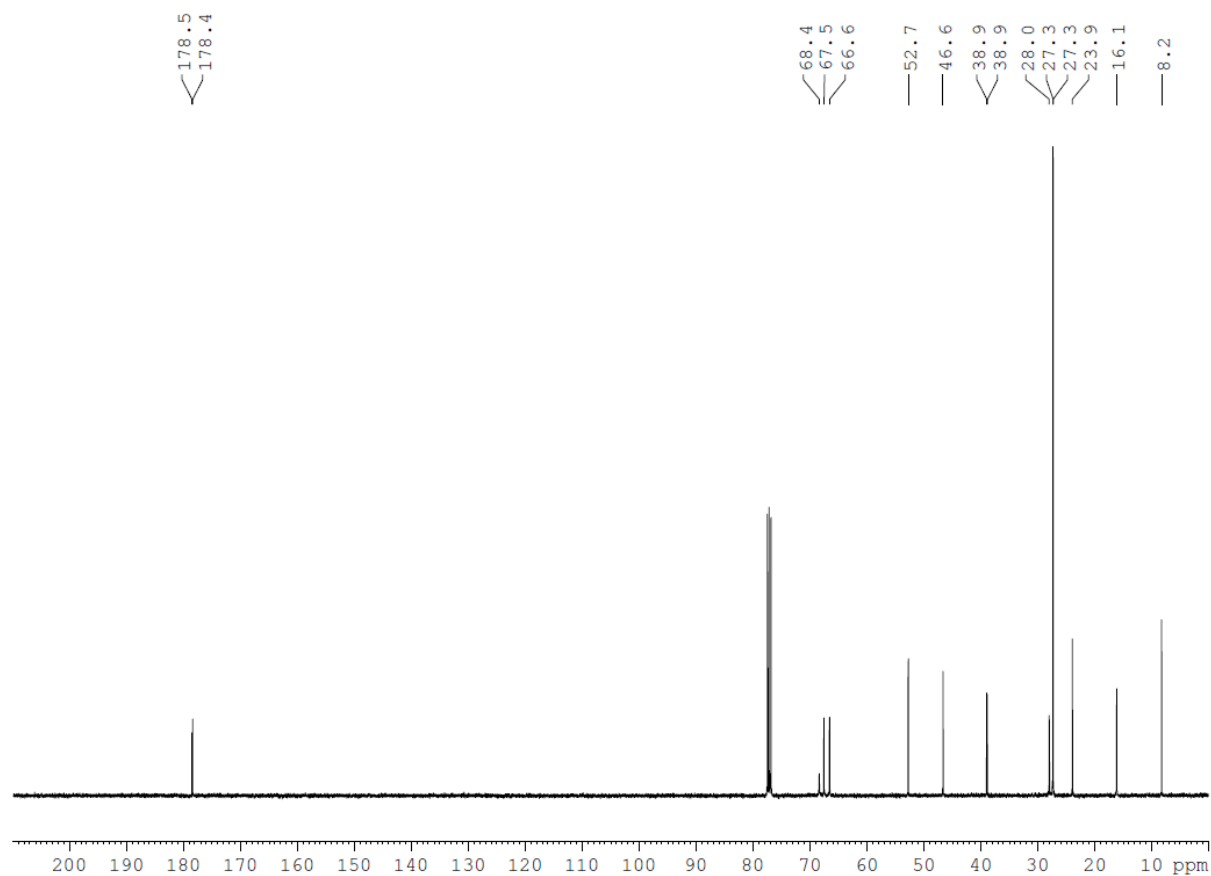
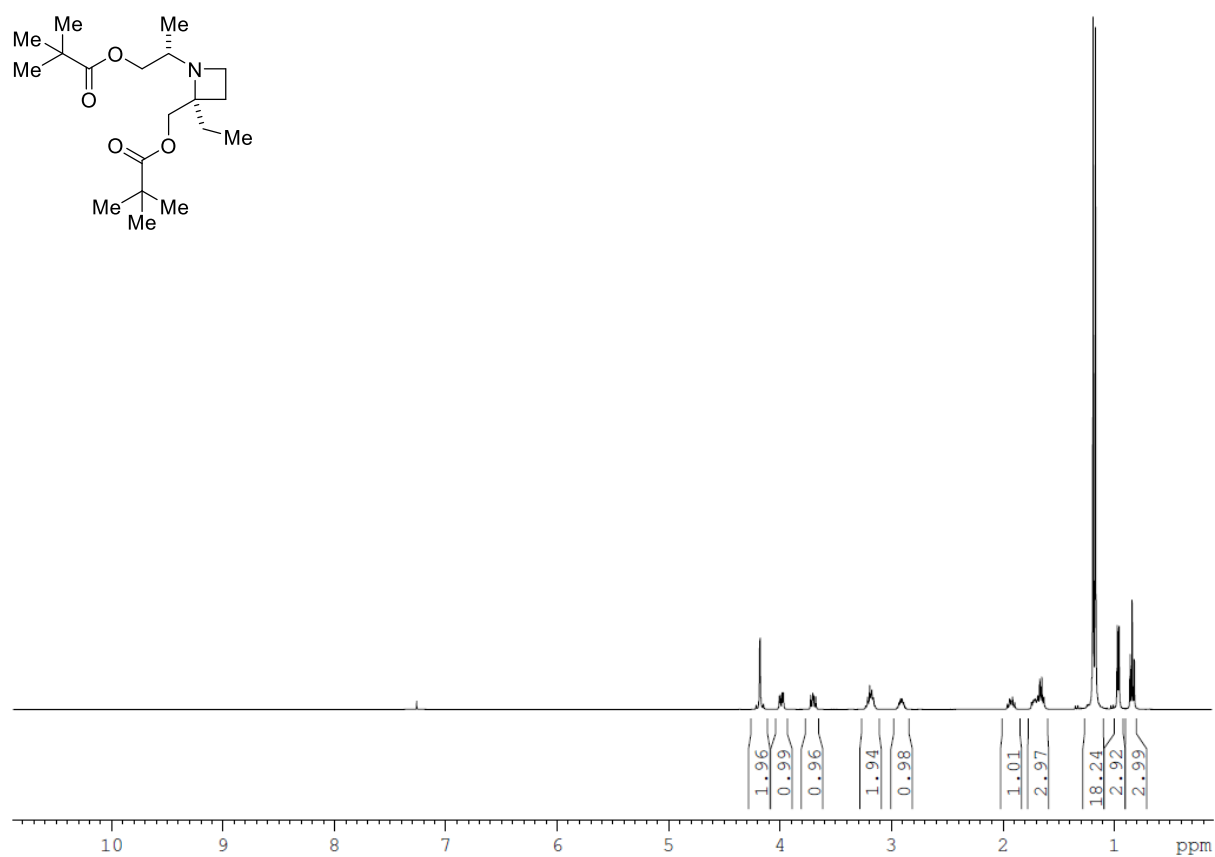


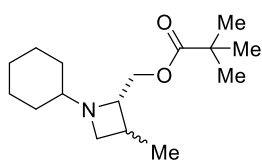
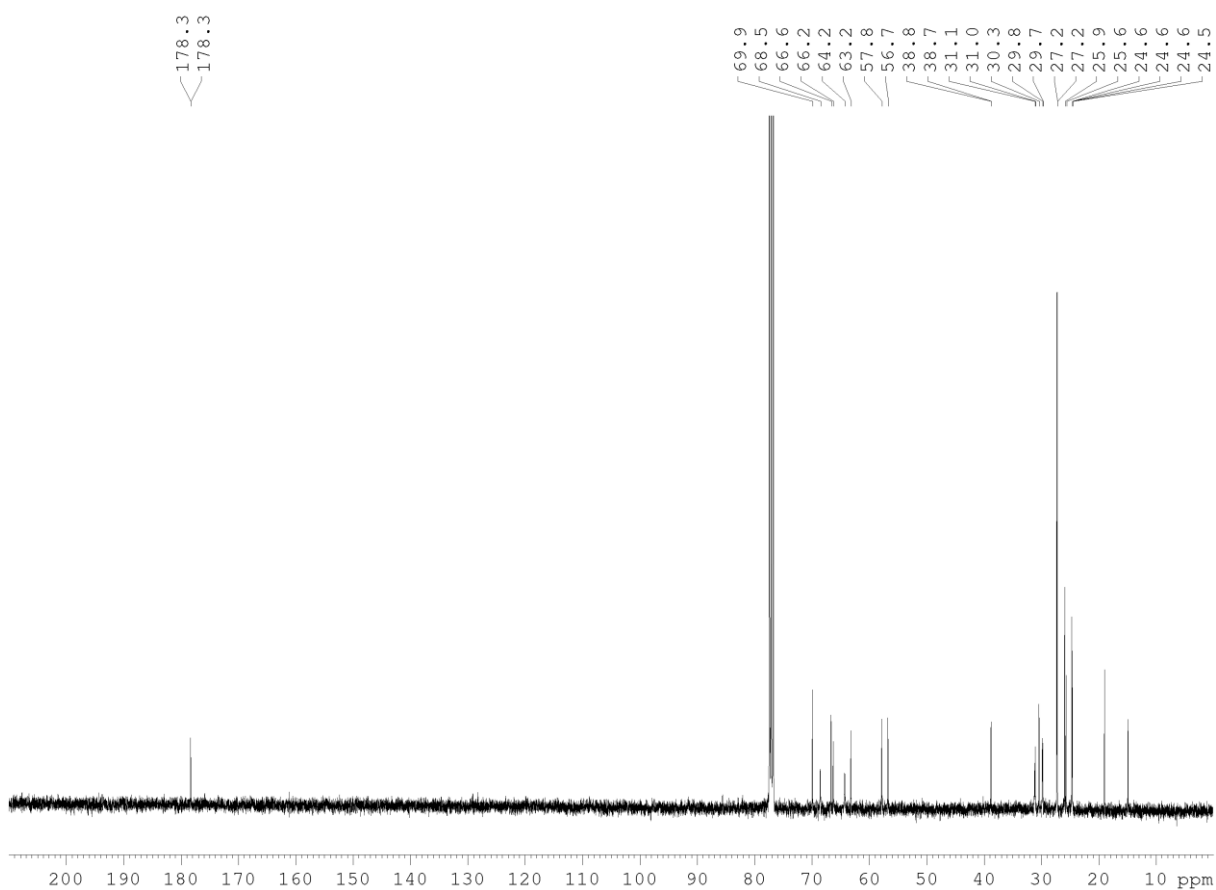
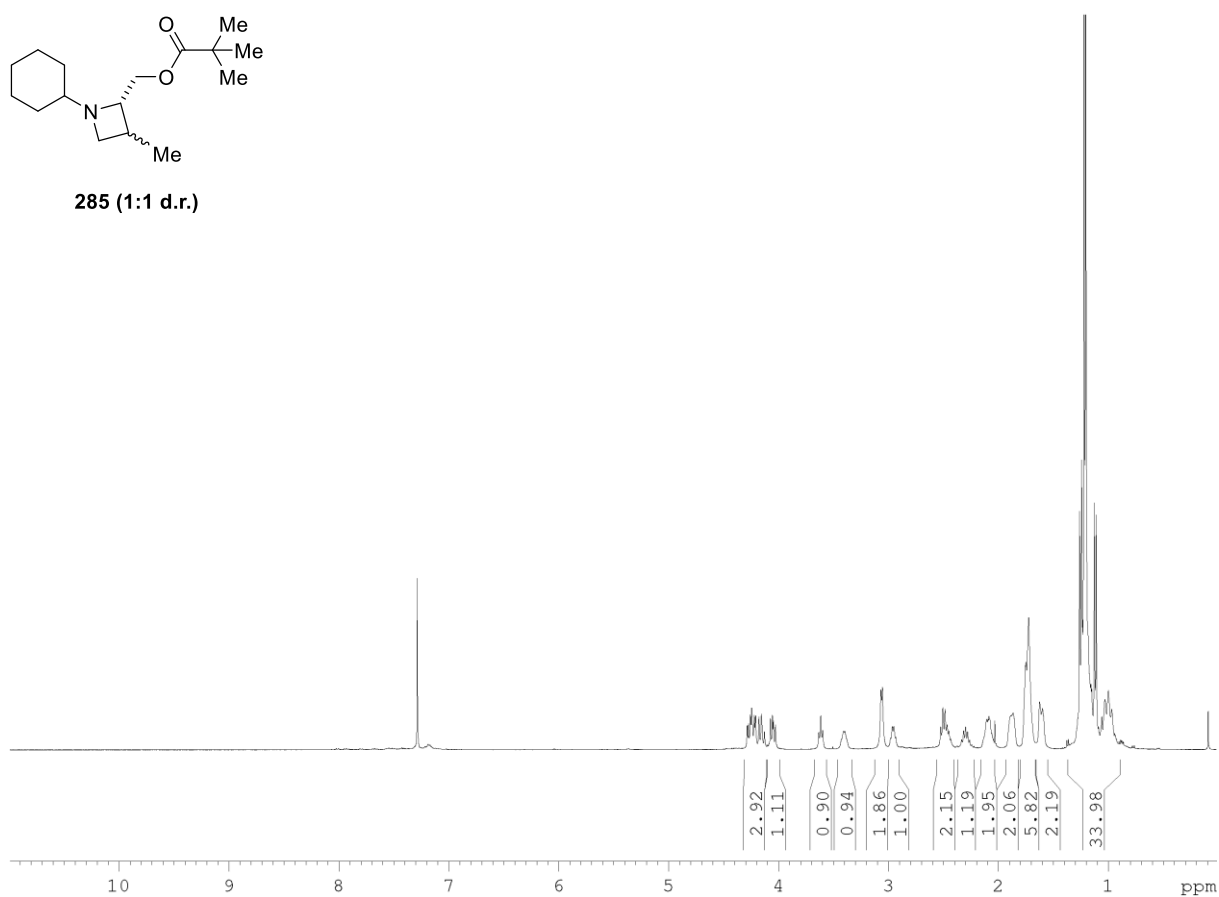


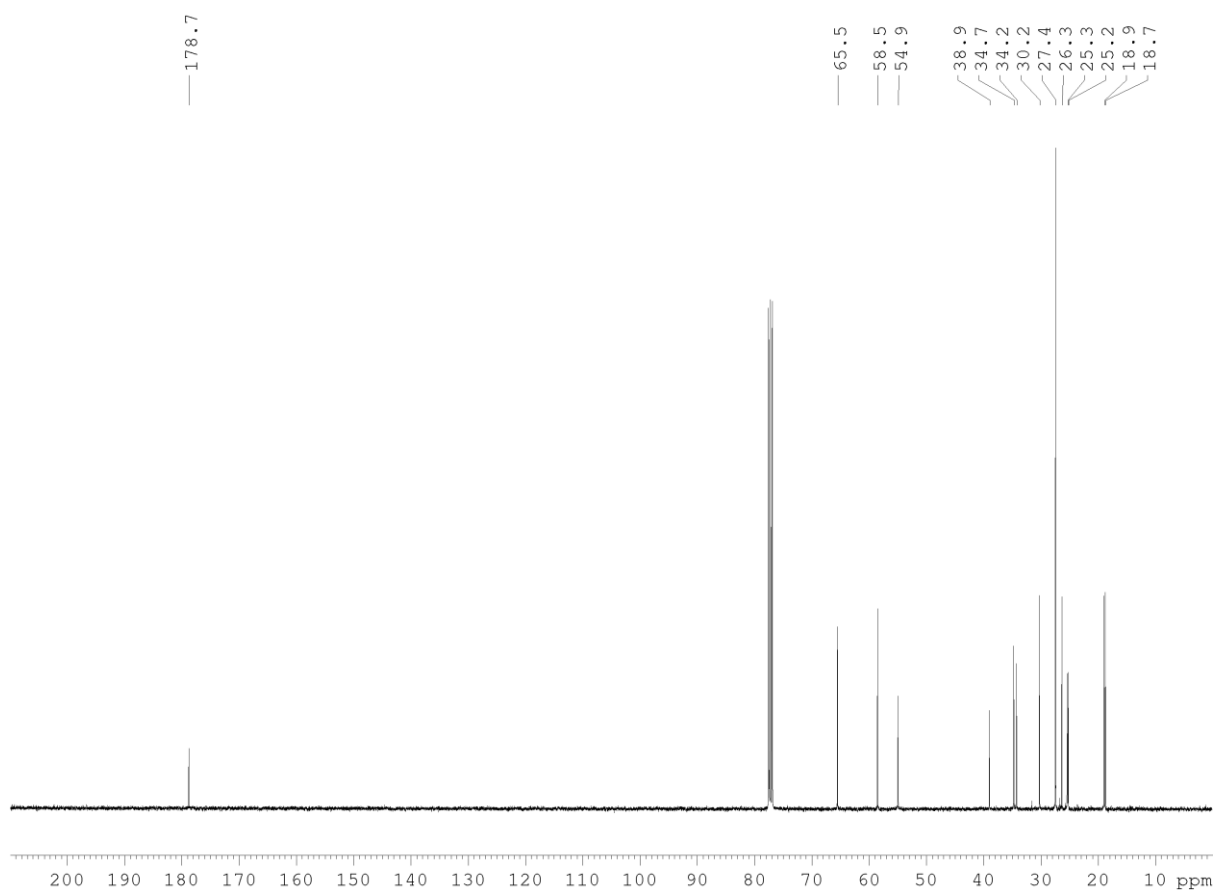
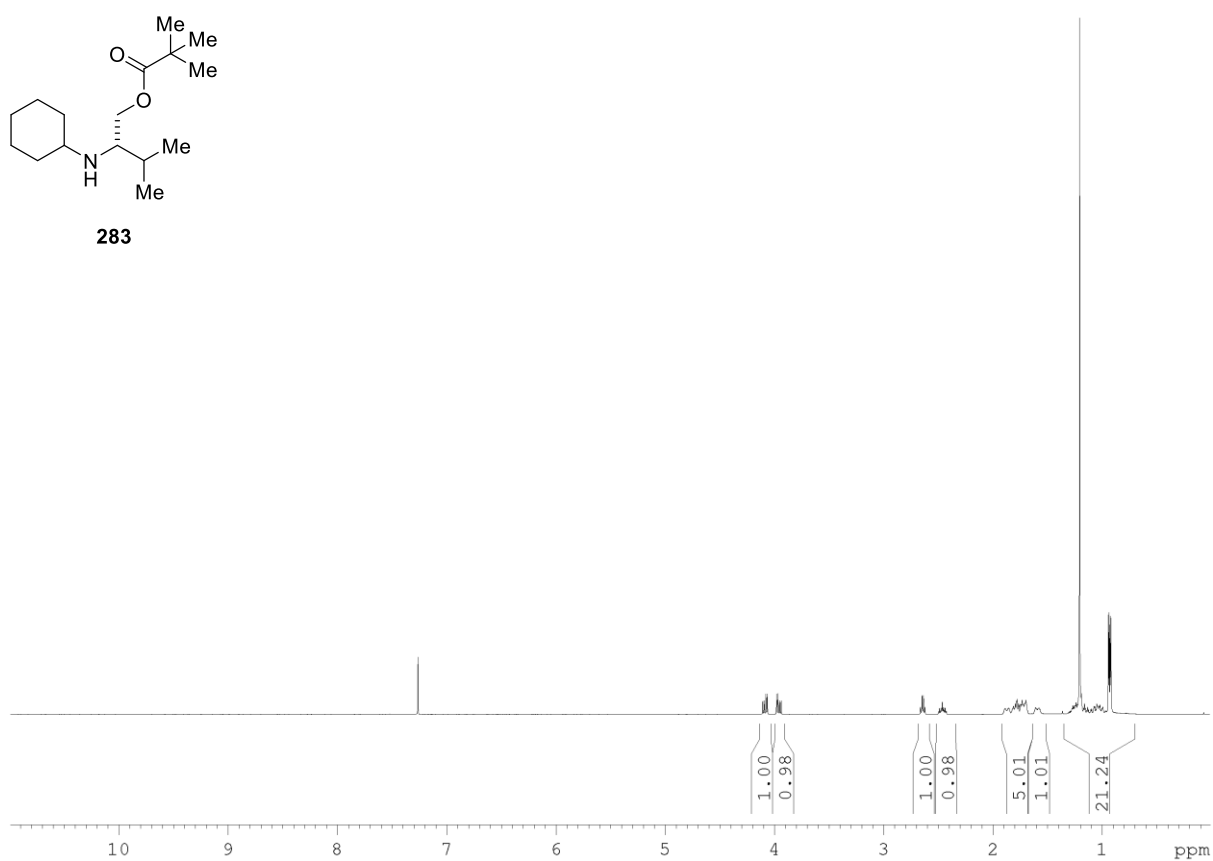


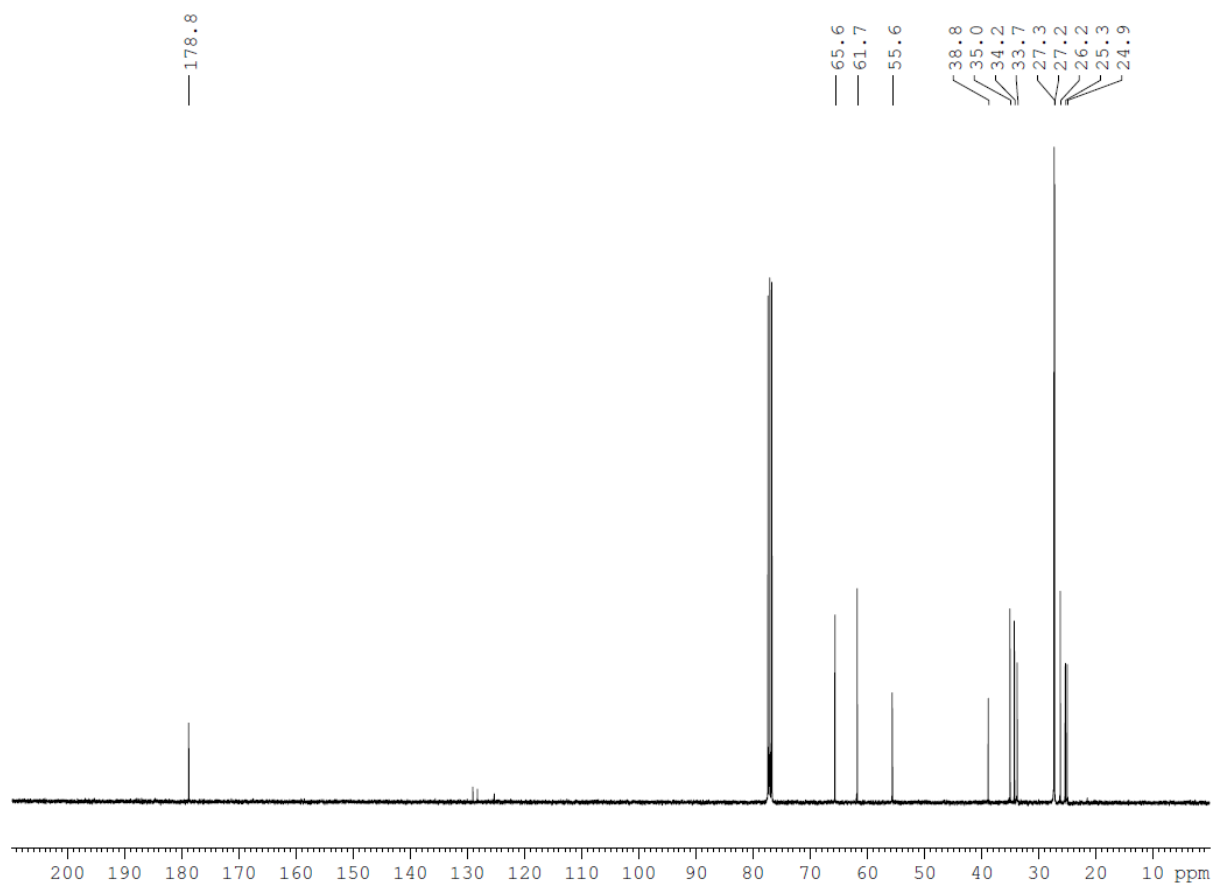
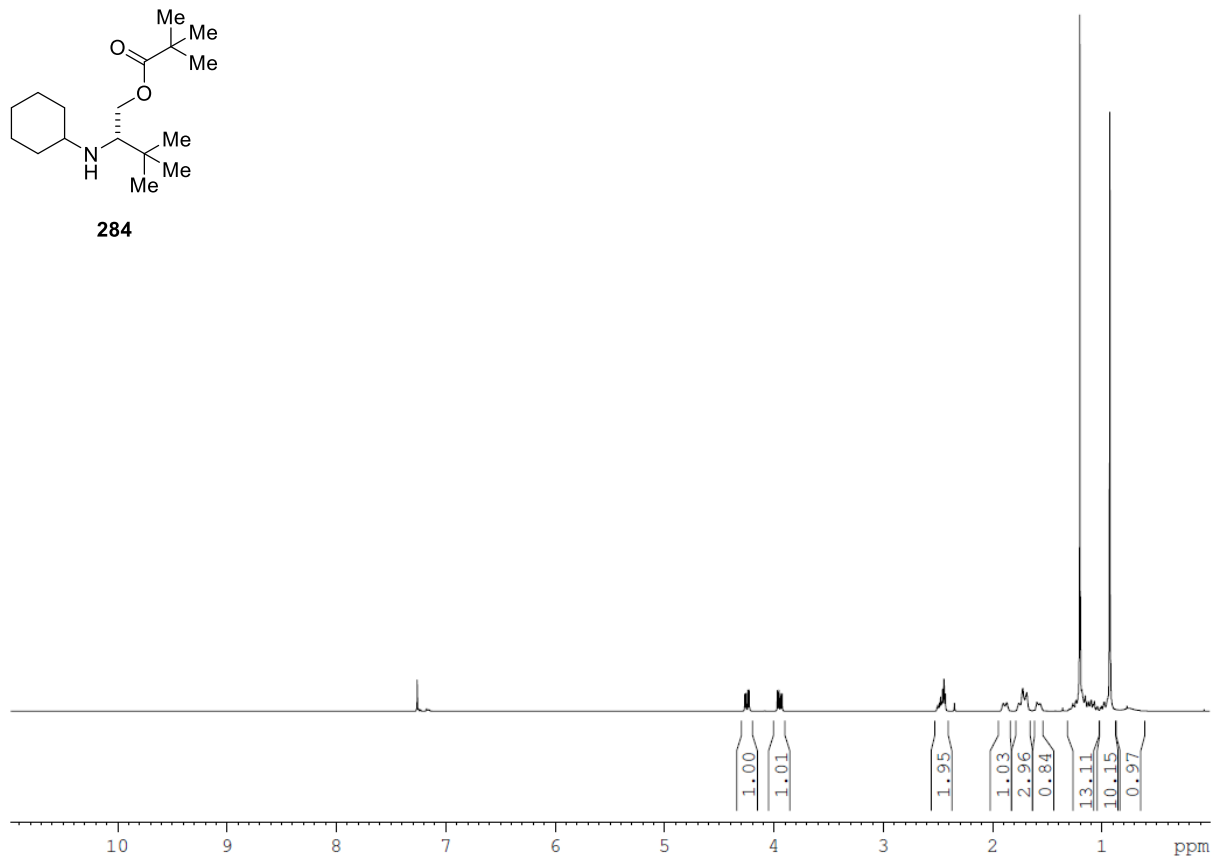
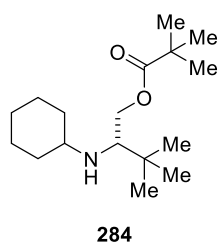
276

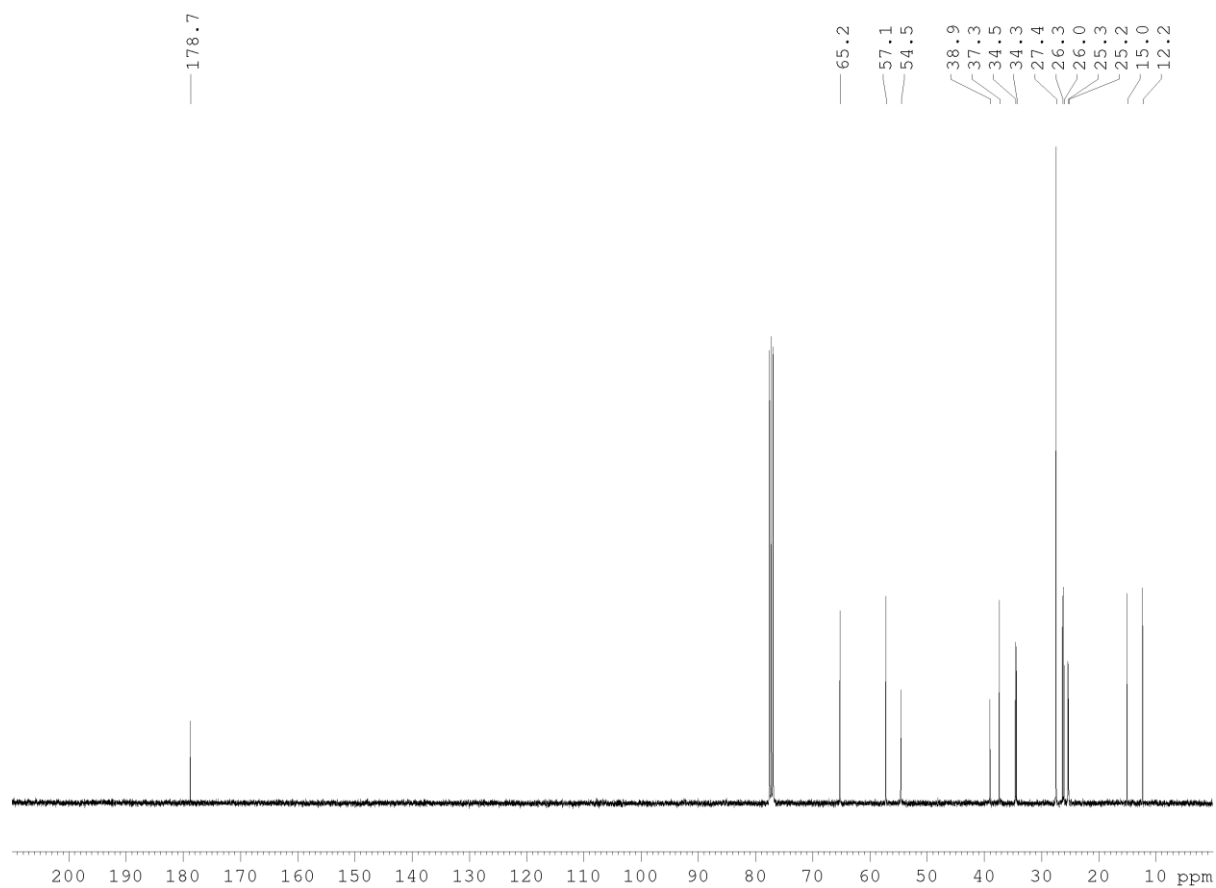
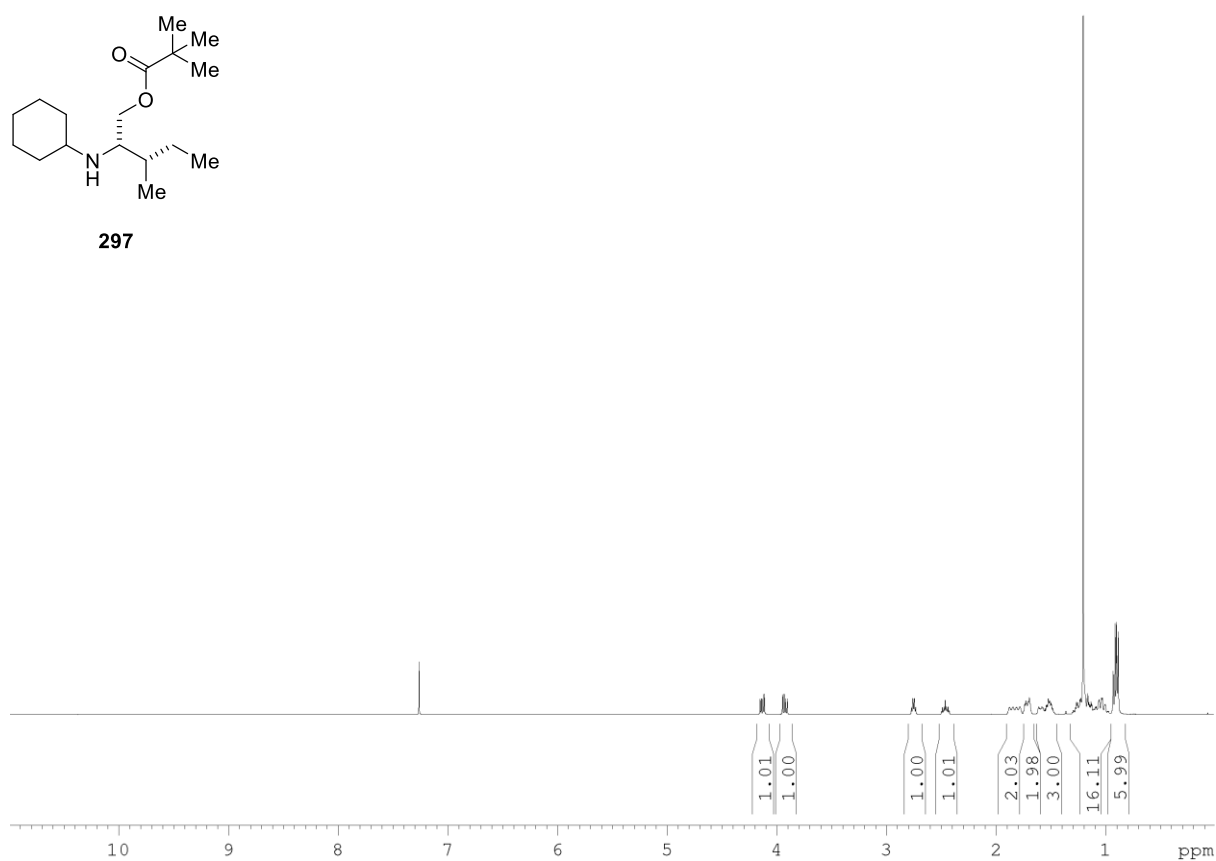
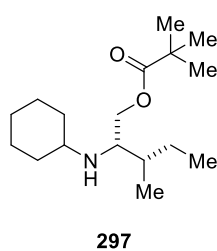


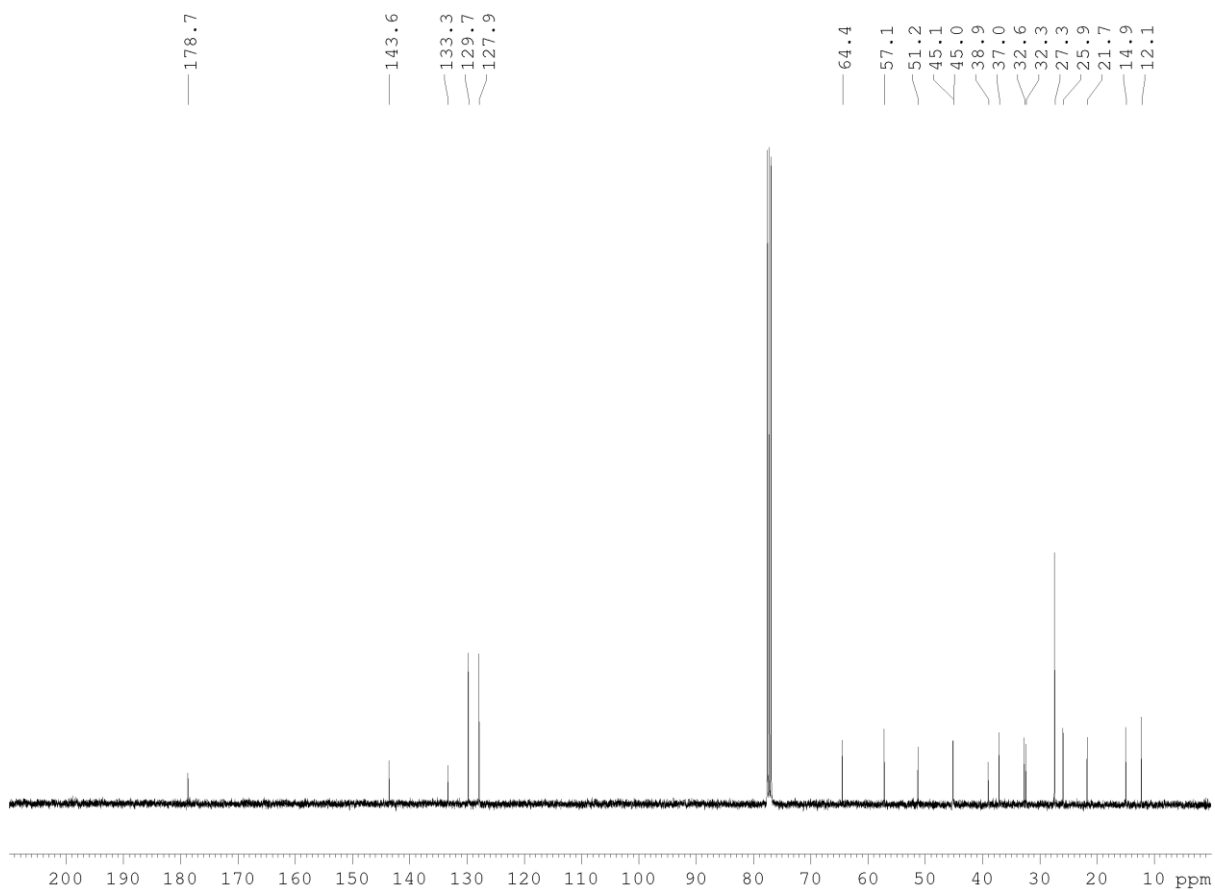
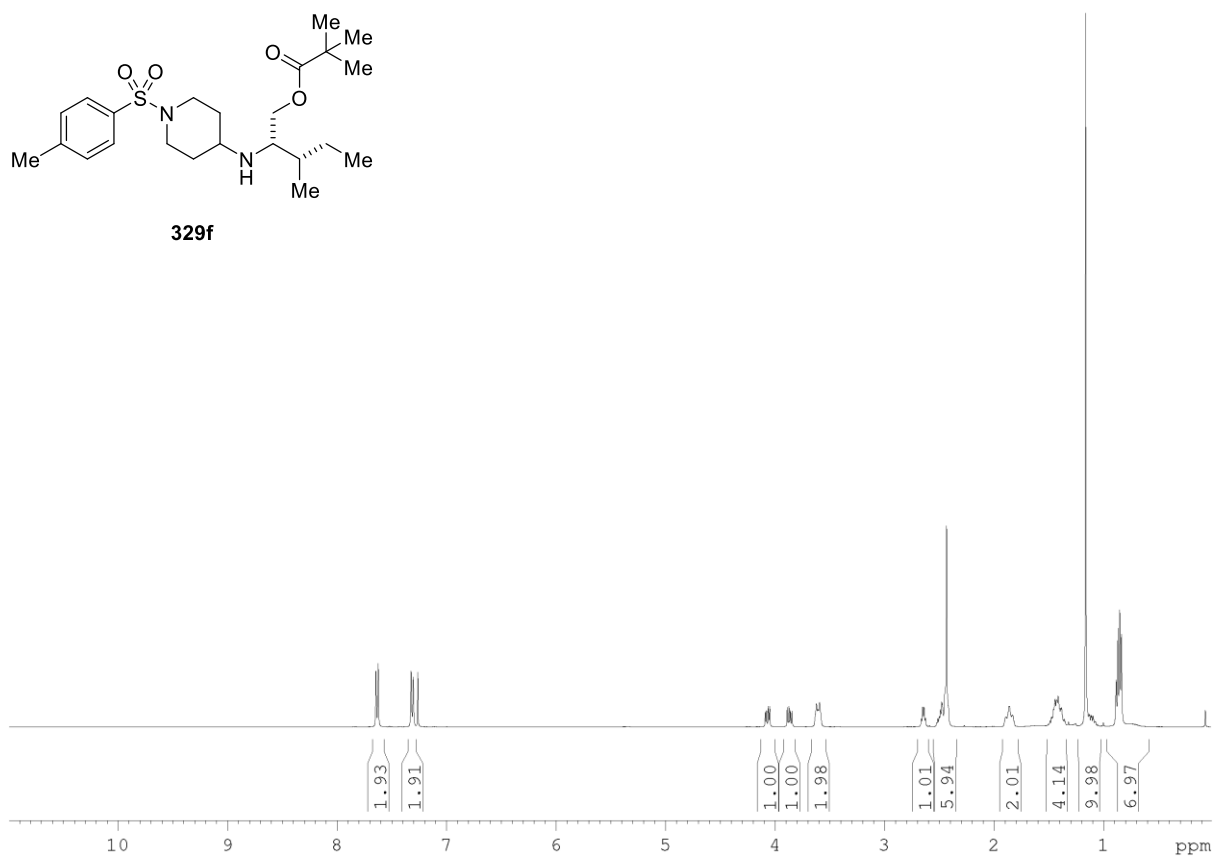
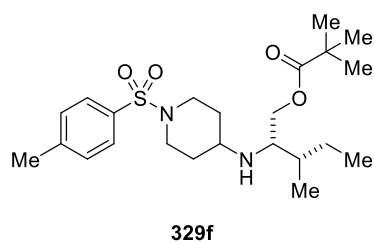


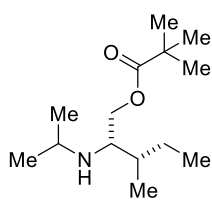
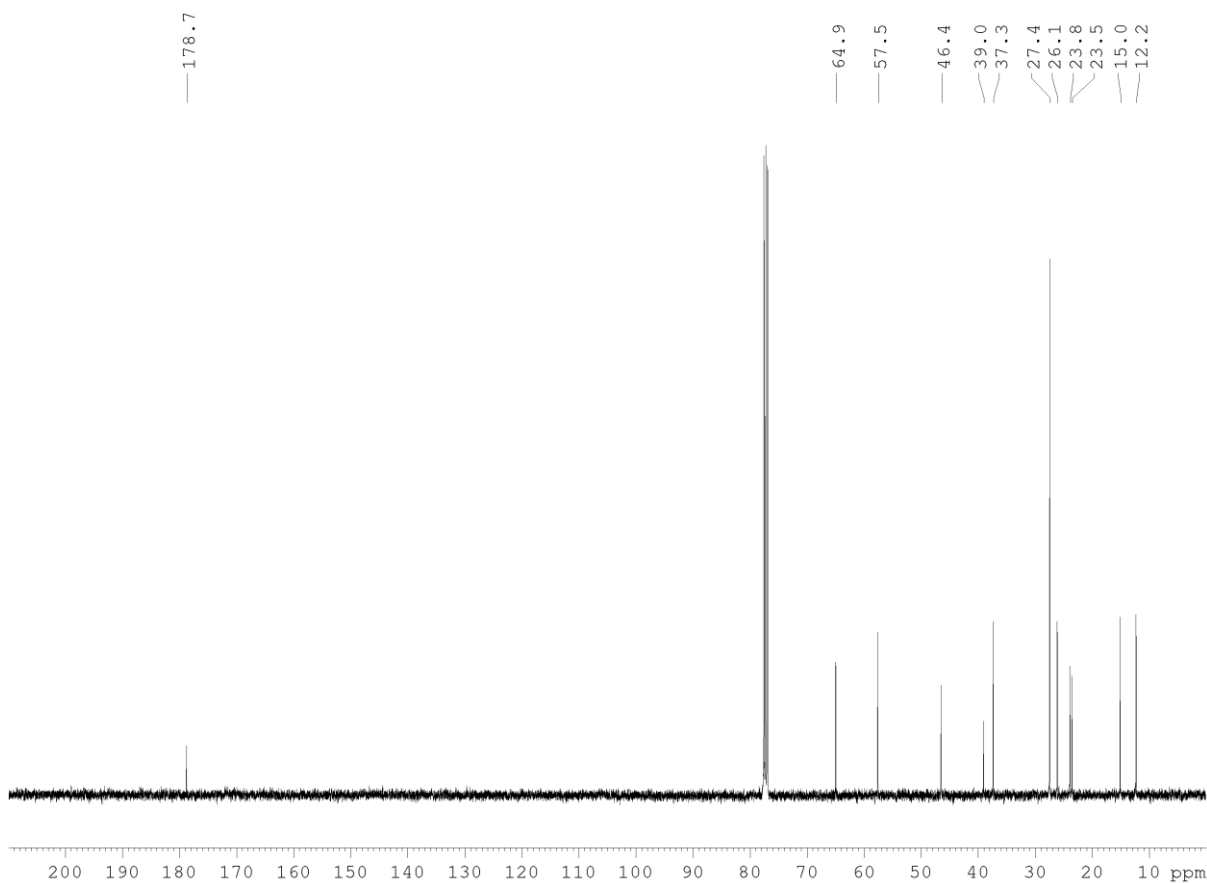
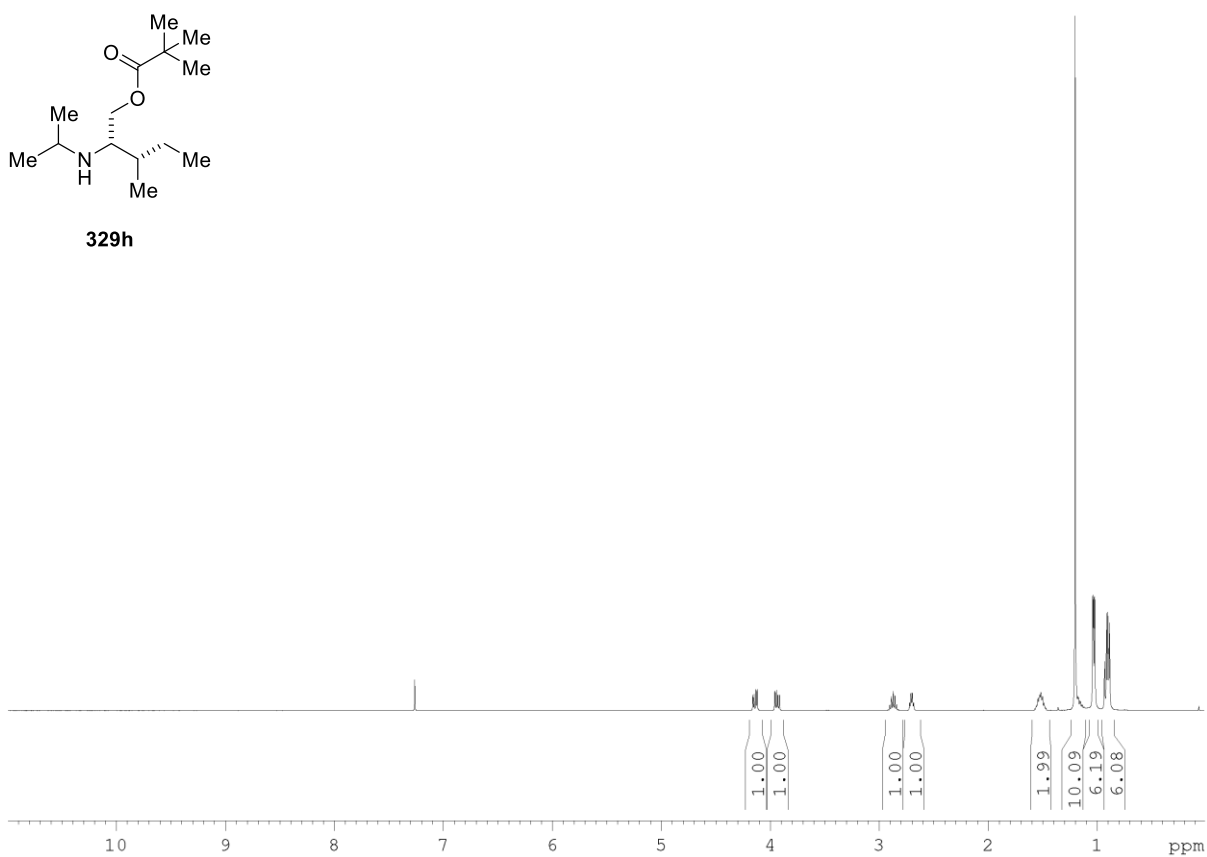
**285 (1:1 d.r.)**

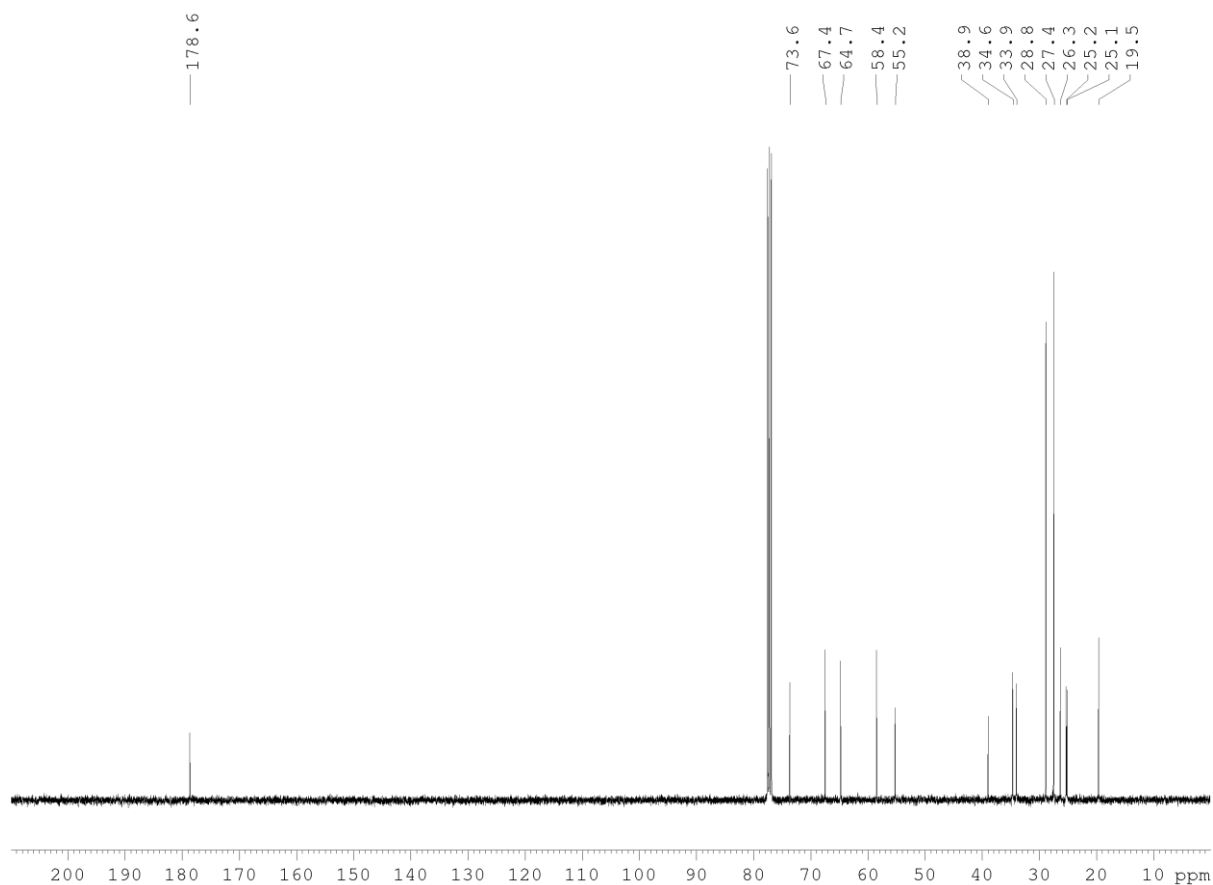
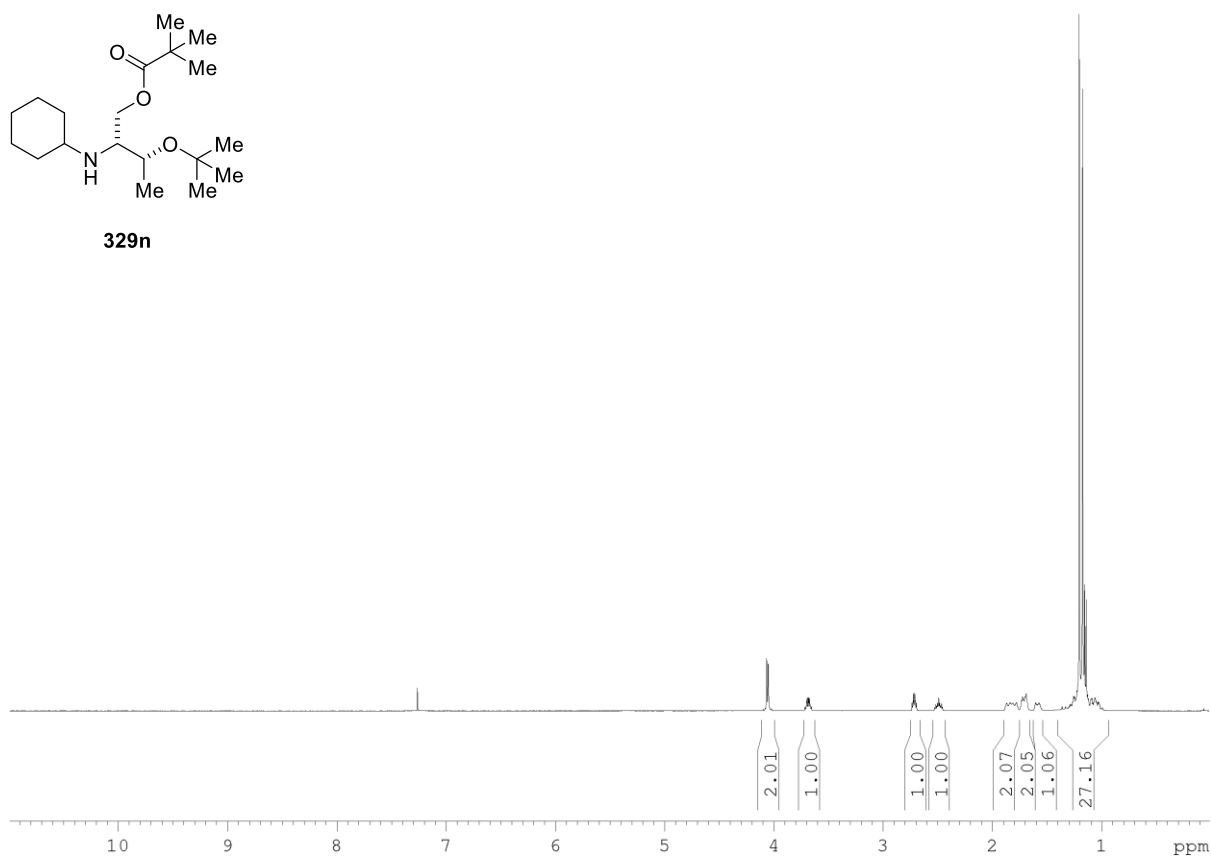
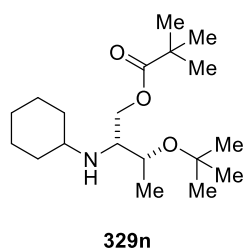


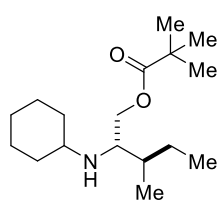




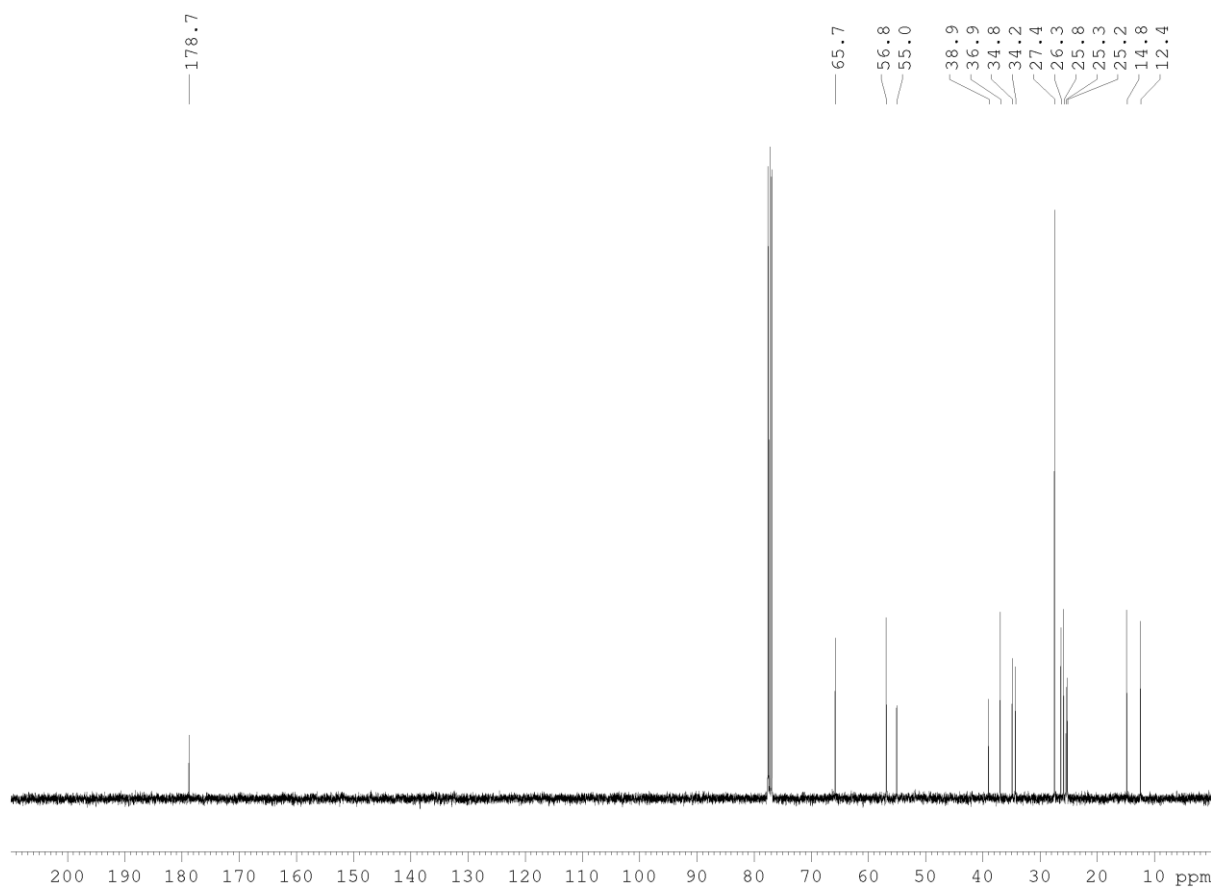
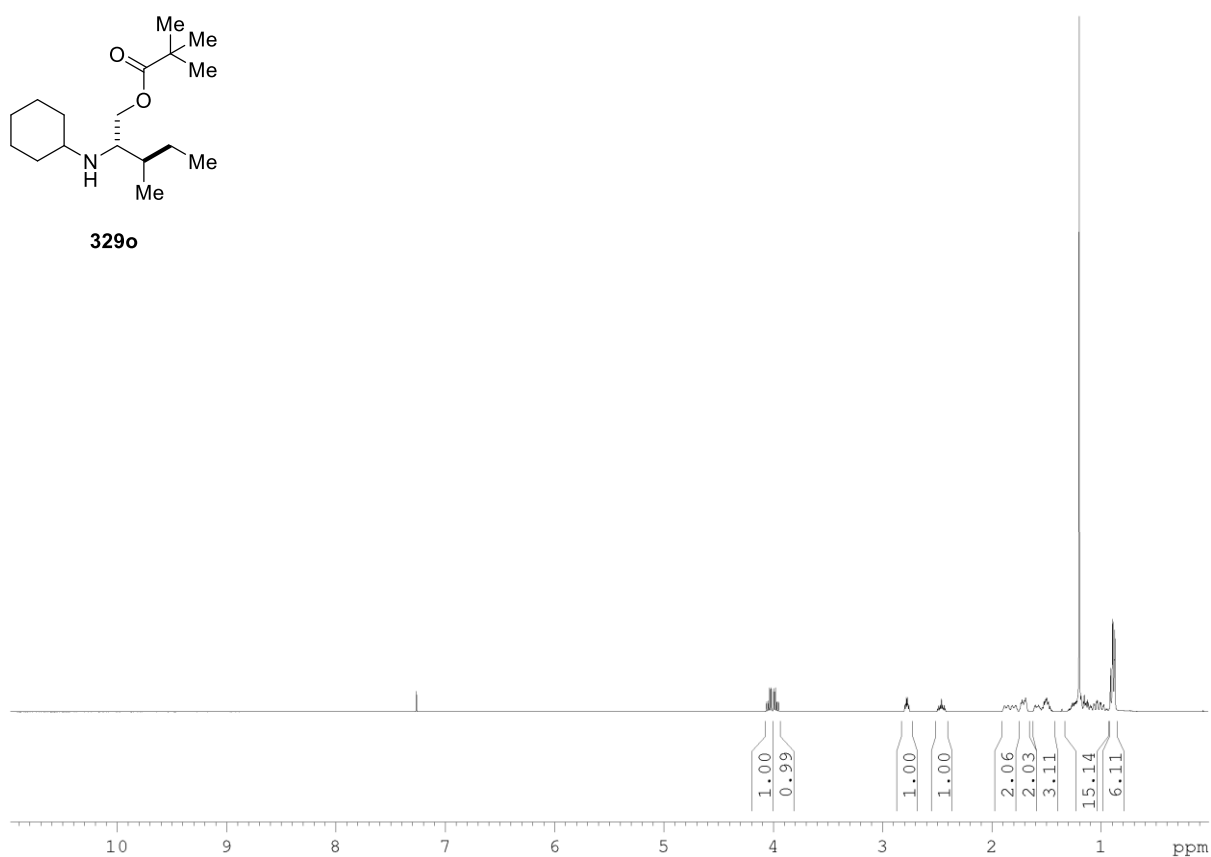


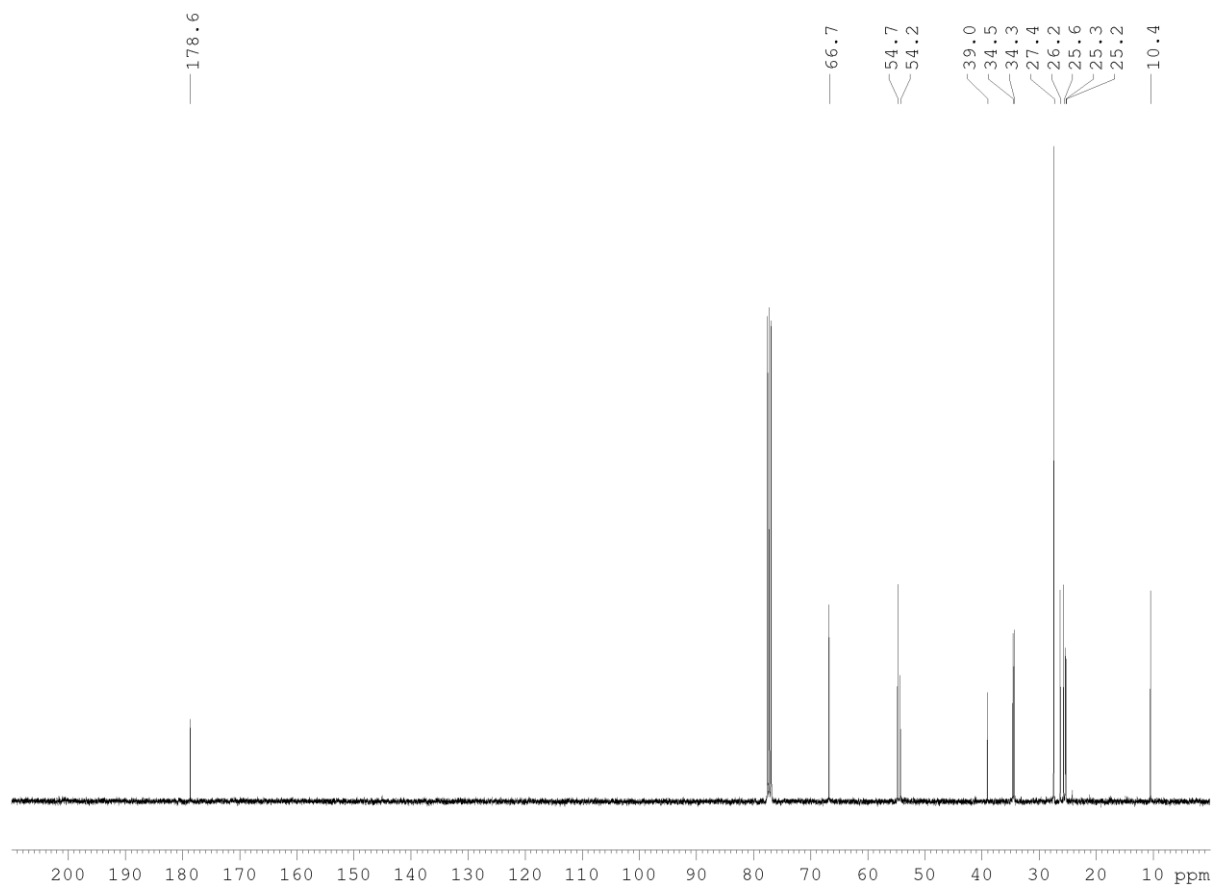
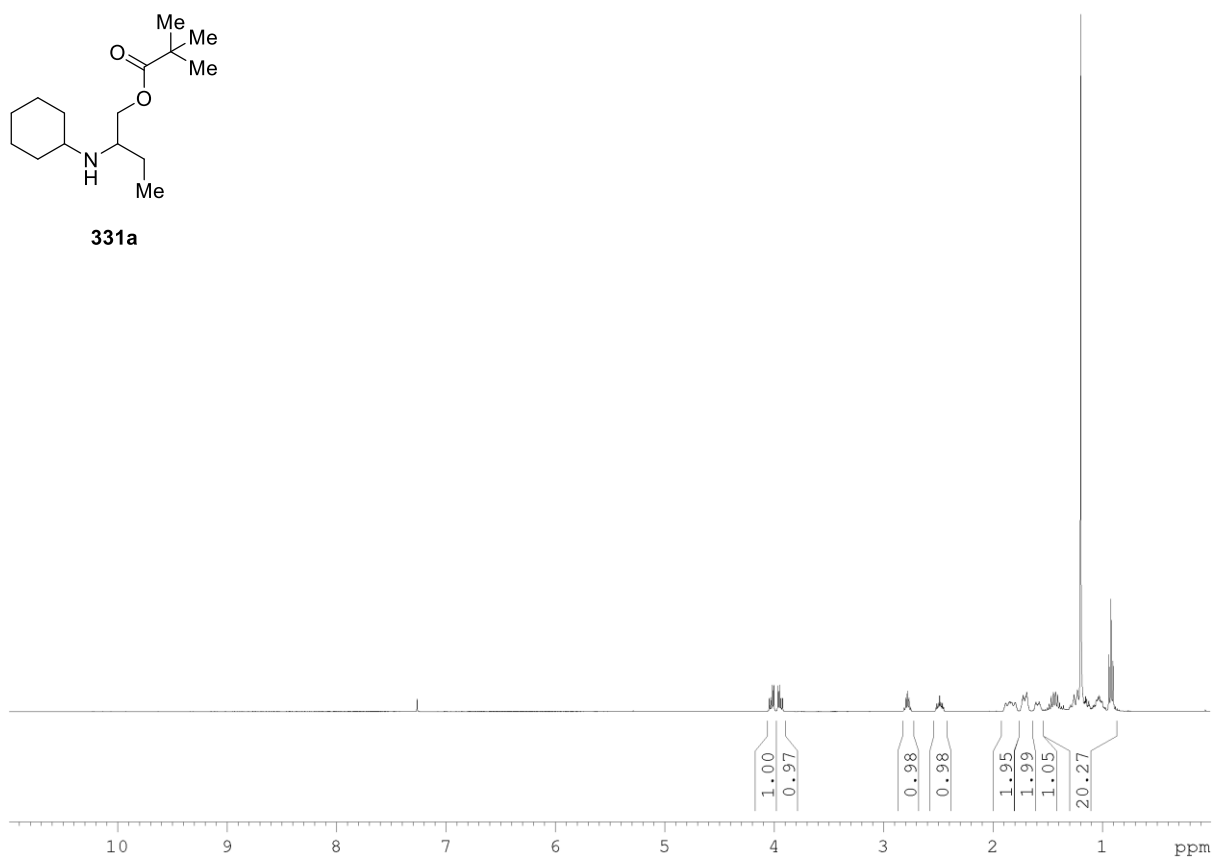
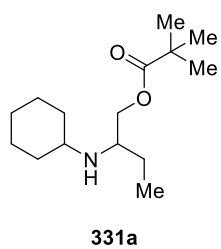
**329h**

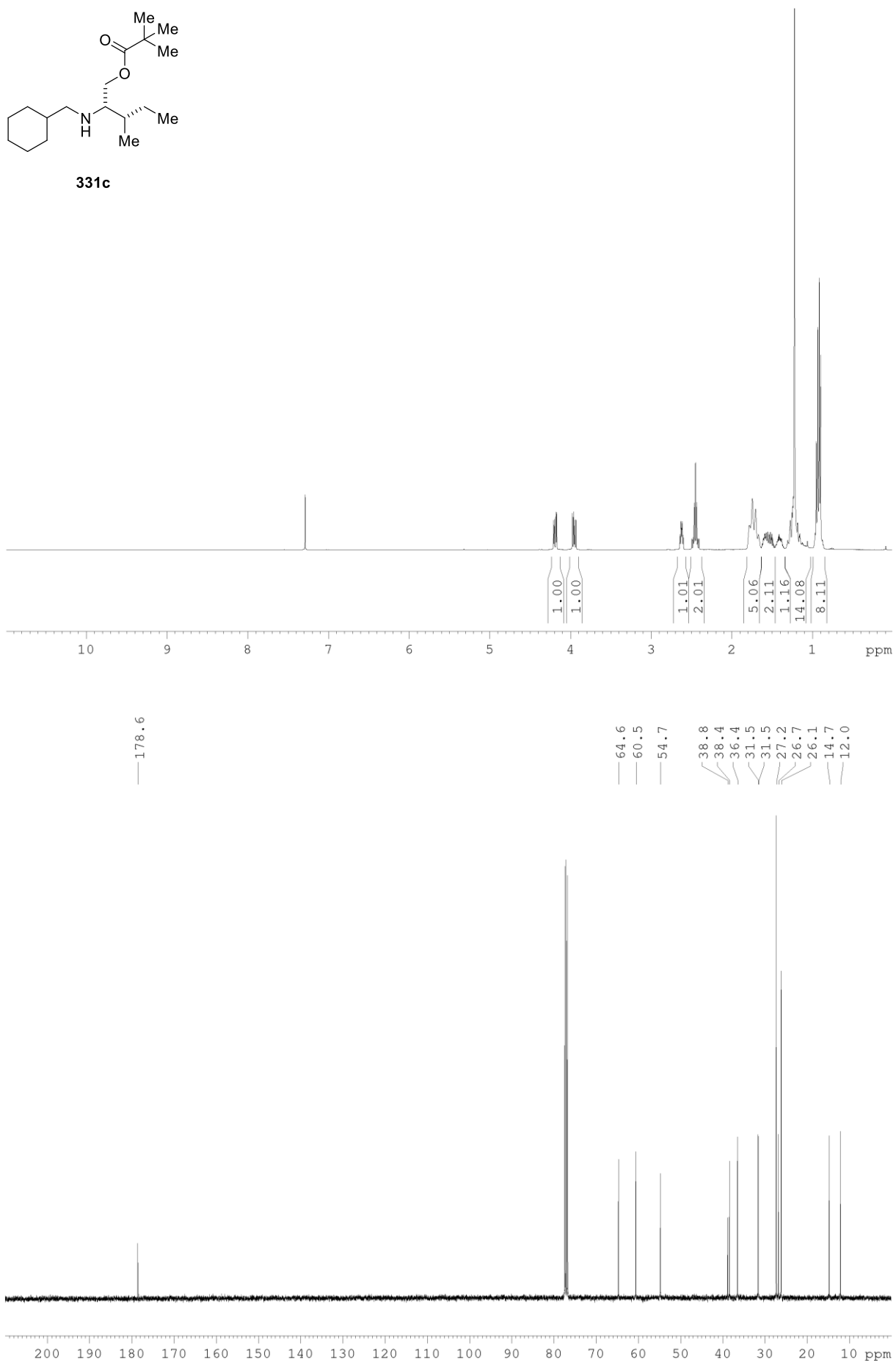


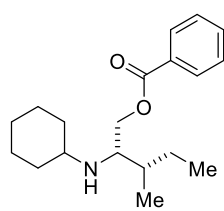
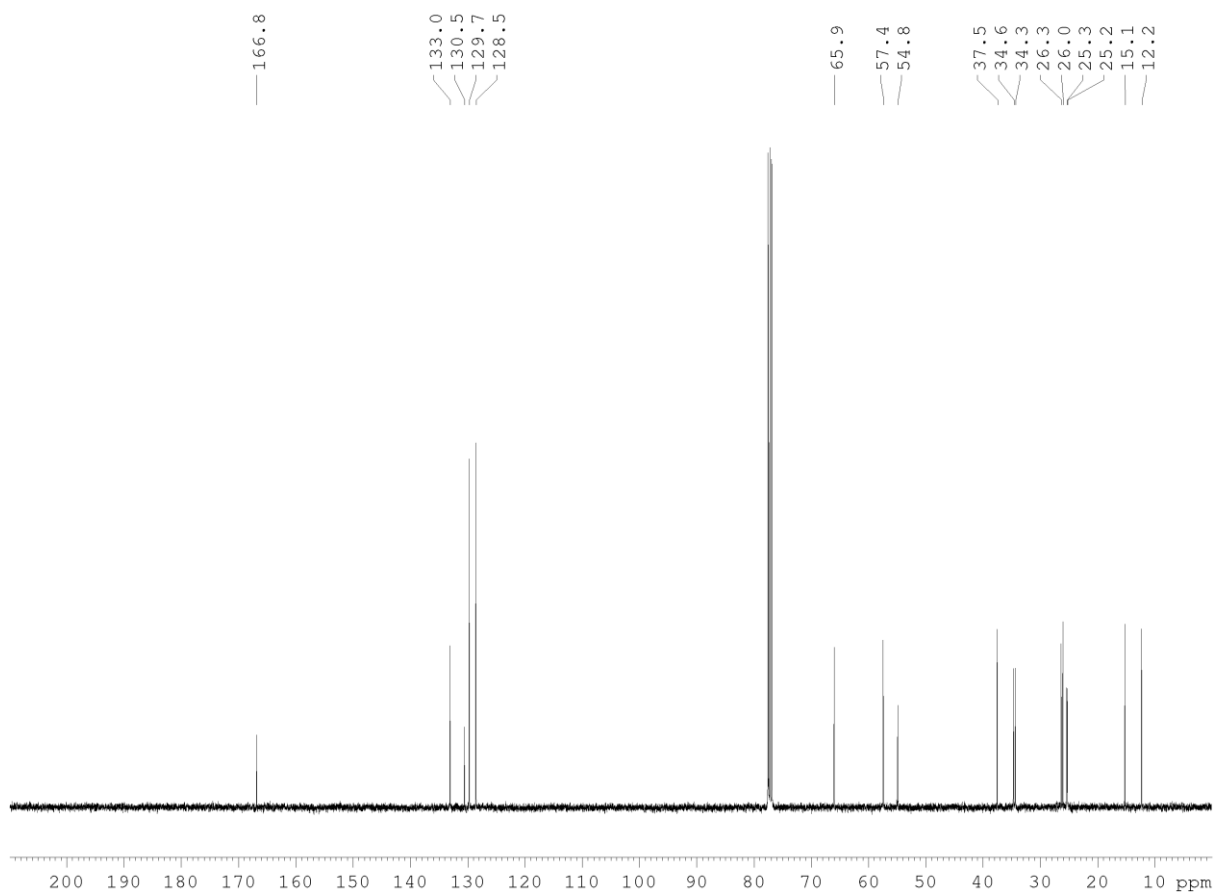
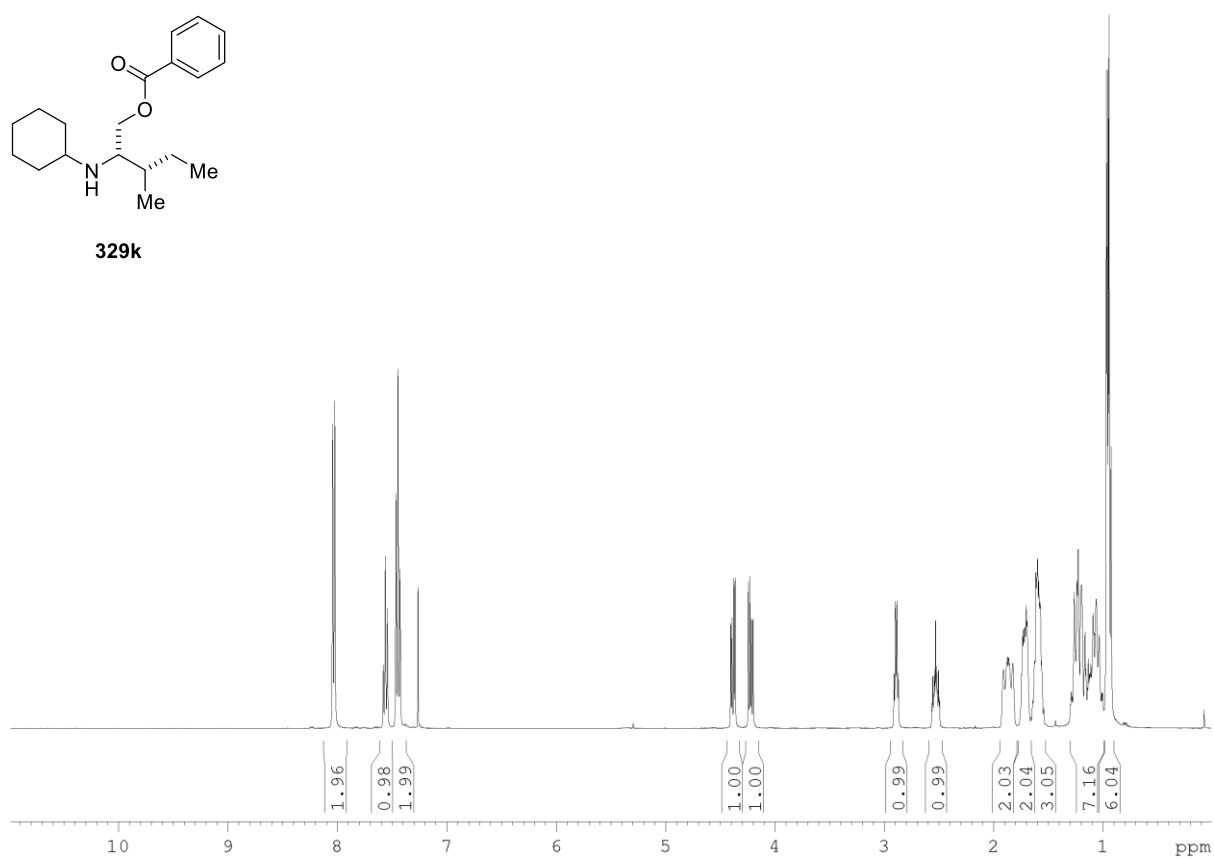


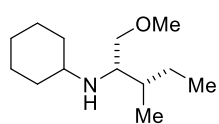
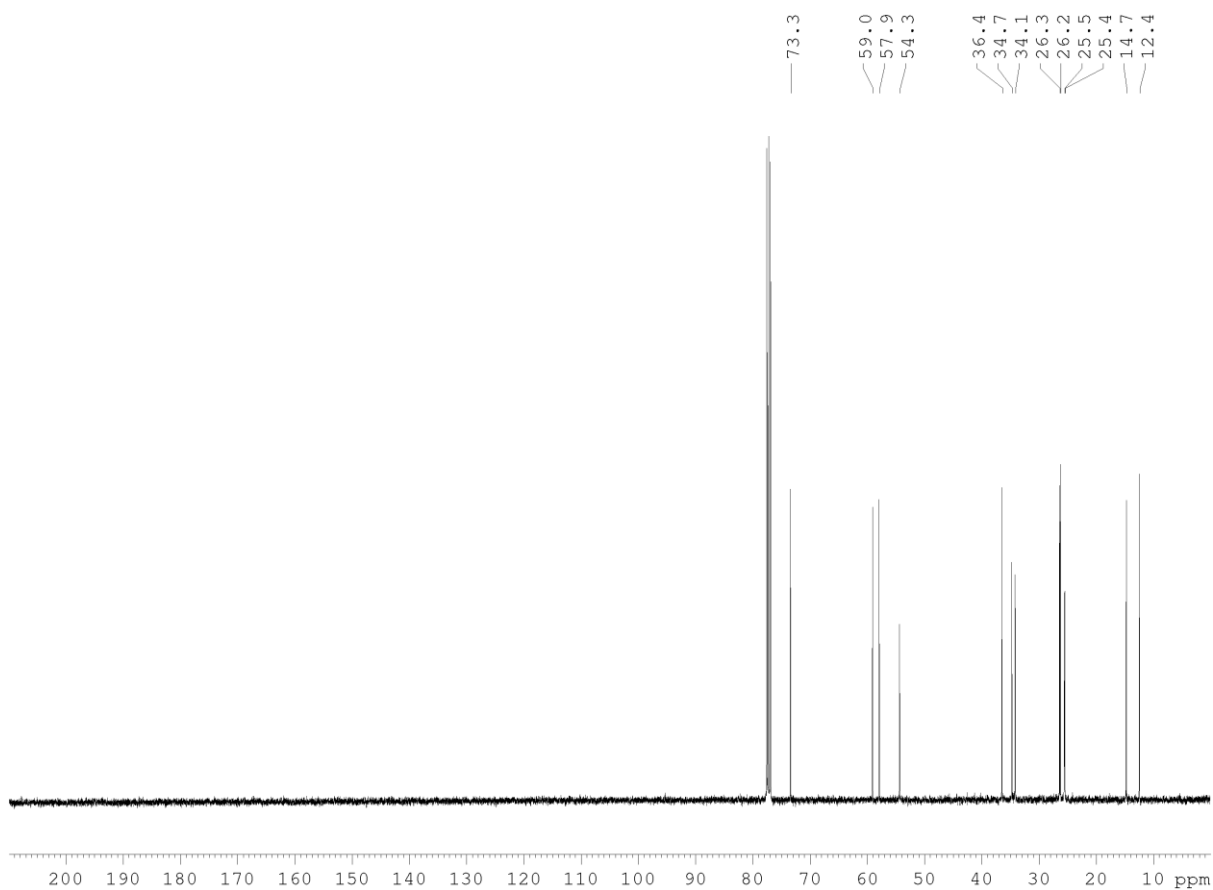
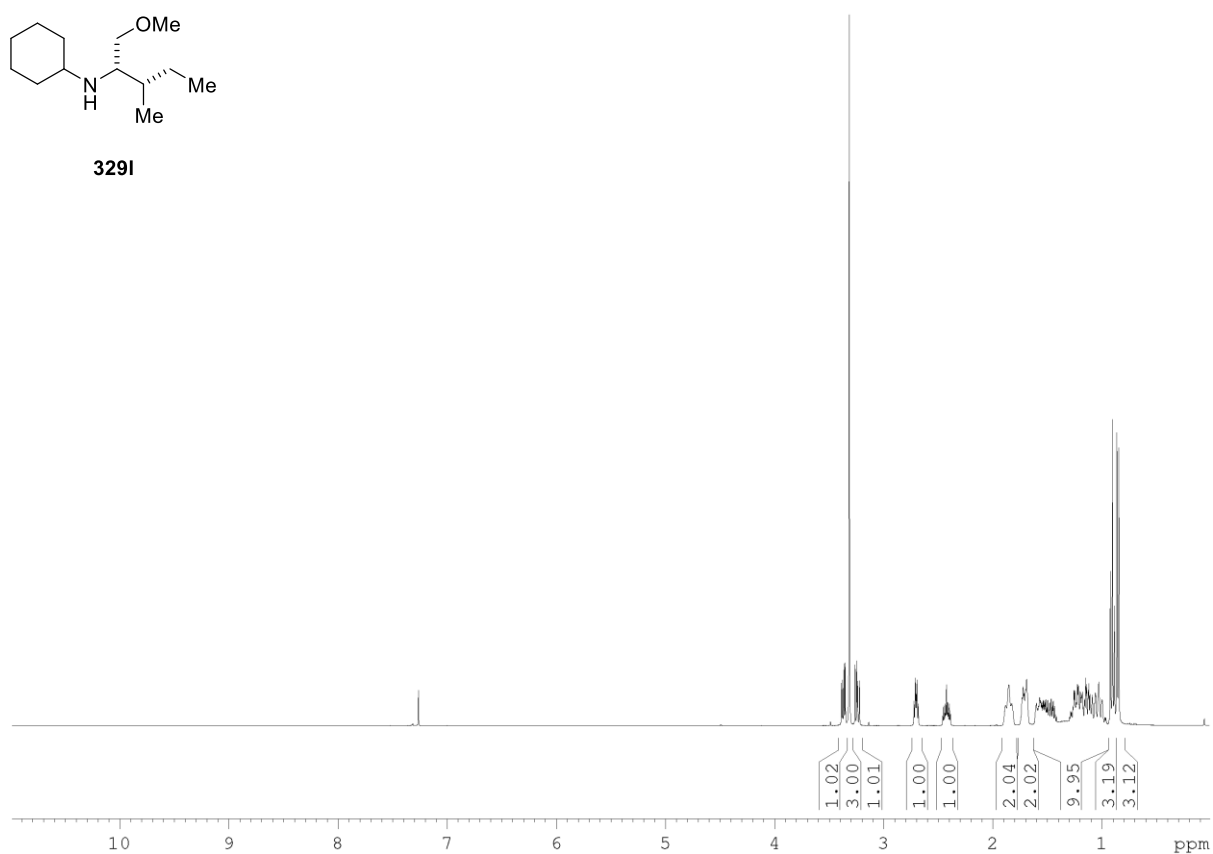
329o

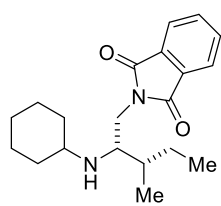
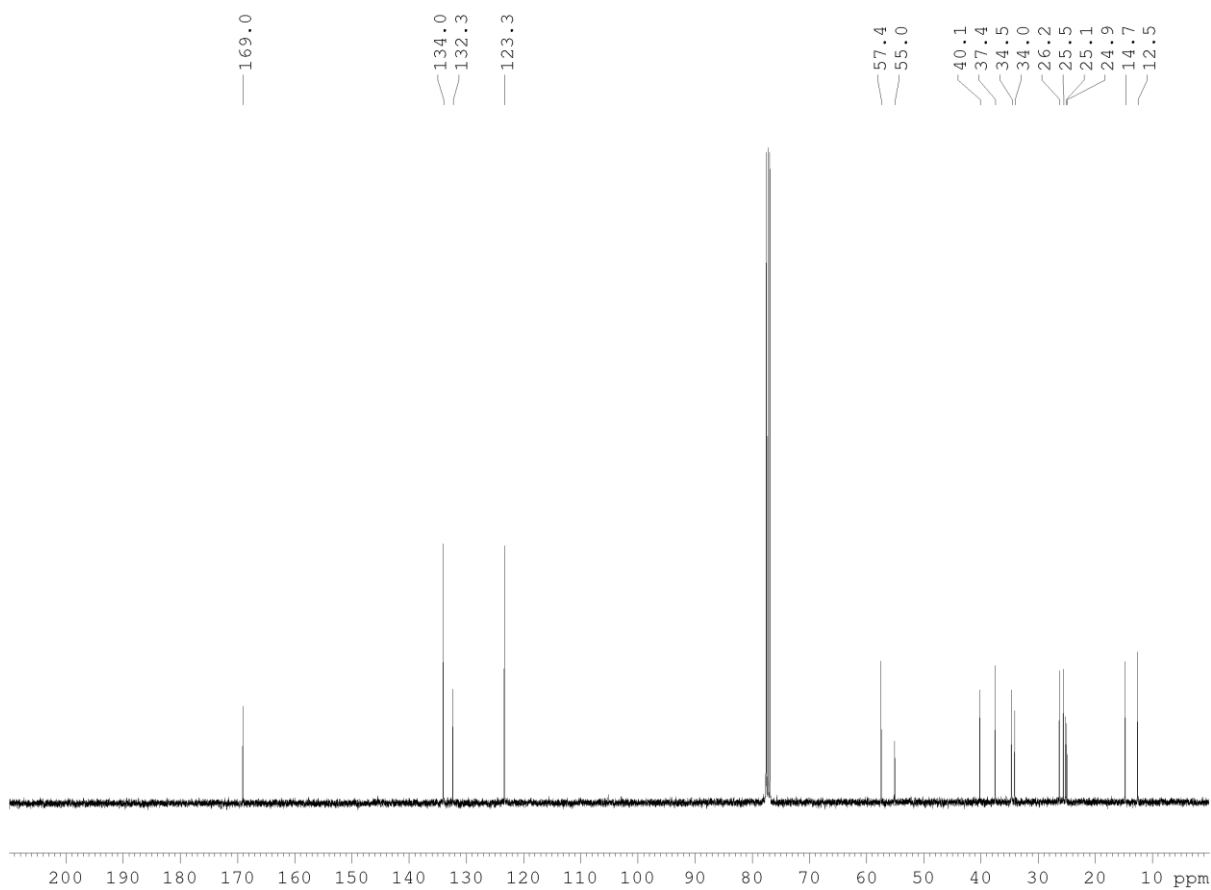
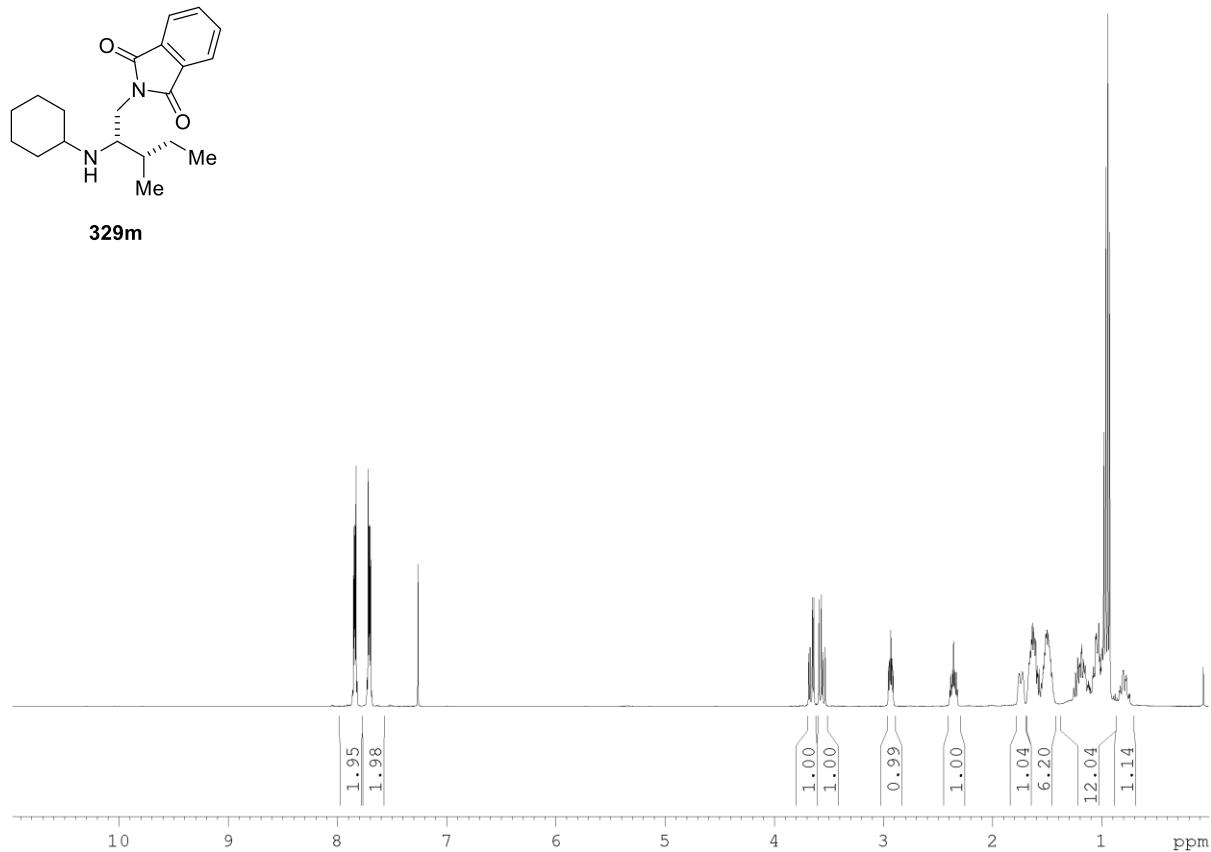


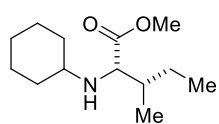
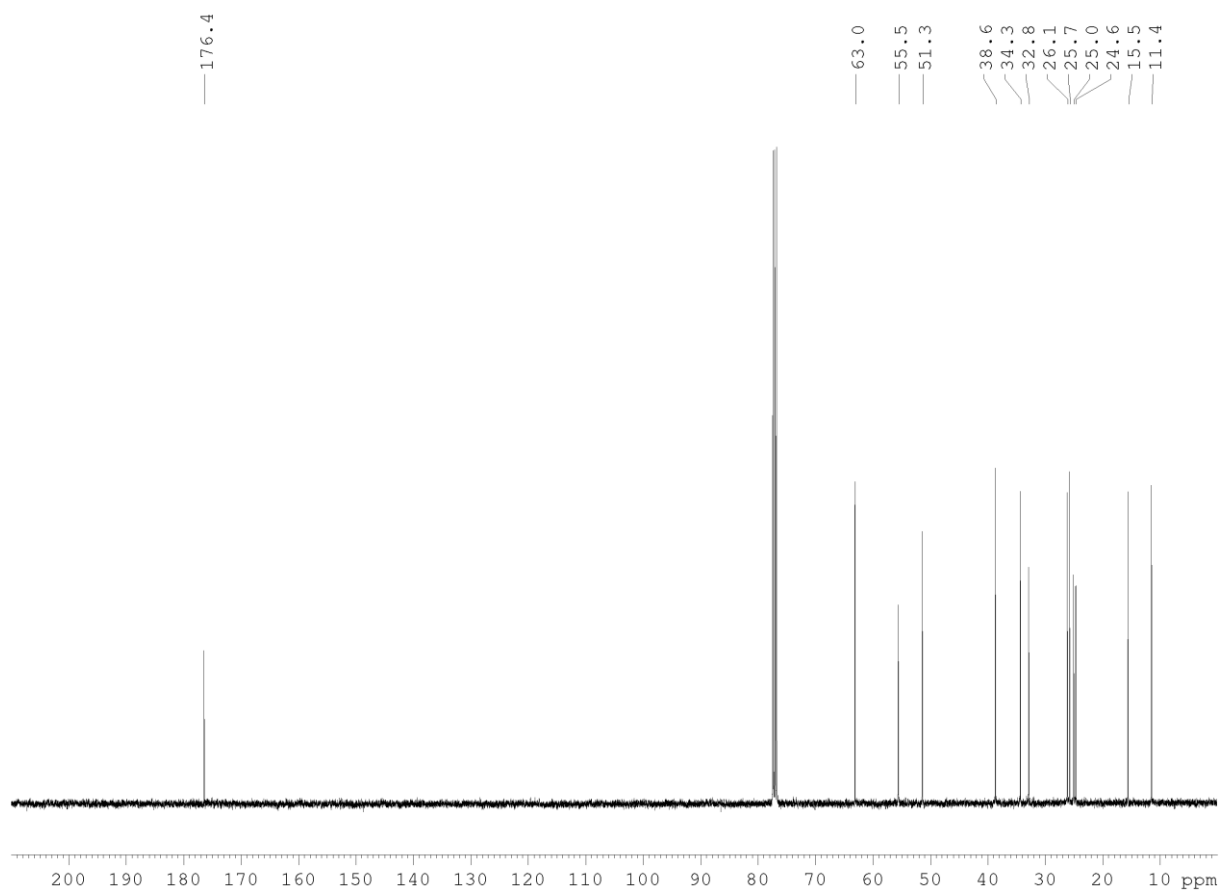
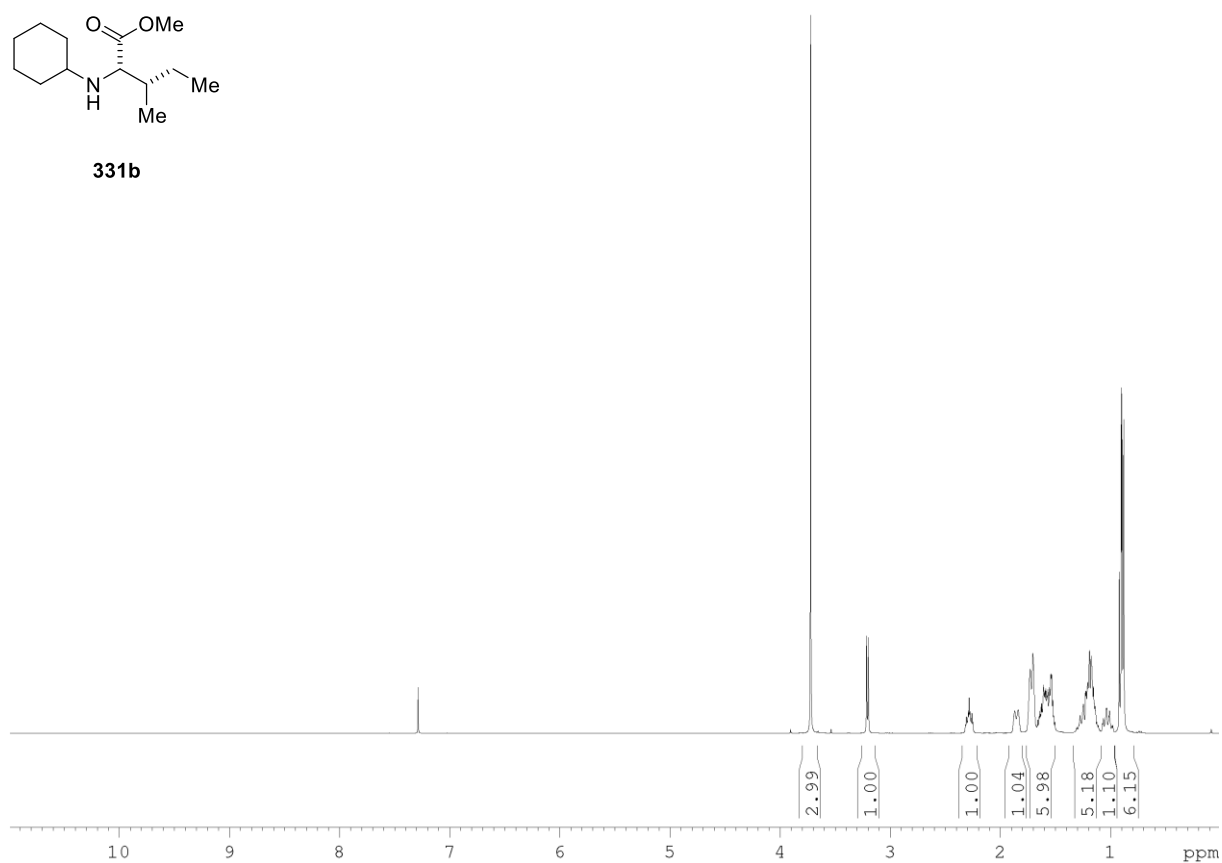


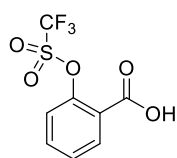


**329k**

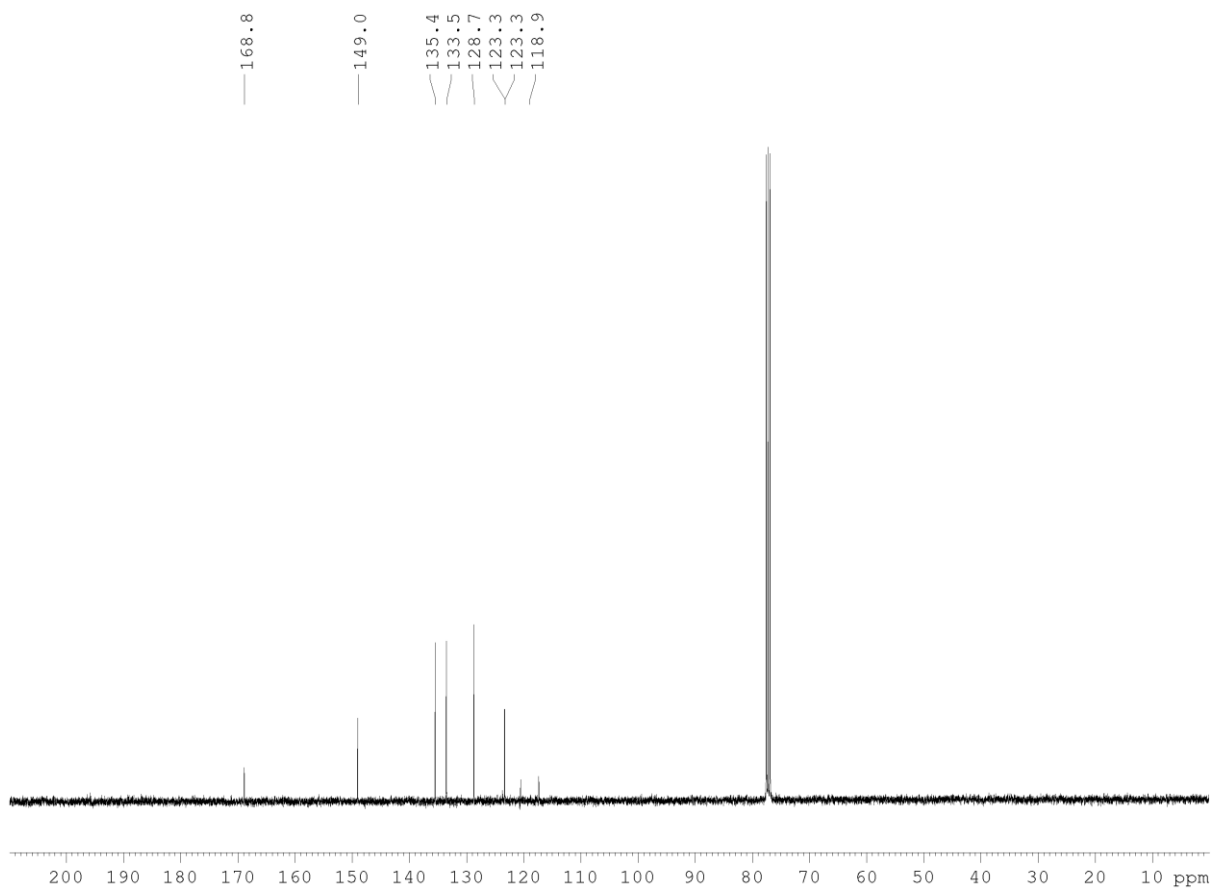
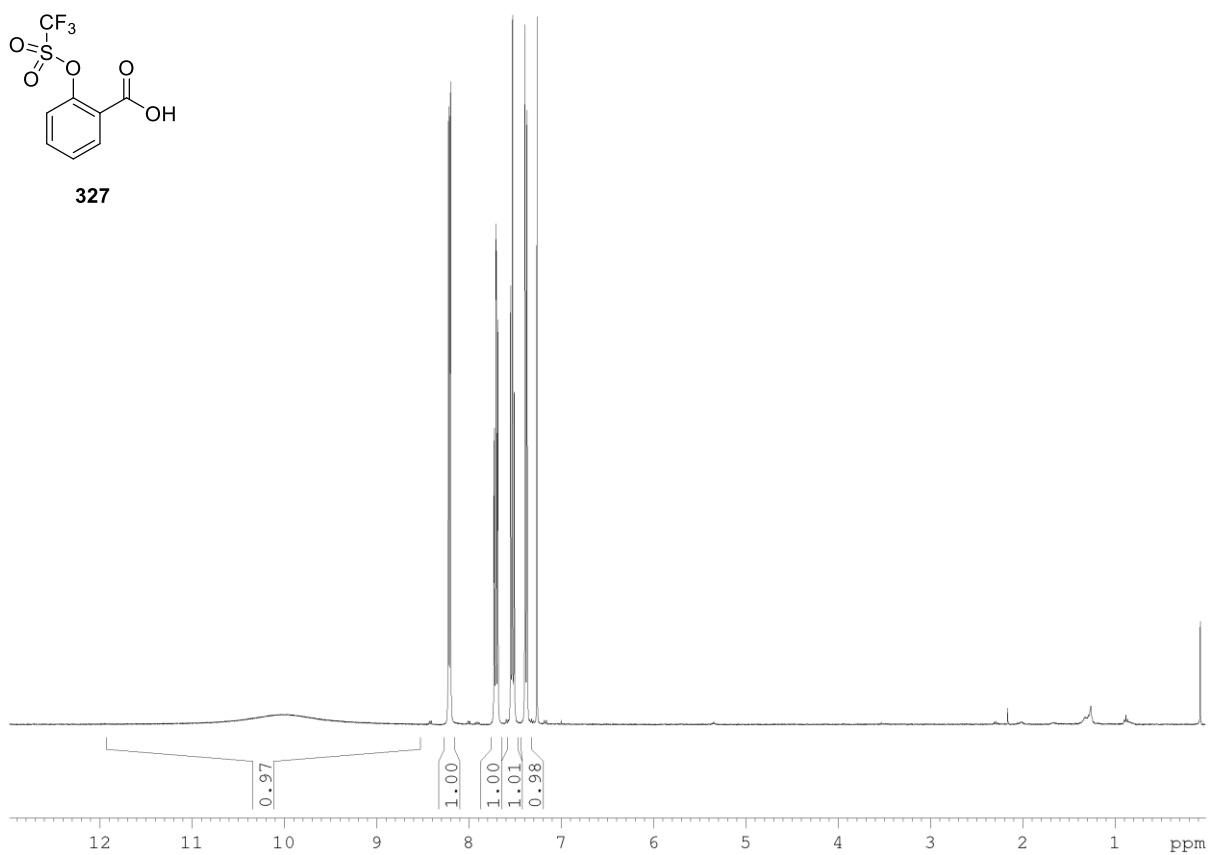
**329I**

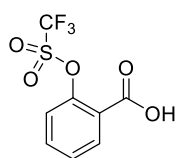
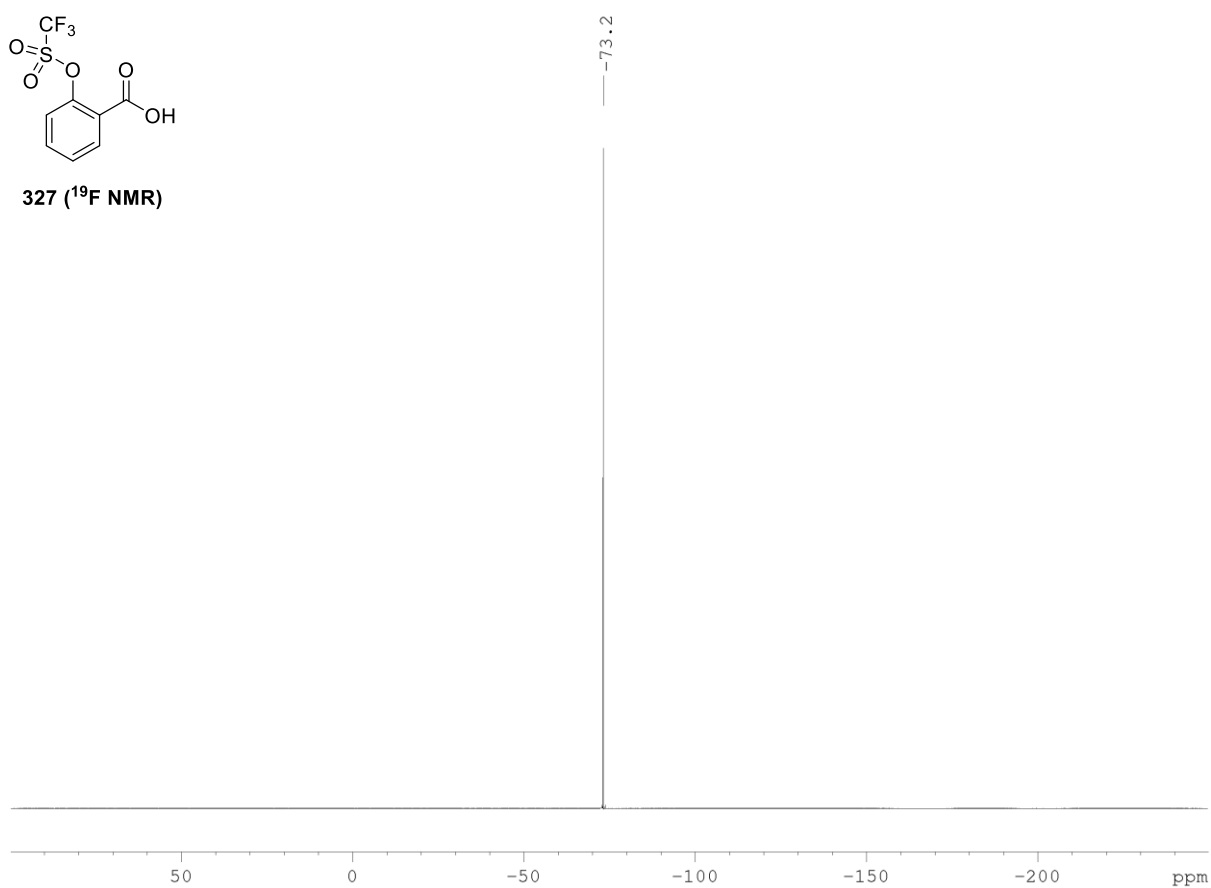
**329m**

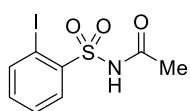
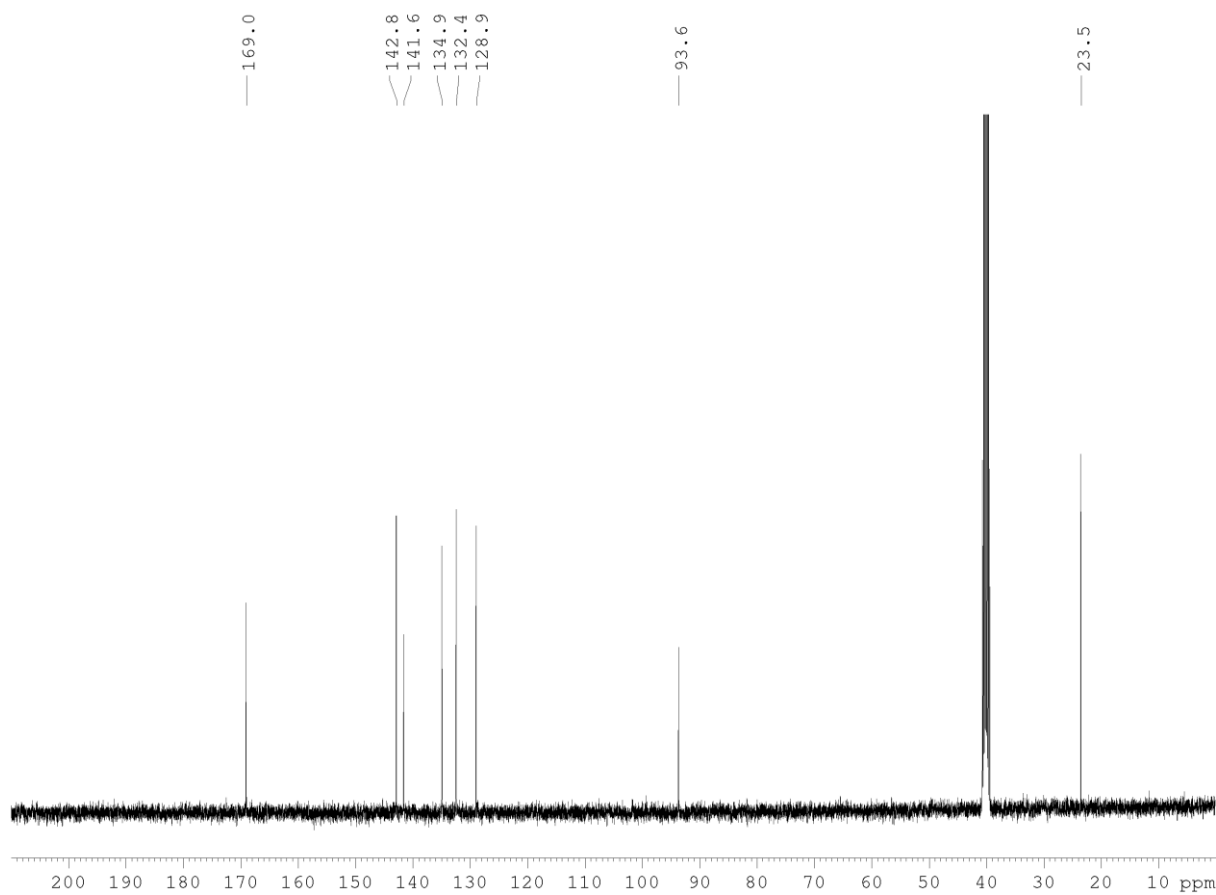
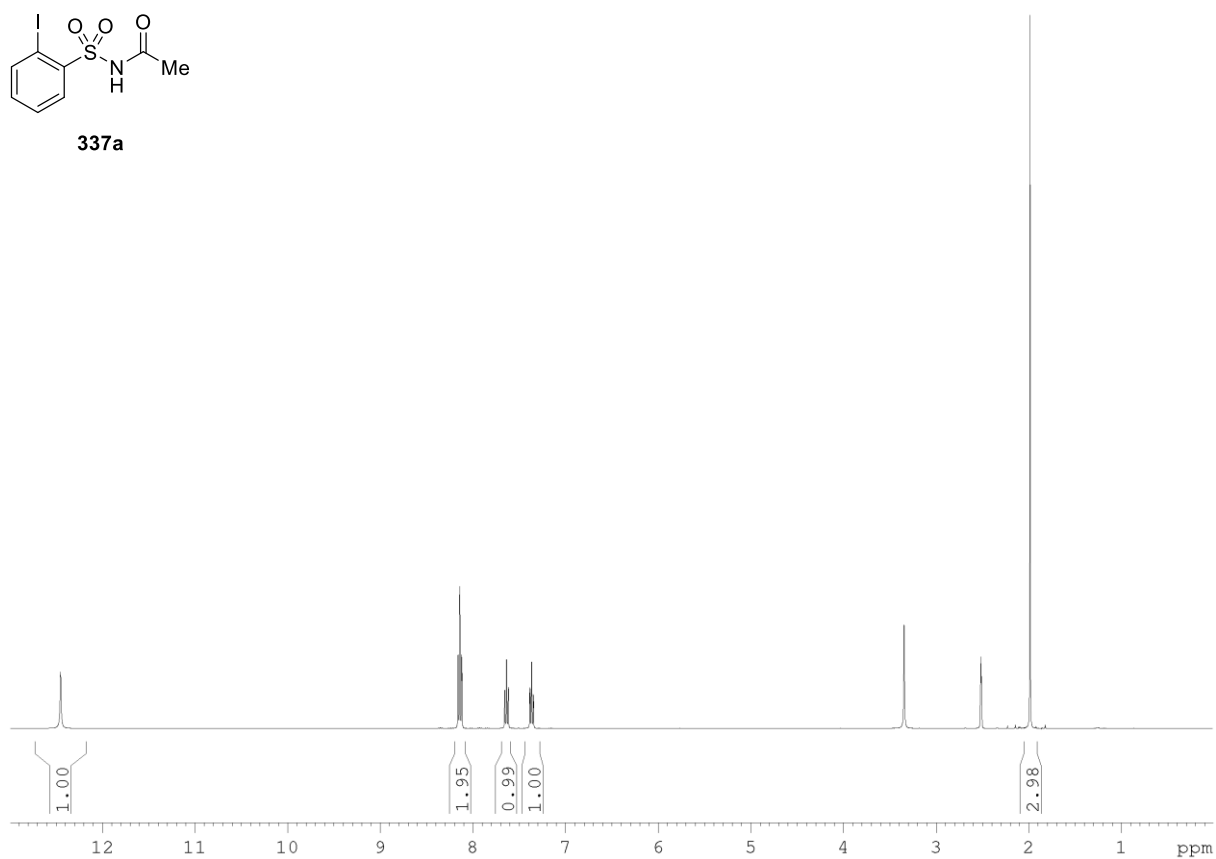
**331b**

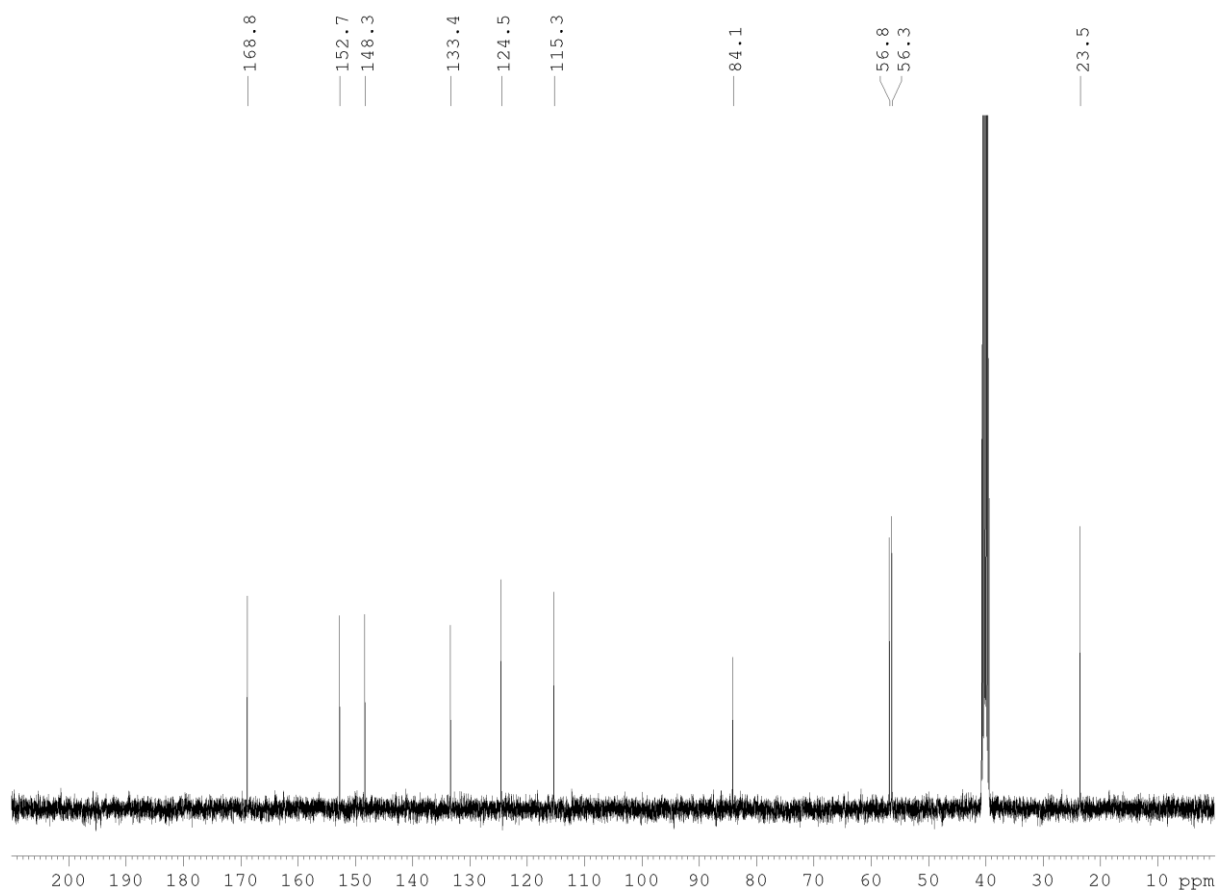
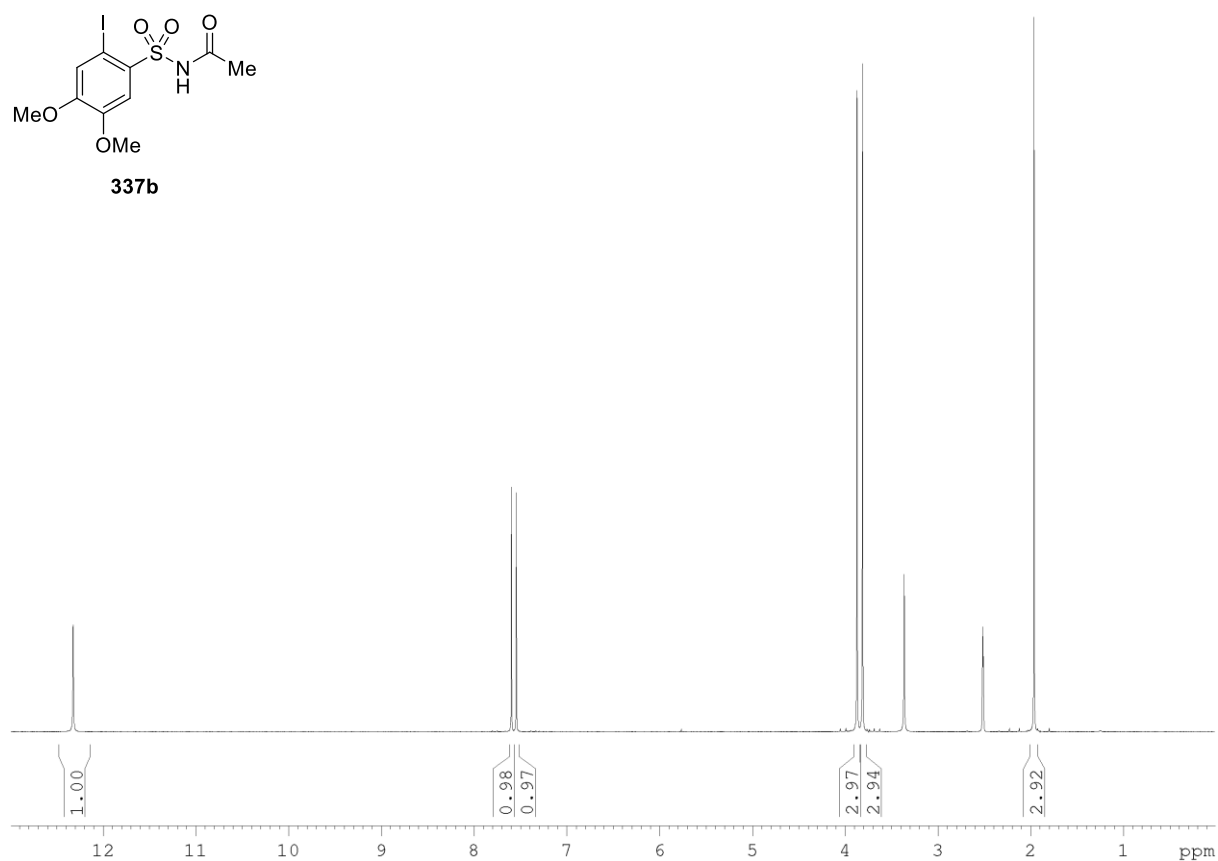
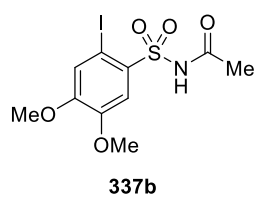


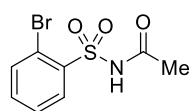
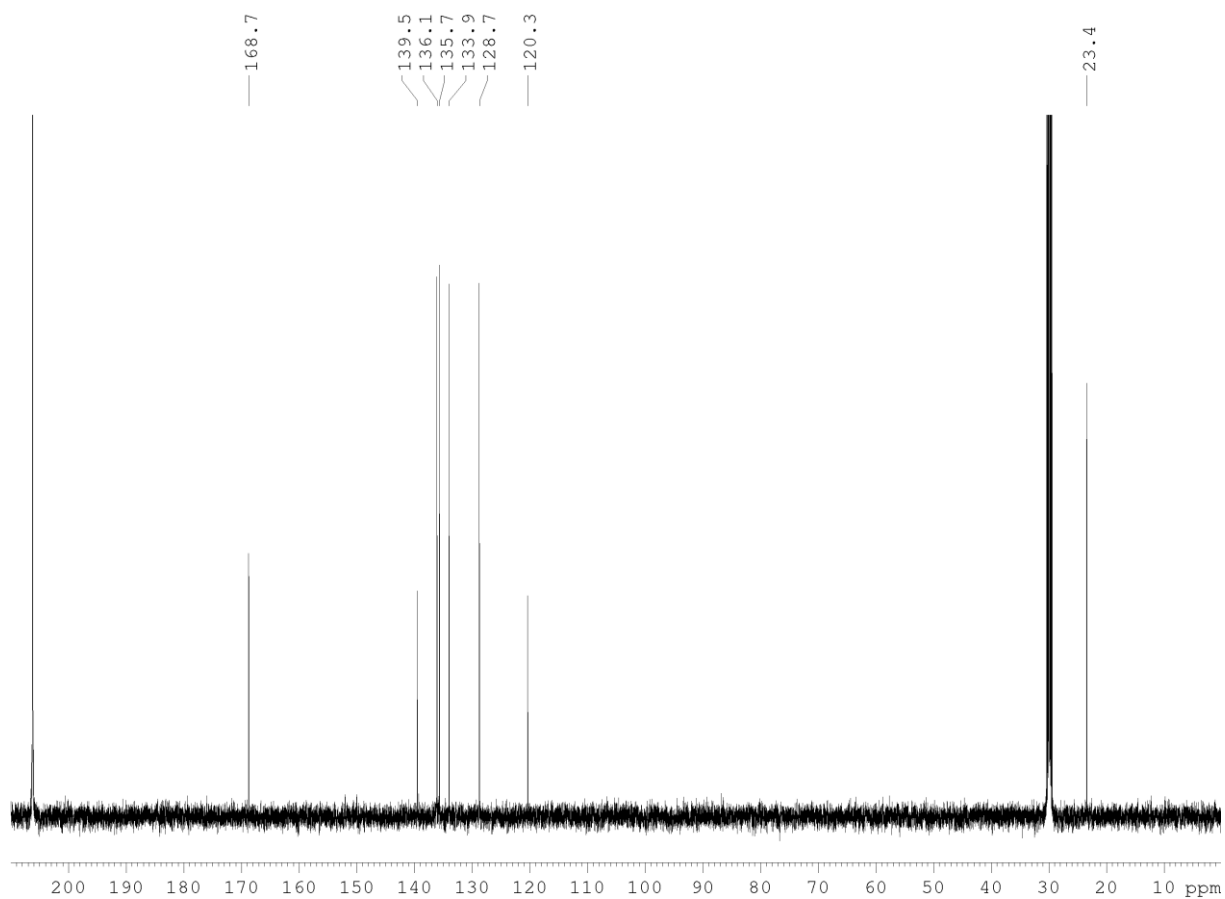
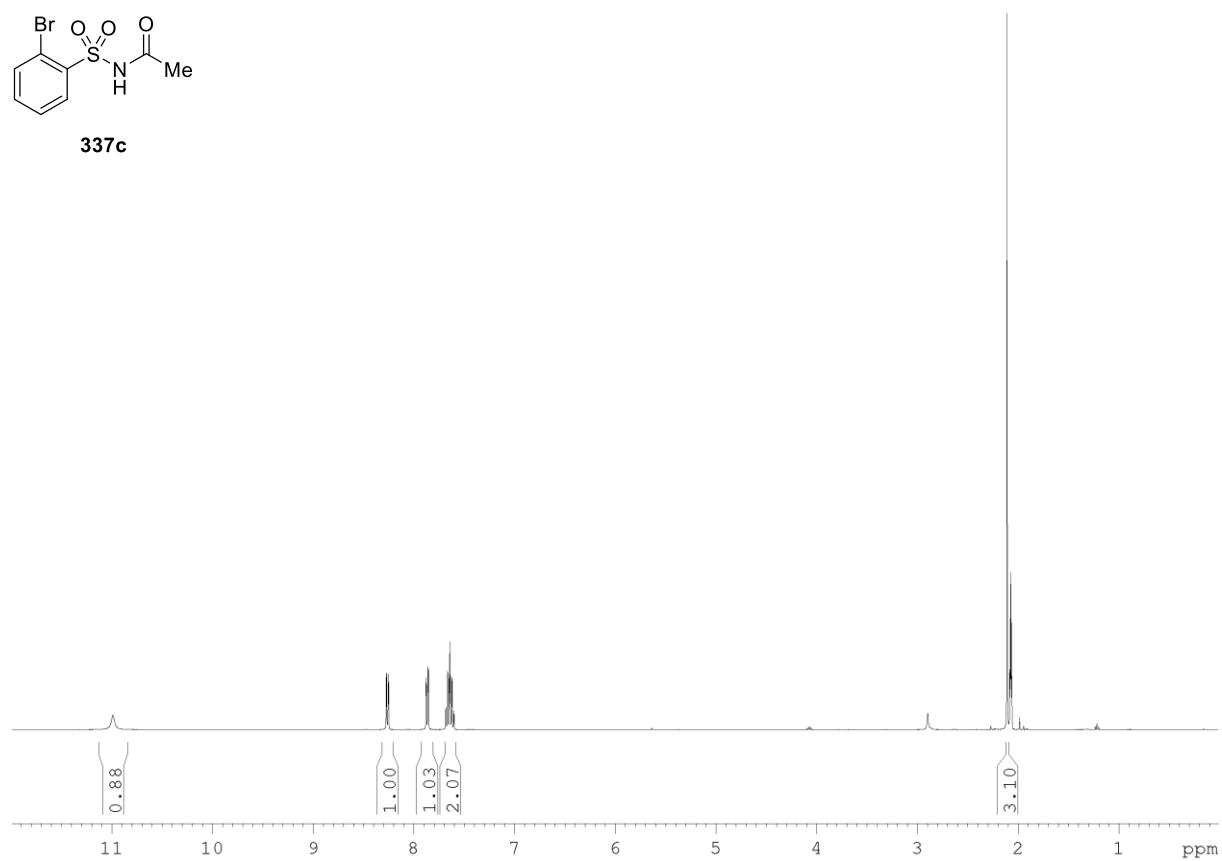
327

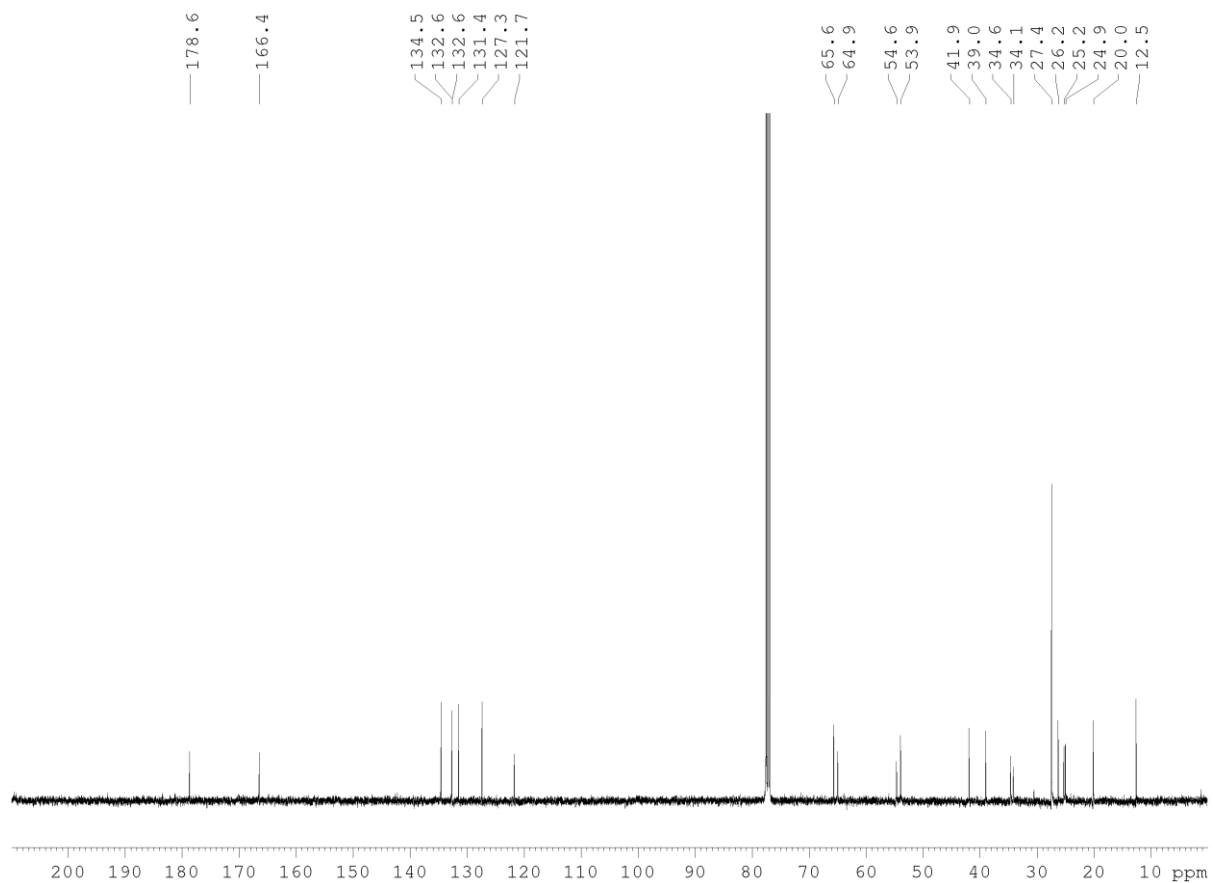
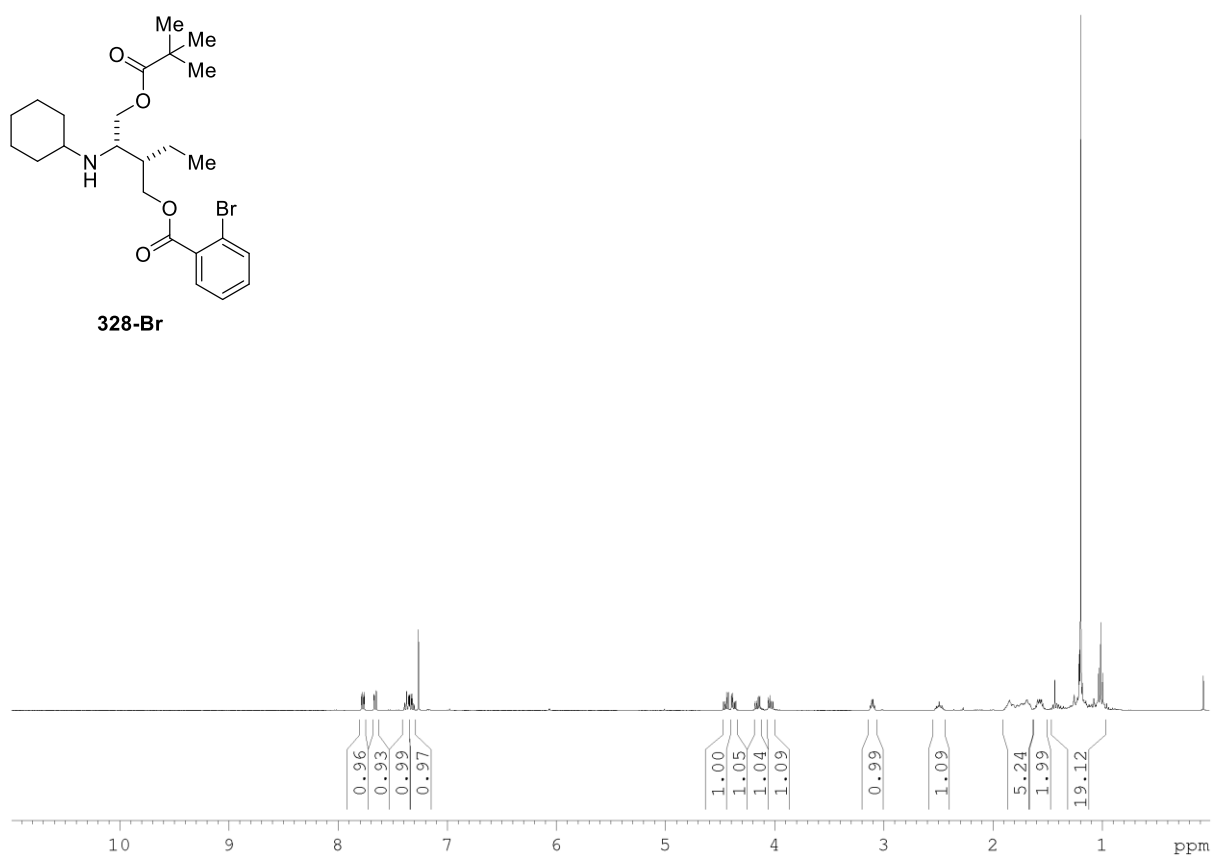


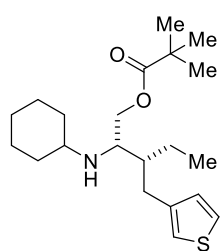
327 (^{19}F NMR)

**337a**

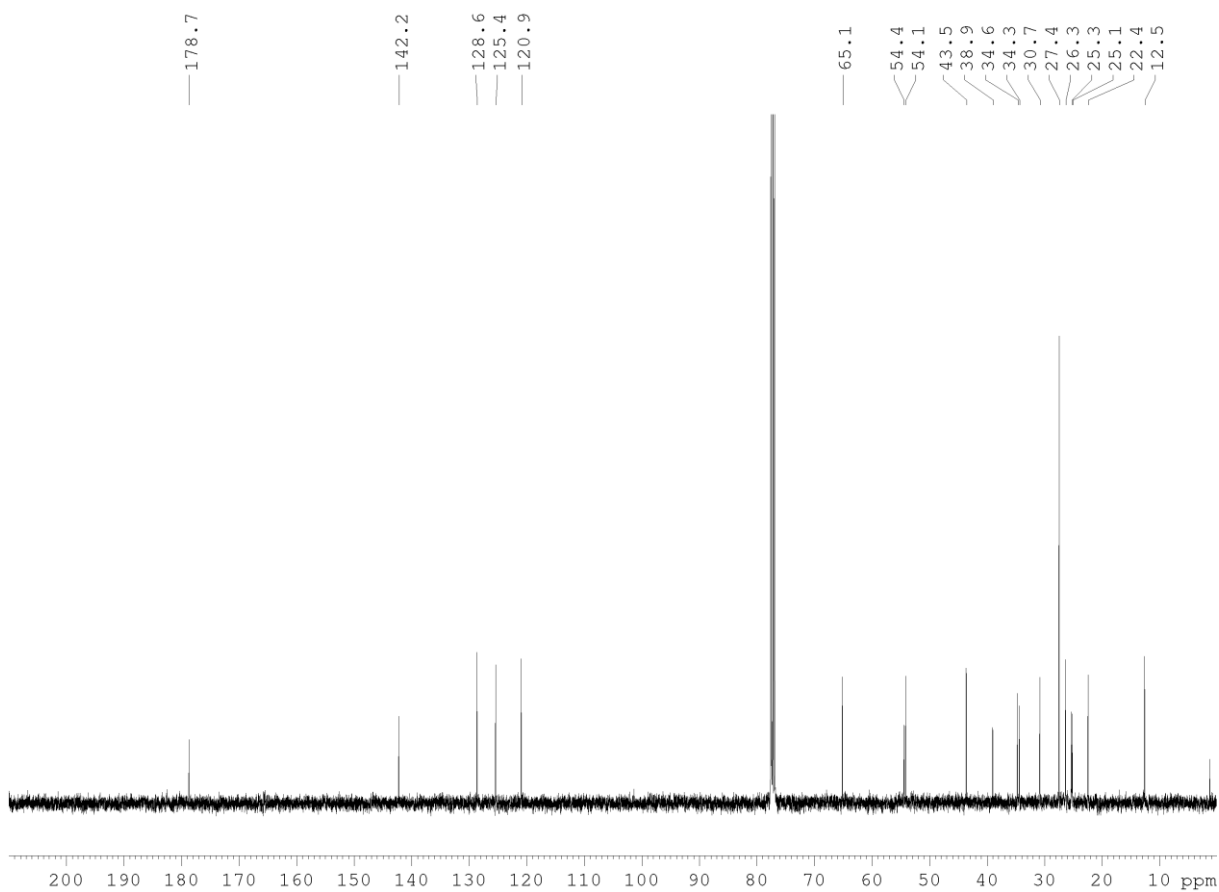
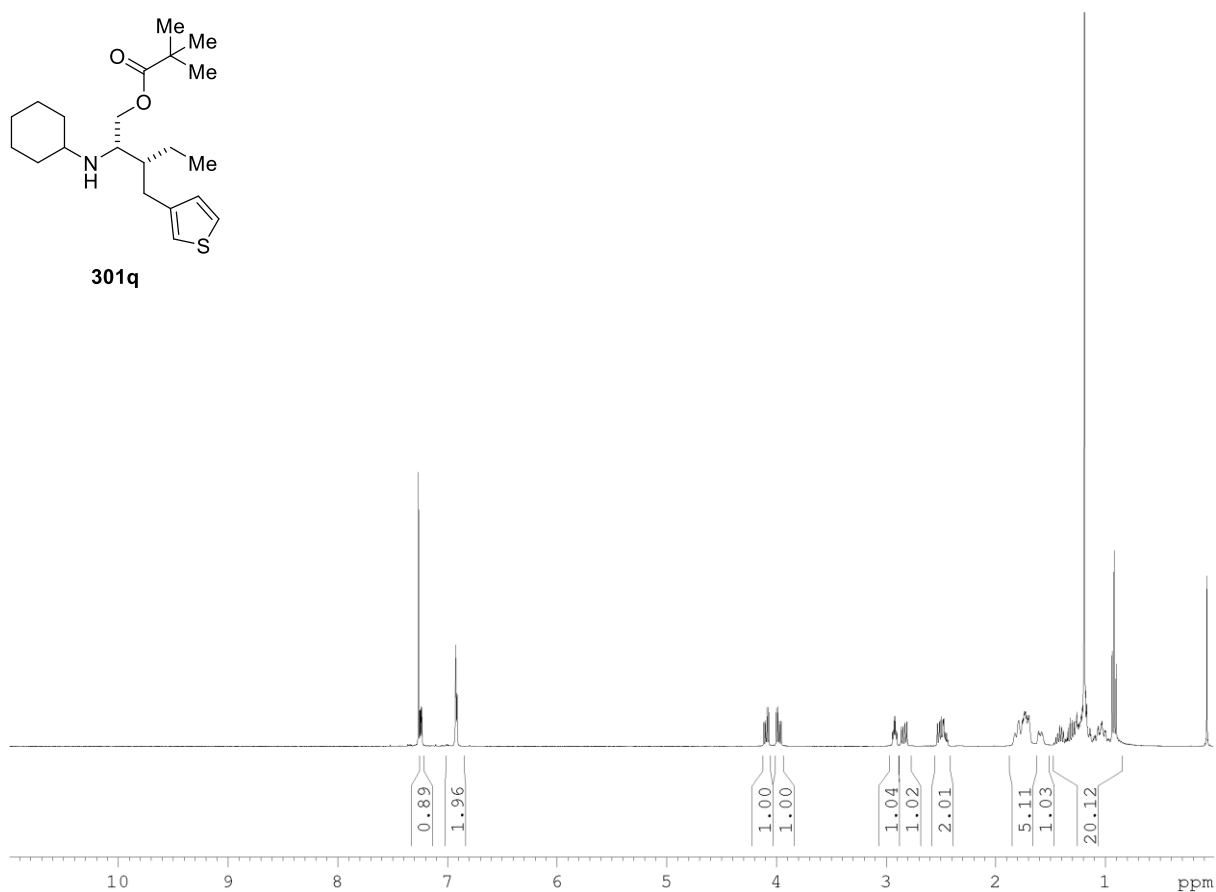


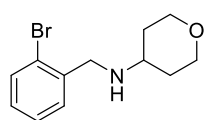
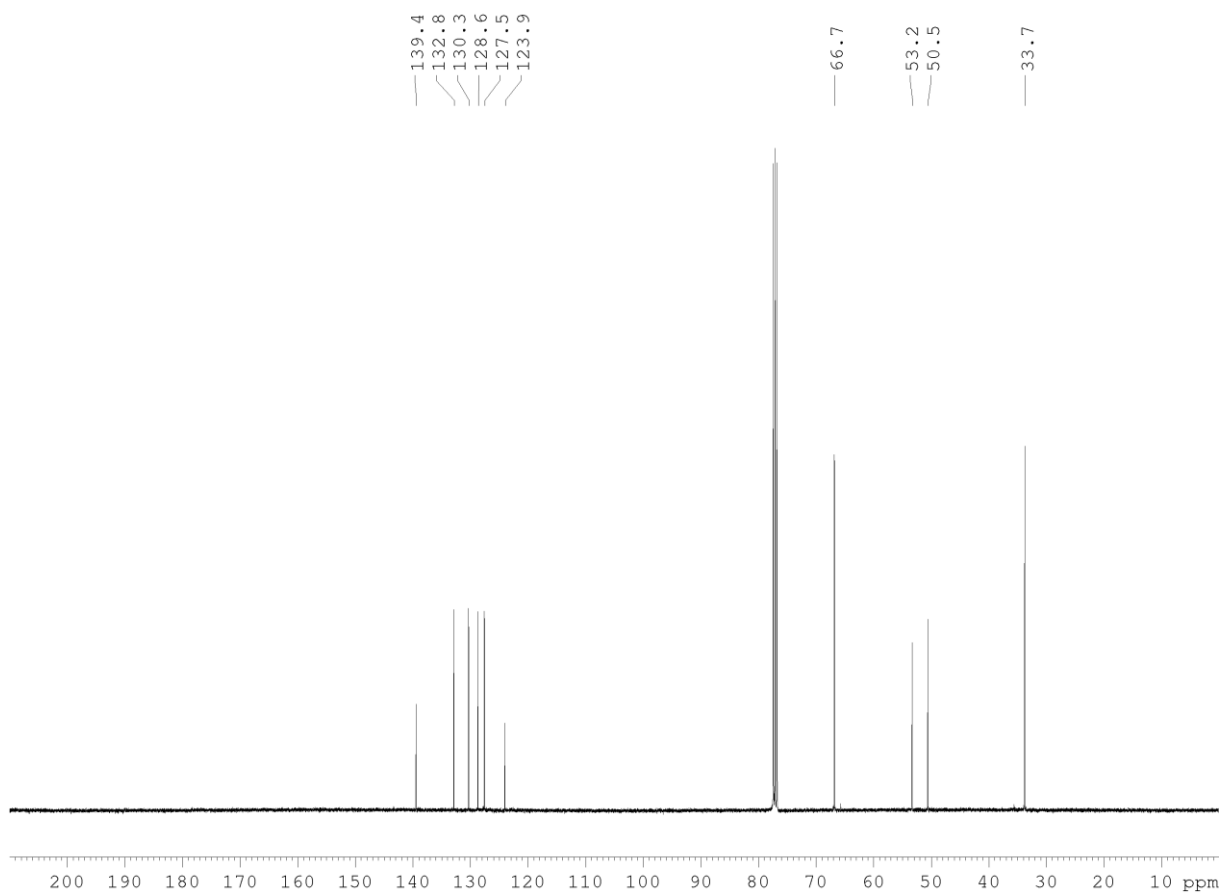
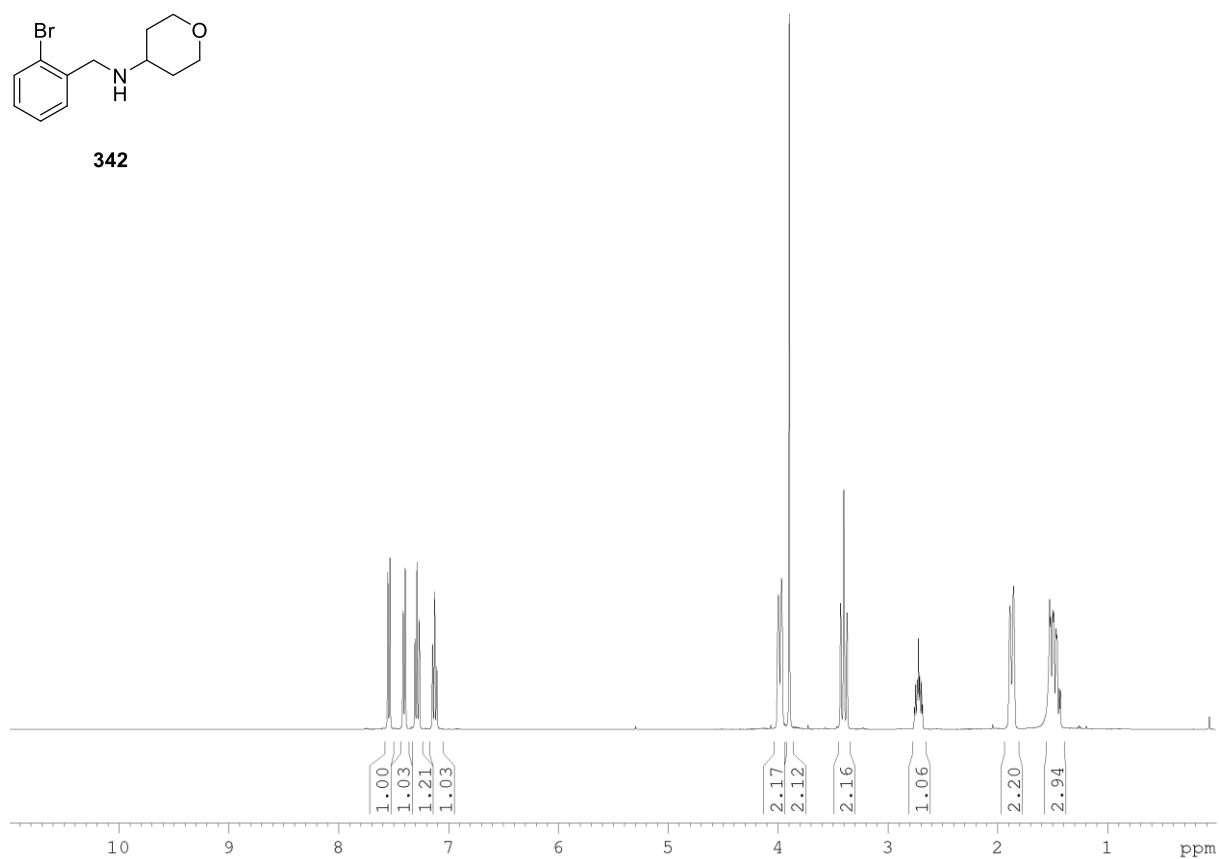
**337c**

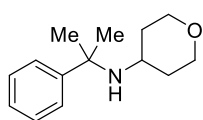




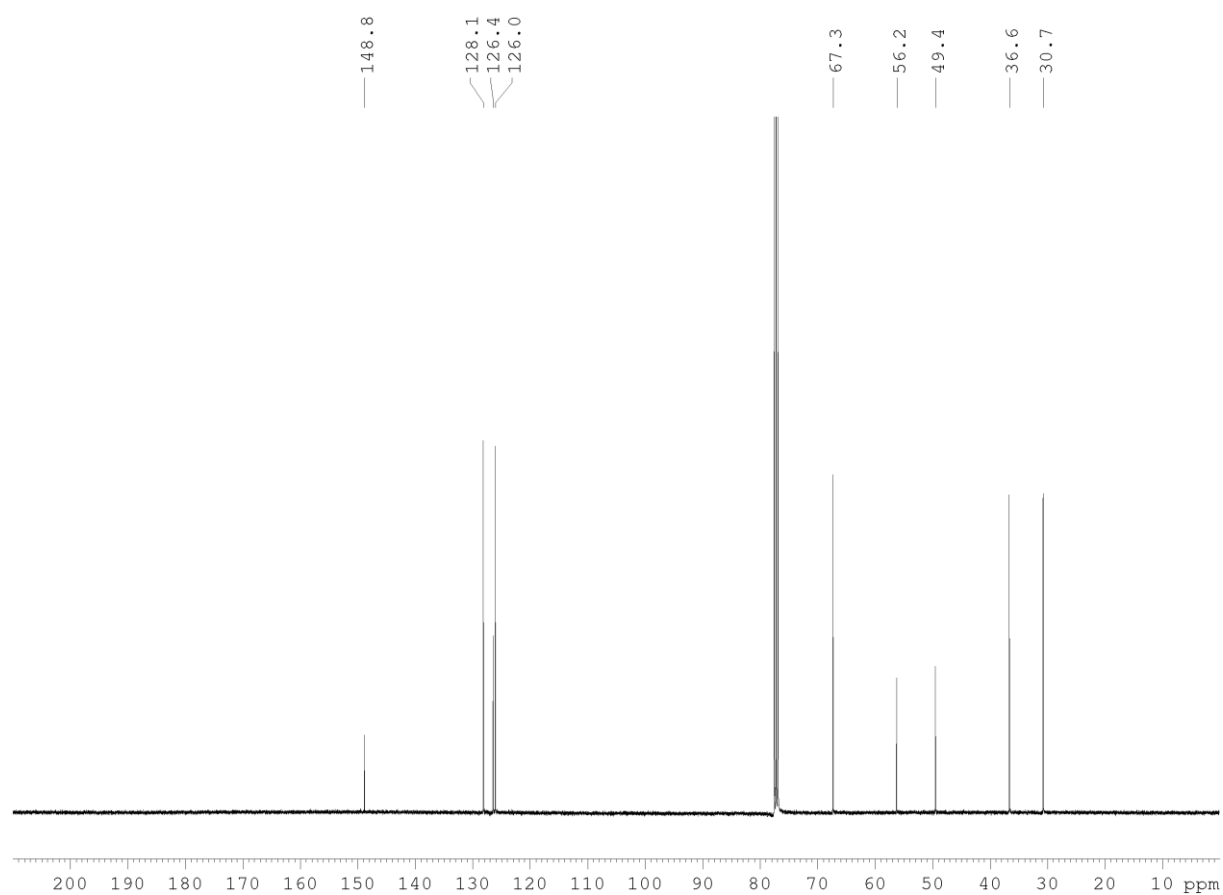
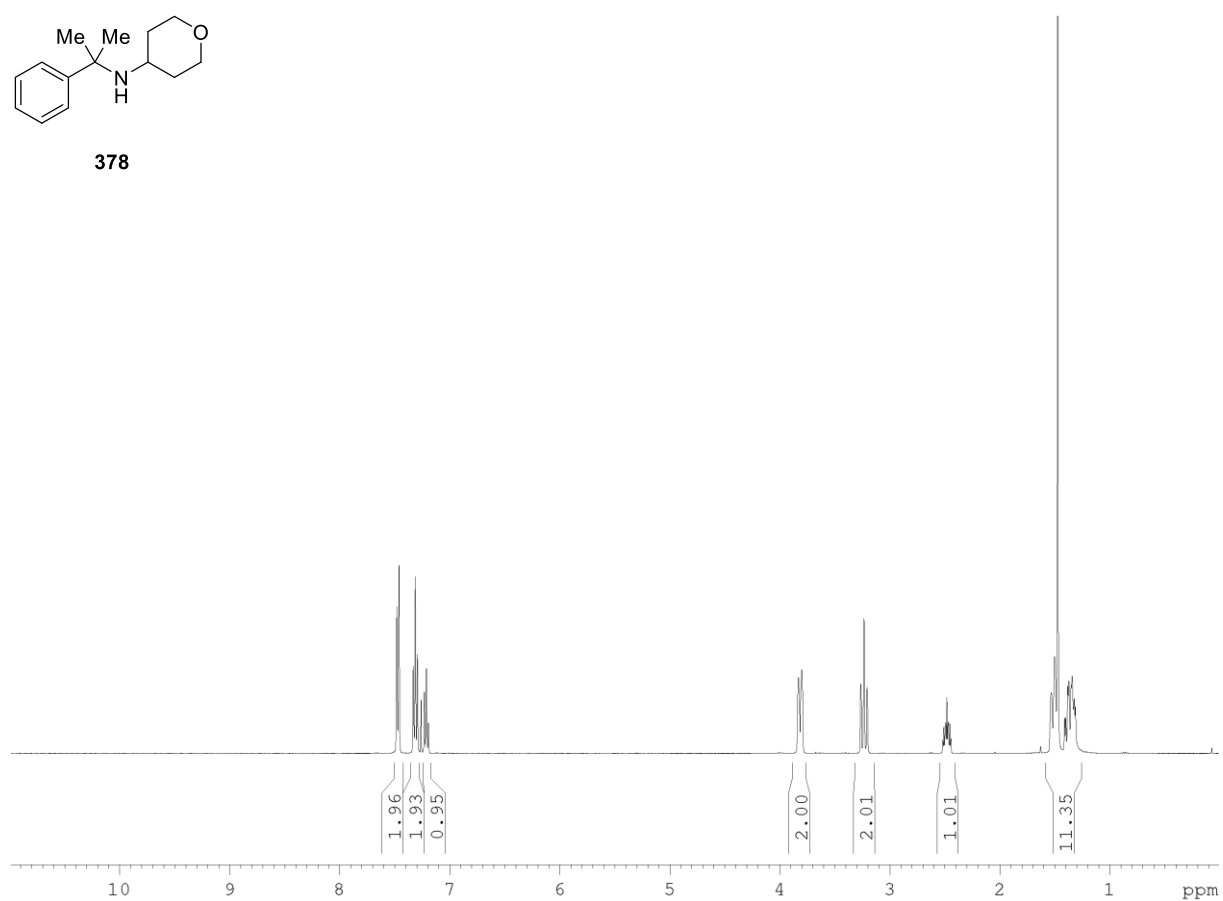
301q



**342**



378



Appendix IV: Published Work



C–H Activation

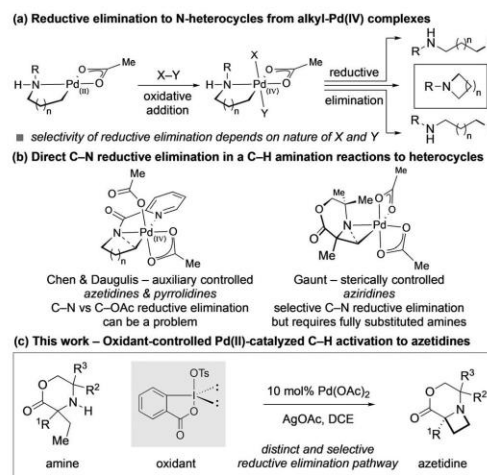
International Edition: DOI: 10.1002/anie.201800519

German Edition: DOI: 10.1002/ange.201800519

 Selective Reductive Elimination at Alkyl Palladium(IV) by
Dissociative Ligand Ionization: Catalytic C(sp³)–H Amination to
Azetidines
Manuel Nappi[†], Chuan He[†], William G. Whitehurst, Ben G. N. Chappell, and Matthew J. Gaunt^{*}

Abstract: A palladium(II)-catalyzed γ -C–H amination of cyclic alkyl amines to deliver highly substituted azetidines is reported. The use of a benziodoxole tosylate oxidant in combination with AgOAc was found to be crucial for controlling a selective reductive elimination pathway to the azetidines. The process is tolerant of a range of functional groups, including structural features derived from chiral α -amino alcohols, and leads to the diastereoselective formation of enantiopure azetidines.

The development of new methods for the synthesis of aliphatic N-heterocycles based on metal-catalyzed C–H activation has stimulated intense research efforts.^[1] Among these processes, intramolecular C–H amination using palladium(II) catalysts represents an attractive way to access saturated N-heterocycles from free(NH) amines. Key to the success of such a strategy would be the oxidation of an amine-ligated palladium(II) palladacycle to an alkyl palladium(IV) species,^[2] from which C–N reductive elimination would form the cyclic amine. Despite its apparent simplicity, the successful realization of this tactic is hindered by two factors. Firstly, oxidation of the amine-ligated palladacycle results in a palladium(IV) species displaying a number of different anionic ligands, meaning that the selectivity of reductive elimination can be difficult to control and leads to multiple products (Scheme 1a).^[3] Secondly, palladium(II)-catalyzed C–H activation on free(NH) alkyl amines can be hampered by substrate degradation connected to the use of the strong oxidants required to affect the transition between Pd^{II/IV} intermediates.^[4] While a number of elegant solutions have emerged for C(sp²)–H amination,^[5] examples of palladium(II)-catalyzed C–H amination to aliphatic N-heterocycles are rare. In 2012, the groups of Daugulis and Chen independently reported that palladium(II)-catalyzed intramolecular C(sp³)–H amination to five- and four-membered N-heterocycles could be affected by a hypervalent iodine oxidant (Scheme 1b).^[6] However, the amine substrate required protection with a picolinamide auxiliary and, in some cases, the reaction led to product mixtures arising from



Scheme 1. Palladium-catalyzed C–H amination to N-heterocycles. DCE = 1,2-dichloroethane, Ts = *p*-toluenesulfonyl.

non-selective reductive elimination. In 2014, our laboratory reported a palladium(II)-catalyzed C–H amination to aziridines, also using an I^{III} oxidant.^[7] In this case, the reaction could not accommodate amine substrates containing C–H bonds at the α -position to the amine. Consequently, the development of catalytic processes to form aliphatic cyclic amine products from aminoalkyl palladium(IV) species remains a challenge.

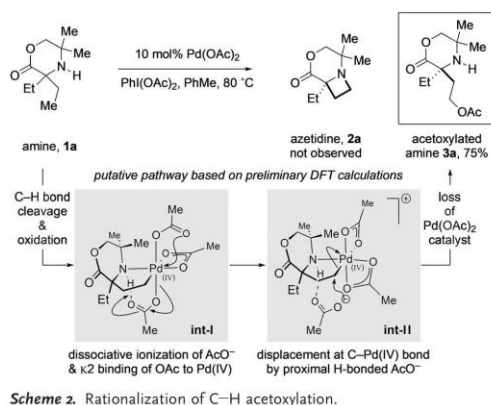
Here, we detail a palladium(II)-catalyzed intramolecular C–H amination process in which a distinct oxidation system exerts control over competitive reductive elimination pathways leading to the formation of azetidines (Scheme 1c). The C–H amination converts a class of synthetically versatile alkyl amines into highly substituted, functionally complex, and stereochemically defined azetidines, which could be useful as novel building blocks.^[8]

Recently, we described a palladium(II)-catalyzed process for β -C–H amination on hindered alkyl amines to form aziridines, which proceeded by direct intramolecular C–N reductive elimination from an aminoalkyl palladium(IV) intermediate.^[7] We speculated that reaction of a related homologated amine (**1a**) should undergo γ -C–H amination to form the corresponding azetidine **2a** (Scheme 2). We were surprised to find, however, that the reaction of **1a** produced

[*] M. Nappi,^[‡] C. He,^[‡] W. G. Whitehurst, B. G. N. Chappell, Prof. Dr. M. J. Gaunt
Department of Chemistry, University of Cambridge
Lensfield Rd, Cambridge CB2 1EW (UK)
E-mail: m.jg32@cam.ac.uk

[†] These authors contributed equally to this work.

Supporting information and the ORCID identification number(s) for the author(s) of this article can be found under:
<https://doi.org/10.1002/anie.201800519>.

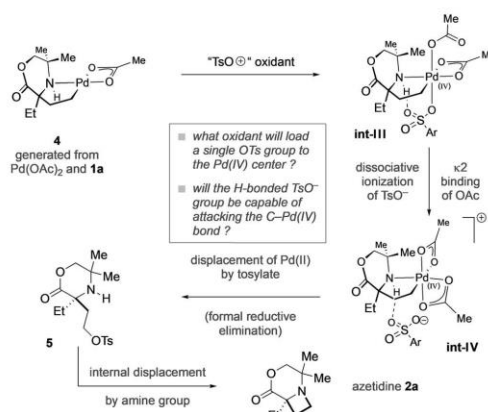


only the γ -C–H acetoxylation product **3a**, with no sign of **2a**, when treated under identical reaction conditions to those of the aziridine-forming process.^[7a] Notably, Chen et al. observed competitive C–H acetoxylation as a (often significant) by-product in their related azetidine-forming reaction.^[6b] Drawing analogy with our mechanistic work on aziridine formation,^[7b] we assumed the aminoalkyl palladium(IV) species **int-I** (from oxidation of palladacycle **4**, see Scheme 3) would precede C–O reductive elimination and provide a starting point for computational studies. We were cognizant of the important effect imparted by the adjacent carbonyl motif. While its precise role remains uncertain, we believe that it modulates the reactivity of the NH group and affects both the steps leading to C–H activation as well as modulating the pathways leading to reductive elimination. Although a number of catalytic C(sp³)–H acetoxylation methods have been reported to proceed via alkyl palladium(IV) intermediates, the salient features of the crucial C(sp³)–O reductive elimination step have proved difficult to elucidate.^[9] Towards the formation of **3a**, computational interrogation of the fate of **int-I** surprisingly showed that the lowest energy pathway did not involve direct C–O reductive elimination.

Instead, we found that **3a** could be formed by a two-step reaction at the palladium(IV) center. Dissociative ionization of an axial acetate from **int-I** and simultaneous κ^2 binding of the axial acetate forms the octahedral complex **int-II**. Notably, the dissociated acetate remains hydrogen bonded to the ligated amino group in **int-II**, which aids the displacement of the high-valent metal group, thus installing the acetoxy motif at the γ -position. This pathway draws an important parallel with the elegant work of Sanford et al., who recently reported C–O reductive elimination from stoichiometric alkyl palladium(IV) complexes based on a dissociative ionization mechanism.^[9c,f] In light of these preliminary computational studies, we re-evaluated our design hypothesis for azetidine formation.

We proposed that replacing one of the acetate ligands on the aminoalkyl palladium(IV) species with a OTs group (**int-III**) would promote dissociative ionization of the better

leaving group (Scheme 3). Accompanied by the anchimeric κ^2 binding of the *trans* (axial) acetate, the dissociation of the OTs from the aminoalkyl palladium(IV) center generates the octahedral palladium(IV) intermediate **int-IV**, in which the hydrogen-bonded tosylate is primed for displacement at the electrophilic C–Pd^{IV} bond to form the γ -amino tosylate **5**.^[9c–L,10] Cyclization of the amine to displace the γ -tosylate completes the formal C–N reductive elimination process to **2a**.



Guided by this mechanistic blueprint, we first considered an oxidant capable of transferring the single tosylate group required to form the crucial **int-III**. We began by testing reaction conditions related to the C–H acetoxylation process (Scheme 2), wherein TsOH was added in expectation that the desired pathway could be triggered by the substitution of acetate on a palladium(IV) intermediate with a TsO ligand (Table 1, entry 1). Unfortunately, none of the desired azeti-

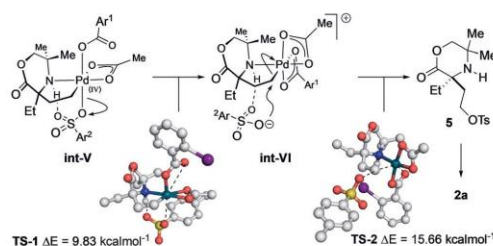
Table 1: Optimization of reaction conditions.

Entry	Catalyst	Oxidant (equiv)	Additive (equiv)	T [°C]	Solvent	Yield [%] ^[a]
1	Pd(OAc) ₂	PIDA (2)	TsOH (2)	80	PhMe	0
2	Pd(OAc) ₂	HTIB (2)	–	80	PhMe	6
3	Pd(OAc) ₂	HTIB (2)	AgOAc (2)	80	PhMe	27
4	Pd(OAc) ₂	6 (2)	AgOAc (2)	80	PhMe	52
5	Pd(OAc) ₂	6 (3)	AgOAc (3)	60	DCE	81
6	Pd(OAc) ₂	6 (3)	–	60	DCE	trace
7	–	6 (3)	AgOAc (3)	60	DCE	–
8	Pd(OAc) ₂	6 (3)	AgOTs (3)	60	DCE	–

[a] Yields determined by ¹H NMR spectroscopy using either Ph₃CH or (Cl₂CH)₂ as an internal standard.

dine was observed. Similarly, the use of NFSI in combination with TsOH, reaction conditions reported independently by Dong and co-workers^[10] as part of C(sp³)-H oxysulfonylation processes, also failed to give **2a**. Our first success was realized through the use of Koser's reagent, a tosylate-containing hypervalent iodine oxidant (entry 2).^[11] We were pleased to observe the formation of **2a**, albeit in 6% yield. We were surprised to find that addition of AgOAc increased the yield of **2a** to 27% with only trace acetoxylation observed (entry 3). With this in mind and based on Rao's use of benziodoxoles in palladium(II) reactions,^[12] reaction of **1a** with a tosylate derivative of these reagents (**6**), retaining AgOAc, increased the yield of **2a** to 52% (entry 4). Further improvements were made by increasing the amount of AgOAc and **6** (entry 5). Reaction without AgOAc gave trace amounts of **2a** and there was no reaction in the absence of Pd(OAc)₂ (entries 6 and 7). These results point to an important role for both the oxidant **6** and AgOAc. The use of **6** suggests oxidative transfer of the tosylate to form **int-III**. Interestingly, use of AgOTs precludes any reaction (entry 8).

Although the precise role of the AgOAc is unclear, it could be responsible for converting any non-acetate palladium(II) species, formed at the end of the cycle, back to the essential Pd(OAc)₂ catalyst.^[13] We validated our hypothesis through computation (Scheme 4). Probing the



Scheme 4. Computational validation of C-H amination.

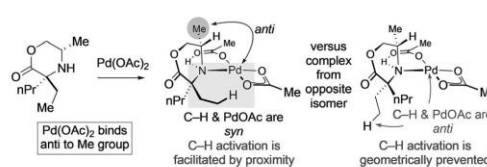
fate of aminoalkyl palladium(IV) species **int-V** (formed from **4** and **6**) revealed a low-energy pathway involving the dissociative ionization of tosylate (TS_{dis} = 9.83 kcal mol⁻¹), via **TS-1**, assisted by the concerted κ_2 binding of the 2-iodobenzoate ligand to form **int-VI**. The tosylate then attacks the γ -carbon atom (in **int-VI**, via **TS-2**), thus displacing the nucleofugal palladium(IV) species (TS_{displ} = 15.66 kcal mol⁻¹) to form the C-OTs bond in **5**.^[10] Following decomplexation of palladium(II), displacement of tosylate with the amine forms **2a**.^[14,15] With the optimal reaction conditions, we examined the scope of the γ -C-H amination.

Table 2 shows that a range of fully substituted morpholinones displaying an α -ethyl group alongside functionalized α' -sidechains undergo efficient C-H amination to the azetidines **2a-h**. Side-chain groups compatible with the reaction comprised hydroxymethyl derivatives (**2c,d**), fluoromethyl (**2e**), protected amines (**2f**), esters (**2g**), and arenes (**2h**). In addition, an amine containing a spiro-cyclohexane motif provided the corresponding azetidine **2i** in 83% yield. The C-

H amination of a cyclic amide derivative led to the piperazinone **2j** in moderate yield.

Typically, the C(sp³)-H functionalization of unprotected alkyl amines by a classical cyclopalladation/palladium(IV) pathway is often restricted to molecules displaying fully substituted carbon atoms around the free(NH) motif. This restriction is in part a result of deleterious oxidation reactions at the α -position to the amine, and are initiated by the requisite oxidant, thus leading to decomposition. On the basis that **6** is less oxidizing than its acyclic counterparts,^[16] we reasoned that amine substrates with fewer substituents might be compatible with the modified reagent. This feature would be attractive for two reasons: chiral amino alcohols could be used to assemble the morpholinones, and a chiral center adjacent to the NH motif would introduce a previously unexplored diastereoselectivity question to the C-H activation step. Accordingly, a range of enantioenriched substrates were prepared starting from different amino alcohols. At 80 °C, the C-H amination delivered the azetidines in useful yields and excellent diastereoselectivity (**2k-x**; Table 2).

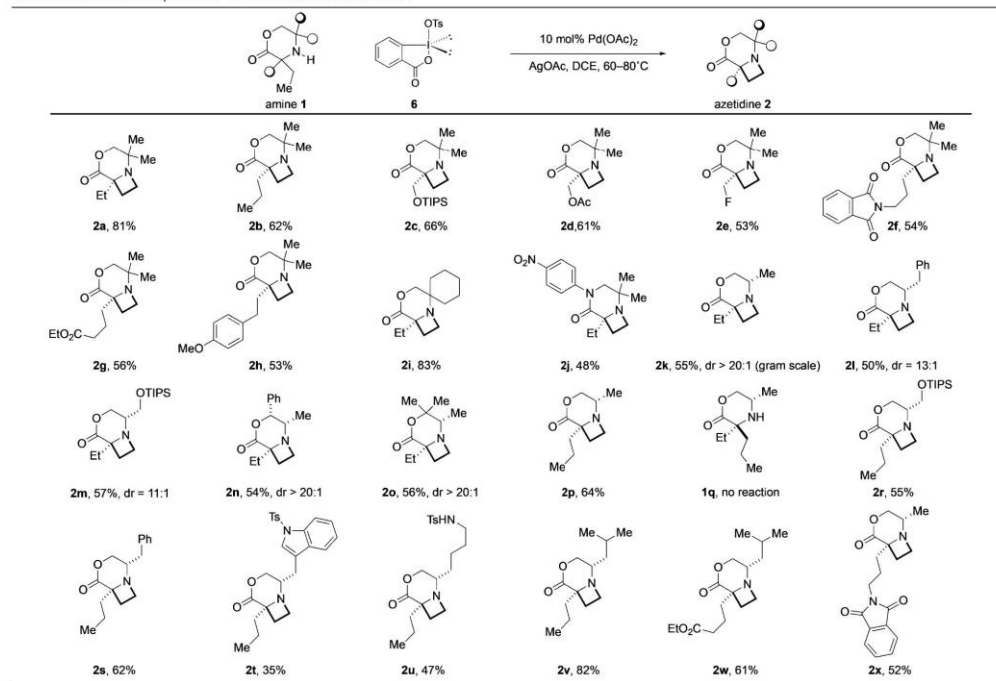
Interestingly, the highest diastereoselectivity was observed when using morpholinones based on alaninol (**2k**), in comparison to phenylalanine- and serine-derived amines (**2l,m**). To probe the stereochemical features of the C-H activation step, we prepared isomeric substrates that displayed the reactive ethyl group both *syn* and *anti* to the stereogenic center. We found that only the *anti* isomer produced the desired azetidine **2p**, with the *syn* isomer returning the starting material **1q**. A possible explanation involves binding Pd(OAc)₂ to the less sterically hindered face of the cyclic amine, and placing the key C-H bond in a *syn* orientation to the palladium(II) center (Scheme 5).



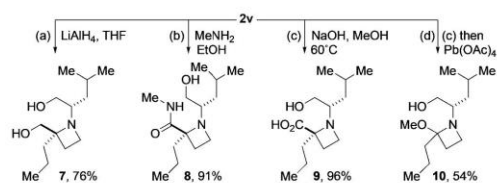
Scheme 5. Stereoselective C-H activation.

Further examples of the C-H amination demonstrated that substituents can be accommodated on either side of the amine linkage, thus forming the azetidines **2r-x** which display functional groups useful for downstream synthetic modification (Table 2). The azetidine **2x** was crystalline, thus enabling unambiguous confirmation of the absolute configuration of the product by X-ray diffraction.^[17] Acyclic amines proved to be poor substrates, and required stoichiometric amounts of Pd(OAc)₂ to afford **2y** in a modest yield.^[18]

Finally, we showed that the azetidine products serve as substrates for a selection of simple transformations to potentially useful products (Scheme 6). Reduction of the lactone of **2v** with LiAlH₄ generated the diol **7**. Aminolysis of the lactone gave amide **8** in very good yield. Hydrolysis of the morpholinone delivered the corresponding hydroxy acid **9**. We also found that oxidative decarboxylation of **9** delivered

Table 2: Substrate scope for C–H amination to azetidines.^[a]

[a] Yields are of isolated products. See the Supporting Information for details. [b] Stoichiometric reaction over two steps. TIPS = triisopropylsilyl.



Scheme 6. Derivatization of azetidines. THF = tetrahydrofuran.

the four-membered ring cyclic hemiaminal **10** as a stable, single diastereomer.

In conclusion, we have developed a palladium(II)-catalyzed γ -C–H amination process in which cyclic secondary alkyl amines are converted into highly substituted azetidines. The use of a benzodioxole tosylate as an oxidant, in combination with AgOAc, was crucial in delivering the azetidines. We propose that the C–H amination to azetidines is facilitated by a selective reductive elimination that involves dissociative ionization of a tosylate and anchimeric κ^2 carboxylate binding to form an octahedral aminoalkyl palladium(IV) complex. Nucleophilic attack of the tosylate at the carbon atom bearing the palladium(IV) group forms the C–OTs bond, which in turn is displaced by the proximal

amino group to form the azetidine. The reaction displays a broad tolerance to functional groups, including structural features derived from chiral α -amino alcohols, which leads to a diastereoselective process forming enantiopure azetidines. We believe that the distinct reductive elimination pathway will be applicable to other C–H functionalization processes.

Acknowledgements

We are grateful to EPSRC (EP/N031792/1), the Royal Society for a Wolfson Merit Award (M.J.G.), H2020 European Research Council (M.N. & C.H.), the Herchel Smith Foundation (B.G.N.C.), EPSRC, and AstraZeneca (W.G.W.) for funding. Mass spectrometry data were acquired at the EPSRC UK National Mass Spectrometry Facility at Swansea University.

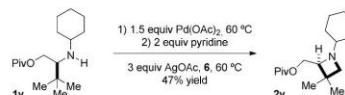
Conflict of interest

The authors declare no conflict of interest.

Keywords: azetidines · C–H activation · hypervalent compounds · palladium · reaction mechanisms

How to cite: *Angew. Chem. Int. Ed.* **2018**, *57*, 3178–3182
Angew. Chem. **2018**, *130*, 3232–3236

- [1] a) P. Thansandote, M. Lautens, *Chem. Eur. J.* **2009**, *15*, 5874–5883; b) J. L. Jeffrey, R. Sarpong, *Chem. Sci.* **2013**, *4*, 4092–4106; c) J. Yuan, C. Liu, A. Lei, *Chem. Commun.* **2015**, *51*, 1394–1409; d) W. A. Nack, G. Chen, *Synlett* **2015**, 26, 2505–2511; e) Y. Park, Y. Kim, S. Chang, *Chem. Rev.* **2017**, *117*, 9247–9301.
- [2] a) K. Muñoz, *Angew. Chem. Int. Ed.* **2009**, *48*, 9412–9423; *Angew. Chem.* **2009**, *121*, 9576–9588; b) P. Sehnal, R. J. K. Taylor, I. J. S. Fairlamb, *Chem. Rev.* **2010**, *110*, 824–889; c) K. M. Engle, T.-S. Mei, X. Wang, J.-Q. Yu, *Angew. Chem. Int. Ed.* **2011**, *50*, 1478–1491; *Angew. Chem.* **2011**, *123*, 1514–1528; d) A. J. Hickman, M. S. Sanford, *Nature* **2012**, *484*, 177–185.
- [3] a) S. R. Neufeldt, M. S. Sanford, *Acc. Chem. Res.* **2012**, *45*, 936–946; b) M. H. Pérez-Temprano, J. M. Racowski, J. W. Kampf, M. S. Sanford, *J. Am. Chem. Soc.* **2014**, *136*, 4097–4100.
- [4] a) K. C. Nicolaou, C. J. N. Mathison, T. Montagnon, *Angew. Chem. Int. Ed.* **2003**, *42*, 4077–4082; *Angew. Chem.* **2003**, *115*, 4211–4216; b) C. de Graaff, L. Bensch, M. J. van Lint, E. Ruijter, R. V. A. Orru, *Org. Biomol. Chem.* **2015**, *13*, 10108–10112.
- [5] a) J. Jiao, K. Murakami, K. Itami, *ACS Catal.* **2016**, *6*, 610–633; b) R. Narayan, S. Manna, A. Antonchick, *Synlett* **2015**, 26, 1785–1803; c) M. Baeten, B. U. W. Maes, *Adv. Organomet. Chem.* **2017**, *67*, 401–481. See also ref. [1].
- [6] a) E. T. Nades, O. Daugulis, *J. Am. Chem. Soc.* **2012**, *134*, 7–10; b) G. He, Y. Zhao, S. Zhang, C. Lu, G. Chen, *J. Am. Chem. Soc.* **2012**, *134*, 3–6; c) G. He, G. Lu, Z. Guo, P. Liu, G. Chen, *Nat. Chem.* **2016**, *8*, 1131–1136. For related studies, see: X. Ye, Z. He, T. Ahmed, K. Weise, N. G. Akhmedov, J. L. Petersen, X. Shi, *Chem. Sci.* **2013**, *4*, 3712–3716.
- [7] a) A. McNally, B. Haffemayer, B. S. L. Collins, M. J. Gaunt, *Nature* **2014**, *510*, 129–133; b) A. P. Smalley, M. J. Gaunt, *J. Am. Chem. Soc.* **2015**, *137*, 10632–10641.
- [8] a) A. Brandi, S. Cicchi, F. M. Cordero, *Chem. Rev.* **2008**, *108*, 3988–4035; b) B. Alcaide, P. Almendros, C. Aragoncillo, *Curr. Opin. Drug Discov. Devel.* **2010**, *13*, 685–697; c) F. Couty, G. Evano, *Synlett* **2009**, 3053–3064.
- [9] a) L. V. Desai, K. L. Hull, M. S. Sanford, *J. Am. Chem. Soc.* **2004**, *126*, 9542–9543; b) R. Giri, J. Liang, J.-G. Lei, J.-J. Li, D.-H. Wang, X. Chen, I. C. Naggar, C. Guo, B. M. Foxman, J.-Q. Yu, *Angew. Chem. Int. Ed.* **2005**, *44*, 7420–7424; *Angew. Chem.* **2005**, *117*, 7586–7590; c) S. L. Marquard, J. F. Hartwig, *Angew. Chem. Int. Ed.* **2011**, *50*, 7119–7123; *Angew. Chem.* **2011**, *123*, 7257–7261; d) A. J. Canty, *Dalton Trans.* **2009**, 10409–10417; e) N. M. Camasso, M. H. Perez-Temprano, M. S. Sanford, *J. Am. Chem. Soc.* **2014**, *136*, 12771–12775; f) A. J. Canty, A. Ariafard, N. M. Camasso, A. T. Higgs, B. F. Yates, M. S. Sanford, *Dalton Trans.* **2017**, 46, 3742–3748; g) G. Yin, X. Mu, G. Liu, *Acc. Chem. Res.* **2016**, *49*, 2413–2423; h) H. Peng, Z. Yuan, H.-Y. Wang, Y.-I. Guo, G. Liu, *Chem. Sci.* **2013**, *4*, 3172–3178.
- [10] a) Y. Xu, G. Yan, Z. Ren, G. Dong, *Nat. Chem.* **2015**, *7*, 829–834; b) R. Zhao, W. Lu, *Org. Lett.* **2017**, *19*, 1768–1771.
- [11] G. F. Koser, R. H. Wettach, *J. Org. Chem.* **1980**, *45*, 4988–4989.
- [12] a) G. Shan, X. Yang, Y. Zong, Y. Rao, *Angew. Chem. Int. Ed.* **2013**, *52*, 13606–13610; *Angew. Chem.* **2013**, *125*, 13851–13855; b) J. Hu, T. Lan, Y. Sun, H. Chen, J. Yao, Y. Rao, *Chem. Commun.* **2015**, *51*, 14929–14932; c) V. V. Zhdankin, C. J. Kuehl, J. T. Bolz, M. S. Formanek, A. J. Simonsen, *Tetrahedron Lett.* **1994**, *35*, 7323–7326; d) J. P. Brand, D. F. Gonzalez, S. Nicolai, J. Waser, *Chem. Commun.* **2011**, 47, 102–115.
- [13] See the Supporting Information for details. See also: a) X. Chen, C. E. Goodhue, J.-Q. Yu, *J. Am. Chem. Soc.* **2006**, *128*, 12634–12635; b) J.-J. Li, T.-S. Mei, J.-Q. Yu, *Angew. Chem. Int. Ed.* **2008**, *47*, 6452–6455; *Angew. Chem.* **2008**, *120*, 6552–6555.
- [14] Alternative mechanisms for direct C–O or C–N reductive elimination (to **3a** and **2a**, respectively) from **int-V** were significantly higher in energy. See the Supporting Information (Figure S2) for details.
- [15] Although we were unable to isolate **5**, support for the proposed pathway is demonstrated by the preparation of the corresponding chloride, by the same pathway, and observation of the formation of **2a**. See the Supporting Information for details.
- [16] M. S. Yusubov, T. Wirth, *Org. Lett.* **2005**, *7*, 519–521.
- [17] **2x** was obtained as a single crystal, whose structure was confirmed by X-ray diffraction. See the Supporting Information for details.
- [18] Acyclic amine (**1y**) formed the corresponding azetidine (**2y**) in 47% yield over two steps using a stoichiometric amount of palladium.



Manuscript received: January 13, 2018

Accepted manuscript online: January 30, 2018

Version of record online: February 22, 2018

C–H Activation

International Edition: DOI: 10.1002/anie.201902838

German Edition: DOI: 10.1002/ange.201902838

Carboxylate-Assisted Oxidative Addition to Aminoalkyl Pd^{II} Complexes: C(sp³)–H Arylation of Alkylamines by Distinct Pd^{II}/Pd^{IV} Pathway

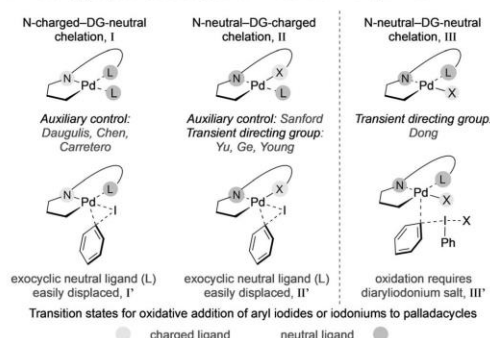
William G. Whitehurst, J. Henry Blackwell, Gary N. Hermann, and Matthew J. Gaunt*

Abstract: Reported is the discovery of an approach to functionalize secondary alkylamines using 2-halobenzoic acids as aryl-transfer reagents. These reagents promote an unusually mild carboxylate-assisted oxidative addition to alkylamine-derived palladacycles. In the presence of Ag^I salts, a decarboxylative C(sp³)–C(sp²) bond reductive elimination leads to γ -aryl secondary alkylamines and renders the carboxylate motif a traceless directing group. Stoichiometric mechanistic studies were effectively translated to a Pd-catalyzed γ -C(sp³)–H arylation process for secondary alkylamines.

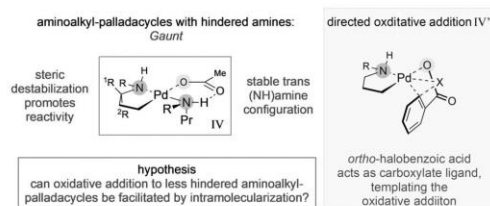
The transformation of unactivated C(sp³)–H bonds into C–aryl bonds using transition-metal catalysts has been the focus of intense academic research over the past decade.^[1] Within this field, Pd-catalyzed C(sp³)–H arylation of alkylamines has stimulated significant interest as the products of such a transformation display structural features that are highly represented in pharmaceutical agents.^[2,3] As a general premise, amine-directed C–H activation leads to the formation of a palladacycle intermediate, from which arylation can be promoted through a variety of pathways. Yu and co-workers have established that sulfonamide and thioamide derivatives of alkylamines undergo C–H arylation with arylboronic acids and esters.^[4] Similarly aryl iodides have been commonly employed reagents for C(sp³)–H arylation of auxiliary-derived amine derivatives, wherein the selective nature of the oxidative addition to electron-rich Pd^{II} centres in the corresponding palladacycles affords broad substrate scope and functional-group compatibility.^[5] An important aspect to the reactivity of aryl iodides is the necessary complexation of either the iodide or π system to the metal in advance of the C–I bond cleavage.^[6] Consequently, the ligand environment in the key palladacyclic intermediate must allow the displacement of a neutral ligand to promote the oxidative functionalization. In consideration of this requirement, a number of subtly distinct strategies have been developed for Pd-catalyzed C(sp³)–H arylation in alkylamine derivatives and can be defined by the coordinating nature of the directing group. Firstly, the groups of Daugulis, Chen, and Carretero^[5a–c] reported amide- and sulfonamide-linked pyridyl auxiliaries which enable C–H activation to palladacycles compris-

ing a bidentate directing motif with anionic and neutral coordinating groups. The remaining site, *exo* to the palladacycle motif, is occupied by a neutral ligand that can be displaced by an aryl iodide, leading to arylation (Figure 1 a, I and I'). Secondly, Sanford and co-workers^[5d] equipped a hindered, neutral tertiary amine derivative with an additional anionic amide to promote the formation of a palladacycle (Figure 1 a, II and II'). In a related class of C–H activation reactions, the groups of Yu, Ge, and Young^[5j–m] have reported a series of transient directing groups that lead to conceptually similar intermediates. In these cases, a neutral-amino derivative forms a palladacycle in conjunction with

a. Directing group-assisted strategies for C–H activation in alkylamines



b. Palladacycles of less hindered alkylamines are stable complexes – this work



c. Catalytic C–H arylation of less hindered amines via directed oxidative addition

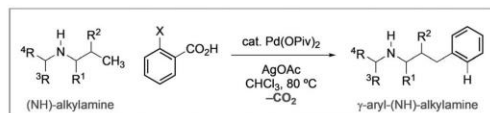


Figure 1. Towards a carboxylate-assisted C–H arylation of alkylamines.

* W. G. Whitehurst, J. H. Blackwell, G. N. Hermann, M. J. Gaunt
Department of Chemistry, University of Cambridge
Lensfield Road, Cambridge CB2 1EW (UK)
E-mail: m.jg32@cam.ac.uk

Supporting information and the ORCID identification number(s) for the author(s) of this article can be found under:
<https://doi.org/10.1002/anie.201902838>.

a charged ligand, with the remaining site once again occupied by a displaceable neutral ligand. Finally, Dong and co-workers^[7] reported a variant of the transient directing group concept by employing an imine with a tethered neutral ligand, resulting in a palladacycle with an anionic ligand occupying the remaining site (Figure 1 a, III and III'). In this distinct scenario, the use of reactive diaryliodonium salts is required to enable oxidation of the palladacycle because there is no readily displaced neutral ligand available.^[8]

Over the last five years, our group has been engaged in a research program geared towards the use of free (NH) alkylamines in Pd^{II}-catalyzed β and γ C(sp³)-H activation reactions.^[2] The success of these strategies has been dependent on either a) the use of hindered alkylamine substrates, which destabilize rapidly formed bis-amine Pd^{II} complexes and lead to a higher concentration of the mono-amine Pd^{II} species empirically required for C-H activation;^[9] or b) the presence of reagents (such as CO) that strongly impact on the mechanism of the process.^[10] While we have frequently observed stoichiometric C-H activation with a range of alkylamines, we recognized that the structure of a putative monocyclic aminoalkyl palladacycle formed in a catalytic reaction with a secondary alkylamine would likely be reflected by a complex wherein a second molecule of alkylamine acts as a neutral ligand alongside a charged carboxylate ligand (Figure 1 b, IV). The structural integrity of a complex of this nature would be reinforced by the favourable thermodynamic scenario of having oppositely dispersed (NH) amine ligands, which replicates the profoundly stable ligand arrangement that is observed for *trans* bis-amine Pd^{II} complexes.^[10a,11] This effect is particularly pertinent to a potential C-H arylation with aryl iodides, whose weak complexing ability may not be sufficient to displace a tightly ligated (NH) amine. Analogous to the situation of Dong et al., the absence of a readily displaced neutral ligand precludes the straightforward reaction of the palladacycle with aryl iodides. However, strongly oxidizing iodine(III) reagents are typically incompatible with less hindered free (NH) alkylamines because of the presence of α -hydrogen atoms in facilitating decomposition pathways.^[9a,c]

Therefore, a conceptually distinct approach from both our previous works and the approaches of others would be required to enable free (NH) amine directed C(sp³)-H arylation. To address the lack of reactivity of these aminoalkyl palladacycles towards oxidative addition, we speculated that installing a carboxylate group at the *ortho* position to the C-I bond in the aryl iodide would displace an anionic group on the aminoalkyl palladacycle and promote a proximity-driven oxidative addition that could lead to C(sp³)-H arylation (Figure 1 b, IV').

Herein we report the successful realization of these ideals, culminating in the development of a Pd^{II}-catalyzed C(sp³)-H arylation of less hindered alkylamines. Key to the success of this strategy is the deployment of an *ortho*-carboxylate-substituted aryl halide as the coupling partner, which facilitates a templated oxidative addition to the stable aminoalkyl palladacycle. Furthermore, the reaction proceeds by a distinct pathway involving a spontaneous decarboxylation and palladium migration step, which renders the overall

process traceless with respect to the activating carboxylate motif.

At the outset of these studies, we focused on investigating the reactivity of a representative five-membered mononuclear γ -aminoalkyl palladacycle (**3**), formed from the reaction of the secondary alkylamine **1** and Pd(OAc)₂, followed by treatment of the initially formed polynuclear species **2** with pyridine (Figure 2 a). This complex served as a characterizable

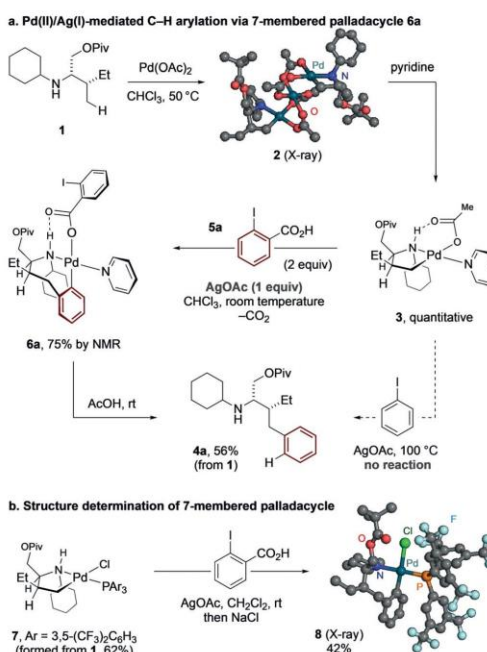


Figure 2. Stoichiometric studies from the mononuclear palladacycles **3** and **7**. The X-ray structure of **8** is shown.^[22]

model for the putative catalytic species that would have a second molecule of the alkylamine in place of the pyridine. Treatment of **3** under reaction conditions commonly used in C-H arylation reactions, namely phenyl iodide and AgOAc (as additive) at 100 °C in either DCE, AcOH, or as a neat reaction, gave no conversion into the corresponding γ -aryl alkylamine **4a**. As highlighted in Figure 1 b, a possible reason for the lack of reactivity of **3** is the stability imparted by the *trans* orientation of nitrogen ligands on Pd^{II}, meaning the iodoarene cannot displace the ligated pyridine. To disrupt this apparently stable complex, we tested the reactivity of an aryl iodide containing an *ortho* carboxylic acid, which we reasoned would displace the acetate ligand and locate the aryl iodide in proximity to the Pd^{II} center (Figure 1 b, IV'), facilitating the oxidative addition to give the putative γ -aminoalkyl Pd^{IV} complex required for C-C bond reductive elimination. When **3** was treated with 2 equivalents of 2-iodobenzoic acid (**5a**) in the presence of one equivalent of AgOAc at room

temperature, we observed complete conversion into a seven-membered palladacycle (**6a**, 75% yield by NMR; Figure 2a).^[12] Formally, the overall transformation from **3** into **6a** corresponds to a 1,2-insertion of an aryl group into the Pd–C bond of the five-membered palladacycle, wherein C(sp³)–C(sp²) bond formation and an unusually facile decarboxylation event have taken place. The palladacycle **6a** was isolable and could be characterized by ¹H and ¹³C NMR spectroscopy. Although **6a** was not a crystalline compound, the structure of a related phosphine-ligated seven-membered palladacycle **8** could be confirmed through X-ray diffraction of a single crystal (Figure 2b). Consequently, treatment of **6a** with AcOH gave **4a** (56% yield from **1**), completing the overall C–H arylation process.

Intrigued by the formation of the seven-membered palladacycle, we conducted a series of control experiments to shed light on the mechanistic steps underpinning the decarboxylative arylation process. Firstly, subjecting **3** to 2-bromobenzoic acid instead of 2-iodobenzoic acid simply resulted in a ligand exchange of acetate for 2-bromobenzoate at room temperature, with the five-membered (NH) amine palladacycle remaining intact.^[13] Stirring the reaction at 80 °C restored reactivity analogous to that of the aryl iodide, and is consistent with a Pd^{II}–Pd^{IV} mechanism based on the diminished reactivity of the aryl bromide relative to the iodide.^[14] Secondly, using 5-methyl-2-iodobenzoic acid (**5b**) as a coupling partner, the arylated product was formed as a single regioisomer (**4b**) in which the newly formed C–C bond is derived from the C–I bond in the reagent (Figure 3a). The exclusive regioselectivity observed cannot be accounted for by a mechanism invoking aryne intermediates, as this would

generate regioisomeric product mixtures.^[15] Further evidence opposing aryne formation was provided by trapping experiments employing aryneophile additives in the stoichiometric arylation procedure, and did not lead to the formation of cycloaddition by-products.^[16] Thirdly, we investigated the point at which decarboxylation occurs along the reaction pathway. Intuitively, one might assume that C–C bond reductive elimination from a putative Pd^{IV} species would initially install an aryl-2-carboxylic acid group at the γ position, giving an amino-acid intermediate that may then undergo either a Pd^{II}- or Ag^I-mediated decarboxylation process to form the γ -arylated amine.^[17] To test this hypothesis, the amino-acid **9** was synthesized and subjected to stoichiometric quantities of Pd(OAc)₂ and AgOAc (Figure 3b). Although minimal conversion occurred at room temperature, stirring the reaction at 80 °C led to the formation of a new palladacyclic species (**10**) resulting from a methylene C–H activation. Crucially, given that the product of decarboxylation (**4a**) was not observed, the hypothesis invoking **9** as an intermediate was not supported. Rather, it became apparent that decarboxylation must occur prior to C–C bond reductive elimination and therefore from a high-valent Pd^{IV} species, which could explain the facile nature of this process compared to reported decarboxylation procedures that typically require high temperatures (> 100 °C).^[17] Lastly, replacing AgOAc with NaOAc led to a significant change in the distribution of products (Figure 3c). The C–O coupled products **11** (43%) and **12** (10%), as well as the elimination product **13** (10%) were obtained. According to literature precedence, C–O reductive elimination is expected to proceed by external attack of an O-centred nucleophile at the

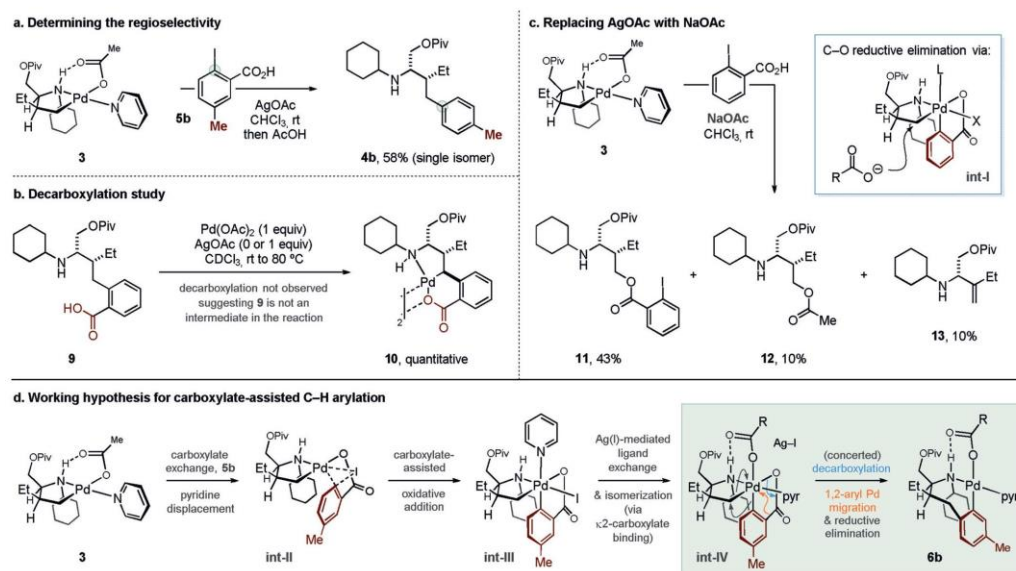


Figure 3. Control experiments and proposed mechanism for carboxylate-assisted C–H arylation.

Pd^{IV}-bound carbon atom (**int-I**),^[18] thus accounting for the presence of the *ortho*-iodide moiety in major product **11**. Notably, **4a** was not observed in the reaction with NaOAc, and therefore in the current system Ag^I was found to be an essential additive for C–C bond reductive elimination.

Based on these preliminary mechanistic studies, we propose a pathway that first involves carboxylate-directed oxidative addition (via **int-II**) to form the bis-palladacyclic γ -aminoalkyl Pd^{IV} species **int-III** (Figure 3d). Presumably, Ag^I-mediated iodide-to-carboxylate ligand exchange generates the corresponding Pd^{IV} carboxylate complex, which through pyridine-displacing κ^2 -carboxylate binding, can trigger a series of geometric isomerisations to form the hydrogen-bond-stabilized Pd^{IV} intermediate **int-IV**. Direct C(sp³)–C(sp²) bond reductive elimination from **int-IV** does not occur, most likely because of the geometric constraints of the bis-palladacycle. However, based on the observed regioselectivity and the absence of aryne intermediates, we believe a decarboxylation triggers a concerted 1,2-arylpalladium migration and reductive elimination, forging i) the C(sp³)–C(sp²) bond between the alkylamine and aryl group and ii) the *ortho* C(sp²)–Pd bond, giving the seven-membered palladacycle (**6b**). To the best of our knowledge, 1,2-arylpalladium migration have been rarely observed outside the context of norbornene-assisted Catellani processes,^[19] despite the analogy with commonly encountered 1,2-palladium migrations of indole or alkenyl Pd^{II} species.^[20]

Next, we tested the decarboxylative C–H arylation under catalytic conditions. Gratifyingly, using 10 mol % Pd(OAc)₂ in the presence of **1**, **5a**, and AgOAc in CHCl₃ at 80 °C gave **4a** in 51% yield as determined by NMR spectroscopy. C–O coupling was observed as a minor side-reaction (**11**, 8%). Significantly, the use of 2-bromobenzoic acid gave an increased yield of **4a**, whereas 2-Cl- and 2-OTf benzoic acid resulted in zero product formation.^[21] Optimal reaction conditions required the treatment of **1** with 10 mol % Pd(OPiv)₂, 2 equivalents of 2-bromobenzoic acid, and 2 equivalents of AgOAc in CHCl₃ at 80 °C for 20 hours, affording **4a** in 74% yield as determined by NMR spectroscopy (70% yield upon isolation, Table 1). With the optimal reaction conditions for C–H arylation identified, the scope with respect to the aryl reagents was investigated (Table 1). Electron-donating and electron-withdrawing substituents at the 4- and 5-positions of the 2-bromobenzoic acid were well tolerated, affording *meta*- and *para*-substituted arylated products in moderate to good yields (**4b–i**). Interestingly, 2-bromo-6-methylbenzoic acid was an effective reagent, demonstrating that increased steric bulk *ortho* to the carboxylic acid is tolerated. The *meta*-methyl product was formed in similar yield (60%, **4fb**) to the reaction using 2-bromo-4-methylbenzoic acid (63%, **4fa**), which gives the same product after decarboxylation. Conversely, the reaction was sensitive to steric effects at the position *ortho* to the C–Br bond. While *ortho*-fluoride and *ortho*-methoxy derivatives could be

Table 1: Scope of the Pd-catalyzed C(sp³)–H arylation of alkylamines.^[a]

aryl scope	amine scope
<p>4a, R = H, 70% 4b, R = Me, 68% 4c, R = F, 54% 4d, R = OMe, 54% 4e, R = CF₃, 39%</p> <p>4fa, R = Me, 63% 4g, R = F, 58% 4h, R = Cl, 61% 4i, R = Br, 49%^[b]</p> <p>4j, R = F, 46% 4k, R = OMe, 51% (R = Me, 0%)</p> <p>4l, 61%</p>	<p>14a, 65% 14b, 62% 14c, 37% 14d, 72%</p> <p>14e, 72% 14f, 77% 14g, 74% 14h, 56% 14i, 40% 14j, 43%</p> <p>14k, 57% 14l, 58% 14m, 53%^[c]</p> <p>14n, 0%</p> <p>14o, 45% 14p 60%^[d] 2:1 mono:di (mono d.r. 1:1)</p> <p>14q, 65%</p>

[a] Reactions carried out on 0.1 mmol scale. [b] 2.5 equiv ArBr and 2.5 equiv AgOAc were used. [c] Reaction temperature was 70 °C. [d] Yield and d.r. determined by ¹H NMR analysis of the crude reaction mixture.

obtained in moderate yields (**4j**, **4k**), 2-bromo-3-methylbenzoic acid gave no reactivity. Finally, 2-bromo-4,5-dimethoxybenzoic acid gave access to more highly substituted derivative **4l**.

The scope with respect to the amine substrates was also investigated (Table 1). A range of functional groups was tolerated in the non-activating substituent of the substrates (**14a–j**), including alkyl, fluoroalkyl, ketal, ether, and sulfonamide groups. Cyclic as well as acyclic sidechains could be incorporated. Generally, *n*-alkyl substituents were not tolerated, though an *N*-benzyl derivative gave a moderate yield of the arylated product (**14j**, 43%). Various substituents could be tolerated along the activating chain, including benzoate, methyl ether, and phthalimide groups (**14k–m**). A substrate without β -branching gave no conversion into the corresponding arylated product (**14n**), whereas a substrate derived from the non-natural diastereomer of isoleucine gave an average yield in the reaction (**14o**, 45%). A valinol derivative was also suitable and gave **14p** as a mixture of diastereomers and mono/diarylated products (60% by NMR spectroscopy, 2:1 mono/di, mono d.r. = 1:1). Finally, we were pleased to find that a derivative of threoninol gave the γ -aryl amino alcohol product **14q** in good yield (65%).

In summary, we have described a new method for $C(sp^3)$ –H arylation of free (NH) secondary amines mediated by Pd^{II} /Ag⁺ using 2-halobenzoic acid reagents. Stoichiometric studies from the Pd^{II} metallacycle demonstrated a remarkably mild, room-temperature decarboxylative arylation is possible when using 2-iodobenzoic acid in the presence of AgOAc. Mechanistic studies suggest that the decarboxylation occurs from a high-valent Pd^{IV} centre and that a 1,2-arylpalladium migration ultimately leads to the required reductive elimination event. The reaction conditions were found to effectively translate to a catalytic system, providing access to a variety of γ -arylated amine derivatives.

Acknowledgements

We are grateful to EPSRC (EP/N031792/1) and for a studentship (W.G.W.), AstraZeneca for a studentship (J.H.B.), the German Academic Exchange Service (DAAD) for a scholarship (G.N.H.), and the Royal Society for a Wolfson Merit Award (M.J.G.) for funding. We are grateful to the mass spectrometry service at the University of Swansea and to Dr Andrew D. Bond for X-ray crystallographic analysis. We are grateful for useful discussions with Dr. Charlene Fallon and Dr. Thomas Hunt (AstraZeneca).

Conflict of interest

The authors declare no conflict of interest.

Keywords: amines · C–H activation · decarboxylation · palladium · reaction mechanisms

How to cite: *Angew. Chem. Int. Ed.* **2019**, *58*, 9054–9059
Angew. Chem. **2019**, *131*, 9152–9157

- [1] a) O. Daugulis, H.-Q. Do, D. Shabashov, *Acc. Chem. Res.* **2009**, *42*, 1074–1086; b) X. Chen, K. M. Engle, D.-H. Wang, J.-Q. Yu, *Angew. Chem. Int. Ed.* **2009**, *48*, 5094–5115; *Angew. Chem.* **2009**, *121*, 5196–5217; c) T. W. Lyons, M. S. Sanford, *Chem. Rev.* **2010**, *110*, 1147–1169; d) O. Baudoin, *Chem. Soc. Rev.* **2011**, *40*, 4902–4911; e) K. M. Engle, T.-S. Mei, M. Wasa, J.-Q. Yu, *Acc. Chem. Res.* **2012**, *45*, 788–802; f) O. Daugulis, J. Roane, L. D. Tran, *Acc. Chem. Res.* **2015**, *48*, 1053–1064; g) G. Qiu, J. Wu, *Org. Chem. Front.* **2015**, *2*, 169–178; h) G. He, B. Wang, W. A. Nack, G. Chen, *Acc. Chem. Res.* **2016**, *49*, 635–645; i) J. He, M. Wasa, K. S. L. Chan, Q. Shao, J.-Q. Yu, *Chem. Rev.* **2017**, *117*, 8754–8786; j) Y. Xu, G. Dong, *Chem. Sci.* **2018**, *9*, 1424–1432; k) J. C. K. Chu, T. Rovis, *Angew. Chem. Int. Ed.* **2018**, *57*, 62–101; *Angew. Chem.* **2018**, *130*, 64–105; l) T. G. Saint-Denis, R.-Y. Zhu, G. Chen, Q.-F. Wu, J.-Q. Yu, *Science* **2018**, *359*, eaao4798.
- [2] C. He, W. G. Whitehurst, M. J. Gaunt, *Chem* **2019**, *5*, 1031–1058.
- [3] a) S. D. Roughley, A. M. Jordan, *J. Med. Chem.* **2011**, *54*, 3451–3479; b) E. Vitaku, D. T. Smith, J. T. Njardarson, *J. Med. Chem.* **2014**, *57*, 10257–10274; c) D. C. Blakemore, L. Castro, I. Churcher, D. C. Rees, A. W. Thomas, D. M. Wilson, A. Wood, *Nat. Chem.* **2018**, *10*, 383–394.
- [4] a) M. Wasa, K. M. Engle, J.-Q. Yu, *Isr. J. Chem.* **2010**, *50*, 605–616; b) K. S. L. Chan, M. Wasa, L. Chu, B. N. Laforteza, M. Miura, J.-Q. Yu, *Nat. Chem.* **2014**, *6*, 146–150; c) J. E. Spangler, Y. Kobayashi, P. Verma, D.-H. Wang, J.-Q. Yu, *J. Am. Chem. Soc.* **2015**, *137*, 11876–11879; d) Q. Shao, J. He, Q.-F. Wu, J.-Q. Yu, *ACS Catal.* **2017**, *7*, 7777–7782; e) Q. Shao, Q.-F. Wu, J. He, J.-Q. Yu, *J. Am. Chem. Soc.* **2018**, *140*, 5322–5325.
- [5] a) V. G. Zaitsev, D. Shabashov, O. Daugulis, *J. Am. Chem. Soc.* **2005**, *127*, 13154–13155; b) G. He, G. Chen, *Angew. Chem. Int. Ed.* **2011**, *50*, 5192–5196; *Angew. Chem.* **2011**, *123*, 5298–5302; c) N. Rodríguez, J. A. Romero-Revilla, M. A. Fernández-Ibáñez, J. C. Carretero, *Chem. Sci.* **2013**, *4*, 175–179; d) M. Fan, D. Ma, *Angew. Chem. Int. Ed.* **2013**, *52*, 12152–12155; *Angew. Chem.* **2013**, *125*, 12374–12377; e) P.-X. Ling, S.-L. Fang, X.-S. Yin, K. Chen, B.-Z. Sun, B.-F. Shi, *Chem. Eur. J.* **2015**, *21*, 17503–17507; f) J. Han, Y. Zheng, C. Wang, Y. Zhu, D.-Q. Shi, R. Zeng, Z.-B. Huang, Y. Zhao, *J. Org. Chem.* **2015**, *80*, 9297–9306; g) J. J. Topczewski, P. J. Cabrera, N. I. Saper, M. S. Sanford, *Nature* **2016**, *531*, 220–224; h) N. Gulia, O. Daugulis, *Angew. Chem. Int. Ed.* **2017**, *56*, 3630–3634; *Angew. Chem.* **2017**, *129*, 3684–3688; i) A. Yada, W. Liao, Y. Sato, M. Murakami, *Angew. Chem. Int. Ed.* **2017**, *56*, 1073–1076; *Angew. Chem.* **2017**, *129*, 1093–1096; j) Y. Wu, Y.-Q. Chen, T. Liu, M. D. Eastgate, J.-Q. Yu, *J. Am. Chem. Soc.* **2016**, *138*, 14554–14557; k) Y. Liu, H. Ge, *Nat. Chem.* **2017**, *9*, 26–32; l) M. Kapoor, D. Liu, M. C. Young, *J. Am. Chem. Soc.* **2018**, *140*, 6818–6822; m) Y.-Q. Chen, Z. Wang, Y. Wu, S. R. Wisniewski, J. X. Qiao, W. R. Ewing, M. D. Eastgate, J.-Q. Yu, *J. Am. Chem. Soc.* **2018**, *140*, 17884–17894.
- [6] a) F. Barrios-Landeros, J. F. Hartwig, *J. Am. Chem. Soc.* **2005**, *127*, 6944–6945; b) H. M. Senn, T. Ziegler, *Organometallics* **2004**, *23*, 2980–2988; c) P. Sehnal, R. J. K. Taylor, I. J. S. Fairlamb, *Chem. Rev.* **2010**, *110*, 824–889.
- [7] Y. Xu, M. C. Young, C. Wang, D. M. Magness, G. Dong, *Angew. Chem. Int. Ed.* **2016**, *55*, 9084–9087; *Angew. Chem.* **2016**, *128*, 9230–9233.
- [8] a) K. J. Szabó, *J. Mol. Catal. A* **2010**, *324*, 56–63; b) N. R. Deprez, M. S. Sanford, *Inorg. Chem.* **2007**, *46*, 1924–1935.
- [9] a) A. McNally, B. Haffemayer, B. S. L. Collins, M. J. Gaunt, *Nature* **2014**, *510*, 129–133; b) A. P. Smalley, M. J. Gaunt, *J. Am. Chem. Soc.* **2015**, *137*, 10632–10641; c) J. Calleja, D. Pla, T. W. Gorman, V. Domingo, B. Haffemayer, M. J. Gaunt, *Nat. Chem.* **2015**, *7*, 1009–1016.
- [10] a) D. Willcox, B. G. N. Chappell, K. F. Hogg, J. Calleja, A. P. Smalley, M. J. Gaunt, *Science* **2016**, *354*, 851–856; b) J. R. Cabrera-Pardo, A. Trowbridge, M. Nappi, K. Ozaki, M. J.



- Gaunt, *Angew. Chem. Int. Ed.* **2017**, *56*, 11958–11962; *Angew. Chem.* **2017**, *129*, 12120–12124.
- [11] a) A. D. Ryabov, *Chem. Rev.* **1990**, *90*, 403–424; b) R. A. Widenhoefer, S. L. Buchwald, *Organometallics* **1996**, *15*, 3534–3542; c) J. Dupont, C. S. Consorti, J. Spencer, *Chem. Rev.* **2005**, *105*, 2527–2571.
- [12] Reaction of **3** with diphenyliodonium triflate and AgOAc at room temperature gave no conversion into **4a**. Heating to 80 °C for 16 h resulted in full consumption of **3** and 24% yield of **4a** as determined by NMR spectroscopy.
- [13] See the Supporting Information for details of the control experiment of **3** with 2-bromobenzoic acid.
- [14] J. Vicente, A. Arcas, F. Juliá-Hernández, D. Bautista, *Angew. Chem. Int. Ed.* **2011**, *50*, 6896–6899; *Angew. Chem.* **2011**, *123*, 7028–7031.
- [15] a) R. Huisgen, J. Sauer, *Angew. Chem.* **1960**, *72*, 91–108; b) E. R. Biehl, E. Nieh, K. C. Hsu, *J. Org. Chem.* **1969**, *34*, 3595–3599; c) J. L. Henderson, A. S. Edwards, M. F. Greaney, *J. Am. Chem. Soc.* **2006**, *128*, 7426–7427; d) J. L. Henderson, A. S. Edwards, M. F. Greaney, *Org. Lett.* **2007**, *9*, 5589–5592; e) J.-A. García-López, M. F. Greaney, *Chem. Soc. Rev.* **2016**, *45*, 6766–6798.
- [16] See the Supporting Information for aryne trapping experiments.
- [17] a) N. Rodríguez, L. K. Goossen, *Chem. Soc. Rev.* **2011**, *40*, 5030–5048; b) J. Cornella, I. Larrosa, *Synthesis* **2012**, *44*, 653–676; c) G. J. P. Perry, I. Larrosa, *Eur. J. Org. Chem.* **2017**, 3517–3527; d) M. Font, J. M. Quibell, G. J. P. Perry, I. Larrosa, *Chem. Commun.* **2017**, 53, 5584–5597.
- [18] a) N. M. Camasso, M. H. Pérez-Temprano, M. S. Sanford, *J. Am. Chem. Soc.* **2014**, *136*, 12771–12775; b) M. Nappi, C. He, W. G. Whitehurst, B. G. N. Chappell, M. J. Gaunt, *Angew. Chem. Int. Ed.* **2018**, *57*, 3178–3182; *Angew. Chem.* **2018**, *130*, 3232–3236.
- [19] a) E. A. Filatova, A. V. Gulevskaya, A. F. Pozharskii, V. A. Ozeryanskii, *Tetrahedron* **2016**, *72*, 1547–1557; b) M. Catellani, E. Motti, N. Della Ca', *Acc. Chem. Res.* **2008**, *41*, 1512–1522.
- [20] a) B. S. Lane, M. A. Brown, D. Sames, *J. Am. Chem. Soc.* **2005**, *127*, 8050–8057; b) J.-P. Ebran, A. L. Hansen, T. M. Gøgsig, T. Skrydstrup, *J. Am. Chem. Soc.* **2007**, *129*, 6931–6942; c) A. T. Lindhardt, T. M. Gøgsig, T. Skrydstrup, *J. Org. Chem.* **2009**, *74*, 135–143.
- [21] See the Supporting Information for full details of the optimization of the Pd-catalyzed C(sp³)-H arylation reaction.
- [22] CCDC 1850705 (**8**) contains the supplementary crystallographic data for this paper. These data can be obtained free of charge from The Cambridge Crystallographic Data Centre.

Manuscript received: March 6, 2019
 Revised manuscript received: April 23, 2019
 Accepted manuscript online: May 1, 2019
 Version of record online: May 23, 2019